AD-782 179

POLARIZED RADIANCE. VOLUME III: WAVELENGTH DEPENDENCE OF POLARIZED BIDIRECTIONAL REFLECTANCE

J. R. Maxwell, et al

Environmental Research Institute of Michigan

Prepared for:

Ballistic Research Laboratories

May 1974

DISTRIBUTED BY:

NTIS

National Technical Information Service
U. S. DEPARTMENT OF COMMERCE
5285 Port Royal Road, Springfield Va. 22151

AD782179

BRL CR 156

BRL

AD

CONTRACT REPORT NO. 156

POLARIZED RADIANCE VOL III: WAVELENGTH DEPENDENCE OF POLARIZED BIDIRECTIONAL REFLECTANCE

Prepared by

Environmental Institute of Michigan
P. O. Box 616
Ann Arbor, Michigan

May 1974

DDC
RECEIVED
JUL 19 1974
B

Approved for public release; distribution unlimited.

USA BALLISTIC RESEARCH LABORATORIES
ABERDEEN PROVING GROUND, MARYLAND

NATIONAL TECHNICAL
INFORMATION SERVICE

Destroy this report when it is no longer needed.
Do not return it to the originator.

Secondary distribution of this report by originating or sponsoring activity is prohibited.

Additional copies of this report may be obtained from the National Technical Information Service, U.S. Department of Commerce, Springfield, Virginia 22151.

ACCESSION for
NTIS White Section
D D Buff Section
UNANNOUNCED
JUSTIFICATION
BY
DISTRIBUTION/AVAILABILITY CODES
Dist. AVAIL. and/or SPECIAL

The findings in this report are not to be construed as an official Department of the Army position, unless so designated by other authorized documents.

The use of trade names or manufacturers' names in this report does not constitute indorsement of any commercial product.

SECURITY CLASSIFICATION OF THIS PAGE (When Data Entered)

REPORT DOCUMENTATION PAGE

READ INSTRUCTIONS BEFORE COMPLETING FORM

1. REPORT NUMBER
CONTRACT REPORT NO. 156

2. GOVT ACCESSION NO.

3. RECIPIENT'S CATALOG NUMBER
AD-782179

4. TITLE (and Subtitle)
POLARIZED RADIANCE (VOL.III): WAVELENGTH DEPENDENCE OF POLARIZED BIDIRECTIONAL REFLECTANCE

5. TYPE OF REPORT & PERIOD COVERED
Final
10 Apr 72 - 31 May 73

6. PERFORMING ORG. REPORT NUMBER
192500-1T(1) (Vol.III)

7. AUTHOR(s)
J. R. Maxwell
S. Weiner

8. CONTRACT OR GRANT NUMBER(s)
DAAD05-72-C-0246

9. PERFORMING ORGANIZATION NAME AND ADDRESS
Environmental Institute of Michigan
P. O. Box 616
Ann Arbor, Michigan 48107

10. PROGRAM ELEMENT, PROJECT, TASK AREA & WORK UNIT NUMBERS
6.11.02B
RDT&E 1T061102B11A

11. CONTROLLING OFFICE NAME AND ADDRESS
USA Ballistic Research Laboratories
Aberdeen Proving Ground, Maryland 21005

12. REPORT DATE
MAY 1974

13. NUMBER OF PAGES
322

14. MONITORING AGENCY NAME & ADDRESS (if different from Controlling Office)

15. SECURITY CLASS. (of this report)
UNCLASSIFIED

15a. DECLASSIFICATION/DOWNGRADING SCHEDULE

16. DISTRIBUTION STATEMENT (of this Report)
Approved for public release; distribution unlimited.

17. DISTRIBUTION STATEMENT (of the abstract entered in Block 20, if different from Report)

18. SUPPLEMENTARY NOTES
The work reported herein was conducted by the Environmental Research Institute of Michigan for the USA Ballistic Research Laboratories, Aberdeen Proving Ground, MD 21005 under Contract No. DAAD05-72-C-0246. Dr. Lawrence VandeKieft is Technical Monitor. Contracts and grants to the Institute for the support of sponsored research are administered through the Office of Contracts Administration.

19. KEY WORDS (Continue on reverse side if necessary and identify by block number)
Bidirectional Reflectance
Wavelength Dependence
Polarized Reflectance
Modeling

Reproduced by
NATIONAL TECHNICAL
INFORMATION SERVICE
U. S. Department of Commerce
Springfield VA 22161

20. ABSTRACT (Continue on reverse side if necessary and identify by block number)
Volume III of this report provides the Ballistic Research Laboratories with a method for extracting information from a limited set of directional and bi-directional reflectance measurements so as to provide a wavelength-corrected input to the volume component of the bidirectional reflectance model described in Volume I. It is shown that the surface component of the bidirectional reflectance has little wavelength dependence for the materials studied from 0.63μm through 3.39μm. Data resulting from extensive measurements performed
(Continued on reverse side)

DD FORM 1 JAN 73 1473 EDITION OF 1 NOV 65 IS OBSOLETE

UNCLASSIFIED

SECURITY CLASSIFICATION OF THIS PAGE (When Data Entered)

Block 20. Abstract

at 0.63μm, 1.06μm, 3.39μm and 10.6μm under this contract are included and are used for the model validation which is also described.

FOREWORD

The work reported herein, covering the period 10 April 1972 to 31 May 1973, was carried out by the Infrared and Optics Division of the Environmental Research Institute of Michigan (formerly the Willow Run Laboratories of The University of Michigan), Ann Arbor, Michigan. The work was performed under Contract DAAD05-72-C-0216 for the Army Ballistic Research Laboratories, and was done in three parts, each of which represent one volume.

The three volumes are:

I - Polarized Bidirectional Reflectance With Lambertian or Non-Lambertian Diffuse Component.

II - Polarized Spectral Emittance From 4 to 14 μm.

III - Wavelength Dependence of Polarized Bidirectional Reflectance.

The internal number of volume III of this report is 192500-1-T(III).

TABLE OF CONTENTS

FORWORD..... 3

LIST OF FIGURES..... 7

LIST OF TABLES..... 9

1.0 INTRODUCTION..... 11

2.0 MEASUREMENTS..... 16
2.1 Beckman Spectrometer Directional Reflectance Measurements..... 17
2.2 Gonioreflectometer Bidirectional Reflectance Measurements..... 21

3.0 MODEL DESCRIPTION..... 23
3.1 Extraction From Directional Reflectance Data..... 26
3.2 Extraction From Bidirectional Reflectance Data..... 28

4.0 MODEL VALIDATION..... 28

REFERENCES..... 50

APPENDIX A: MEASUREMENT DATA FOR A01610, A02022 AND A02023 AT 0.63 μm, 1.06 μm, 3.39 μm AND 10.6 μm..... 51

DISTRIBUTION LIST..... 325

Preceding page blank

LIST OF FIGURES

1. SPECTRAL BIDIRECTIONAL REFLECTANCE FOR GREEN PAINT (SAMPLE NO. 1027) FOR A SPECULAR GEOMETRY WHERE $\theta_i = 55°$ 12

2. SPECTRAL BIDIRECTIONAL REFLECTANCE FOR GREEN PAINT (SAMPLE NO. 1027) FOR A SPECULAR GEOMETRY WHERE $\theta_i = 55°$ 13

3. SPECTRAL BIDIRECTIONAL REFLECTANCE FOR GREEN PAINT (SAMPLE NO. 1027) FOR NORMAL INCIDENCE AND $\theta_r = 50°$ 14

4. SPECTRAL BIDIRECTIONAL REFLECTANCE FOR GREEN PAINT (SAMPLE NO. 1027) FOR NORMAL INCIDENCE AND $\theta_r = 50°$ 15

5. SPECTRAL DIRECTIONAL REFLECTANCE FOR AO 1610 18

6. SPECTRAL DIRECTIONAL REFLECTANCE FOR AO 2022 19

7. SPECTRAL DIRECTIONAL REFLECTANCE FOR AO 2023 20

8. SURFACE COMPONENT OF SPECTRAL DIRECTIONAL REFLECTANCE FOR AO 1610 29

9. SURFACE COMPONENT OF SPECTRAL DIRECTIONAL REFLECTANCE FOR AO 2022 30

10. SURFACE COMPONENT OF SPECTRAL DIRECTIONAL REFLECTANCE FOR AO 2023 31

11(a). FIXED BISTATIC BIDIRECTIONAL REFLECTANCE FOR AO 1610 AT 0.63 μm 33

11(b). FIXED BISTATIC BIDIRECTIONAL REFLECTANCE FOR AO 1610 AT 0.63 μm 34

12(a). FIXED BISTATIC BIDIRECTIONAL REFLECTANCE FOR AO 1610 AT 1.06 μm 35

12(b). FIXED BISTATIC BIDIRECTIONAL REFLECTANCE FOR AO 1610 AT 1.06 μm 36

13(a). FIXED BISTATIC BIDIRECTIONAL REFLECTANCE FOR AO 2022 AT 0.63 μm 37

13(b). FIXED BISTATIC BIDIRECTIONAL REFLECTANCE FOR AO 2022 AT 0.63 μm 38

14(a). FIXED BISTATIC BIDIRECTIONAL REFLECTANCE FOR AO 2022 AT 1.06 μm 39

14(b). FIXED BISTATIC BIDIRECTIONAL REFLECTANCE FOR AO 2022 AT 1.06 μm 40

15. BIDIRECTIONAL REFLECTANCE MEASUREMENT FOR AO 1610 AT 0.63 μm with $\theta_i = 0$ .. 42

16. BIDIRECTIONAL REFLECTANCE, CROSS-POLARIZED COMPONENT CALCULATION FOR AO 1610 AT 0.63 μm WITH $\theta_i = 0$ 43

Preceding page blank

17. BIDIRECTIONAL REFLECTANCE MEASUREMENT FOR AO 1610 AT 0.63 μm WITH θ_i = 40° 44

18. BIDIRECTIONAL REFLECTANCE, CROSS-POLARIZED COMPONENT CALCULATION FOR AO 1610 μm WITH θ_i = 40° 45

19. BIDIRECTIONAL REFLECTANCE MEASUREMENT FOR AO 2022 AT 0.63 μm WITH θ_i = 0 46

20. BIDIRECTIONAL REFLECTANCE CROSS-POLARIZED COMPONENT CALCULATION FOR AO 2022 AT 0.63 μm WITH θ_i = 0 47

21. BIDIRECTIONAL REFLECTANCE MEASUREMENT FOR AO 2022 AT 0.63 μm WITH θ_i = 40° 48

22. BIDIRECTIONAL REFLECTANCE CROSS-POLARIZED COMPONENT CALCULATION FOR AO 2022 at 0.63 μm WITH θ_i = 40° 49

LIST OF TABLES

1. POLARIZATION CODE CORRECTIONS FOR 3.39 μm BIDIRECTIONAL REFLECTANCE REFLECTANCE AND DATA..... 22

2. ACTUAL RECEIVED POLARIZATION ANGLES FOR 3.39 μm BIDIRECTIONAL REFLECTANCE DATA..... 24

1.0 INTRODUCTION

The comprehensive bidirectional reflectance modeling which has been described in Volume I of this report [1] was performed without regard to wavelength dependence. Measurements were made at 1.06 μm, and model calculations were made on the basis of the fixed bistatic data of those measurements plus the assumption of a purely real index of refraction, $n = 1.65$.

Based on measurements made under other contracts [2] there was, at the outset of this effort, reason to believe that the surface reflectance has no discernible wavelength dependence between .63 μm and 1.06 μm. The volume component, however, does.

The foregoing statements are supported by Figures 1 - 4 where the spectral bidirectional reflectance for a green paint is given in two different source-receiver geometries and with two different source polarizations in each case.

Figures 1 and 2 illustrate the situation for a specular geometry with $\theta_i = \theta_r = 55^\circ$. For the perpendicular source polarization (Figure 1) the parallel-polarized receiver return is about two orders of magnitude below that of the perpendicular-polarized receiver. In this case, the surface reflectance ($\rho|_{\perp,\perp} - \rho|_{\perp,||}$) (see Volume I, [1]) is approximately the same as the like-polarized component ($\rho|_{\perp,\perp}$) which is seen to be essentially flat between 0.63 and 1.06 μm. (If the cross-polarized component is subtracted out, it becomes even flatter.) Therefore, with a perpendicular-polarized source, the bidirectional surface reflectance in a specular geometry for this sample appears wavelength independent from .63 to beyond 1.06 μm.

The spectral return with a parallel-polarized source (Figure 2) looks different. This is so because at $\theta_i = 55^\circ$ we are very close to the Brewster angle and the reflectance from a parallel-polarized source nears its minimum. However, in this case too, when the surface component is calculated by subtracting the cross-polarized component from the like-polarized component ($\rho|_{||,||} - \rho|_{||,\perp}$) it is seen to be essentially wavelength independent

Preceding page blank

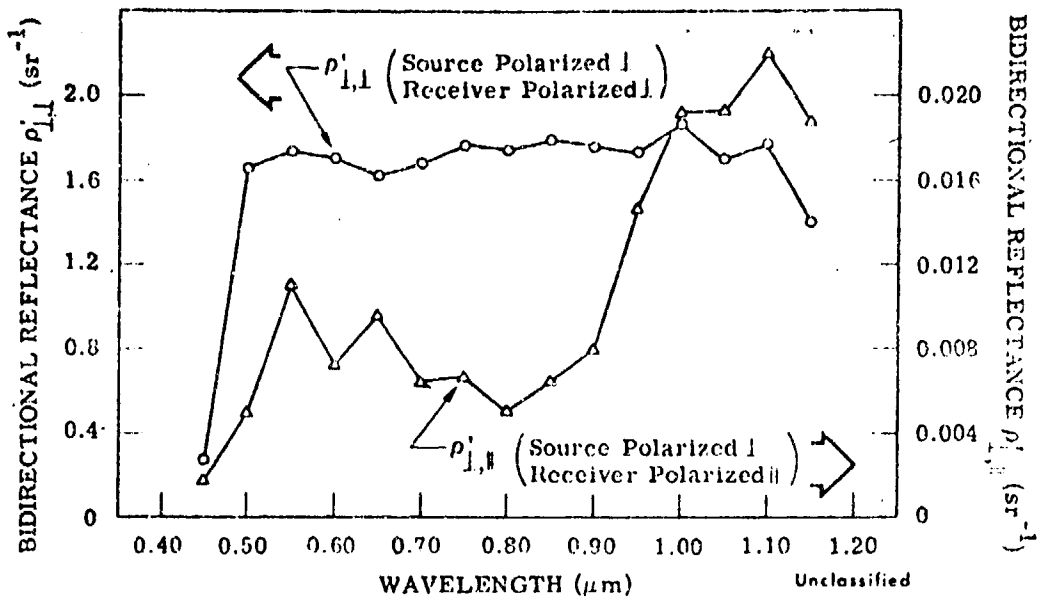

Source Polarization ⊥

FIGURE 1 SPECTRAL BIDIRECTIONAL REFLECTANCE FOR GREEN PAINT (SAMPLE NO. 1027) FOR A SPECULAR GEOMETRY WHERE $\theta_i = 55^o$

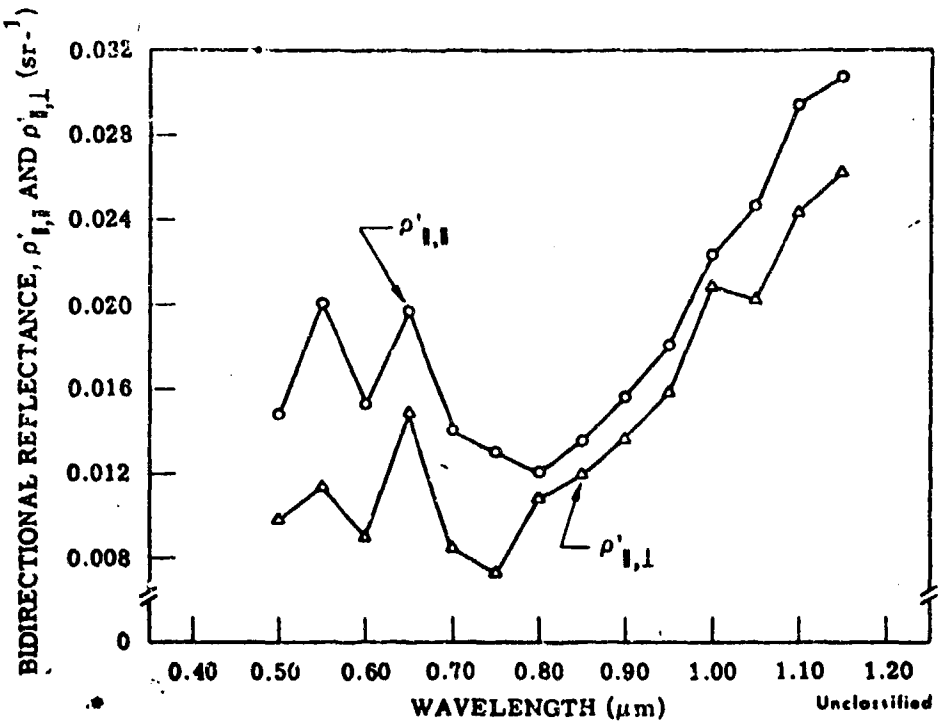

Source Polarization ||

FIGURE 2 SPECTRAL BIDIRECTIONAL REFLECTANCE FOR GREEN PAINT (SAMPLE NO. 1027) FOR A SPECULAR GEOMETRY WHERE $\theta_i = 55^o$

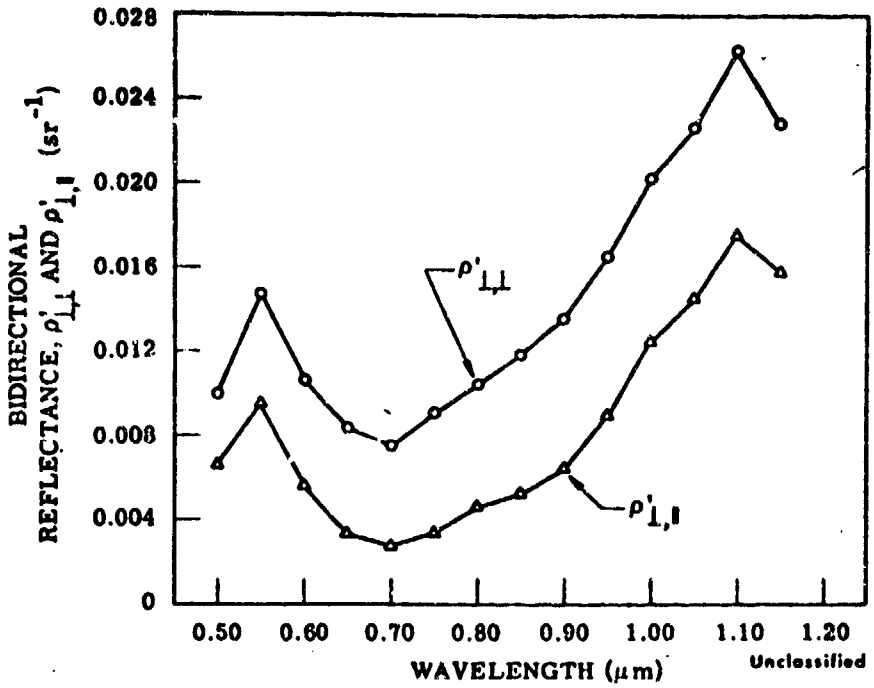

Source Polarization ⊥

FIGURE 3 SPECTRAL BIDIRECTIONAL REFLECTANCE FOR GREEN PAINT (SAMPLE NO. 1027) FOR NORMAL INCIDENCE AND $\theta_r = 50^o$

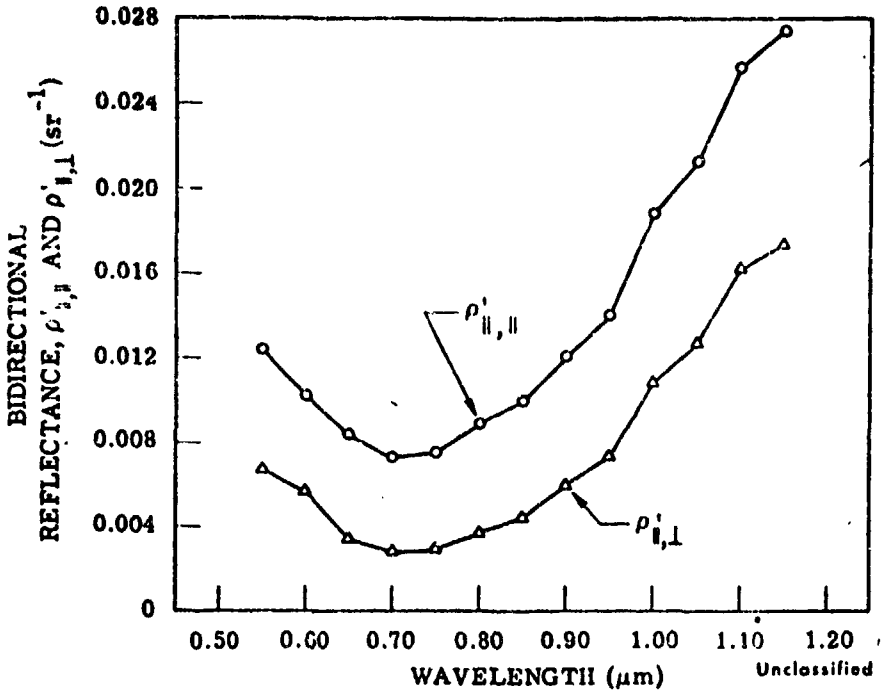

Source Polarization ||

FIGURE 4 SPECTRAL BIDIRECTIONAL REFLECTANCE FOR GREEN PAINT (SAMPLE NO. 1027) FOR NORMAL INCIDENCE AND $\vartheta_r = 50^o$

between .63 and 1.06 μm. However, it is obvious in both Figure 1 and Figure 2 that there is a spectral dependence in the volume, or cross-polarized, component itself.

The same sample is described in Figure 3 and 4 with a different source-receiver geometry; this time $\theta_i = 0$ and $\theta_r = 50°$. Now the case with perpendicular source polarization (Figure 3) looks almost identical to that with parallel source polarization. In both cases, the surface component ($\rho'_{\alpha\alpha} - \rho'_{\alpha\beta}$) is clearly flat throughout the graph, while the volume (corss-polarized) component contains the spectral dependence. It will be seen in Section 2 that a similar situation exists for the samples studied in this work.

The program for this modeling effort was to assume that the wavelength variation of the volume component of the bidirectional reflectance was the same as that for the directional reflectance. If the bidirectional volume reflectance for a given surface is known at one wavelength and the directional reflectance can be obtained at that wavelength and a second wavelength, then the bidirectional volume reflectance for the second wavelength can be obtained from:

$$\rho'_V(\theta_i,\phi_i,\theta_r,\phi_r;\ \lambda_2) = \frac{\rho_D(\lambda_2)}{\rho_D(\lambda_1)}\,\rho'_V(\theta_i,\phi_i,\theta_r,\phi_r;\ \lambda_1)$$

Description of the model is given in Section 3 and of the validation in Section 4. Measurement data are discussed in Section 2.

2.0 MEASUREMENTS

The purpose of the measurement program was to obtain sufficient data to validate the model and to extract input information, based on wavelength dependence, for the RHOPRIME program described in Volume I. In particular, it was important to determine a) the surface reflectance dependence on wavelength in the wavelength region of .63 μm to beyond 3.39 μm and, b) whether the assumption that the bidirectional reflectance varies as the directional reflectance in the volume component is valid.

To accomplish the above objectives extensive measurements were performed on three different sample surfaces at four different wavelengths. The samples are code-numbered: A01610, A02022, and A02023. All are metallic surfaces coated with varying shades and textures of green paint.

The measurements carried out under this contract were bidirectional reflectance measurements performed on the ERIM gonioreflectometer [3]. However, in order to determine directional reflectance ratios, it was necessary to have direct directional reflectance measurement data. Such measurements have been performed by ERIM on the same samples with a Beckman DKII spectrometer under other contracts. (Samples A02022 and A02023 were measured under Contract DAAF03-72-C-0115 with Rock Island Arsenal [4] while Sample A01610 was measured under Contract F33615-68-C-1281 with the Air Force Avionics Laboratory [5].)

2.1 Beckman Spectrometer Directional Reflectance Measurements

The purpose of these measurements was to obtain data for $\rho_D(\lambda)$ so that the ratio of the directional reflectances at two different wavelengths could be used to predict the bidirectional reflectance at one of the wavelengths, given the bidirectional reflectance at the other. (The description of the model is detailed in Section 3.)

Figures 5, 6, and 7 show the directional reflectance measurements from .4 μm to 2.6 μm for samples A01610, A02022 and A02023, respectively. All three samples are shades of green in color and should be expected to increase reflectance sharply in the green wavelength range. That this happens between about .49 and .53 μm is shown in all three figures. In the infrared, A01610 becomes extremely bright at about .75 μm and remains highly reflecting to the 2.6 μm limit of the Beckman measurement. Both A02022 and A02023 show no further rise beyond the increase at .49 μm.

In all three cases, reflectance includes both surface and volume contributions and further reduction had to be performed before the data could be used.

A01610 002

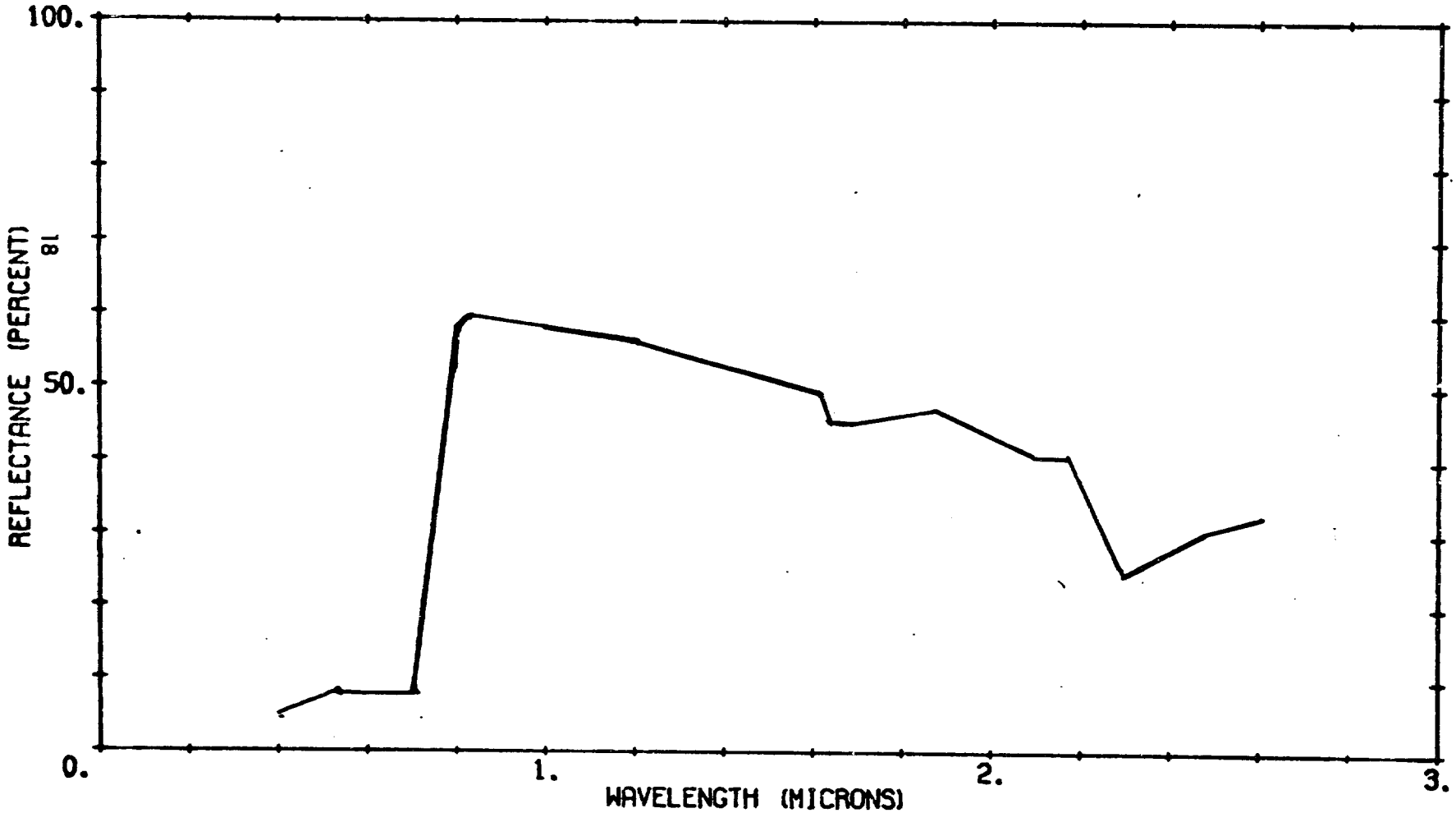

FIGURE 6

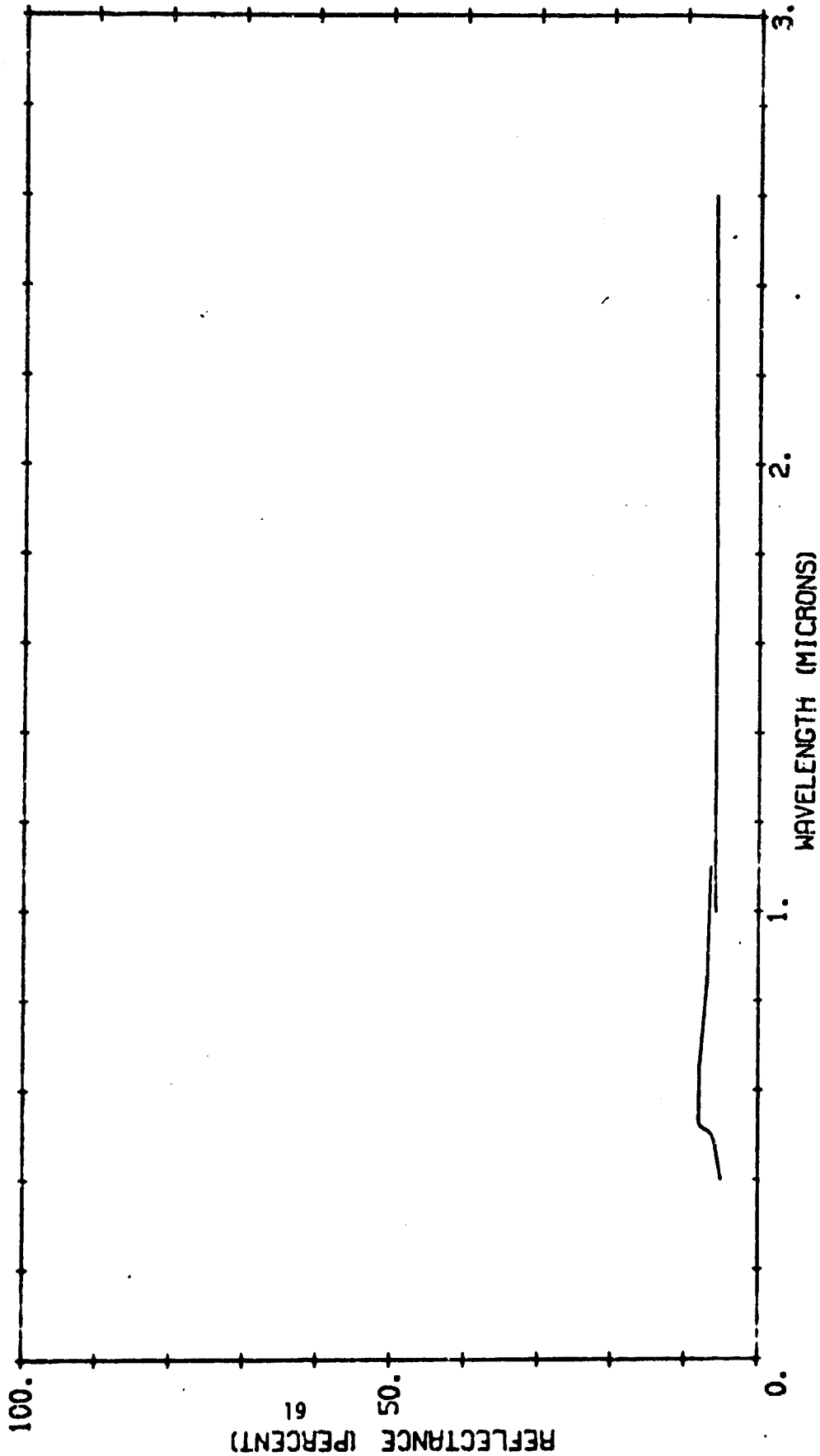

A02022 001

FIGURE 7

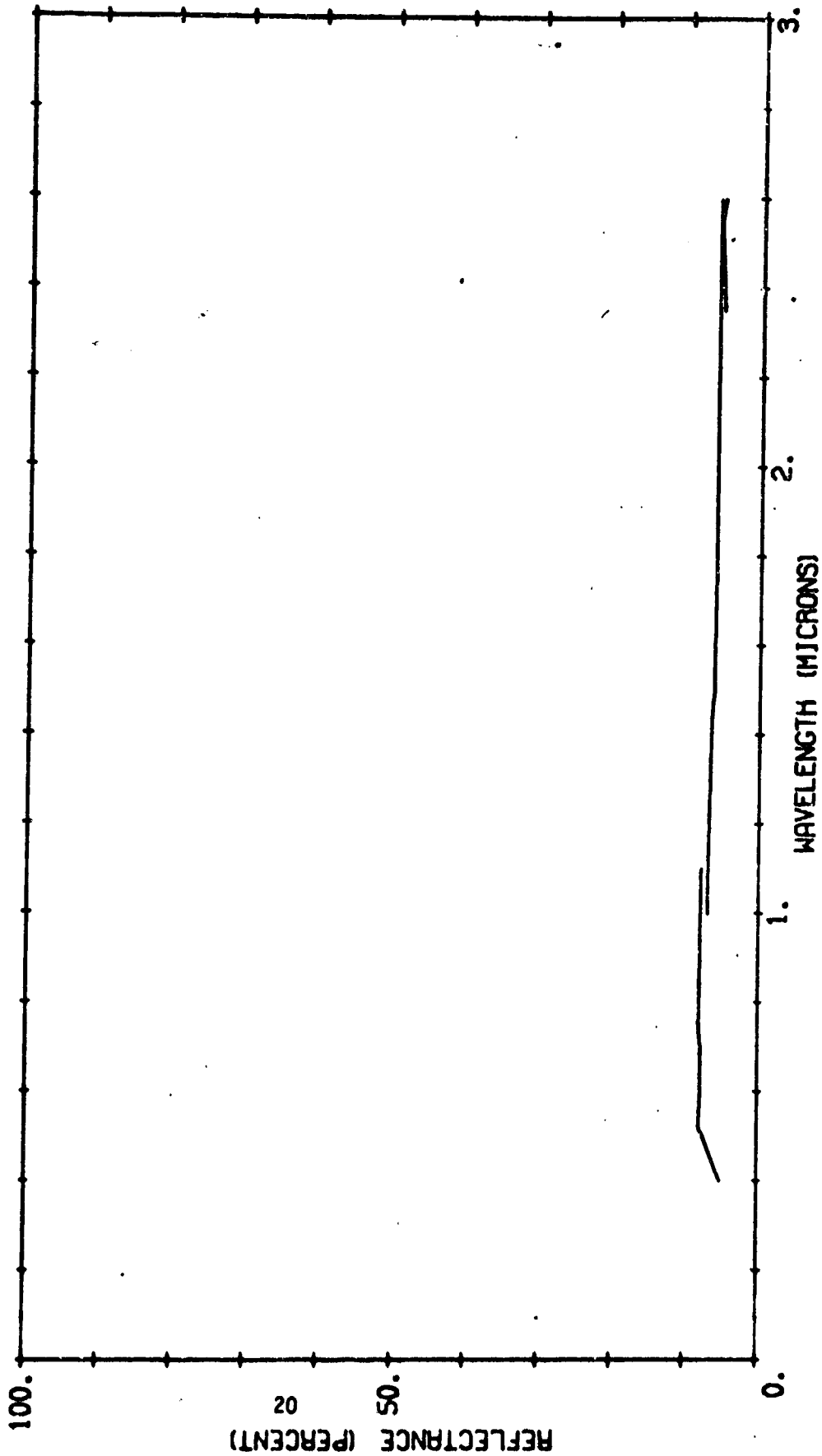

A02023 003

2.2 Gonioreflectometer Bidirectional Reflectance Measurements

Data from the bidirectional reflectance measurements are given in Appendix A. When using the bidirectional reflectance data, the following observations should be noted:

1. There is no significant variation of the surface component of ρ' as a function of wavelength between 0.63 μm and 1.06 μm. (There are, however, significant variations in the volume components in the same spectral region.) That a linear relation is reasonable between 0.63 μm and 10.6 μm is discussed in section 4 where it is shown that for sample AO 1610, the greatest error is about 40% and for the other two samples, the greatest error is about 17%. Therefore, we conclude that for the surface component there is no more than a weak wavelength dependence which is approximately linear with a small enough slope that variations are not significant between 0.63 μm and 10.6 μm.
2. For Samples A01610 and A02022, the volume component varies with wavelength and the measurements are unambiguous and suitable for parameter extraction at 0.63 μm and 1.06 μm. However, at 3.39 μm and 10.6 μm, the volume component falls to below the noise level of the system and hence cannot be used for validation. At 0.63 μm the volume component for Sample A02023 is also below the system noise and therefore this sample was not used in the validation.

   The result is that two samples (A01610 and A02022) were used for model validation at two wavelengths (0.63 μm and 1.06 μm).
3. Difficulties encountered in aligning the receiver polarization analyzer for the 3.39 μm measurements make necessary the following corrections when working with the data:
   a) All ±45° source polarization data must be multiplied by a scale factor of 0.38.
   b) Polarization symbols on the 3.39 μm data are incorrect because of the alignment problems. Table 1 shows what the symbols, as they are, represent and what the correct symbols (with their representative polarizations) should be.

TABLE 1. POLARIZATION CODE CORRECTIONS FOR 3.39 μm BIDIRECTIONAL REFLECTANCE AND DATA

Present Code	Correct Code
• (⊥, 45)	◊ (⊥, -45)
⌘ (||, 45)	K (||, -45)
X (45, ⊥)	A (-45, ⊥)
B (45, 45)	M (-45, -45)
⊡ (45, ||)	★ (-45, ||)
◊ (⊥, -45)	✱ (⊥, 45)
K (||, -45)	⌘ (||, 45)
A (-45, ⊥)	X (45, ⊥)
M (-45, -45)	B (45, 45)
S (-45, ||)	⊡ (45, ||)

c) Nominal receiver polarization angles are presented with the actual polarization angles in Table 2.

Because the receiver is not really at 90° (||) when so referred to, there is no pure cross-polarized measurement with the source at 0° (⊥). Therefore, there appears to be a larger cross-polarized component than there should be in these cases. The increase, however, really represents that part of the 0° polarized return which is not stopped by the analyzer and should be disregarded.

4. In the fixed bistatic data for Sample A02022 at 3.39 μm it should be noted that the ⊥,⊥ component truncates at about $\theta_r = 7°$ because of instrumental saturation.

3.0 MODEL DESCRIPTION

The wavelength dependence model for the volume component of the bidirectional reflectance is based on the assumption that the volume bidirectional reflectance varies with wavelength in the same manner as the directional reflectance. (This assumption has been discussed in [2].) The plausibility of this assumption is borne out by the measurements as described in Section 2. Therefore, if we are able to obtain the directional reflectance, $\rho_D(\lambda)$, at two wavelengths, we can take the ratio of the two and say that the volume bidirectional reflectance varies by the same ratio. In mathematical terms:

$$\rho'_V(\theta_i,\phi_i,\theta_r,\phi_r;\lambda_1) = \frac{\rho_D(\lambda_1)}{\rho_D(\lambda_2)} \rho'_V(\theta_i,\phi_i,\theta_r,\phi_r;\lambda_2)$$

where ρ'_V is the volume component of the bidirectiona reflectance.

As shown in Volume I, the volume component of the bidirectional reflectance always contains a multiplicative factor, ρ_V in the non-Lambertian case and ρ_χ in the Lambertian case, where ρ_V (or ρ_χ), is a constant model parameter which is extracted from a fixed-bistatic bidirectional reflectance scan.

TABLE 2.

Actual Receiver Polarization Angles for 3.39 μm
Bidirectional Reflectance Data

Nominal Polarization Angle		Actual Polarization Angle
0 (⊥)	FIXED BISTATIC	-7
-45		-58.5
-90 (||)		-90
	IN-PLANE	
0(⊥)		0
+45		+41.5
+90 (||)		+83
	OUT-OF-PLANE	
0 (⊥)		0
+45		+41.5
+90 (||)		+83

Therefore, the wavelength dependence is included in the model as a wavelength dependent variation of the parameter, ρ_V (or ρ_X), which is extracted from directional reflectance data. No modification of the model as described in Volume I is necessary.

Parameter Extraction

The model depends upon the assumption that the surface bidirectional reflectance (also the surface directional reflectance) varies linearly with wavelength. Under this assumption, if one knows the surface reflectance at two points, it is possible to interpolate at any point in between. Therefore, it is possible to eliminate the surface component from the directional reflectance at any point. The volume directional reflectance is then used to construct the ratio of directional reflectances at two wavelengths. This ratio is then used to derive the bidirectional reflectance at one of the wavelengths if it is known at the other.

The parameter to be extracted consists of the directional reflectance (ρ_D) at two different wavelengths for a material of interest. It is clear that measurements on a spectrometer such as the Beckman DKII are ideal for this purpose, if they can exclude the surface component or if it can be determined independently and eliminated.

Alternatively, the same information can be extracted from bidirectional reflectance measurements, preferably from a bidirectional scan where the source is normal to the target plane ($\theta_i = 0$). In this case one works only with the cross-polarized components ($\rho'_{\perp,||}$ and $\rho'_{||,\perp}$) and integrates (or sums) over all receiver angles to get return.

As will be shown later in this section, the two methods yield the same results to within about 10%. The agreement is important because it tends to verify the reliability of the method, which means that one has a way to predict bidirectional reflectance wavelength dependence as long as a directional reflectance spectral scan and a bidirectional scan with normal source is available. Details of procedures follow.

3.1 Extraction From Directional Reflectance Data

It has been stated earlier that the directional reflectance measurement includes a surface reflection component which must be eliminated. This can be done if independent data are available from which the surface component can be taken. In the case of this work, the information is included in the bidirectional reflectance measurement of the surface component, i.e. the like-polarized component ($\rho'_{\perp,\perp}$ or $\rho'_{||,||}$). However, there is a non-surface contribution present in the like-polarized components which must first be subtracted out [1]. Also, since an unpolarized directional reflectance can be regarded as a sum of perpendicular and parallel polarized reflectances, we average over both of these cases in the bidirectional reflectance data and obtain:

$$\rho'_{surface} = \frac{\rho'_{\perp\perp} + \rho'_{||\,||}}{2} - \frac{\rho'_{\perp\,||} + \rho'_{||\,\perp}}{2}$$

where $\rho'_{surface}$ is the surface contribution of the bidirectional reflectance. To obtain the surface contribution to the directional reflectance, $\rho'_{surface}$ must be integrated or summed over the entire hemisphere so that, [3]:

$$\rho_{surface} = \int \rho'_{surface}(\theta_i,\phi_i,\theta_r,\phi_r)\sin\theta_r \cos\theta_r d\phi_r d\theta_r$$

If we now make the reasonable assumption that there is no ϕ - dependence in ρ_D, then:

$$\rho_{surface} = 2\pi \int \rho'(\theta_i,\phi_i,\theta_r,\phi_r)\sin\theta_r \cos\theta_r d\theta_r$$

Since there is no easily expressible analytical form for ρ' it is necessary to resort to numerical or graphical methods. The method actually used was graphical and is described in [3]. Using a bidirectional reflectance scan with $\theta_i = 0$, the functions

$$\frac{\rho'_{\perp\perp}(\theta_r) + \rho'_{||}(\theta_r) - \rho'_{||\perp}(\theta_r) - \rho'_{\perp||}(\theta_r)}{2} \sin\theta_r \cos\theta_r$$

was plotted on linear graph paper every 5° for each wavelength of interest. A planimeter was then used to obtain a relative area (or integration) for each plot.

Let $\rho_d(\lambda_1)$ = area of volume component (cross-polarized) plot for wavelength $_1$.

$\rho_s(\lambda_1)$ = area of surface component (like-polarized minus cross-polarized) plot for wavelength λ_1.

Then:

$$\rho_D(\lambda_1) = \left[\frac{\rho_d(\lambda_1)}{\rho_s(\lambda_1) + \rho_d(\lambda_1)}\right] \rho_{DB}(\lambda_1)$$

where

$\rho_D(\lambda_1)$ is the true directional reflectance for λ_1, and

$\rho_{DB}(\lambda_1)$ is the directional reflectance including the surface component as measured in the spectrometer.

Therefore:

$$\rho'(\theta_i,\phi_i,\theta_r,\phi_r;\lambda_1) = \frac{\rho_D(\lambda_1)}{\rho_D(\lambda_2)} \quad \rho'_V(\theta_i,\phi_i,\theta_r,\phi_r;\lambda_2)$$

$$= \frac{\left[\dfrac{\rho_d(\lambda_1)}{\rho_d(\lambda_1) + \rho_s(\lambda_1)}\right] \rho_{DB}(\lambda_1)}{\left[\dfrac{\rho_d(\lambda_2)}{\rho_d(\lambda_2) + \rho_s(\lambda_2)}\right] \rho_{DB}(\lambda_2)} \quad \rho'_V(\theta_i,\phi_i,\theta_r,\phi_r;\lambda_2)$$

Note that to find ρ'_V at some λ_j between λ_1 and λ_2, we would first find $\rho_s(\lambda_j)$ by linear interpolation between $\rho_s(\lambda_1)$ and $\rho_s(\lambda_2)$. Then assuming that $\rho_D(\lambda_1)$, $\rho_D(\lambda_j)$ and $\rho'_V(\lambda_1)$ are known, we can find $\rho_D(\lambda_1)$ and can calculate:

$$\rho'_V(\lambda_j) = \frac{\rho_D(\lambda_j)}{\rho_D(\lambda_1)} \rho'_V(\lambda_1).$$

3.2 Extraction From Bidirectional Reflectance Data

In this case we use only the bidirectional reflectance scan where the source is normal to the target plane ($\theta_i = 0$).

The function to be integrated is:

$$\rho_D = (\rho_{\perp\,||} + \rho_{||\,\perp}) \sin\theta_r \cos\theta_r$$

Once again the integration is performed graphically after plotting values for the above expression every 5° using the $\theta_i = 0$ bidirectional data. After repeating the procedure for a second wavelength, the expression can be written:

$$\rho'_V(\theta_i,\phi_i,\theta_r,\phi_r;\lambda_1) = \frac{\rho_D(\lambda_1)}{\rho_D(\lambda_2)} \rho'_V(\theta_i,\phi_i,\theta_r,\phi_r;\lambda_2)$$

In both this procedure and the previous one in which directional data were used the wavelength factor is actually applied to the RHOPRIME program input, ρ_V or ρ_X [see Volume I], so that

$$\rho_V(\lambda_1) = \frac{\rho_D(\lambda_1)}{\rho_D(\lambda_2)} \rho_V(\lambda_2)$$

and similarly for ρ_X.

4.0 MODEL VALIDATION

In Figures 8, 9, and 10, the justification for assuming a linear relation between wavelength and surface directional reflectance is shown. Figure 8 shows directional surface reflectance as a function of wavelength for sample AO 1610. (By directional surface reflectance we mean the surface component of the bidirectional reflectance integrated over the hemisphere.) Figures 9 and 10 represent samples AO 2022 and AO 2023 respectively. In all cases the reflectances are normalized so that the value at 0.63 μm is 1. A straight line is drawn between reflectance values at 0.63 μm and 10.6 μm. For sample AO 1610, the largest deviation from linearity is about 40%. For sample AO 2022 the fit to linearity is never worse than 17%, and for AO 2023, never worse than 16%.

As pointed out earlier, validation was done only at 0.63 and 1.06 μm since there was no measurable cross-polarized reflectance for any of the

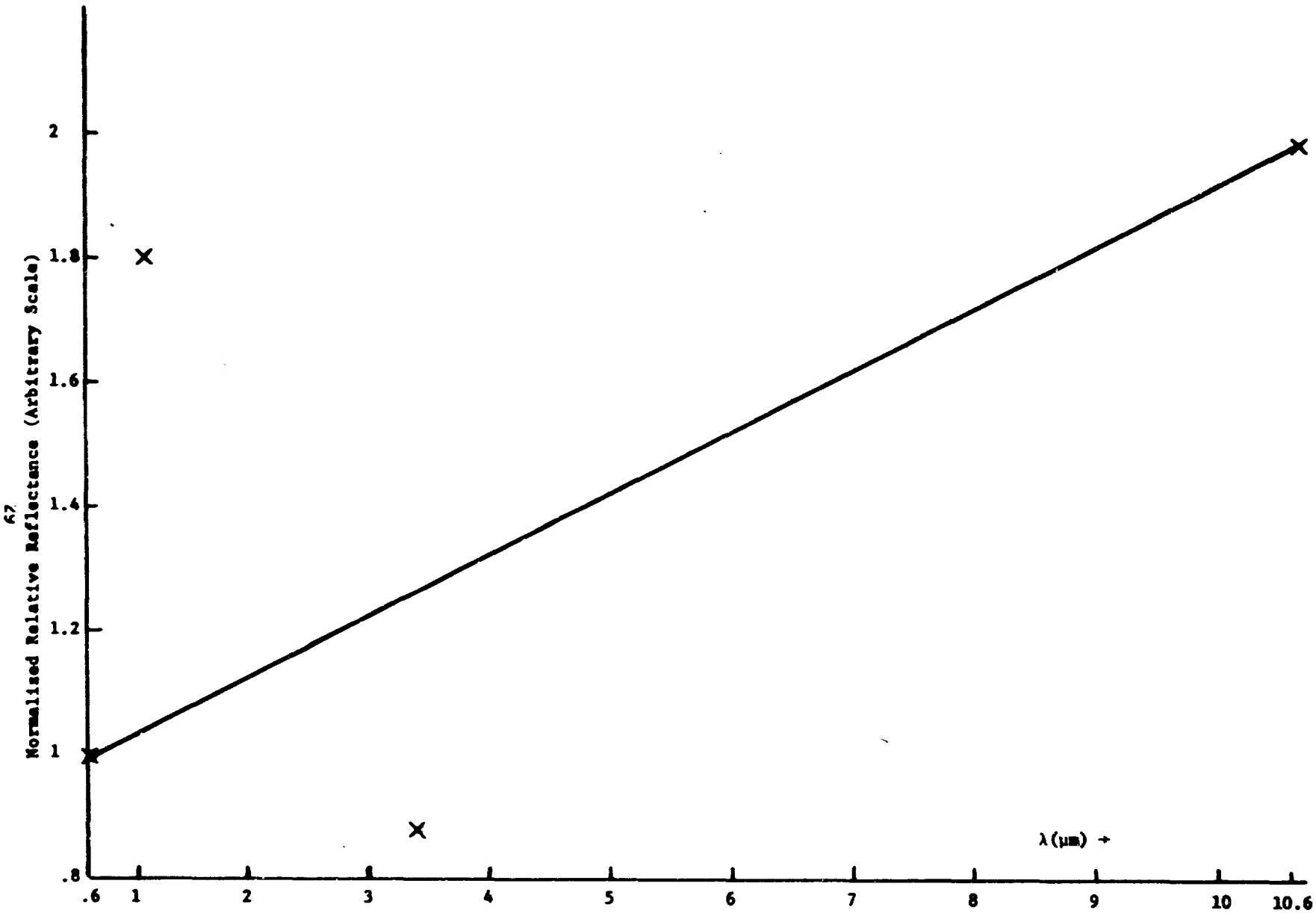

FIGURE 8. Surface Component Of Spectral Directional Reflectance For A01610.

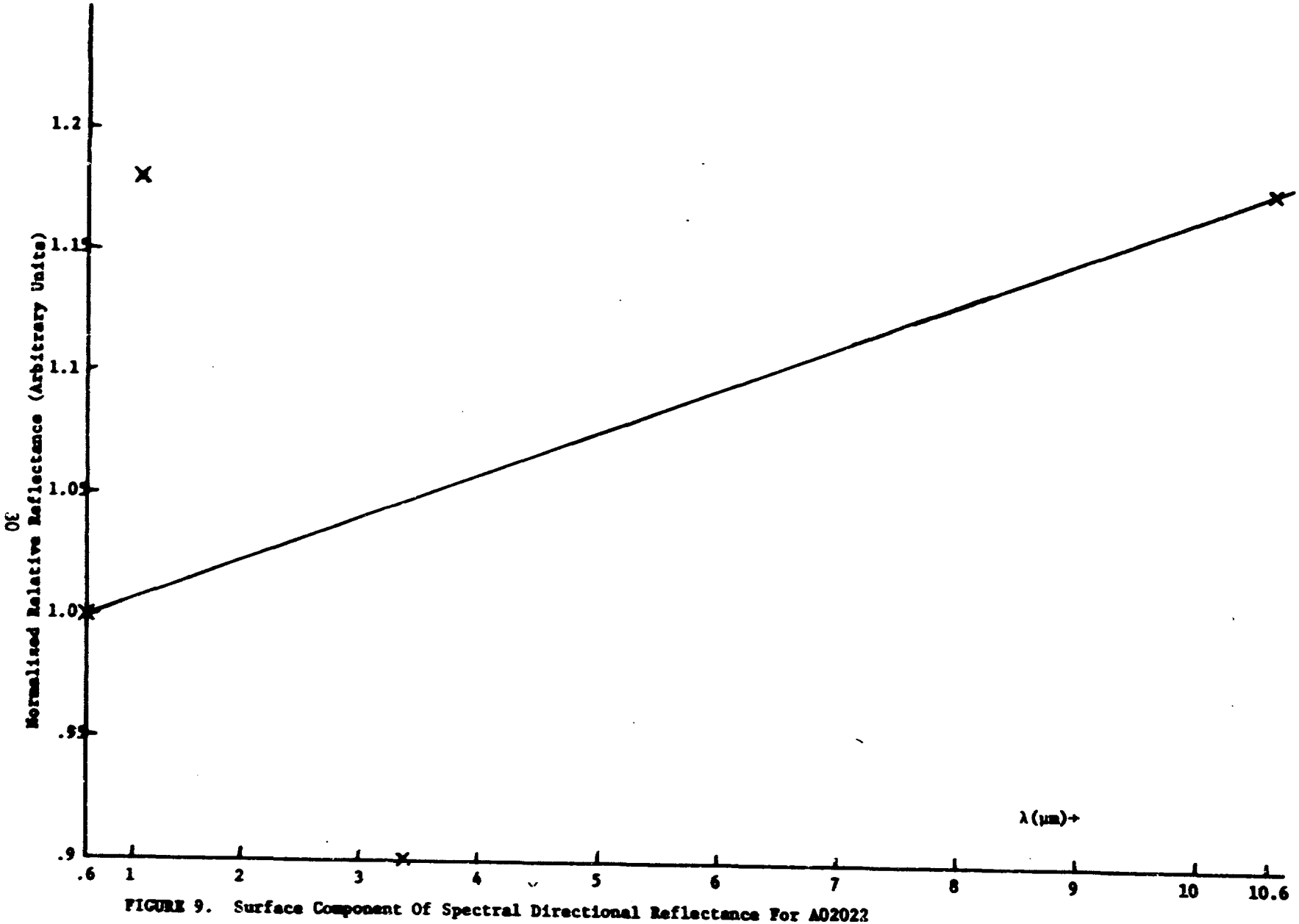

FIGURE 9. Surface Component Of Spectral Directional Reflectance For A02022

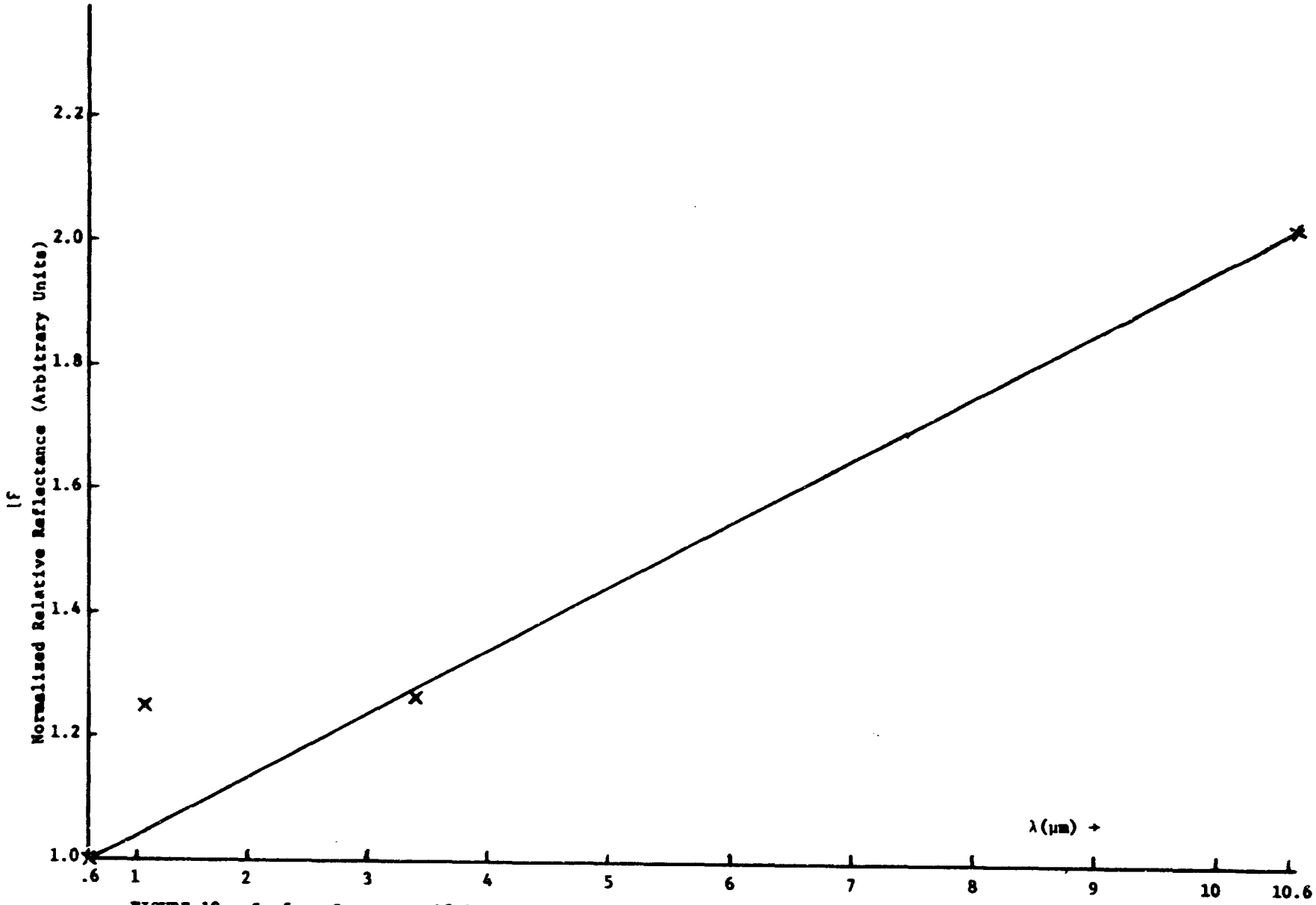

FIGURE 10. Surface Component Of Spectral Directional Reflectance For A02023

samples at 3.39 or 10.6 μm. Therefore validation in this case is a confirmation that the relationship,

$$\rho_V(\lambda_1) = \frac{\rho_D(\lambda_1)}{\rho_D(\lambda_2)} \rho_V(\lambda_2)$$

is valid based on comparison with measurements. If it had turned out that there was a measureable volume component at 3.39 μm the interpolation scheme described in Section 3 could have been more thoroughly validated. Also only samples A01610 and A02022 were used because A02023 had no measurable cross-polarized reflectance at 0.63 μm.

Fixed bistatic bidirectional reflectance scans at both wavelengths (Figures 11, 12, 13 and 14) indicate that both samples follow a non-Lambertian volume reflectance at 0.63 μm. At 1.06 μm the volume component appears to be quite flat for both samples and so in the validation it was assumed that the volume component was Lambertian. Therefore in running the model we use ρ_V for 0.63 μm and ρ_X for 1.06 μm as discussed in Volume 1. In Section 3 it was pointed out the ρ_D, the directional reflectance can be extracted from a combination of bidirectional and directional reflectance measurements where the bidirectional measurement was used to determine and eliminate the effect of the surface reflectance component.

In running the RHOPRIME program, only the cross-polarized contribution was calculated since as stated earlier, only the cross-polarized component has significant wavelength dependence in the spectral region between 0.63 μm and 3.39 μm.

The validation was performed two ways for each sample. In one case, ρ_X was determined from the fixed bistatic data at 1.06 μm and ρ_V for 0.63 μm was then calculated from:

$$\rho_V(0.63) = \frac{\rho_D(0.63)}{\rho_D(1.06)} \rho_X(1.06)$$

In the other case ρ_V was determined from the fixed bistatic data at 0.63 μm and ρ_X for 1.06 μm was then calculated from:

λ = .63
$\phi_i = \phi_n + -1.7$
θ_i = .0

FIGURE 11a
AO 1610

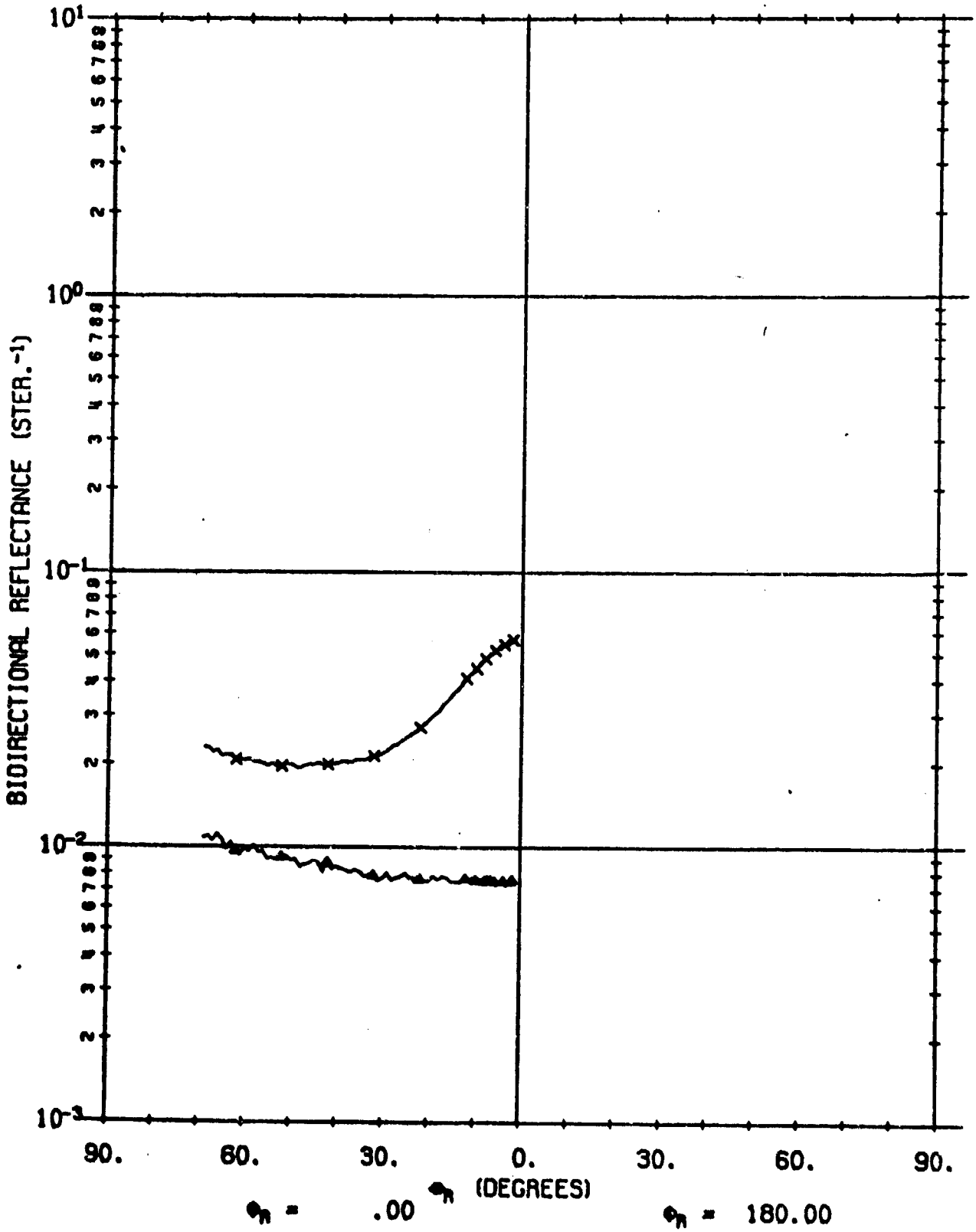

λ = .63
$\Phi_I = \Phi_R +$ 1.7
Φ_I = 180.0

FIGURE 11b
-AO 1610-

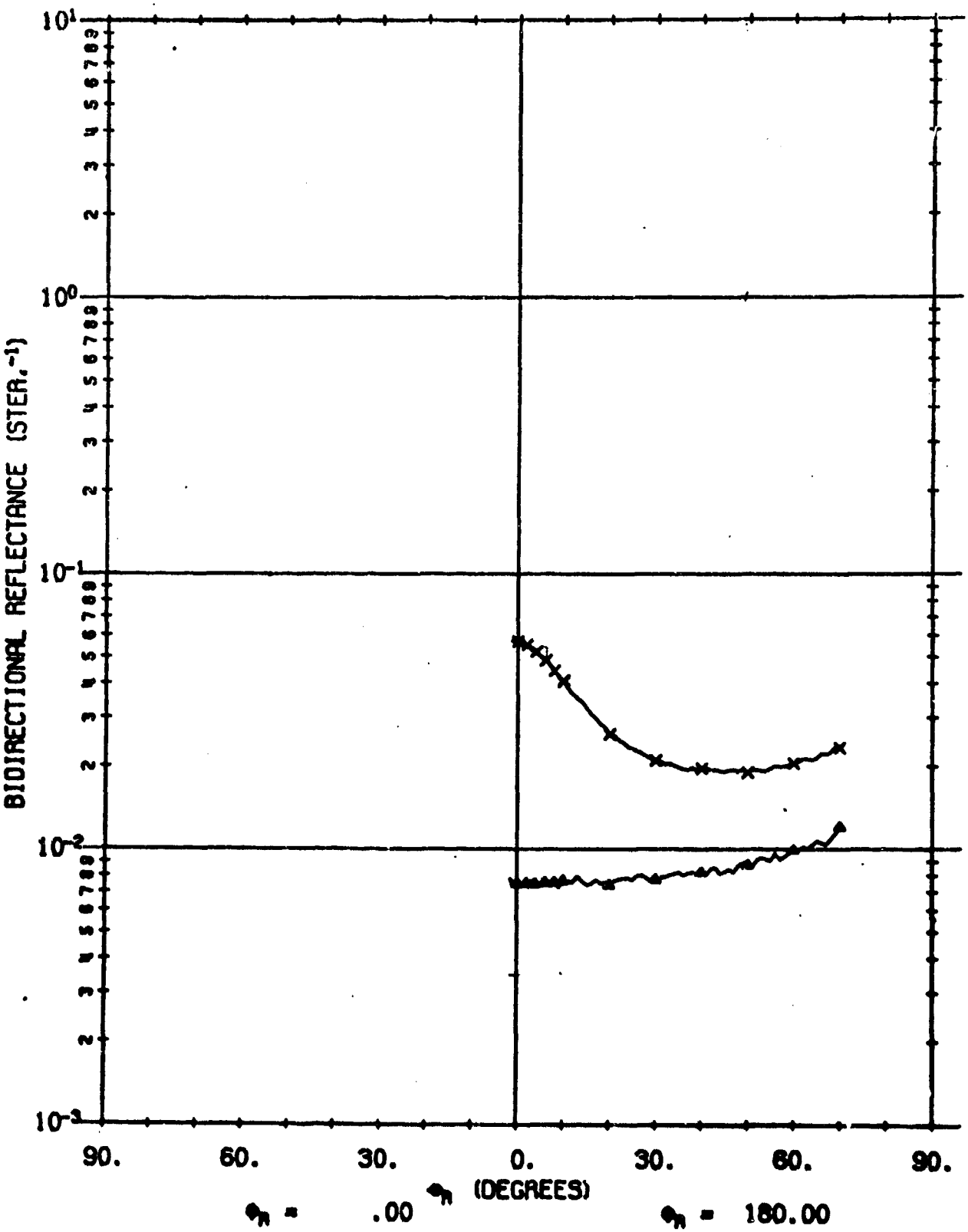

λ = 1.06
$\Phi_I = \Phi_R^+$ -1.7
Φ_I = .0

FIGURE 12a
A0 1610

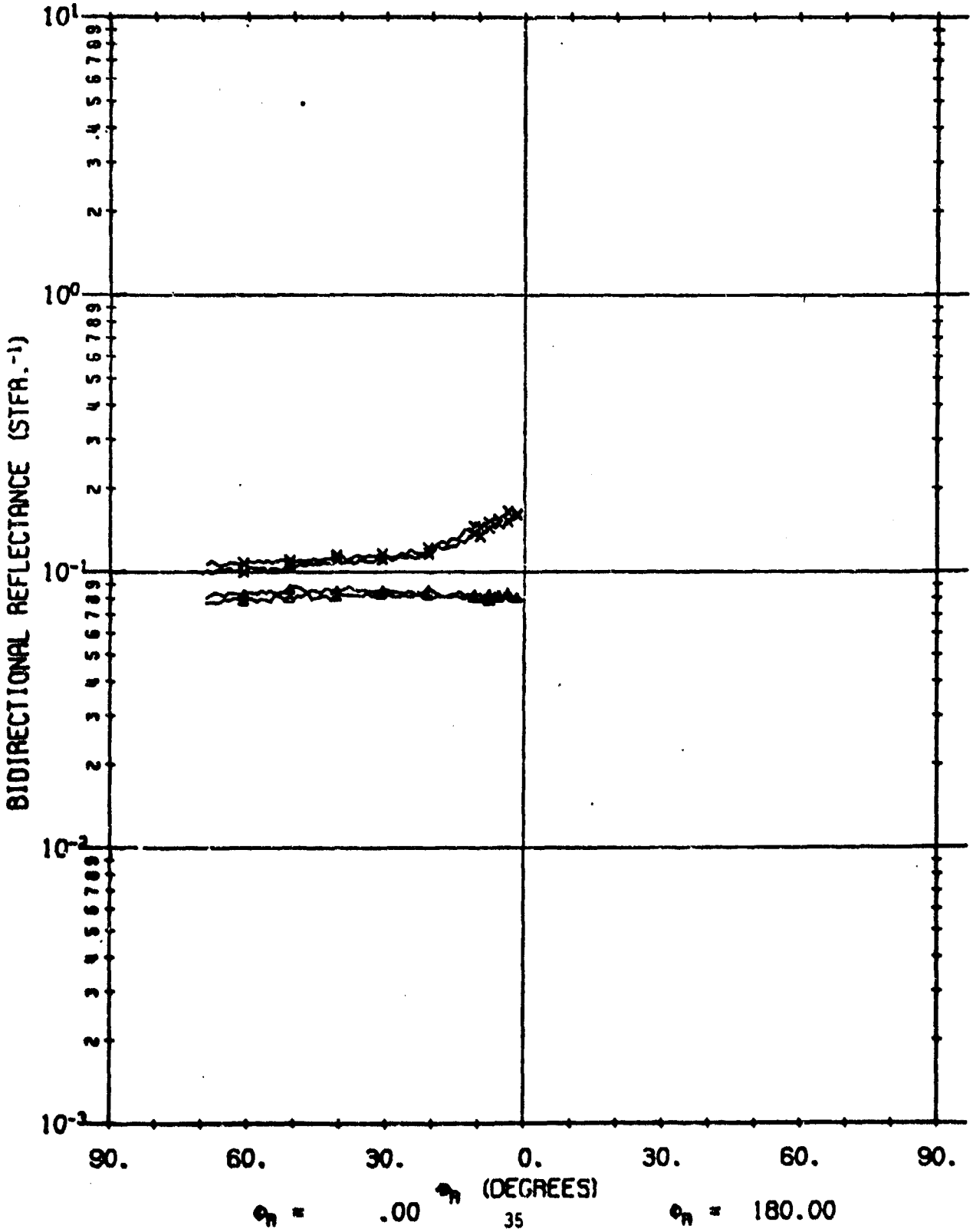

λ = 1.06
$\Phi_I = \Phi_R +$ 1.7
Φ_I = 180.0

FIGURE 12b
AO 1610

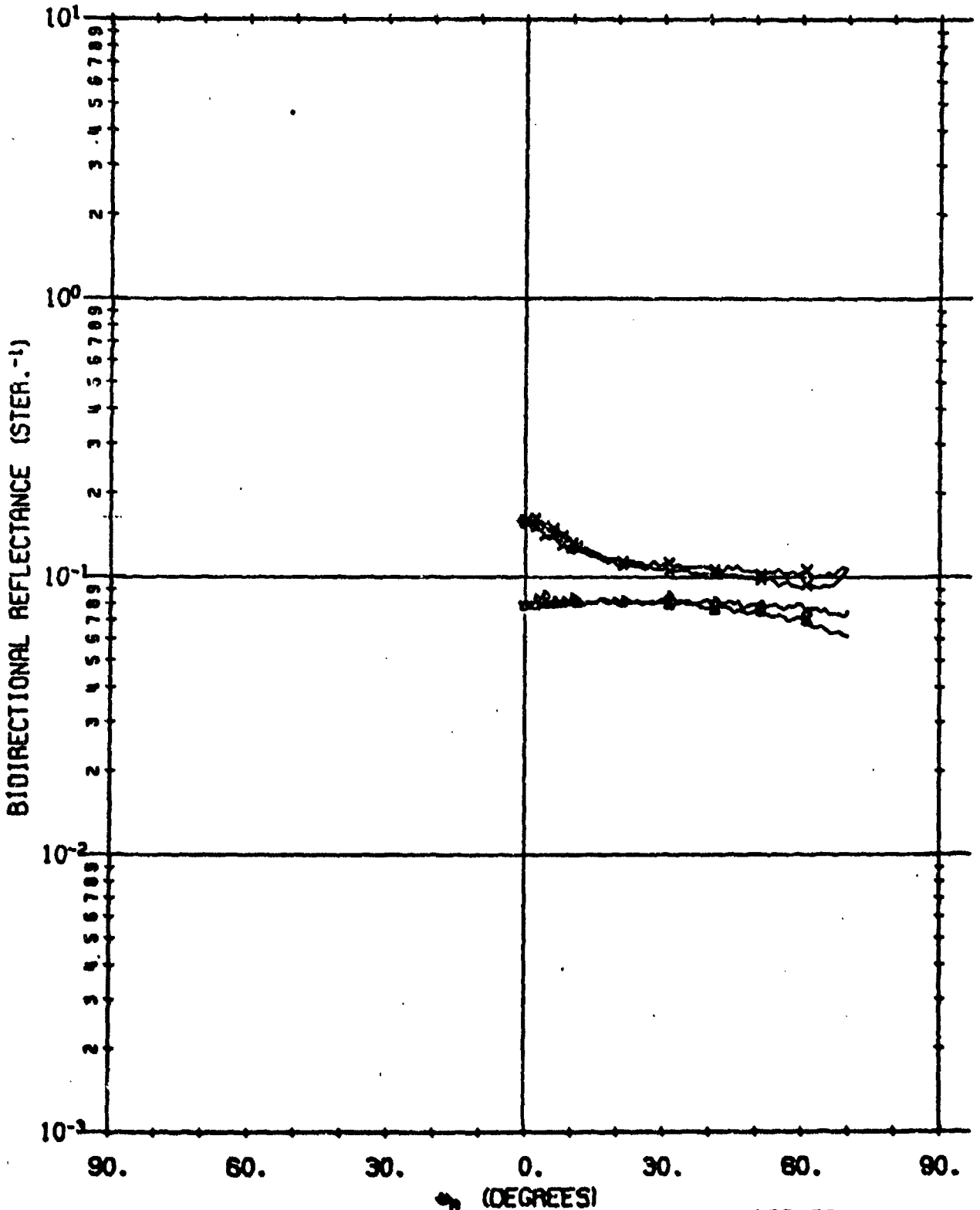

Φ_R = .00 Φ_R = 180.00

λ = .63
$\theta_I = \theta_R +$ 1.7
φ_I = .0

FIGURE 13a
AO 2022

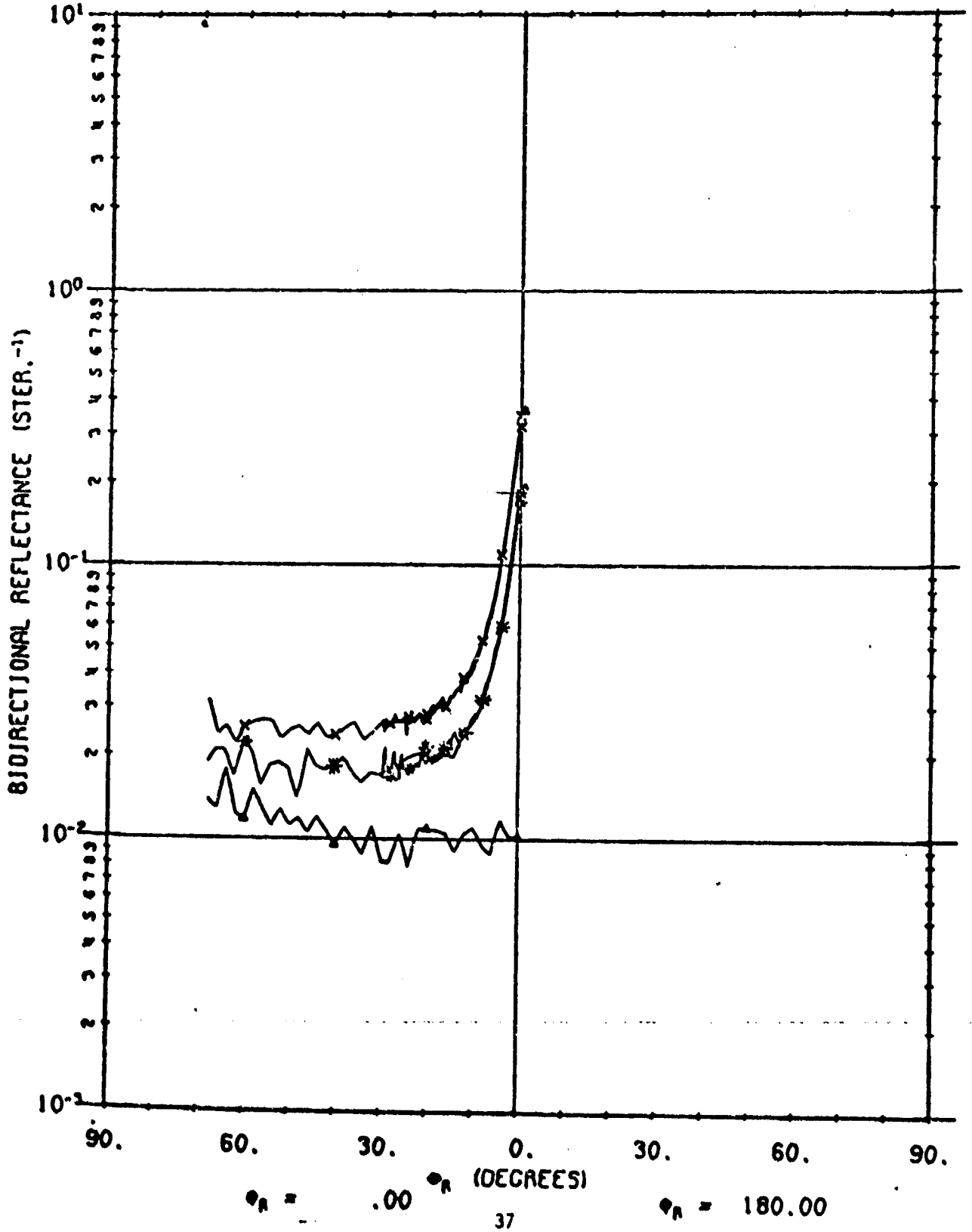

λ = .63
$\theta_I = \theta_R +$ -1.7
φ_I = 180.0

FIGURE 13b
AO 2022

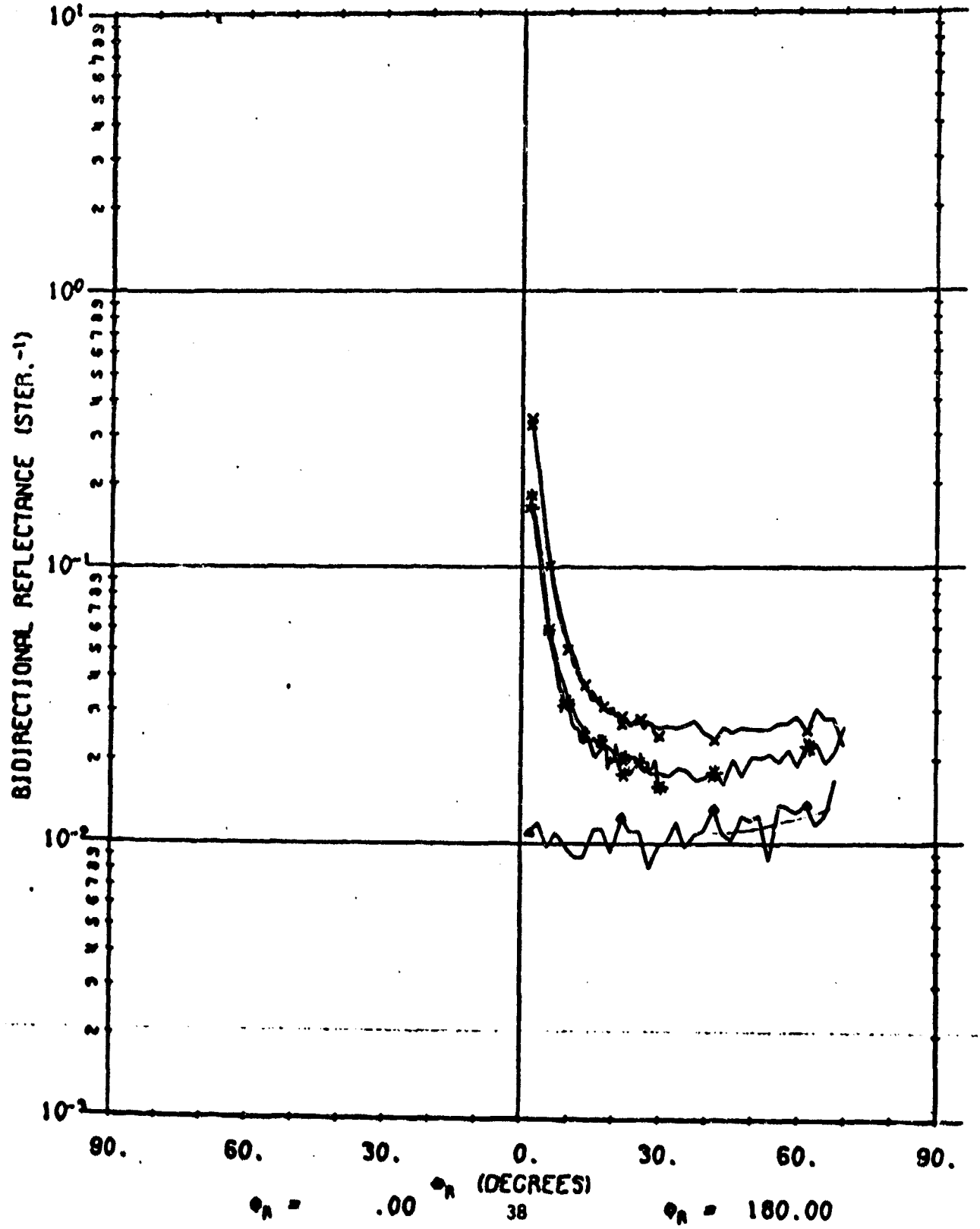

λ = 1.06
$\Theta_I = \Theta_n^+$ 1.7
Φ_I = .0

FIGURE 14a
AO 2022

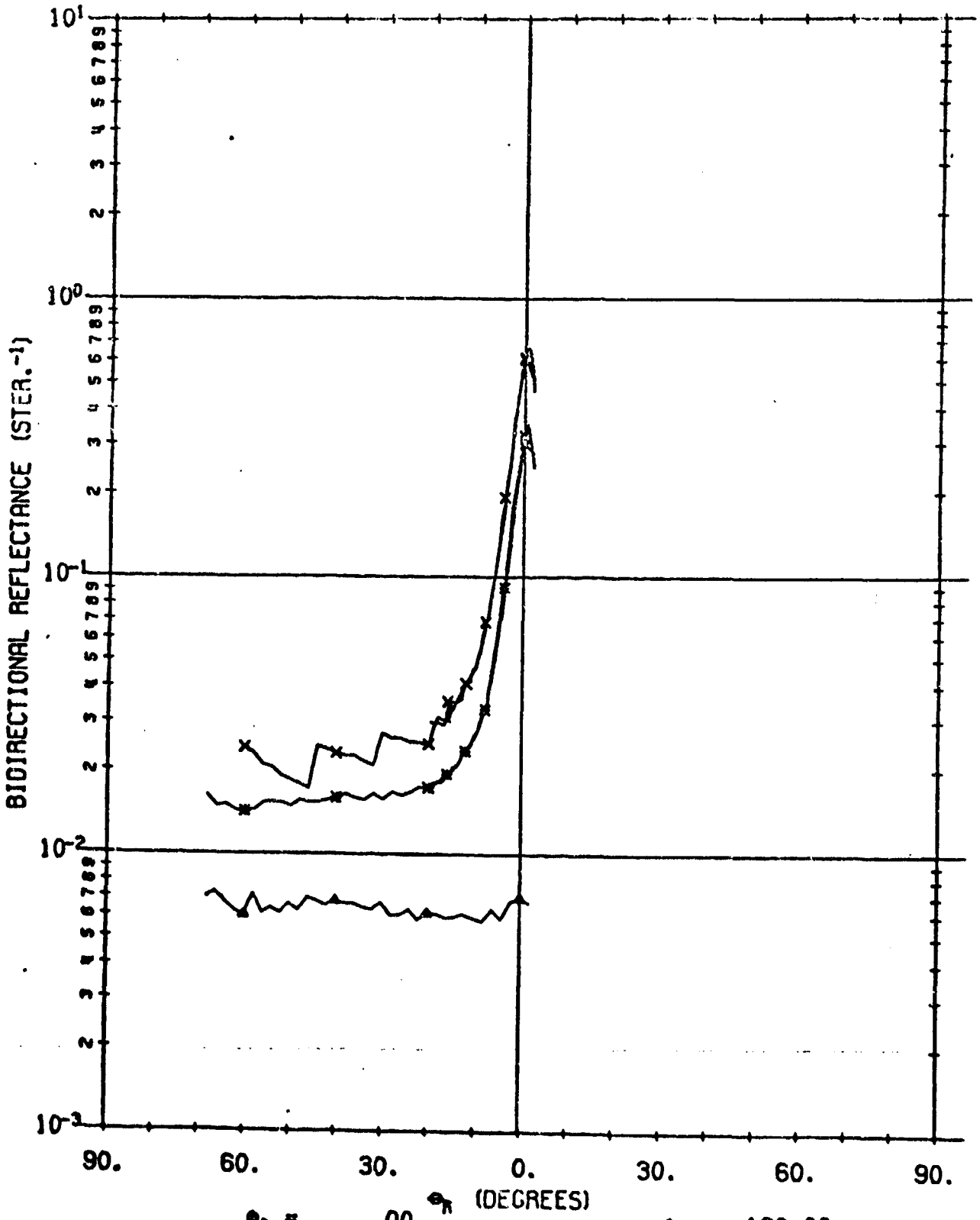

Φ_R = .00 Φ_R = 180.00

λ = 1.06
$\Phi_I = \Phi_R + -1.0$
Φ_I = 180.0

FIGURE 14b
AO 2022

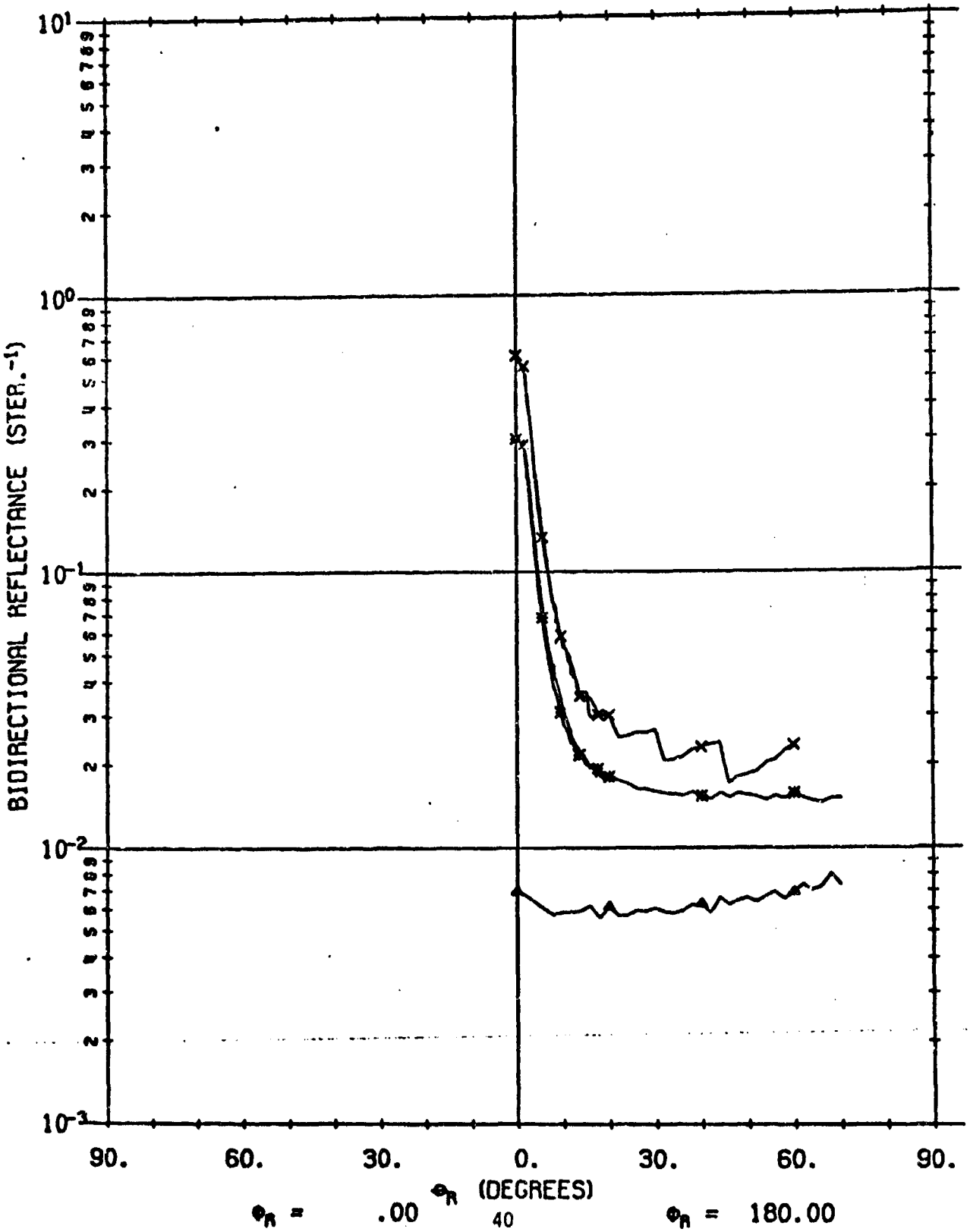

$$\rho_\chi(1.06) = \frac{\rho_D(1.06)}{\rho_D(0.63)} \quad \rho_V(0.63)$$

Results were then compared to the measured data for two different source angles, $\theta_i = 0°$ and $\theta_i = 40°$. For both samples it was decided that behavior was most nearly non-Lambertian at 0.63 μm and most nearly Lambertian at 1.06 μm.

Figure 15 shows the measured data for sample A01610 with "parallel" - polarized source* at $\theta_i = 0$ and at 0.63 μm. Figure 16 shows the calculation for the volume component for 0.63 μm with the ρ_V value extrapolated from 1.06 μm data. The agreement is very close. Figures 17 and 18 provide a similar comparison for $\theta_i = 40°$. Figures 19 - 22 again provide similar comparisons for sample A02022. It should be noted that between 0.63 μm and 1.06 μm the wavelength correction is small. As wavelength increases beyond 1.06 μm, however, the cross-polarized component decreases rapidly. (At 3.39 μm it is effectively zero.) Therefore the wavelength correction will be more important as λ increases beyond 1.06 μm.

*The cross-polarized component for the "parallel"-polarized source is the same as that for the "perpendicular"-polarized source.

λ = .63
θ_I = .0
ϕ_I = 180.0

FIGURE 15
AO 1610

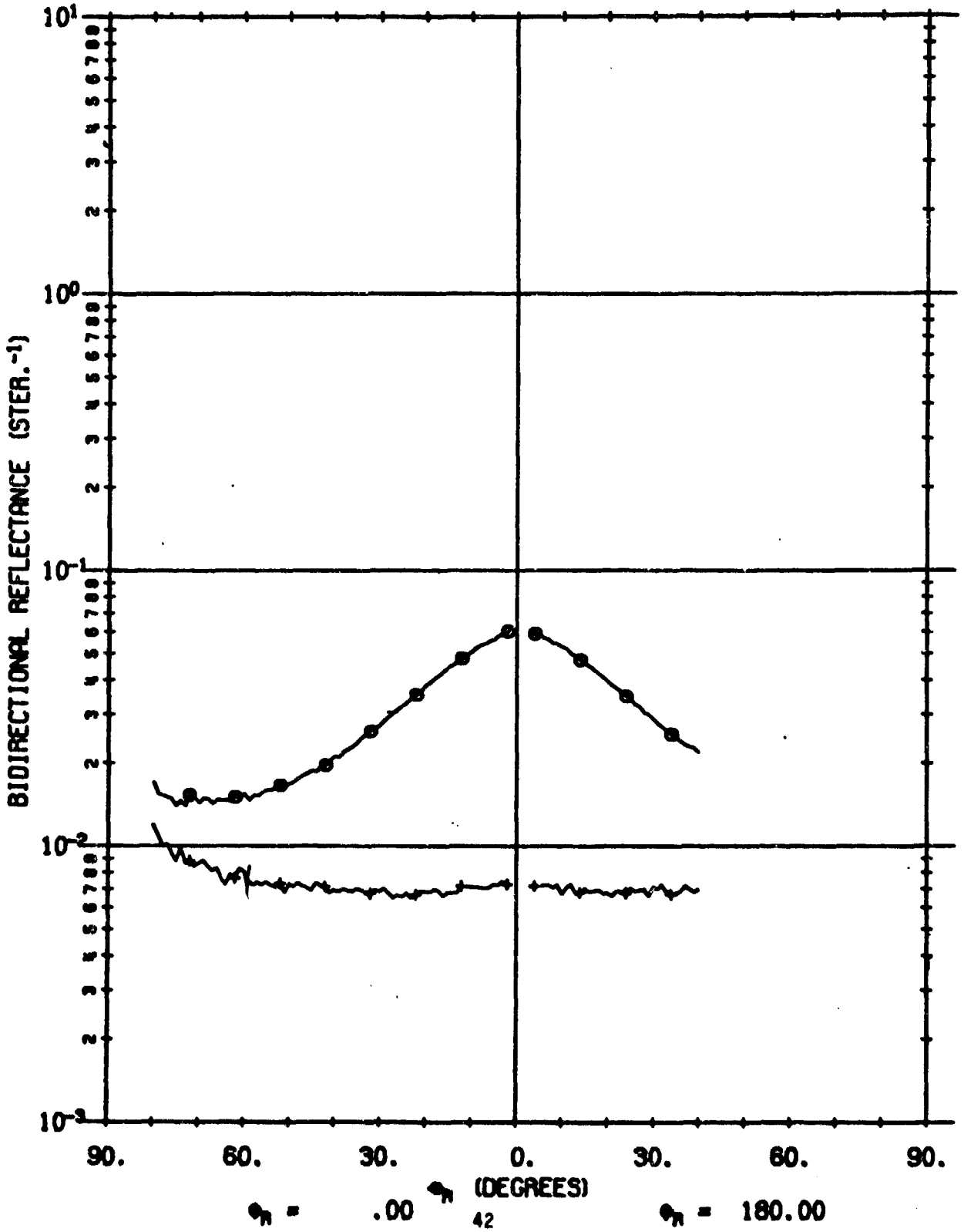

FIGURE 16
AO 1610

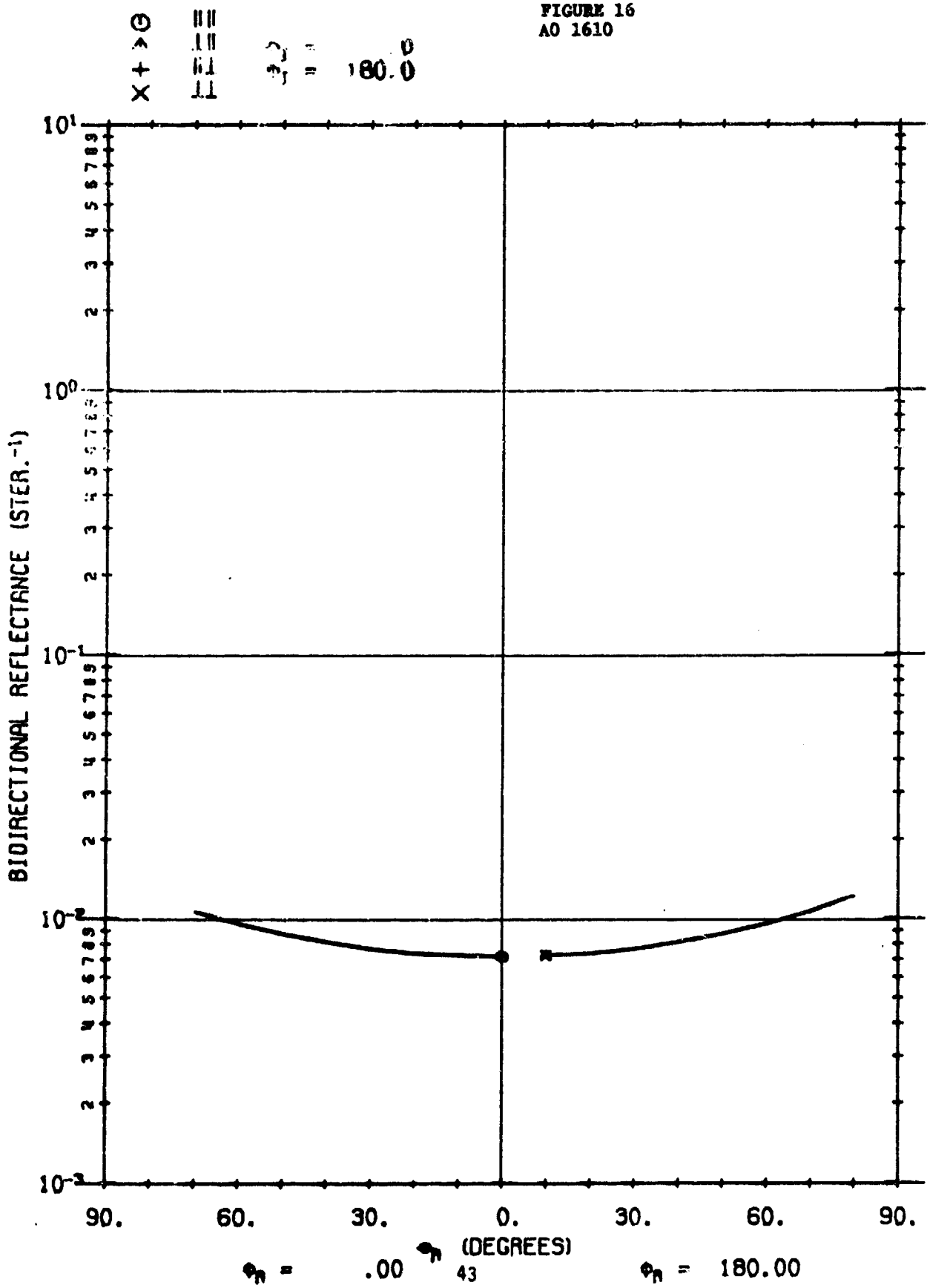

λ = .63
ϕ_I = 40.0
ϕ_I = 180.0

FIGURE 17
AO 1610

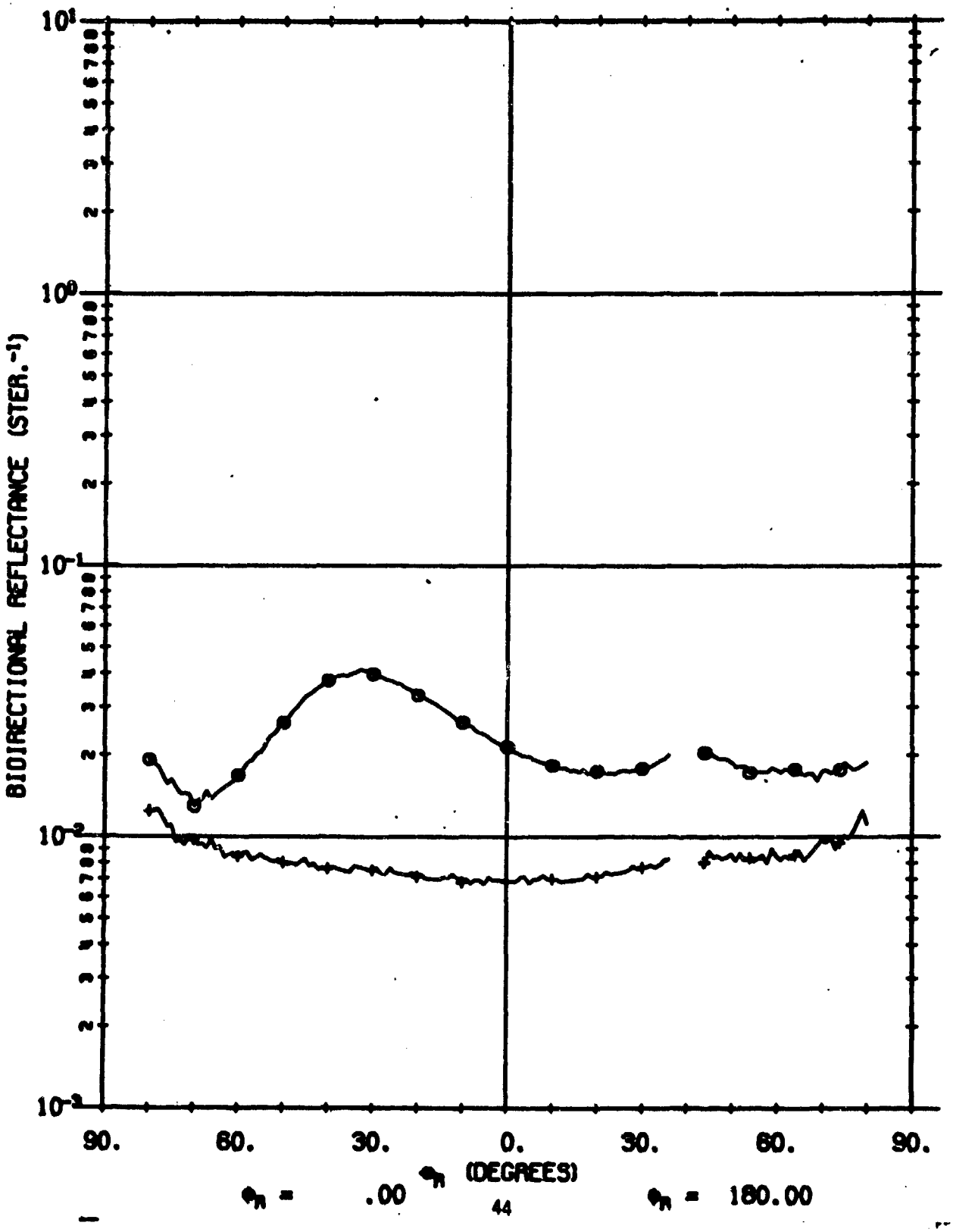

FIGURE 18
AO 1610

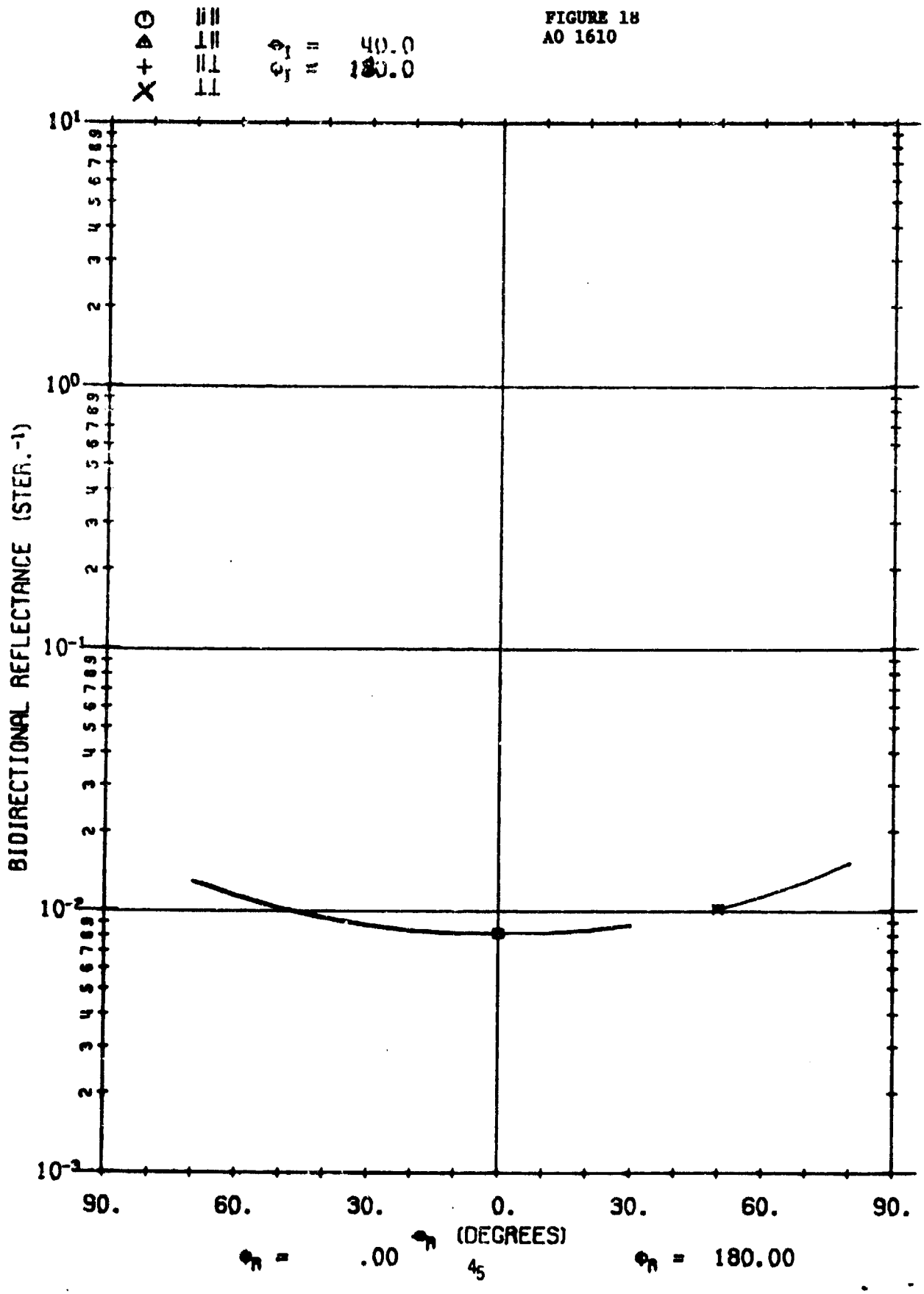

λ = .63
θ_I = .0
φ_I = 180.0

FIGURE 19
AO 2022

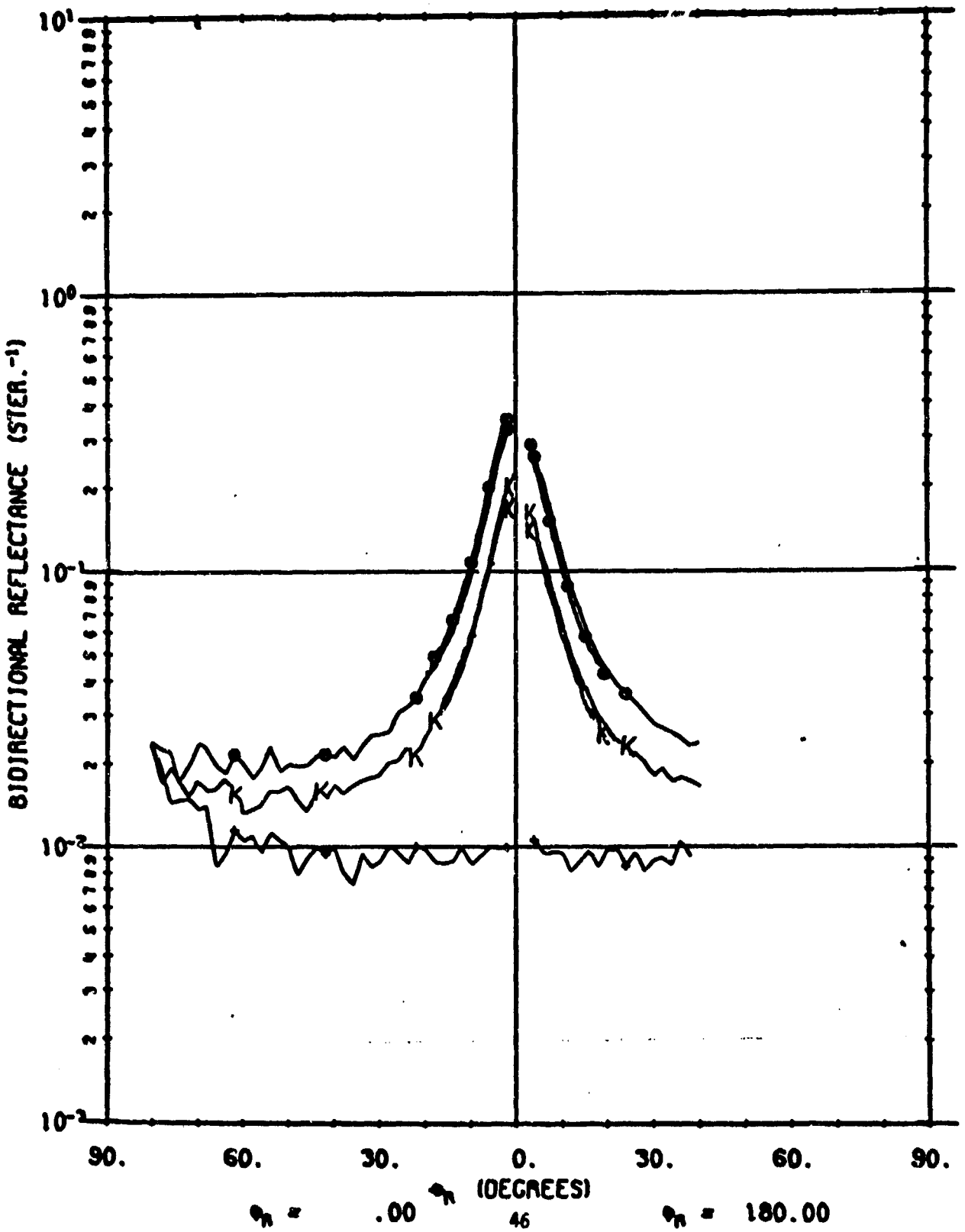

FIGURE 20
AO 2022

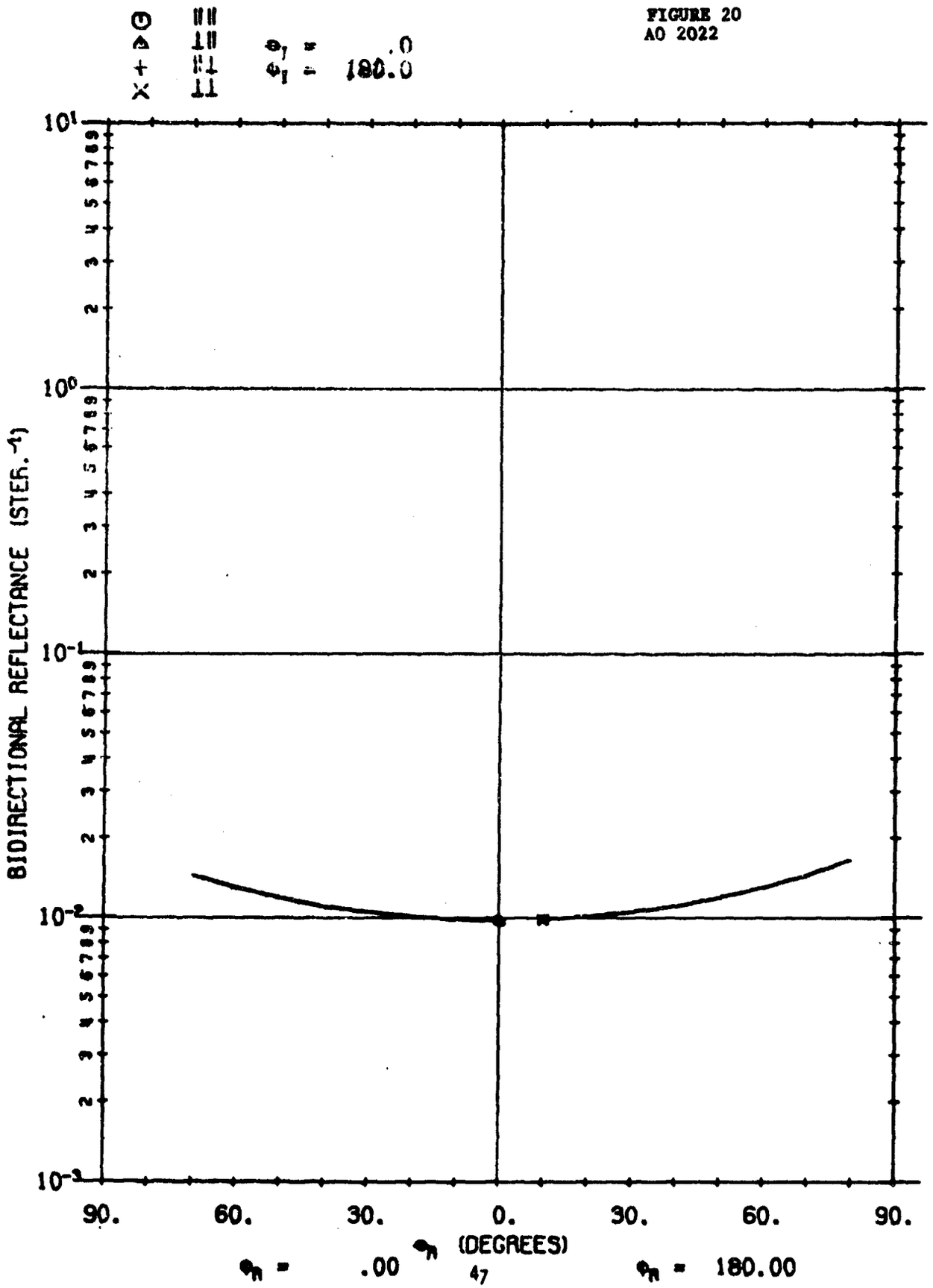

λ = .63
θ_i = 40.0
ϕ_i = 180.0

FIGURE 21
AO 2022

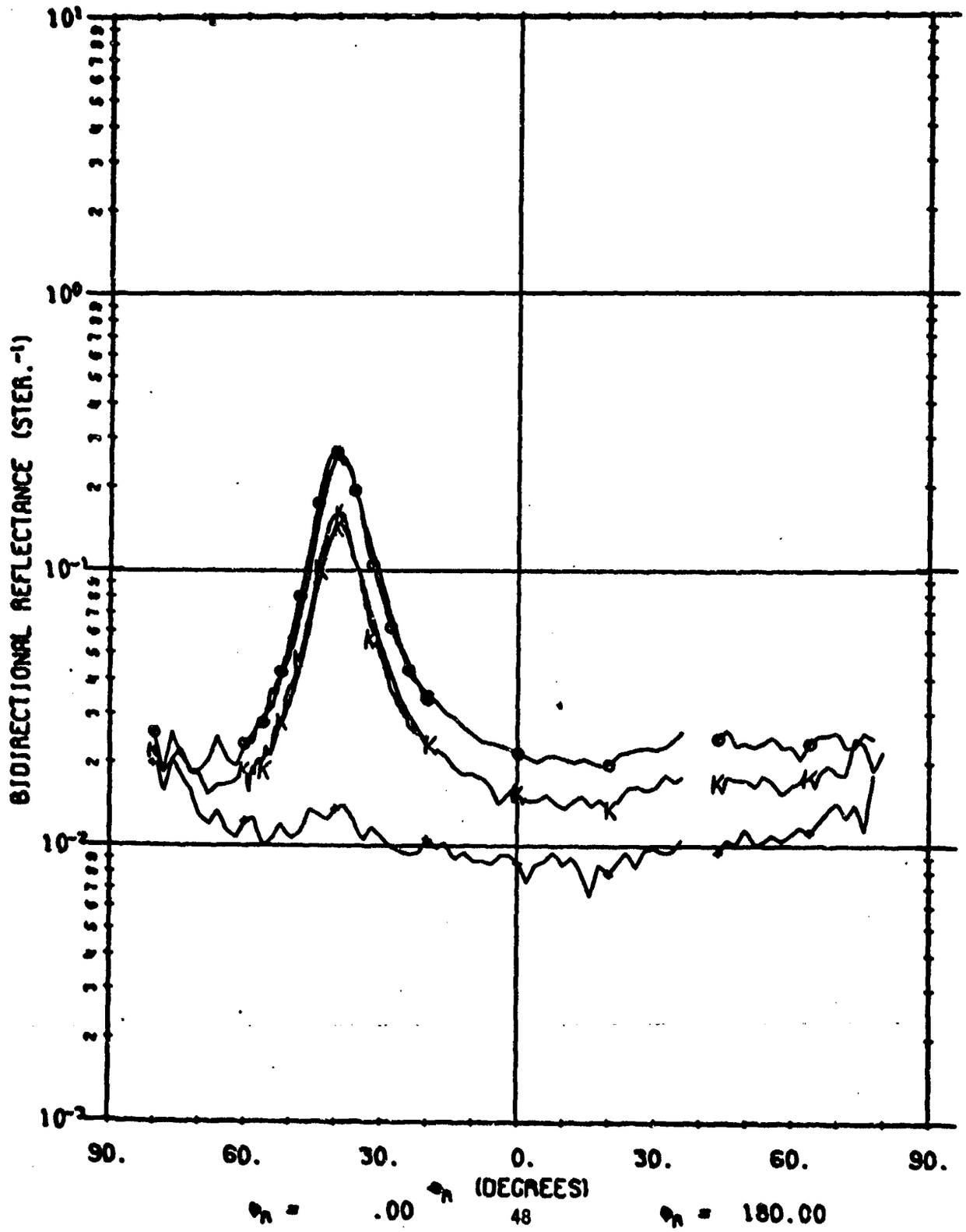

FIGURE 22
AO 2022

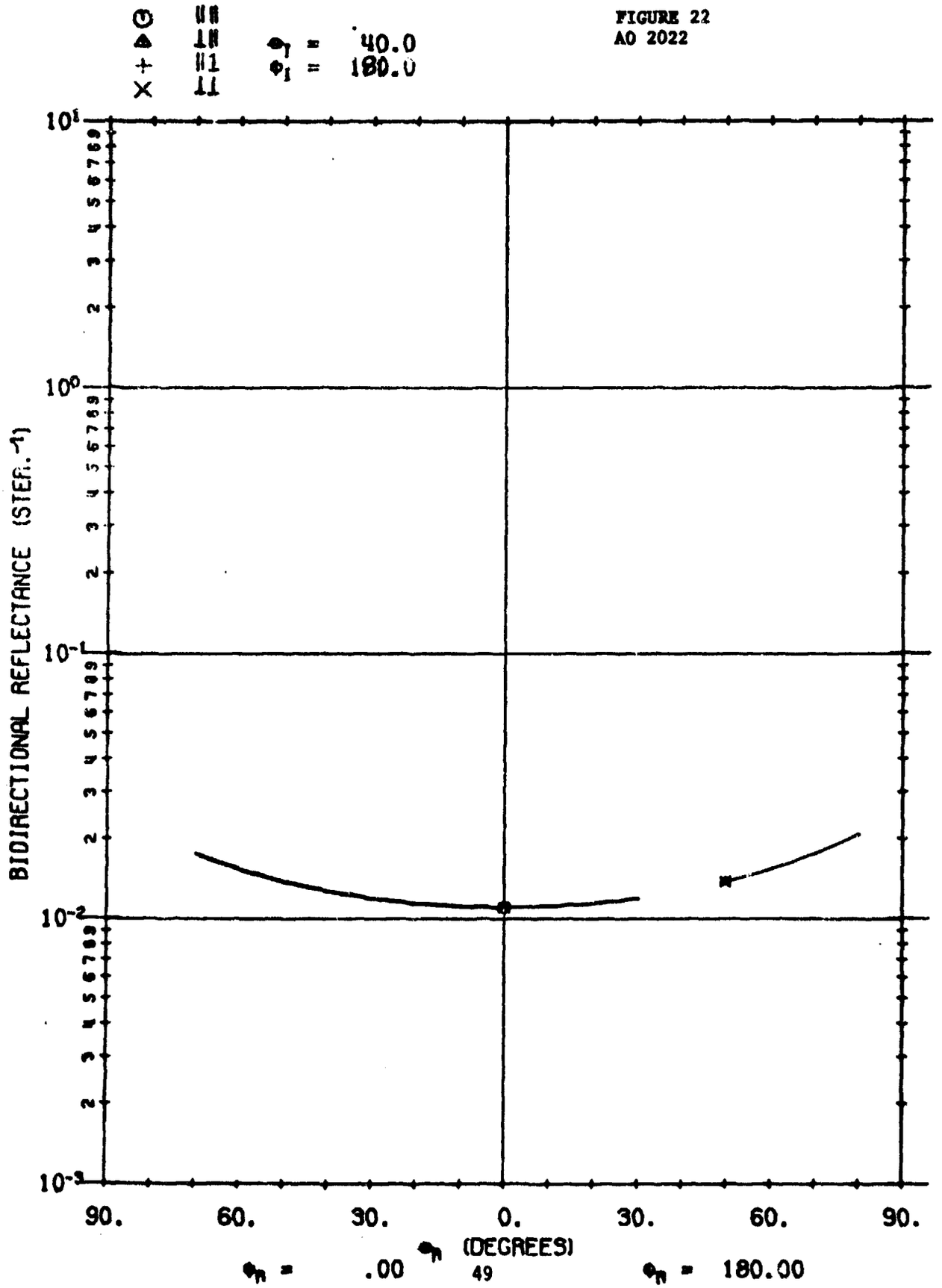

REFERENCES

1. Polarized Radiance, Volume I: Polarized Bidirectional Reflectance With Lambertian Or Non-Lambertian Diffuse Components, Report No. 192500-1-T(I), Environmental Research Institute of Michigan, Ann Arbor, Michigan.

2. Target Signature Program: Measurements and Analyses, Report No. AFAL-TR-70-213, Willow Run Laboratories of The University of Michigan, Ann Arbor, March 1971.

3. A Gonioreflectometer Facility Using Coherent and Incoherent Sources, Report No. AFAL-TR-70-161, Willow Run Laboratories of The University of Michigan, Ann Arbor, August 1970.

4. Target Signature Computer Model For Laser-Designated Tactical Targets, Report No. 192200-2-F, Environmental Research Institute of Michigan, Ann Arbor, July 1973.

APPENDIX A

BIDIRECTIONAL REFLECTANCE DATA FOR SAMPLES A01610, A02022, A02023 AT 0.63, 1.06, 3.39 AND 10.6 μm.

For convenience in using this Appendix, the data are preceeded by an index which outlines the organization and provides page numbers of specific data sets.

Bidirectional Reflectance Data With Fixed Bistatic Angle

Sample	Source Polarization	λ (μm)	ϕ-Plane	Page
A02023	⊥	.63, 1.06, 3.39, 10.6	0, 180	57
	45	3.39, 10.6	0, 180	65
	‖	.63, 1.06, 3.39, 10.6	0, 180	69
	‖	10.6	90, 270	77
A01610	⊥	.63, 1.06, 3.39, 10.6	0, 180	79
	45	3.39	0, 180	87
	‖	.63, 1.06, 3.30	0, 180	89
	‖	10.6	90, 270	95
A02022	⊥	.63, 1.06, 3.39, 10.6	0, 180	97
	45	3.39, 10.6	0, 180	105
	‖	.63, 1.06, 3.39, 10.6	0, 180	109
	‖	10.6	90, 270	117

Preceding page blank

Bidirectional Reflectance Data With Variable Bistatic Angle

Sample	Source Polarization	θ_i	λ (μm)	ϕ-Plane	Page
A01610	⊥	0	.63, 1.06, 3.39, 10.6	0, 180	119
		20	.63, 1.06, 3.39, 10.6	0, 180	123
		20	.63, 1.06, 3.39, 10.6	90, 270	127
		40	.63, 1.06, 3.39, 10.6	0, 180	131
		40	.63, 1.06, 3.39, 10.6	90, 270	135
		60	.63, 1.06, 3.39, 10.6	0, 180	139
		60	.63, 1.06, 3.39, 10.6	90, 270	143
A01610	45°	0	3.39, 10.6	0, 100	147
		20	3.39, 10.6	0, 100	149
		20	3.39, 10.6	90, 270	151
		40	3.39, 10.6	0, 180	153
		40	3.39	90, 270	155
		60	3.30, 10.6	0, 180	156
		60	3.39	90, 270	158
A01610	||	0	.63, 1.06, 3.39, 10.6	0, 180	159
		20	.63, 1.06, 3.39, 10.6	0, 180	163
		20	.63, 1.06, 3.39	90, 270	167
		40	.63, 1.06, 3.39, 10.6	0, 180	170
		40	.63, 1.06, 3.39	90, 270	174
		60	.63, 1.06, 3.39, 10.6	0, 180	177
		60	.63, 1.06, 3.39	90, 270	181

Sample	Source Polarization	θ_i	λ (μm)	ϕ-Plane	Page
A02022	⊥	0	.63, 1.06, 3.39, 10.6	0, 180	184
		0	.63, 1.06	90, 270	188
		20	.63, 1.06, 3.39, 10.6	0, 180	190
		20	.63, 1.06, 3.39, 10.6	90, 270	194
		40	.63, 1.06, 3.39, 10.6	0, 180	198
		40	.63, 1.06, 3.39, 10.6	90, 270	202
		60	.63, 1.06, 3.39, 10.6	0, 180	206
		60	.63, 1.06, 3.39, 10.6	90, 270	210
A02022	45°	0	3.39, 10.6	0, 180	214
		20	3.39, 10.6	0, 180	216
		20	3.39, 10.6	90, 270	218
		40	3.39, 10.6	0, 180	220
		40	3.39, 10.6	90, 270	222
		60	3.39, 10.6	0, 180	224
		60	3.39, 10.6	90, 270	226
A02022	‖	0	.63, 1.06, 3.39, 10.6	0, 180	228
		0	.63, 1.06	90, 270	232
		20	.63, 1.06, 3.39, 10.6	0, 180	234
		20	.63, 1.06, 3.39, 10.6	90, 270	238
		40	.63, 1.06, 3.39, 10.6	0, 180	242
		40	.63, 1.06, 3.39, 10.6	90, 270	246
		60	.63, 1.06, 3.39, 10.6	0, 180	250
		60	.63, 1.06, 3.39	90, 270	254

Sample	Source Polarization	θ_i	λ (μm)	φ-Plane	Page
A02023	⊥	0	1.06, 3.39, 10.6	0, 180	257
		0	1.06	90, 270	260
		20	1.06, 3.30, 10.6	0, 180	261
		20	.63, 1.06, 3.39, 10.6	90, 270	264
		40	1.06, 3.39, 10.6	0, 180	268
		40	.63, 1.06, 3.39, 10.6	90, 270	271
		60	1.06, 3.39, 10.6	0, 180	275
		60	.63, 1.06, 3.39, 10.6	90, 270	278
A02023	45°	0	3.39, 10.6	0, 180	282
		20	3.39, 10.6	0, 180	284
		20	3.39, 10.6	90, 270	286
		40	3.39, 10.6	0, 180	288
		40	3.39, 10.6	90, 270	290
		60	3.39, 10.6	0, 180	292
		60	3.39, 10.6	90, 270	294
A02023	‖	0	.63, 1.06, 3.39, 10.6	0, 180	296
		0	1.06	90, 270	300
		20	.63, 1.06, 3.39, 10.6	0, 180	301
		20	.63, 1.06, 3.39, 10.6	90, 270	305
		40	.63, 1.06, 3.39, 10.6	0, 180	309
		40	.63, 1.06, 3.39, 10.6	90, 270	313
		60	.63, 1.06, 3.39, 10.6	0, 180	317
		60	.63, 1.06, 3.39, 10.6	90, 270	321

A02023 501

λ = .63
$\Phi_I = \Phi_R +$ -1.7
Φ_I = .0

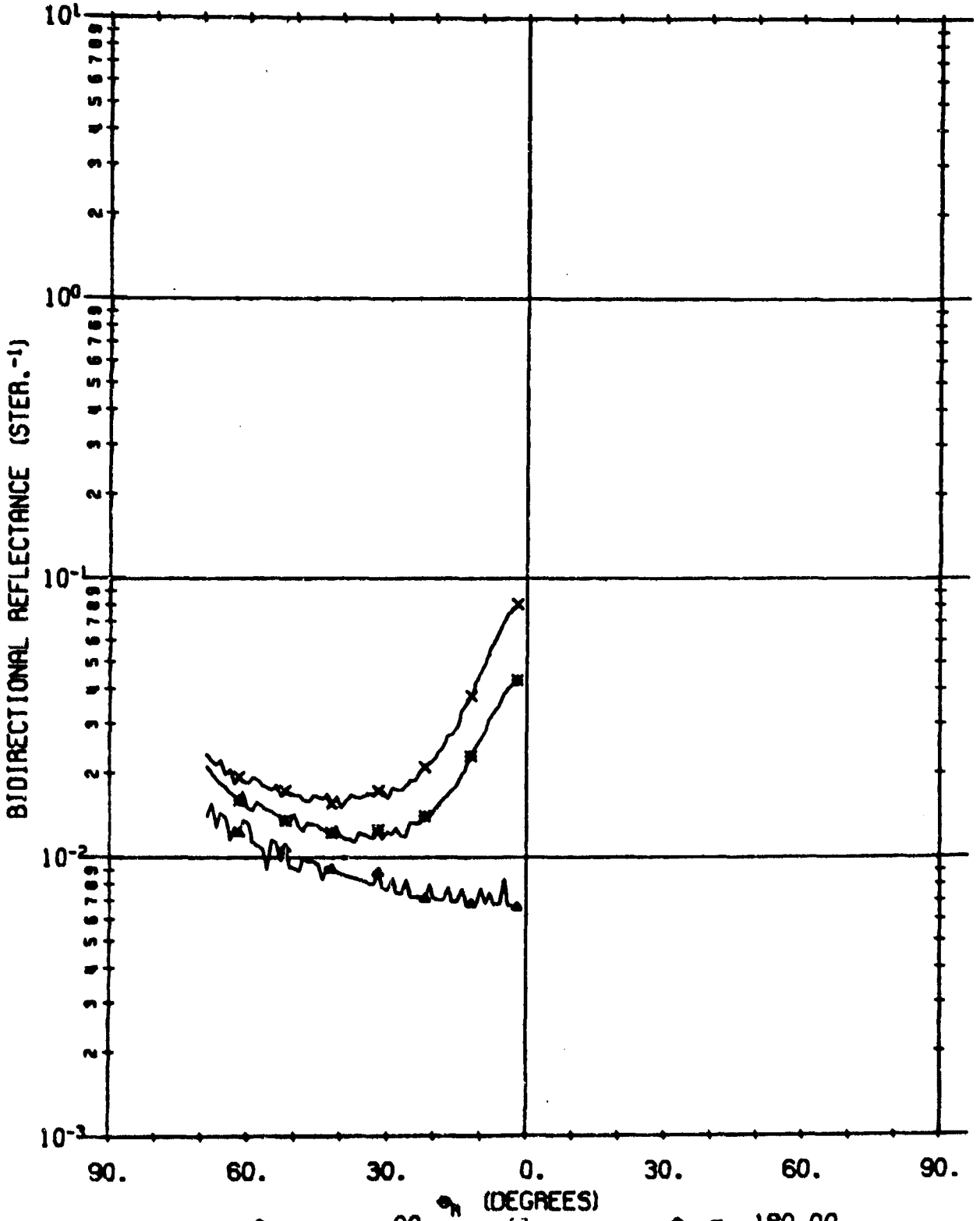

Φ_R = .00 Φ_R = 180.00

A02023 501

λ = .63
$\phi_I = \phi_R + 1.7$
ϕ_I = 180.0

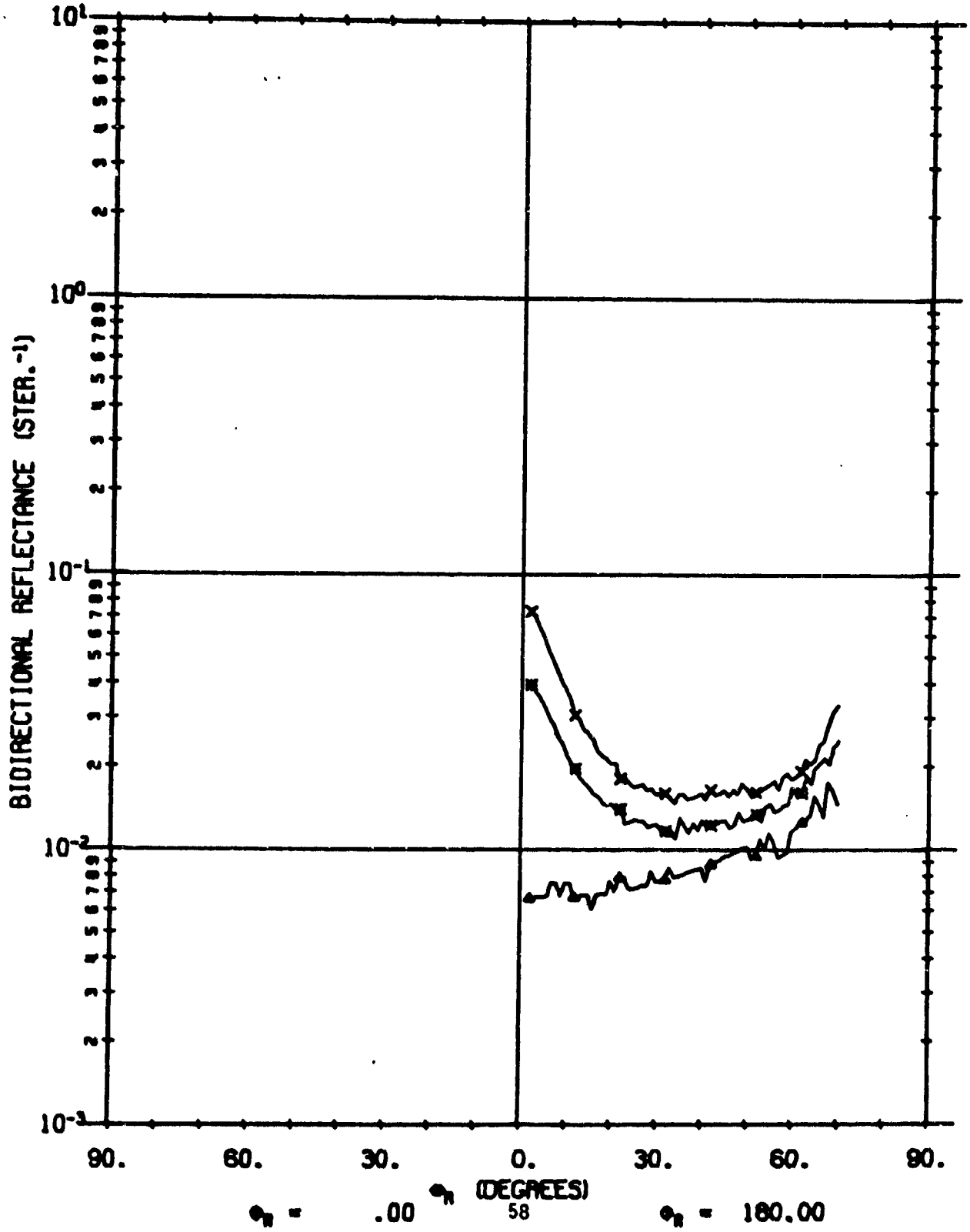

A02023 101

λ = 1.06
$\phi_i = \phi_n$+ 1.7
θ_i = .0

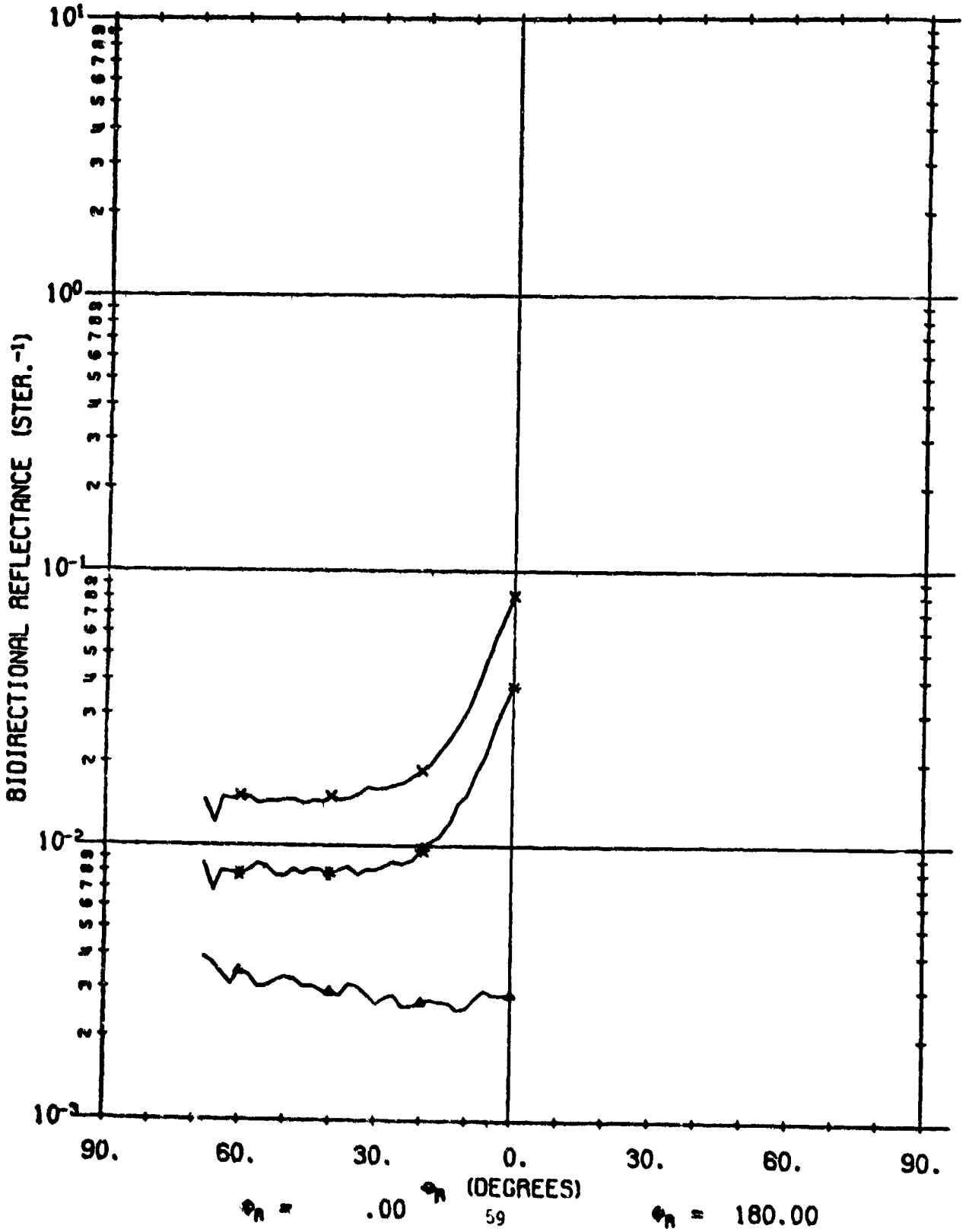

A02023 101

λ = 1.06
$\theta_i = \theta_n^+$ -1.0
ϕ_i = 180.0

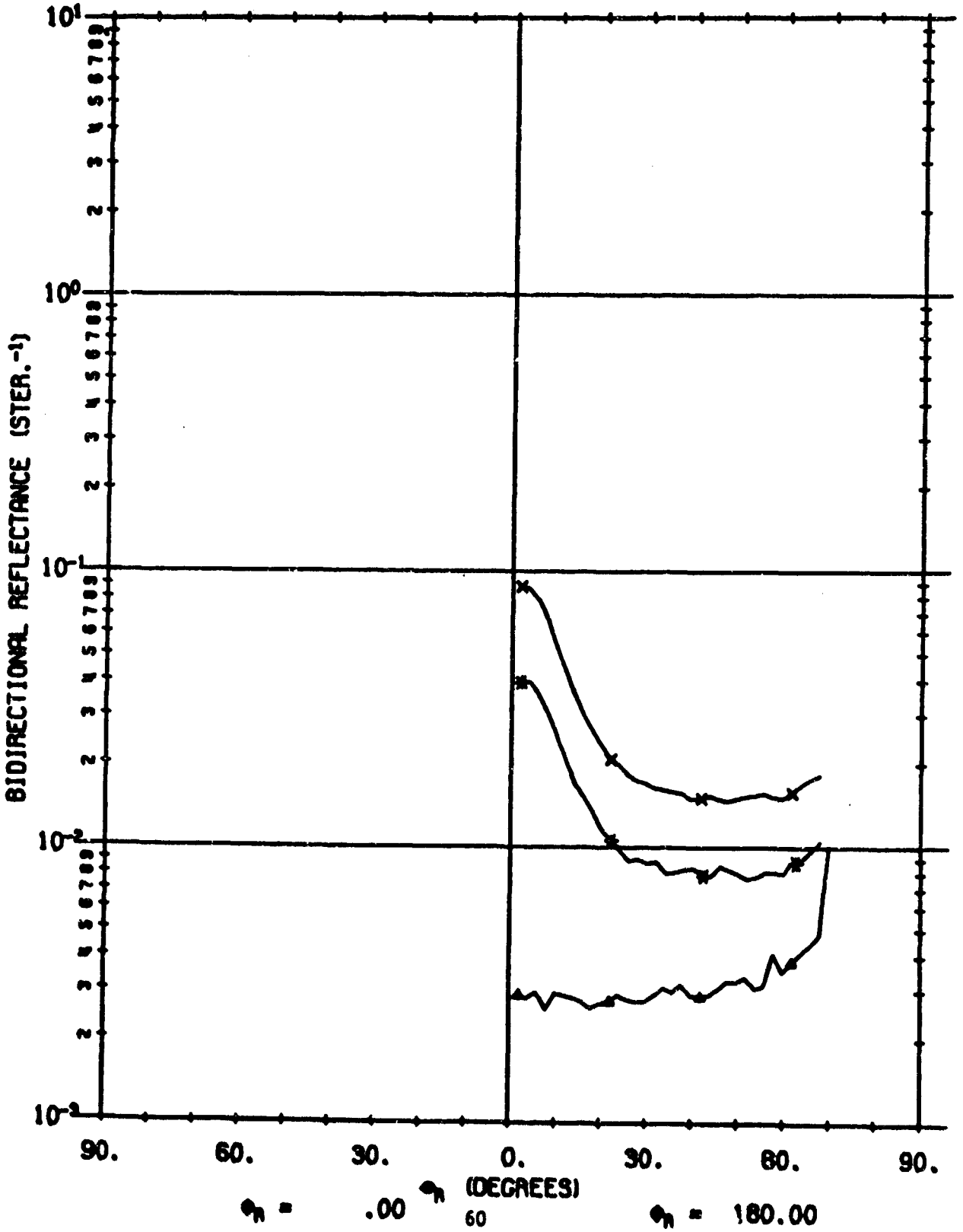

A02023 701

λ = 3.39
$\phi_I = \phi_R$ + 2.0
θ_I = .0

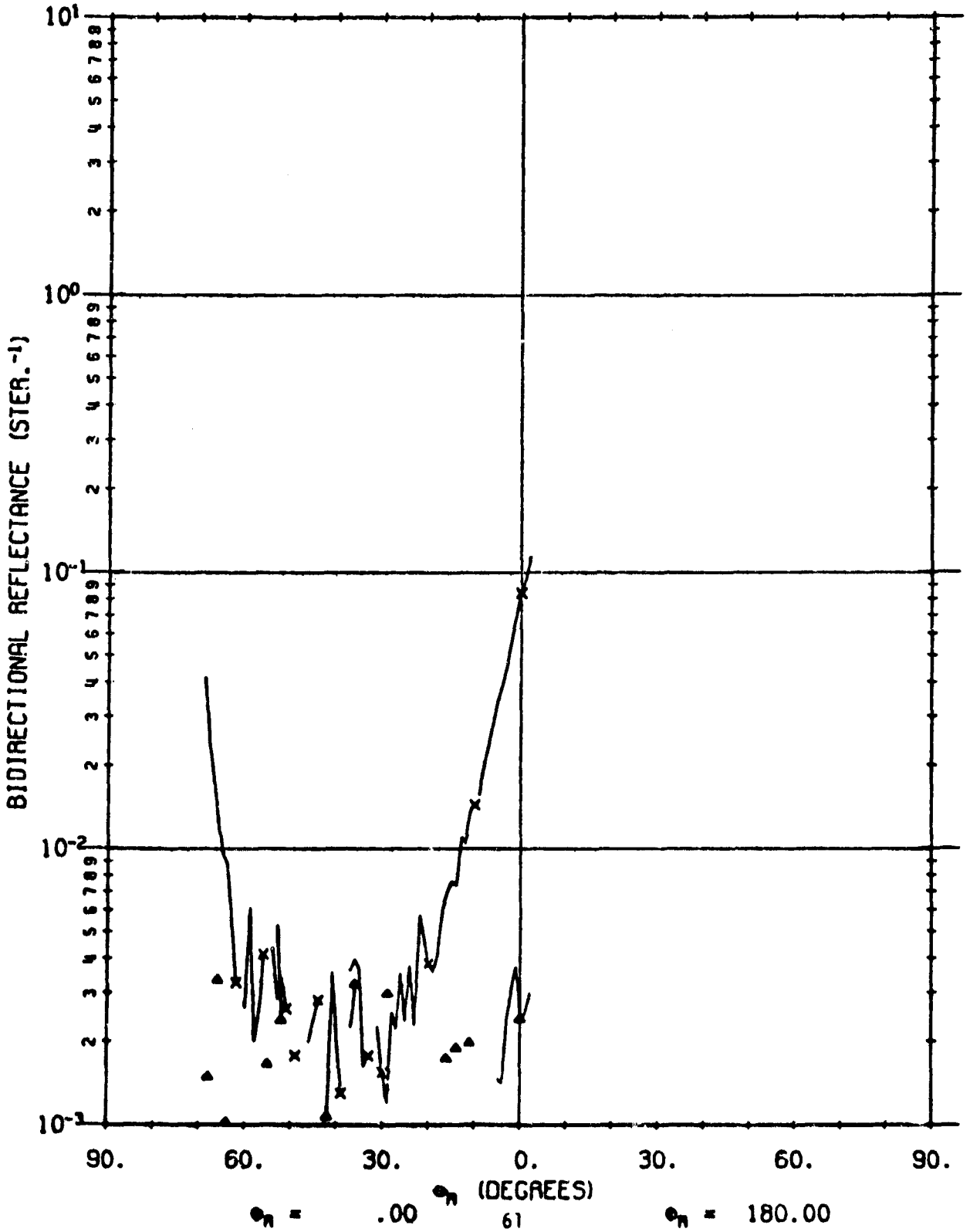

A02023 701

λ = 3.39
$\phi_I = \phi_n + -2.0$
θ_I = 180.0

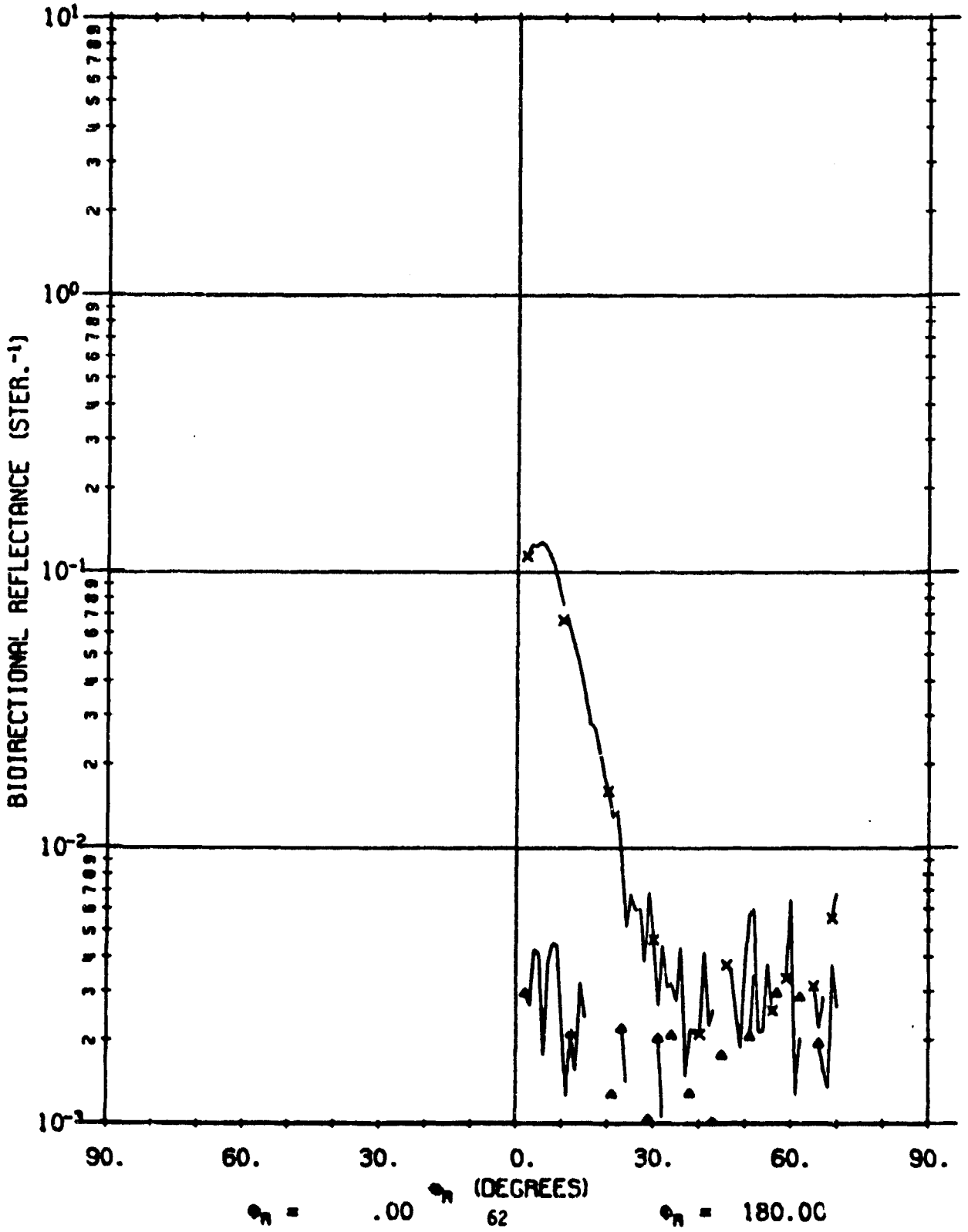

A02023 604

λ = 10.60
$\theta_I = \theta_n$+ 2.5
ϕ_I = .0

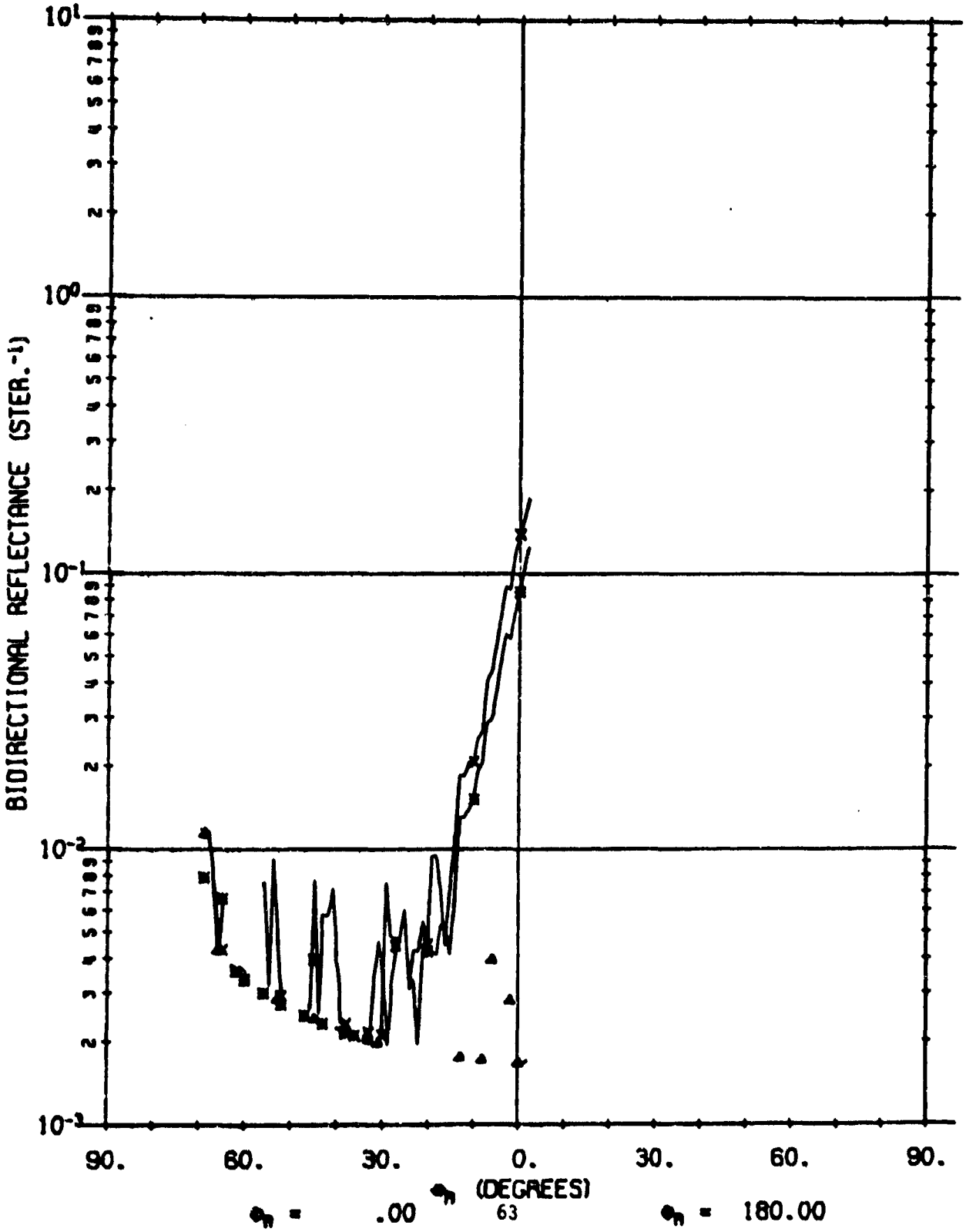

A02023 604

λ = 10.60
$\theta_r = \theta_n + -2.5$
θ_i = 180.0

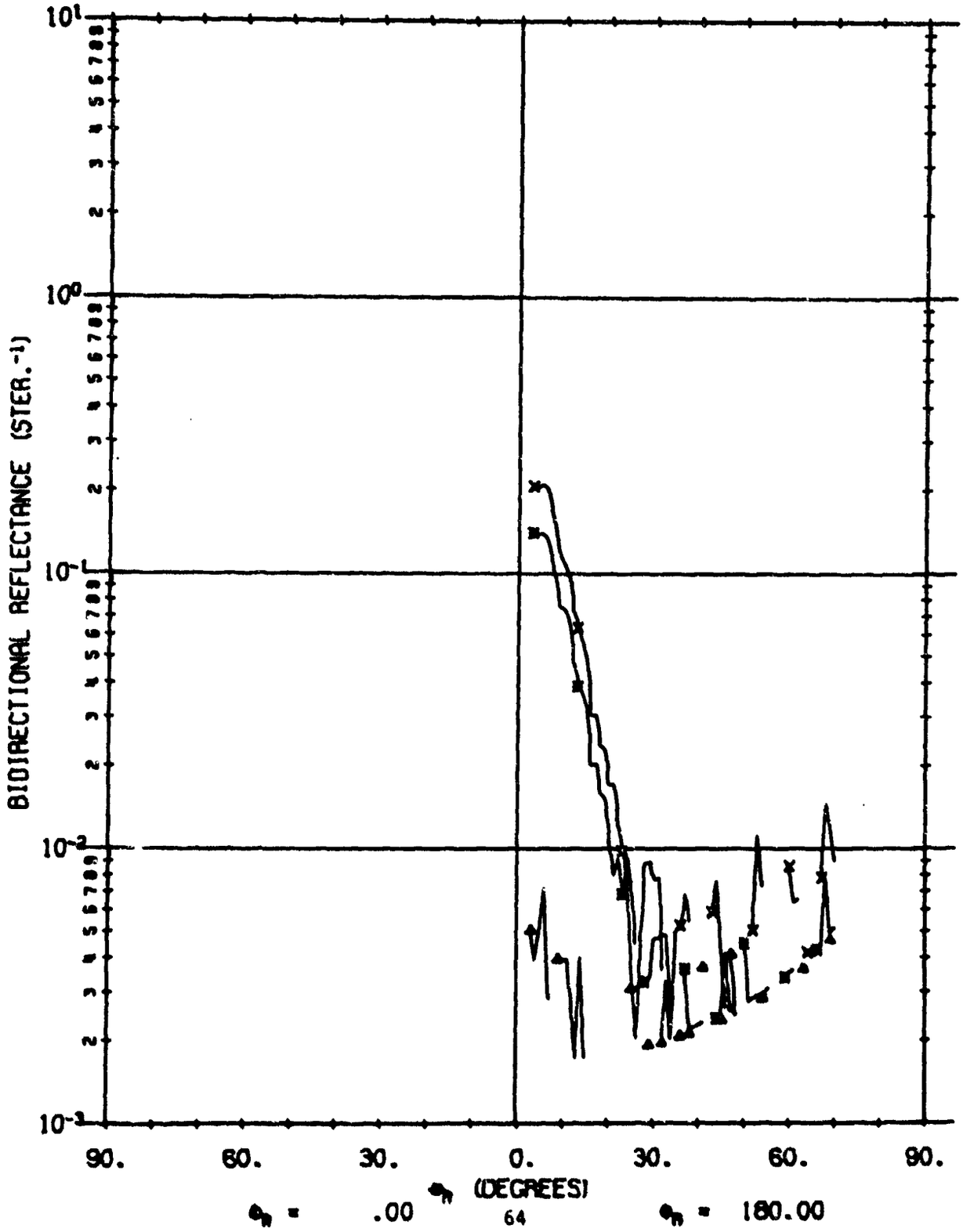

A02023 703

λ = 3.39
$\theta_i = \theta_n +$ 2.0
ϕ_i = .0

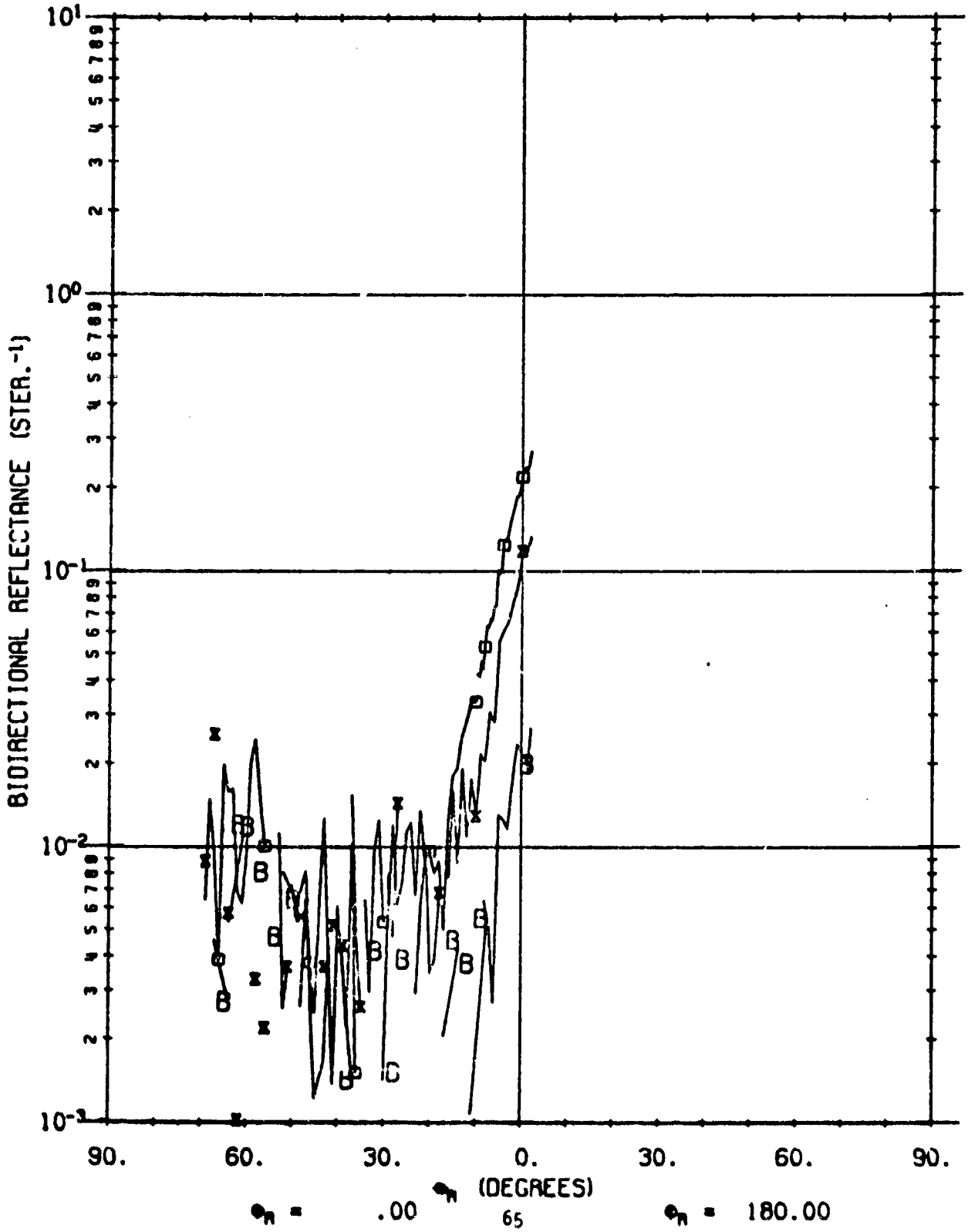

A02023 703

λ = 3.39
$\phi_i = \phi_n +$ -2.0
θ_i = 180.0

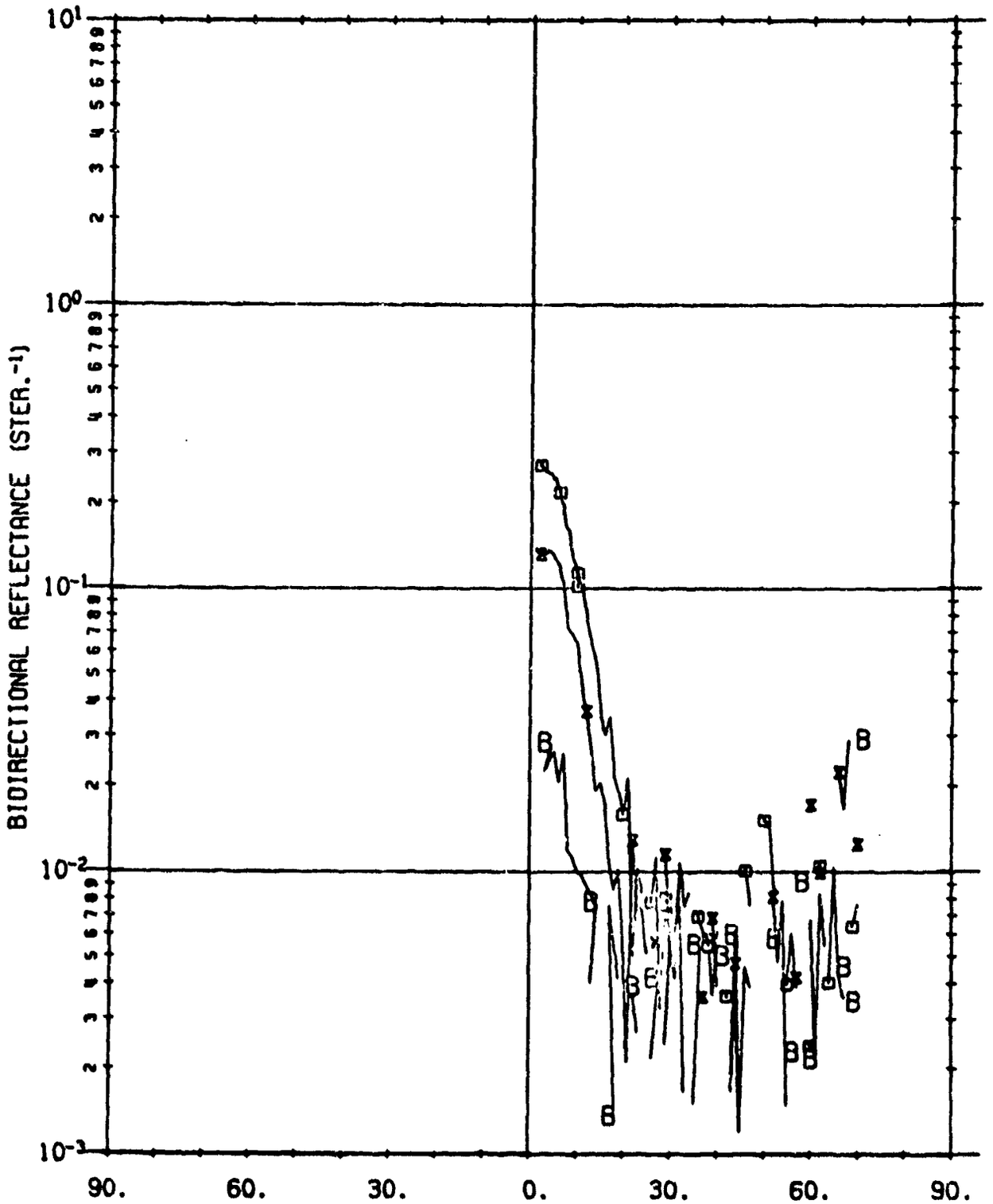

ϕ_n = .00 ϕ_n = 180.00

A02023 603

λ = 10.60
$\phi_i = \phi_n +$ 2.5
θ_i = .0

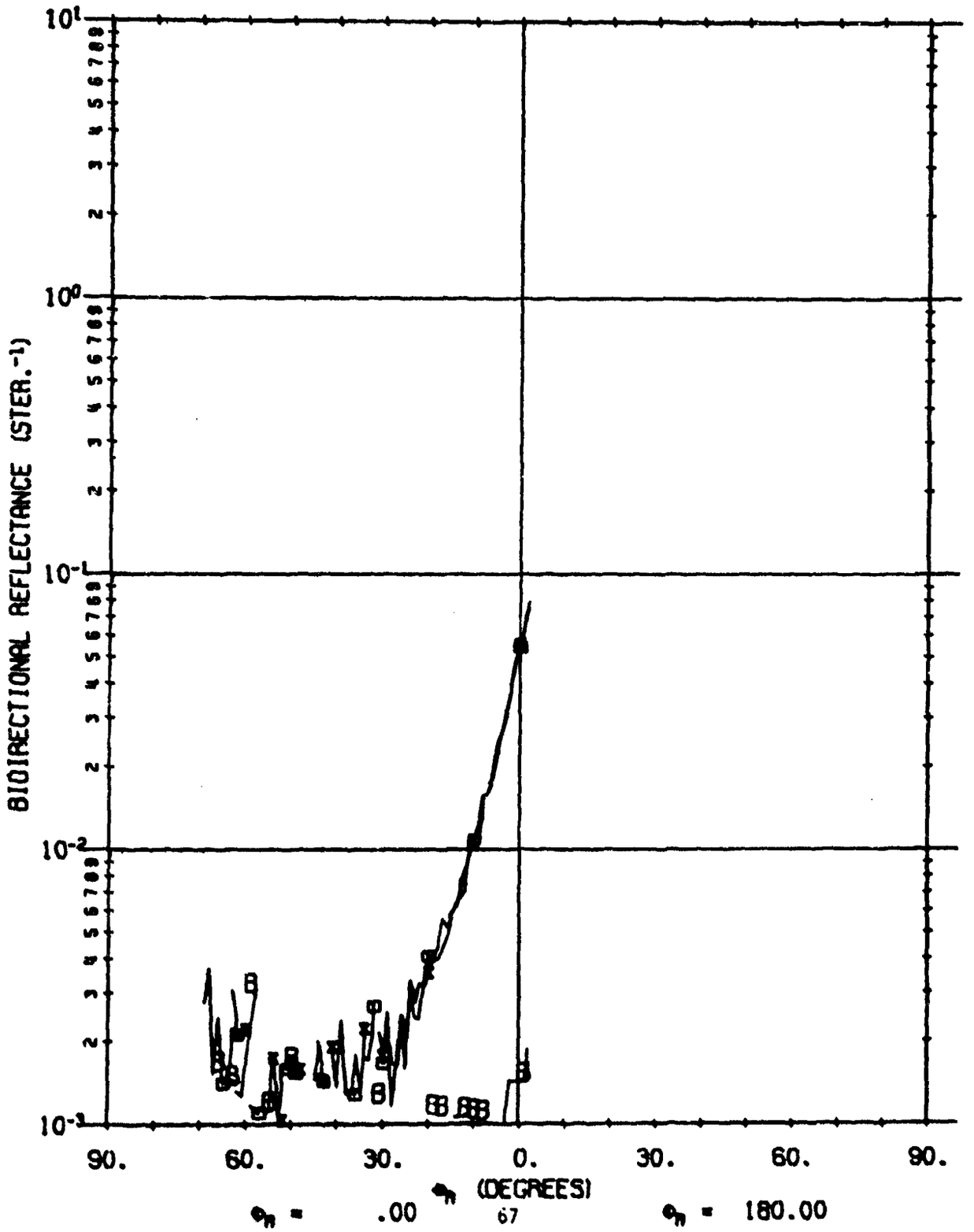

A02023 603

λ = 10.60
$\phi_i = \phi_n +$ -2.5
ϕ_i = 180.0

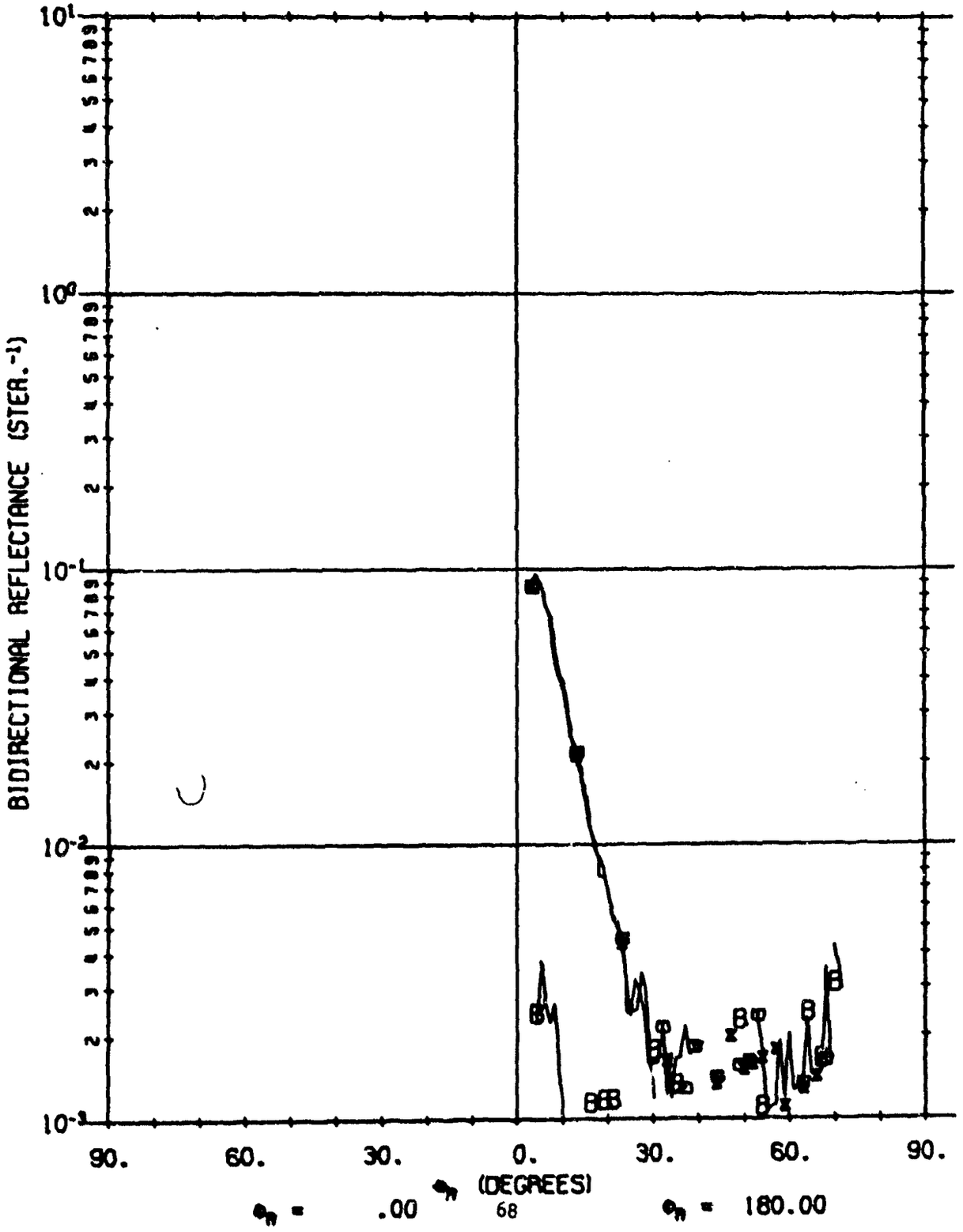

A02023 501

λ = .63
$\Phi_I = \Phi_R +$ -1.7
Φ_I = .0

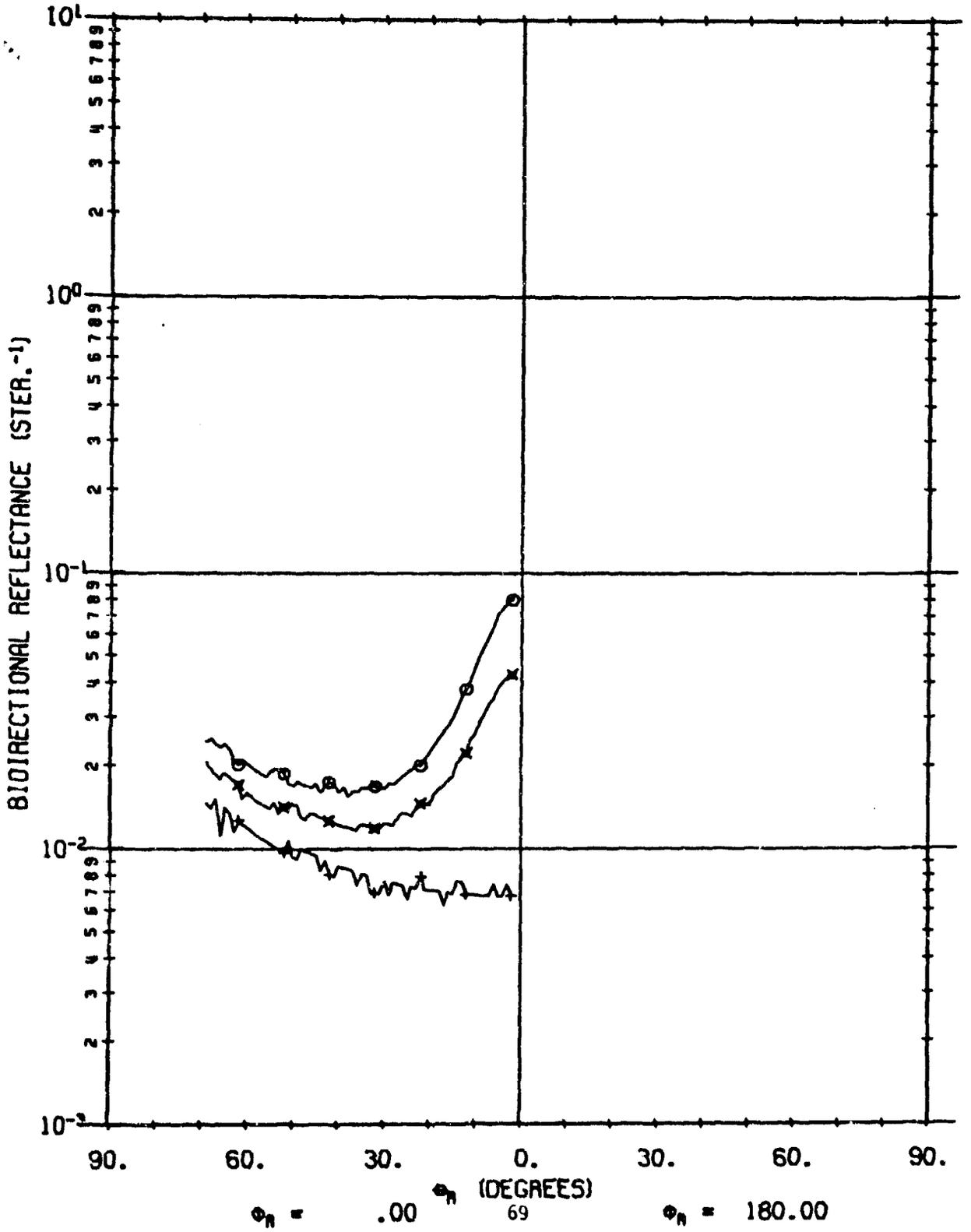

Φ_R = .00 Φ_R = 180.00

A02023 501

λ = .63

$\theta_I = \theta_R$ + 1.7

ϕ_I = 180.0

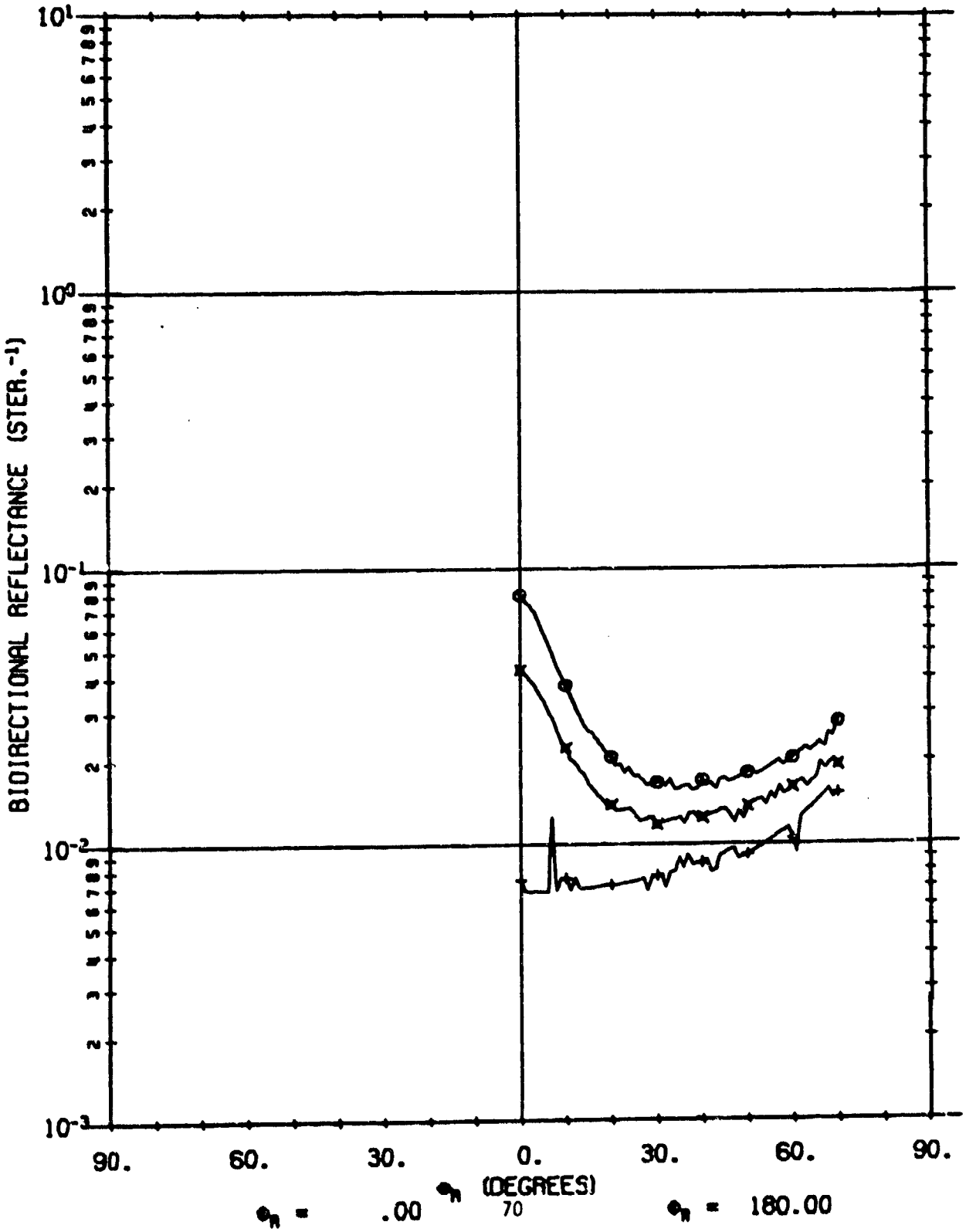

A02023 101

λ = 1.06
$\phi_r = \phi_n +$ 1.7
ϕ_i = .0

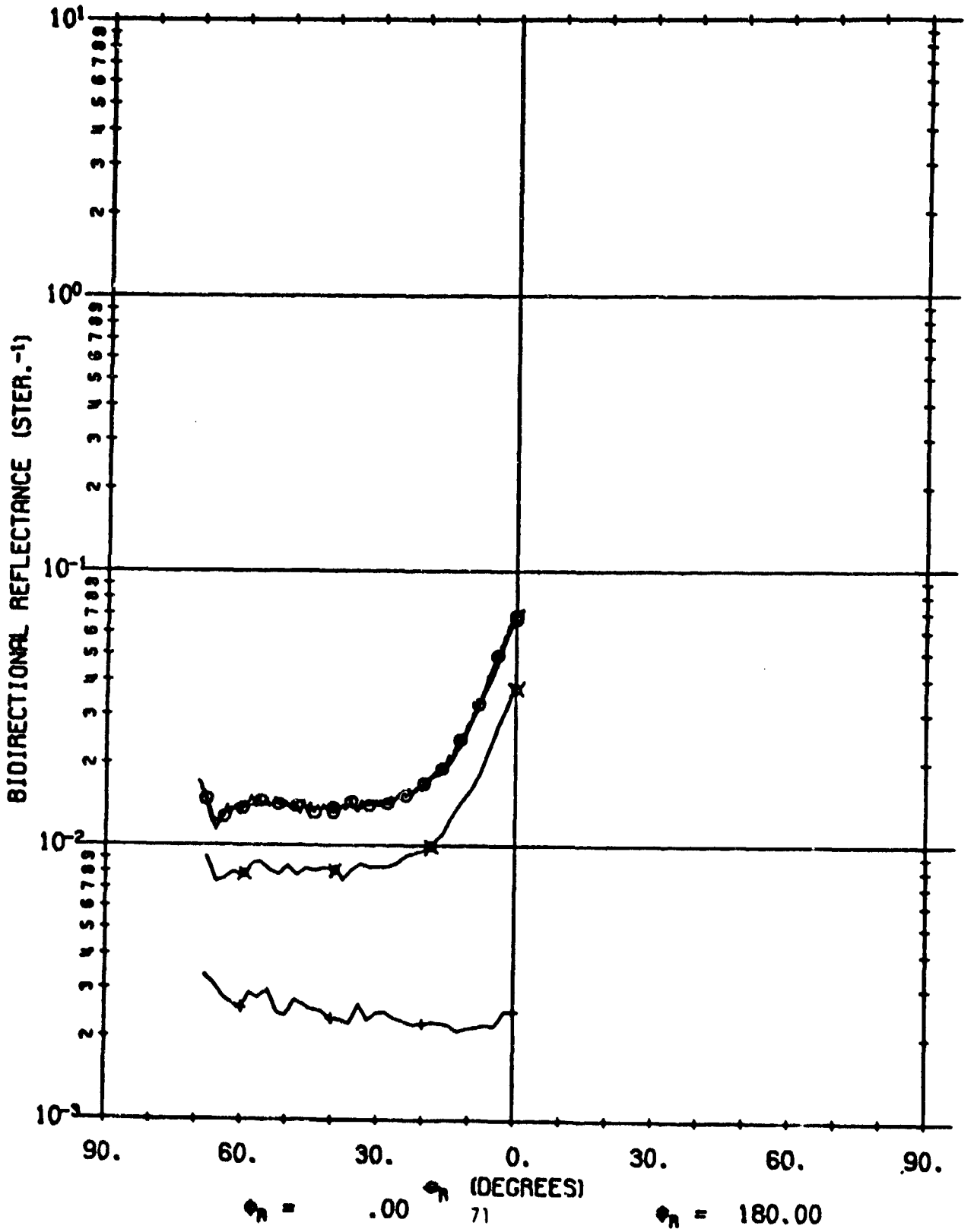

A02023 101

λ = 1.06
$\theta_i = \theta_n$ + -1.0
ϕ_i = 180.0

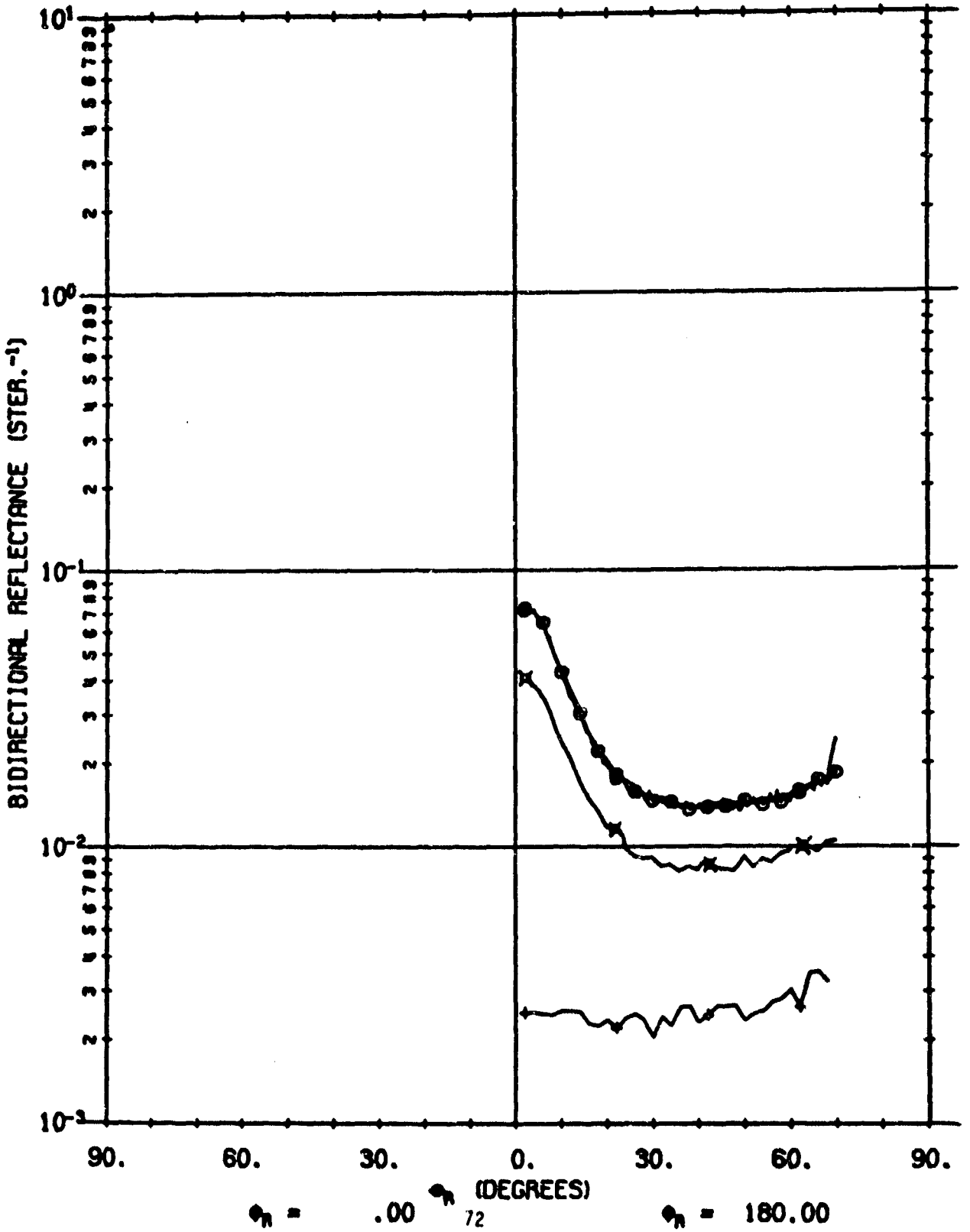

A02023 702

λ = 3.39
$\phi_i = \phi_n +$ 2.0
ϕ_i = .0

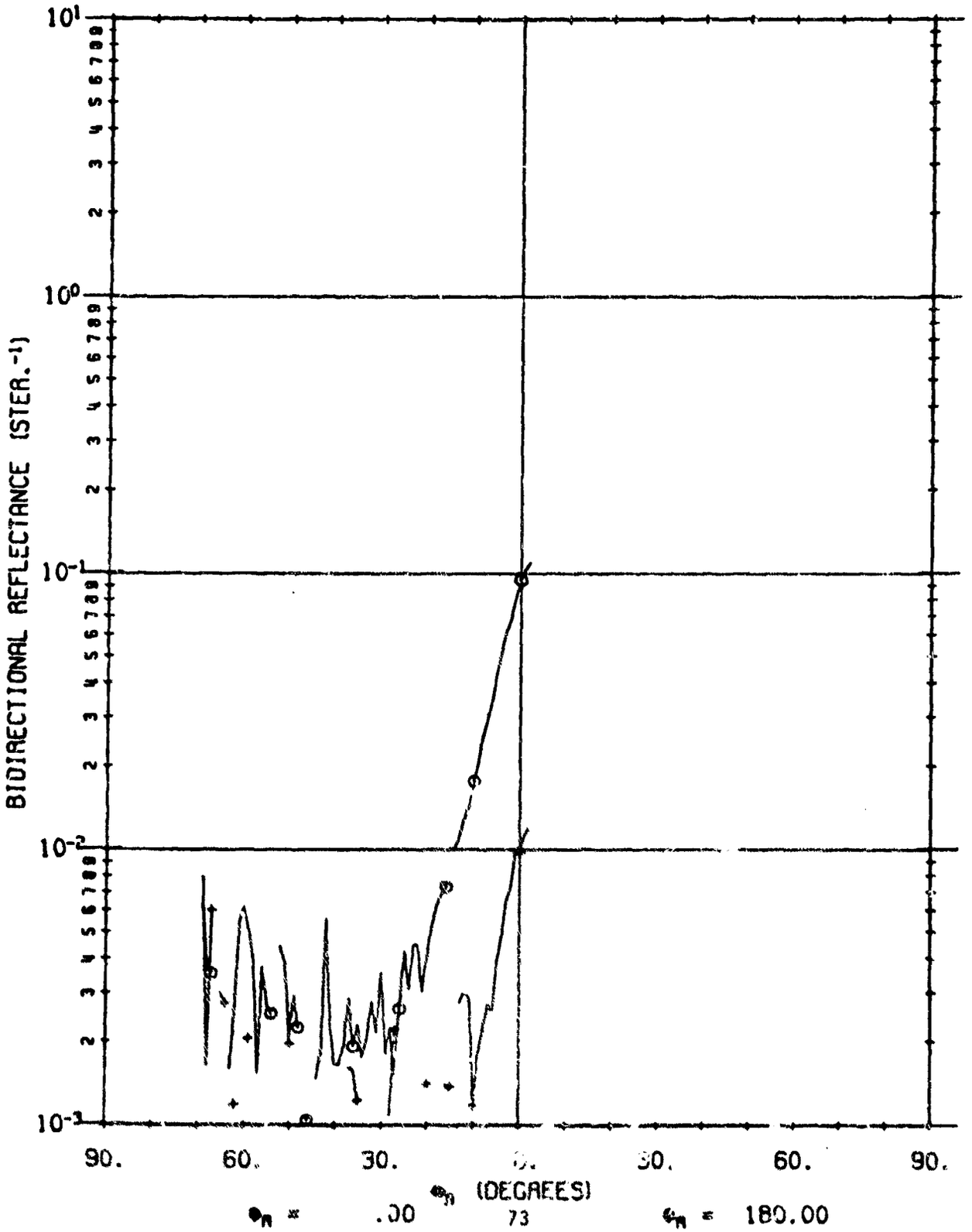

ϕ_n = .00 73 ϕ_n = 180.00

A02023 702

λ = 3.39
$\phi_i = \phi_n +$ -2.0
θ_i = 180.0

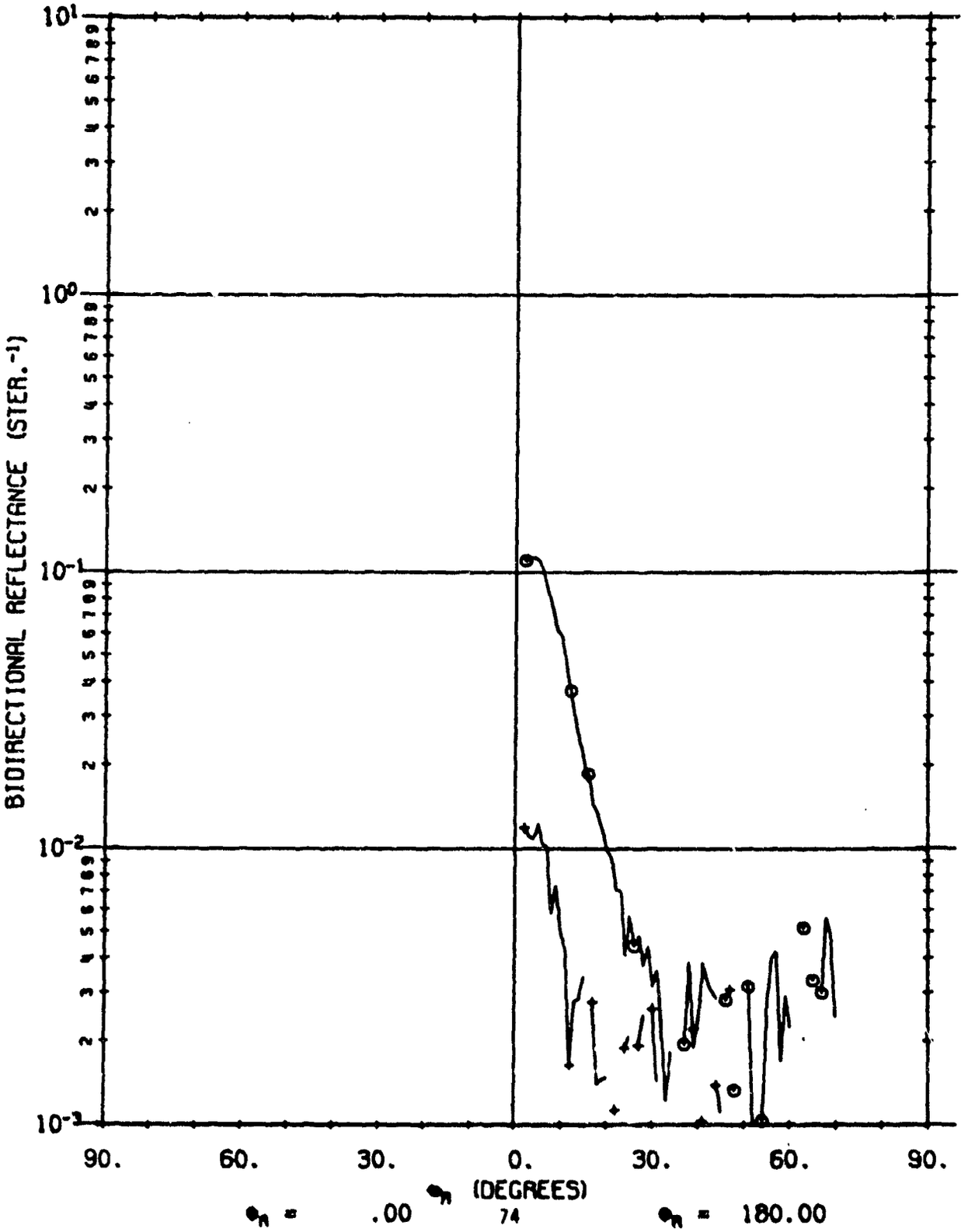

A02023 602

λ = 10.60
$\phi_I = \phi_n +$ 2.5
ϕ_I = .0

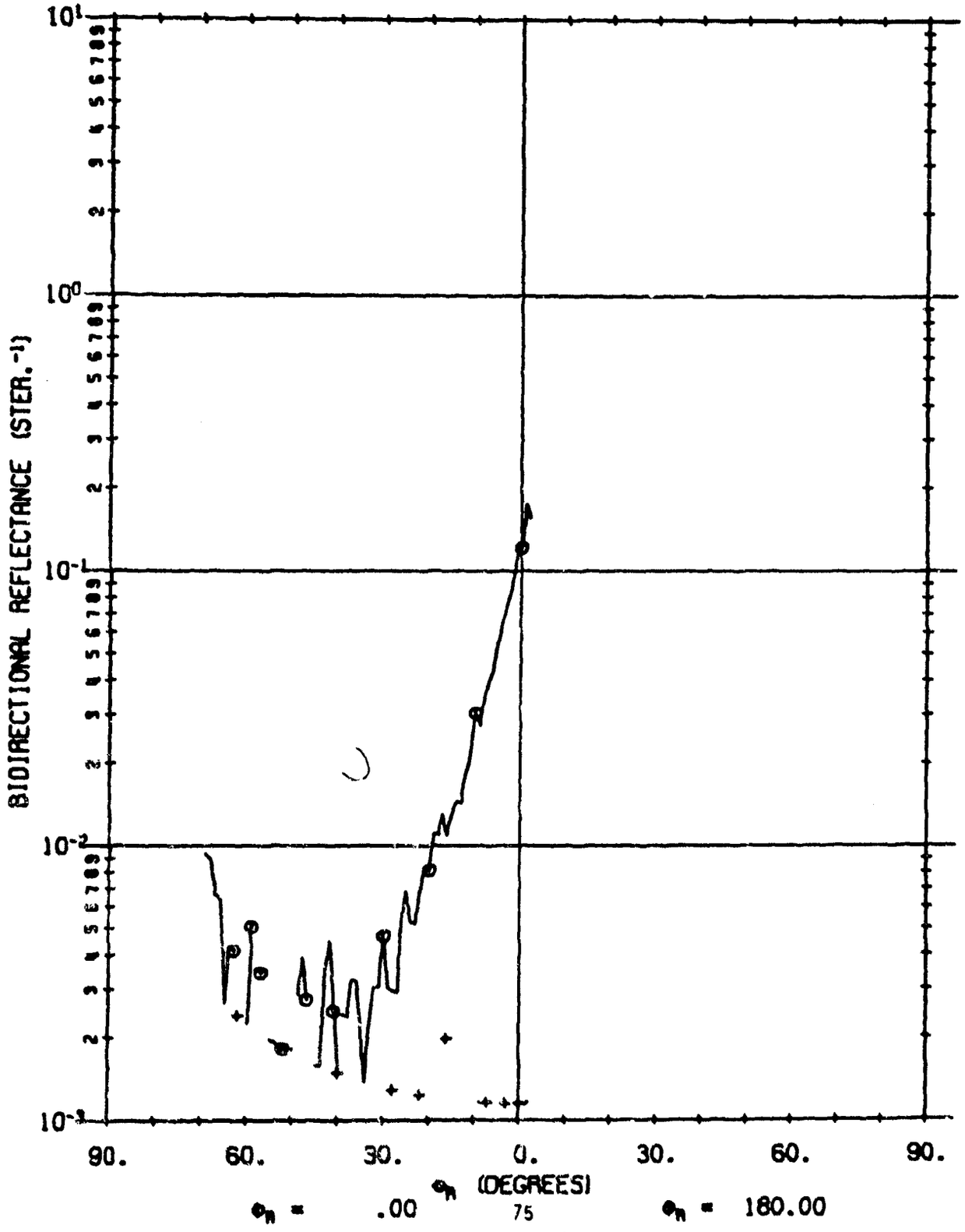

ϕ_n = .00 ϕ_n = 180.00

A02023 602

λ = 10.60
$\phi_I = \phi_R +$ -2.5
ϕ_I = 180.0

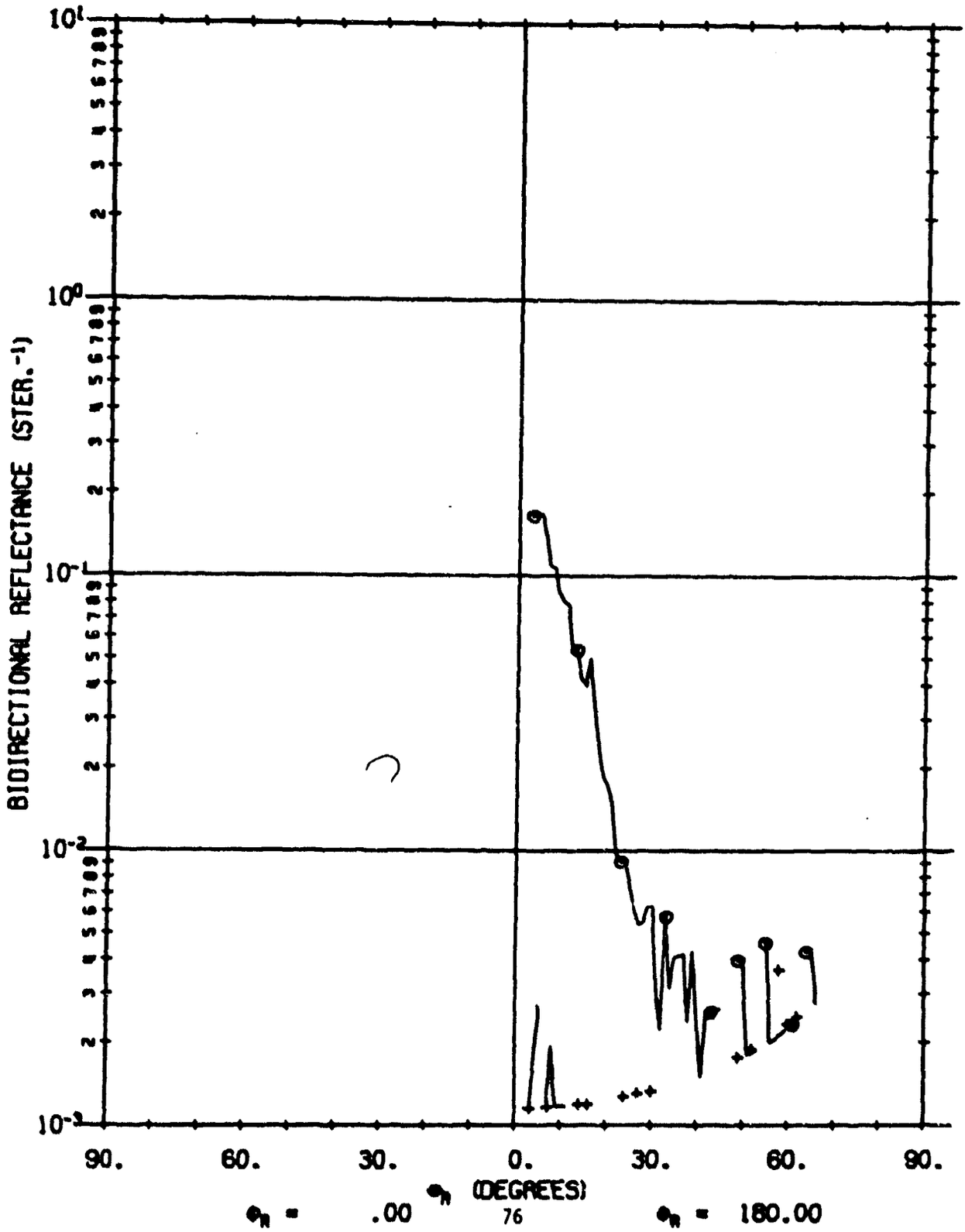

A02023 602

λ = 10.60
$\theta_I = \theta_R + -2.5$
ϕ_I = 90.0

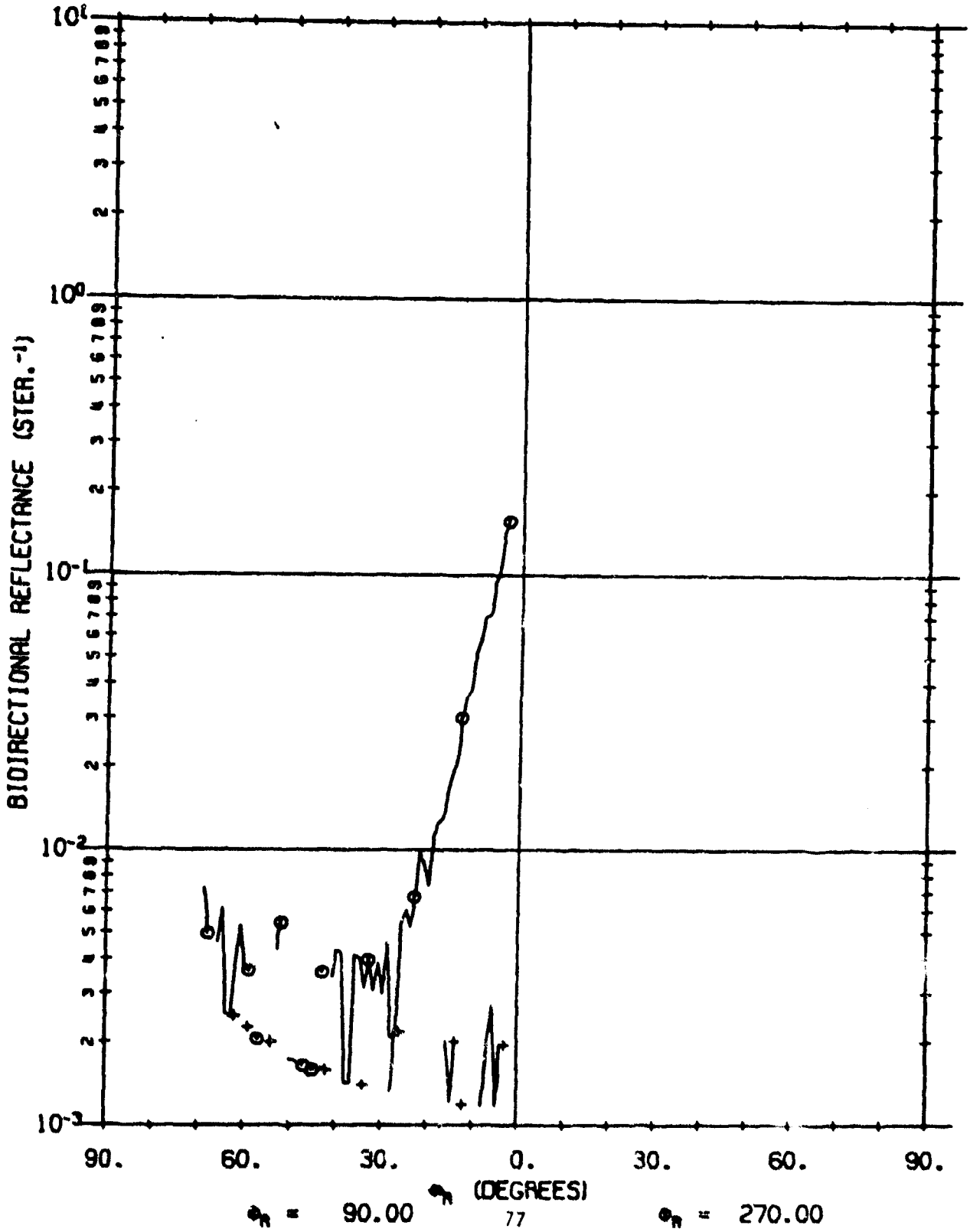

ϕ_R = 90.00 ϕ_R = 270.00

A02023 602

λ = 10.60
$\theta_I = \theta_n +$ 2.5
ϕ_I = 270.0

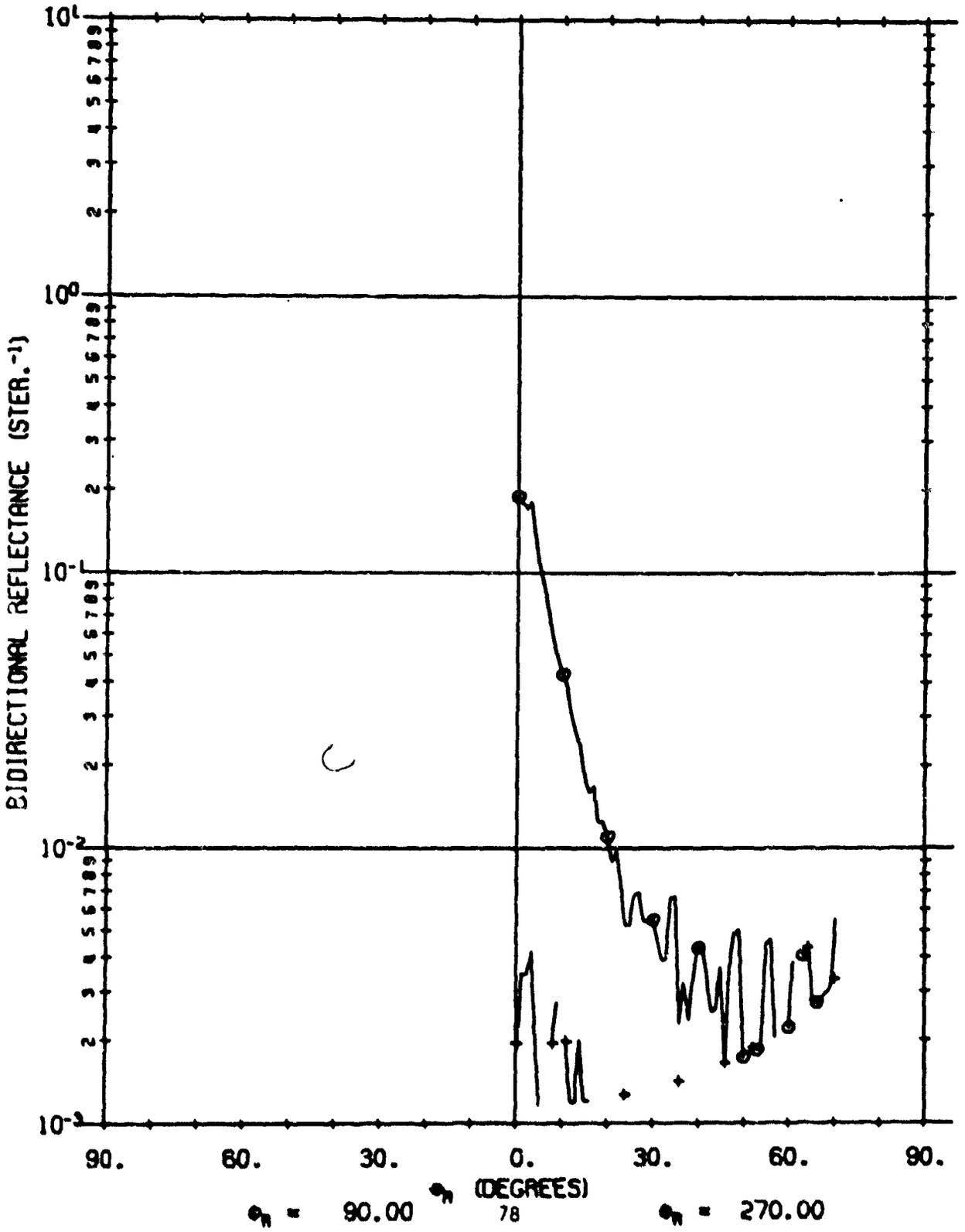

A01610 101

λ = .63
$\phi_I = \phi_R +$ -1.7
θ_I = .0

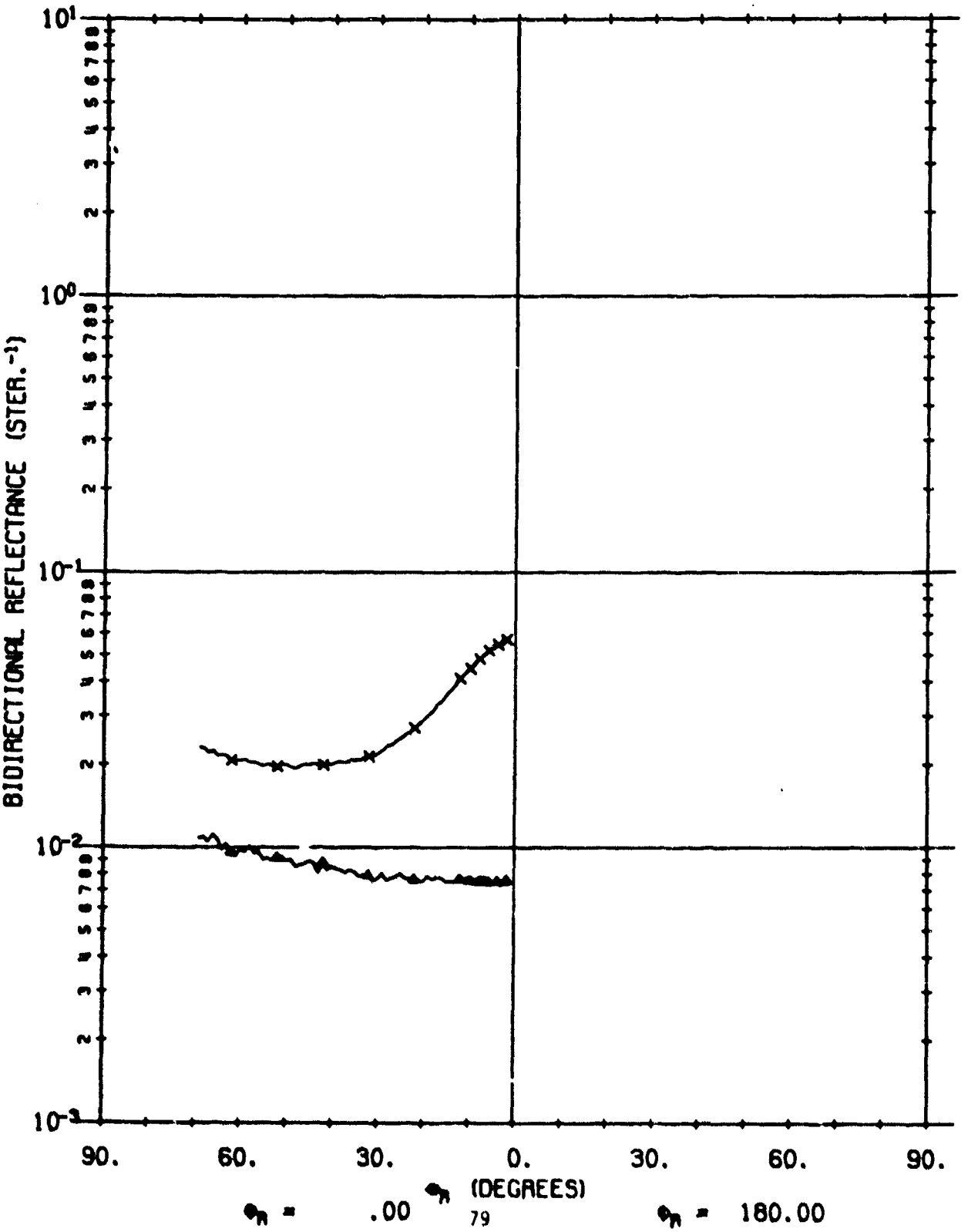

λ = .63
$\theta_i = \theta_n + 1.7$
ϕ_i = 180.0

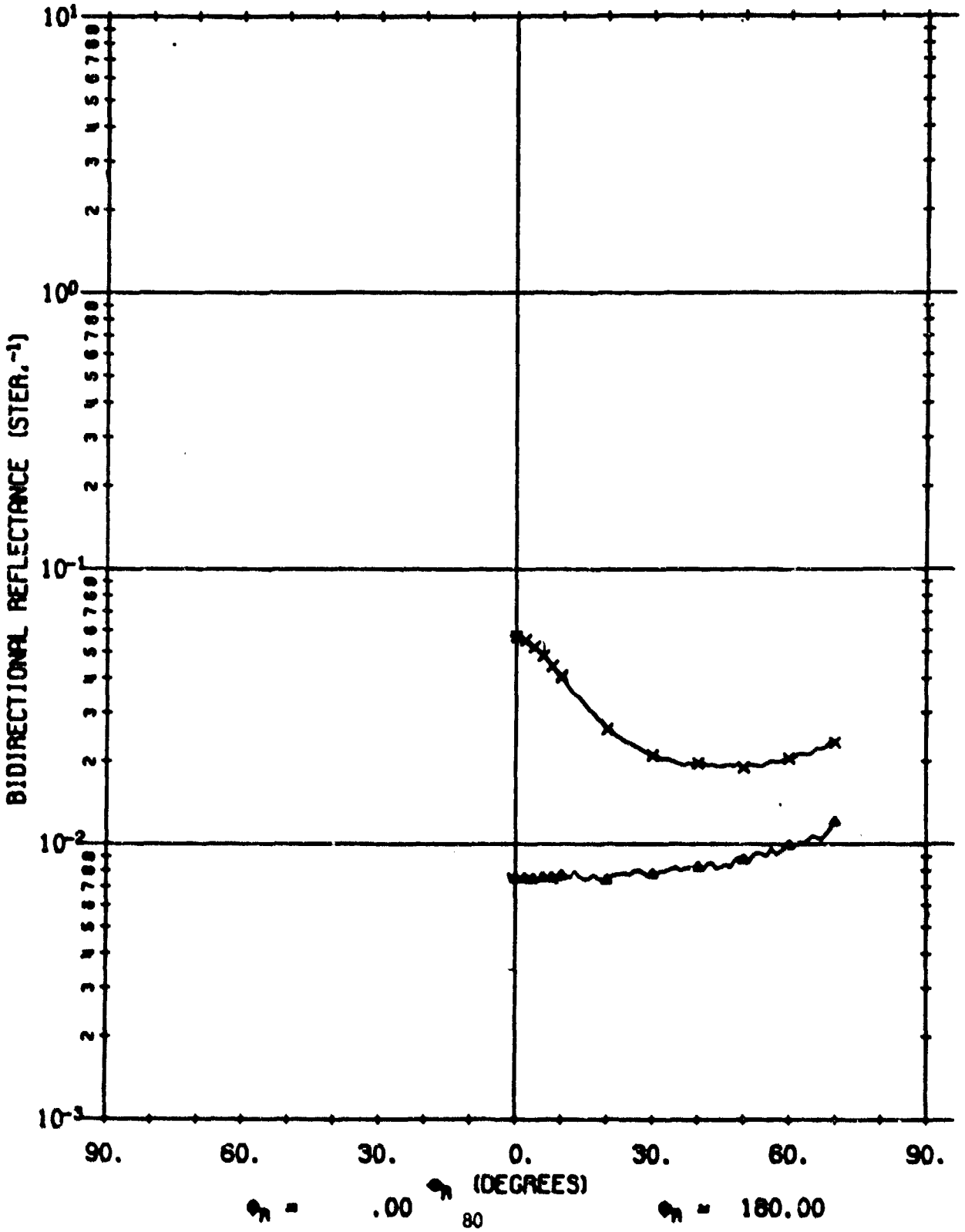

A01610 102

λ = 1.06
$\phi_I = \phi_n^+$ -1.7
θ_I = .0

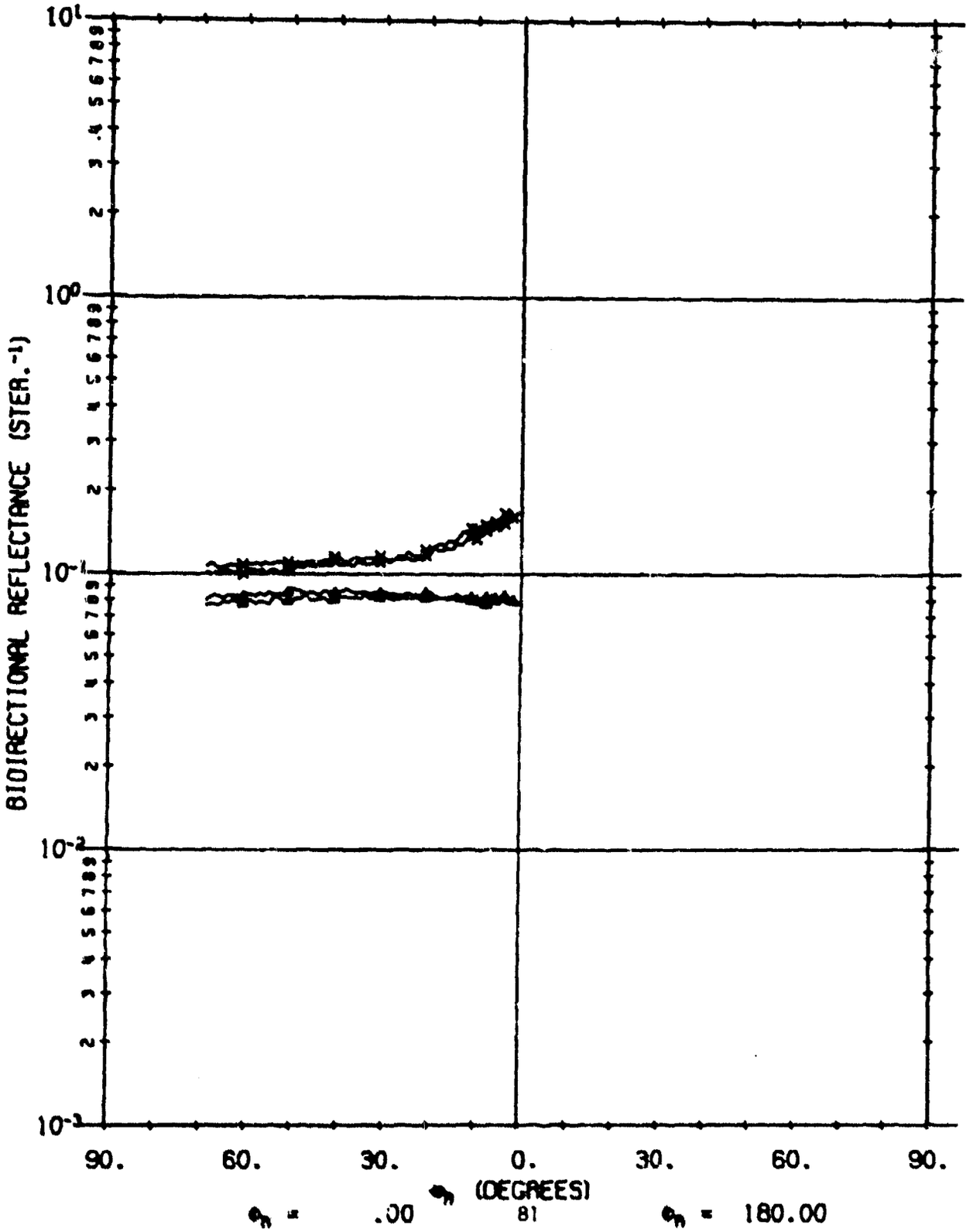

A01610 102

λ = 1.06
θ_i = θ_n + 1.7
ϕ_i = 180.0

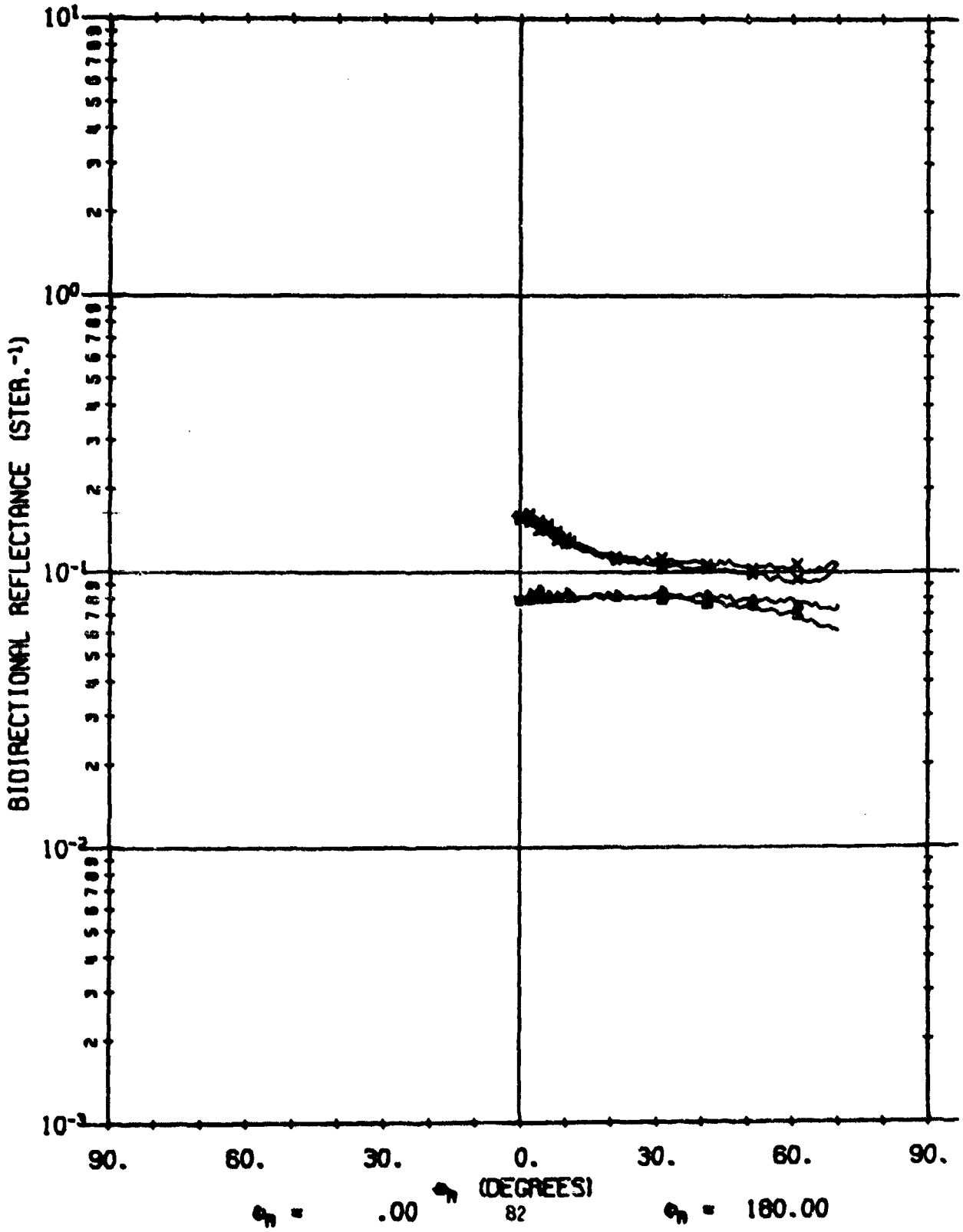

A01610 301

λ = 3.39
$\phi_1 = \phi_R +$ 2.0
θ_1 = .0

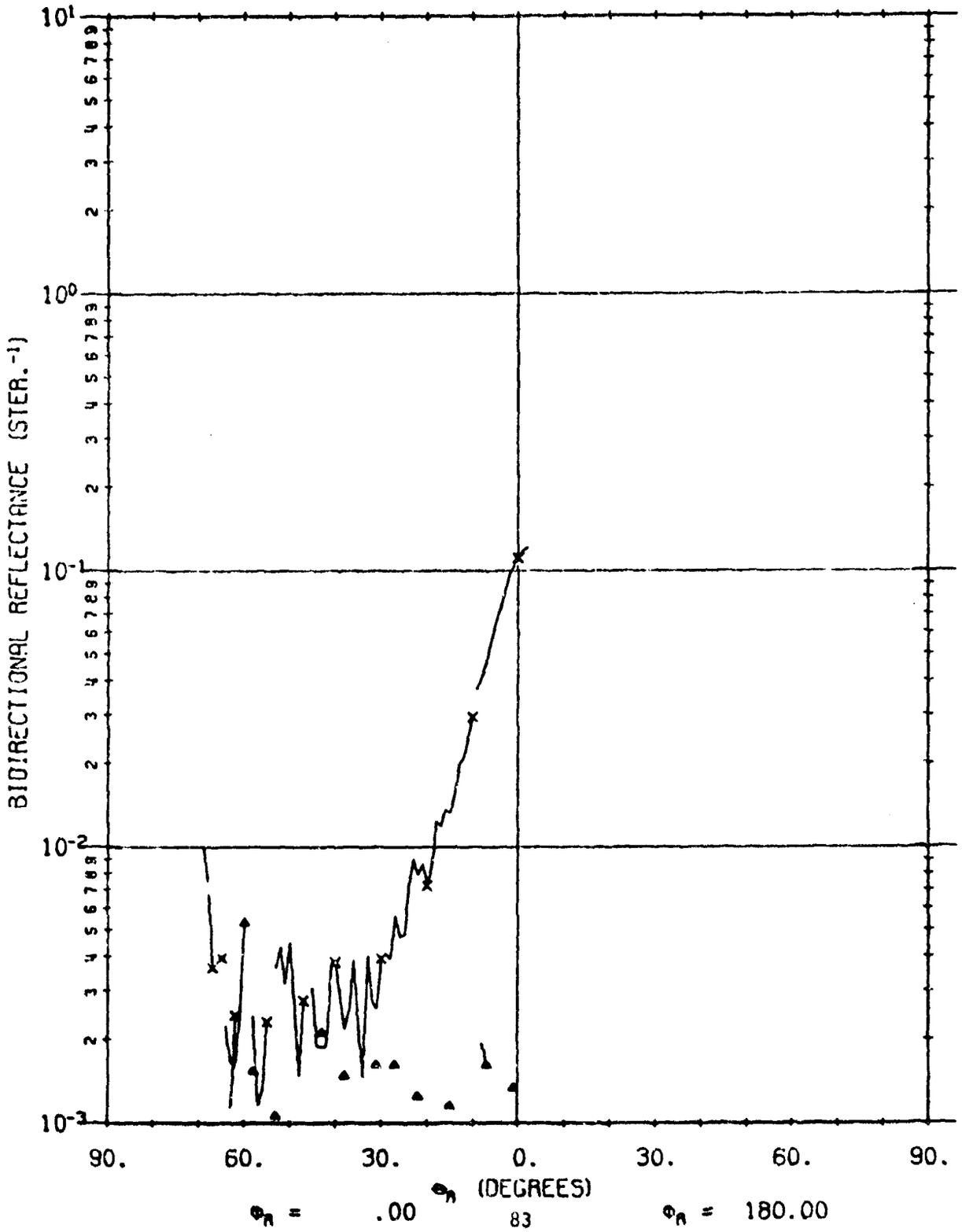

A01610 301

λ = 3.39
$\Phi_I = \Phi_R +$ -2.0
Φ_I = 180.0

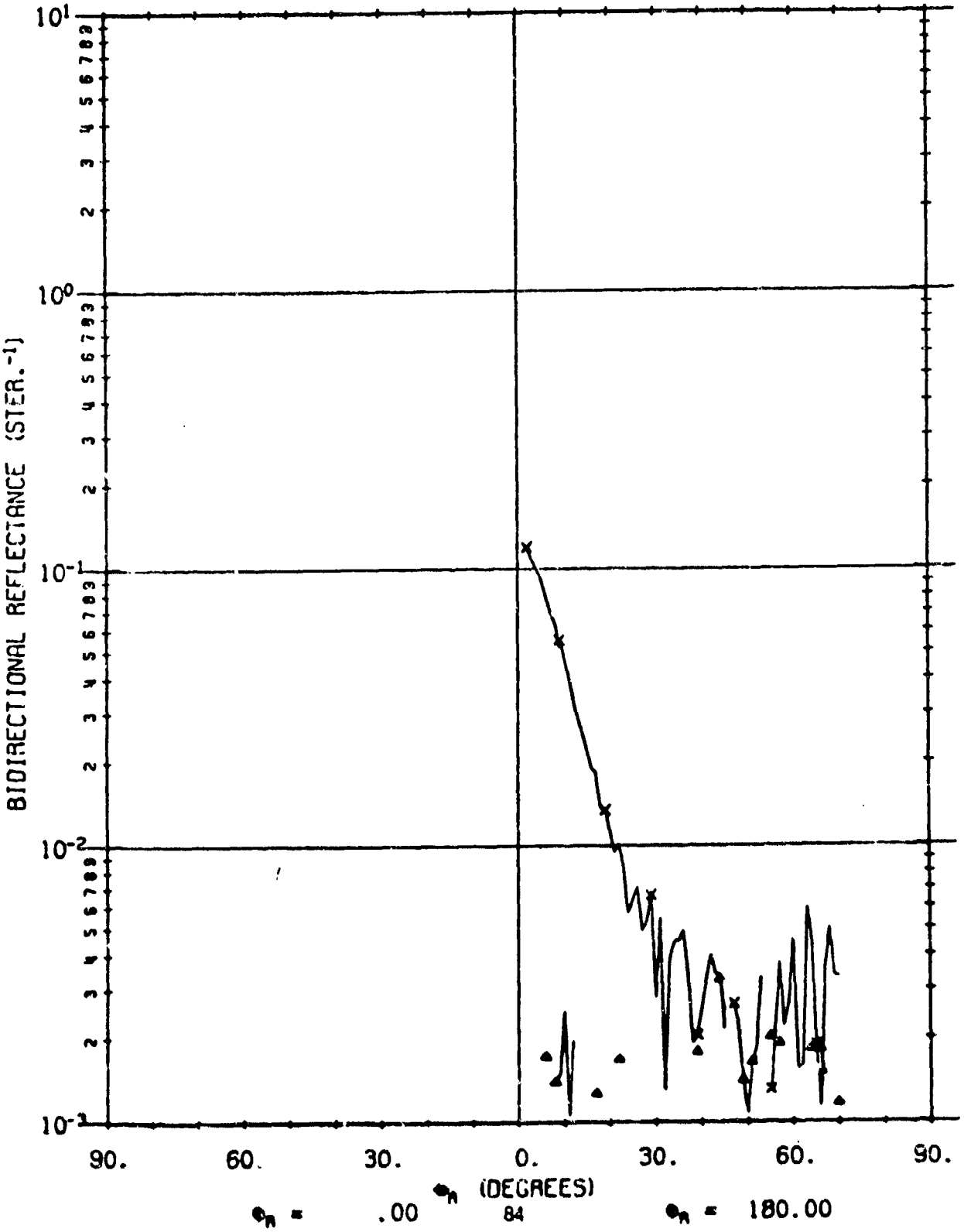

A01610 201

λ = 10.60
$\theta_I = \theta_n +$ 2.5
ϕ_I = .0

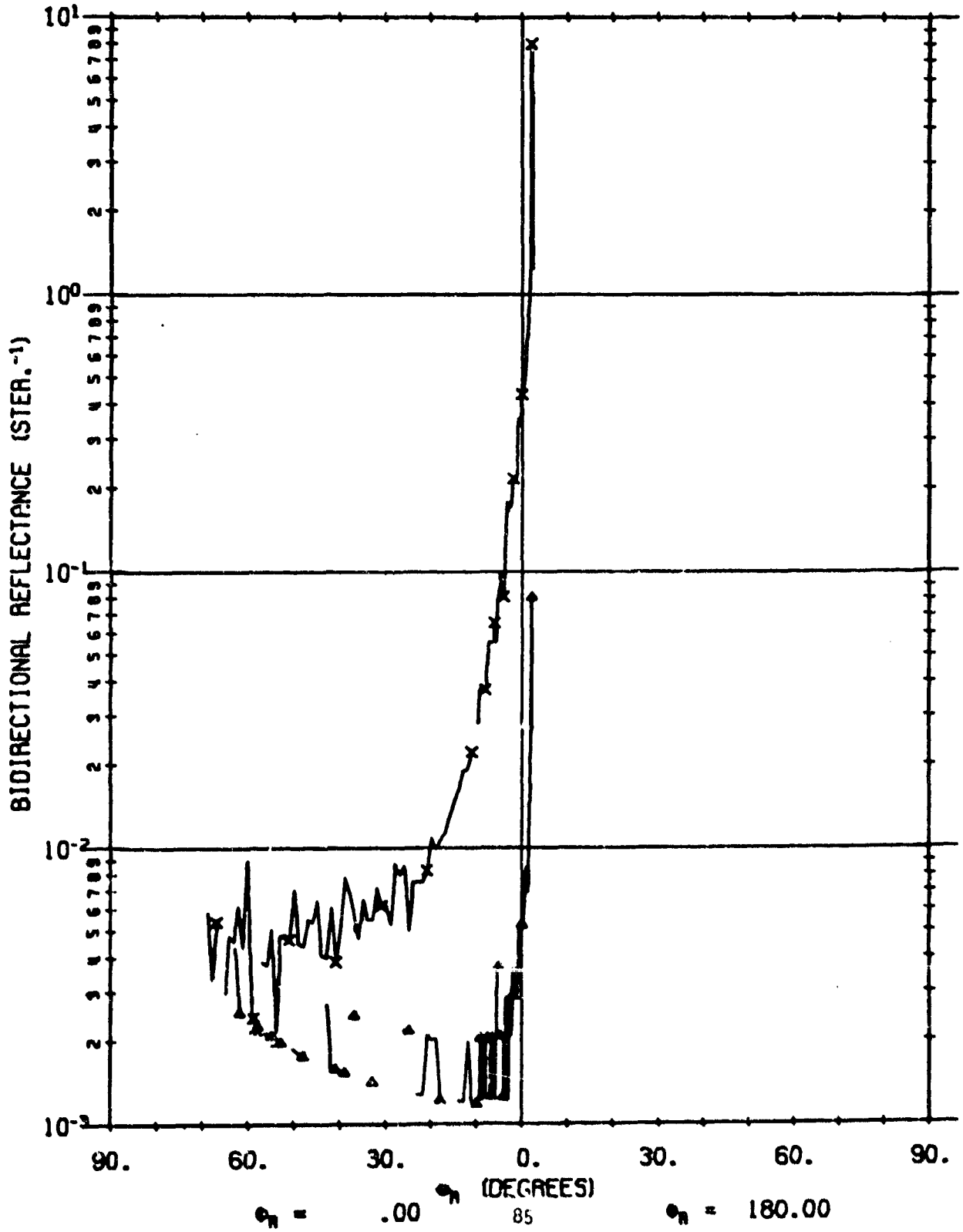

A01610 201

λ = 10.60
$\theta_i = \theta_n + -2.5$
ϕ_i = 180.0

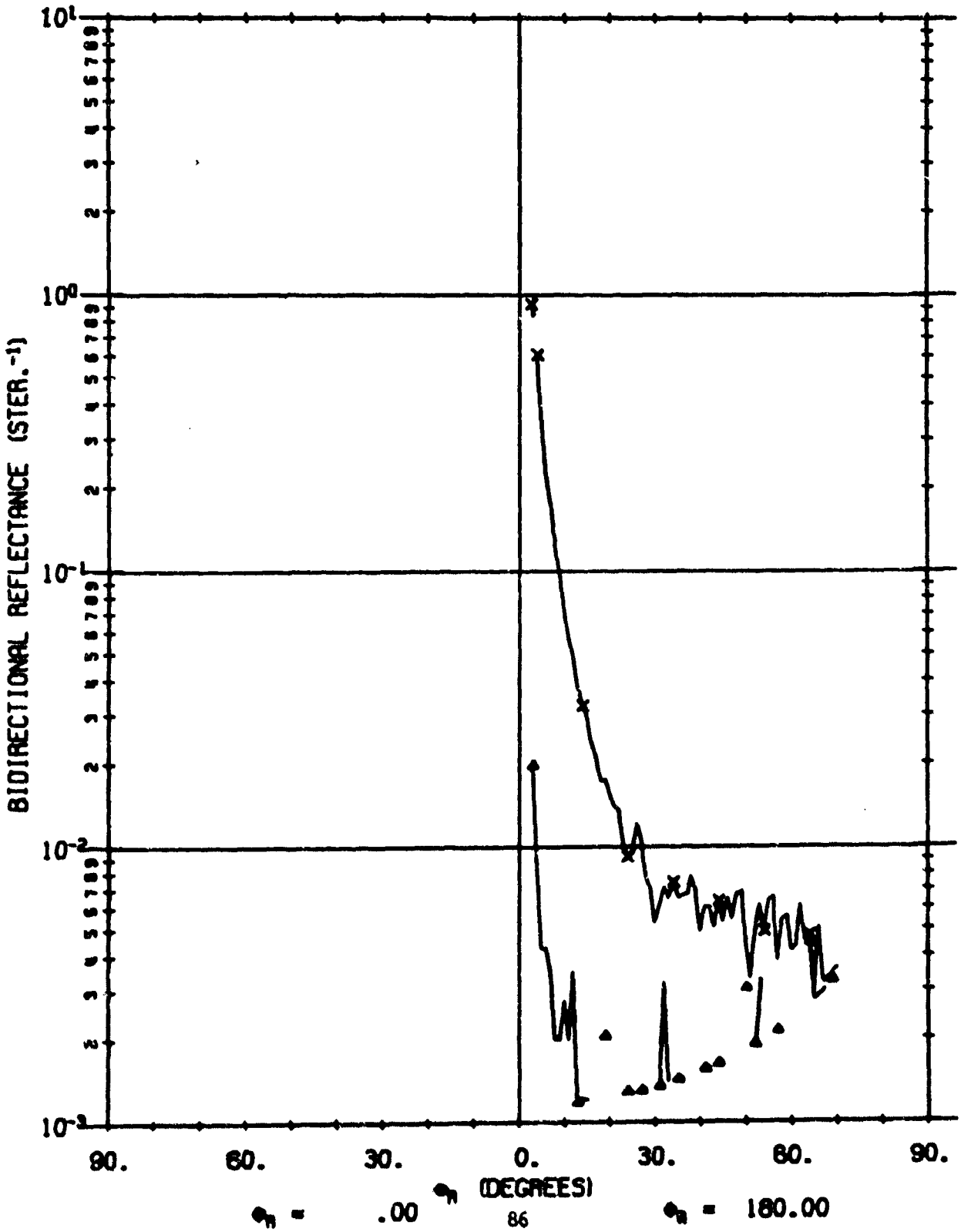

A01610 303

λ = 3.39
$\Phi_I = \Phi_R$ = 2.0
Φ_I = .0

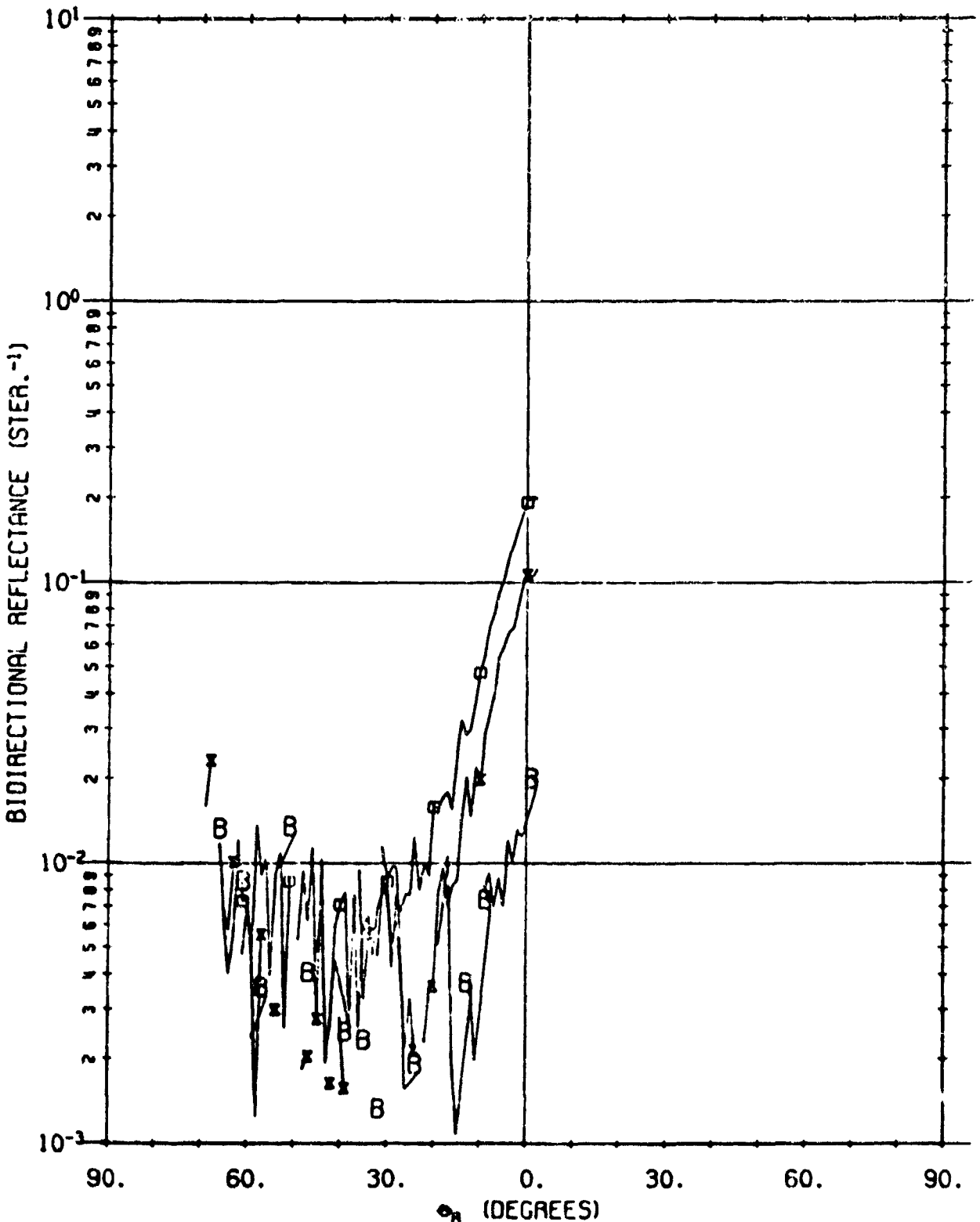

Φ_R = .00 Φ_R = 180.00

A01610 303

λ = 3.39
$\phi_I = \phi_R +$ -2.0
θ_I = 180.0

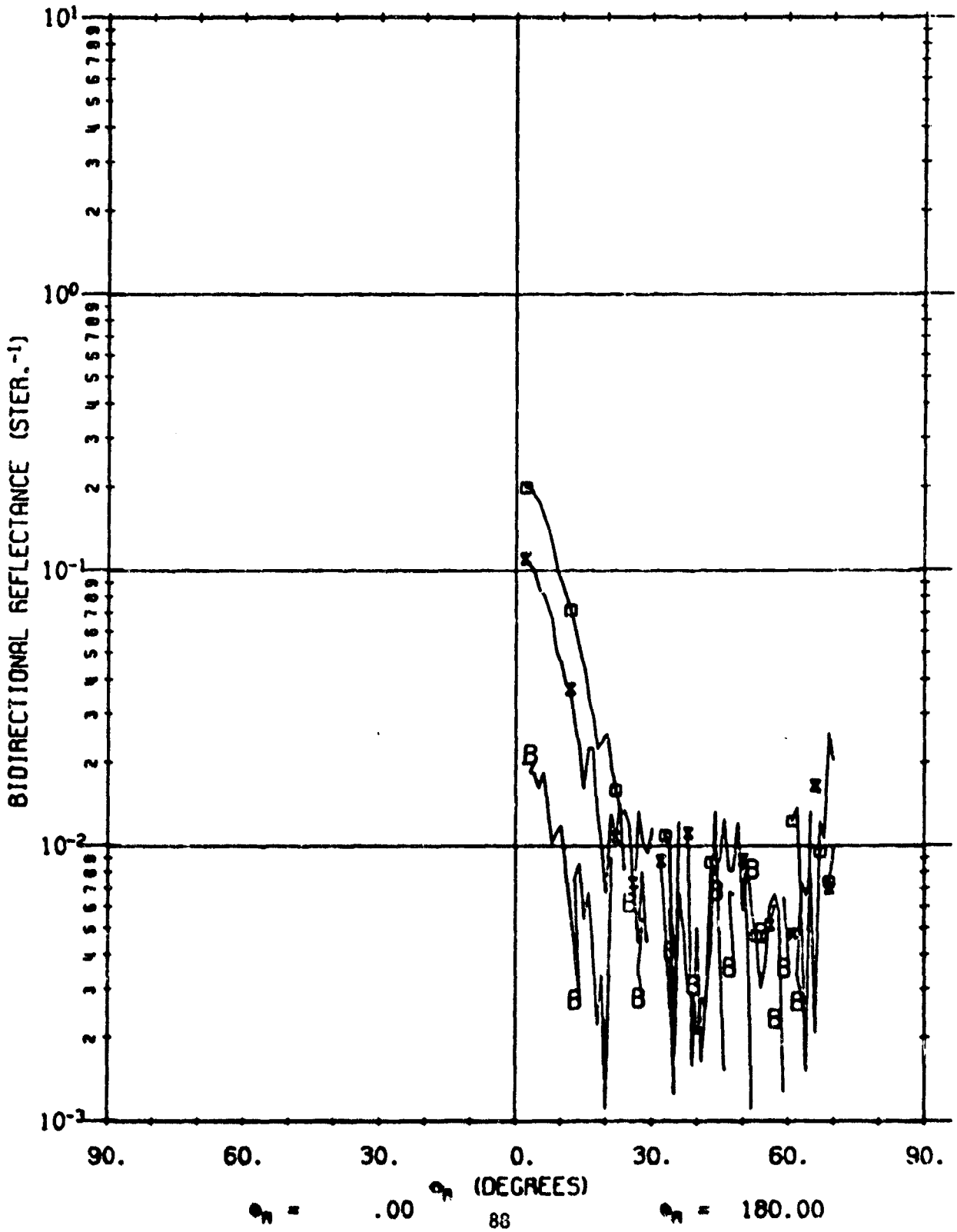

A01610 101

λ = .63
$\theta_I = \theta_R^+$ -1.7
ϕ_I = .0

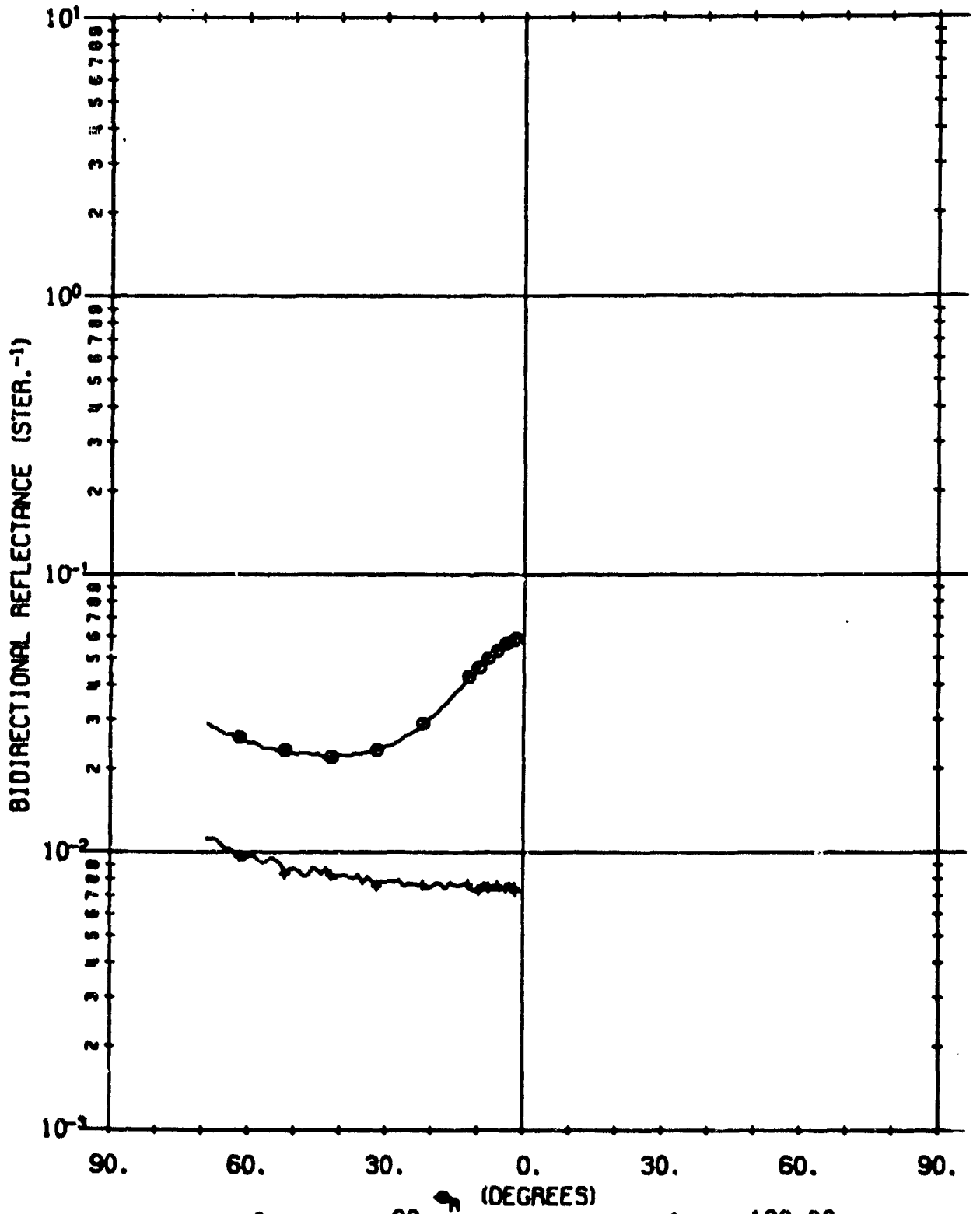

ϕ_R = .00 ϕ_R = 180.00

A01610 101

λ = .63

$\theta_i = \theta_n + 1.7$

ϕ_i = 180.0

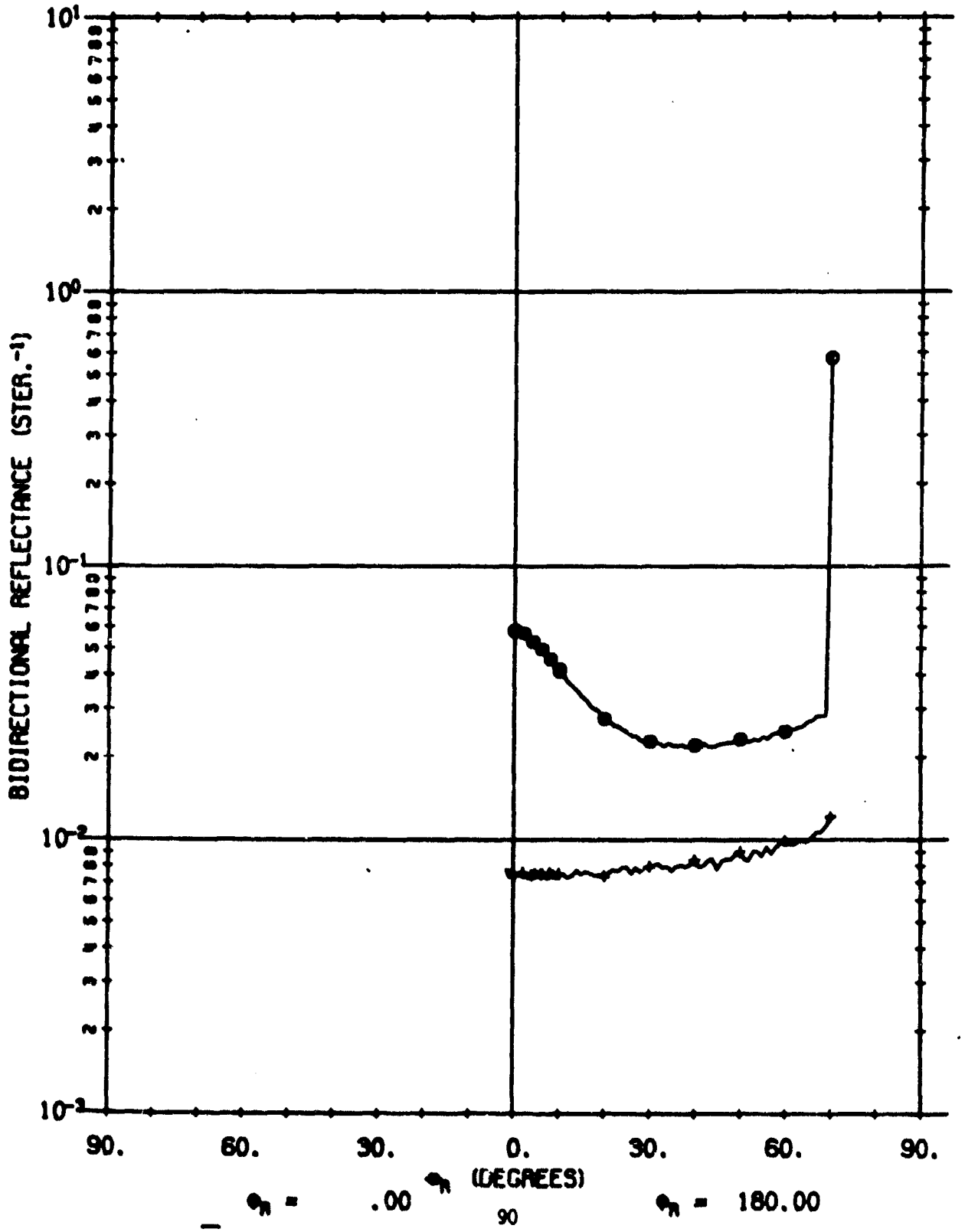

A01610 102

λ = 1.06
$\theta_i = \theta_n +$ -1.7
θ_i = .0

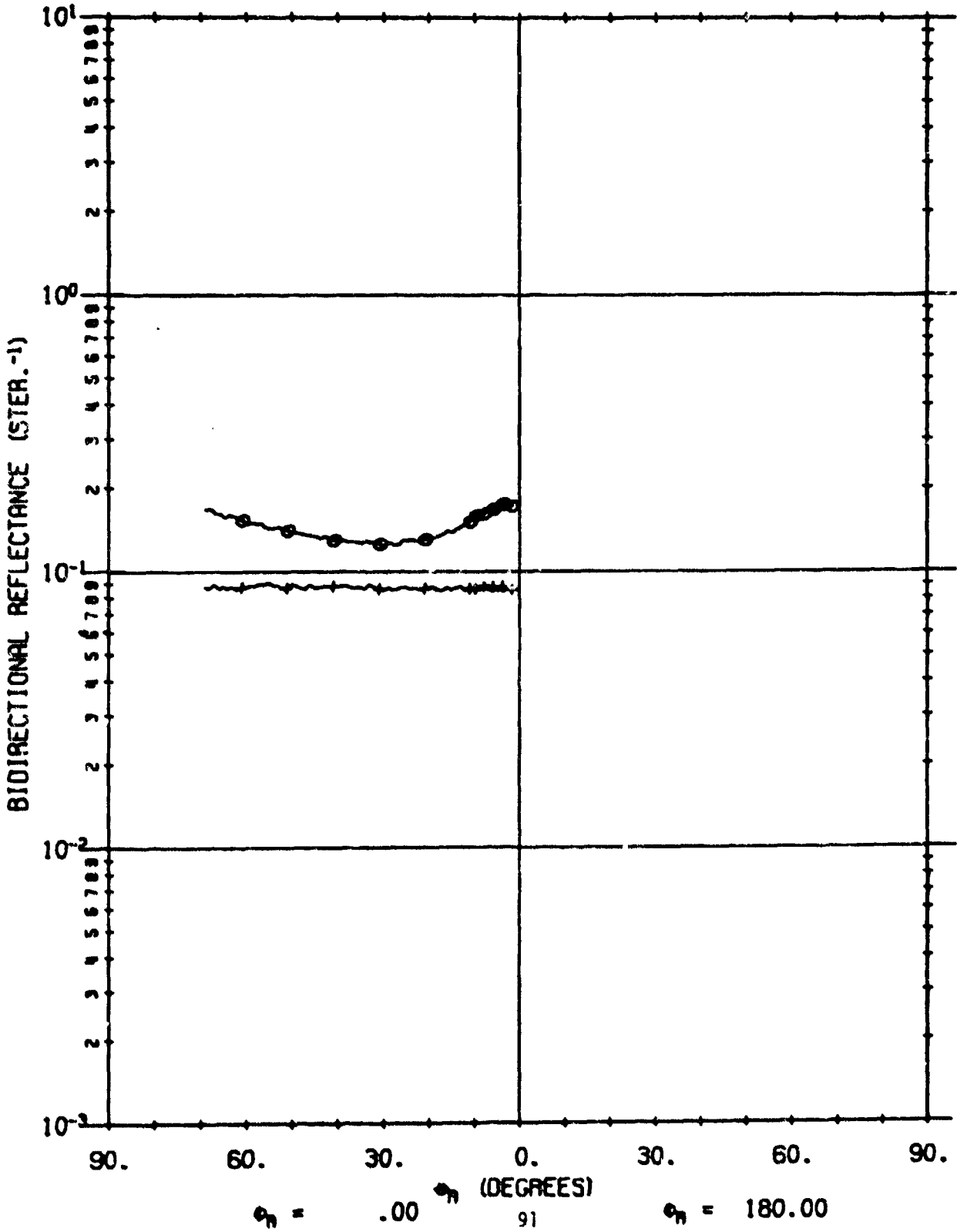

001610 102

λ = 1.06
$\phi_I = \phi_n^+$ +1.7
θ_I = .0

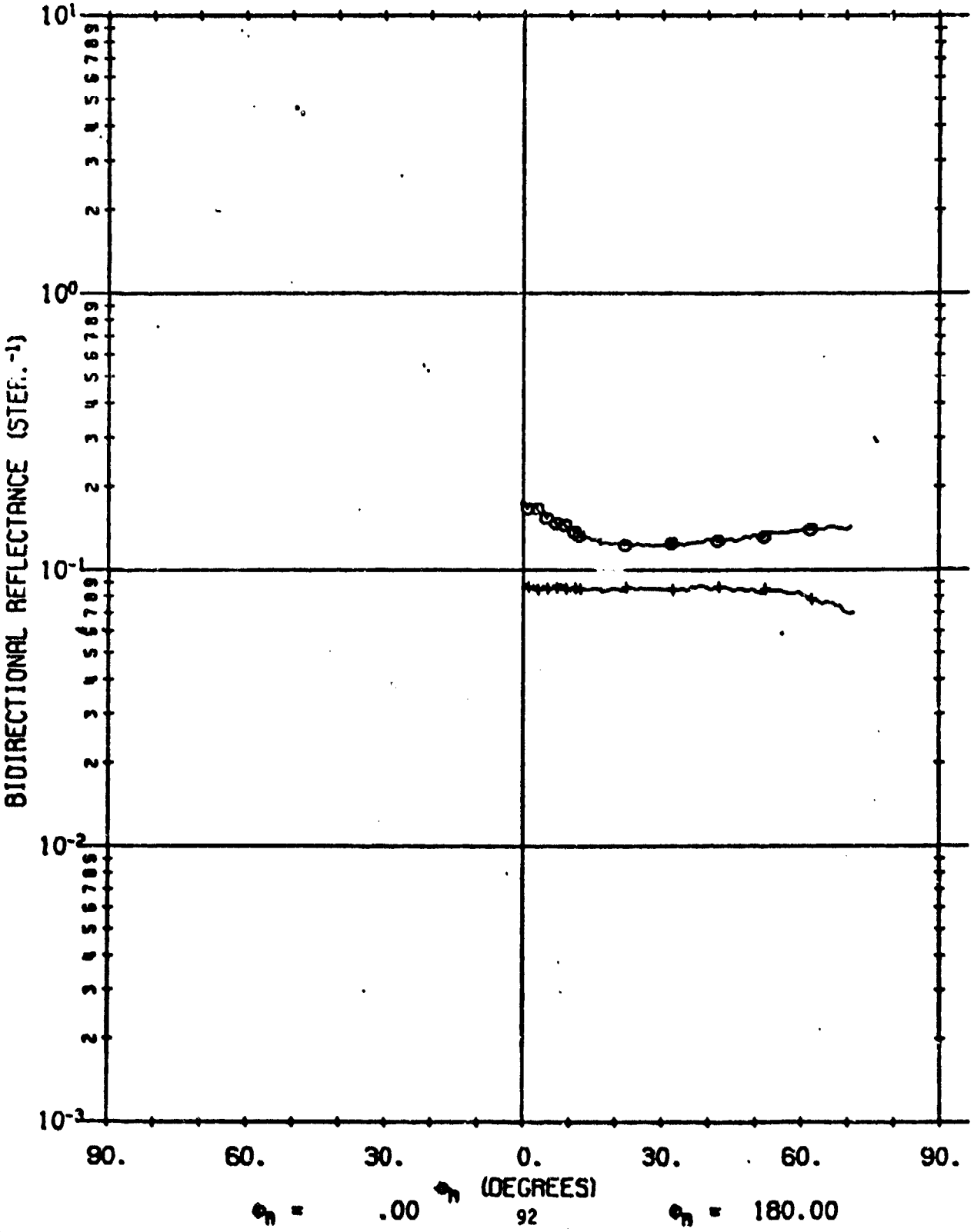

A01610 302

λ = 3.39
$\Phi_I = \Phi_R +$ 2.0
Φ_I = .0

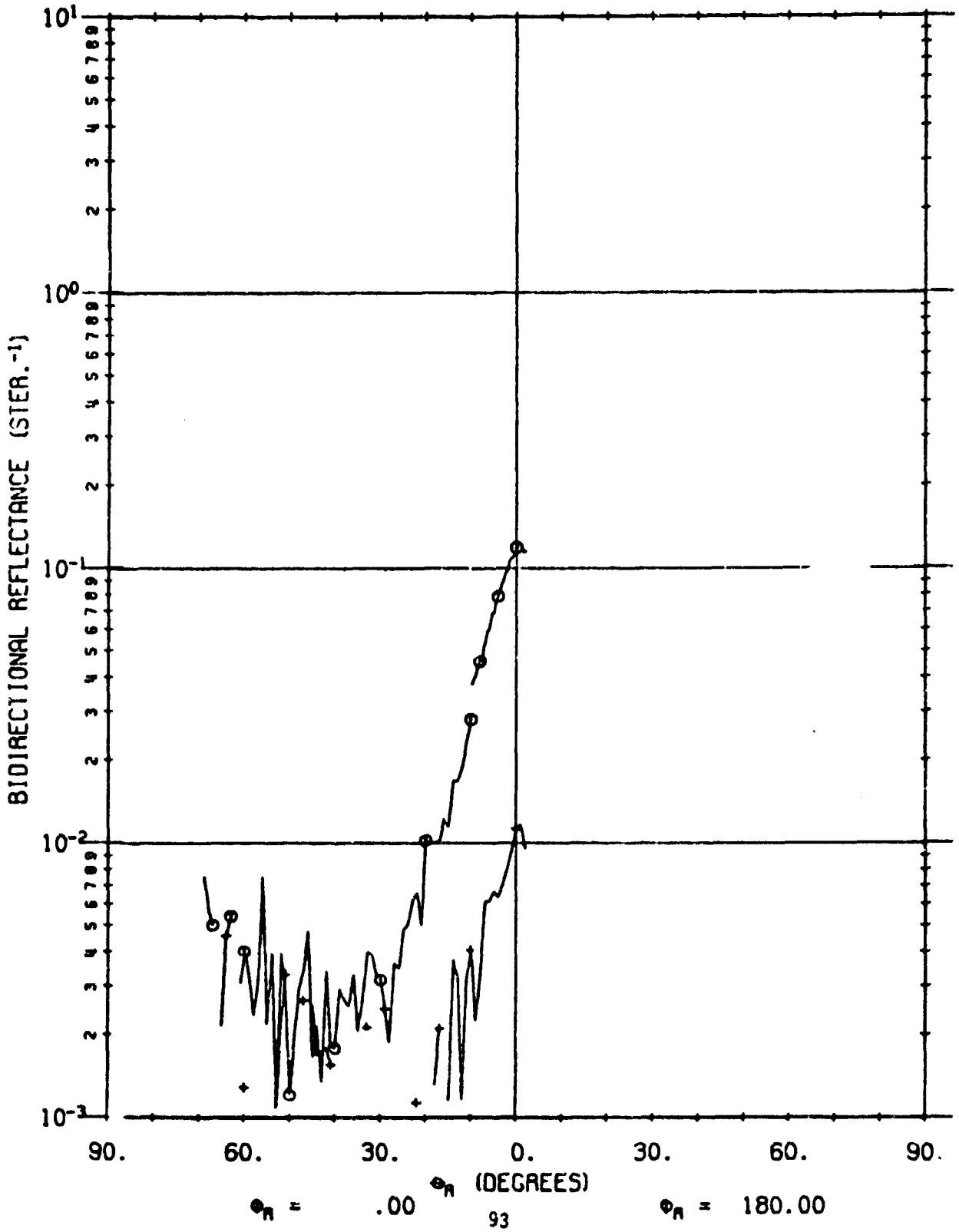

A01610 302

λ = 3.39
$\theta_I = \theta_n +$ -2.0
ϕ_I = 180.0

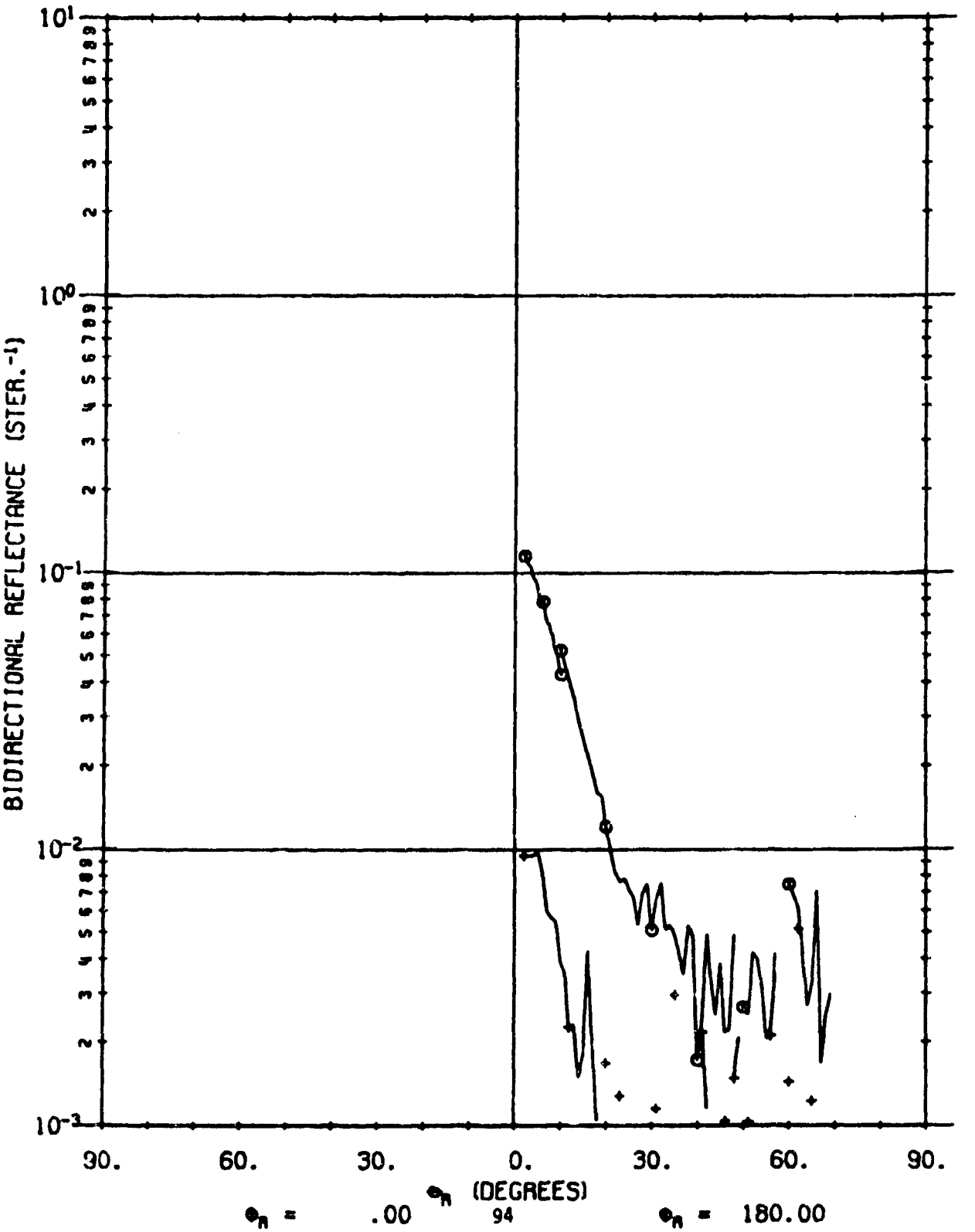

A01610 201

λ = 10.60
$\theta_I = \theta_R^+$ -2.5
ϕ_I = 90.0

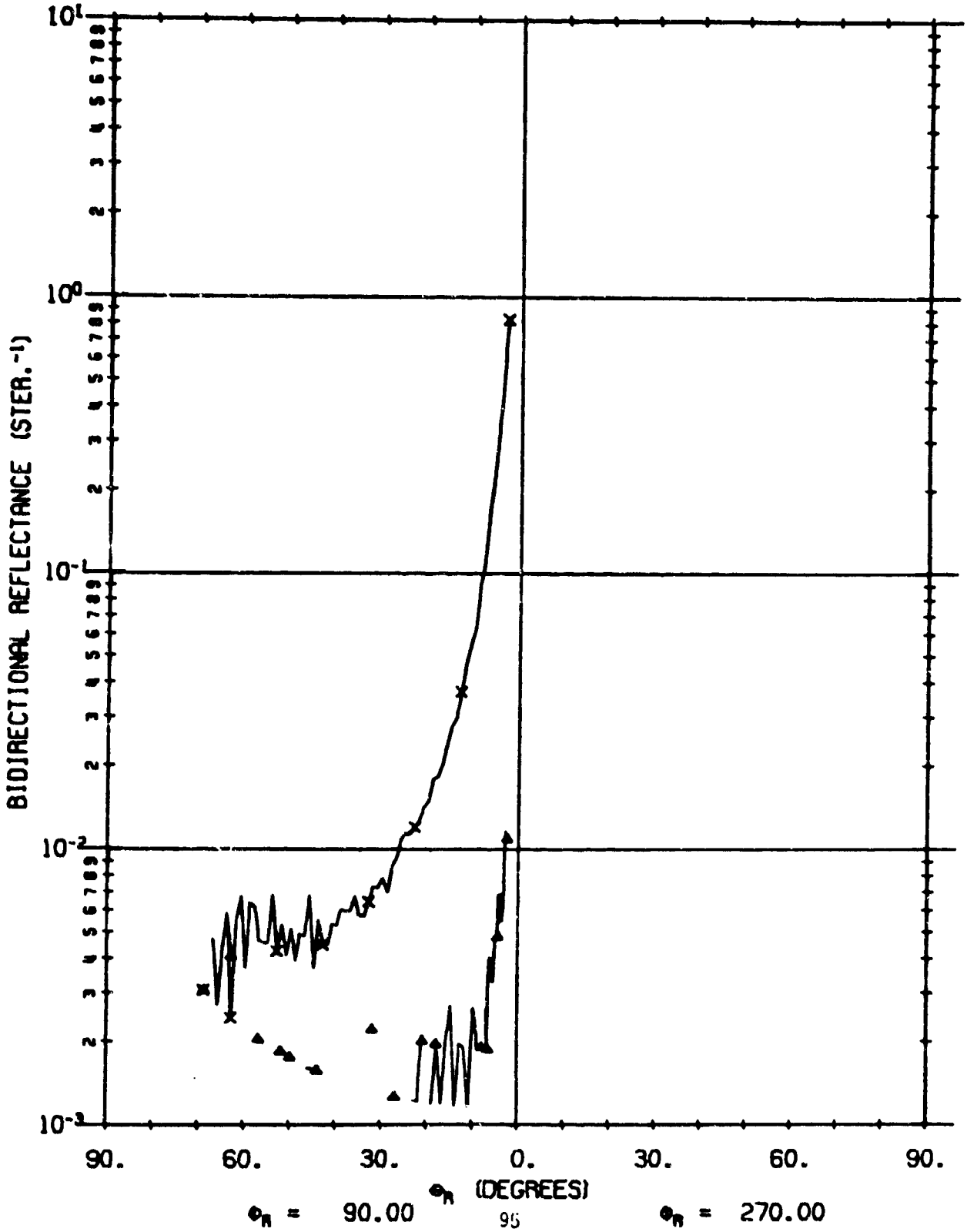

A01610 201

λ = 10.60
$\theta_I = \theta_n +$ 2.5
ϕ_I = 270.0

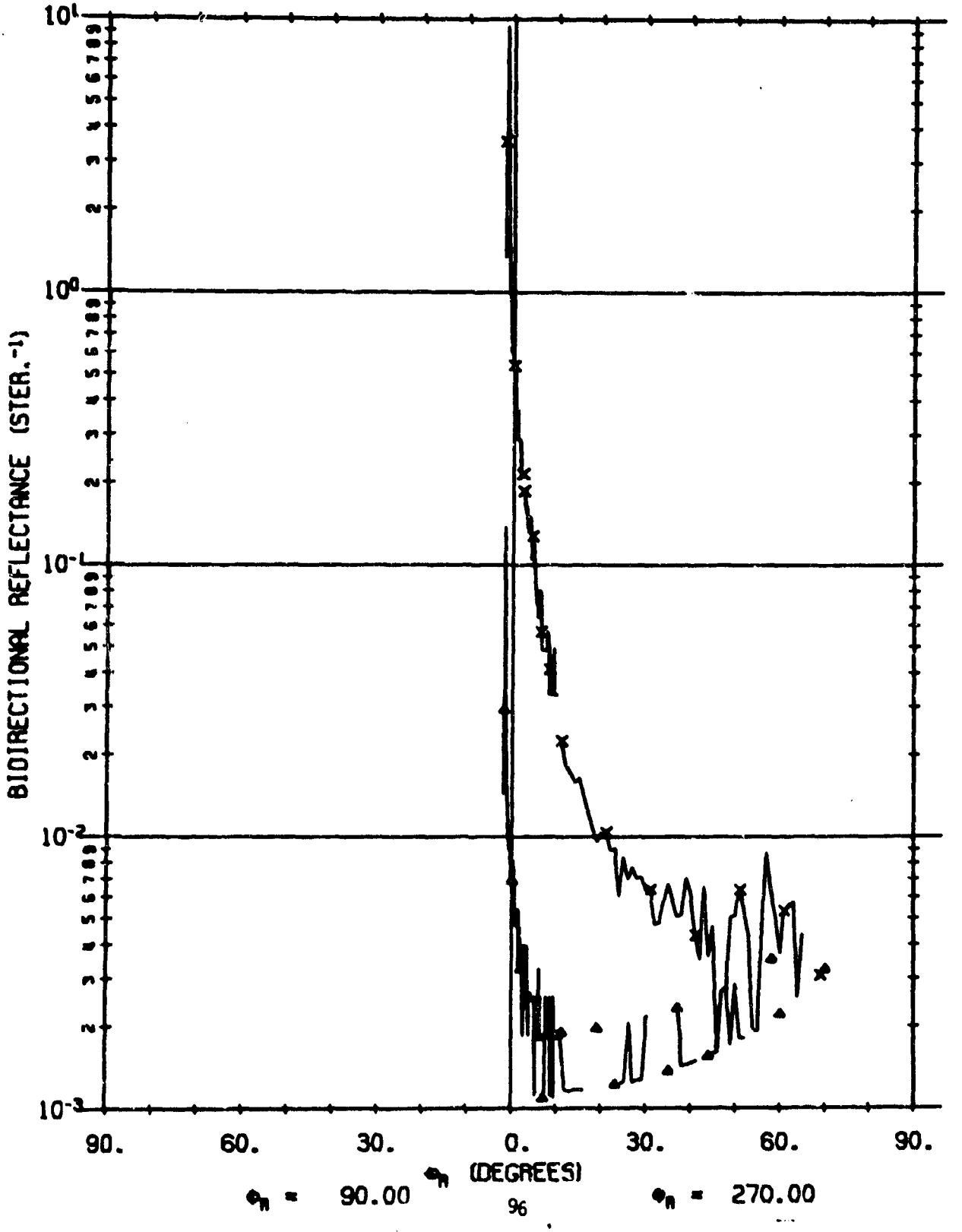

A02022 202

λ = .63
$\theta_i = \theta_R$ 1.7
φ_i = .0

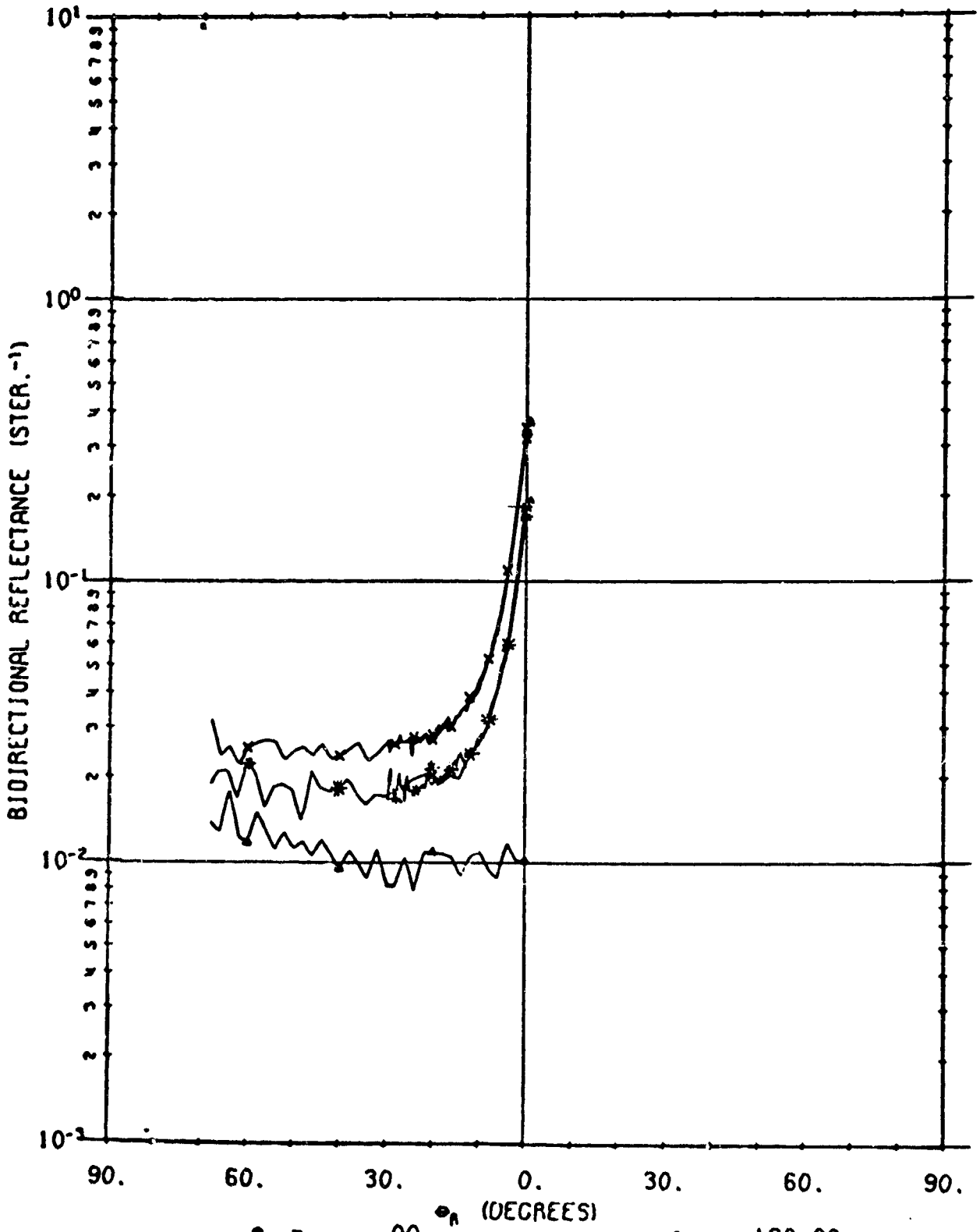

A02022 202

λ = .63
$\theta_I = \theta_R +$ -1.7
ϕ_I = 180.0

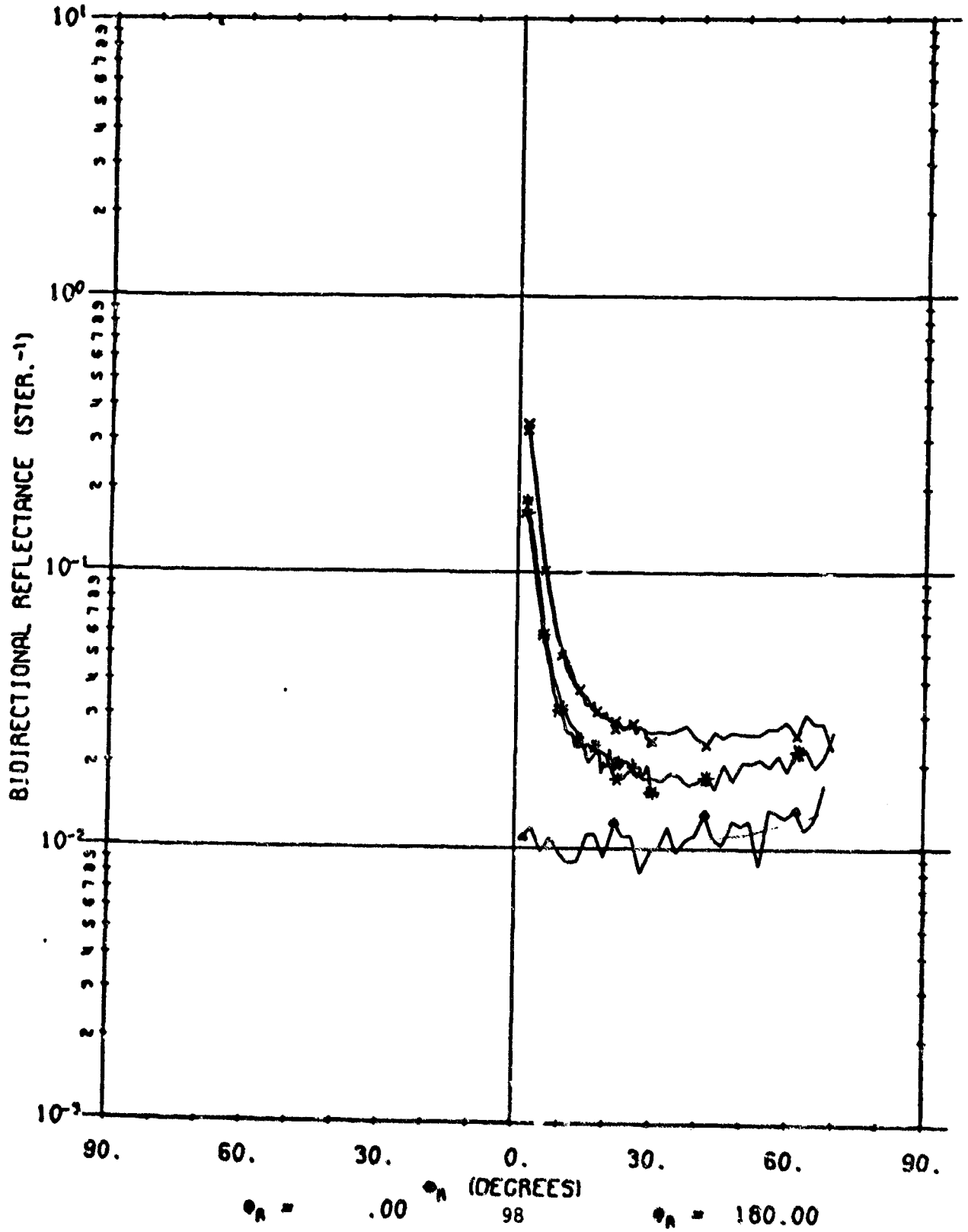

ϕ_R = .00 ϕ_R = 180.00

A02022 201

λ = 1.06
$\phi_1 = \phi_n^+$ 1.7
ϕ_1 = .0

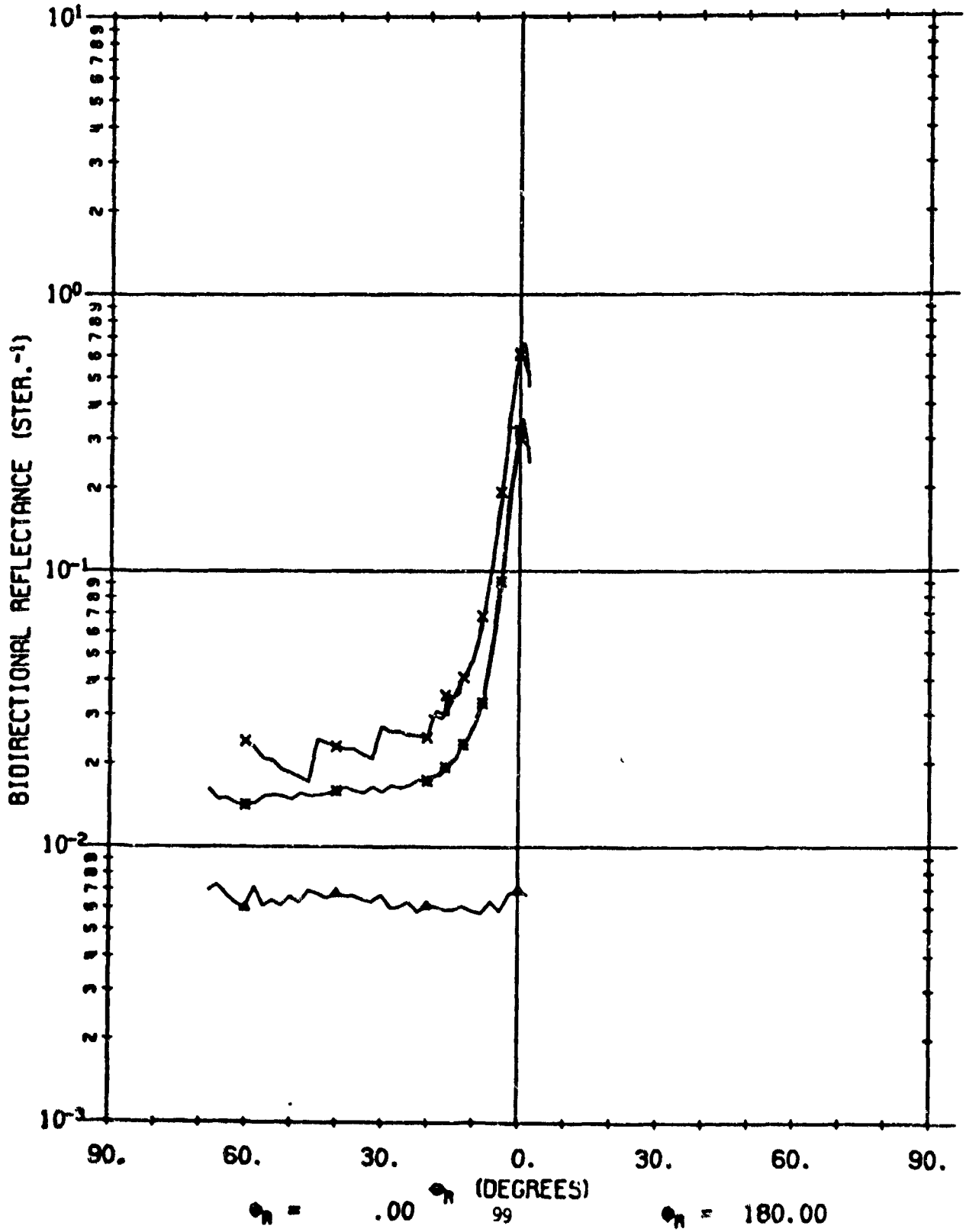

AD2022 201

λ = 1.06
$\theta_i = \theta_r +$ -1.0
ϕ_i = 180.0

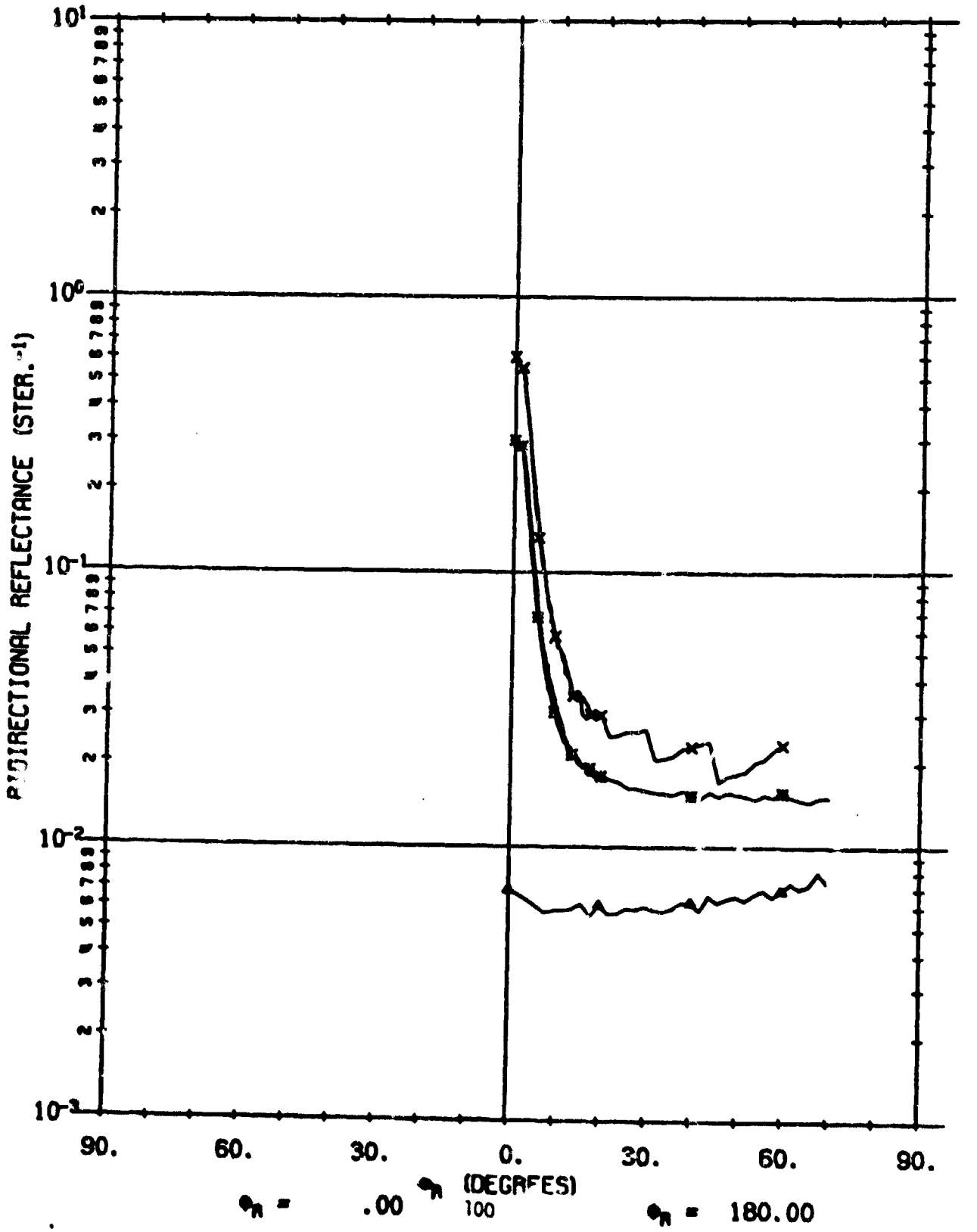

A02022 701

λ = 3.39
$\Phi_I = \Phi_R +$ 2.0
Φ_I = .0

81

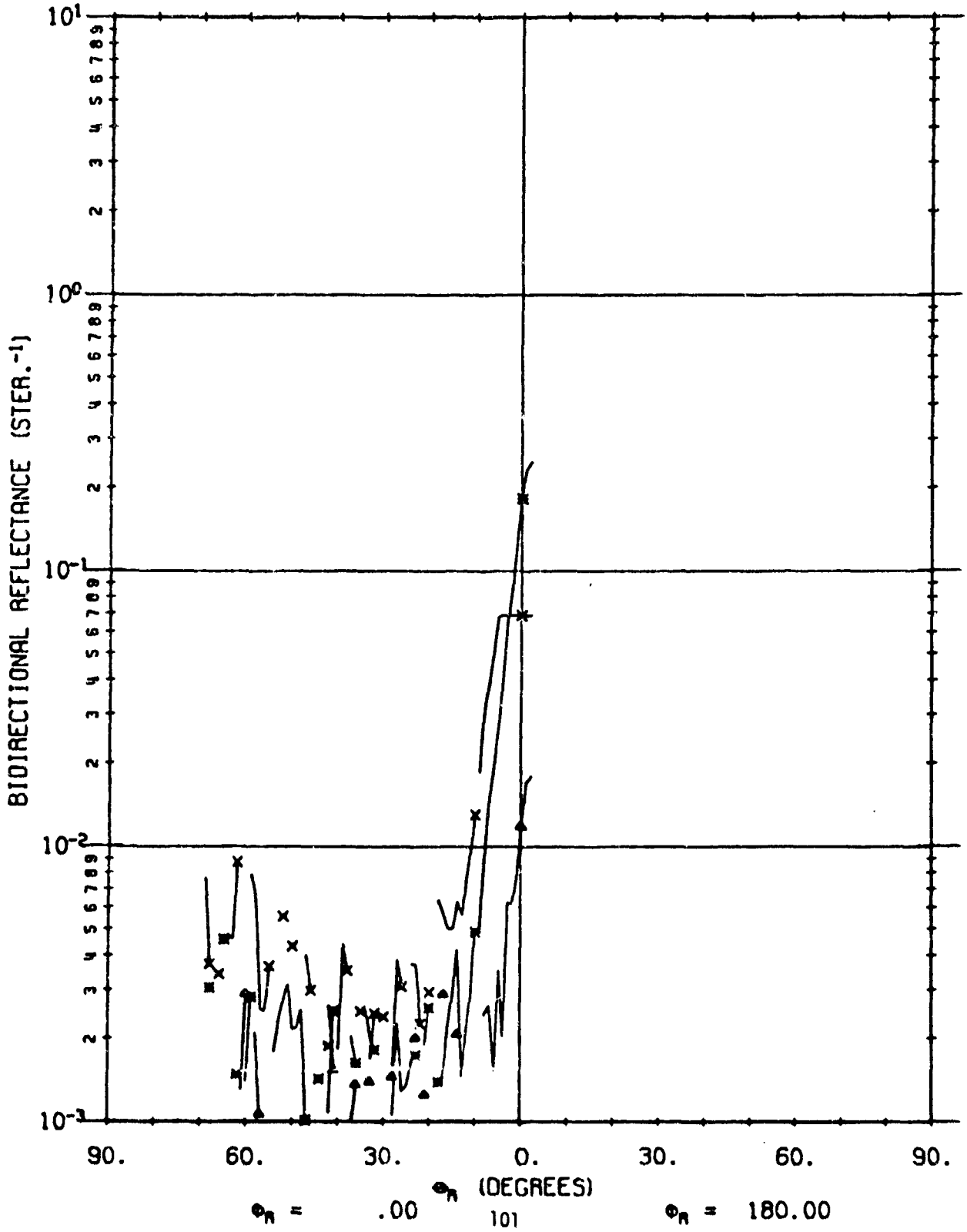

A02022 701

λ = 3.39
$\phi_I = \phi_n +$ -2.0
ϕ_I = 180.0

83

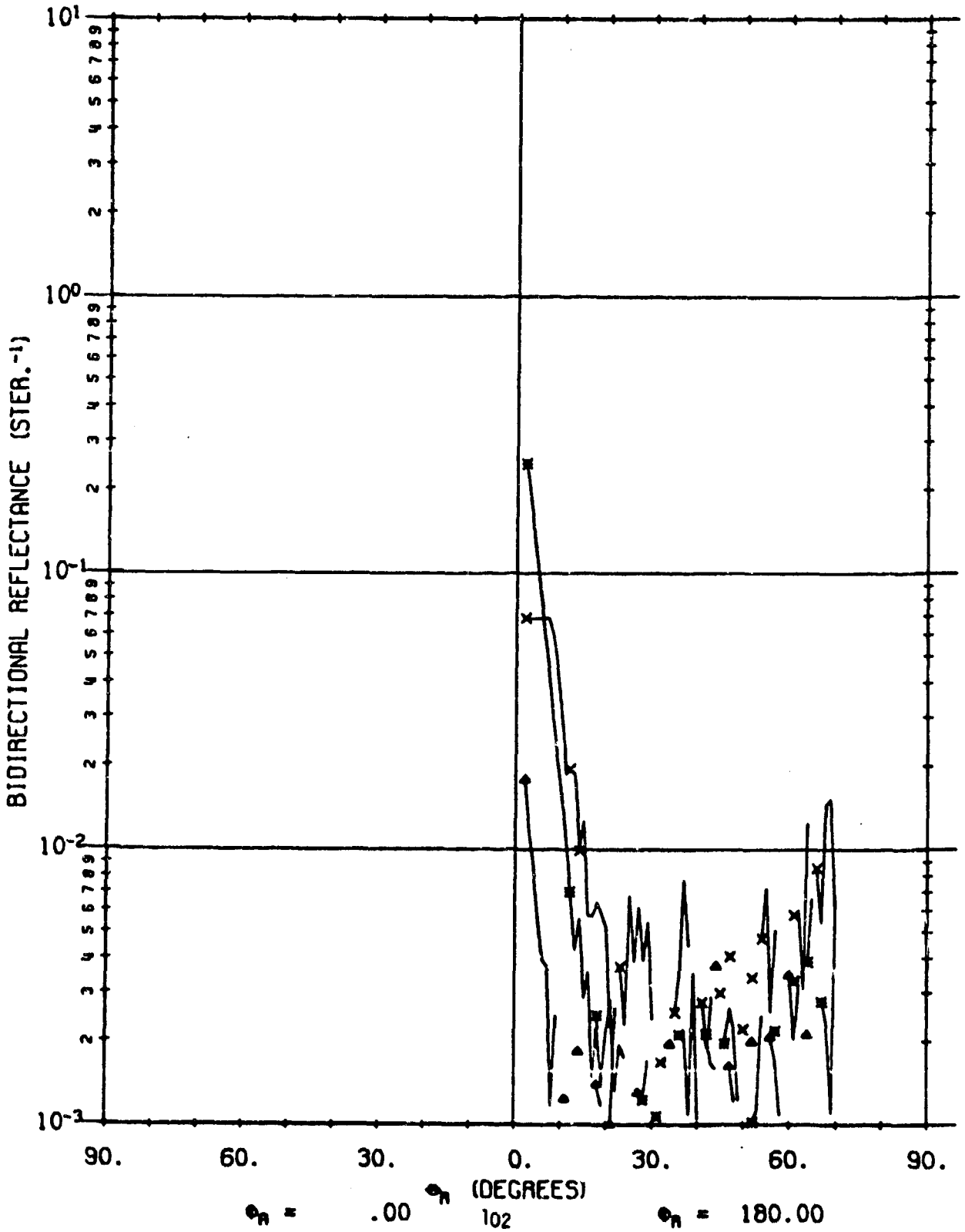

A02022 604

λ = 10.60
$\phi_r = \phi_n +$ 2.5
ϕ_i = .0

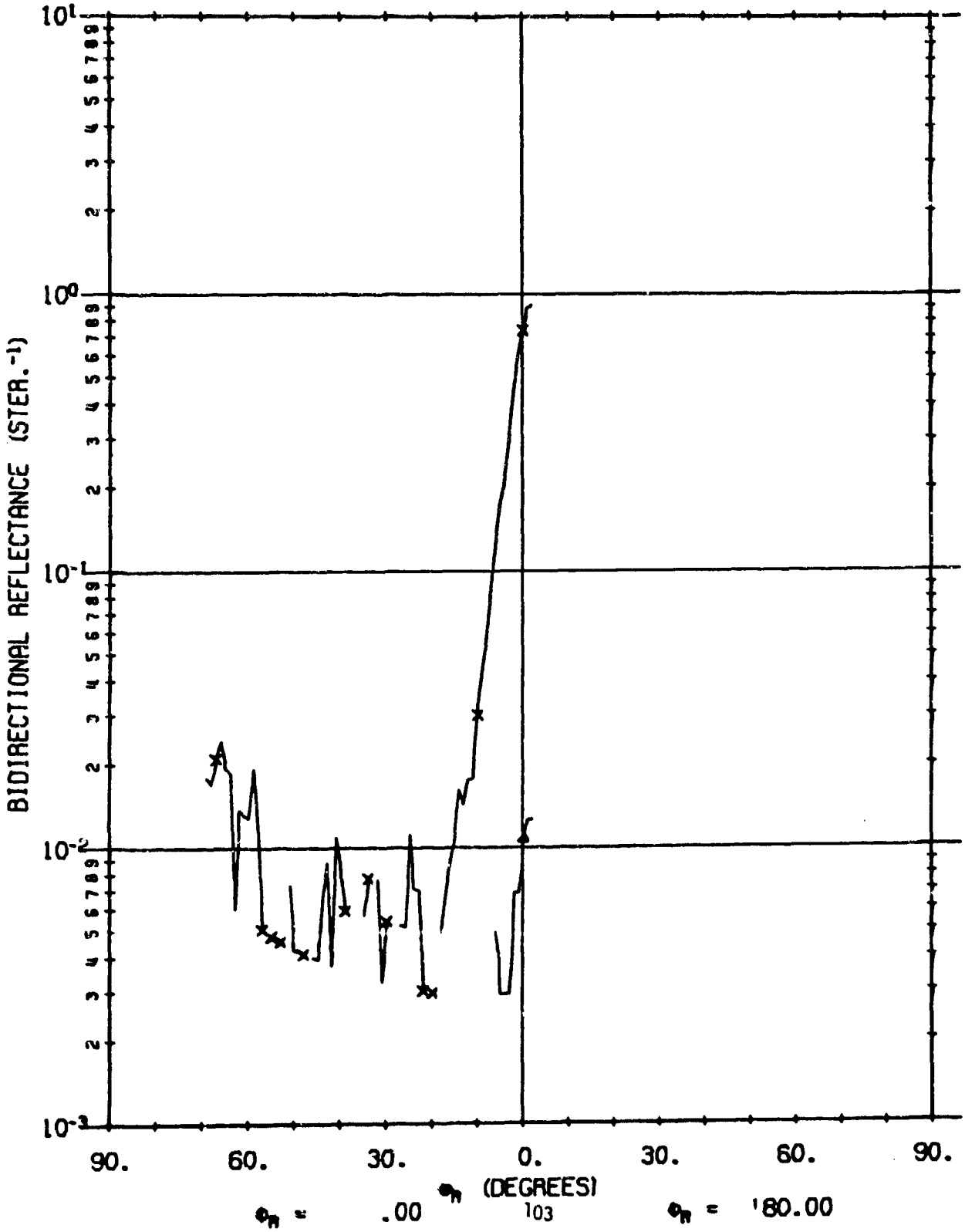

A02022 604

λ = 10.60
$\theta_I = \theta_n + -2.5$
ϕ_I = 180.0

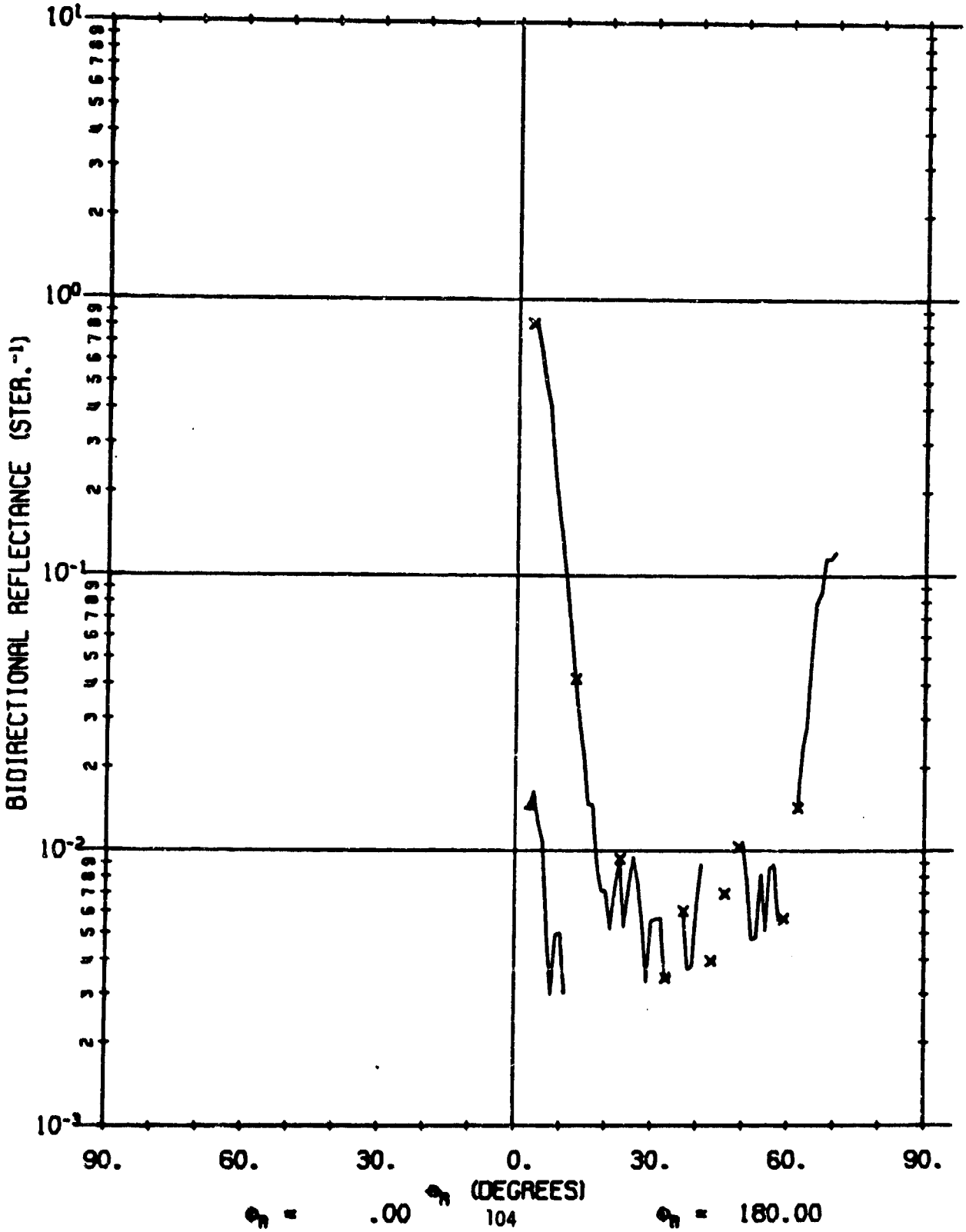

A02022 703

λ = 3.39
$\Theta_I = \Theta_R +$ 2.0
Φ_I = .0

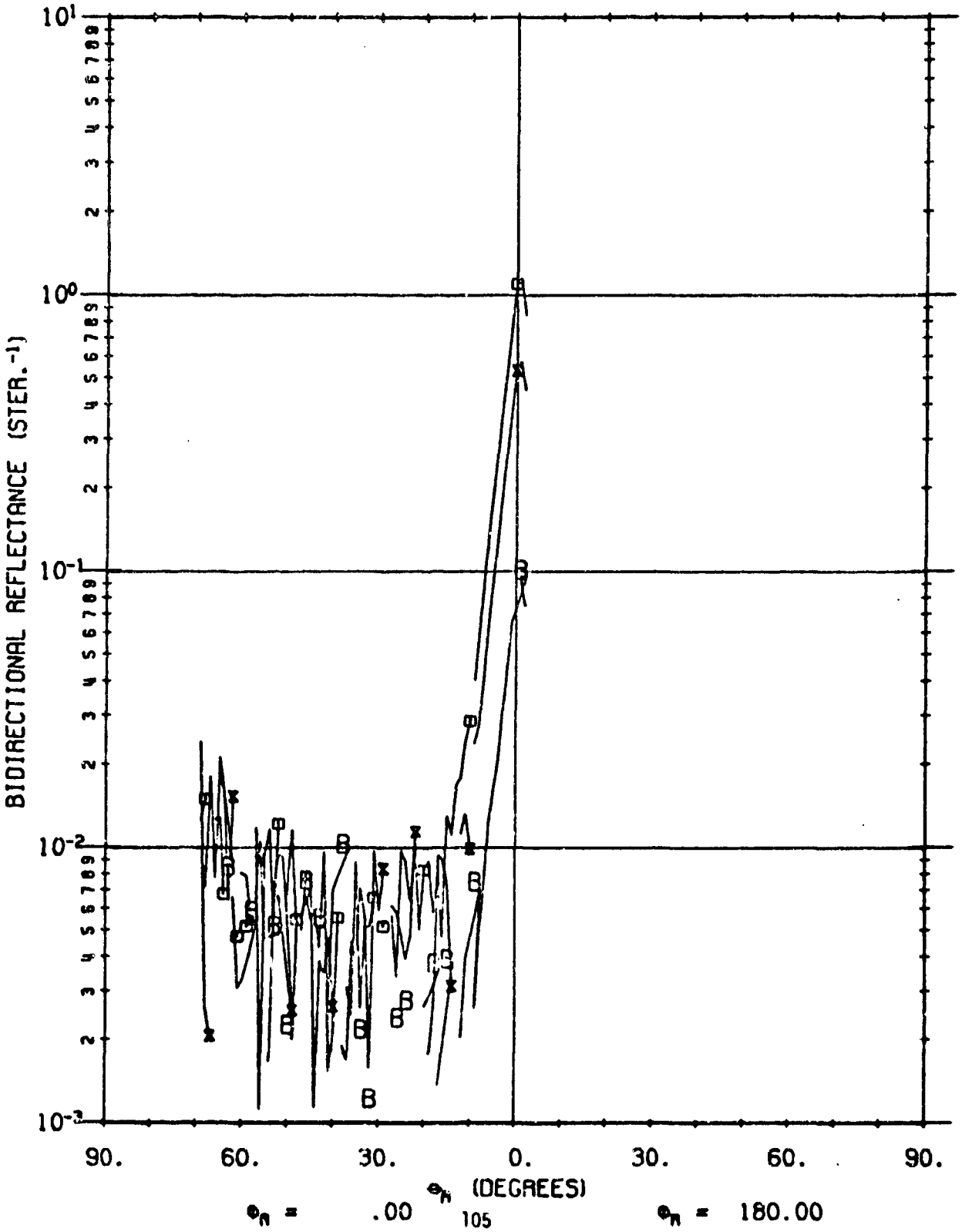

A02022 703

λ = 3.39
$\theta_I = \theta_n +$ -2.0
ϕ_I = 180.0

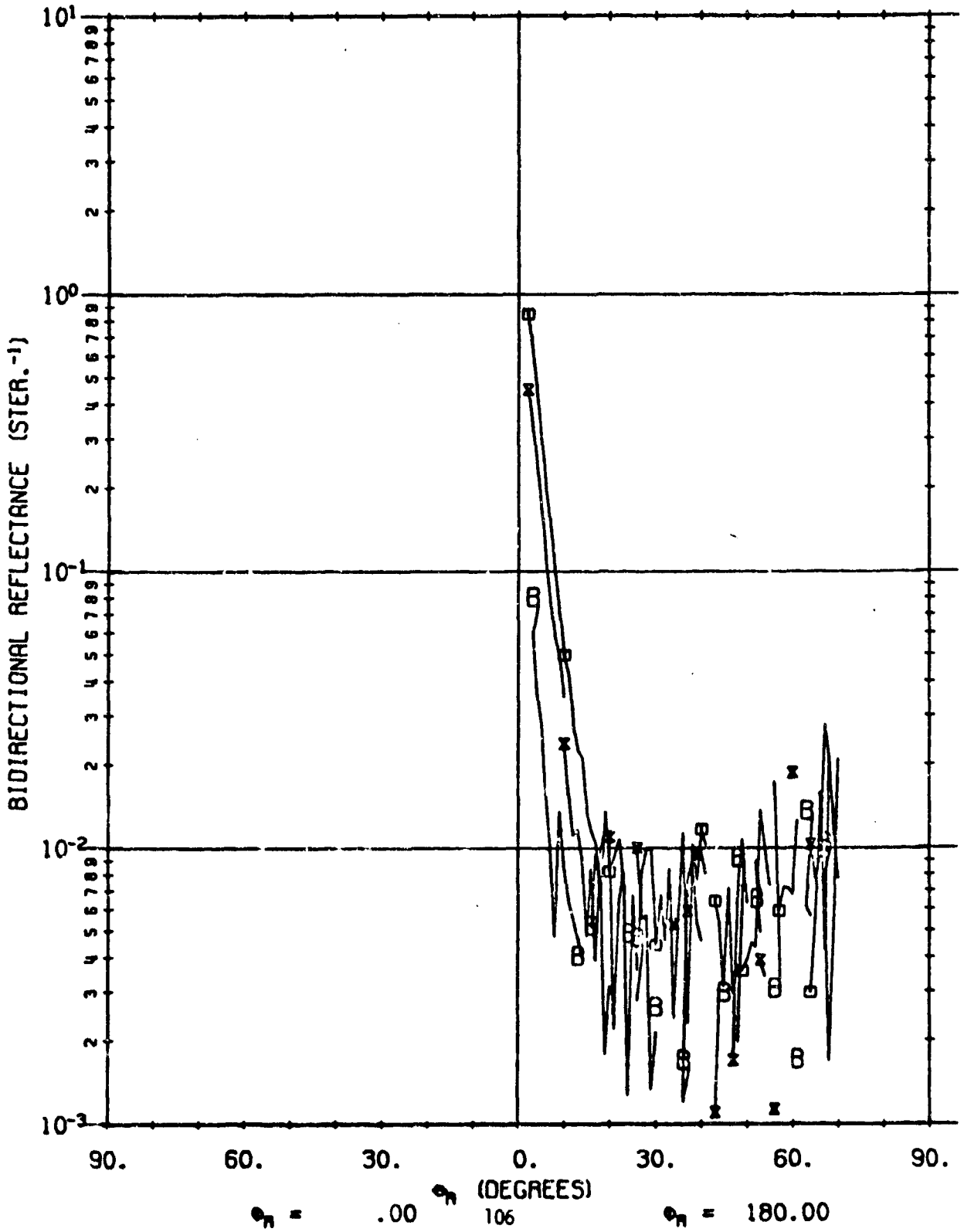

A02022 603

λ = 10.60
$\Phi_I = \Phi_R +$ 2.5
Φ_I = .0

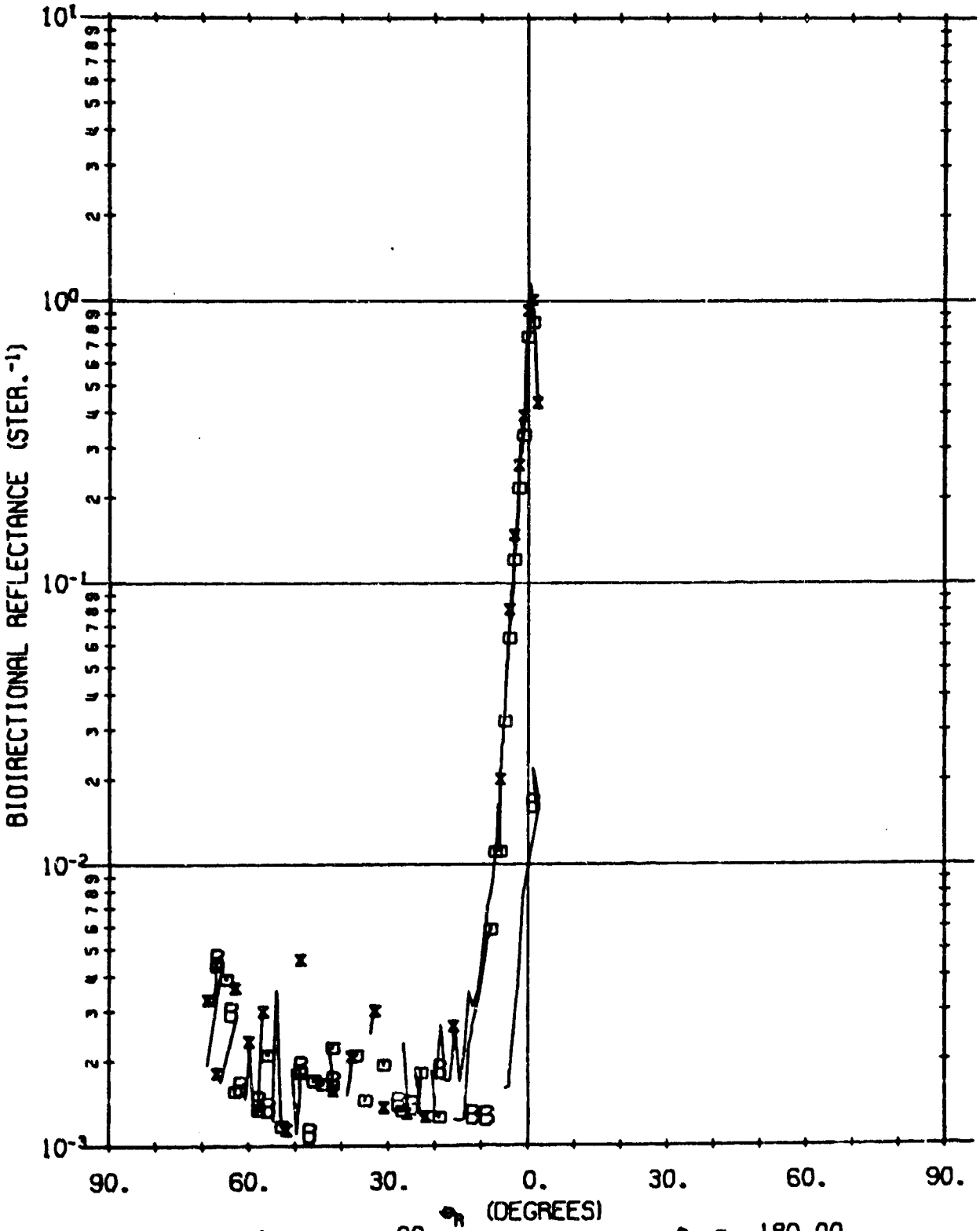

Φ_R = .00 Φ_R = 180.00

.02022 603

λ = 10.60
ϕ_i = ϕ_n + -2.5
ϕ_i = 180.0

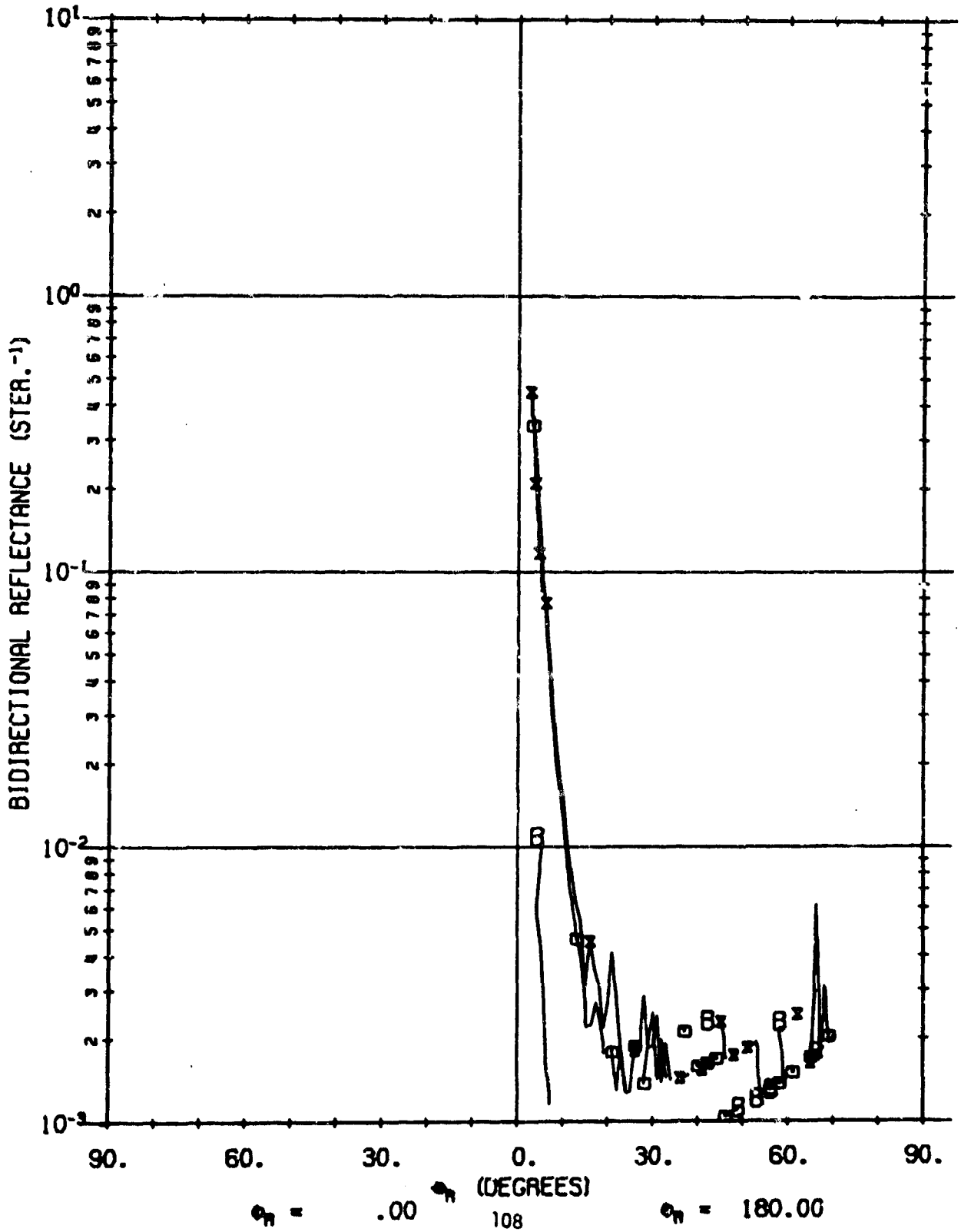

A02022 202

λ = .63
θ_i = θ_n + -1.7
ϕ_i = 180.0

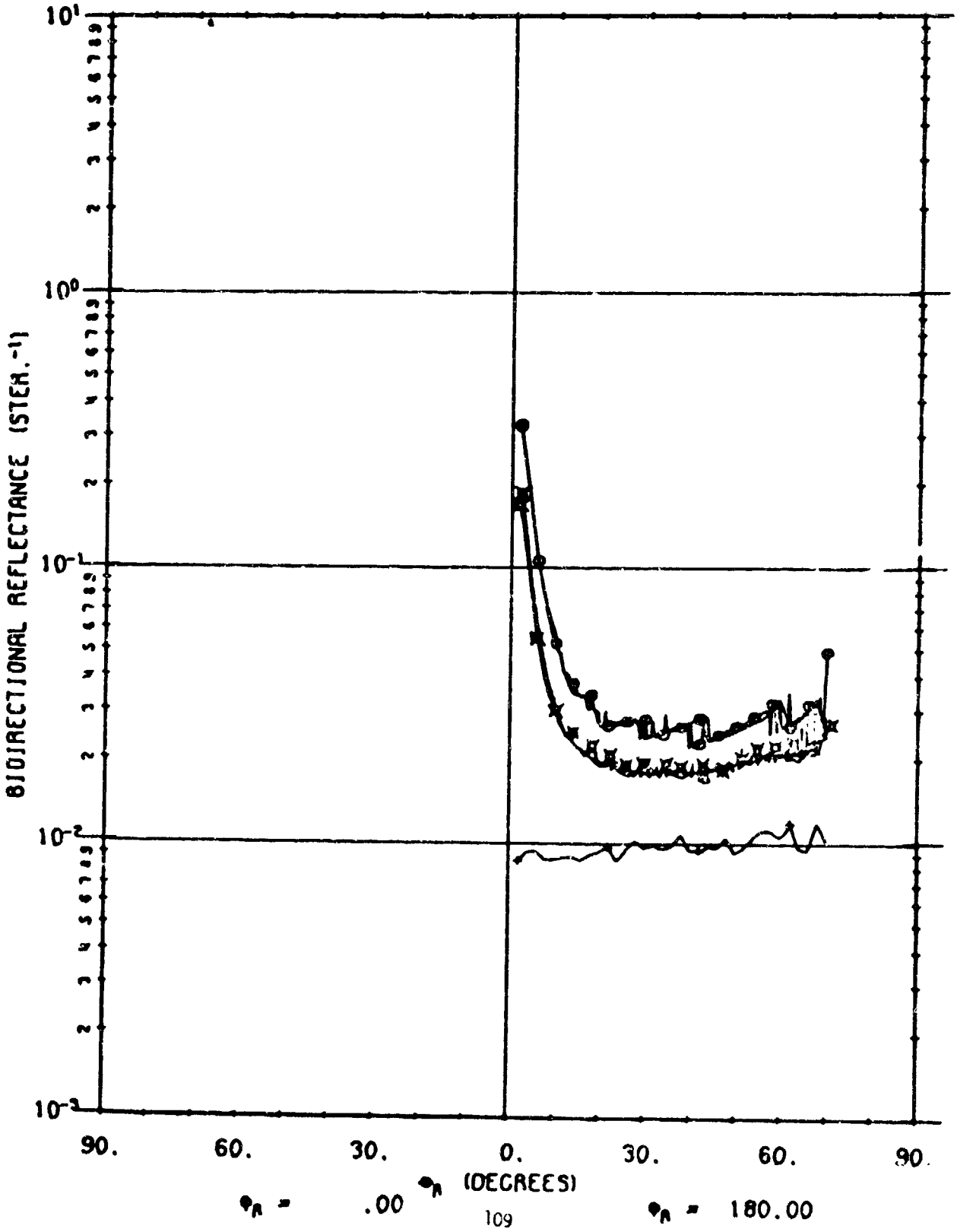

A02022 202

λ = .63

$\theta_I = \theta_n$ 1.7

ϕ_I = .0

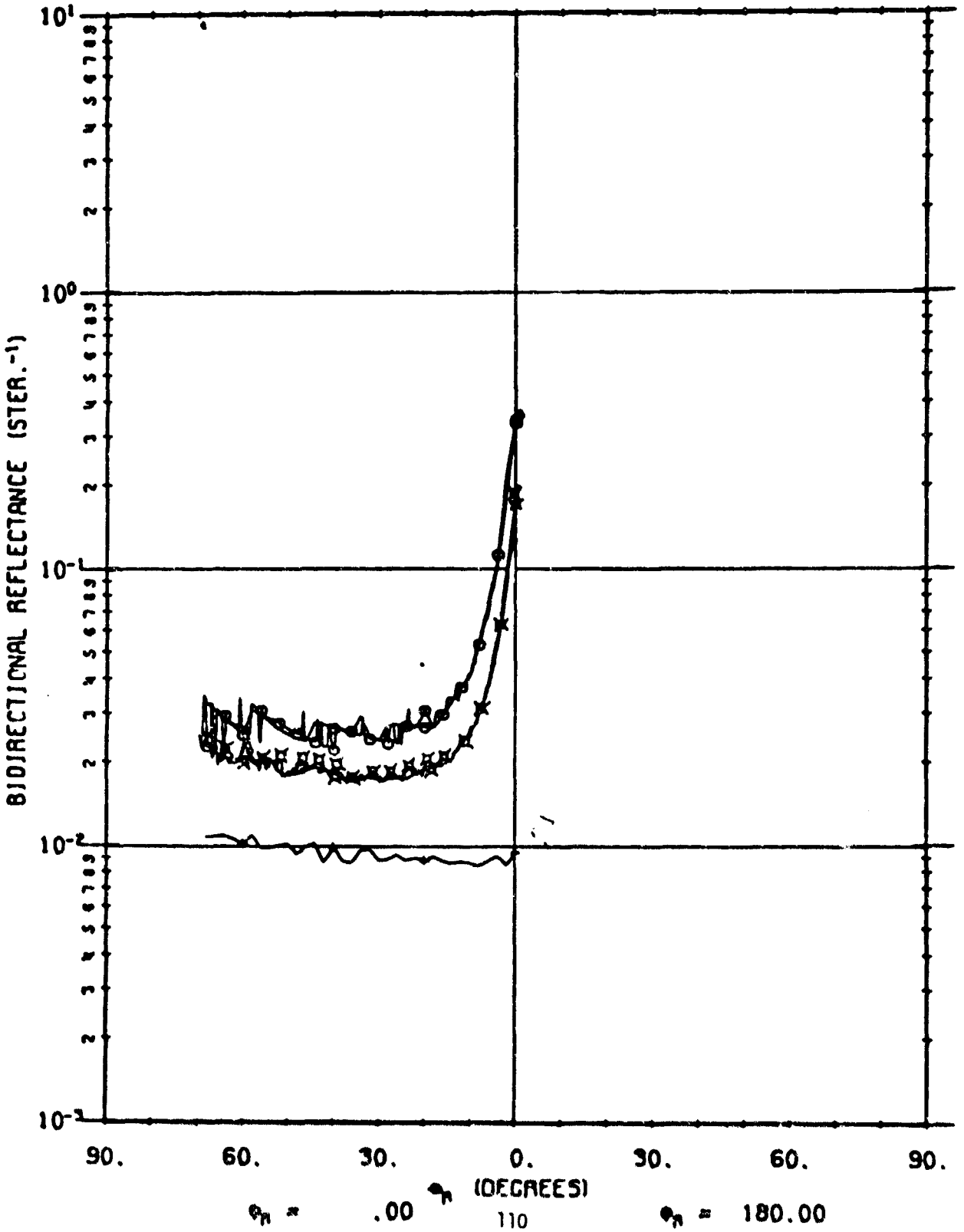

A02022 201

λ = 1.06

$\theta_I = \theta_R$ + 1.7

ϕ_I = .0

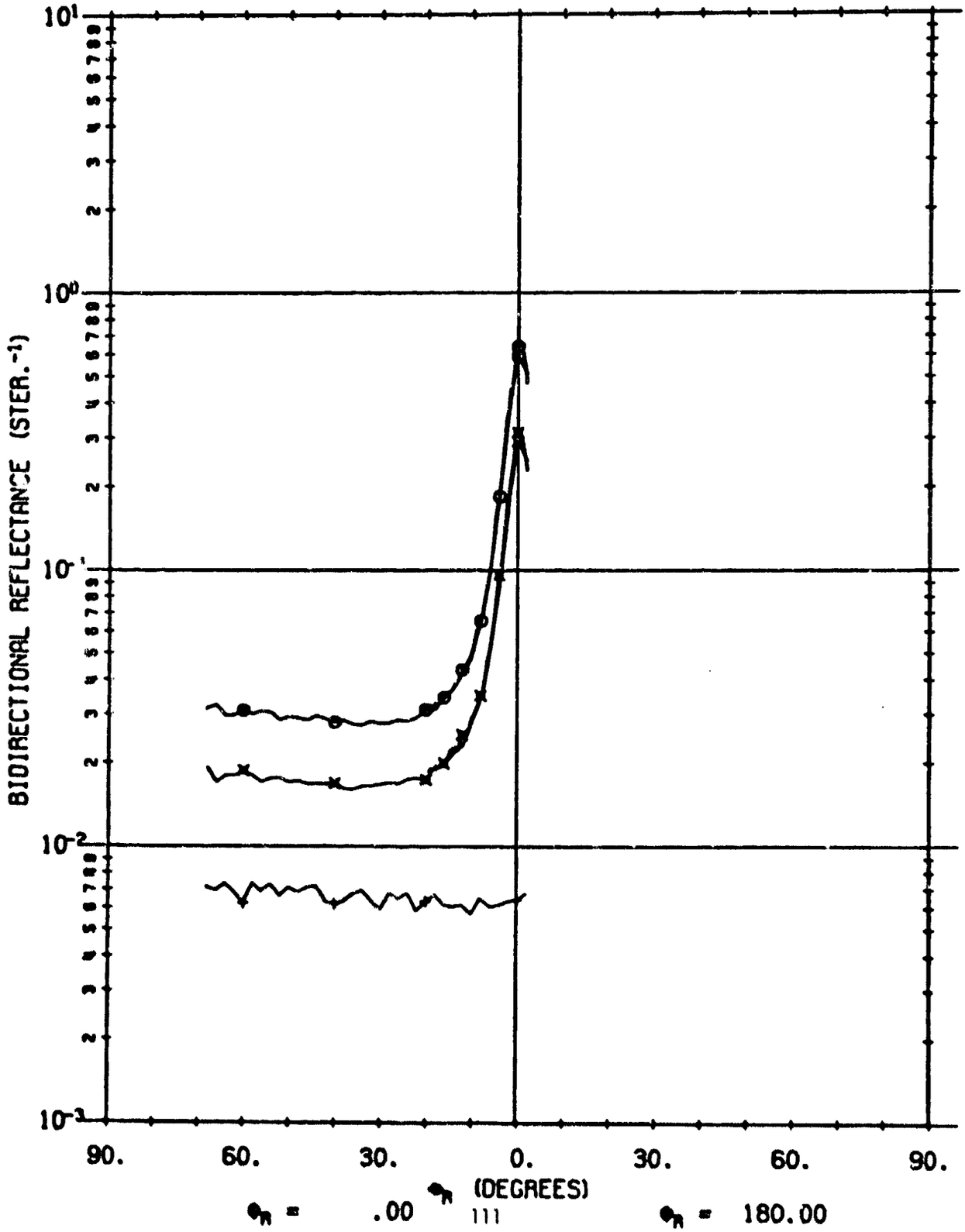

A02022 201

λ = 1.06
$\theta_i = \theta_n$ + -1.0
ϕ_i = 180.0

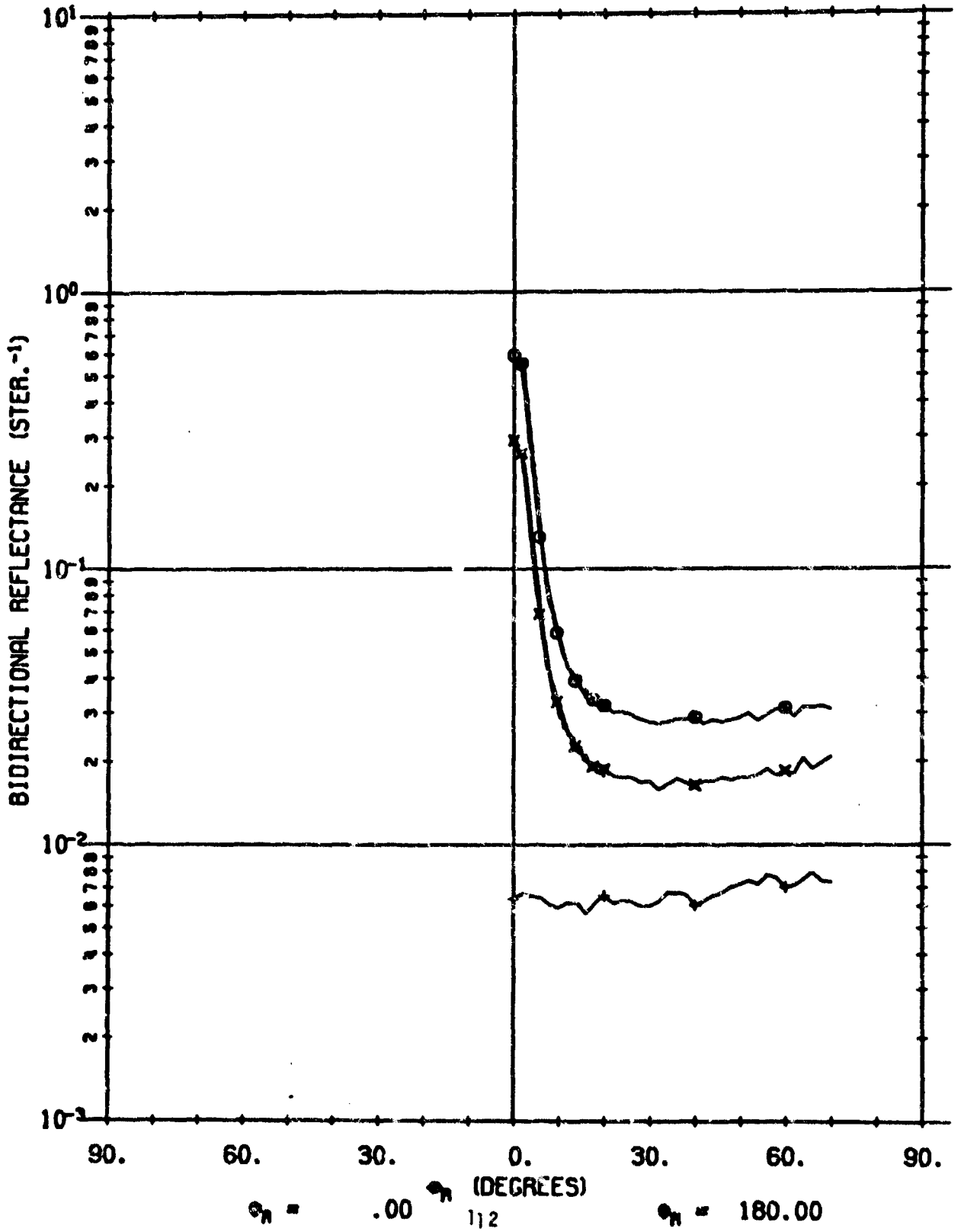

A02022 702

λ = 3.39
$\phi_I = \phi_n +$ 2.0
θ_I = .0

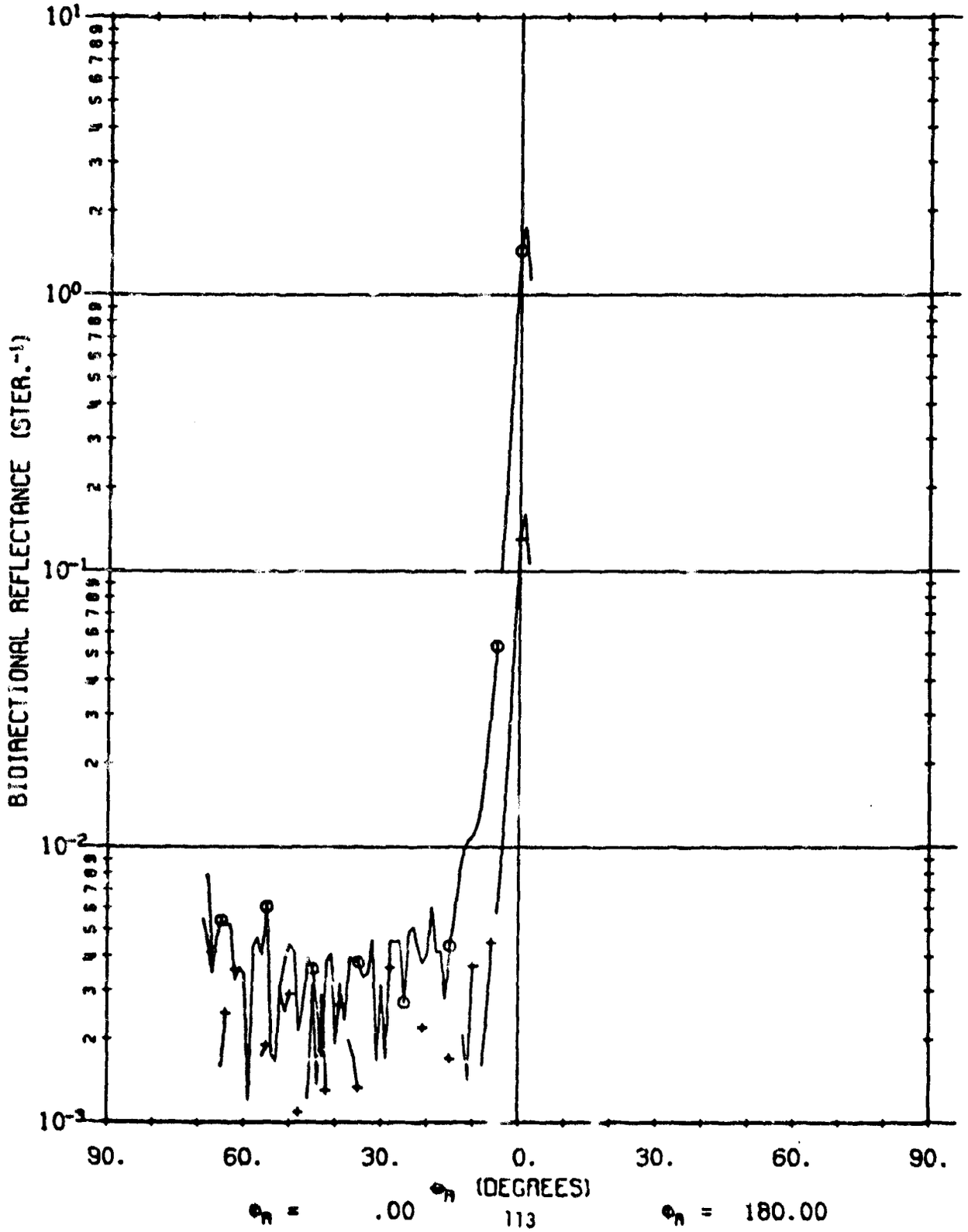

A02022 702

λ = 3.39
$\theta_1 = \theta_n +$ -2.0
ϕ_1 = 180.0

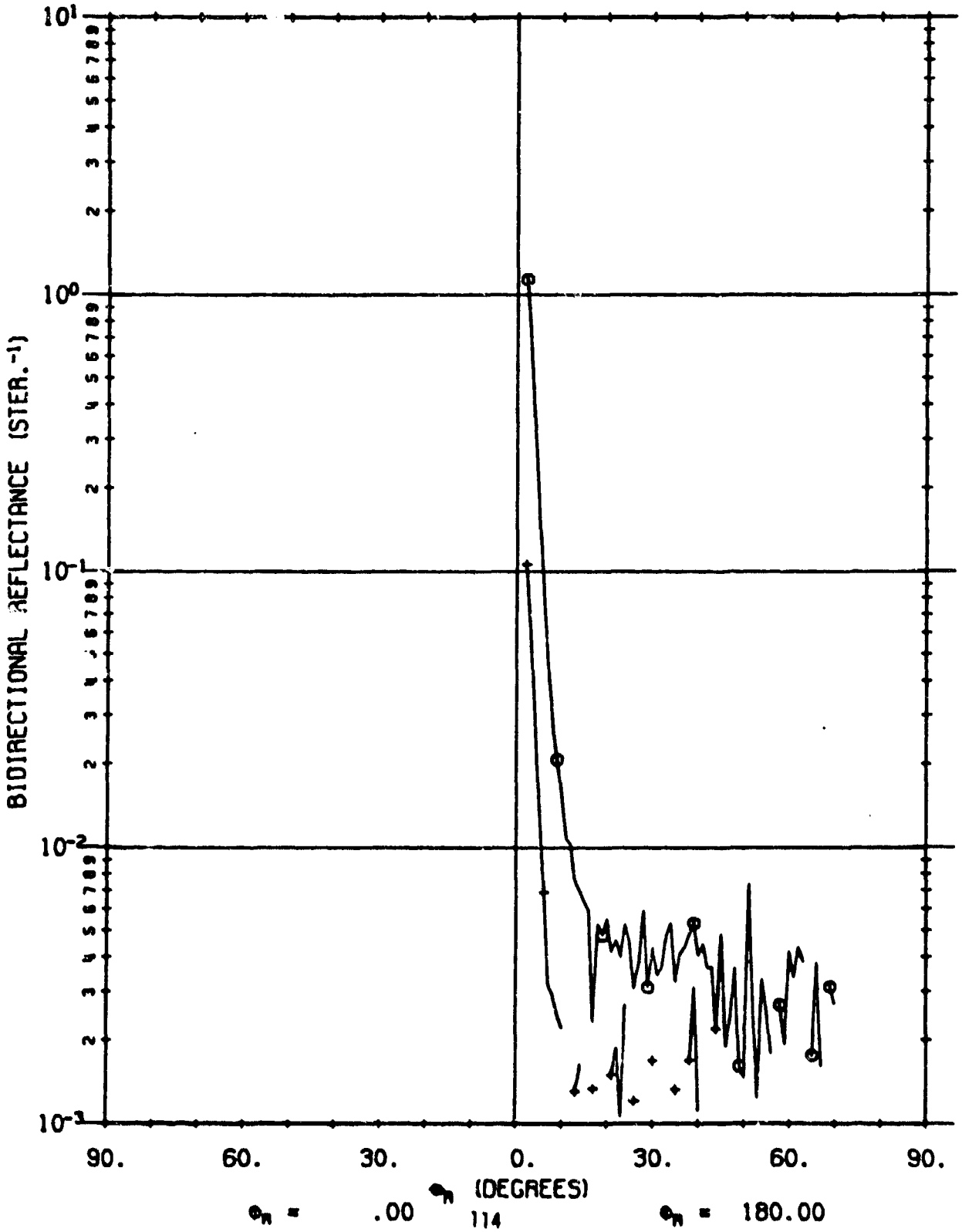

A02022 602

λ = 10.60
$\phi_I = \phi_R + -2.5$
ϕ_I = 180.0

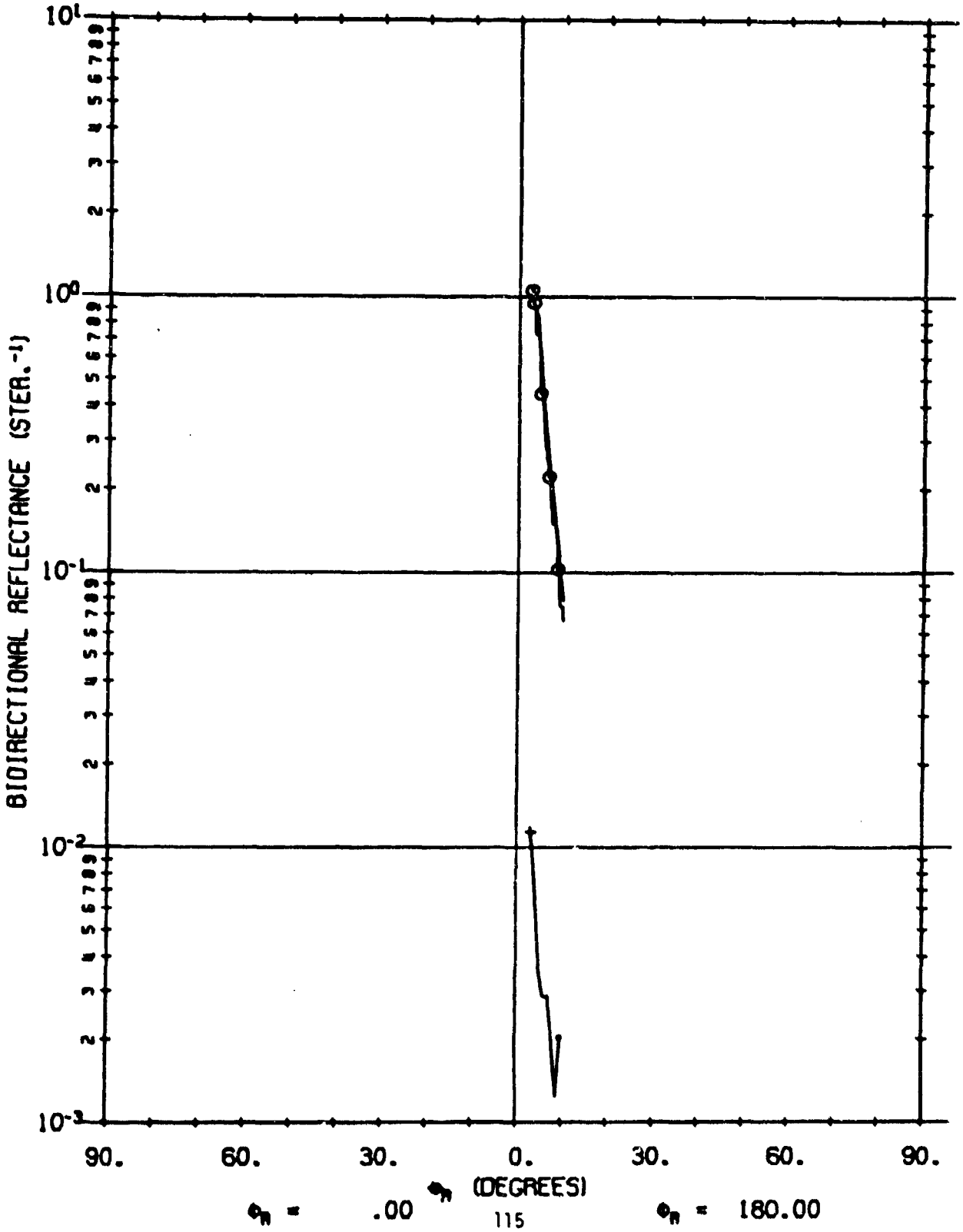

A02022 602

λ = 10.60
$\theta_I = \theta_n +$ 2.5
ϕ_I = .0

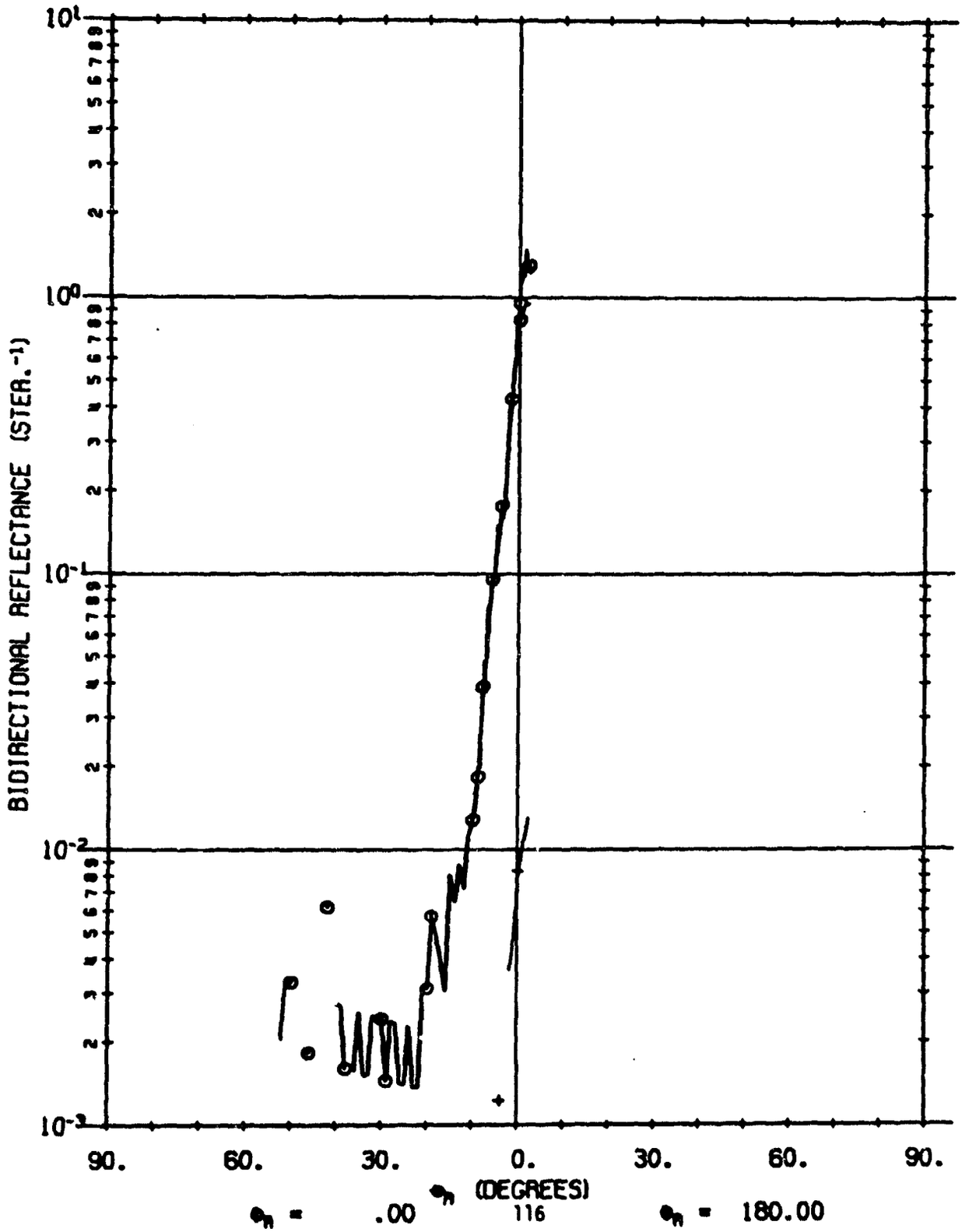

A02022 602

λ = 10.60
$\phi_r = \phi_n +$ -2.5
ϕ_i = 90.0

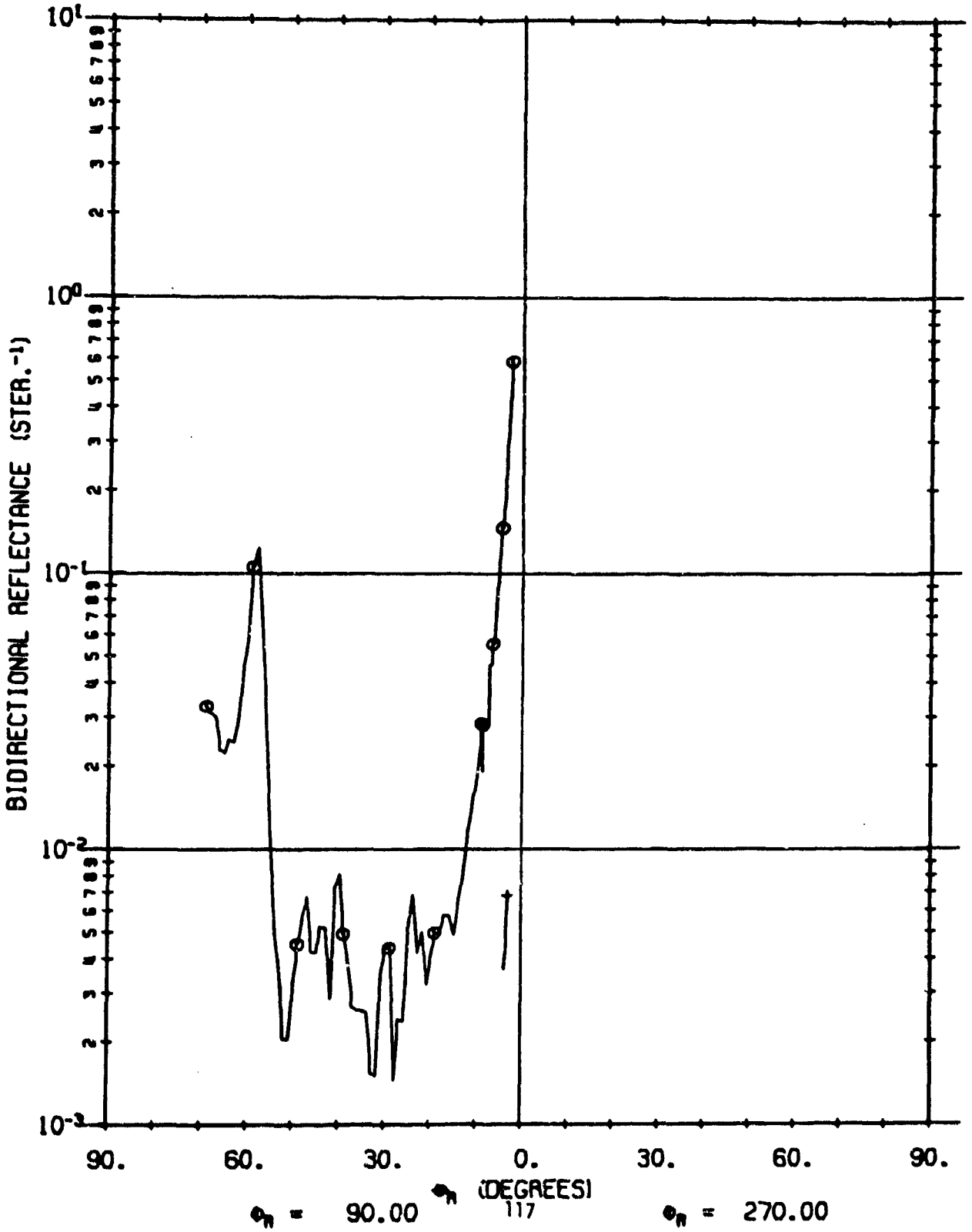

A02022 602

λ = 10.60
$\theta_r = \theta_n + 2.5$
θ_i = 270.0

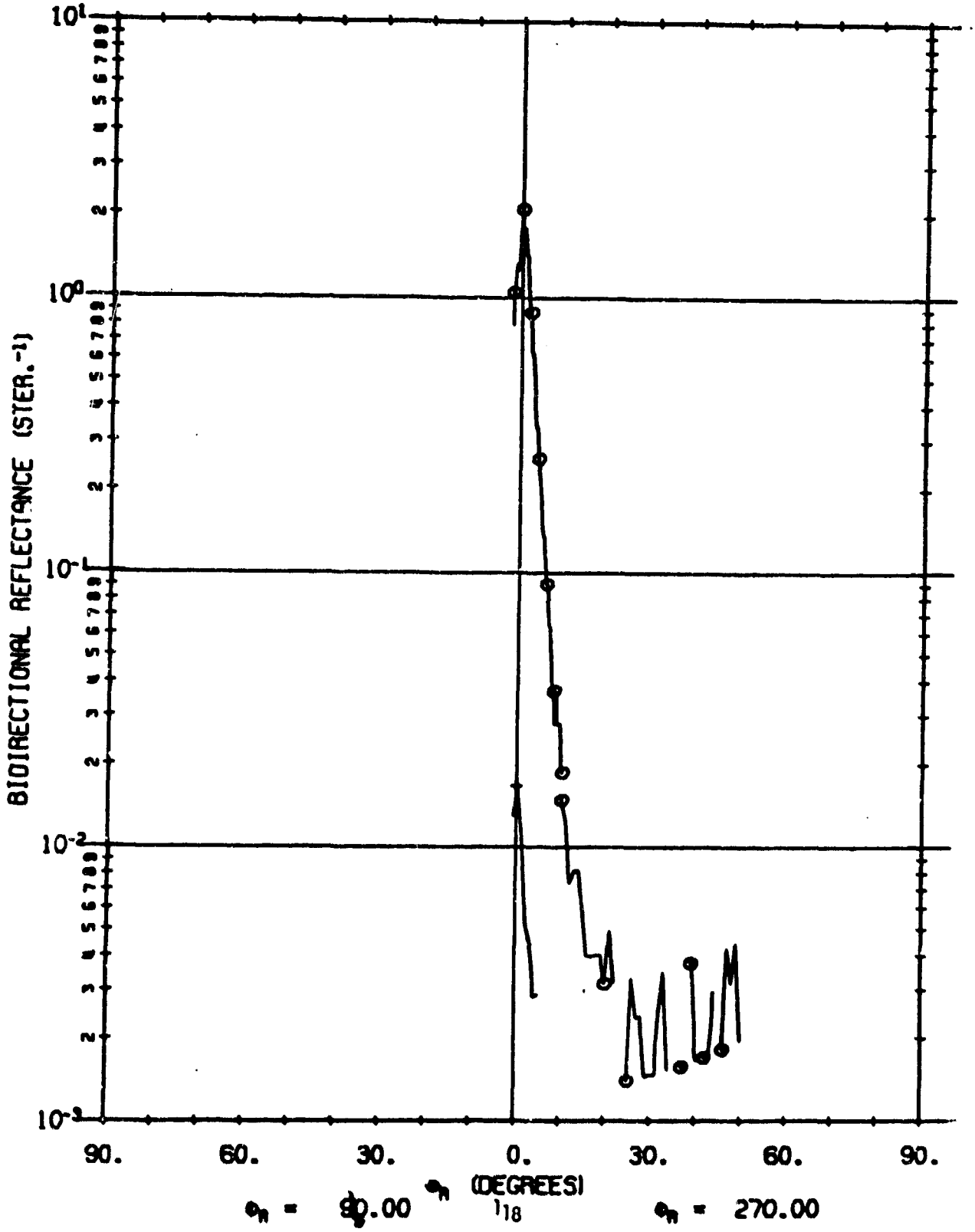

A01610 101

λ = .63
θ_I = .0
ϕ_I = 180.0

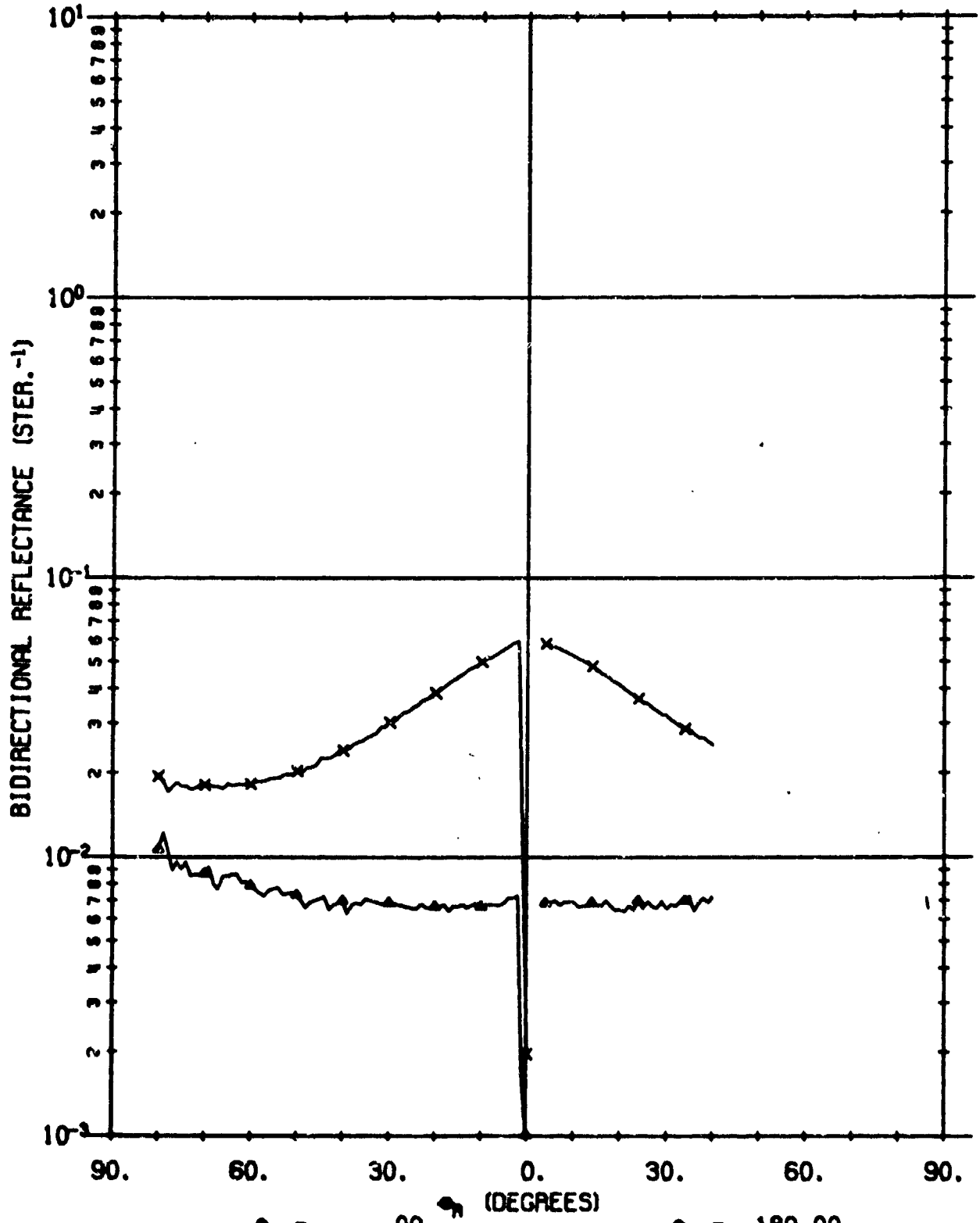

ϕ_R = .00 ϕ_R = 180.00

A01610 102

λ = 1.06
θ_I = .0
ϕ_I = 180.0

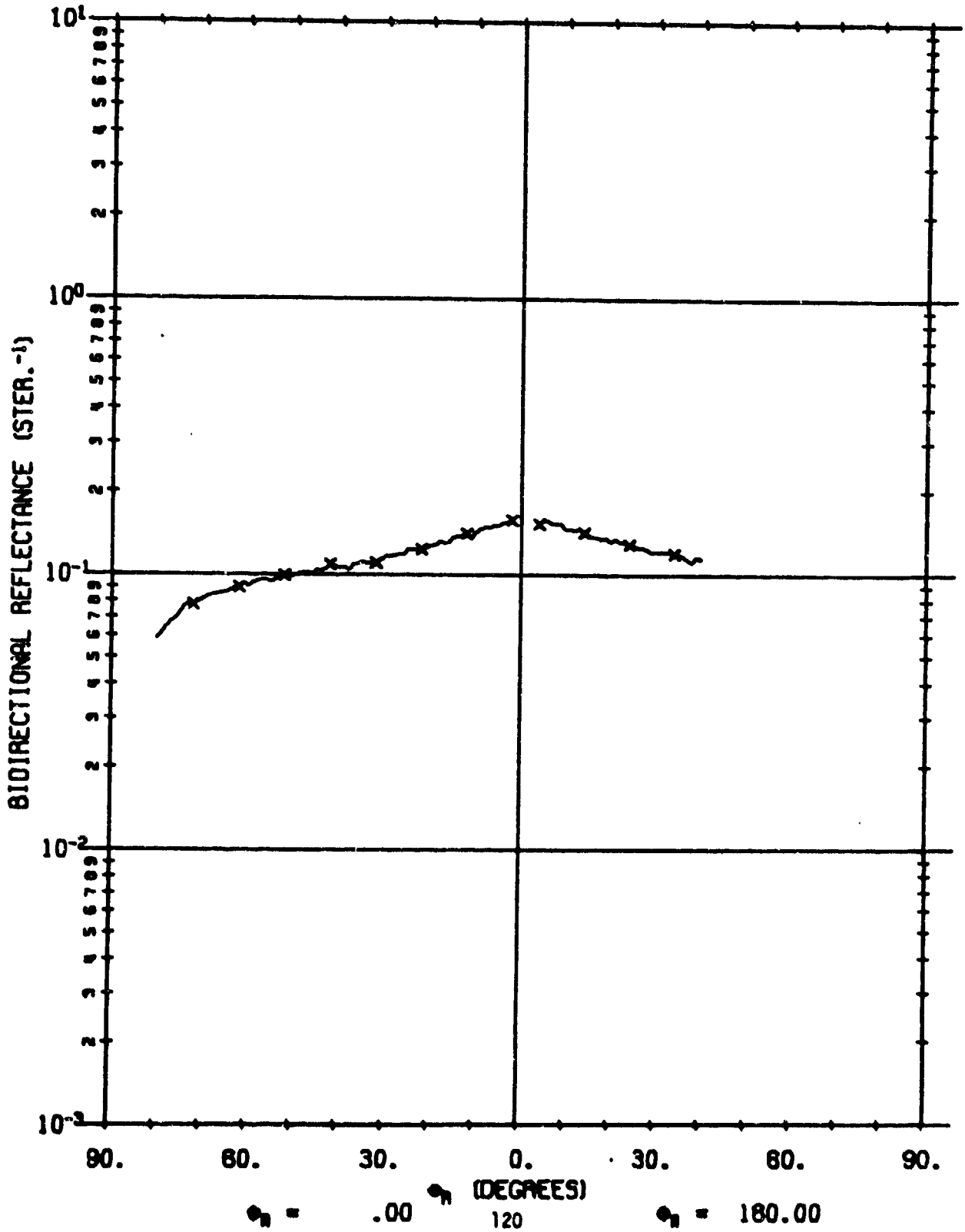

A01610 302

λ = 3.39
Φ_I = .0
Θ_I = 180.0

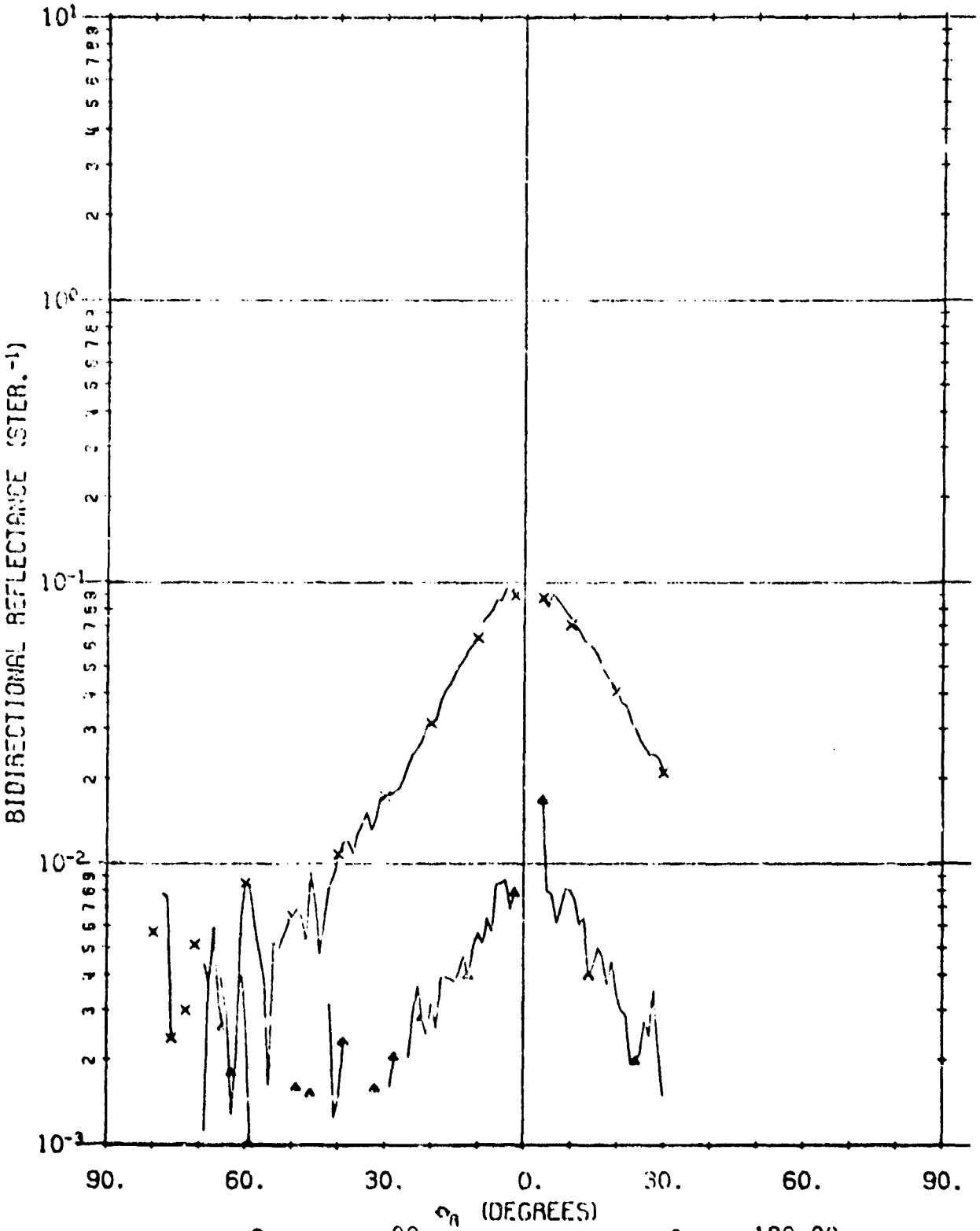

Φ_R = .00 Φ_R = 180.00

A01610 202

λ = 10.60
θ_I = .0
φ_I = 180.0

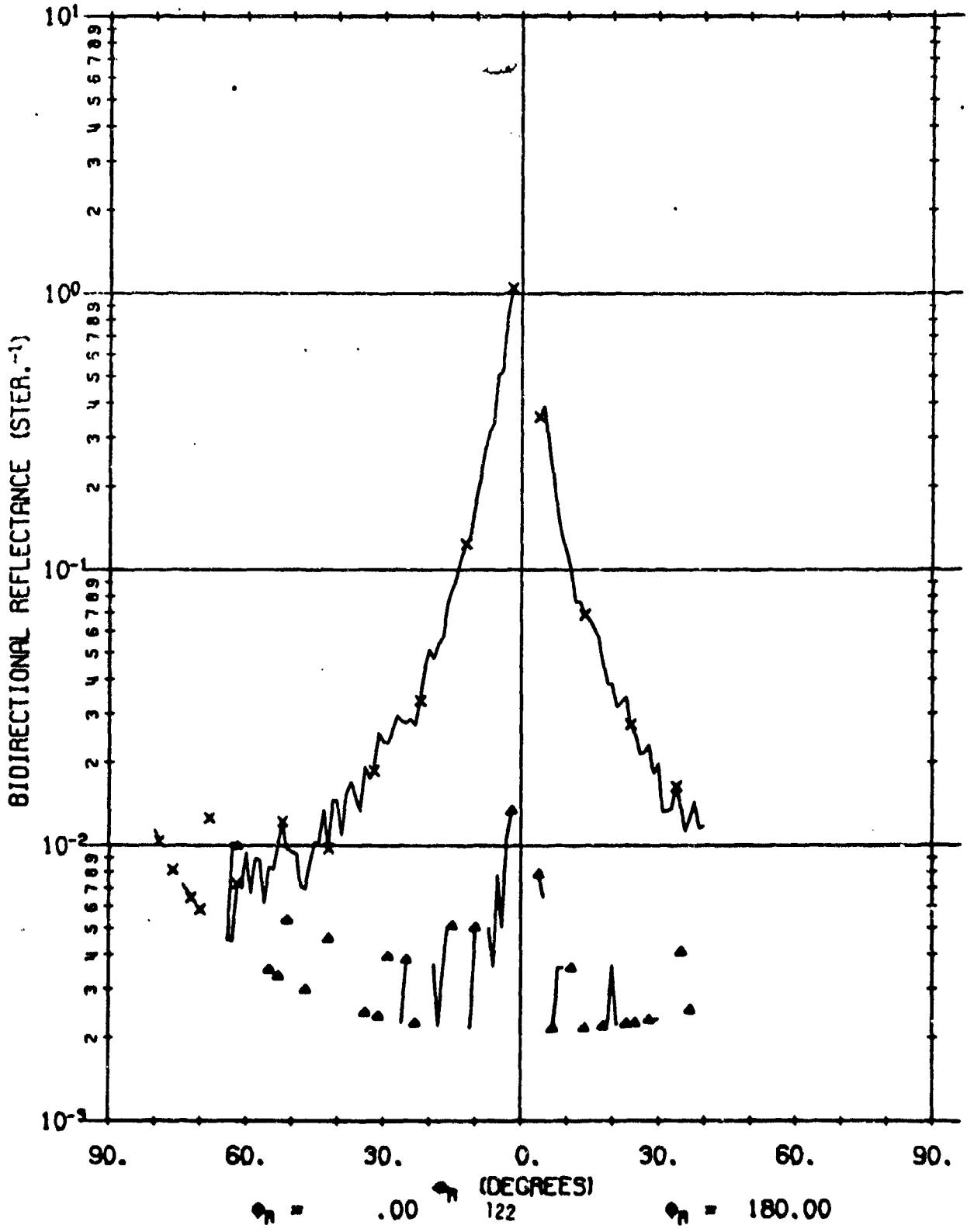

A01610 101

λ = .63
ϕ_1 = 20.0
ϕ_1 = 180.0

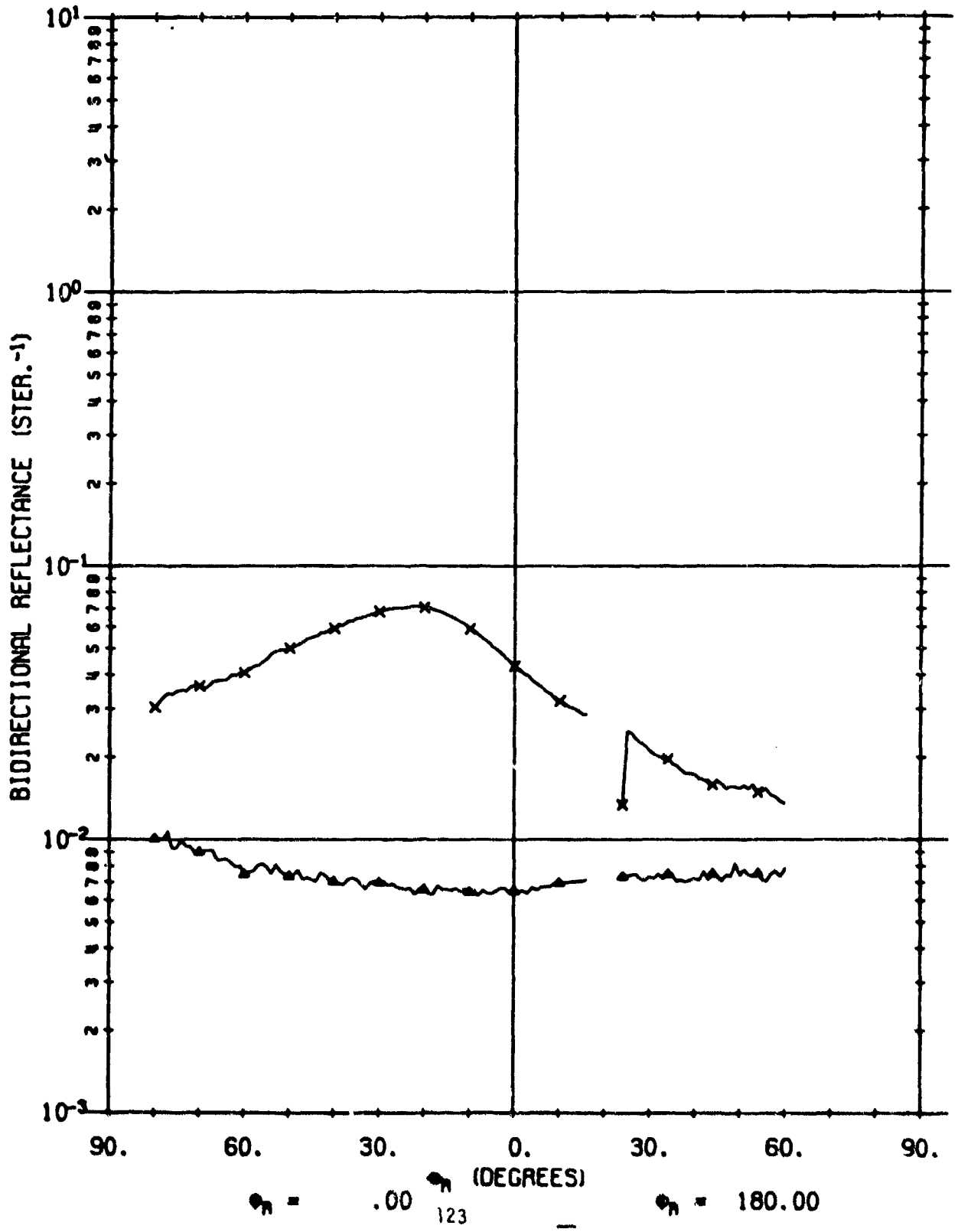

A01610 102

λ = 1.06
θ_I = 20.0
ϕ_I = 180.0

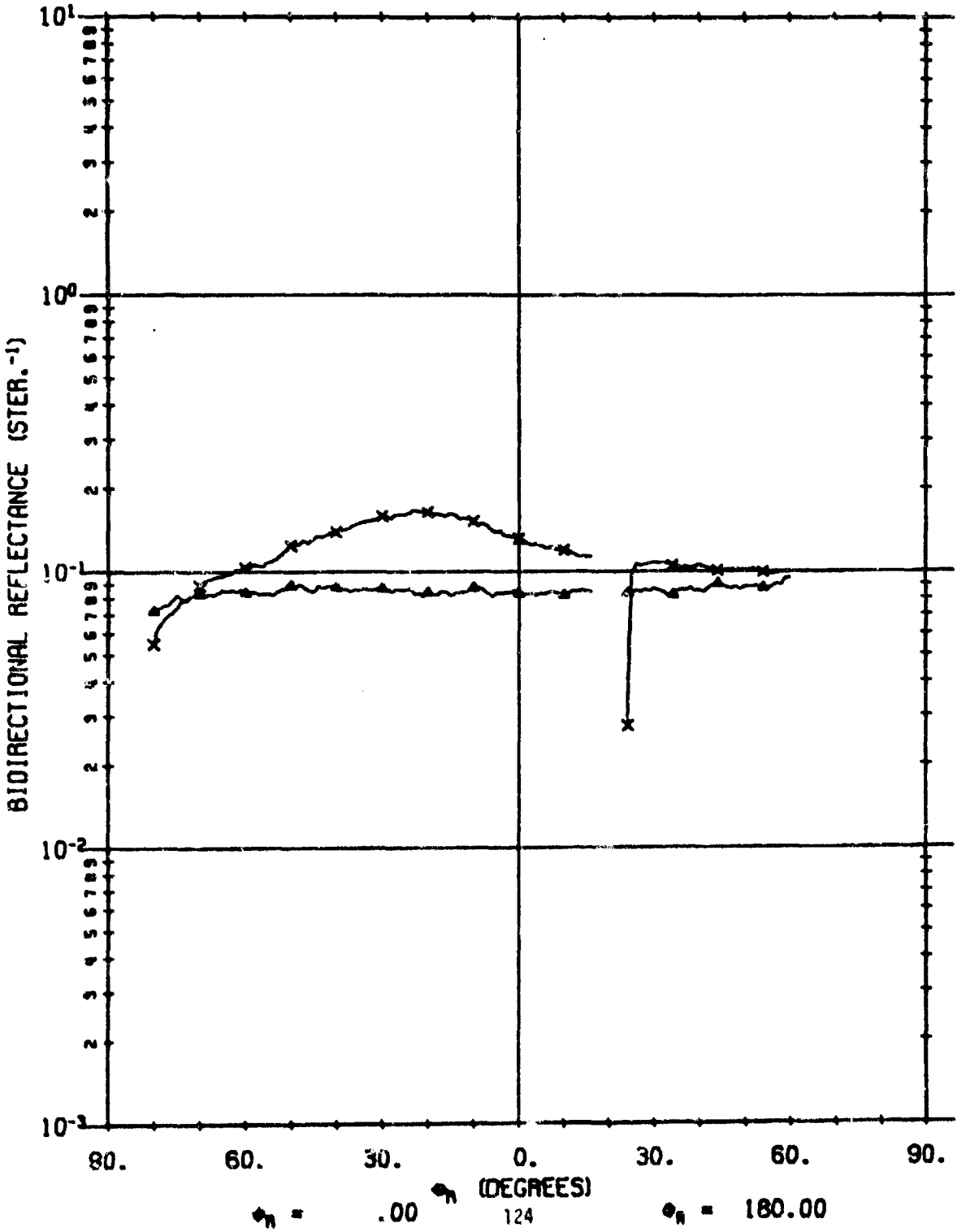

A01610 302

λ = 3.39
Φ_I = 20.0
Φ_I = 180.0

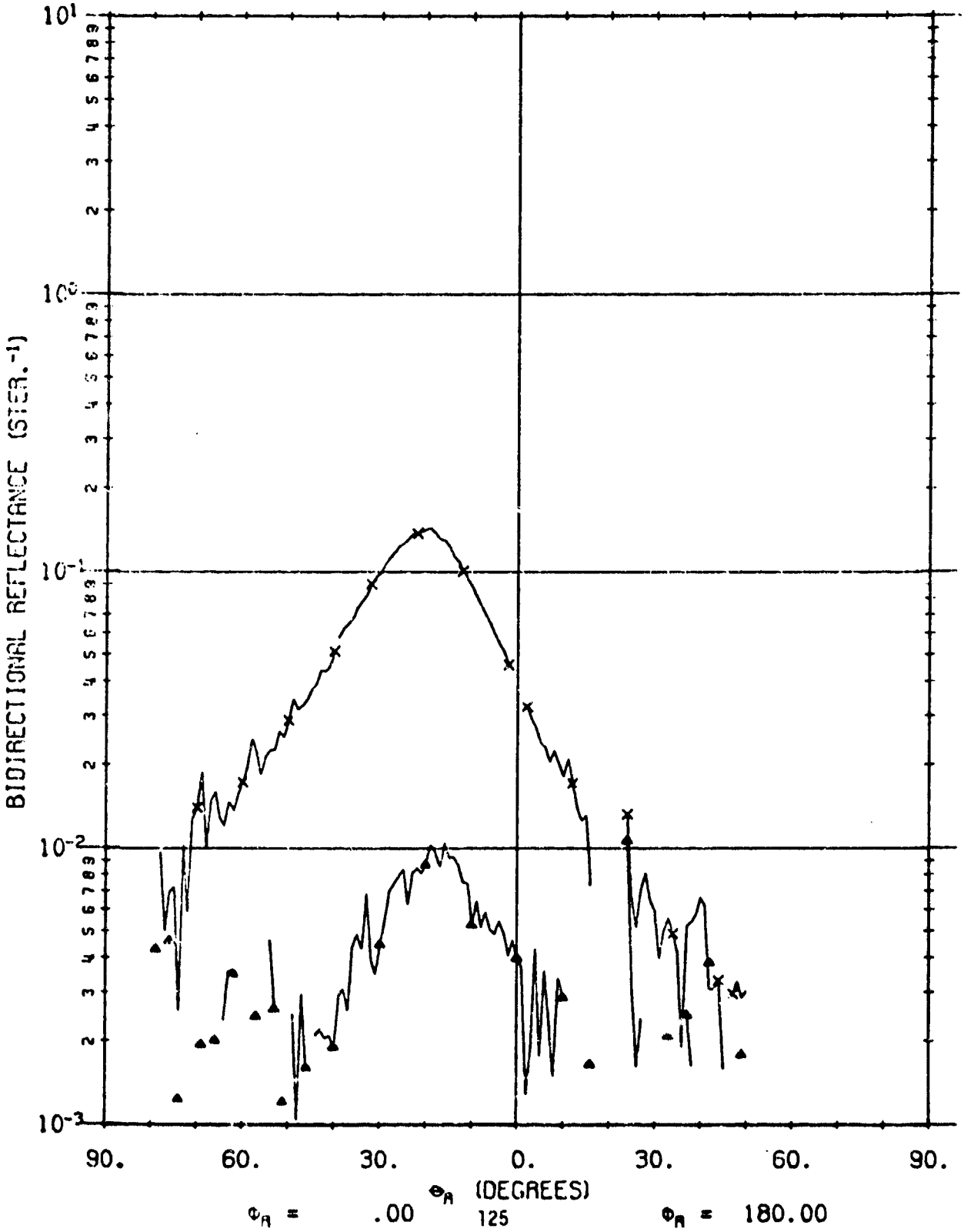

A01610 202

λ = 10.60
Φ_i = 20.0
Φ_i = 180.0

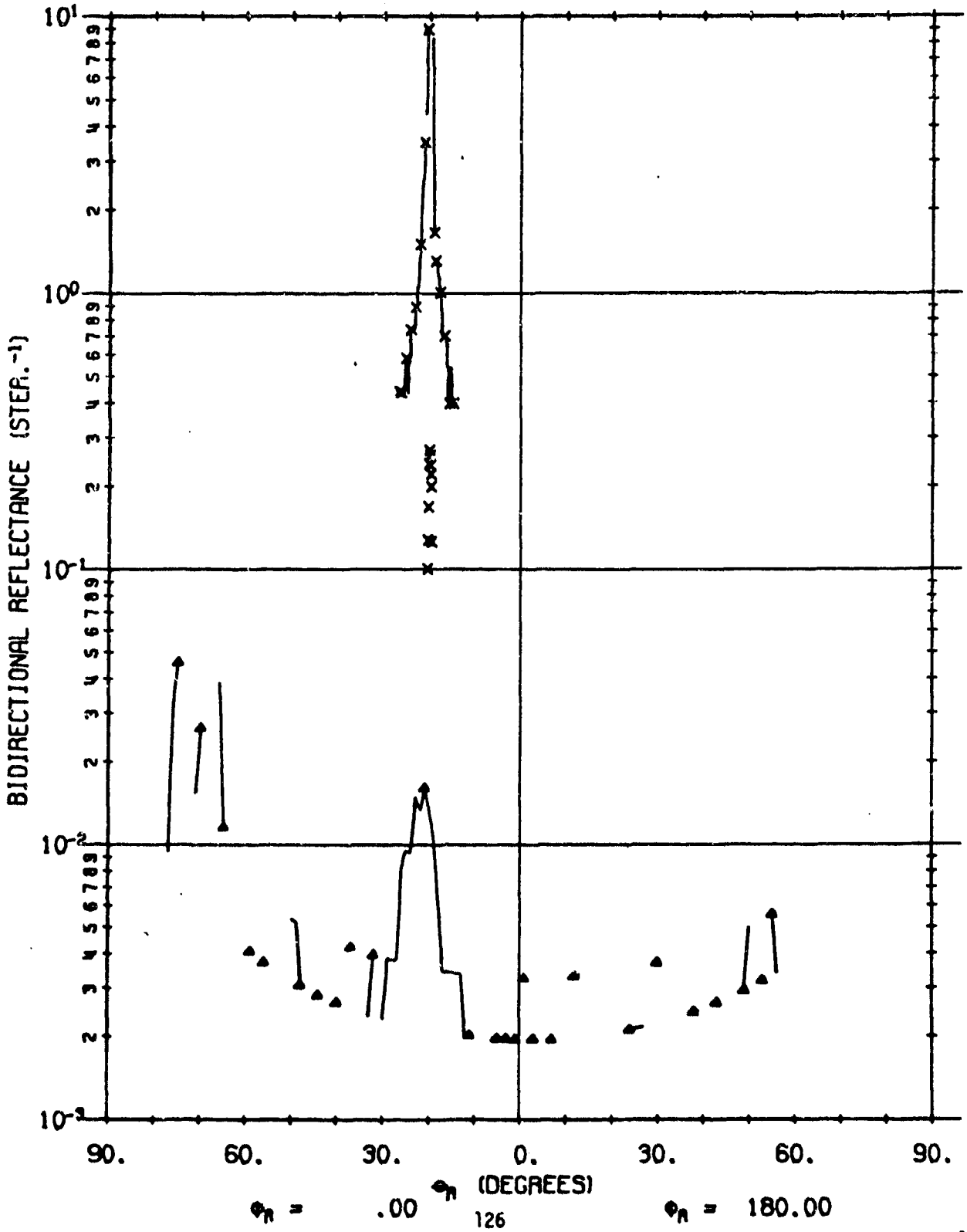

A01610 101

λ = .63
ϕ_I = 20.0
ϕ_I = 180.0

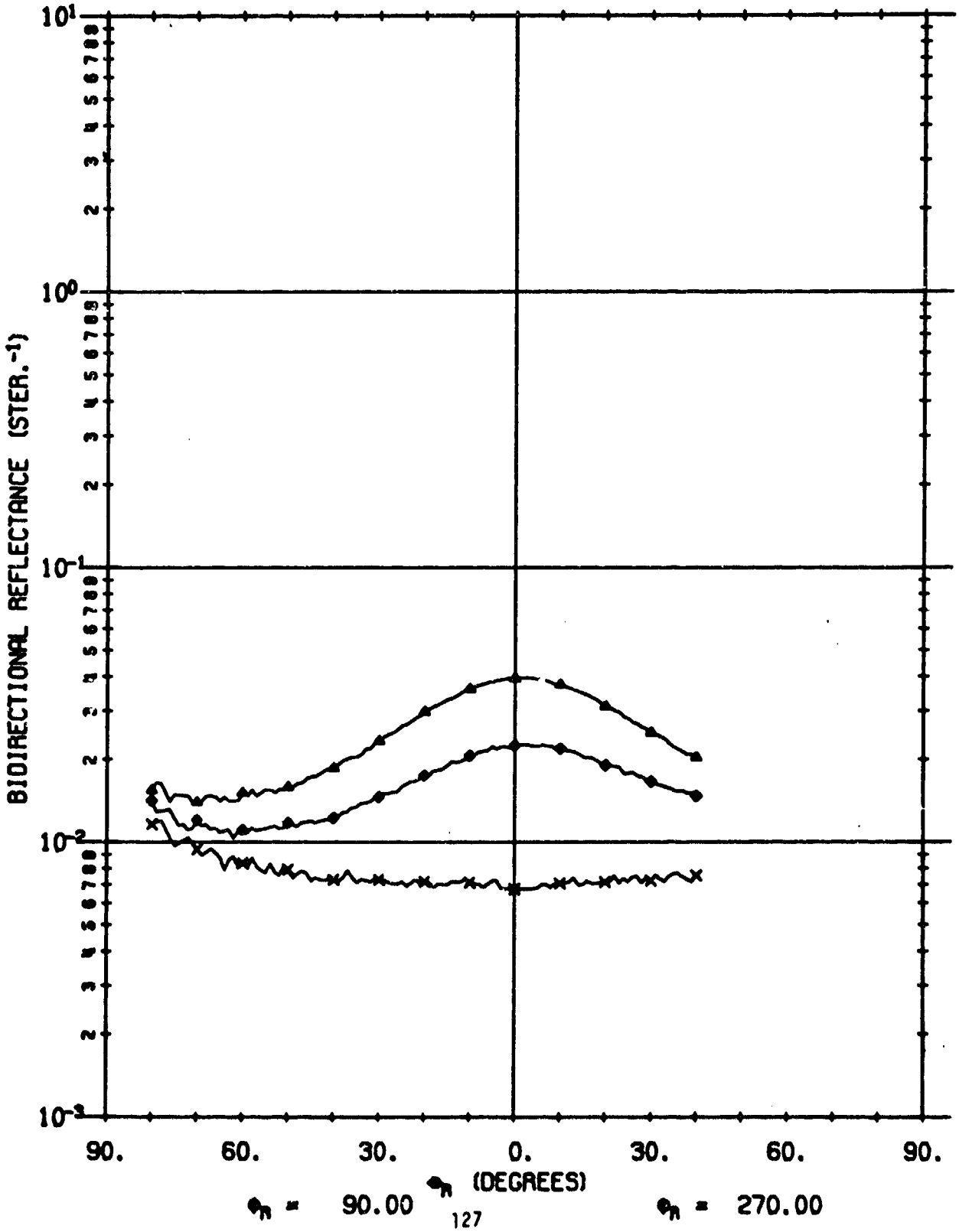

A01610 102

λ = 1.06
ϕ_I = 20.0
θ_I = 180.0

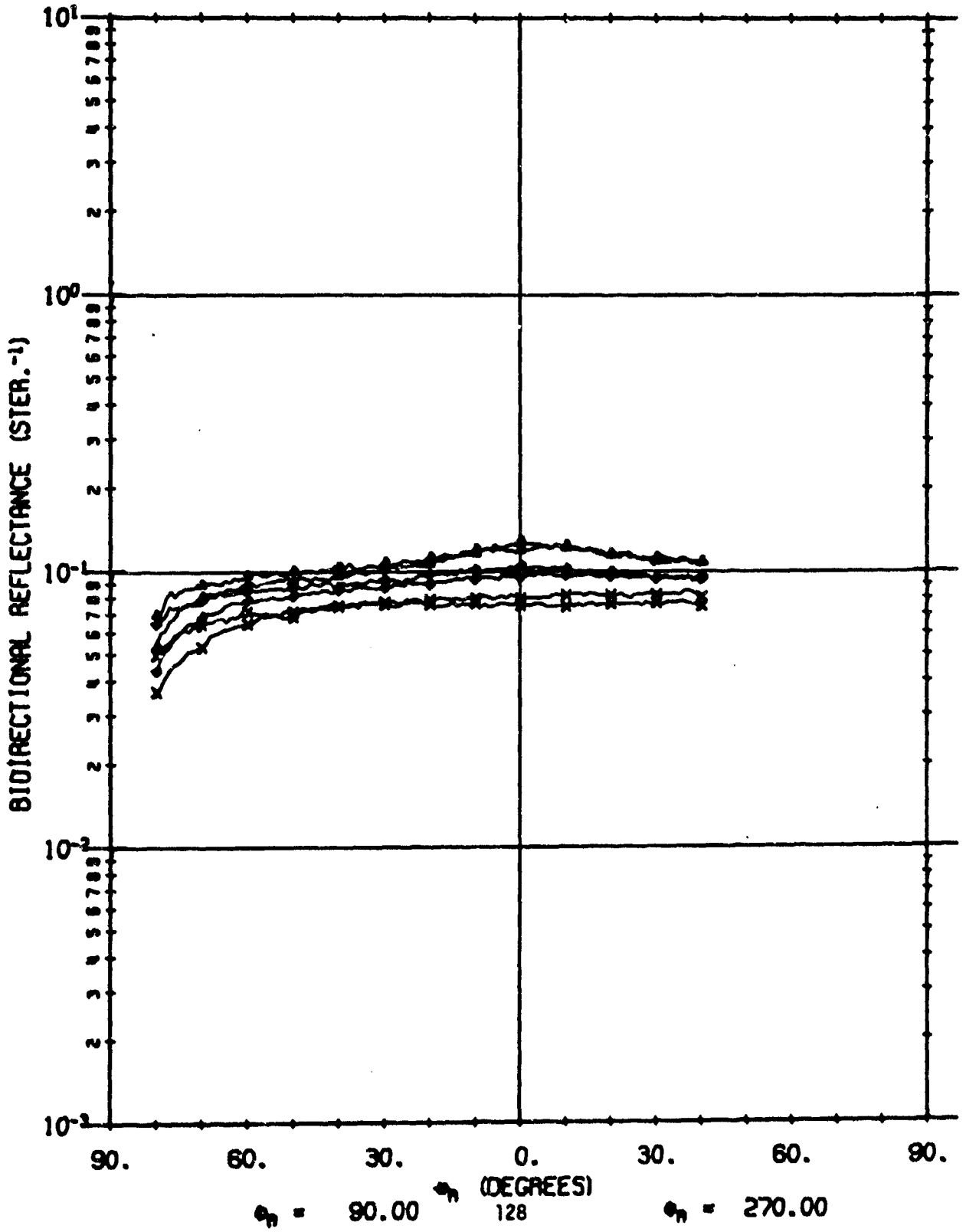

A01610 301

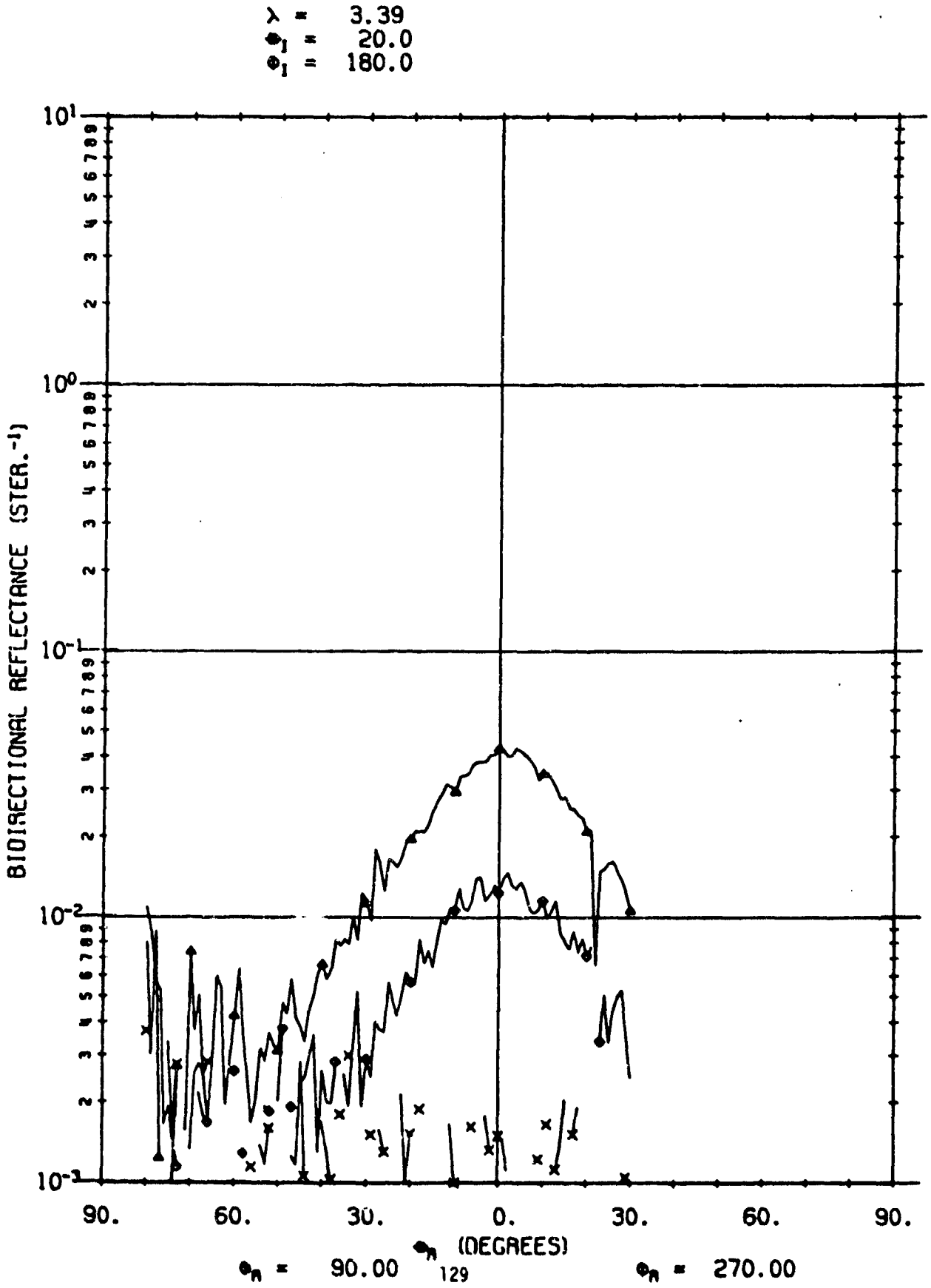
λ = 3.39
θ1 = 20.0
φ1 = 180.0
BIDIRECTIONAL REFLECTANCE (STER.-1)
10^1
10^0
10^-1
10^-2
10^-3
90.
60.
30.
0.
30.
60.
90.
θr (DEGREES)
φr = 90.00
φr = 270.00

A01610 204

λ = 10.60
θ_I = 20.0
ϕ_I = 180.0

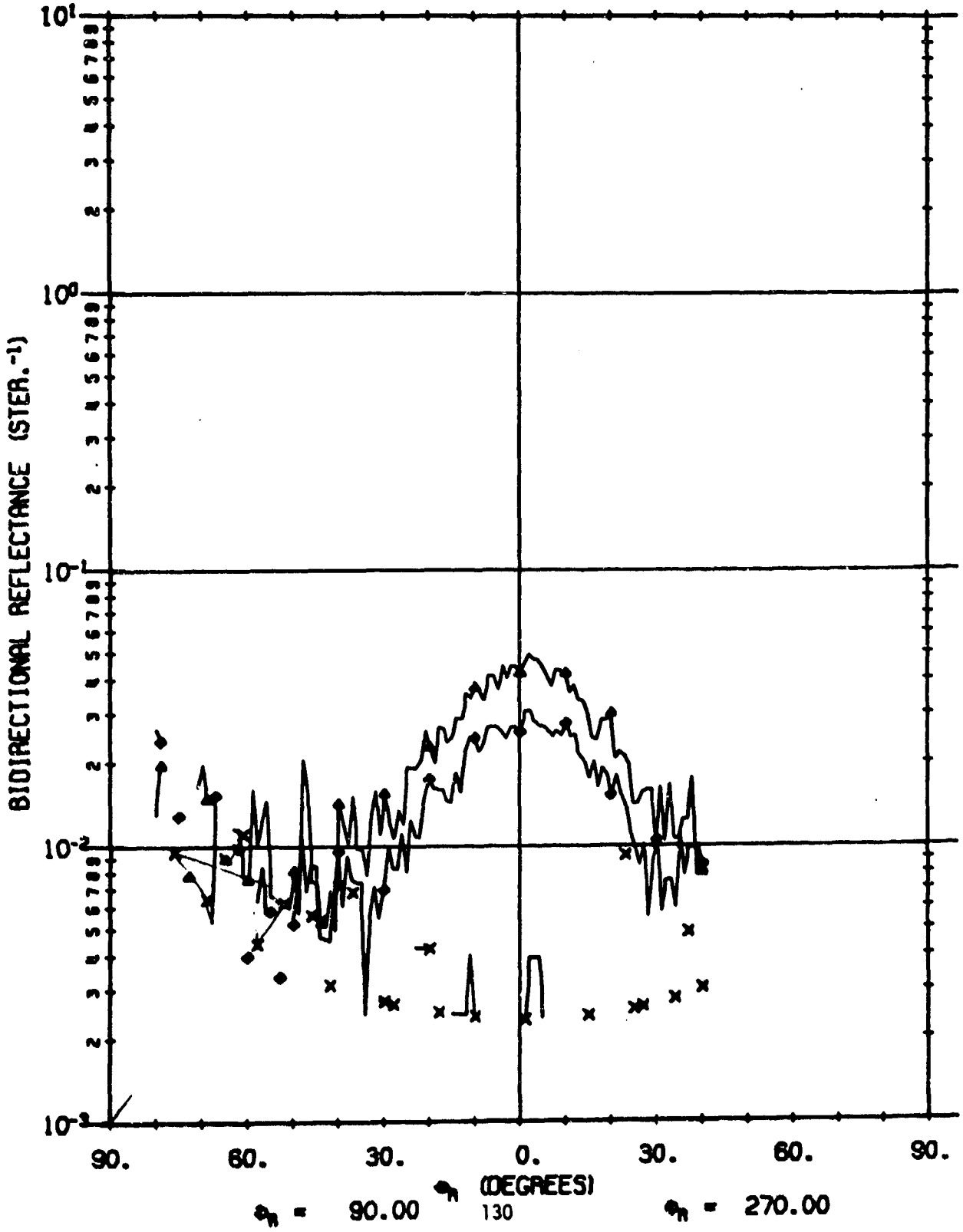

A01610 101

λ = .63
θ_I = 40.0
ϕ_I = 180.0

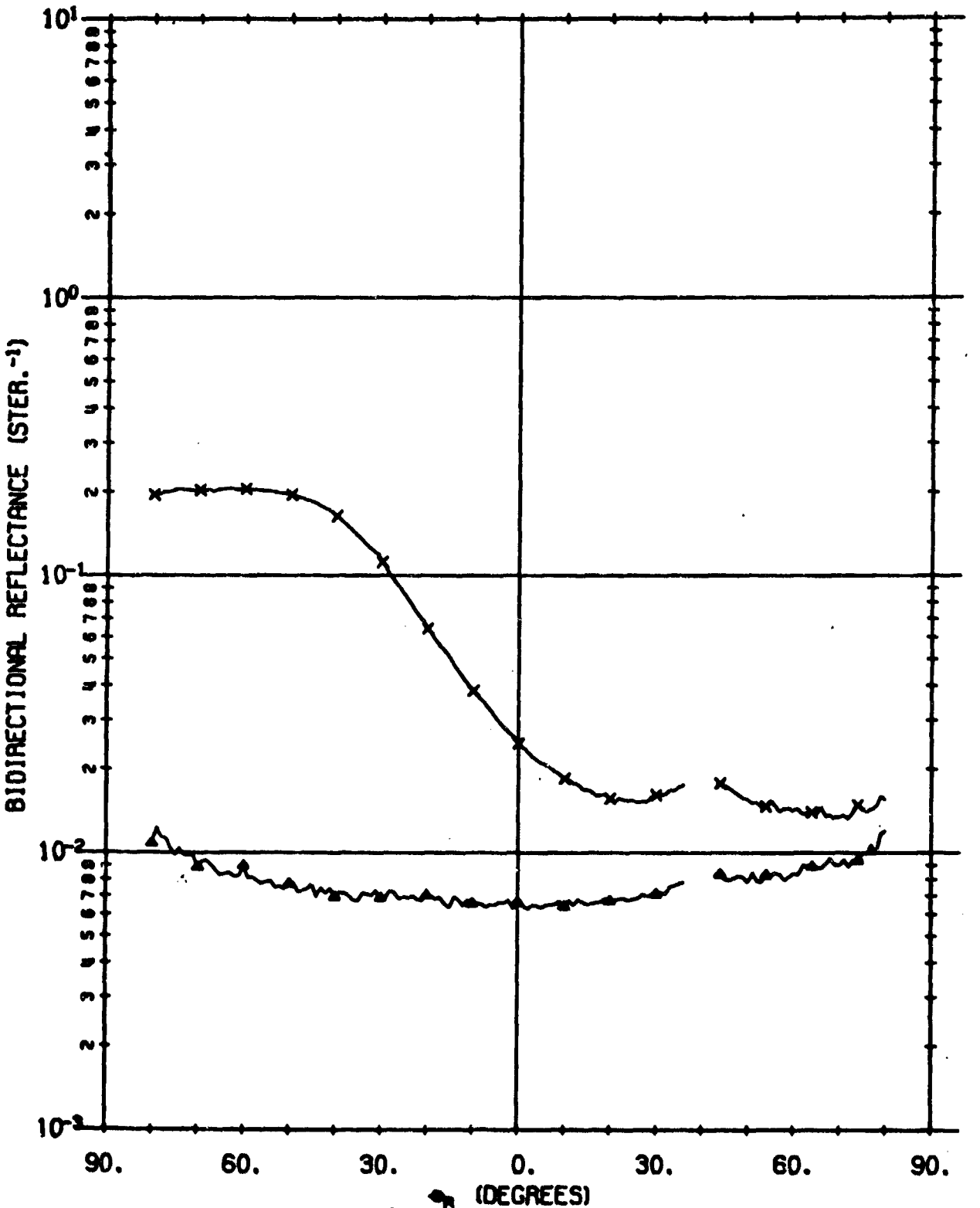

ϕ_R = .00 ϕ_R = 180.00

A01610 102

λ = 1.06
ϕ_I = 40.0
θ_I = 180.0

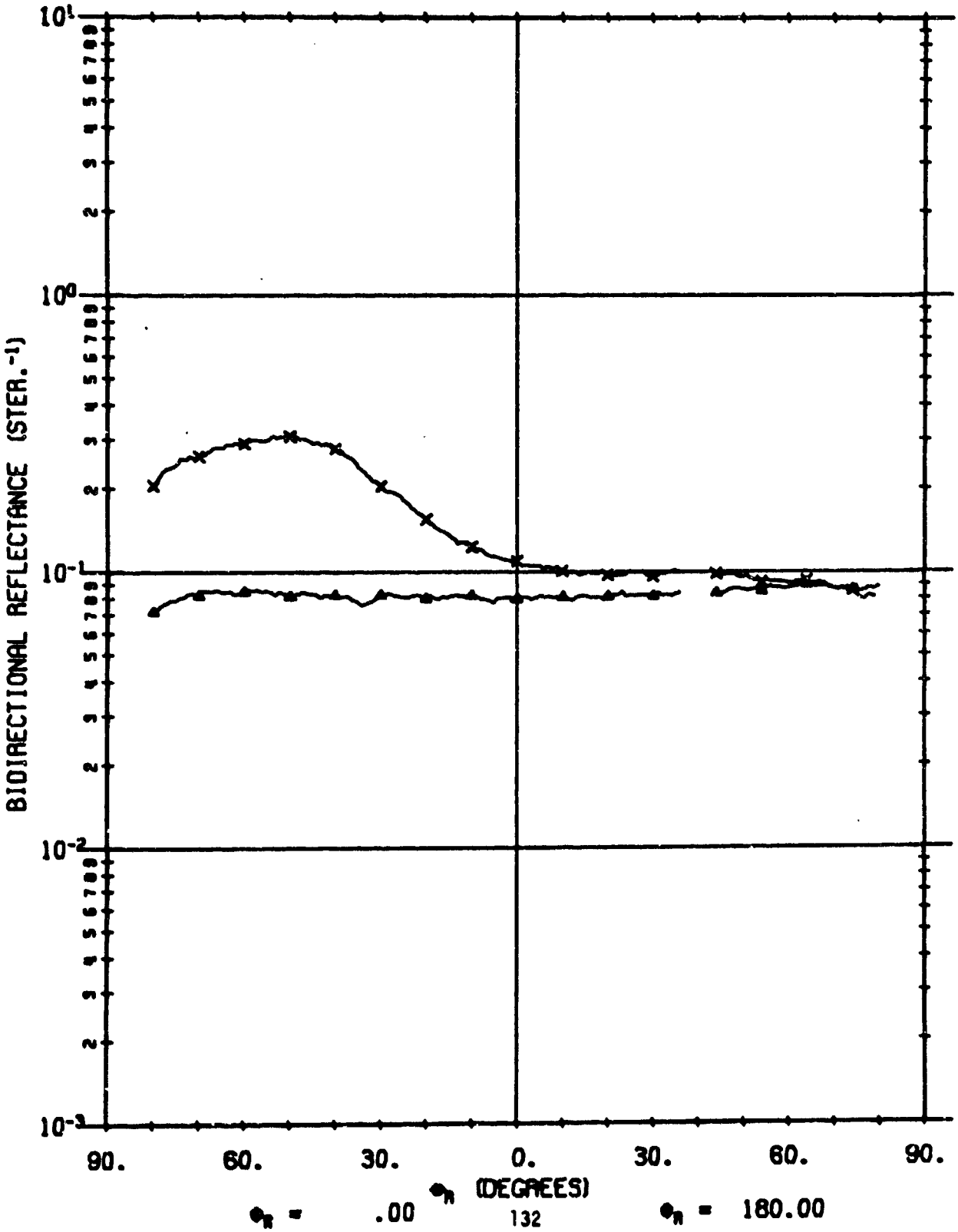

A01610 302

λ = 3.39
ϕ_i = 40.0
θ_i = 180.0

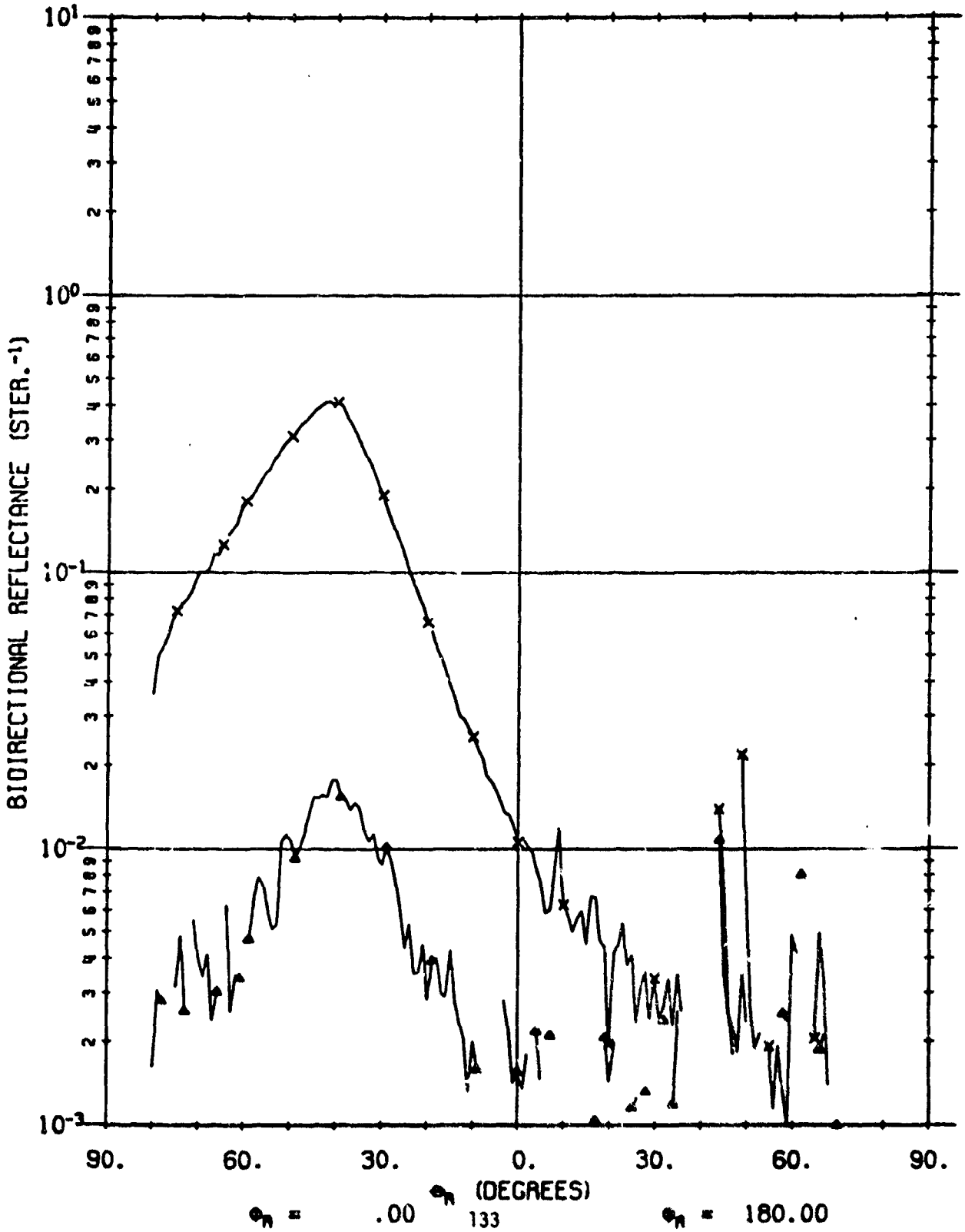

A01610 202

λ = 10.60
θ_I = 40.0
Φ_I = 180.0

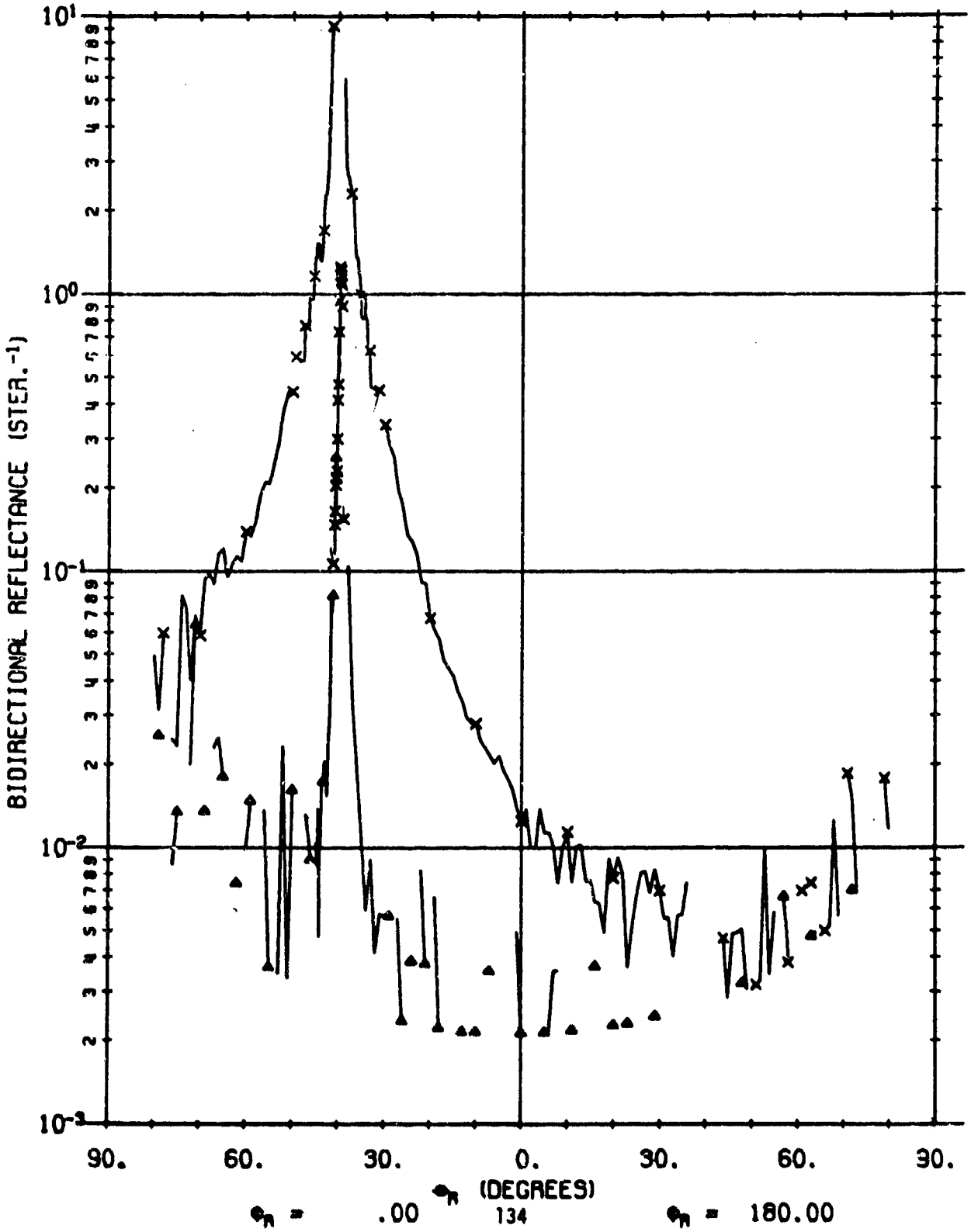

A01610 101

λ = .63
θ_I = 40.0
ϕ_I = 180.0

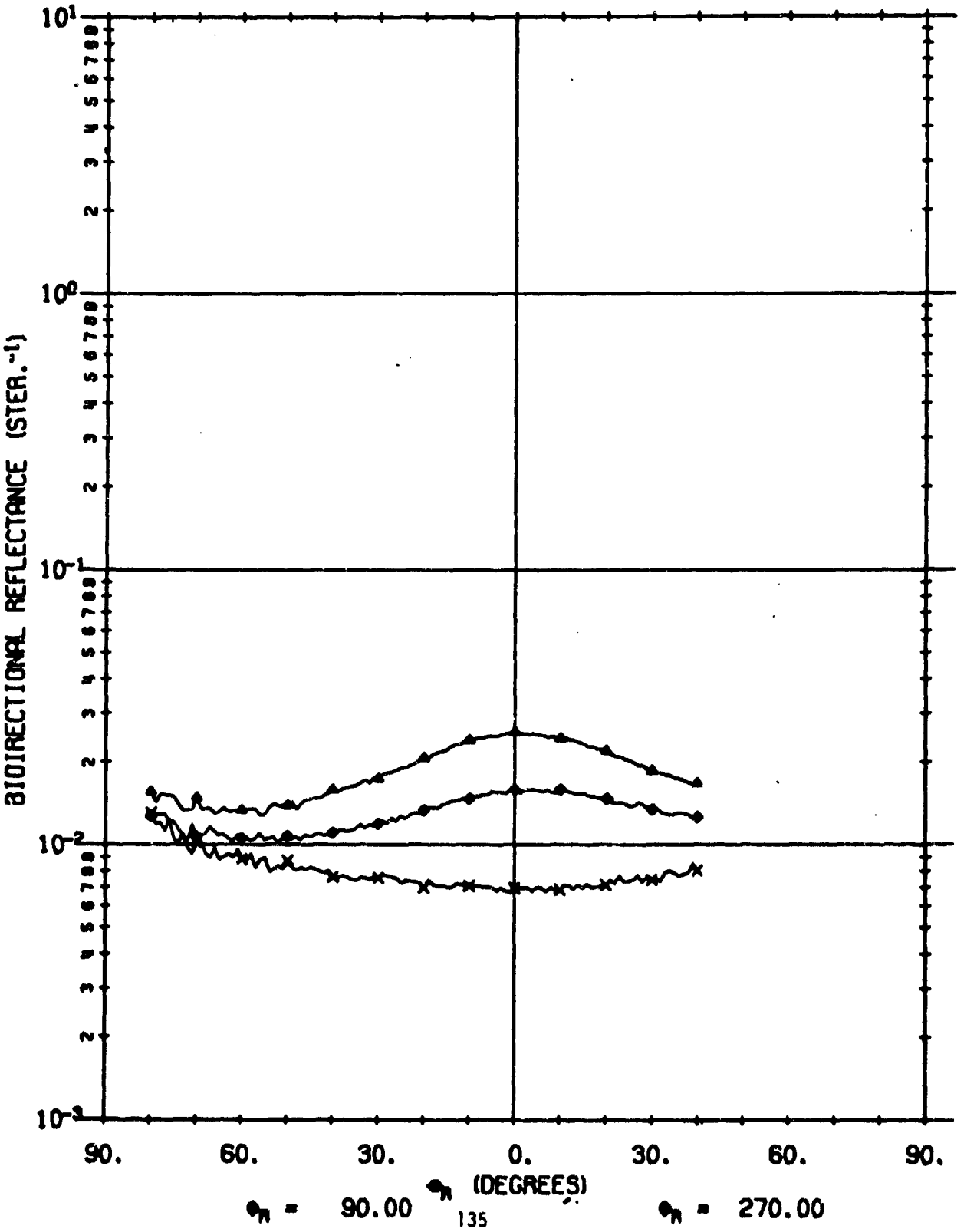

A01610 102

λ = 1.06
θ_I = 40.0
ϕ_I = 180.0

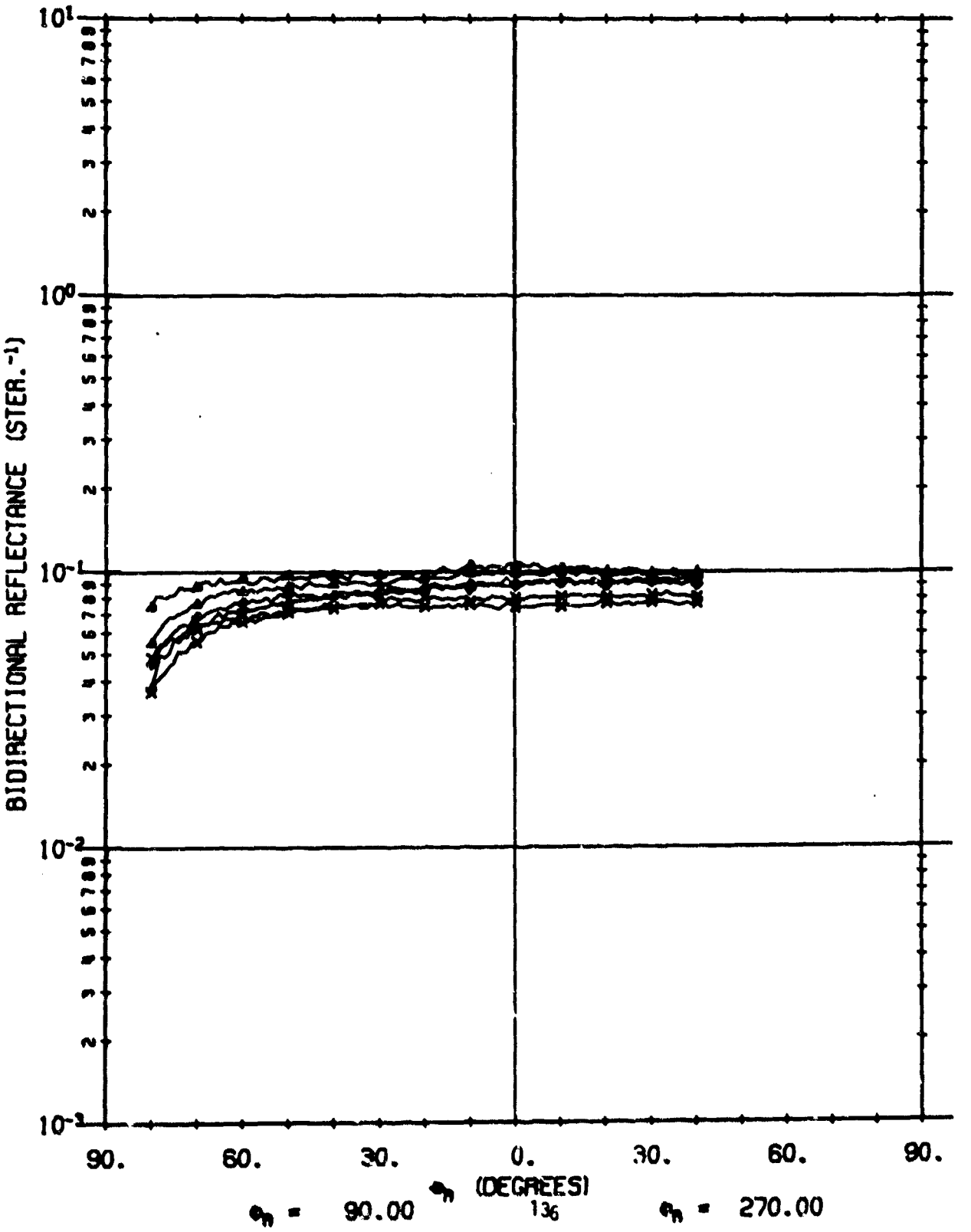

A01610 301

λ = 3.39
ϕ_I = 40.0
θ_I = 180.0

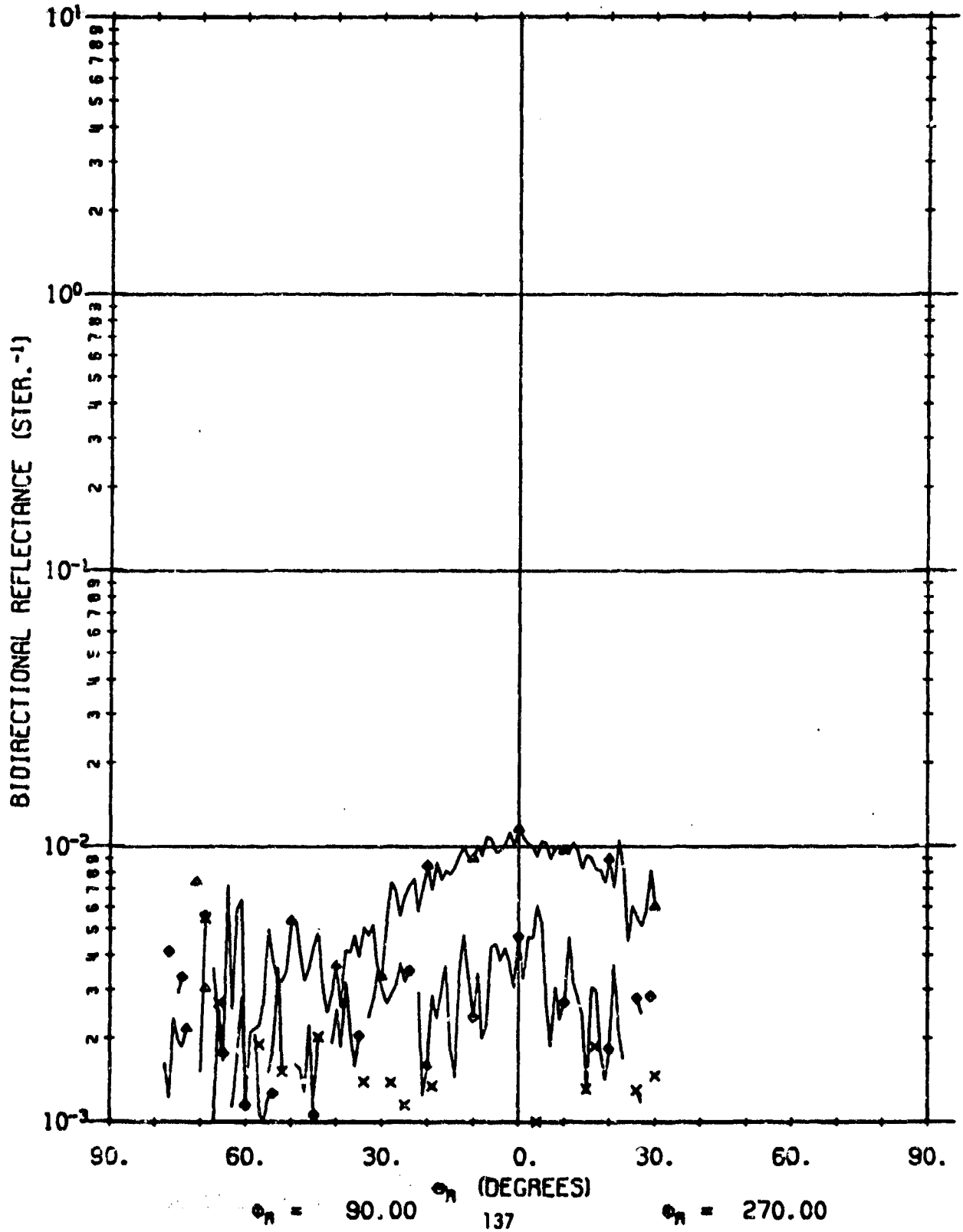

ϕ_R = 90.00 ϕ_R = 270.00

A01610 201

λ = 10.60
θ_I = 40.0
ϕ_I = 180.0

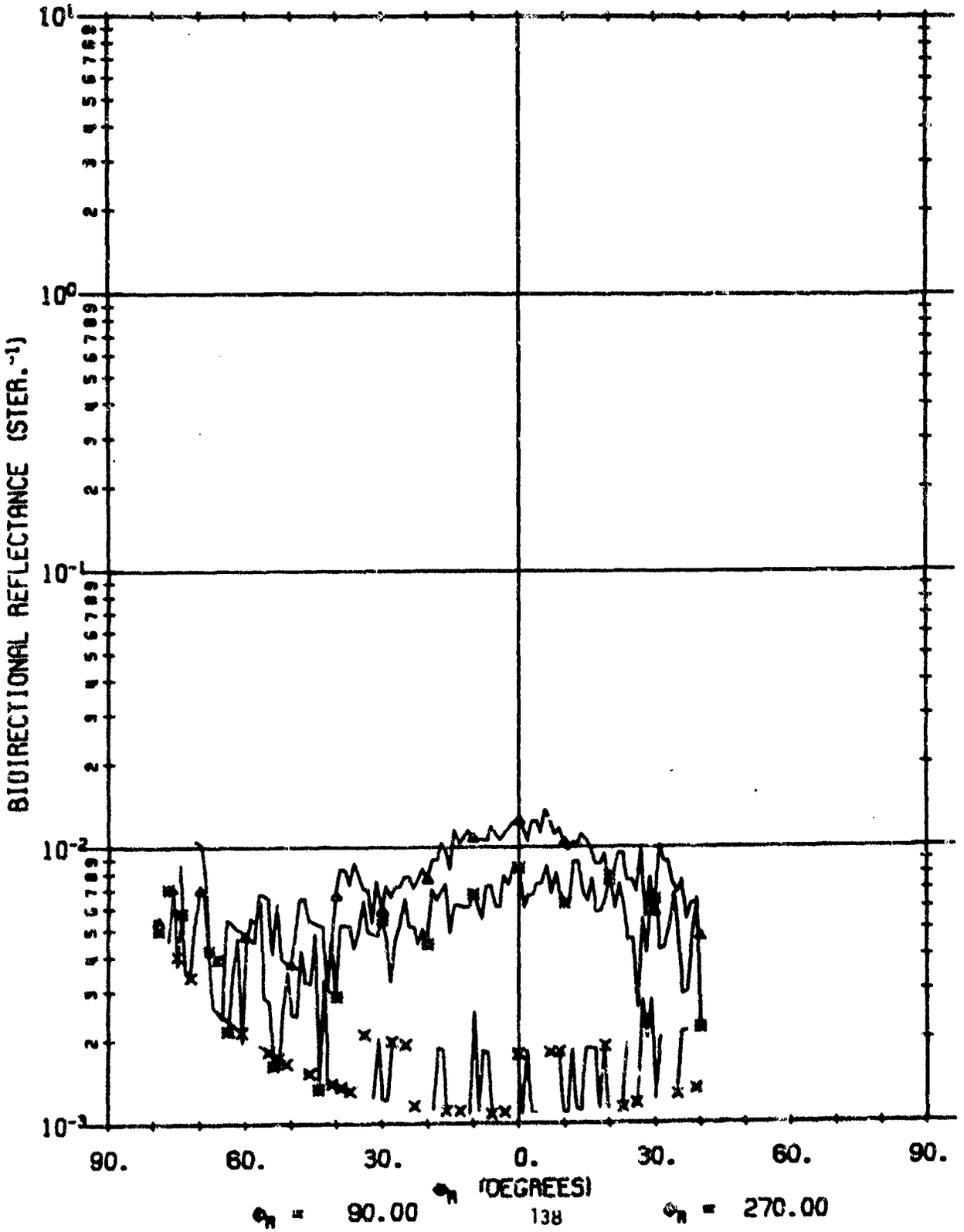

A01610 101

λ = .63
θ_I = 60.0
ϕ_I = 180.0

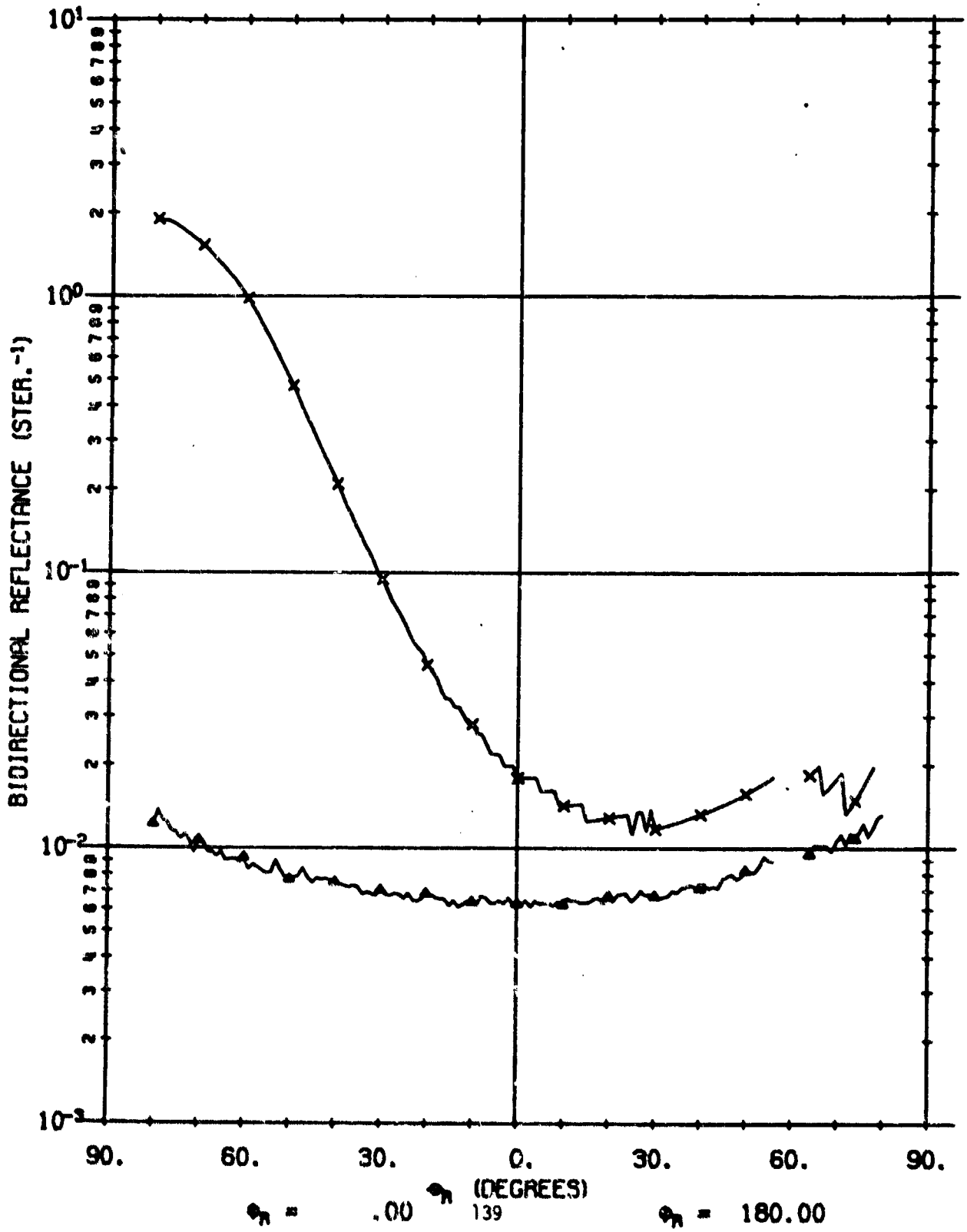

A01610 102

λ = 1.06
θ_i = 60.0
ϕ_i = 180.0

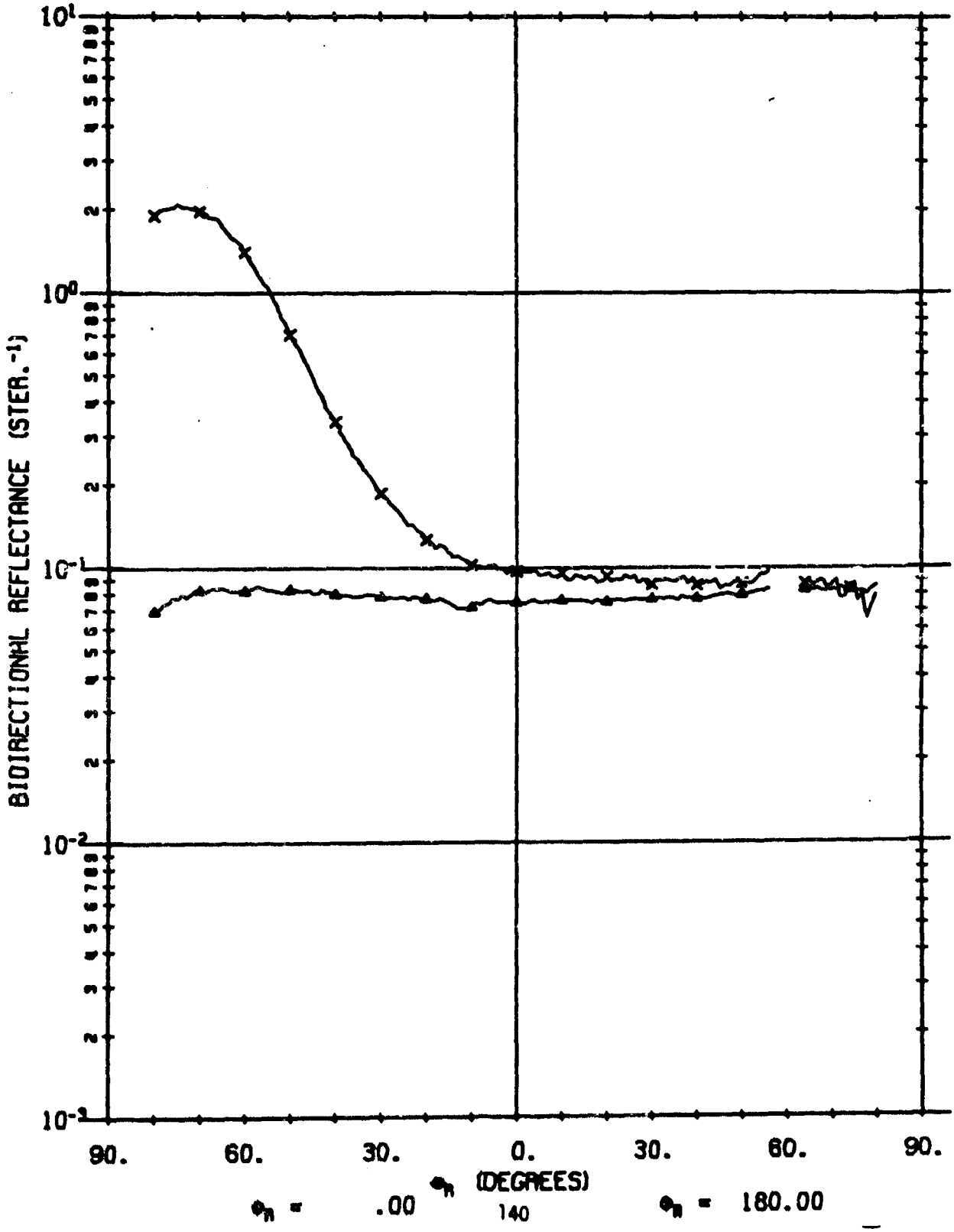

A01610 302

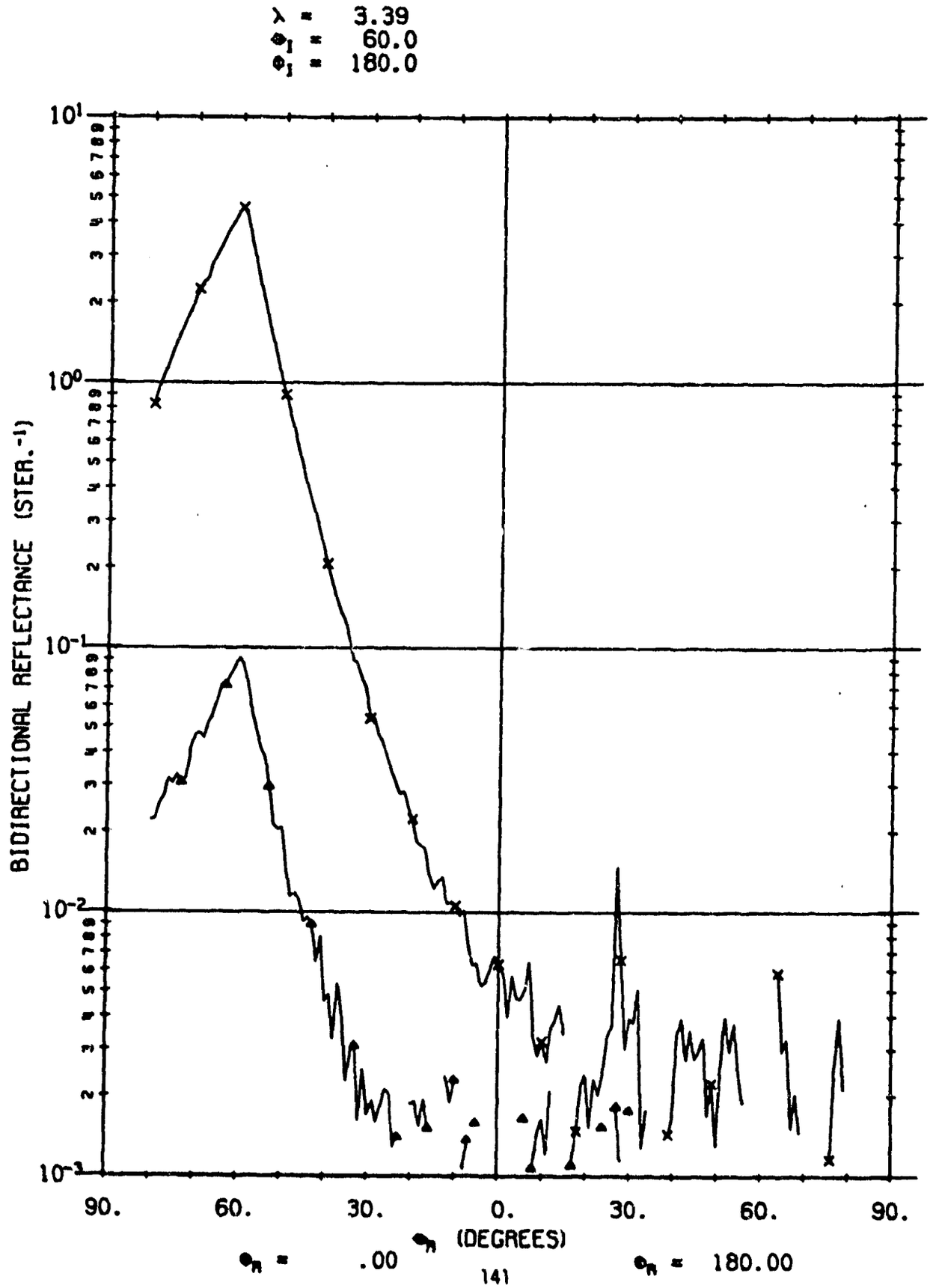
λ = 3.39
Φ_I = 60.0
Θ_I = 180.0
BIDIRECTIONAL REFLECTANCE (STER.$^{-1}$)
10^1
10^0
10^{-1}
10^{-2}
10^{-3}
90.
60.
30.
0.
30.
60.
90.
Θ_R (DEGREES)
Φ_R = .00
Φ_R = 180.00

A01610 202

λ = 10.60
θ_I = 60.0
φ_I = 180.0

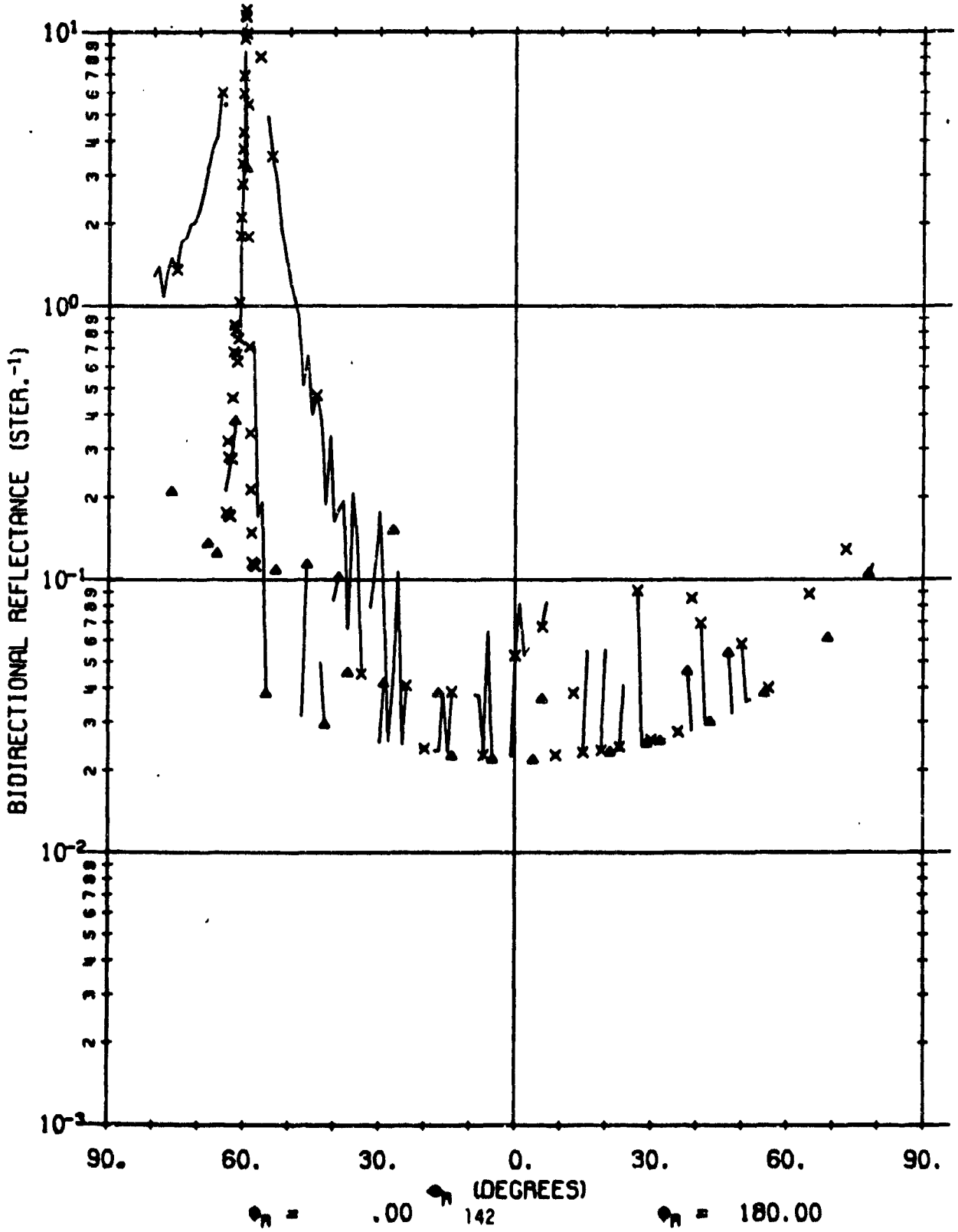

A01610 101

λ = .63
θ_I = 60.0
ϕ_I = 180.0

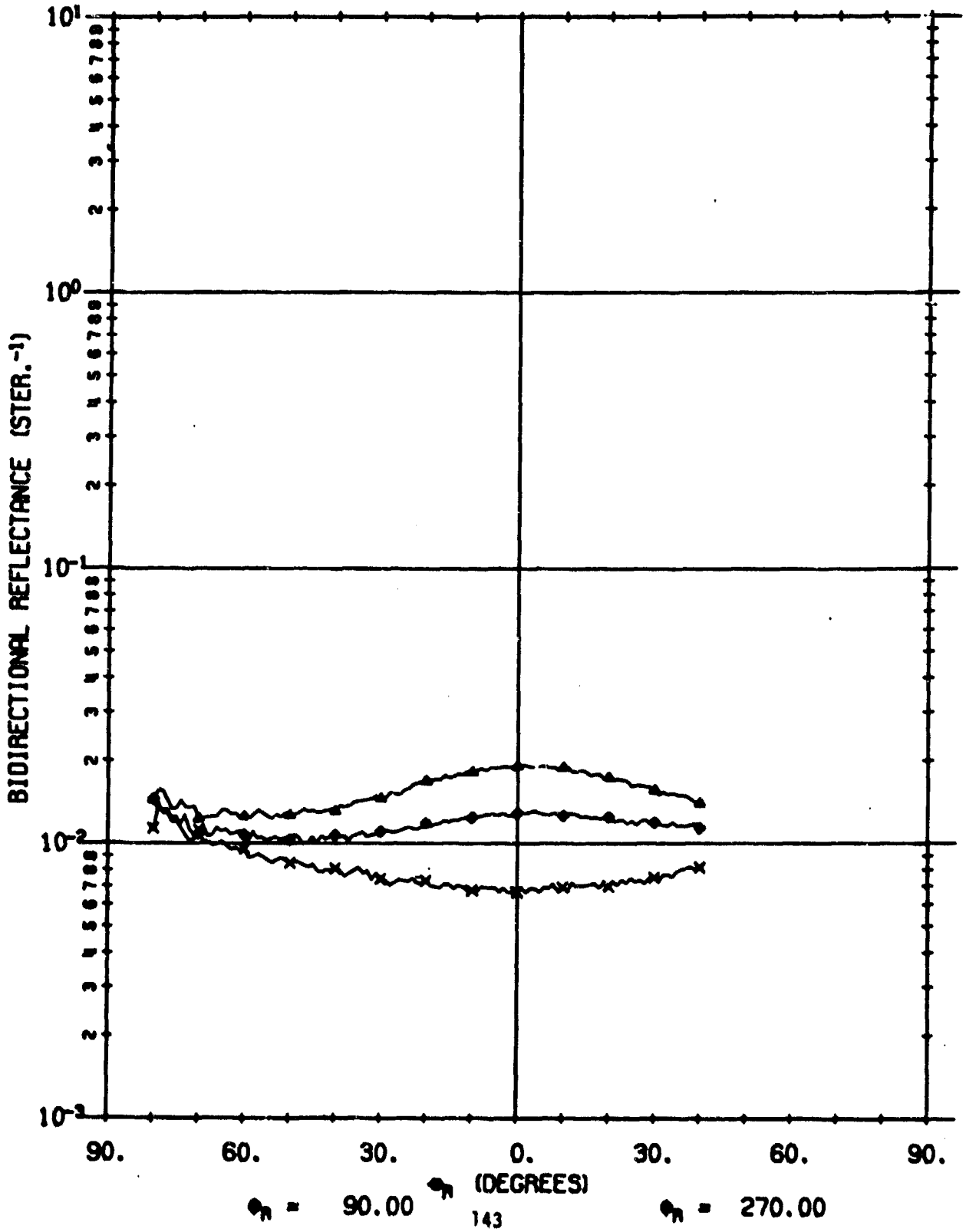

A01610 102

λ = 1.06
θ_I = 60.0
ϕ_I = 180.0

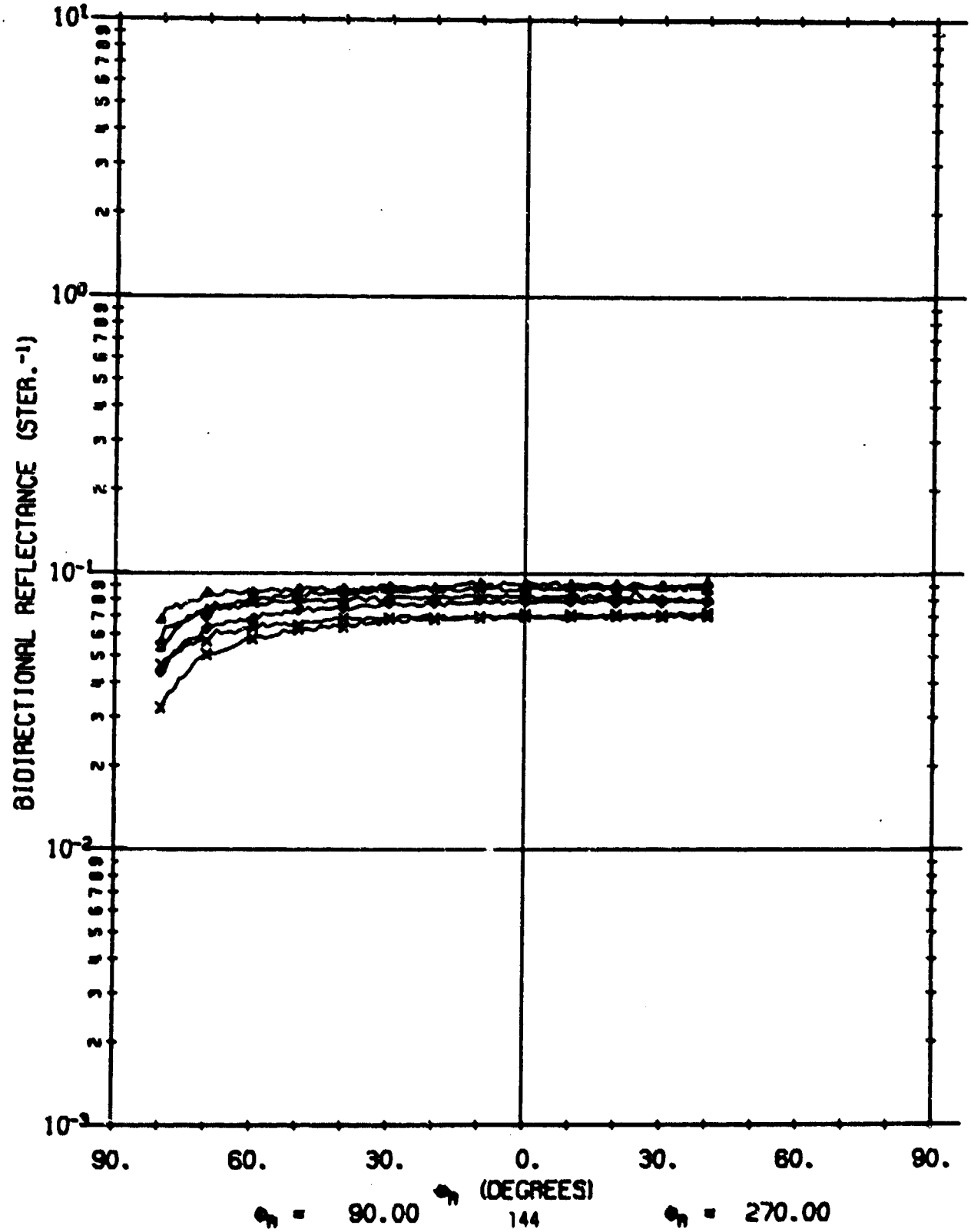

A01610 301

λ = 3.39
Φ_I = 60.0
Φ_I = 180.0

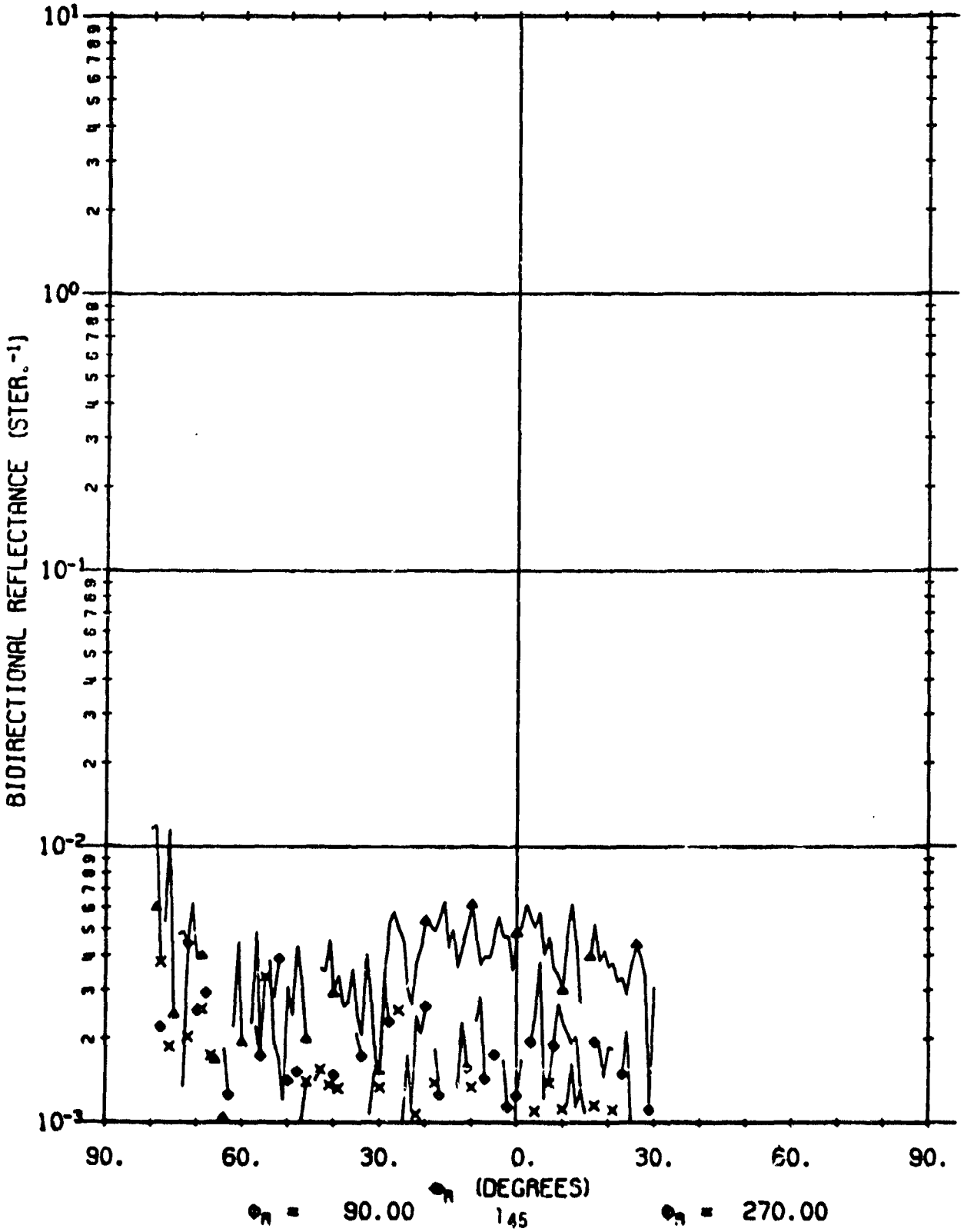

A01610 201

λ = 10.60
θ_I = 60.0
ϕ_I = 180.0

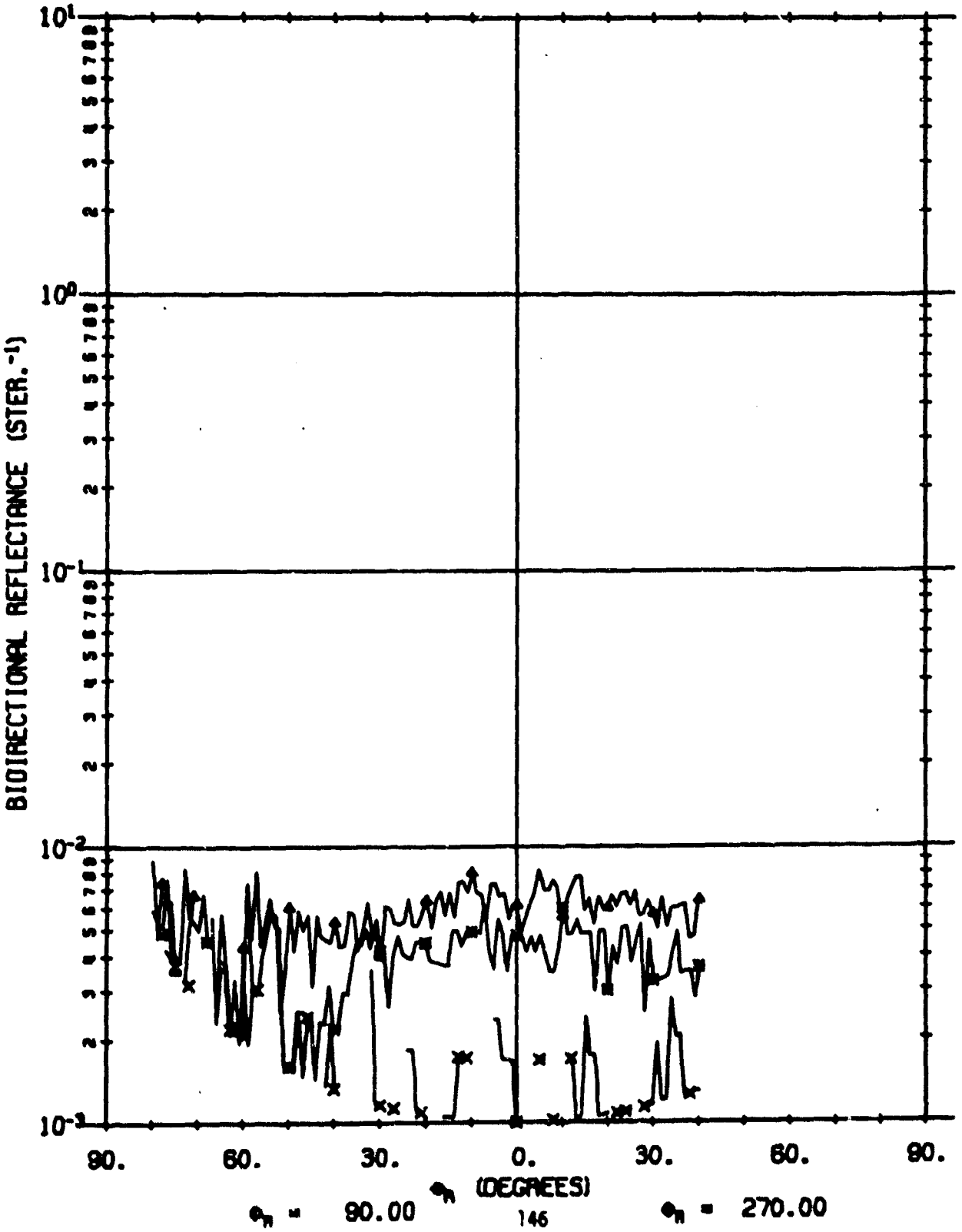

A01610 303

λ = 3.39
Φ_I = .0
Θ_I = 180.0

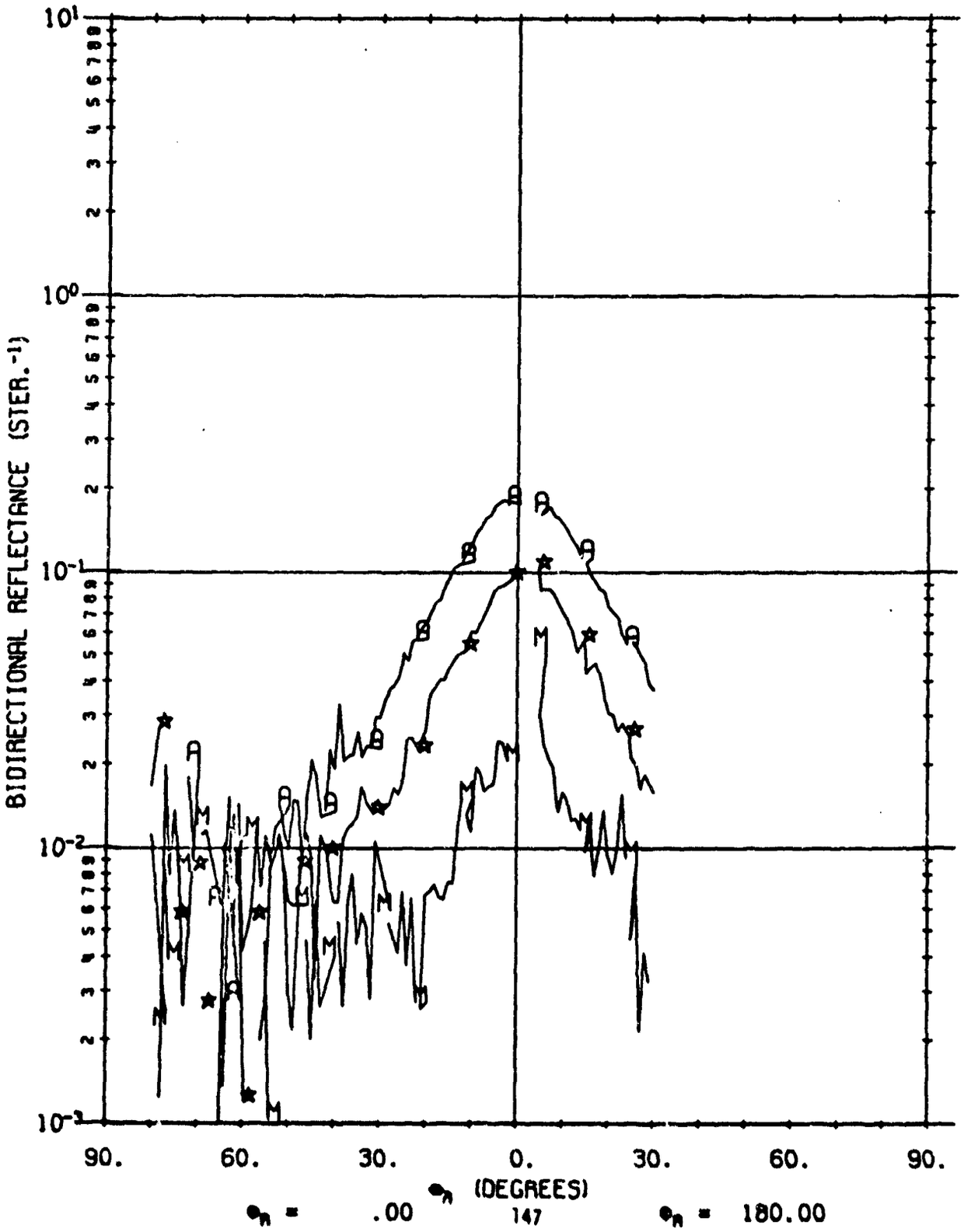

A01610 203

λ = 10.60
θ_I = .0
φ_I = 180.0

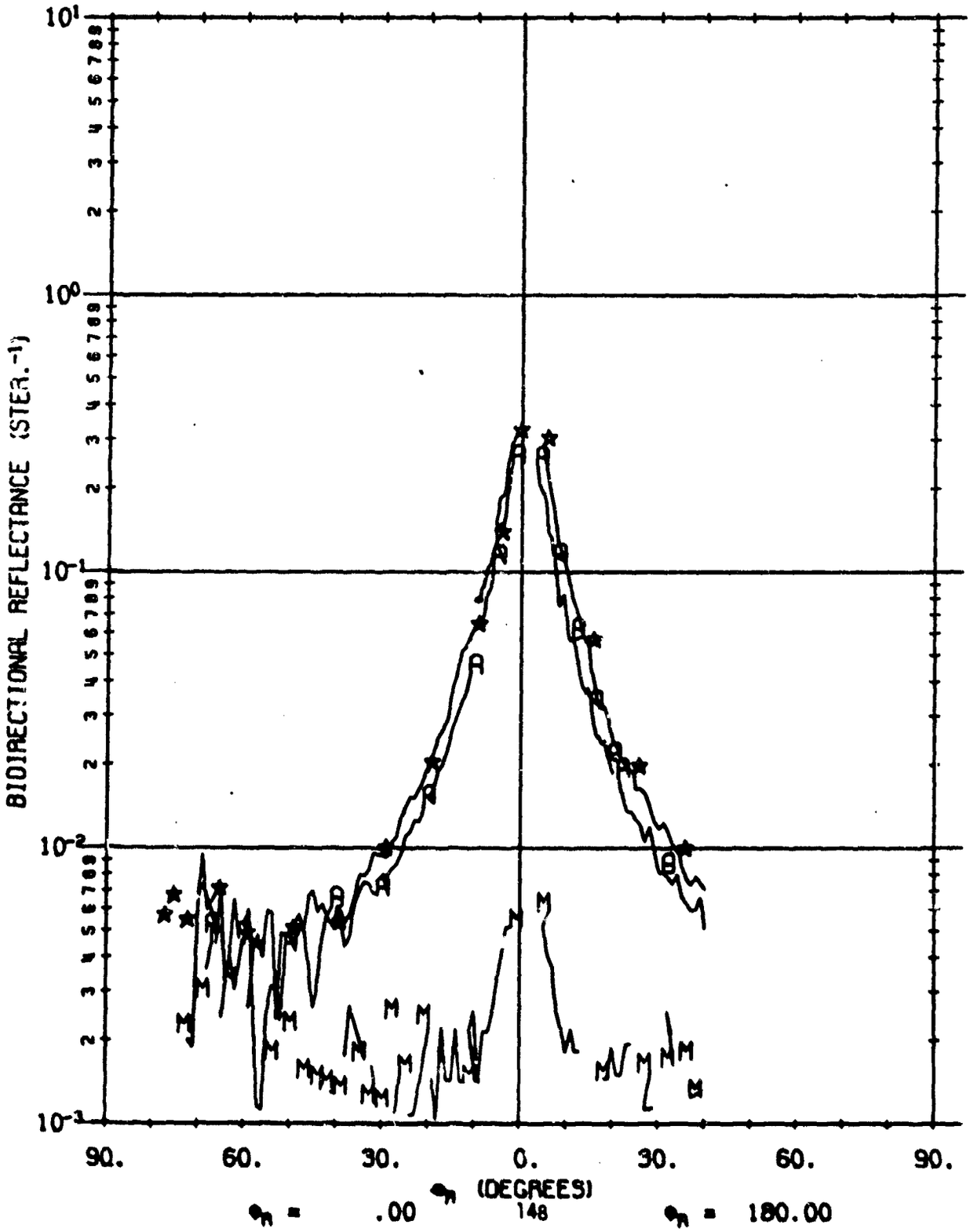

A01610 303

λ = 3.39
Φ_I = 20.0
Φ_I = 180.0

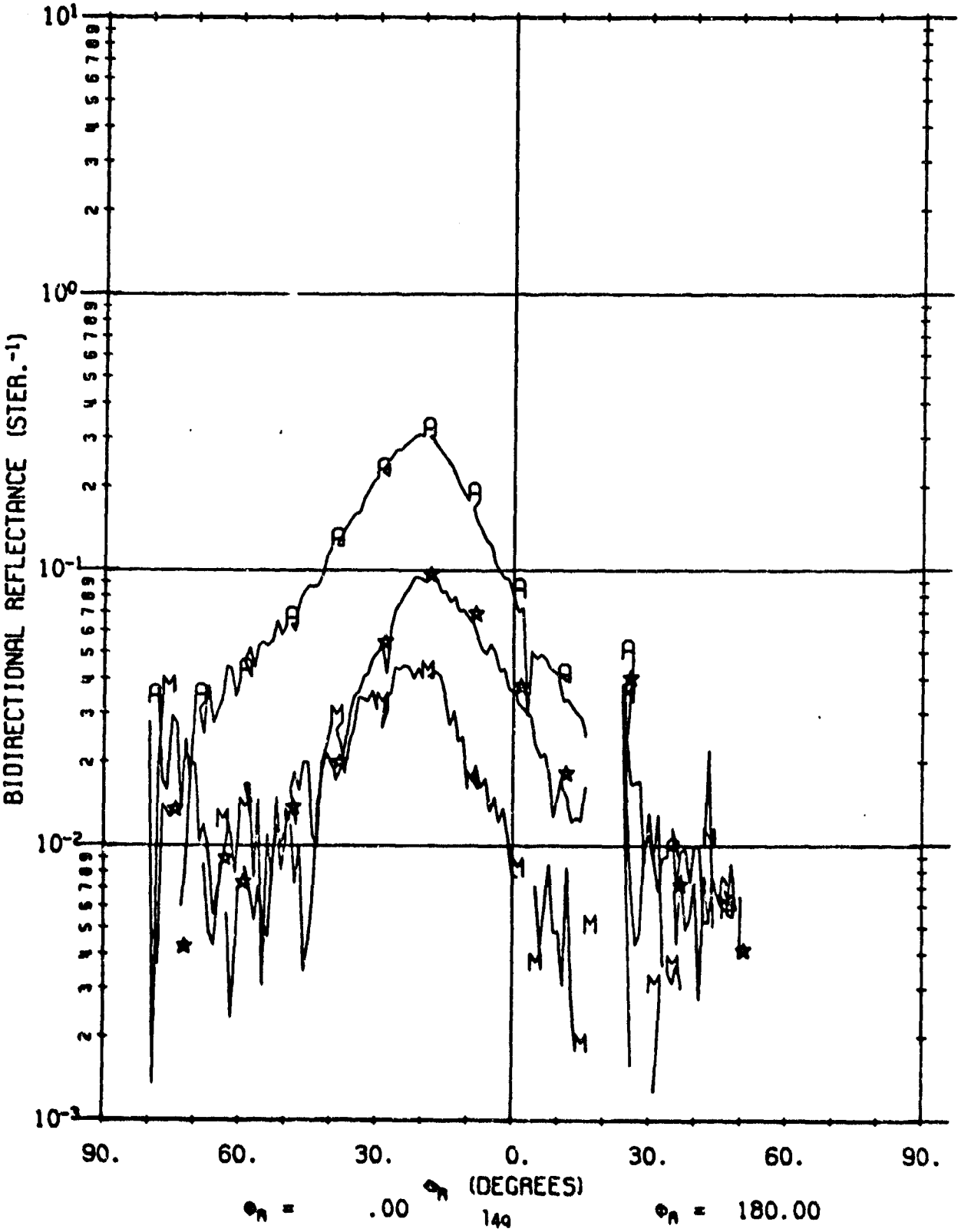

A01610 203

λ = 10.60
θ_I = 20.0
ϕ_I = 180.0

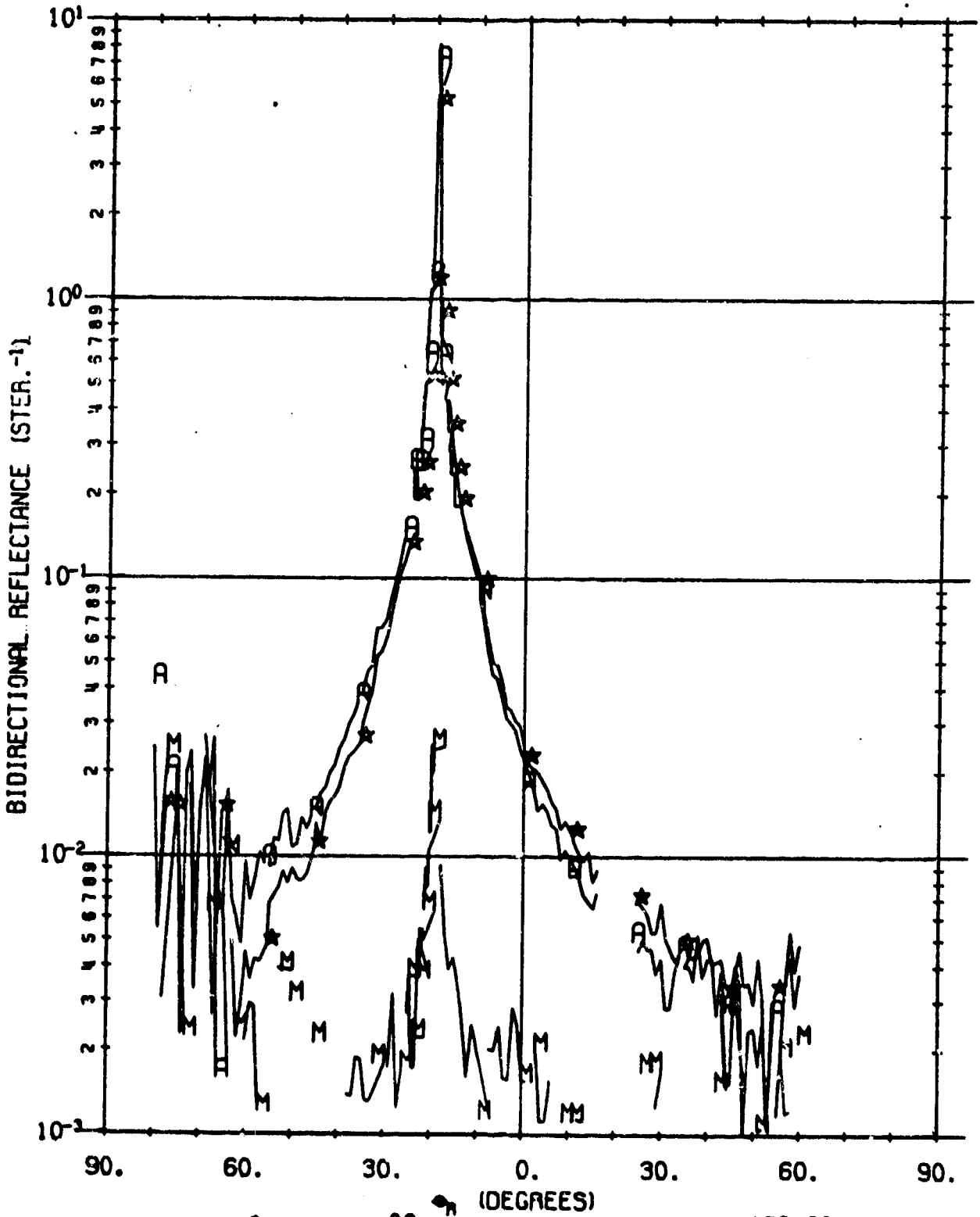

ϕ_R = .00 ϕ_R = 180.00

A01610 303

λ = 3.39
Φ_1 = 20.0
Φ_1 = 180.0

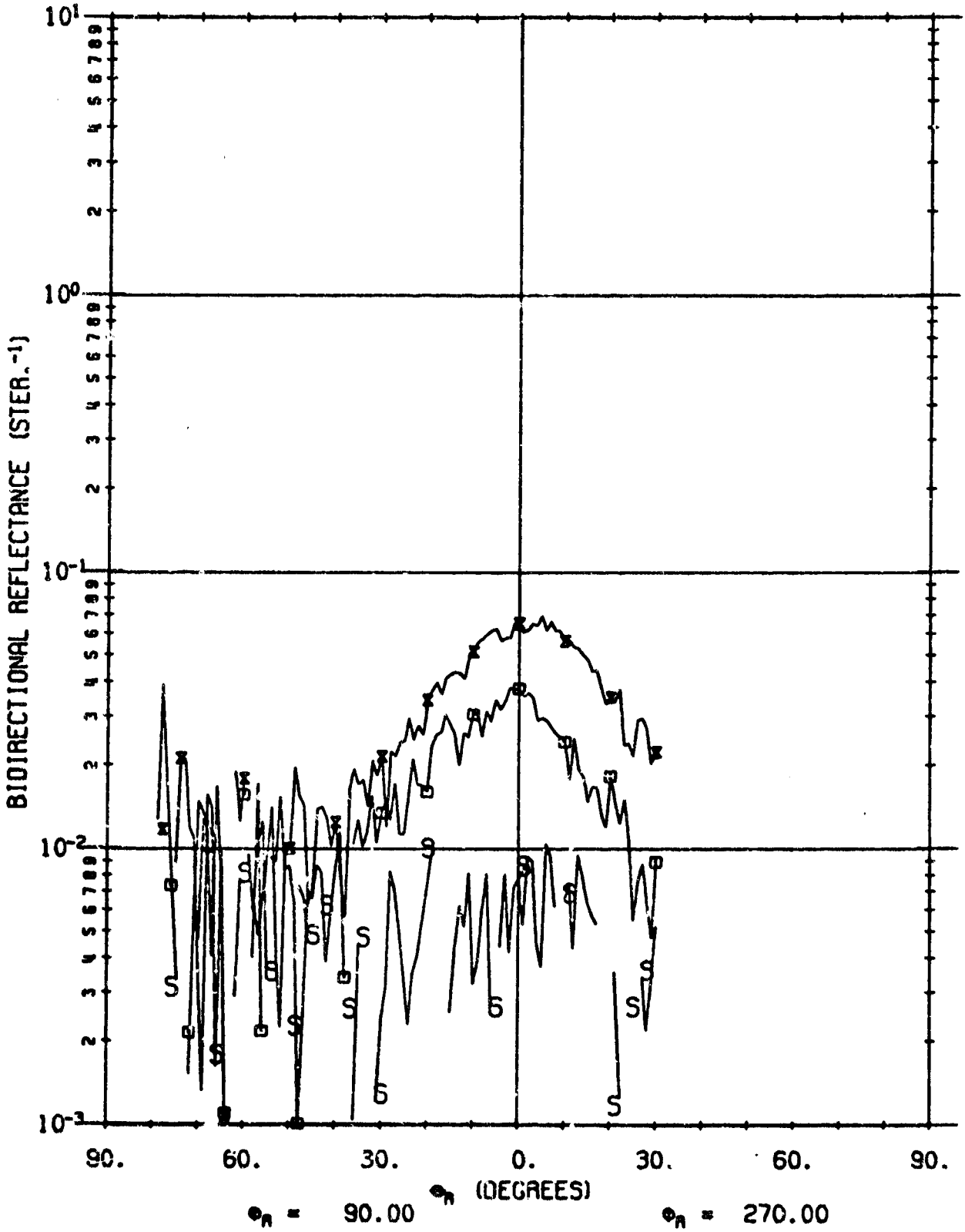

Φ_R = 90.00 Φ_R = 270.00

A01610 203

λ = 10.60
θ_I = 20.0
φ_I = 160.0

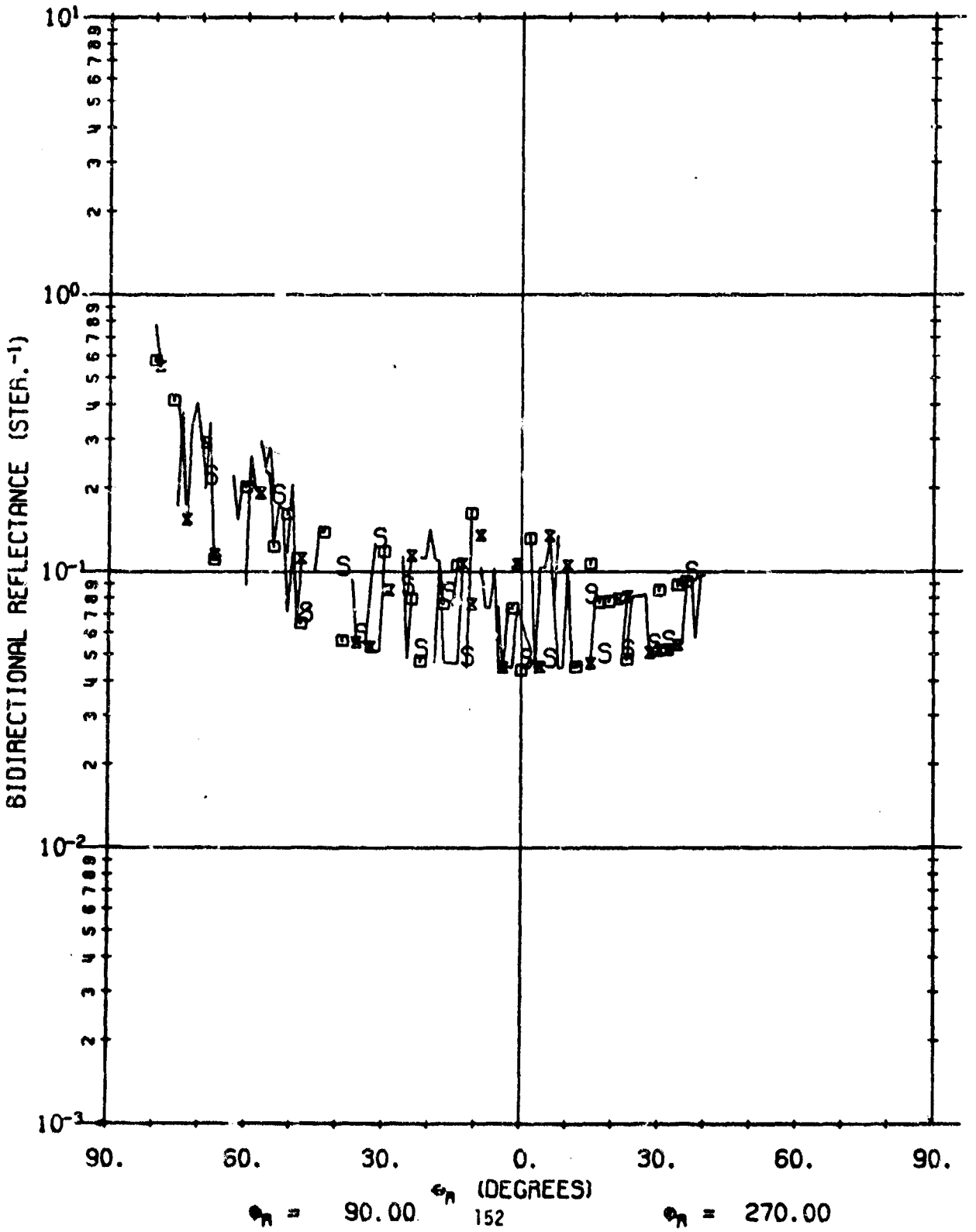

A01610 303

λ = 3.39
Φ_I = 40.0
Φ_I = 180.0

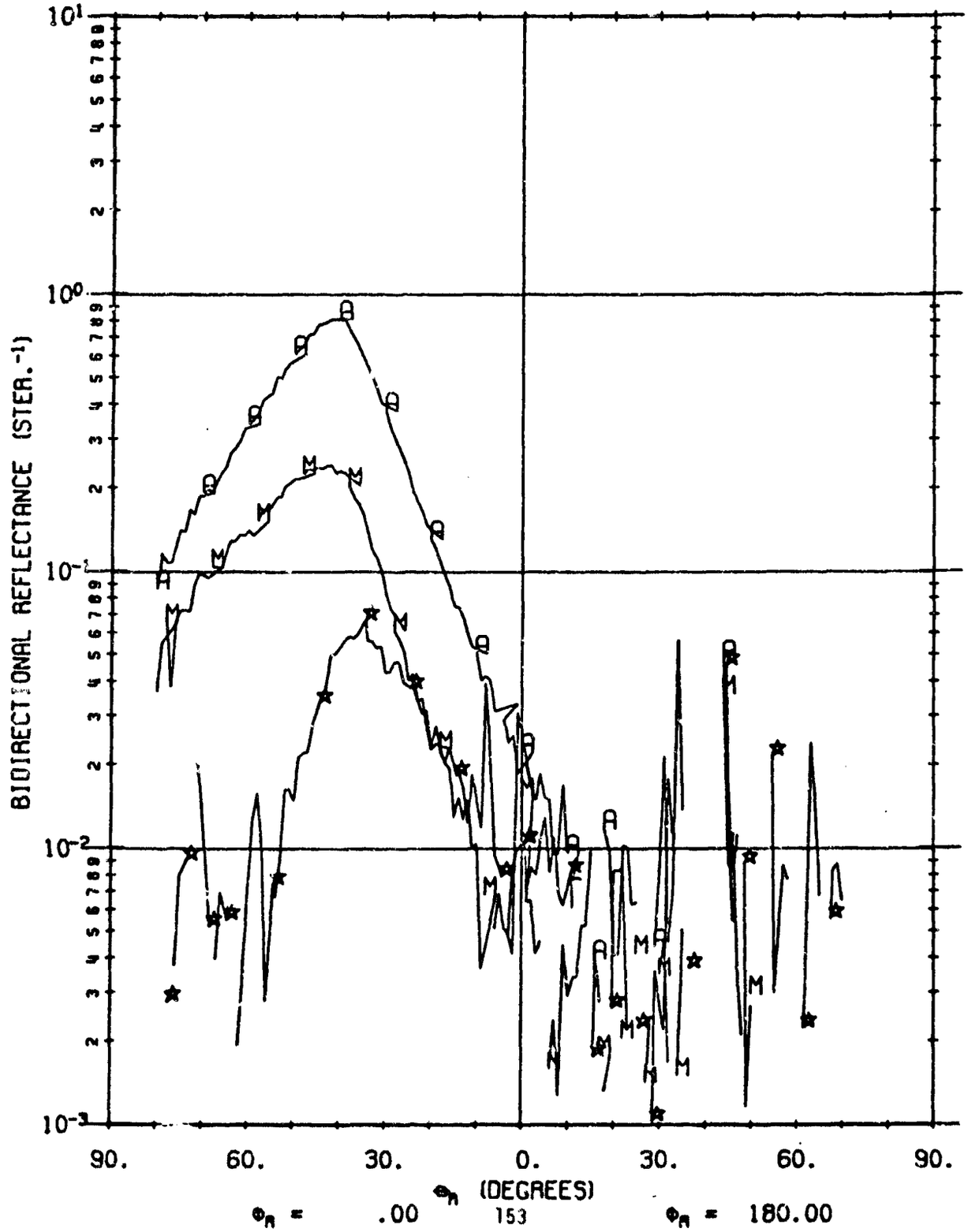

H01610 203

λ = 10.60
Φ_I = 40.0
Φ_I = 180.0

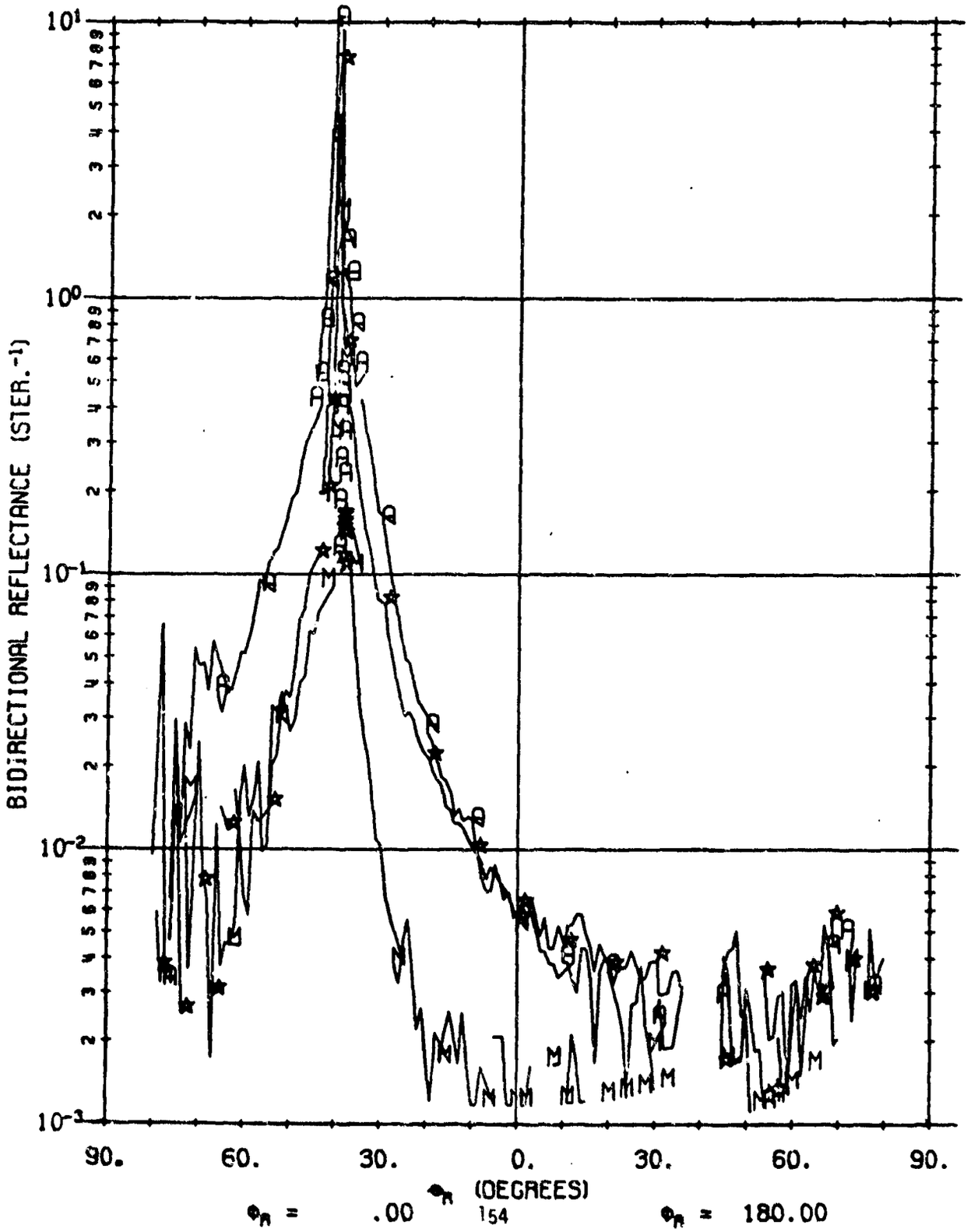

A01610 303

λ = 3.39
Φ_I = 40.0
Φ_I = 180.0

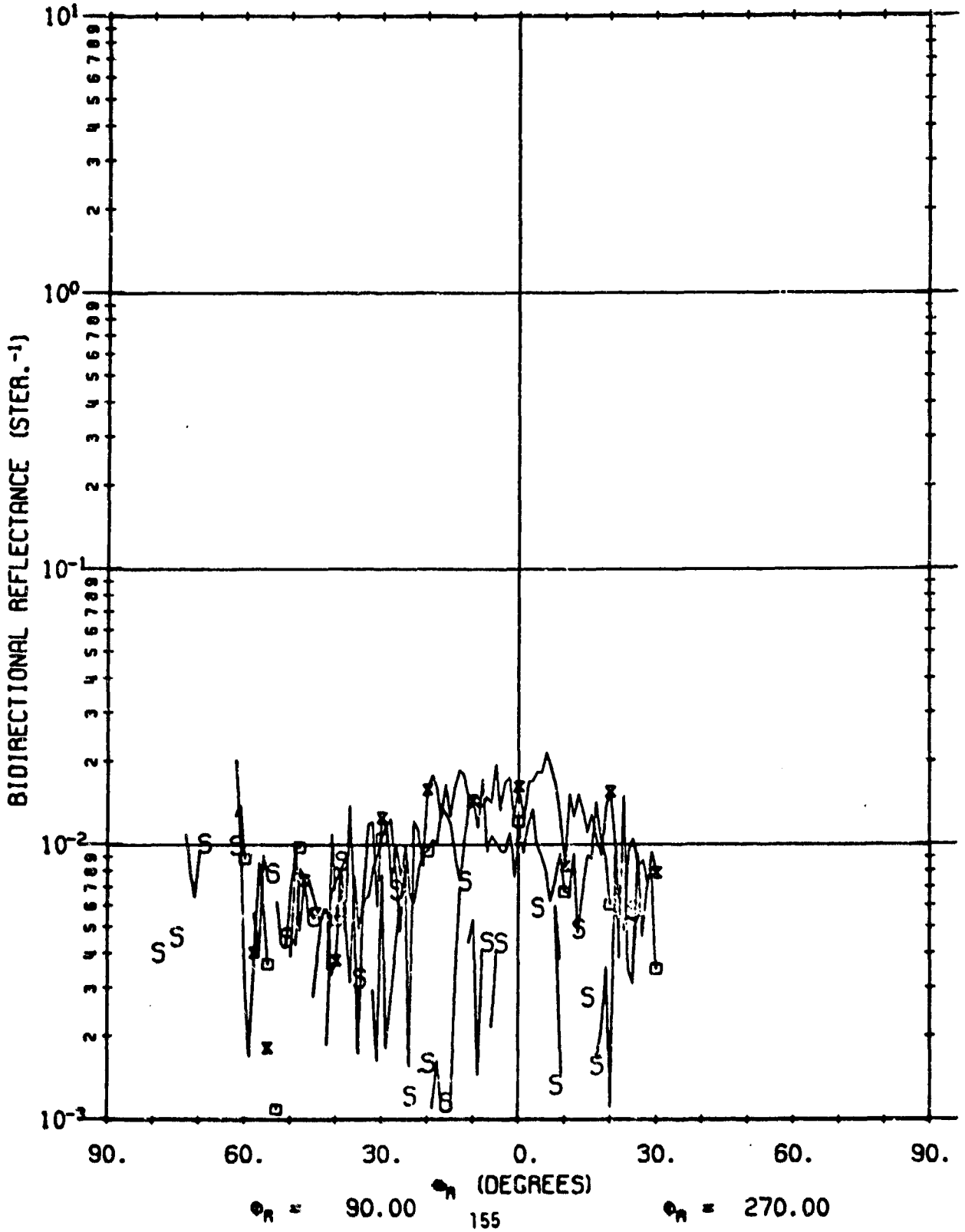

A01610 303

λ = 3.39
Φ_I = 60.0
Θ_I = 180.0

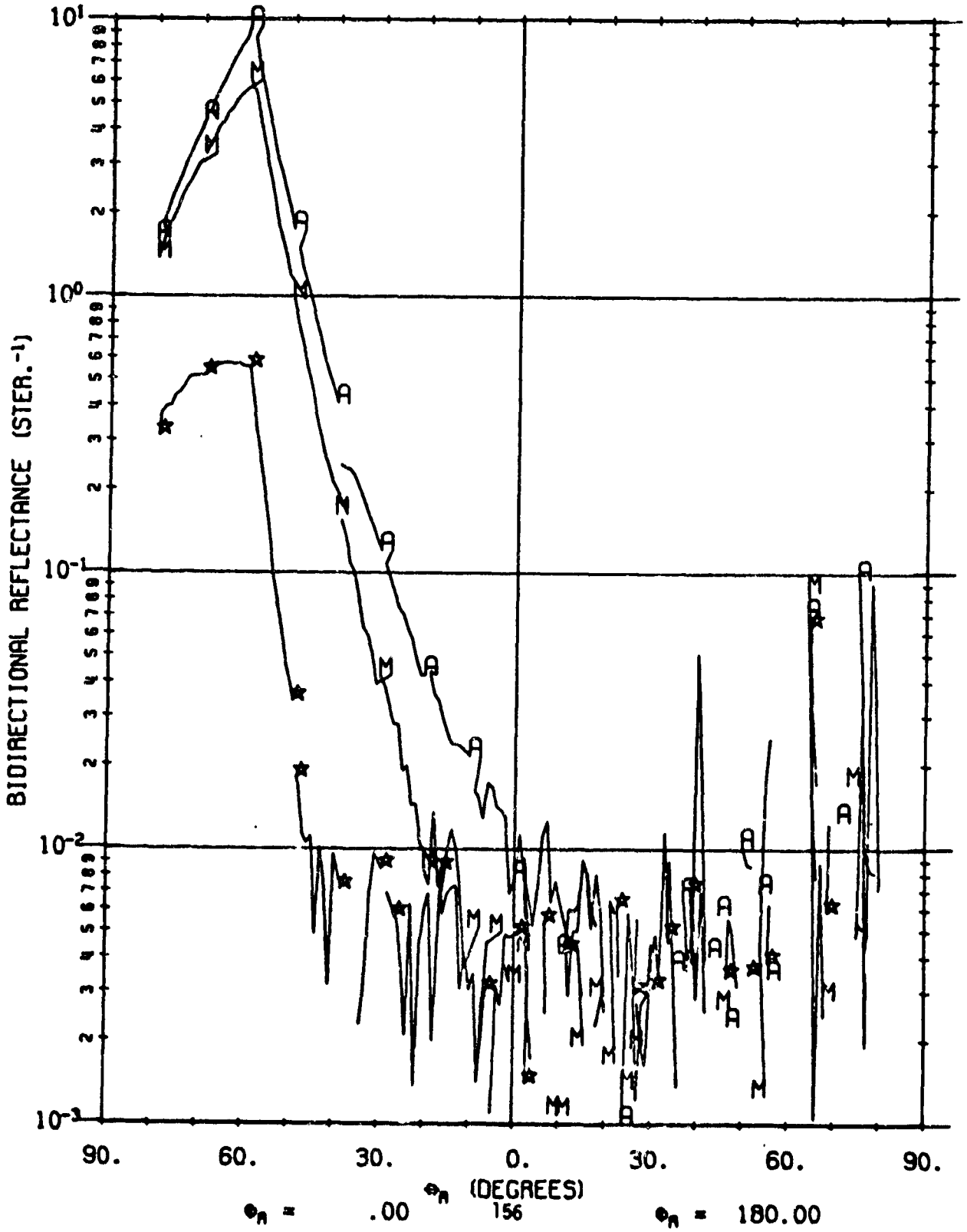

A01610 203

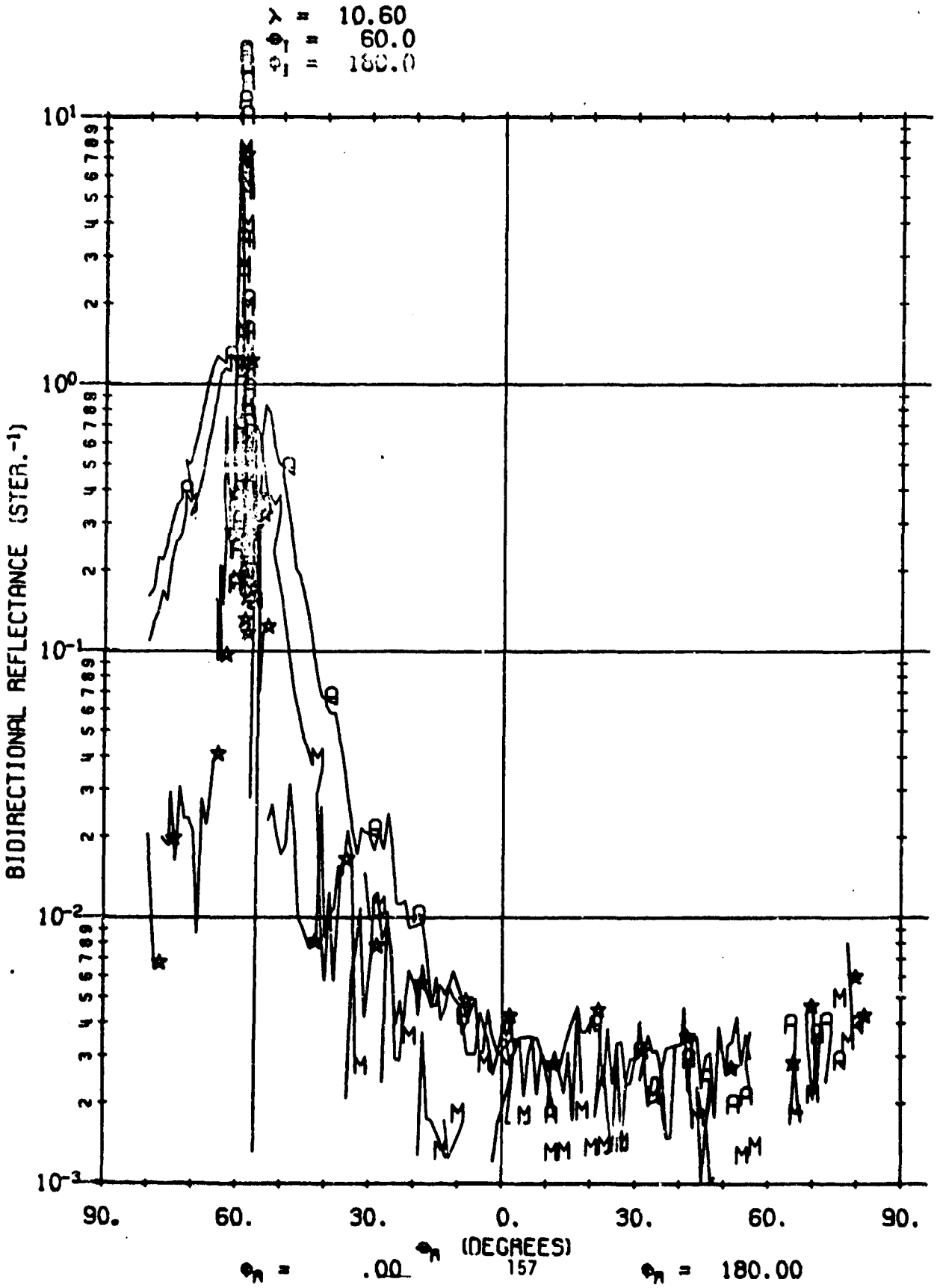
λ = 10.60
θi = 60.0
φi = 180.0
BIDIRECTIONAL REFLECTANCE (STER.-1)
10^1
10^0
10^-1
10^-2
10^-3
90.
60.
30.
0.
30.
60.
90.
θr (DEGREES)
φr = .00
φr = 180.00

A01610 303

λ = 3.39
θ_I = 60.0
ϕ_I = 180.0

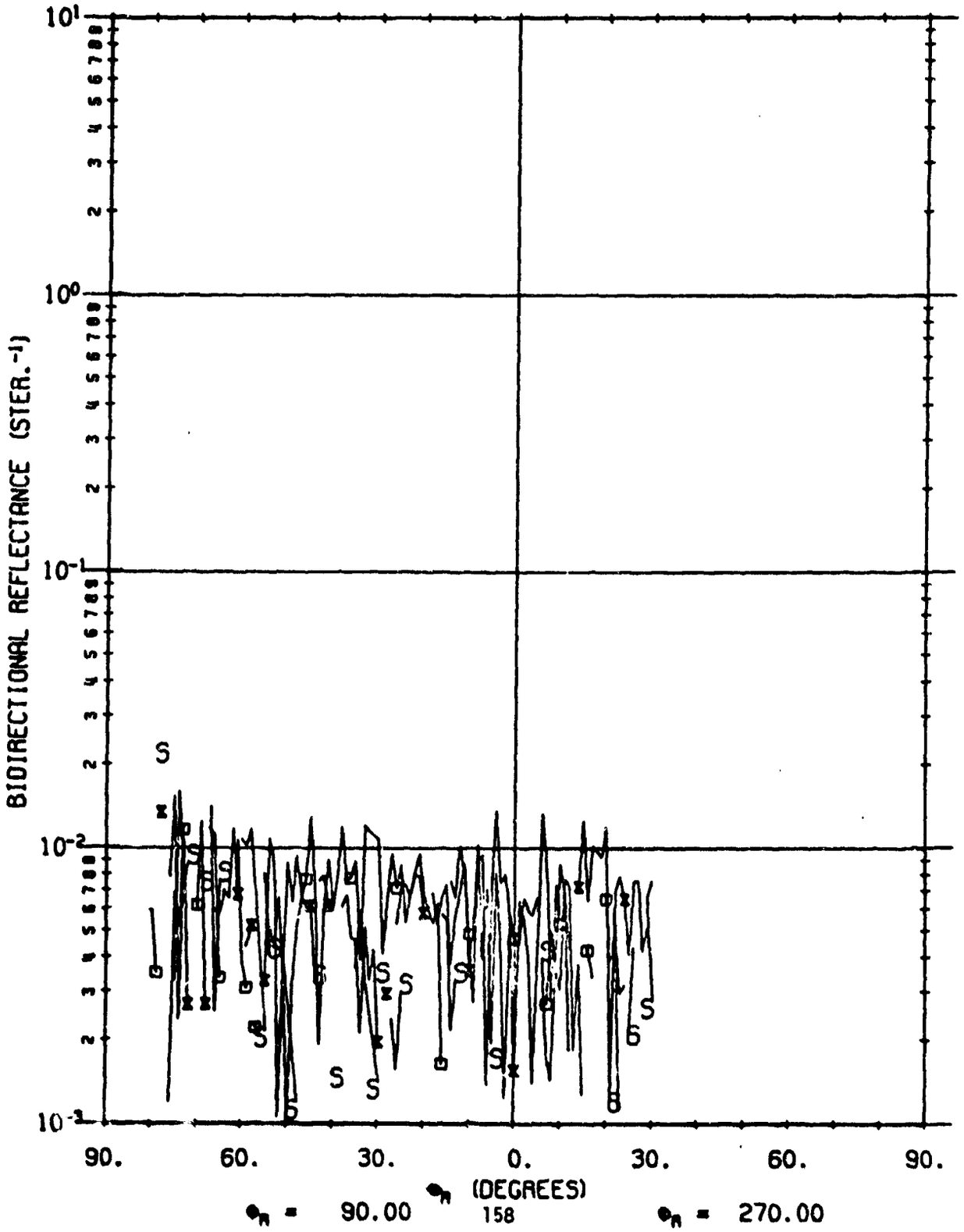

A01610 101

λ = .63
ϕ_J = .0
θ_J = 180.0

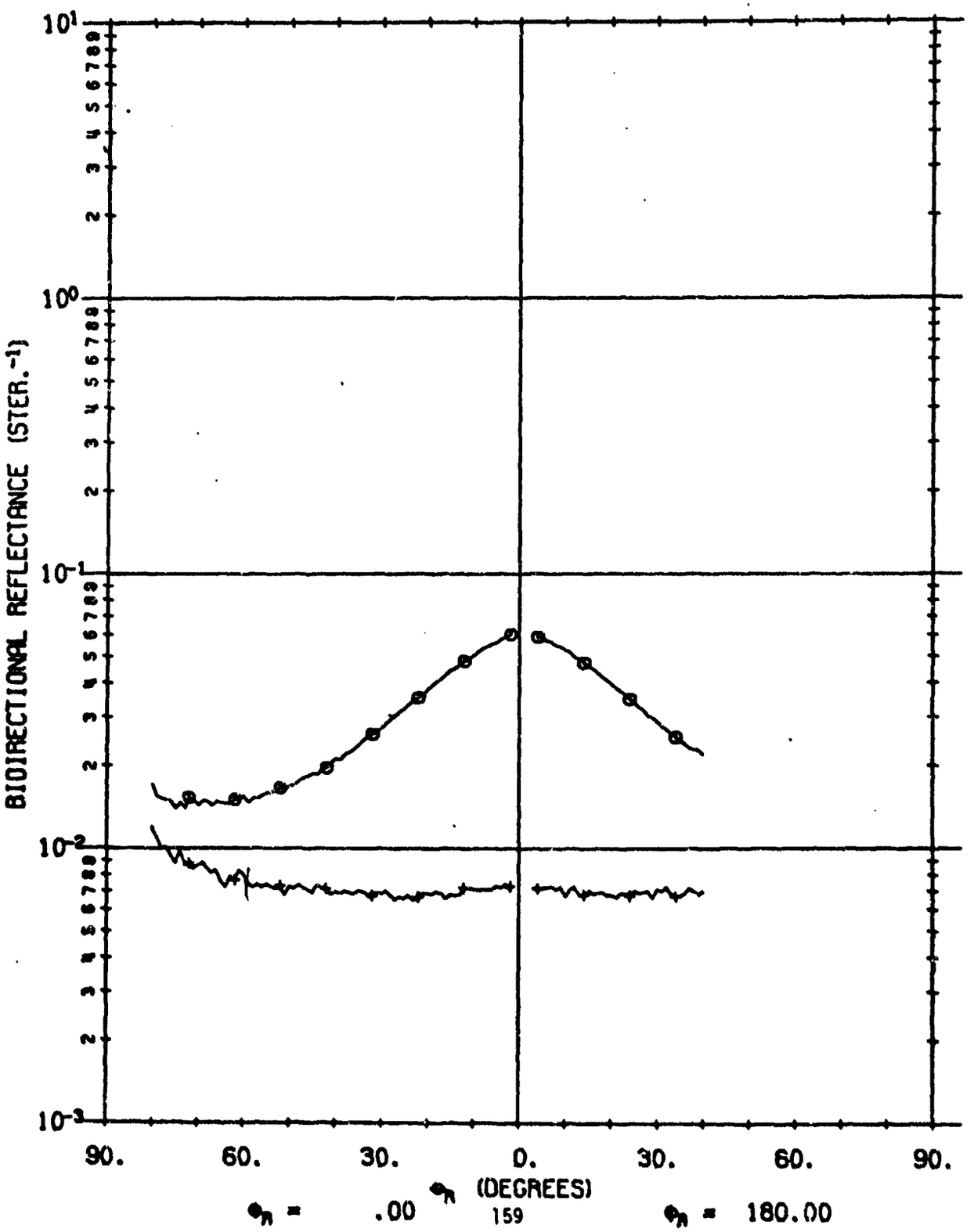

A01610 102

λ = 1.06
θ_i = .0
ϕ_i = 180.0

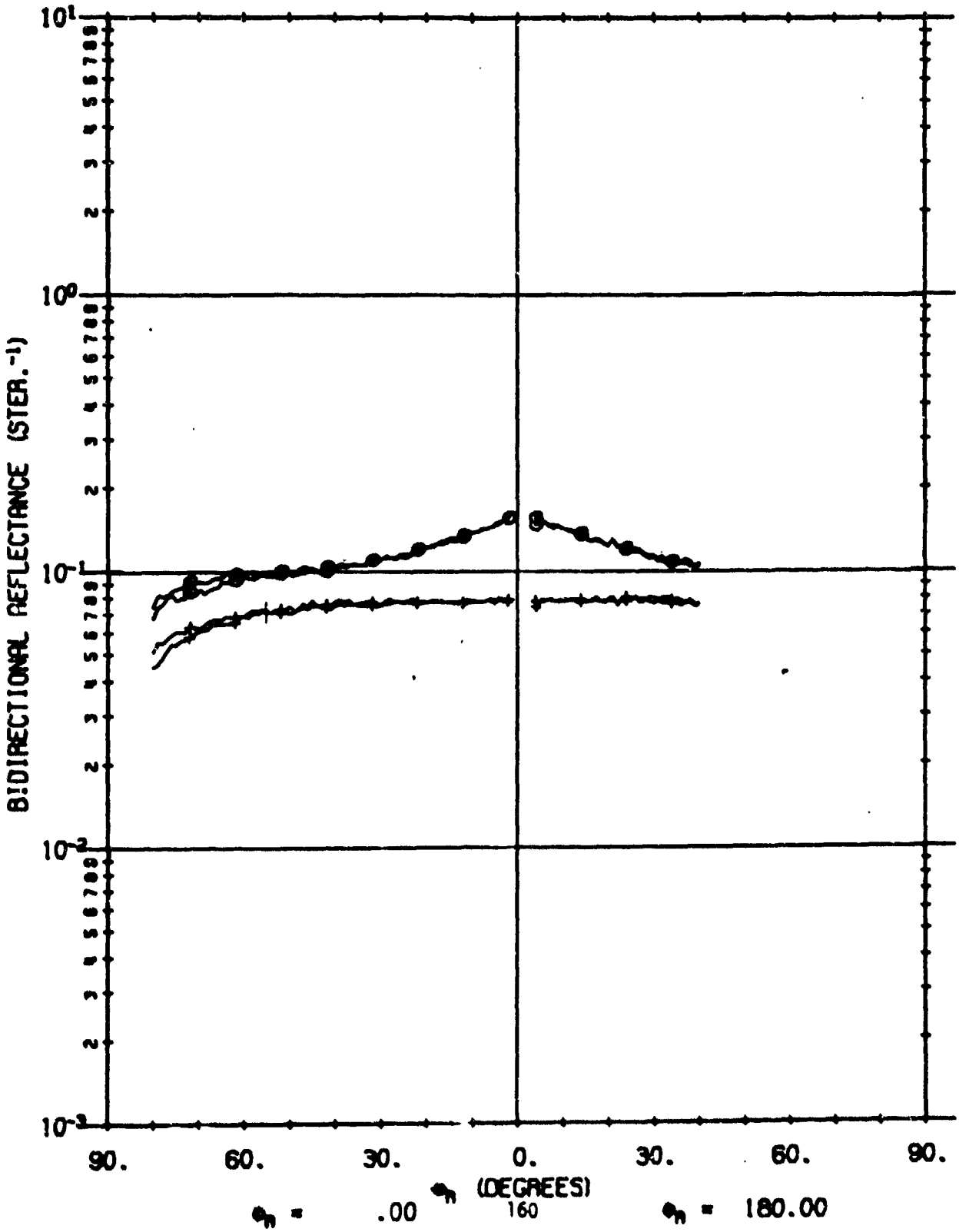

A01610 301

λ = 3.39
ϕ_1 = .0
θ_1 = 180.0

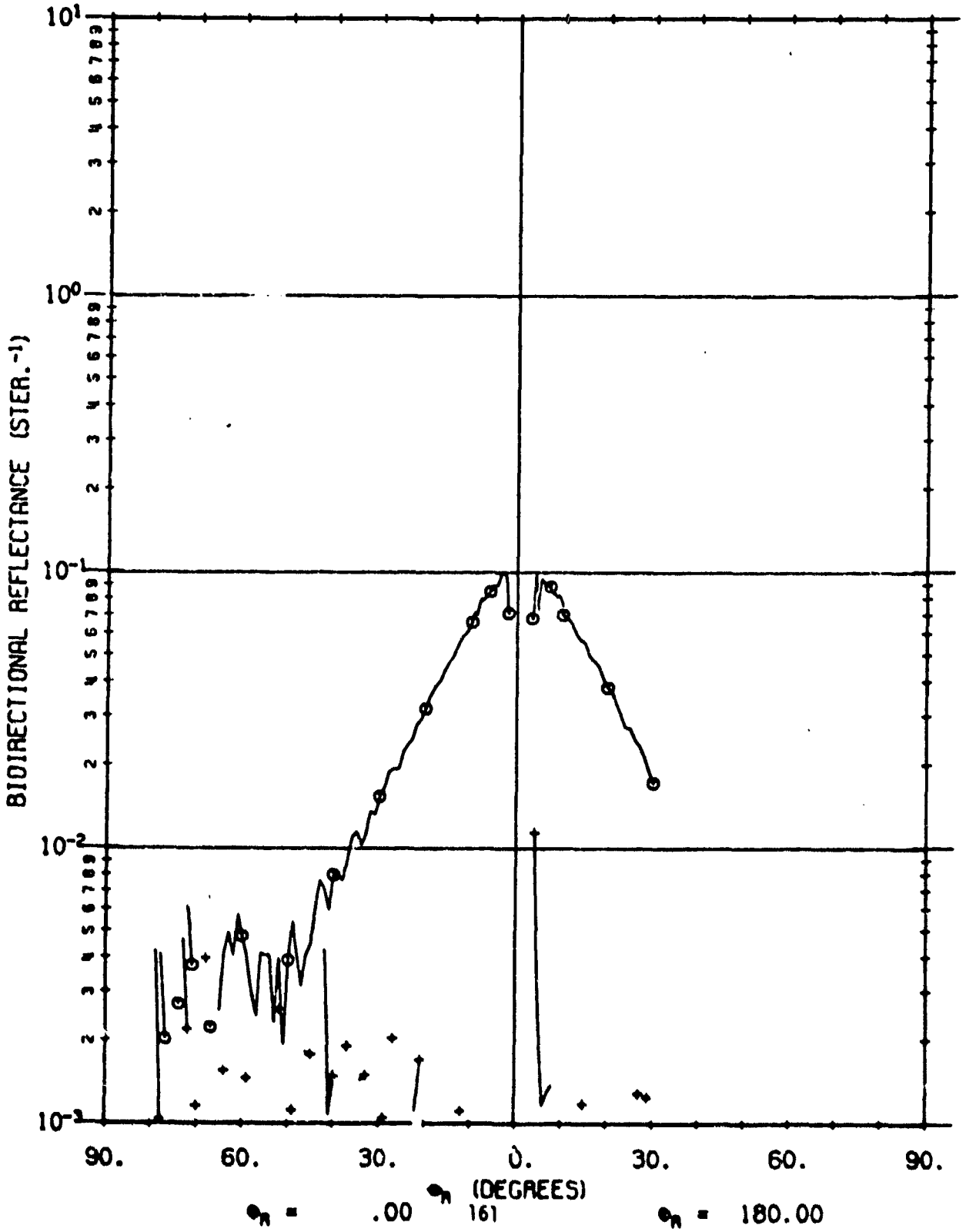

A01610 204

λ = 10.60
ϕ_I = .0
ϕ_t = 180.0

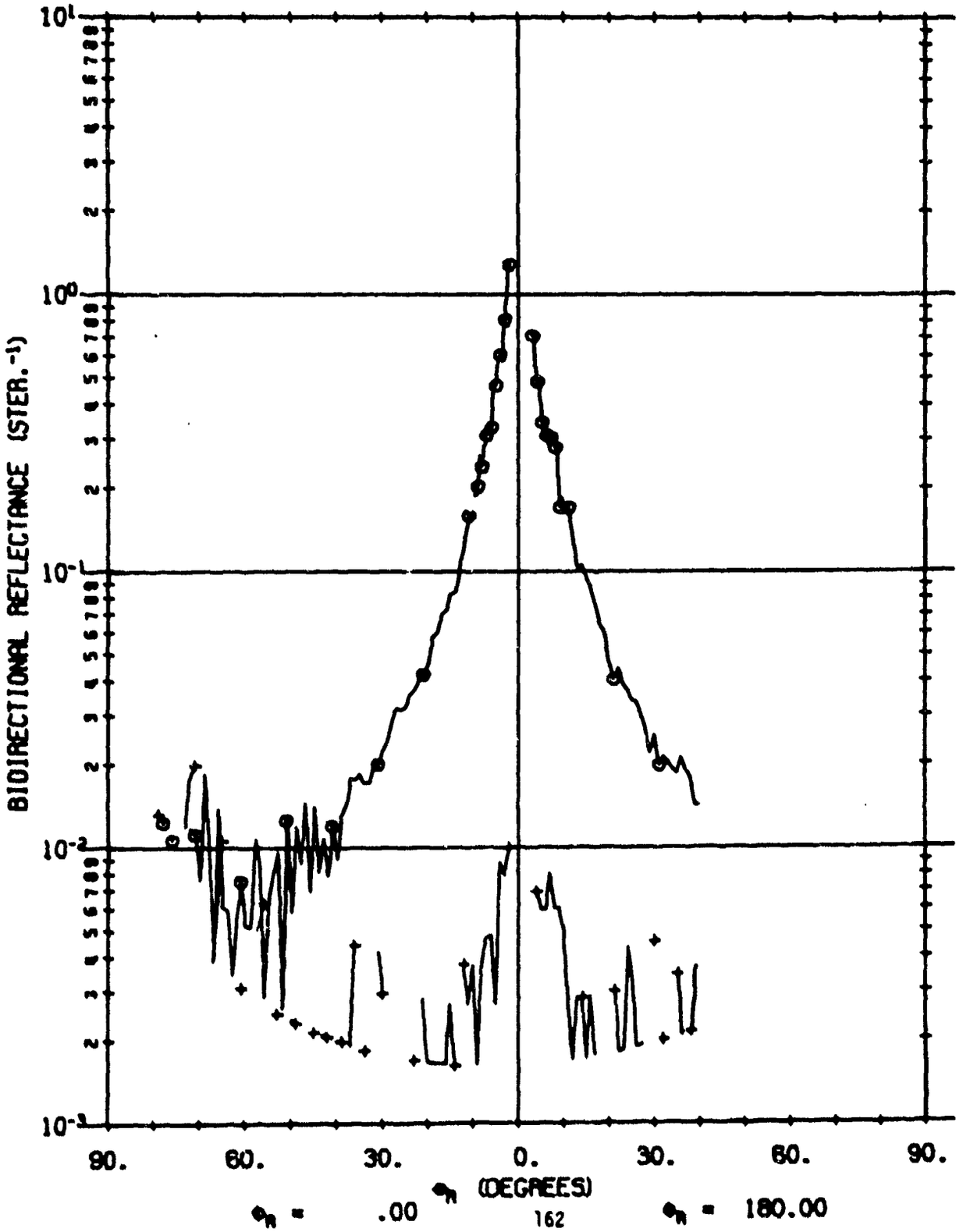

A01610 101

λ = .63
θ_I = 20.0
ϕ_I = 180.0

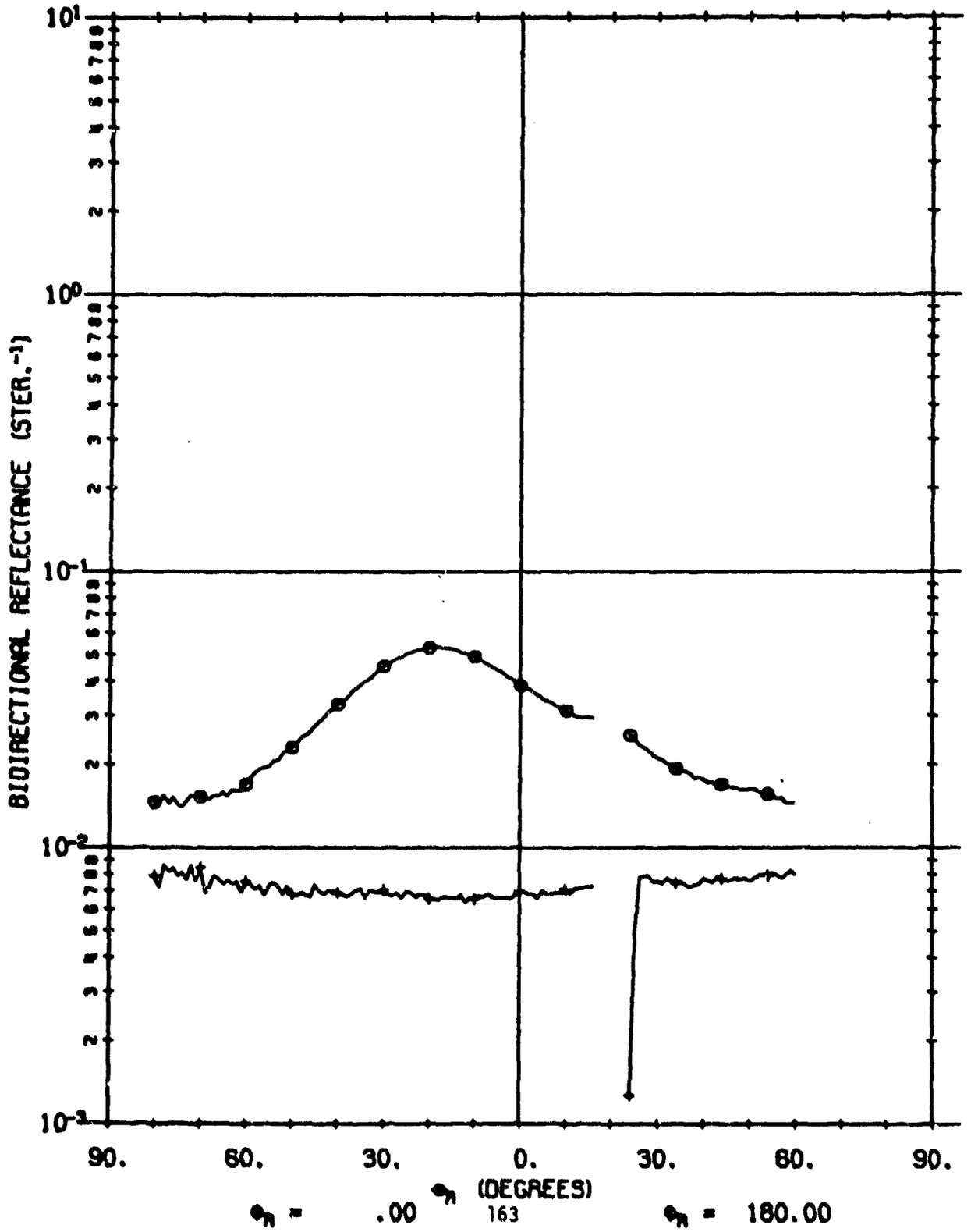

A01610 102

λ = 1.06
θ_I = 20.0
ϕ_I = 180.0

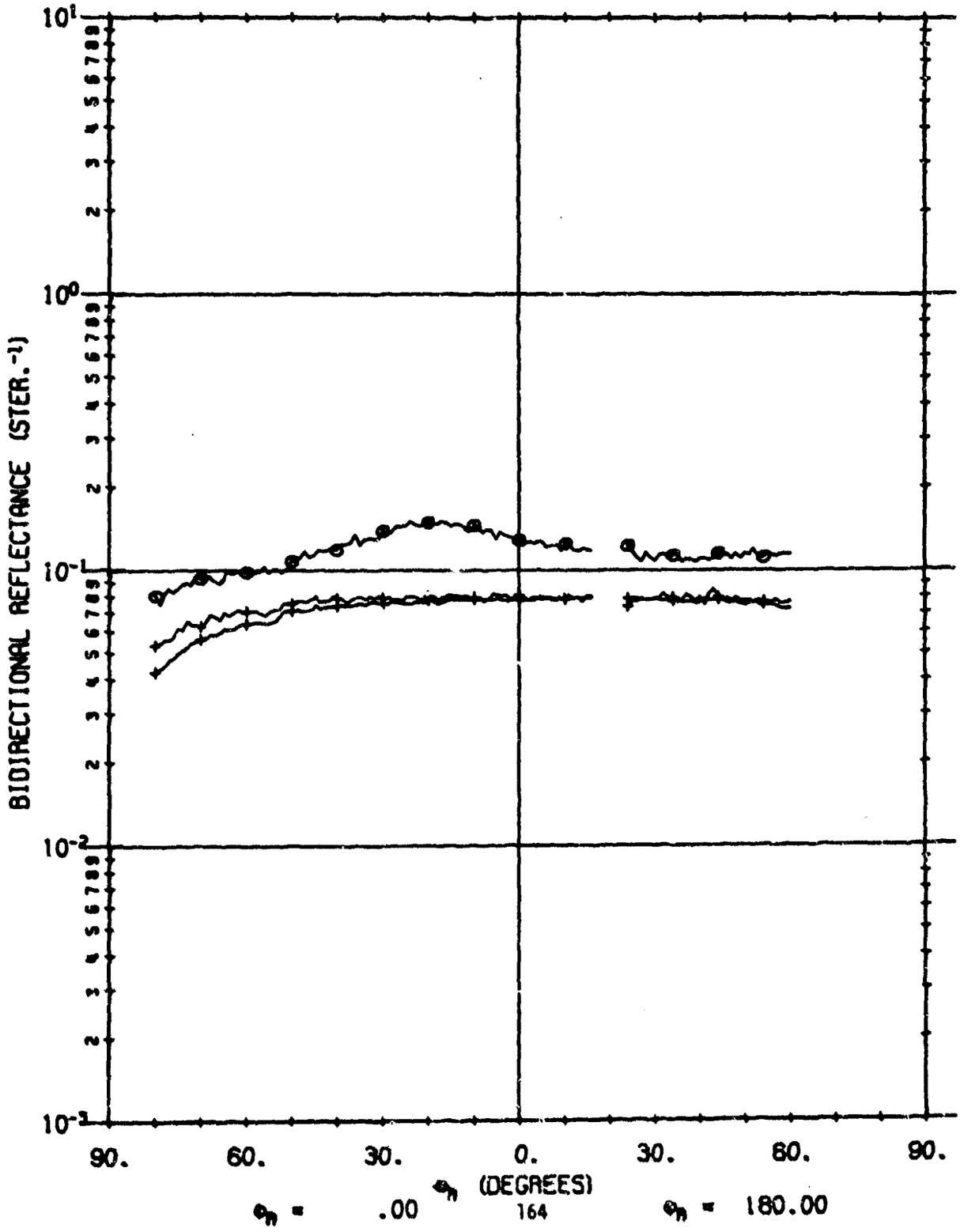

A01610 301

λ = 3.39
θ_I = 20.0
ϕ_I = 180.0

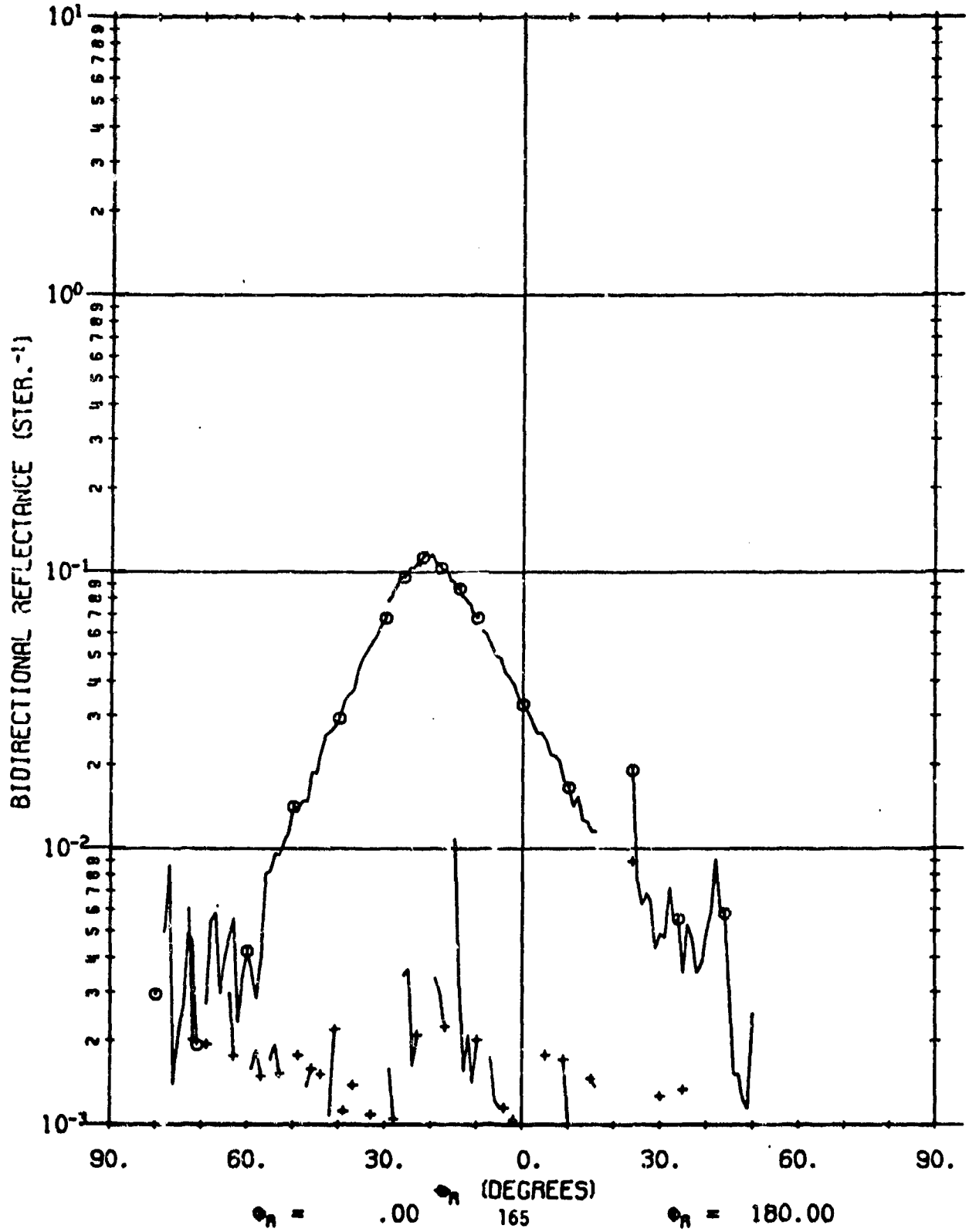

A01610 204

λ = 10.60
θ_I = 20.0
ϕ_I = 180.0

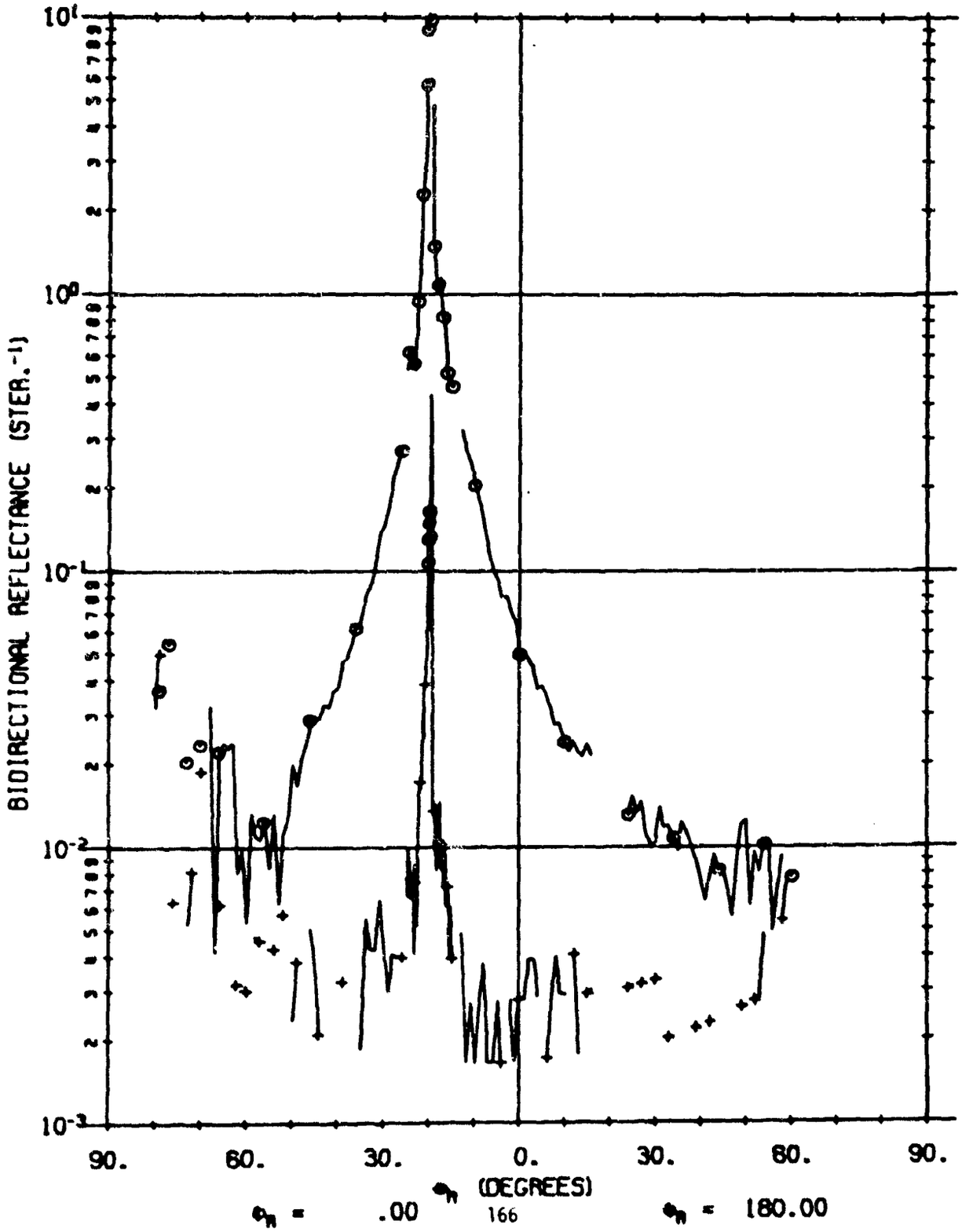

A01610 101

λ = .63
ϕ_I = 20.0
θ_I = 180.0

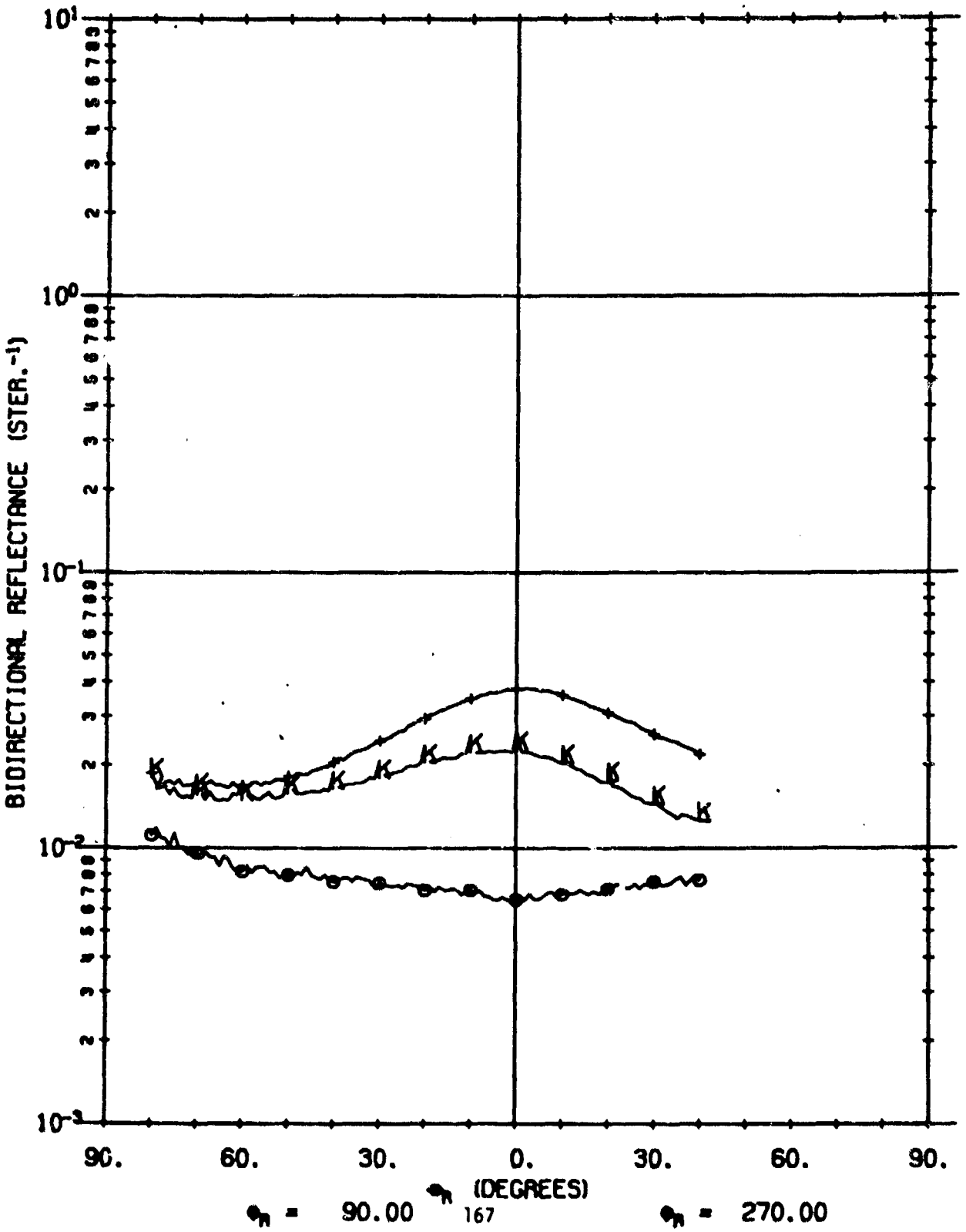

A01610 102

λ = 1.06
θ_r = 20.0
ϕ_i = .0

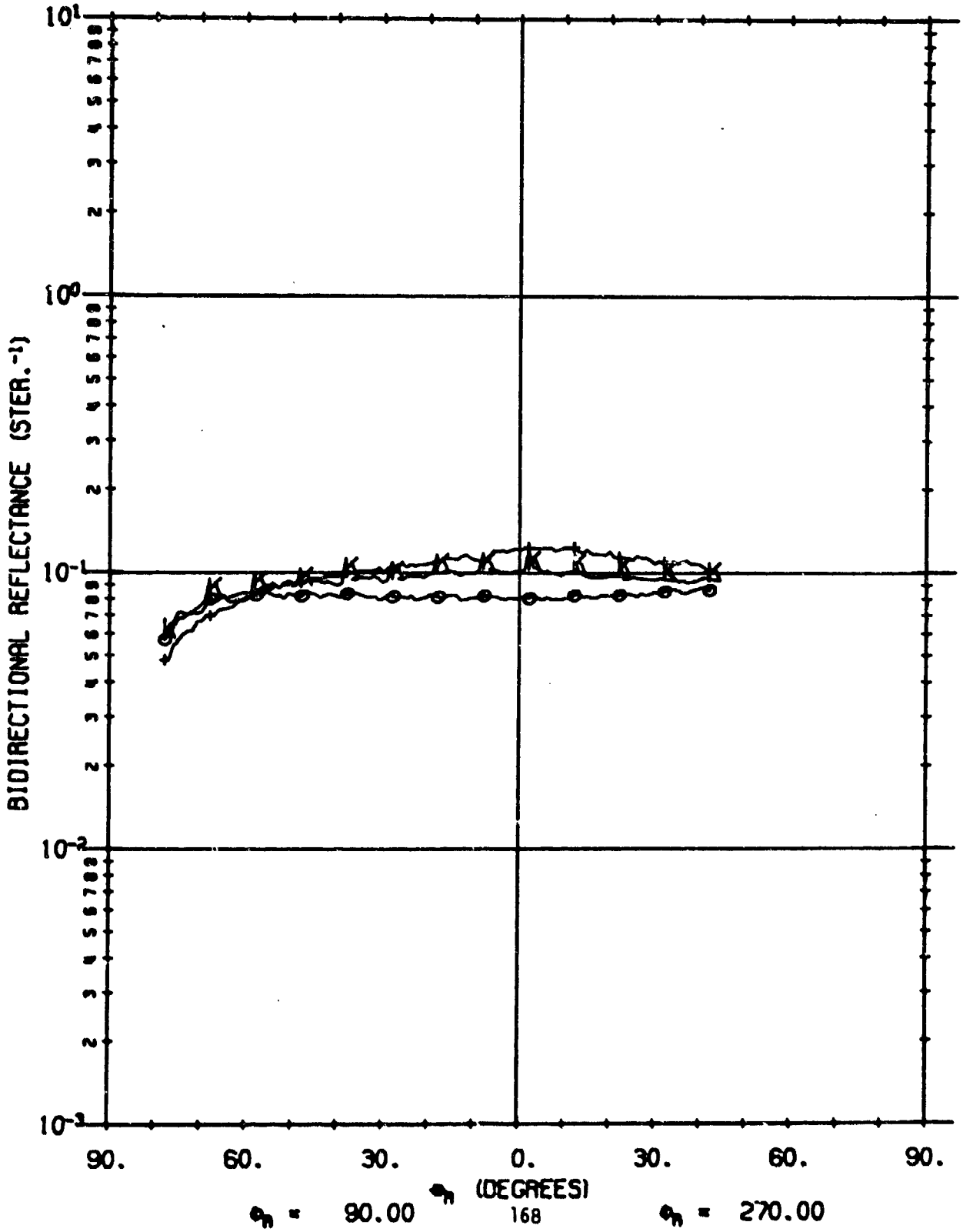

A01610 302

λ = 3.39
θ_I = 20.0
ϕ_I = 180.0

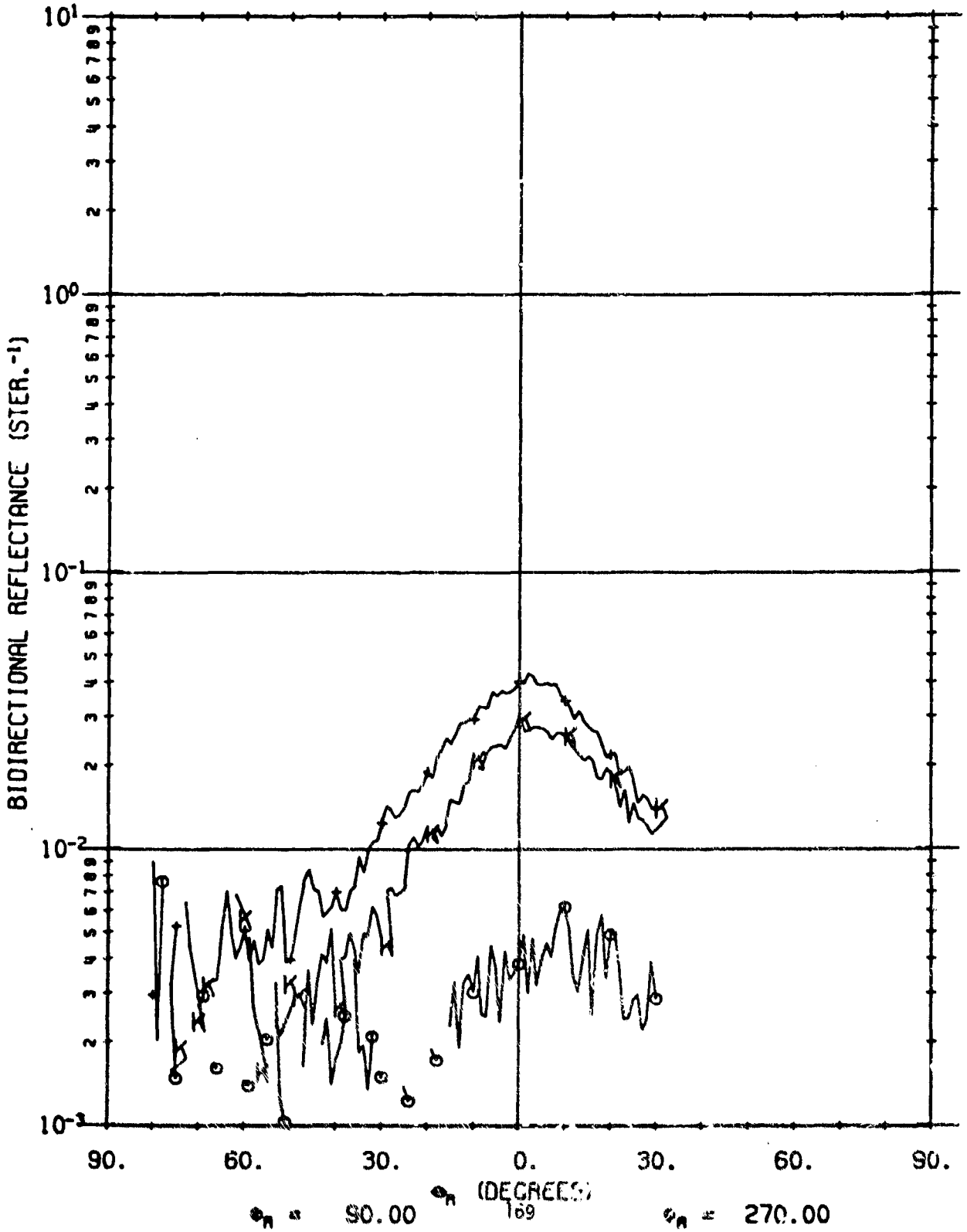

H01610 101

λ = .63
ϕ_1 = 40.0
θ_1 = 180.0

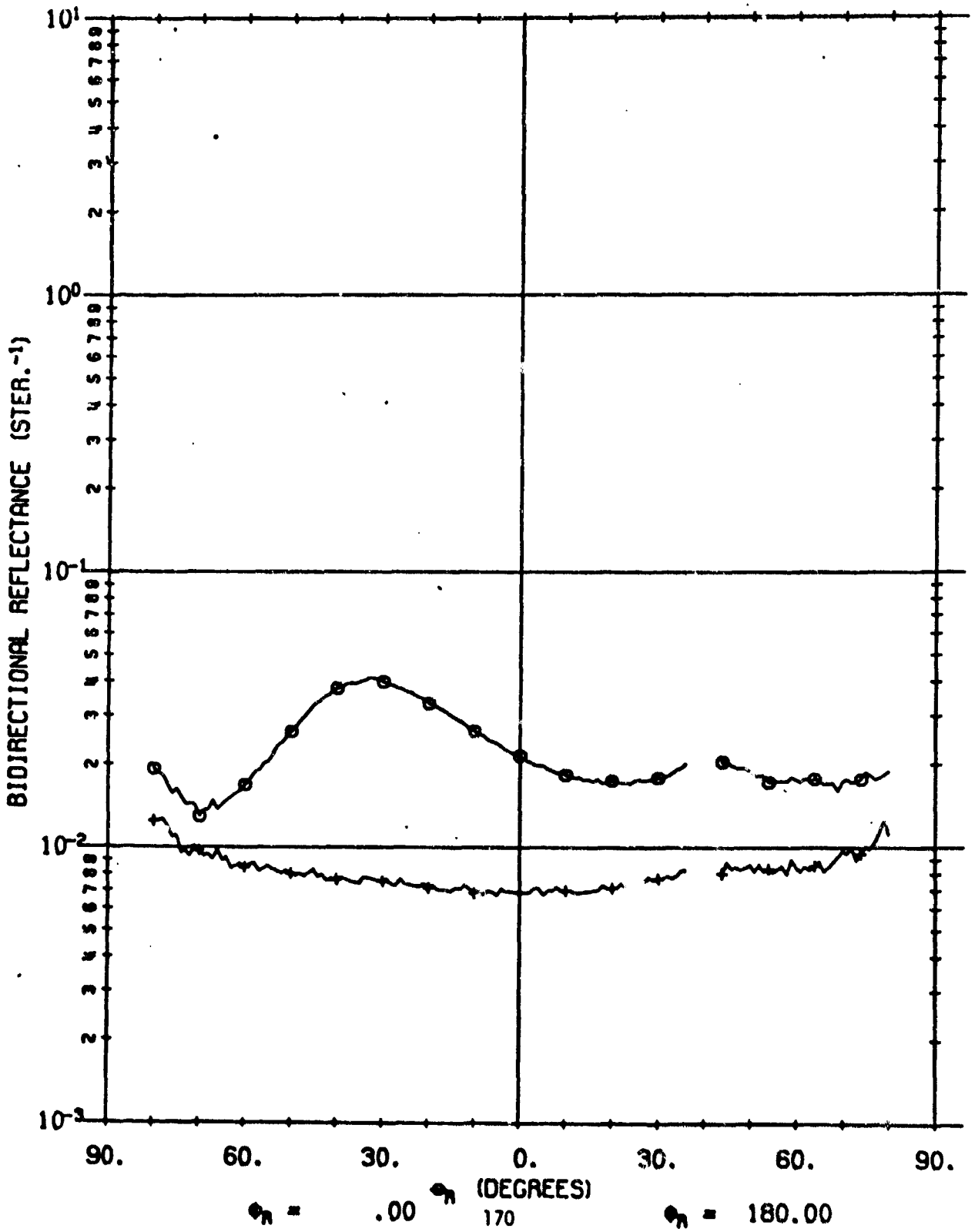

A01610 102

λ = 1.06
θ_I = 40.0
ϕ_I = 180.0

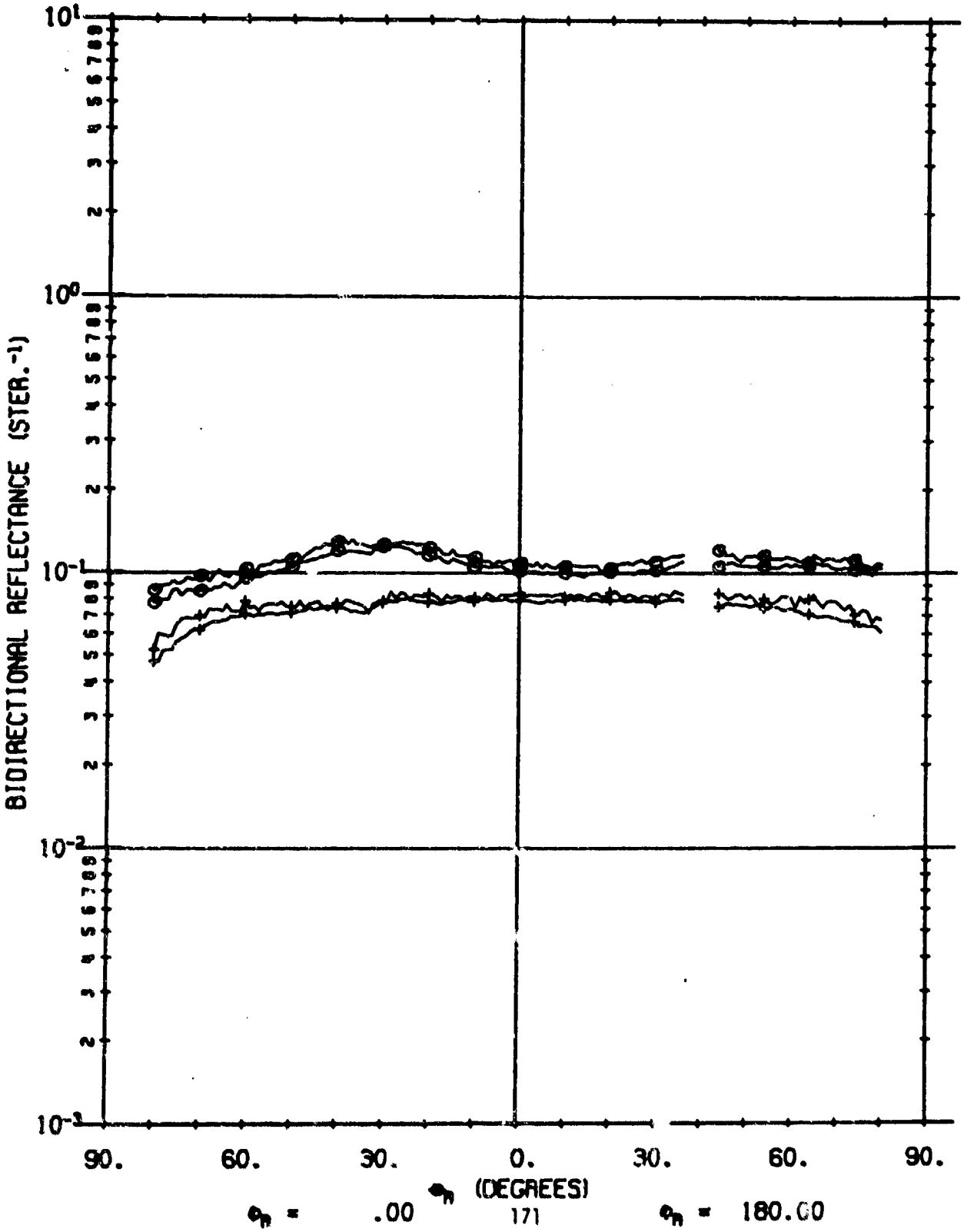

A01610 301

λ = 3.39
θ_I = 40.0
ϕ_I = 180.0

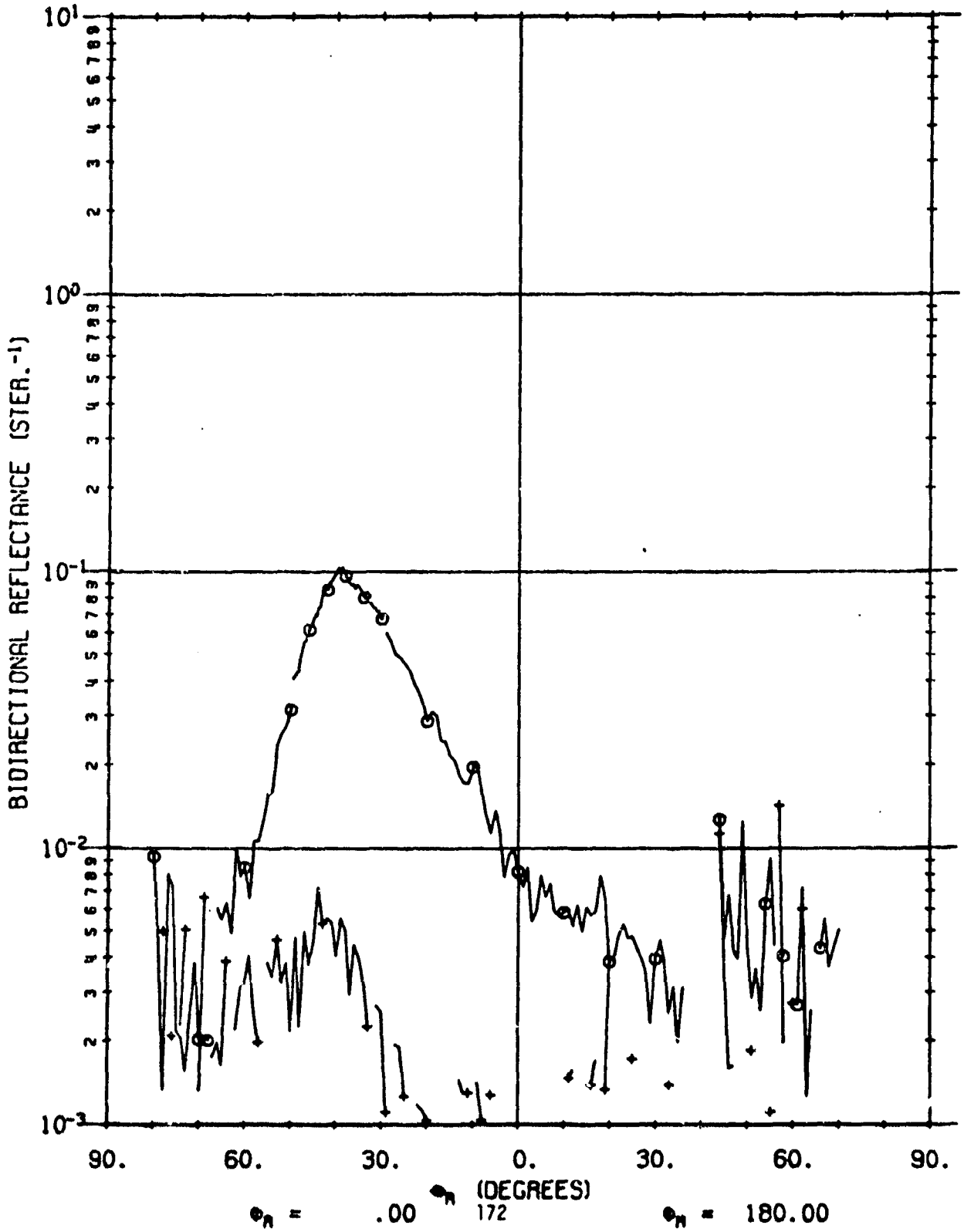

A01610 204

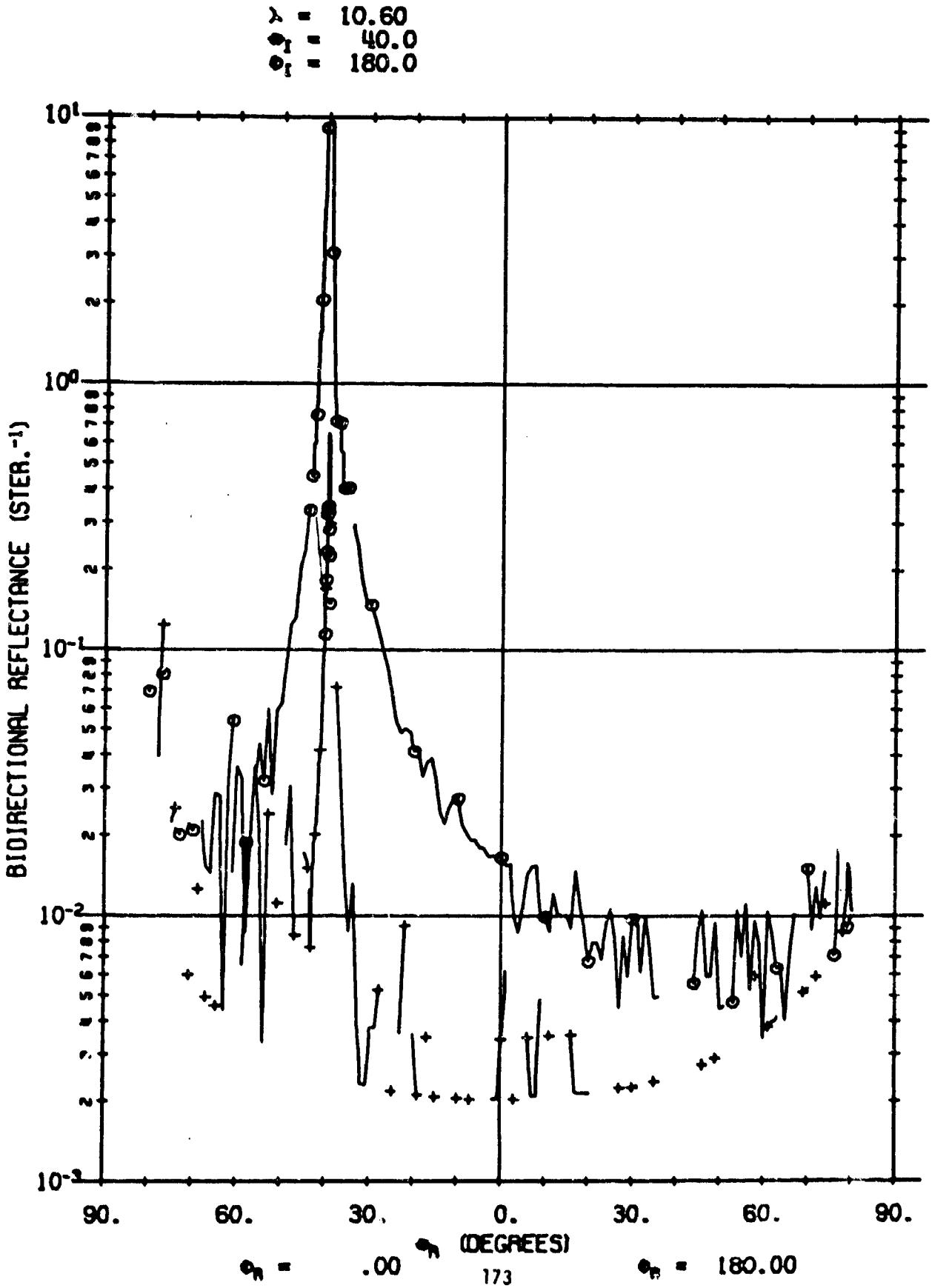
λ = 10.60
θI = 40.0
φI = 180.0
BIDIRECTIONAL REFLECTANCE (STER.-1)
10¹
10⁰
10⁻¹
10⁻²
10⁻³
90.
60.
30.
0.
30.
60.
90.
θR (DEGREES)
φR = .00
φR = 180.00

A01610 101

λ = .63
ϕ_I = 40.0
θ_I = 180.0

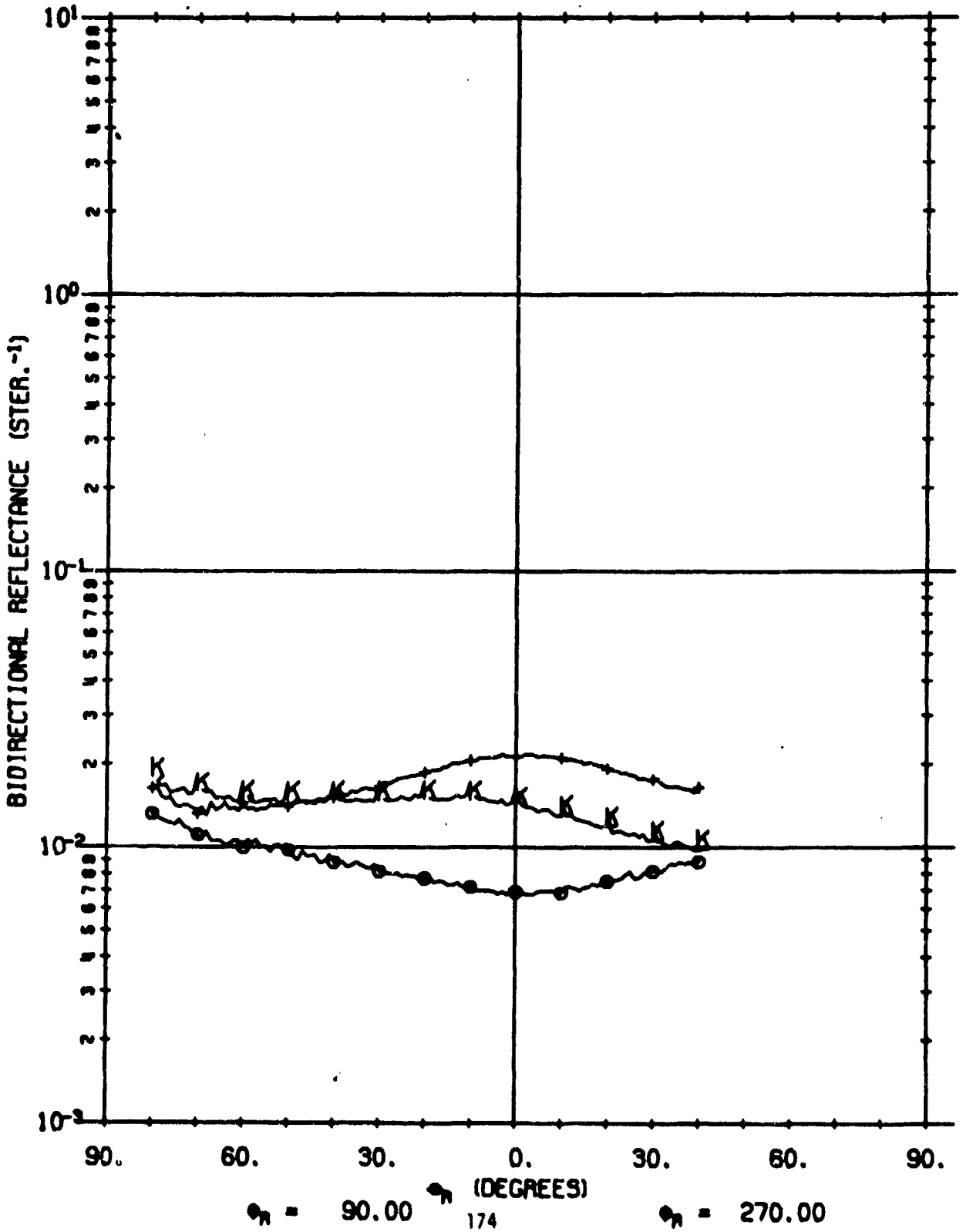

A01610 102

λ = 1.06
Φ_I = 10.0
θ_I = .0

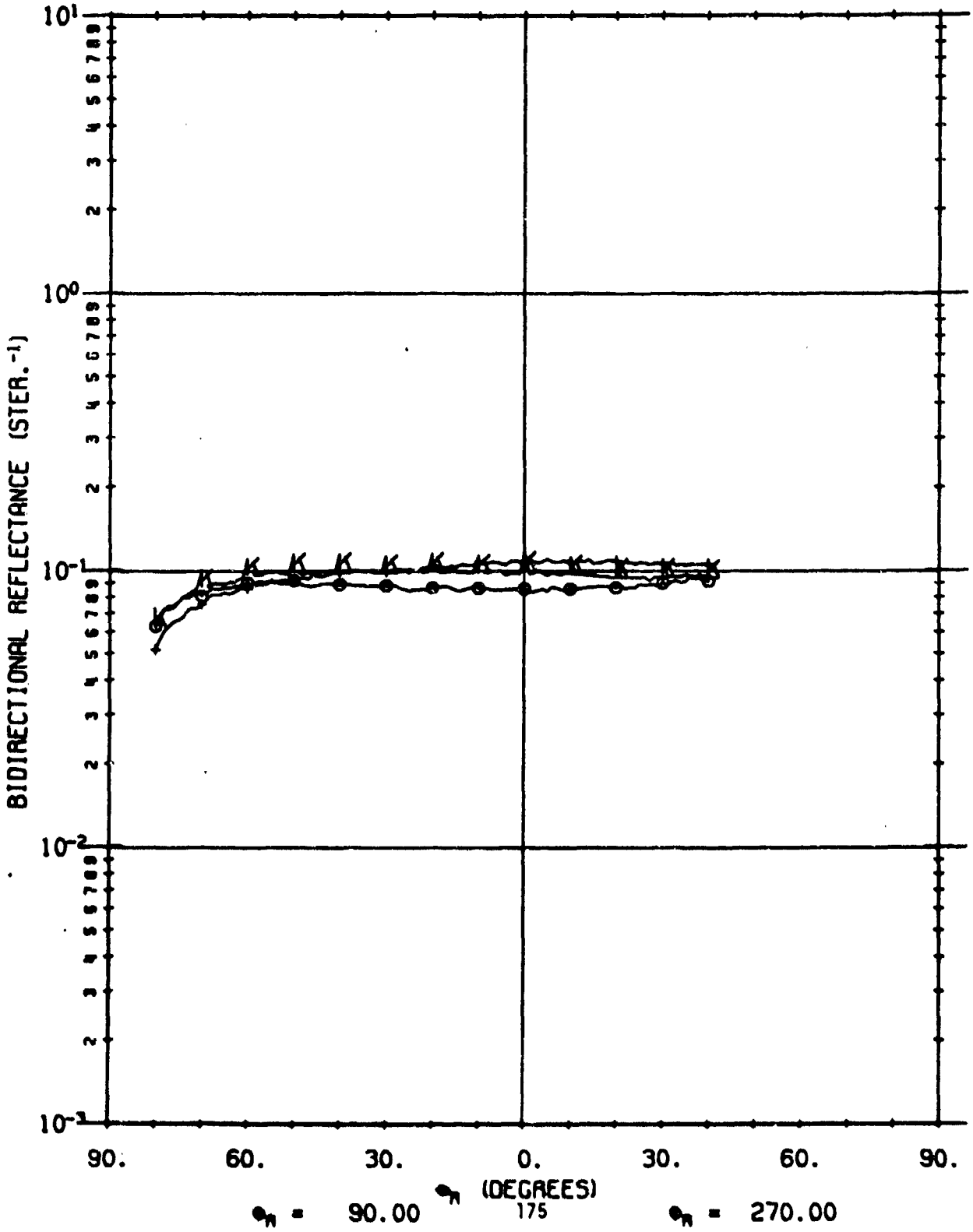

A01610 302

λ = 3.39
θ_I = 40.0
ϕ_I = 180.0

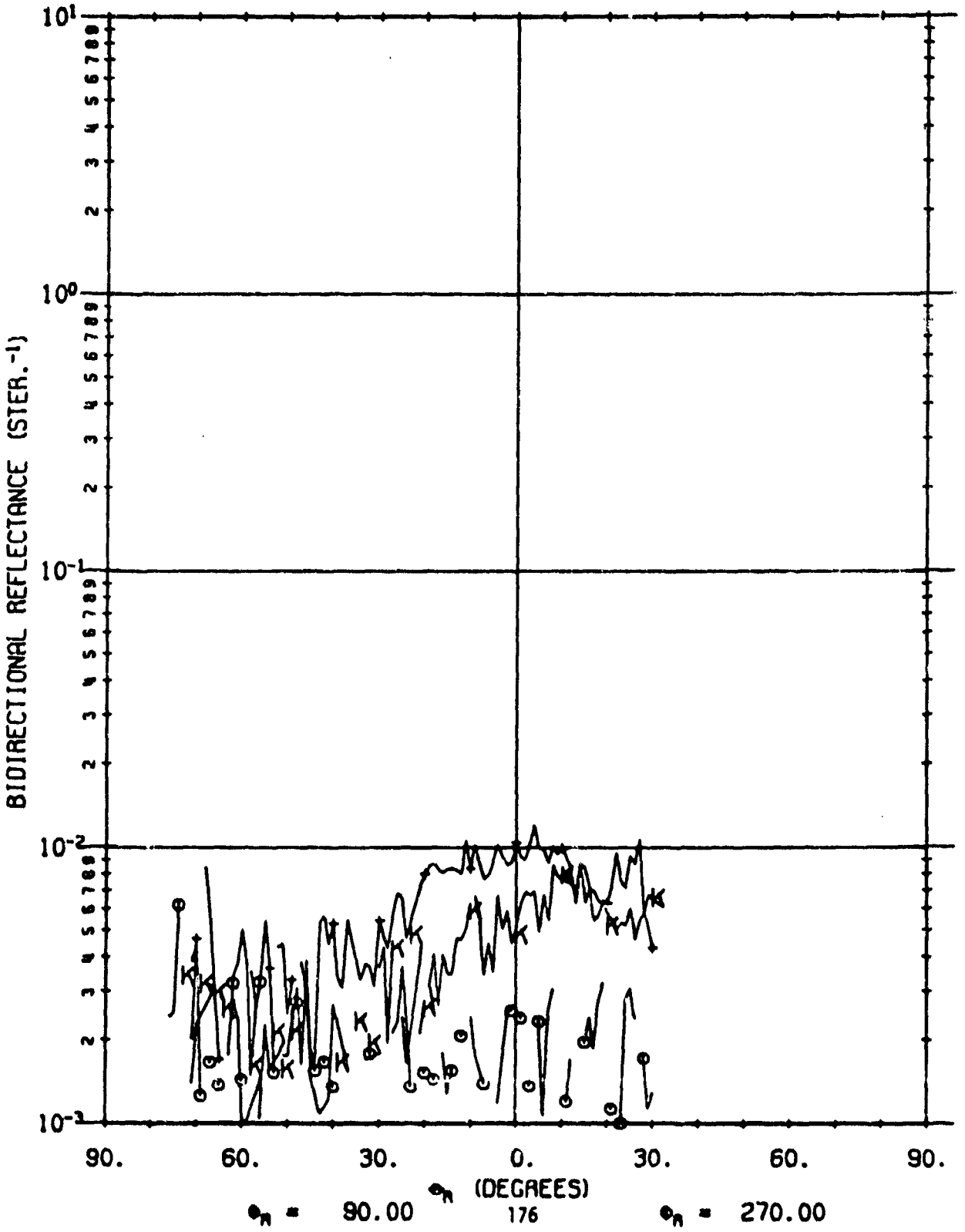

A01610 101

λ = .63
θ_I = 60.0
ϕ_I = 180.0

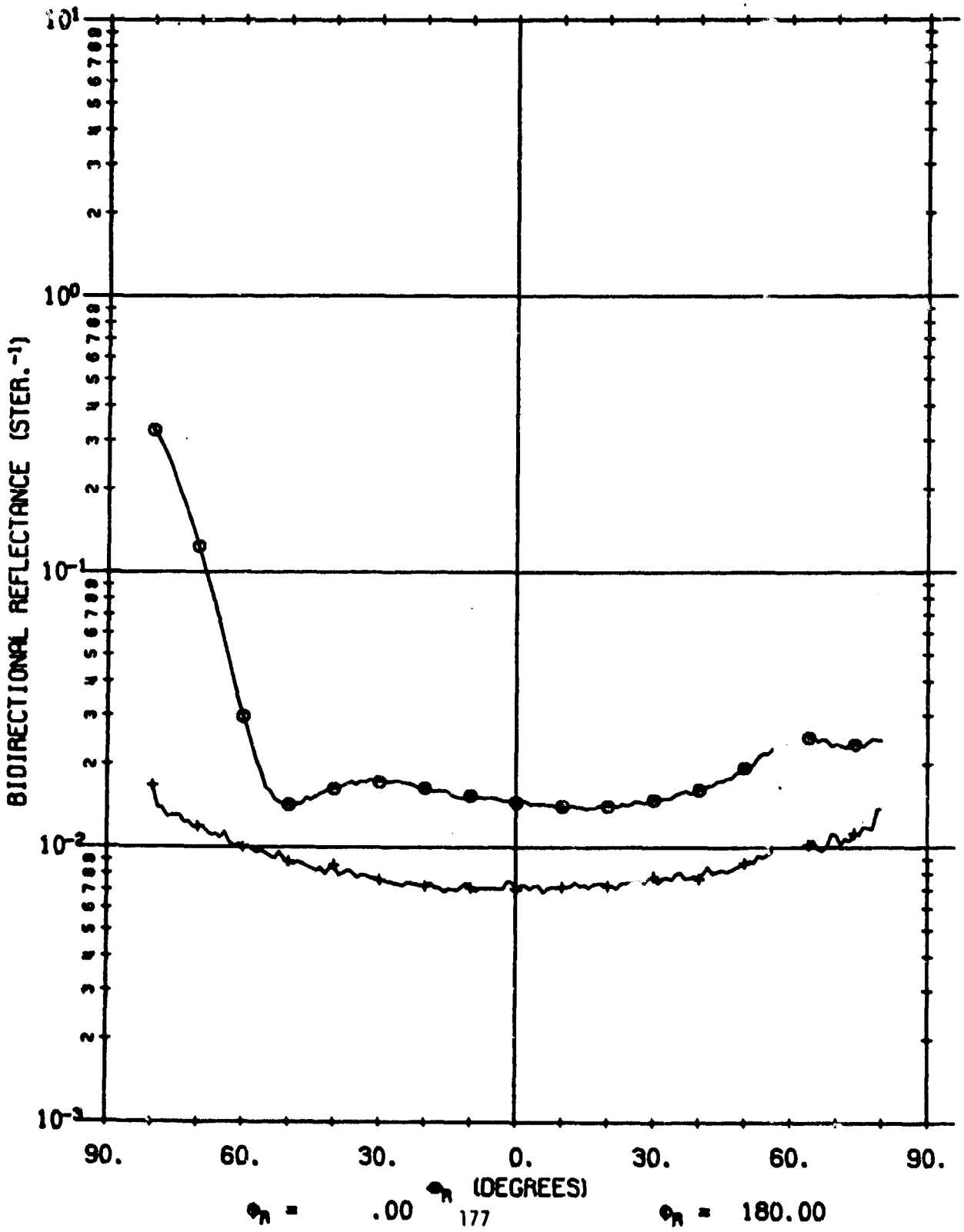

A01610 102

λ = 1.06
θ_I = 60.0
ϕ_I = 180.0

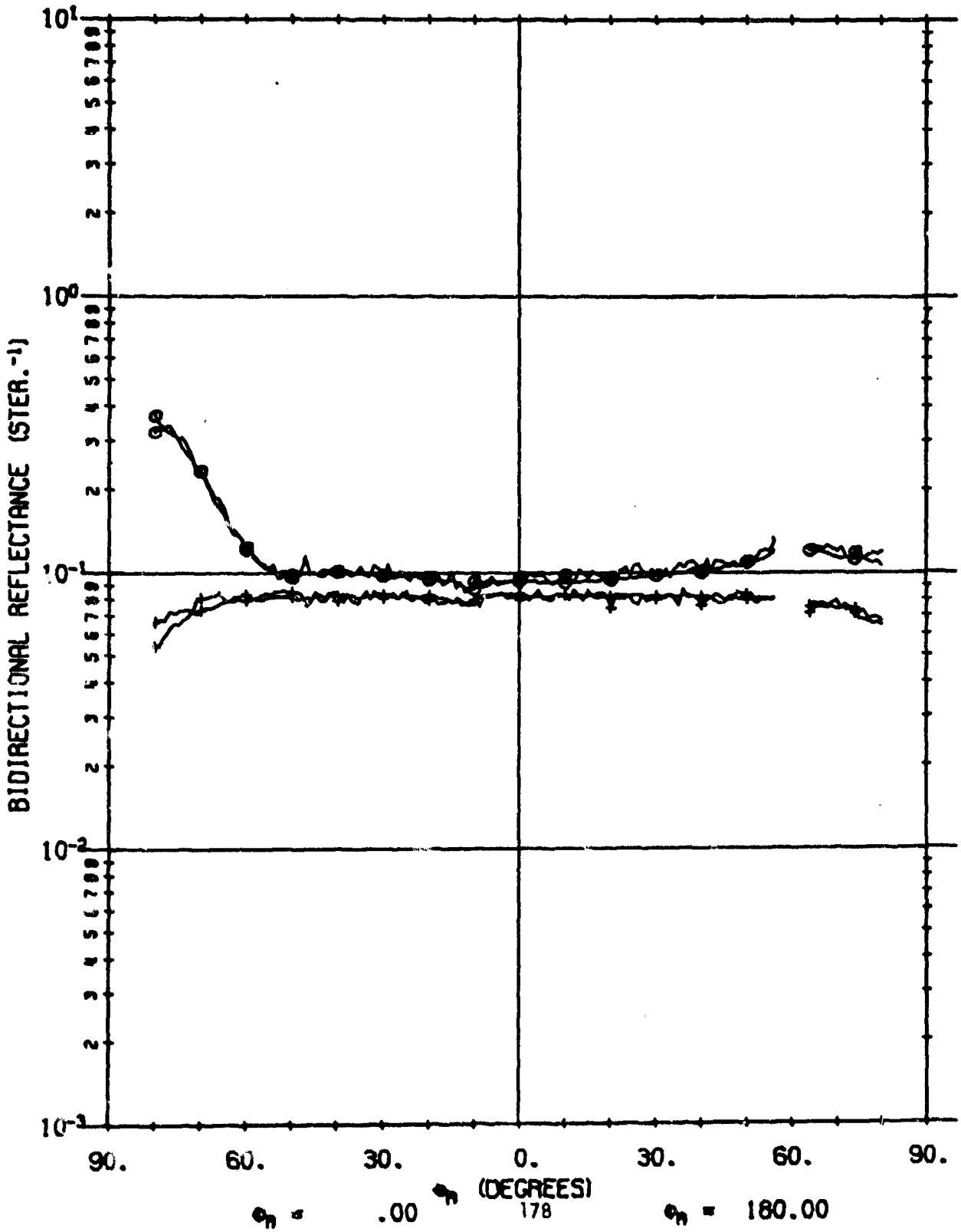

A01610 301

λ = 3.39
θ_i = 60.0
ϕ_i = 180.0

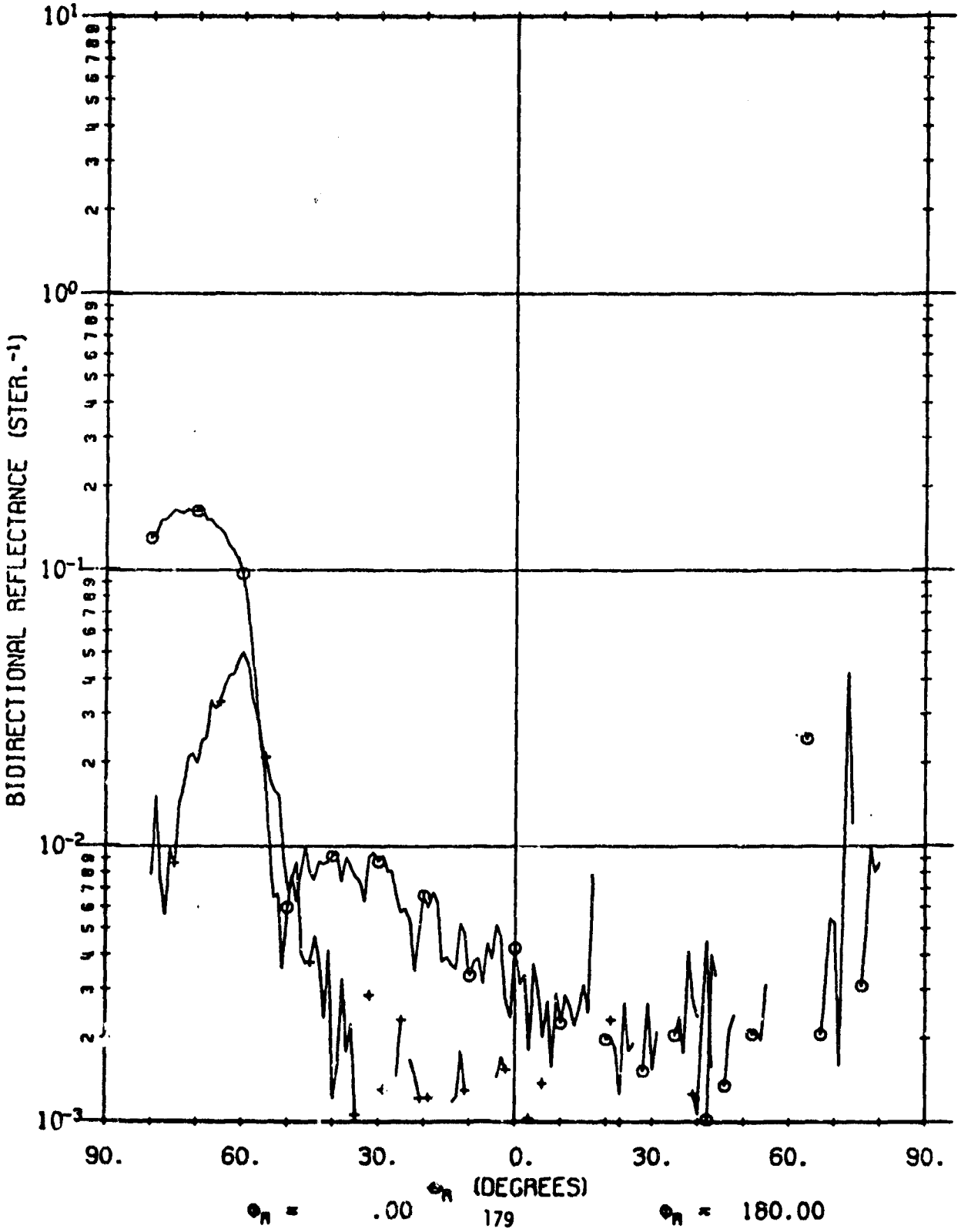

A01610 204

λ = 10.60
Φ_I = 60.0
Φ_I = 180.0

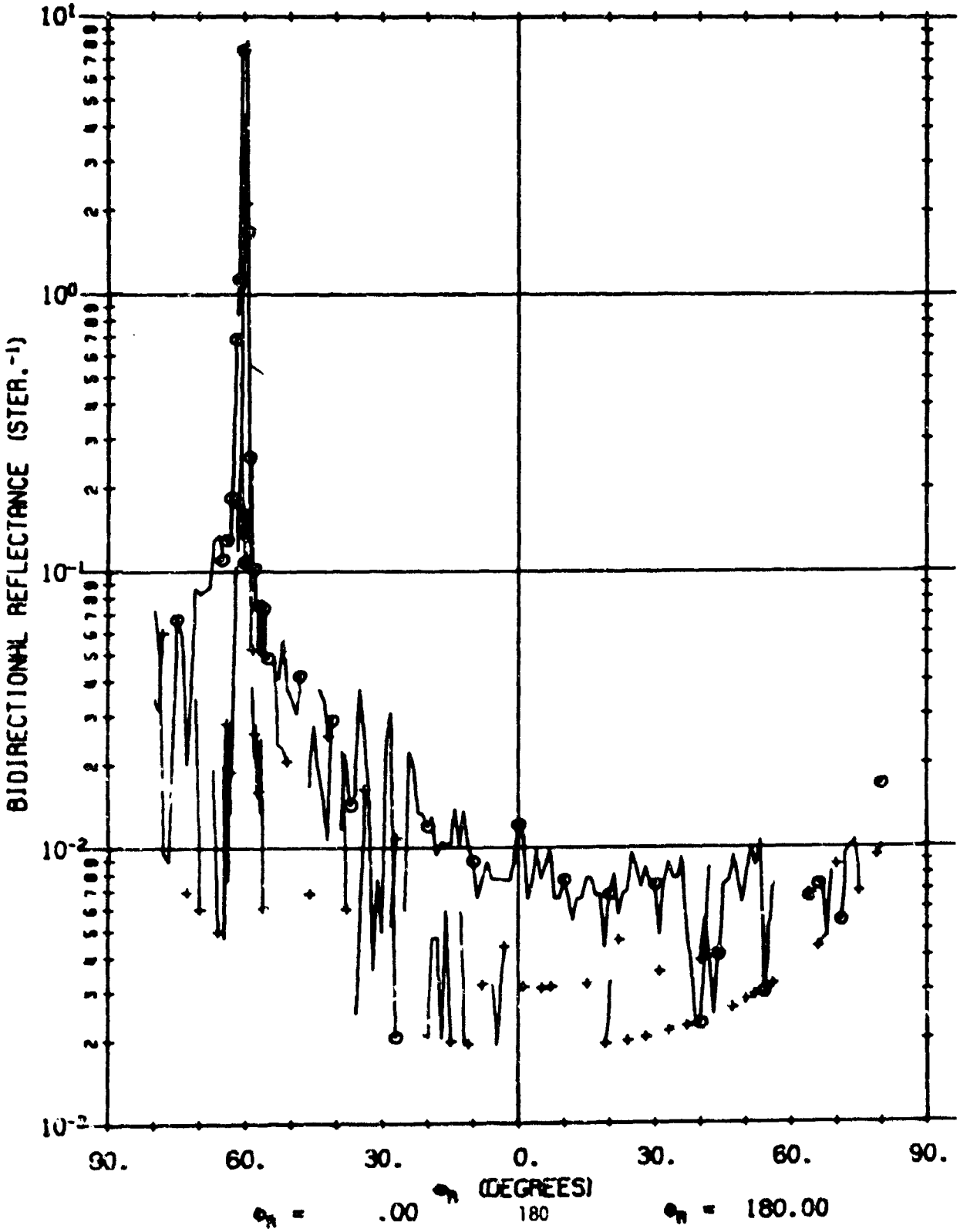

A01610 101

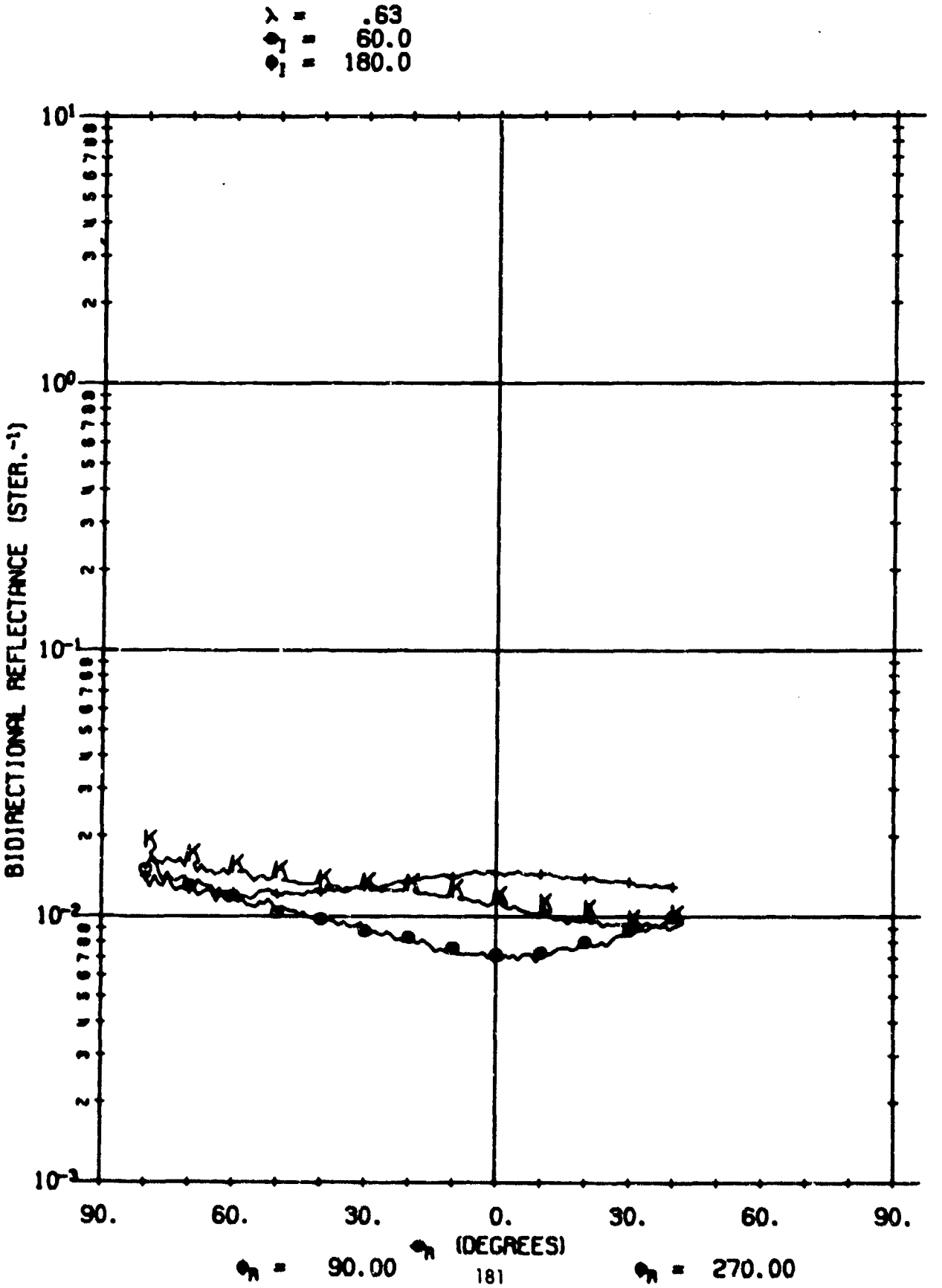
λ = .63
ϕ_I = 60.0
θ_I = 180.0
BIDIRECTIONAL REFLECTANCE (STER.$^{-1}$)
10^1
10^0
10^{-1}
10^{-2}
10^{-3}
90.
60.
30.
0.
30.
60.
90.
θ_R (DEGREES)
ϕ_R = 90.00
ϕ_R = 270.00

A01610 102

λ = 1.06
θ_I = 60.0
ϕ_I = .0

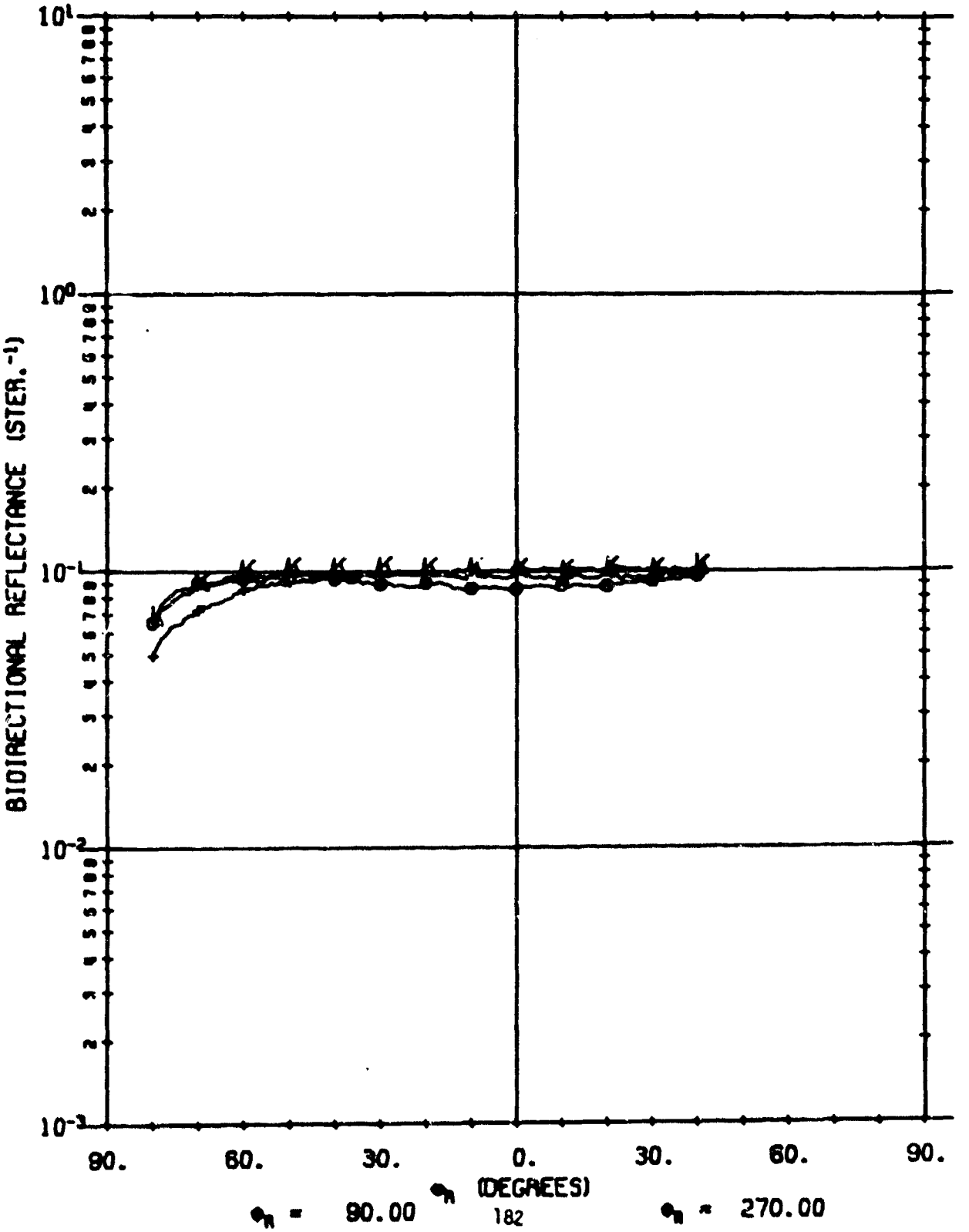

A01610 302

λ = 3.39
Φ_I = 60.0
Φ_I = 180.0

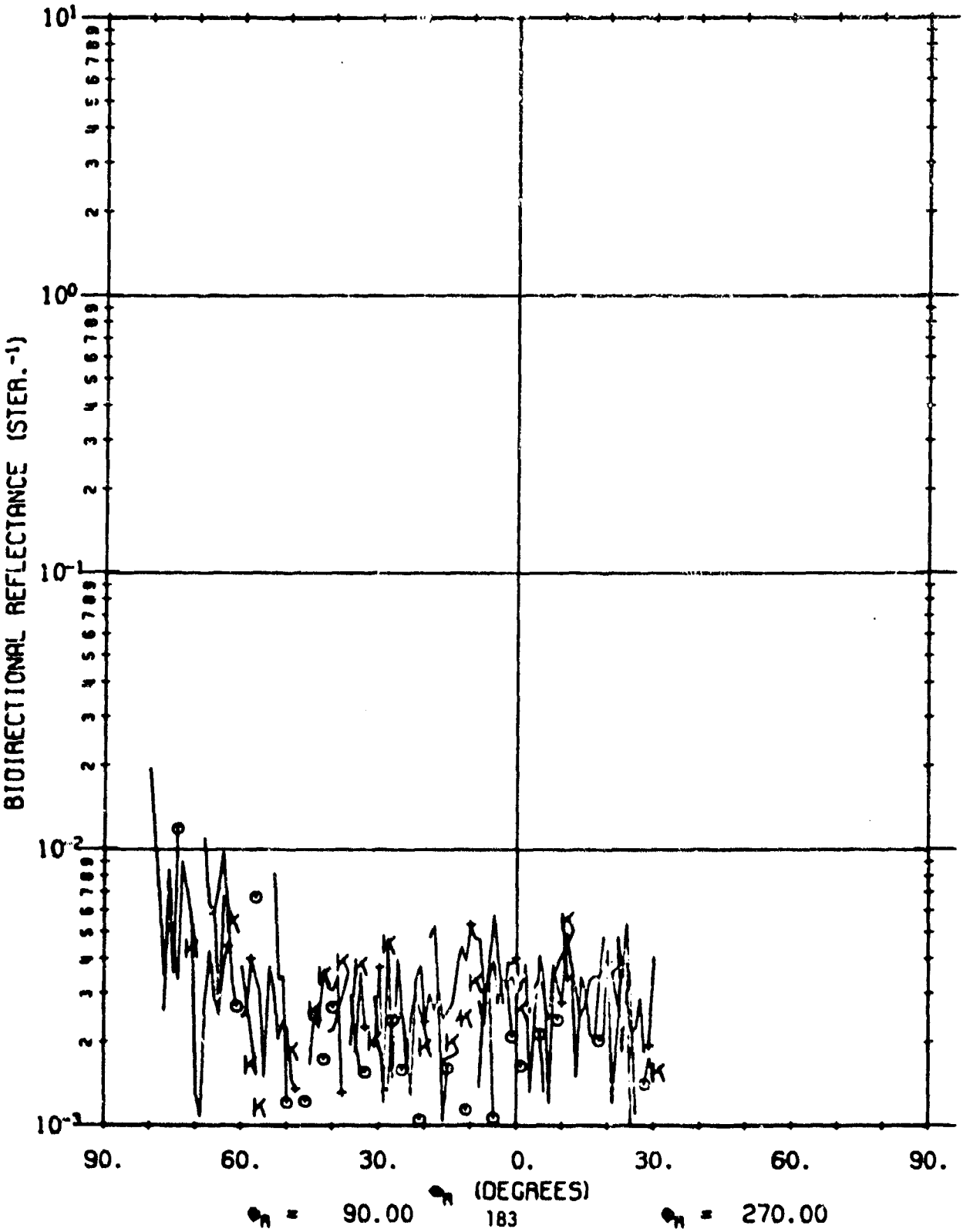

A02022 202

λ = .63
θ_I = .0
ϕ_I = 180.0

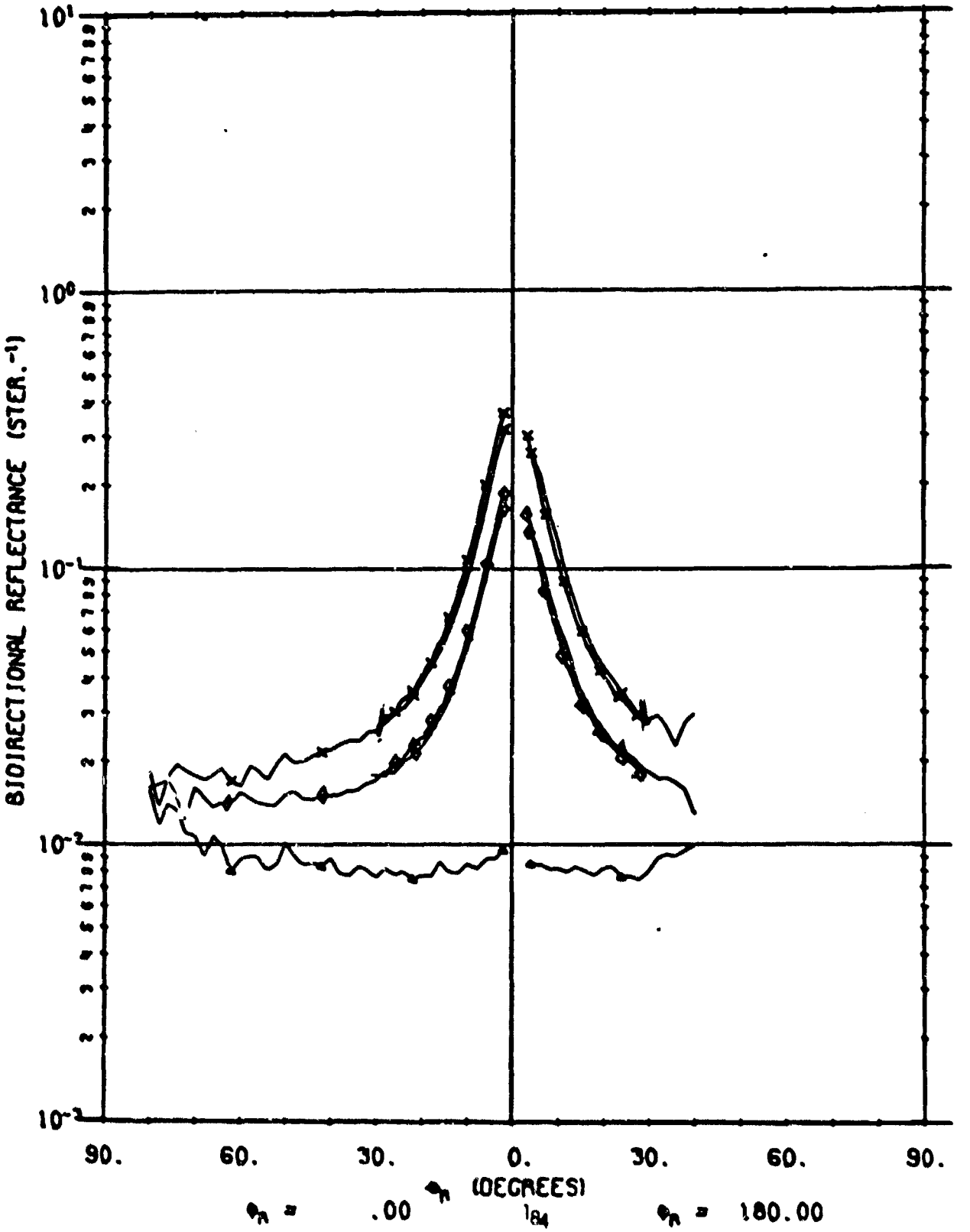

A02022 201

λ = 1.06
ϕ_i = .0
θ_i = 180.0

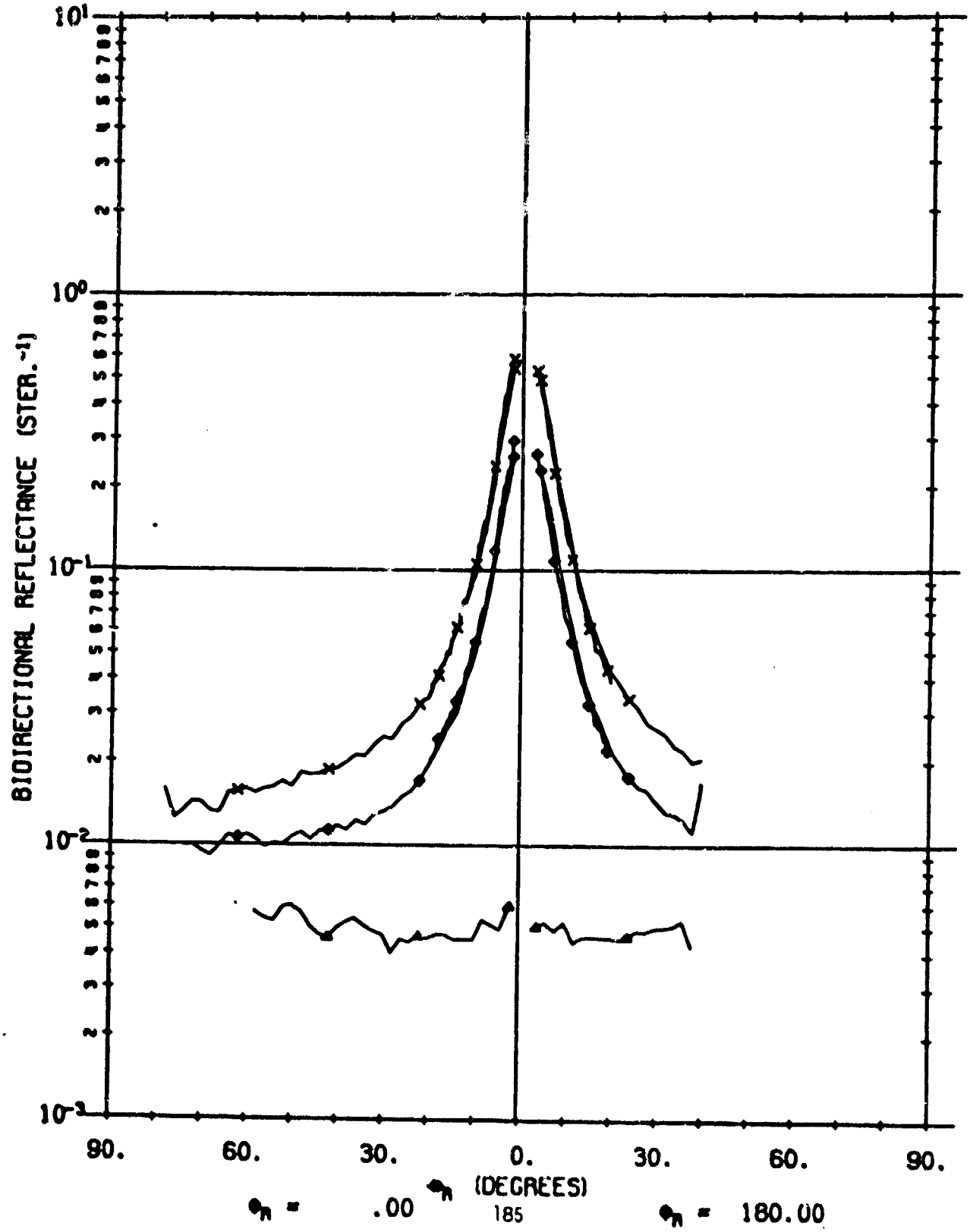

A02022 702

λ = 3.39
ϕ_I = .0
θ_I = 180.0

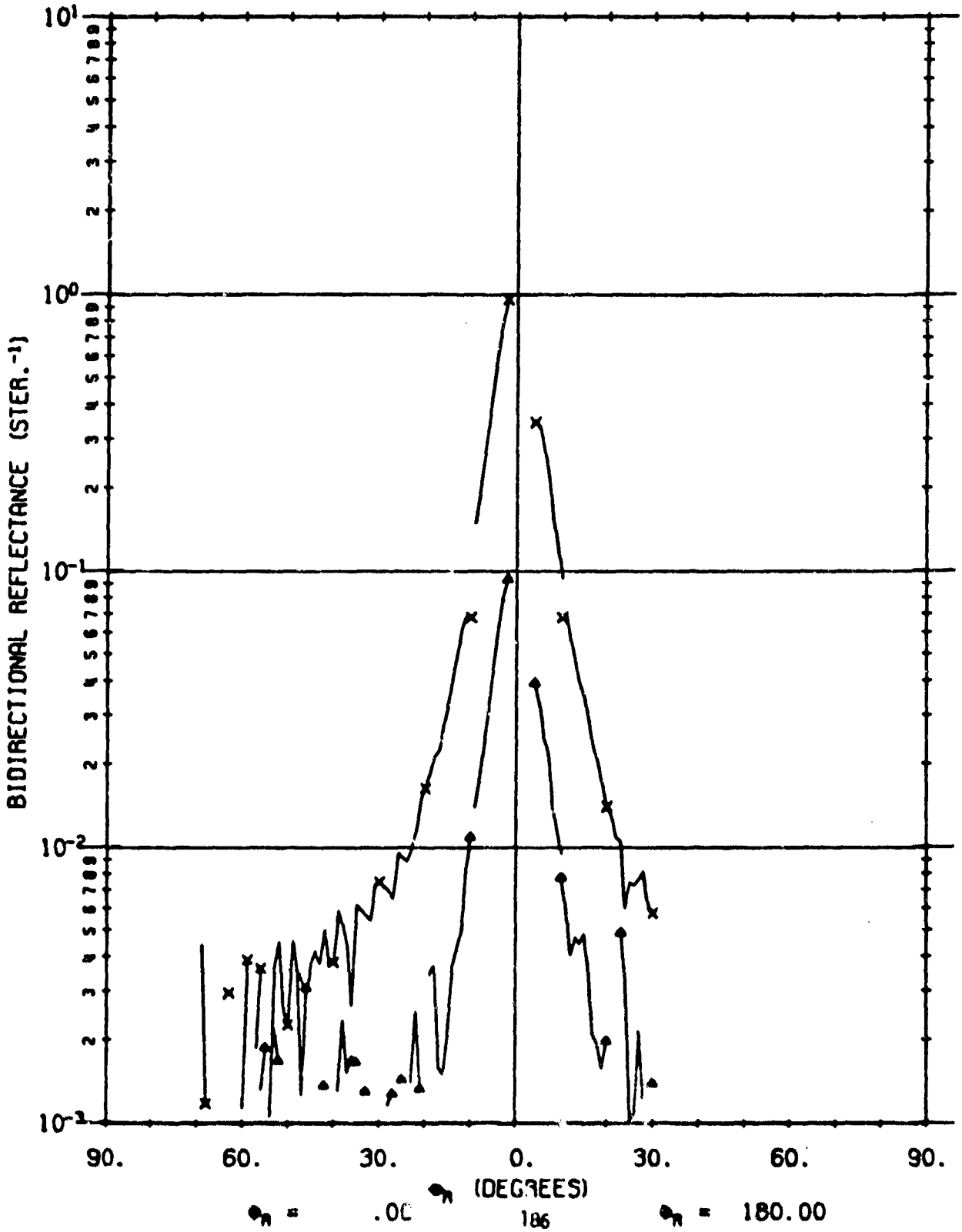

A02022 602

λ = 10.60
ϕ_I = .0
θ_I = 180.0

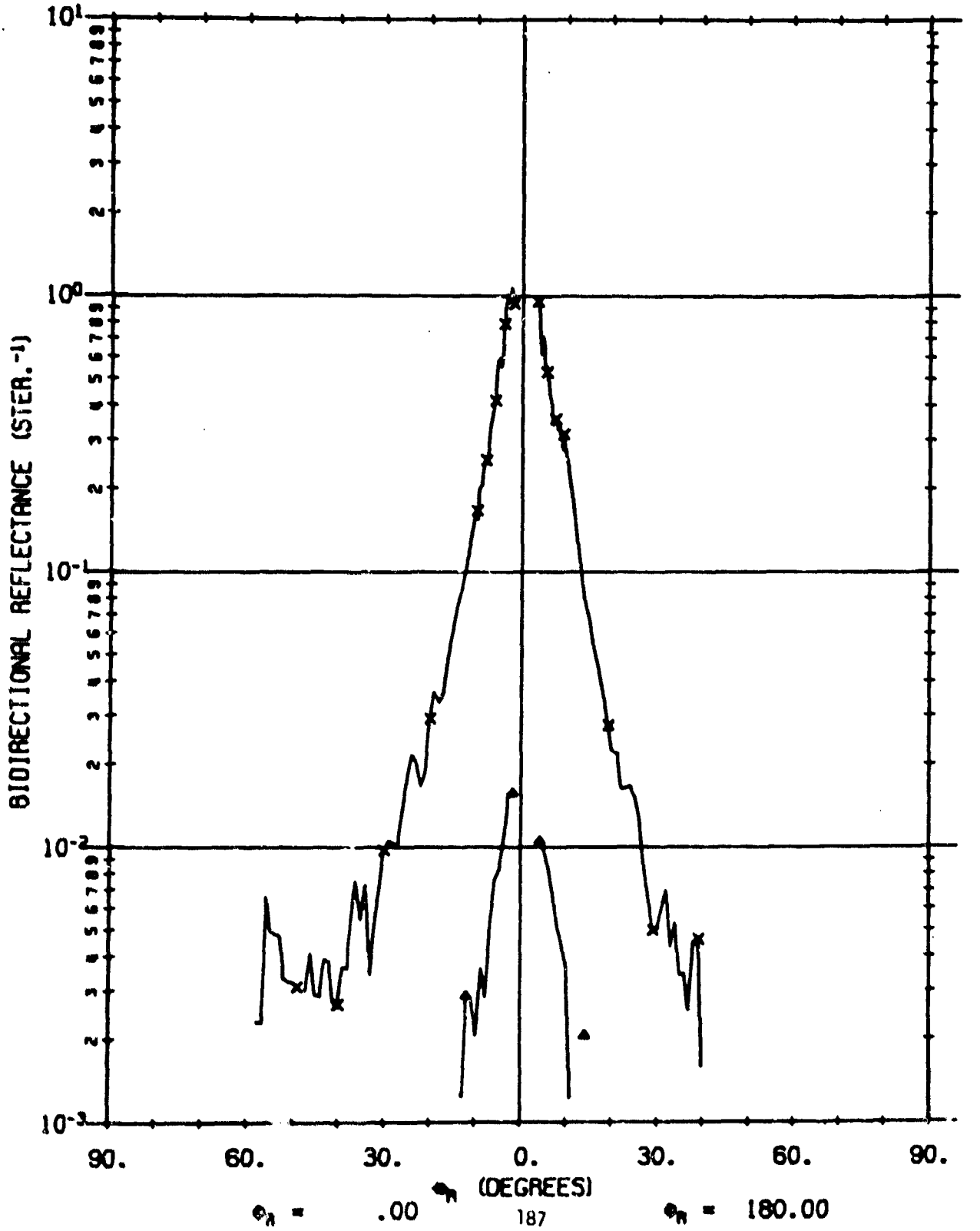

A02022 202

λ = .63
θ_i = .0
ϕ_i = 180.0

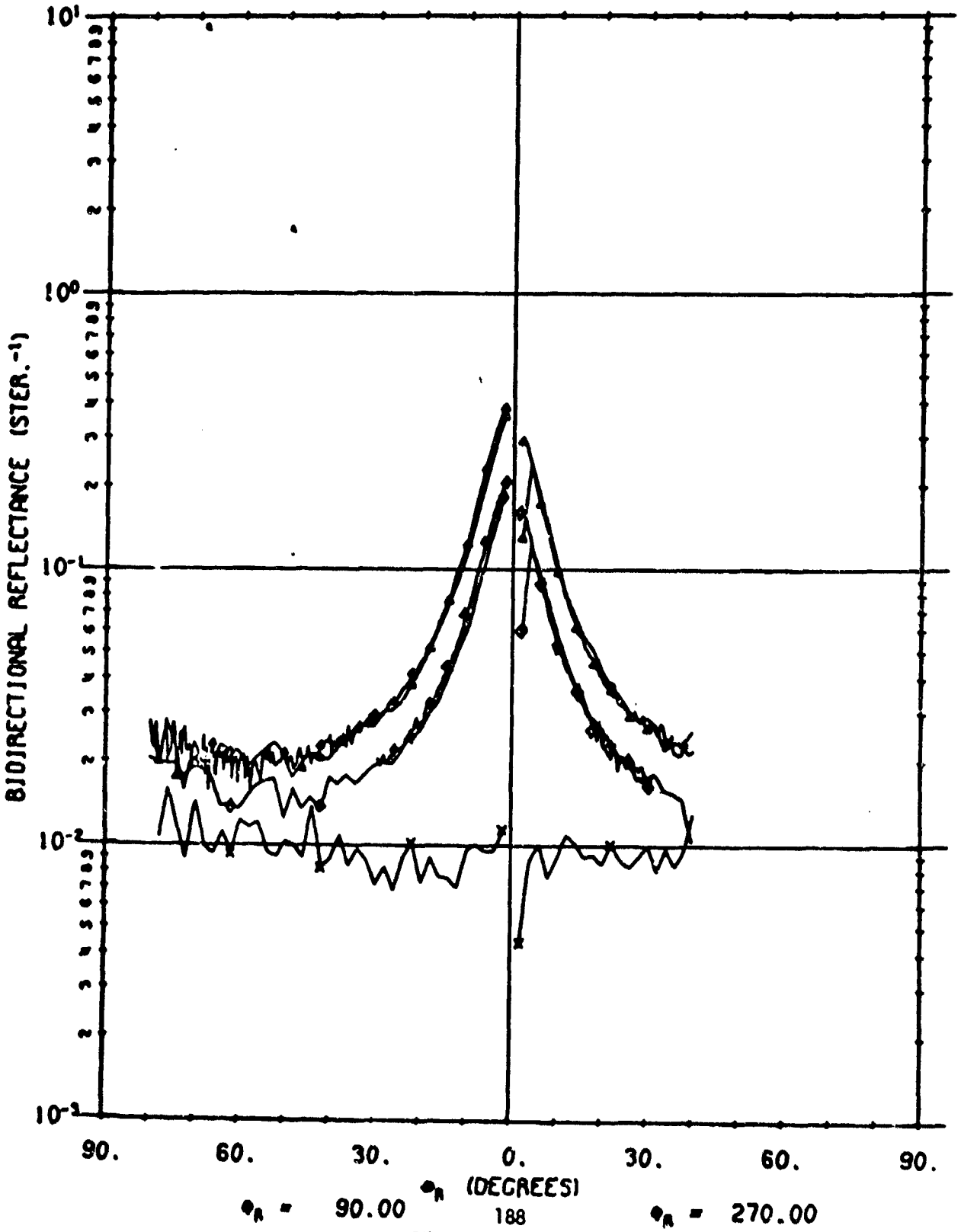

A02022 201

λ = 1.06
ϕ_I = .0
θ_I = 180.0

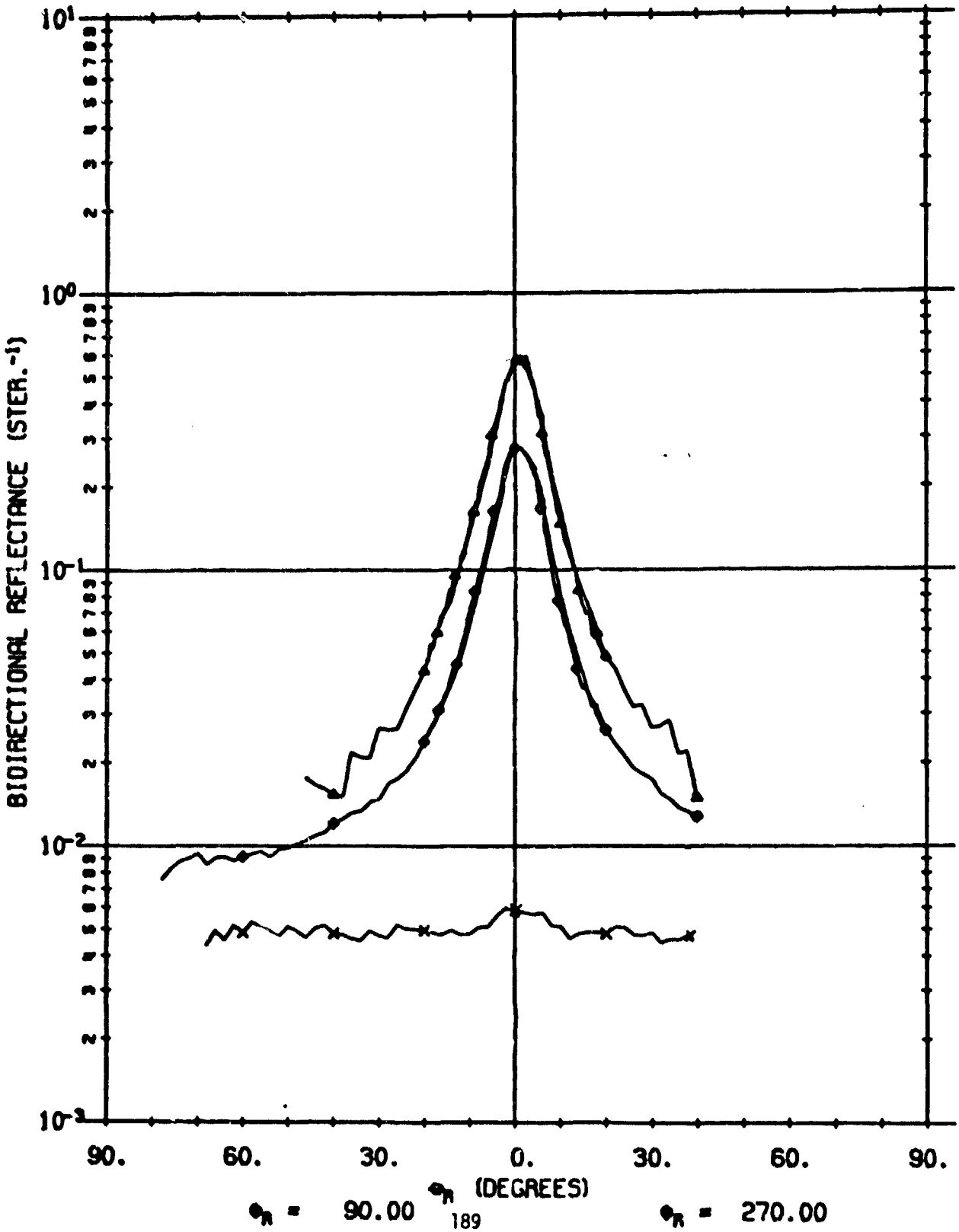

A02022 202

λ = .63
θ_i = 20.0
ϕ_i = 180.0

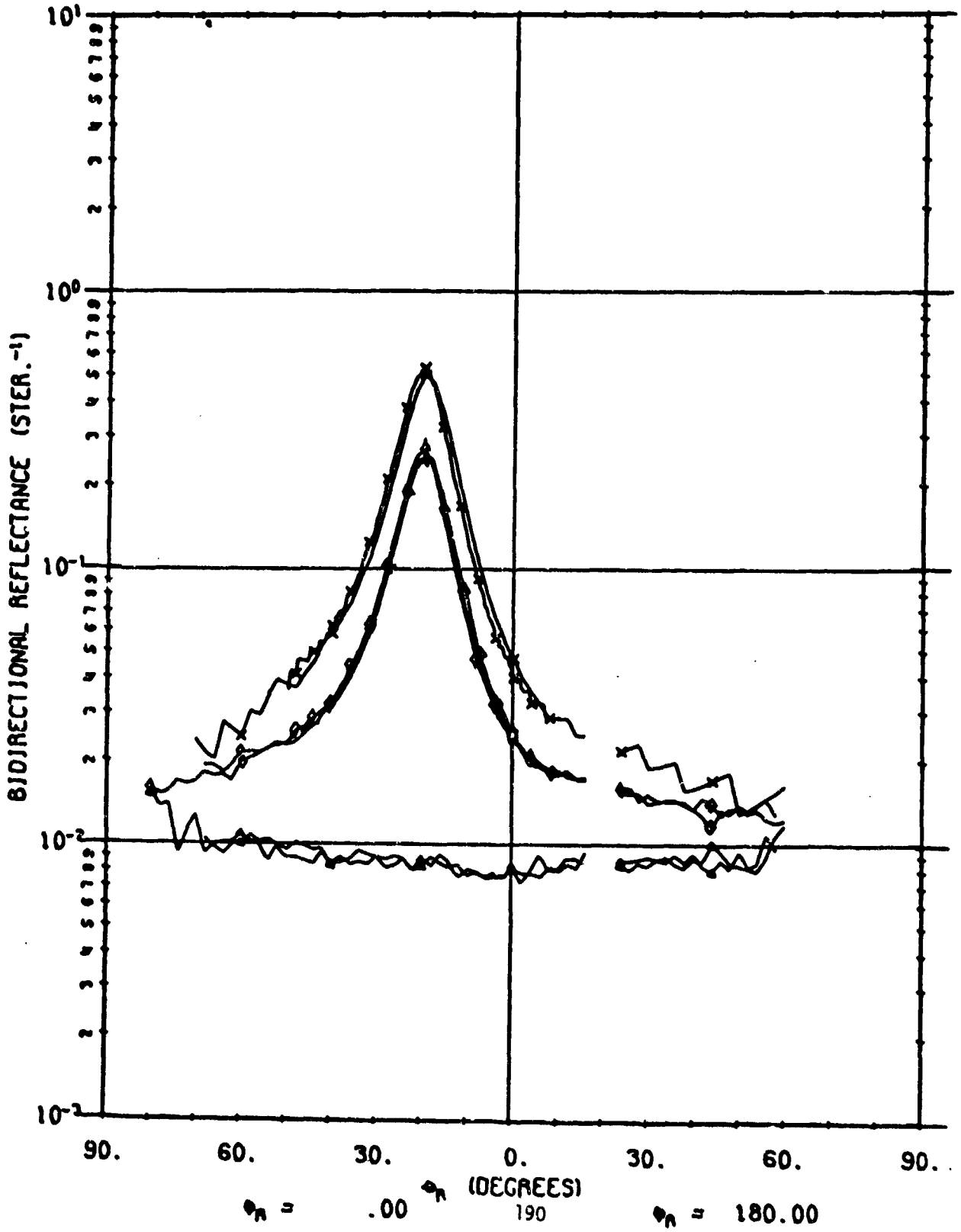

A02022 201

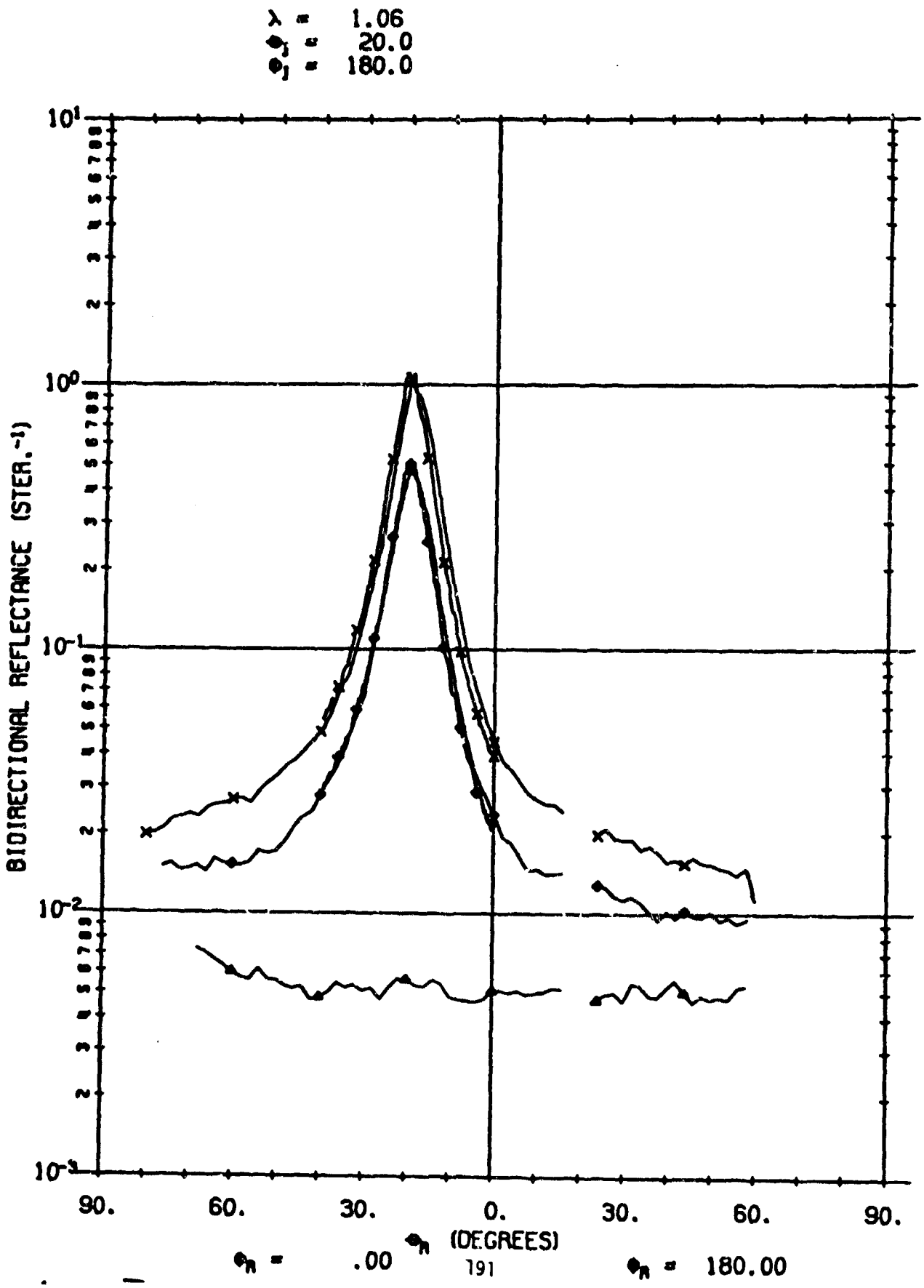
λ = 1.06
ϕ_i = 20.0
ϕ_i = 180.0
BIDIRECTIONAL REFLECTANCE (STER.$^{-1}$)
10^1
10^0
10^{-1}
10^{-2}
10^{-3}
90.
60.
30.
0.
30.
60.
90.
ϕ_R (DEGREES)
ϕ_R = .00
ϕ_R = 180.00

A02022 702

λ = 3.39
ϕ_1 = 20.0
θ_1 = 180.0

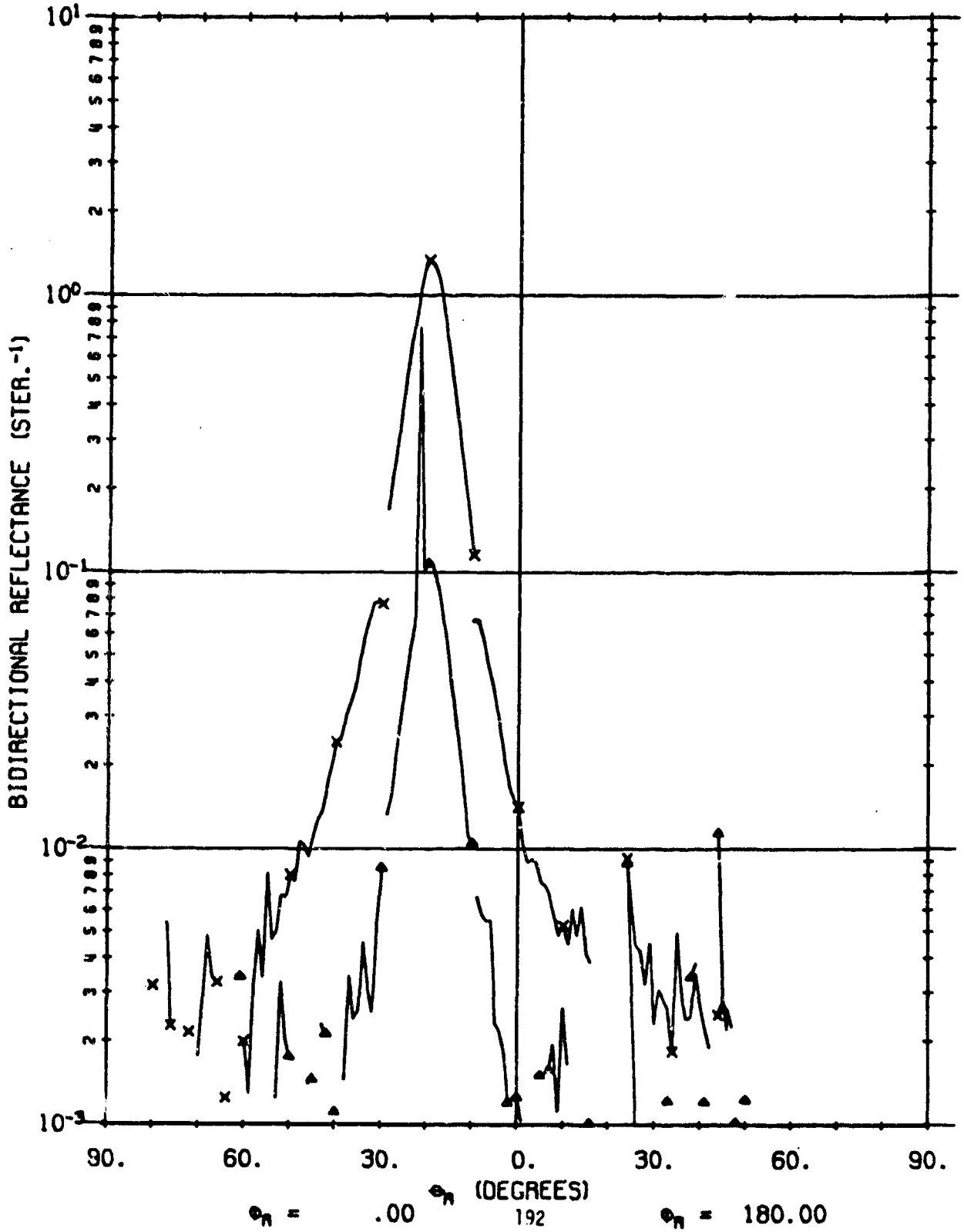

A02022 602

λ = 10.60
Φ_I = 20.0
Φ_t = 180.0

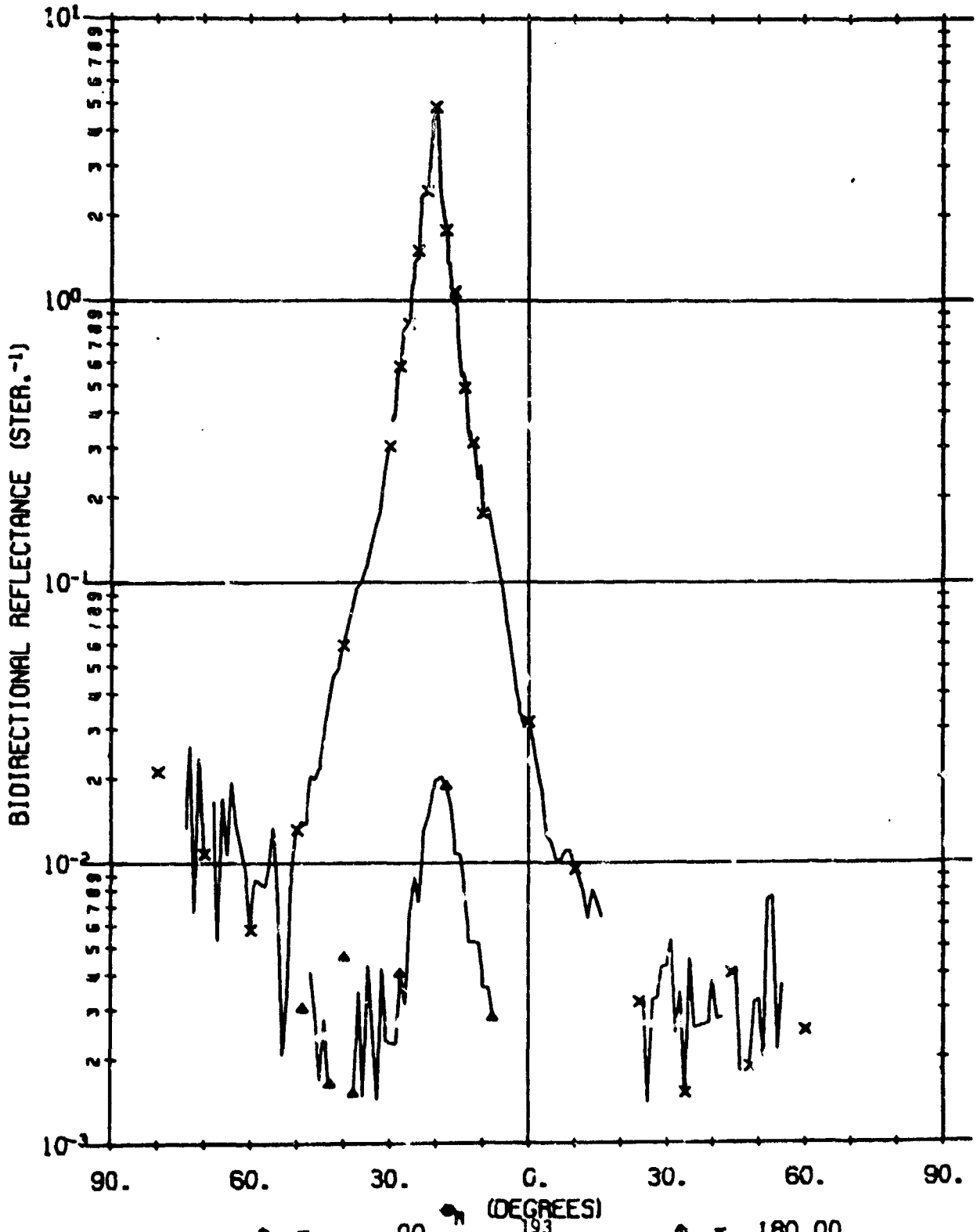

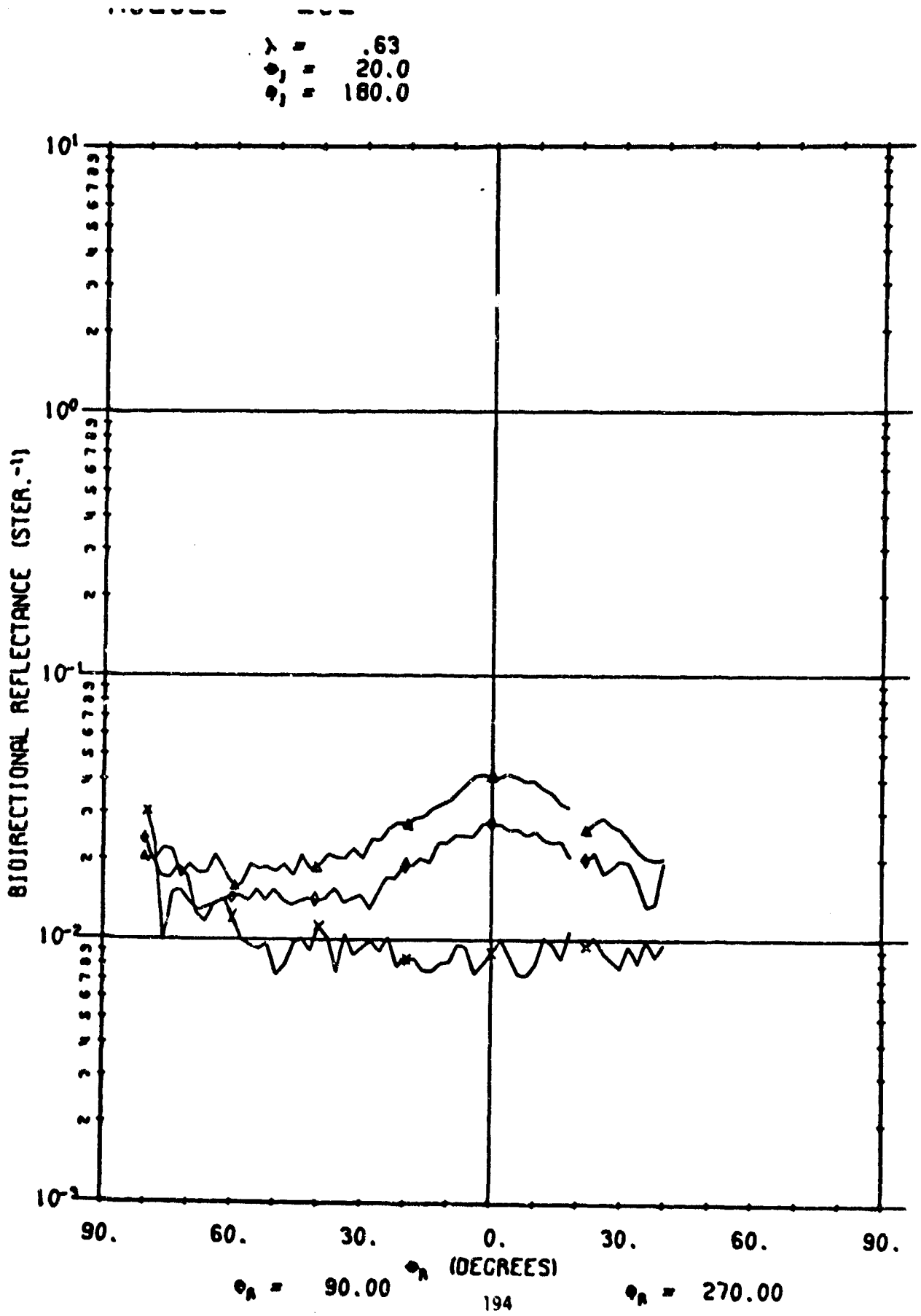
λ = .63
θ_I = 20.0
φ_I = 180.0
BIDIRECTIONAL REFLECTANCE (STER.⁻¹)
10¹
10⁰
10⁻¹
10⁻²
10⁻³
90.
60.
30.
0.
30.
60.
90.
θ_R (DEGREES)
φ_R = 90.00
φ_R = 270.00

A02022 201

λ = 1.06
ϕ_i = 20.0
θ_i = 180.0

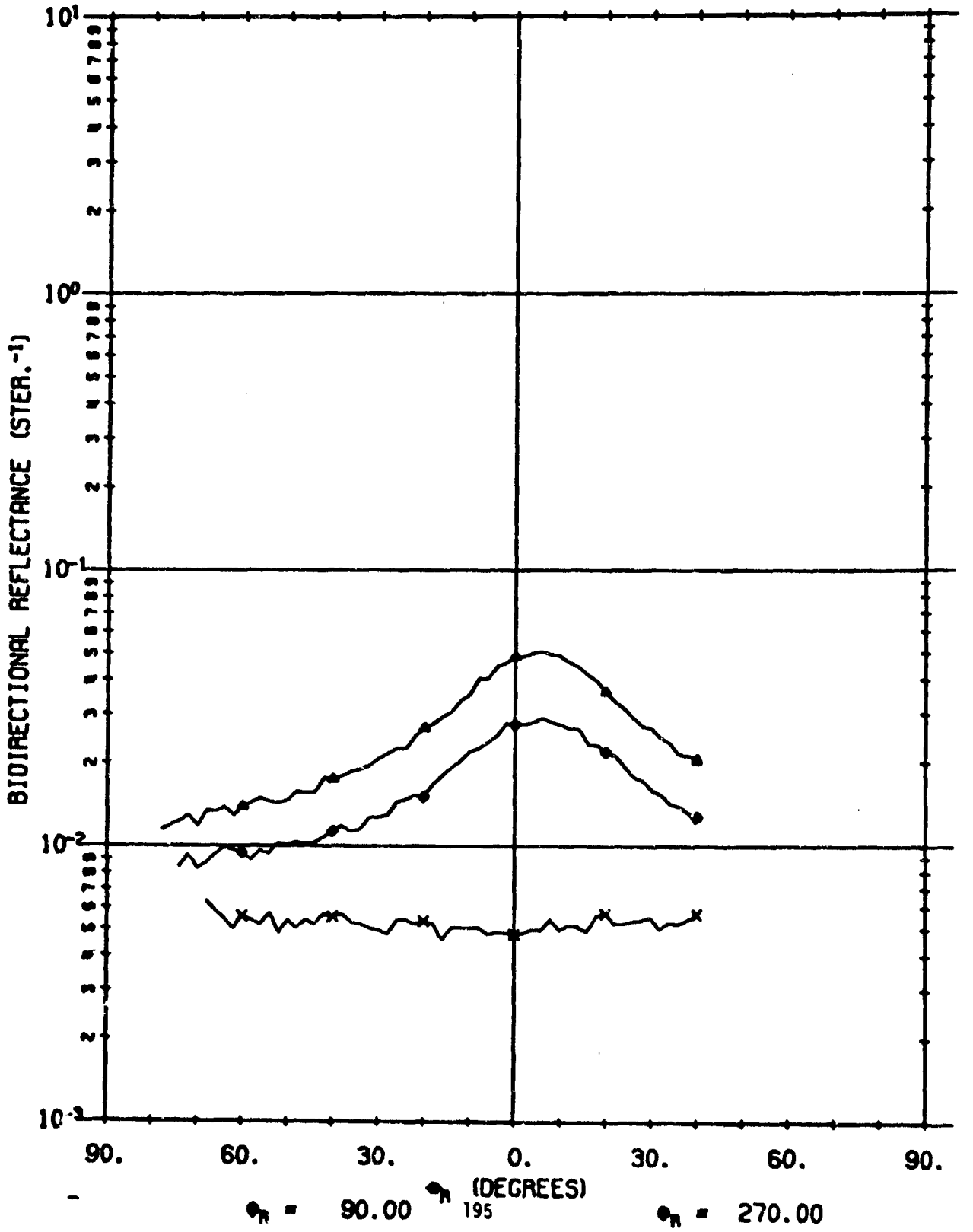

A02022 701

λ = 3.39
θ_I = 20.0
ϕ_I = 180.0

79

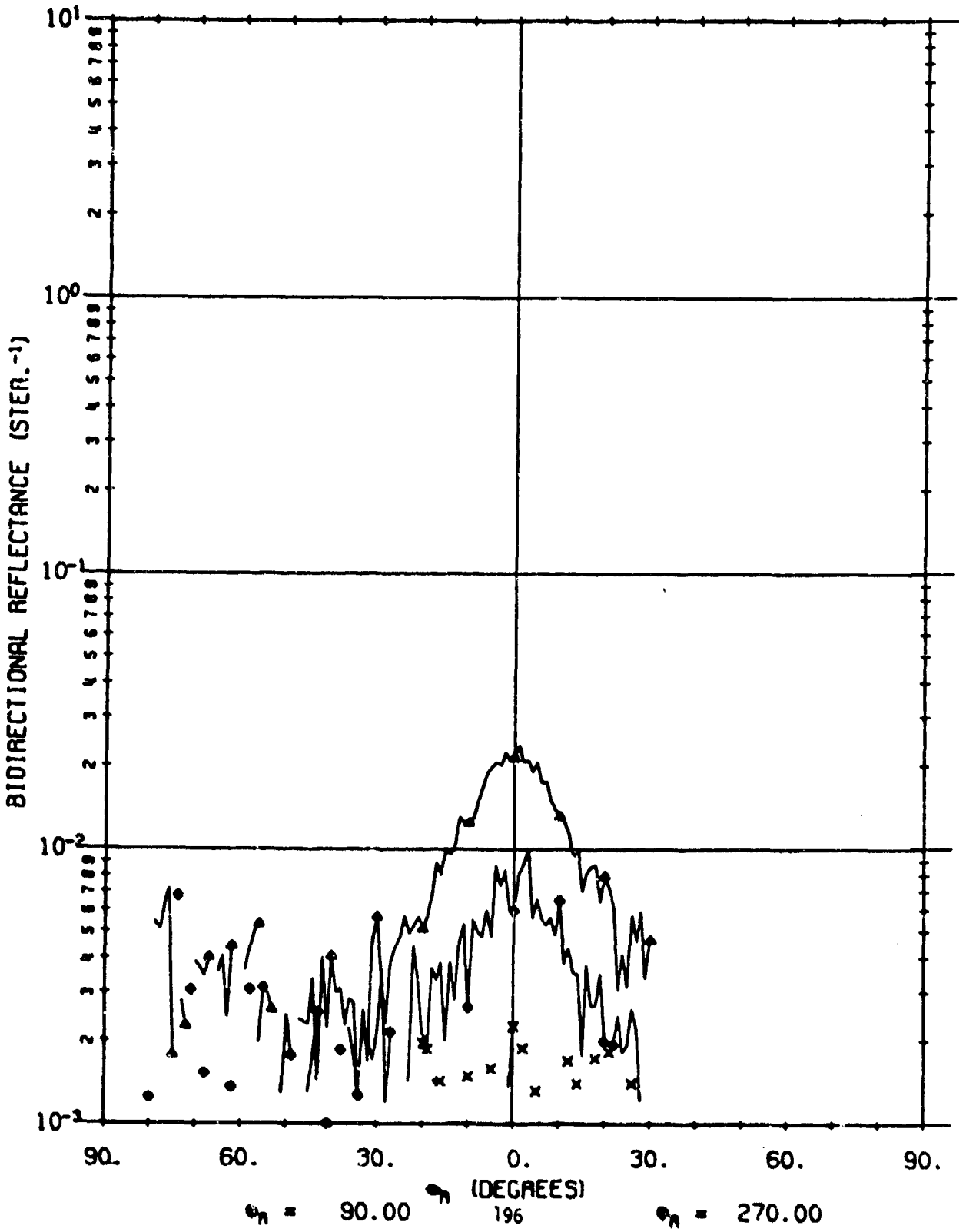

A02022 604

λ = 10.60
ϕ_I = 20.0
ϕ_I = 180.0

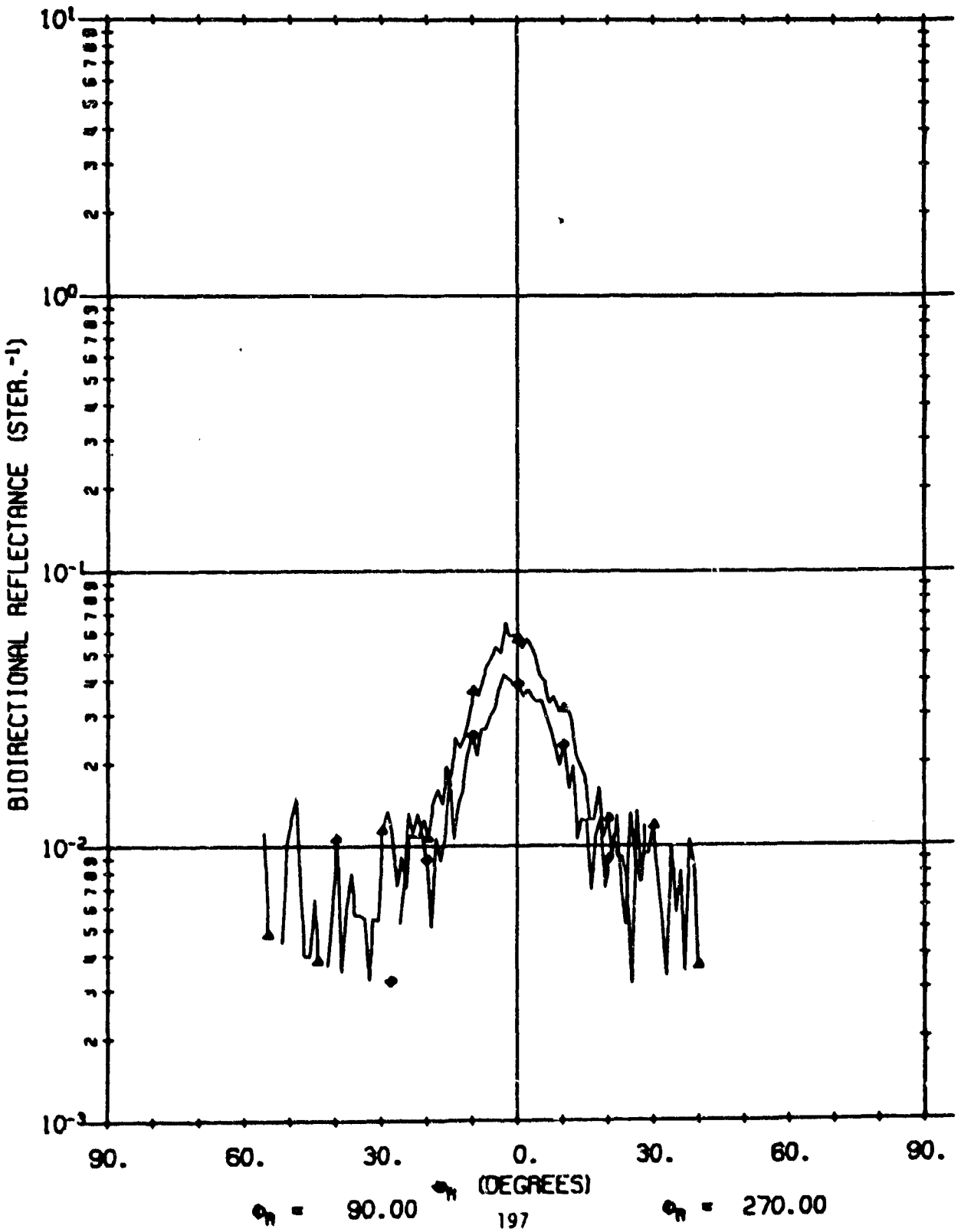

A02022 202

λ = .63
θ_I = 40.0
ϕ_I = 180.0

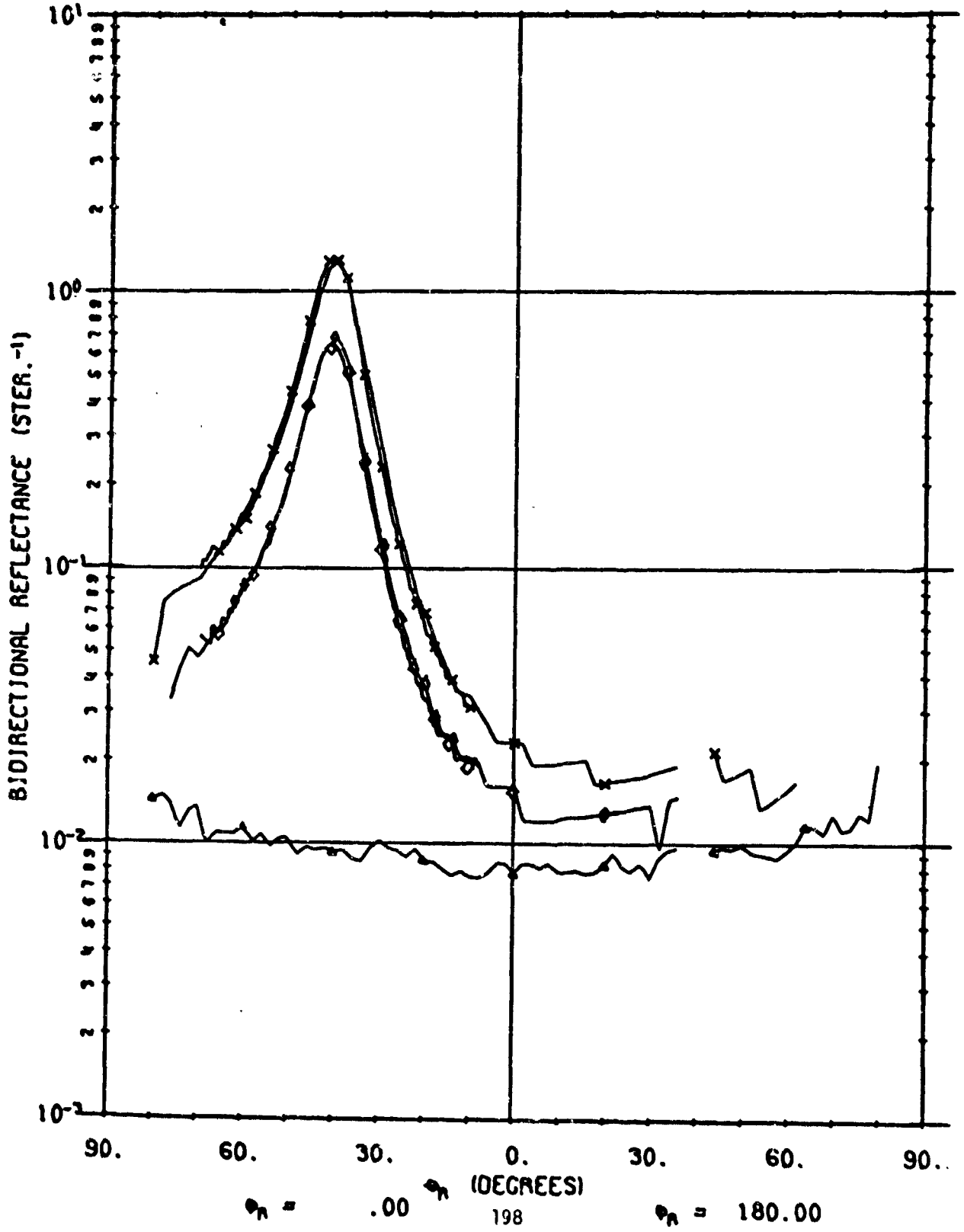

A02022 201

λ = 1.06
θ_i = 40.0
ϕ_i = 180.0

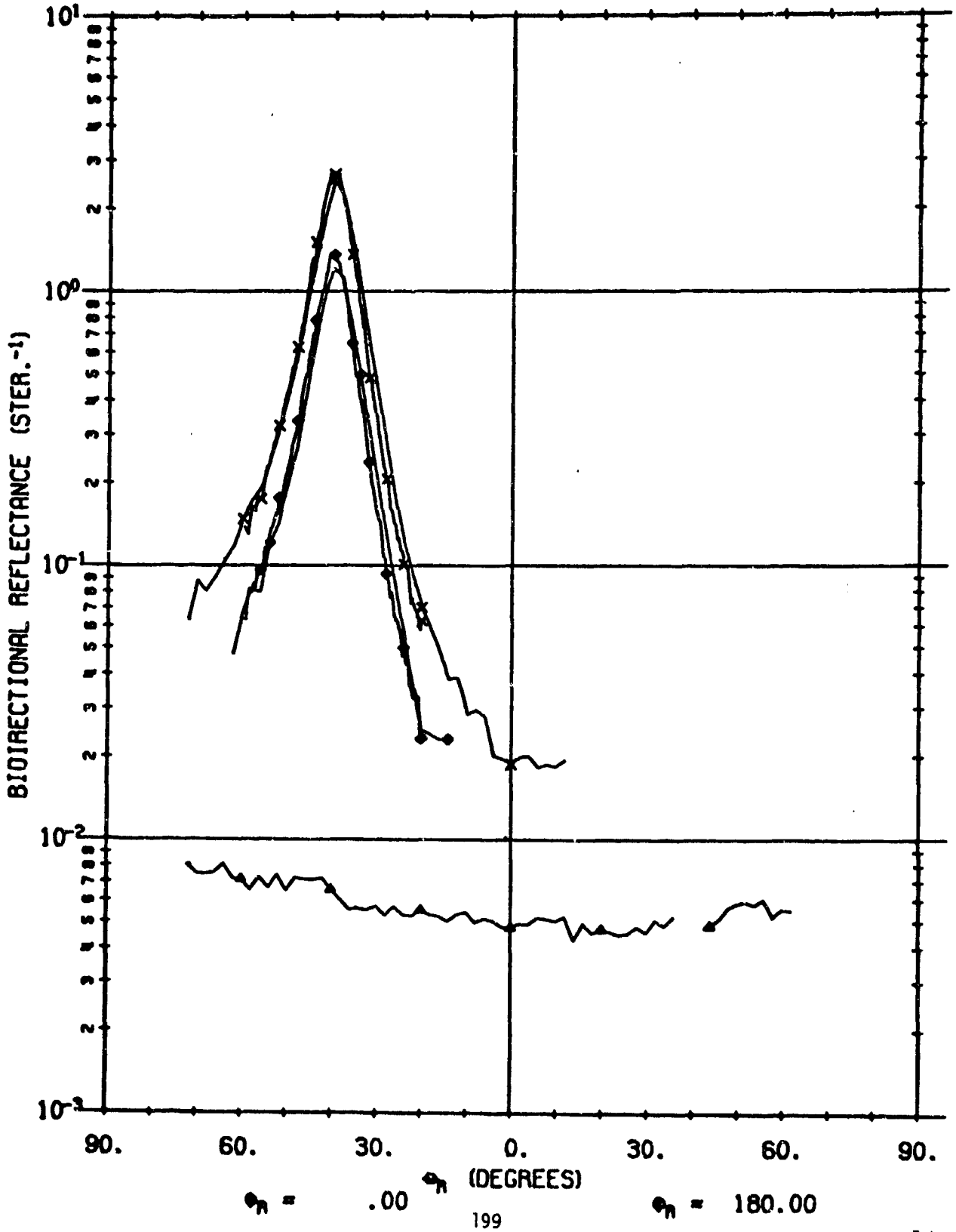

A02022 702

λ = 3.39
θ_i = 40.0
ϕ_i = 180.0

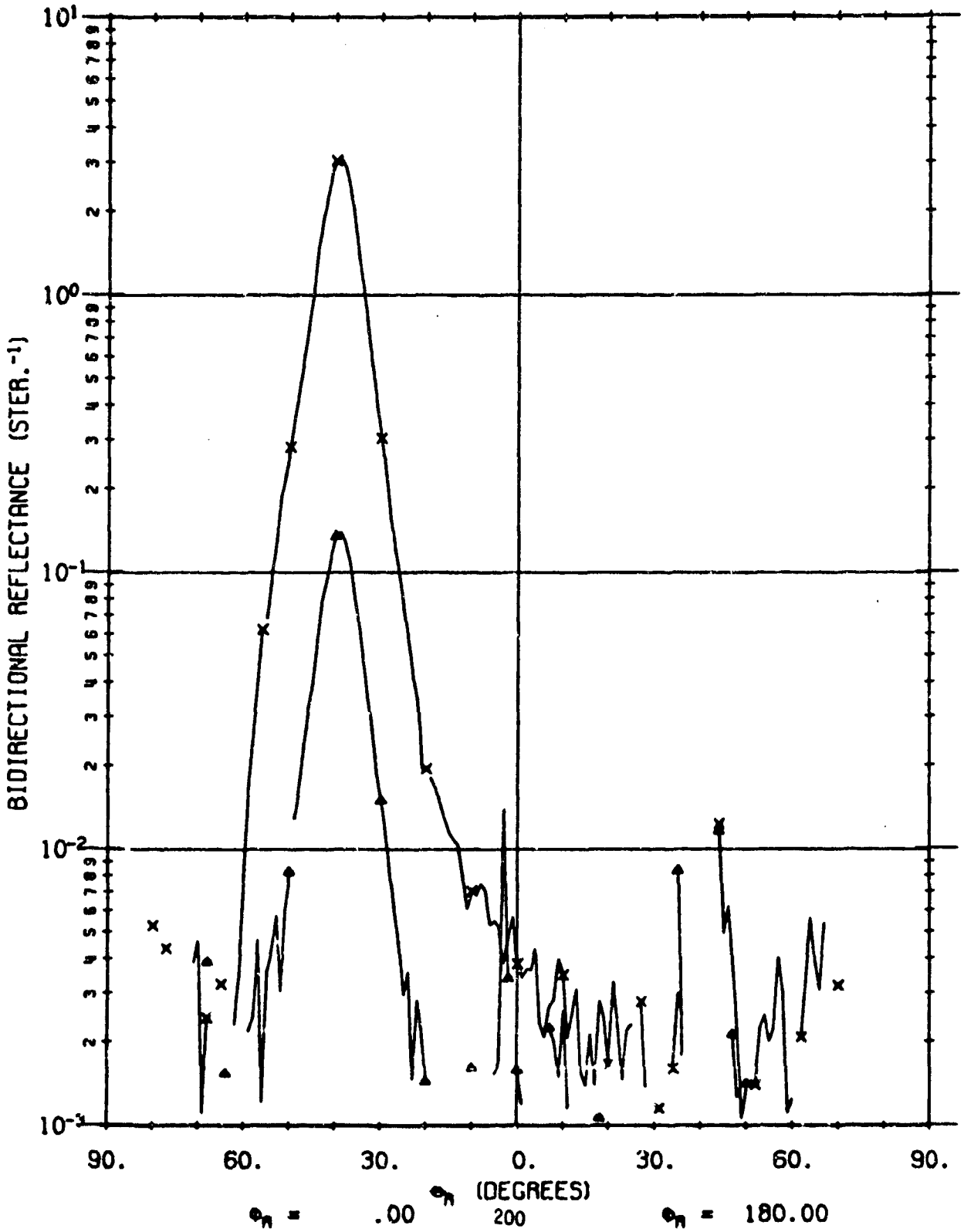

A02022 602

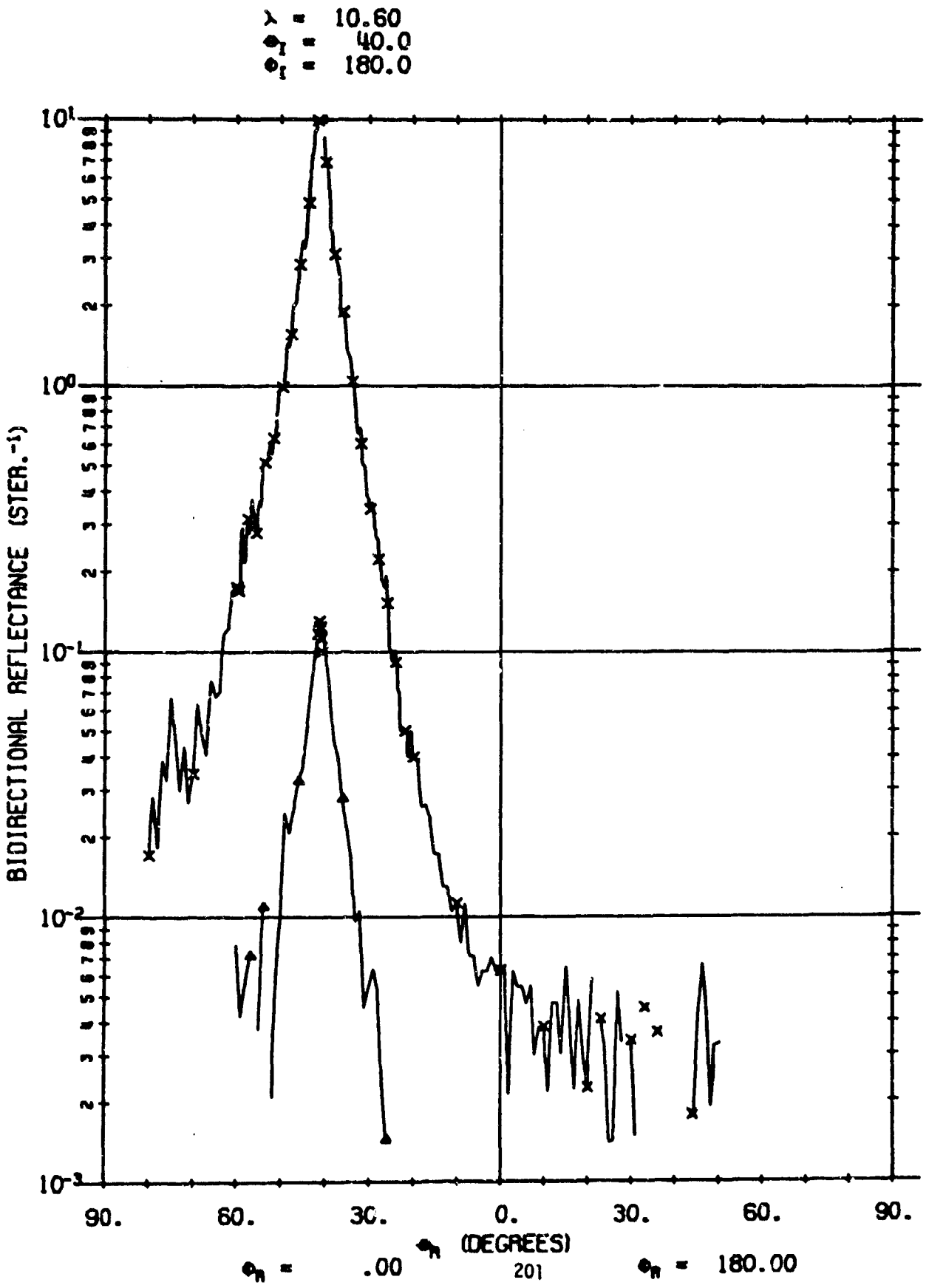
λ = 10.60
Φ_I = 40.0
Φ_I = 180.0
BIDIRECTIONAL REFLECTANCE (STER.$^{-1}$)
10^1
10^0
10^{-1}
10^{-2}
10^{-3}
90.
60.
30.
0.
30.
60.
90.
Φ_R (DEGREES)
Φ_R = .00
Φ_R = 180.00

MUCUCC CUC

λ = .63
θ_i = 40.0
ϕ_i = 180.0

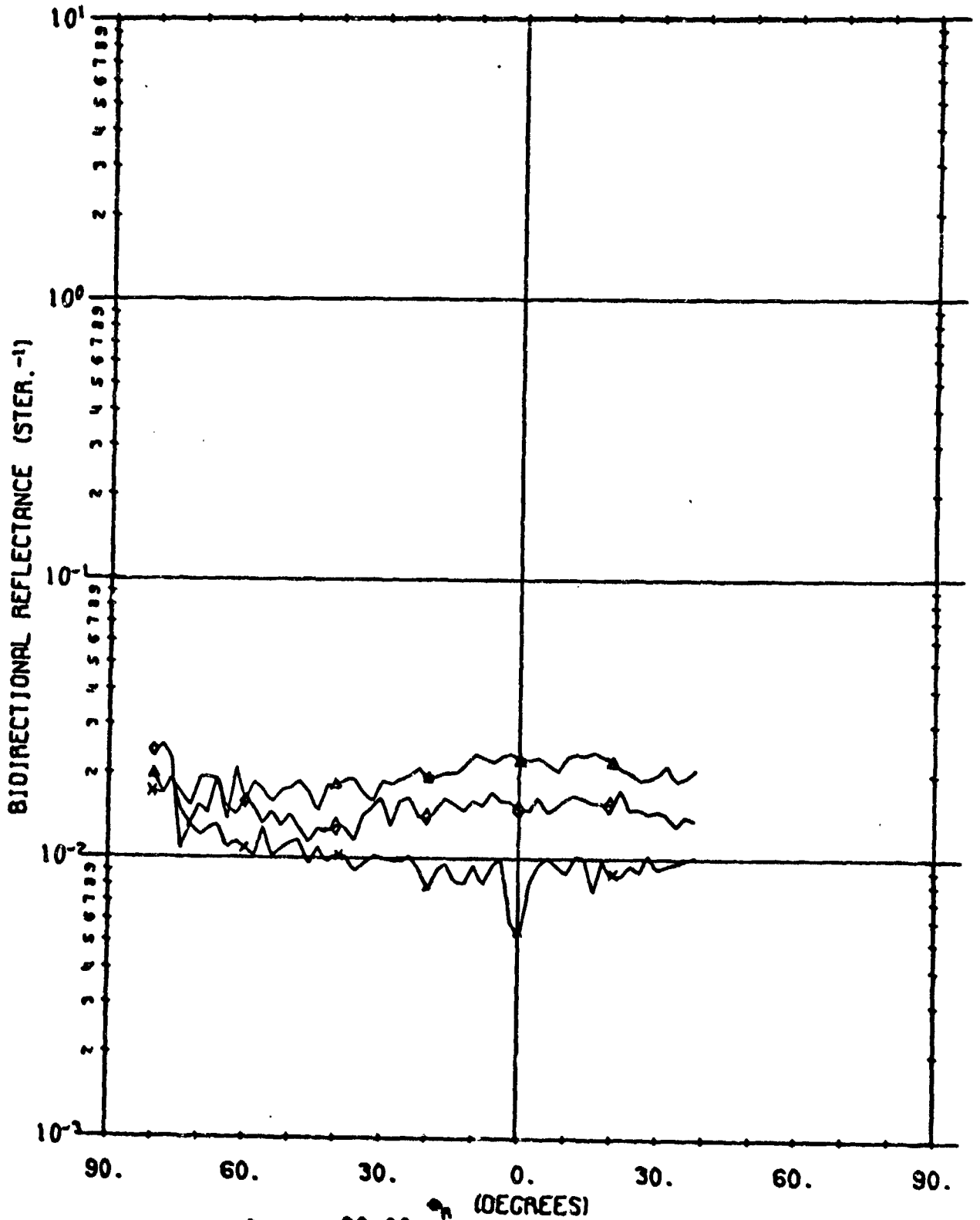

A02022 201

λ = 1.06
ϕ_i = 40.0
θ_i = 180.0

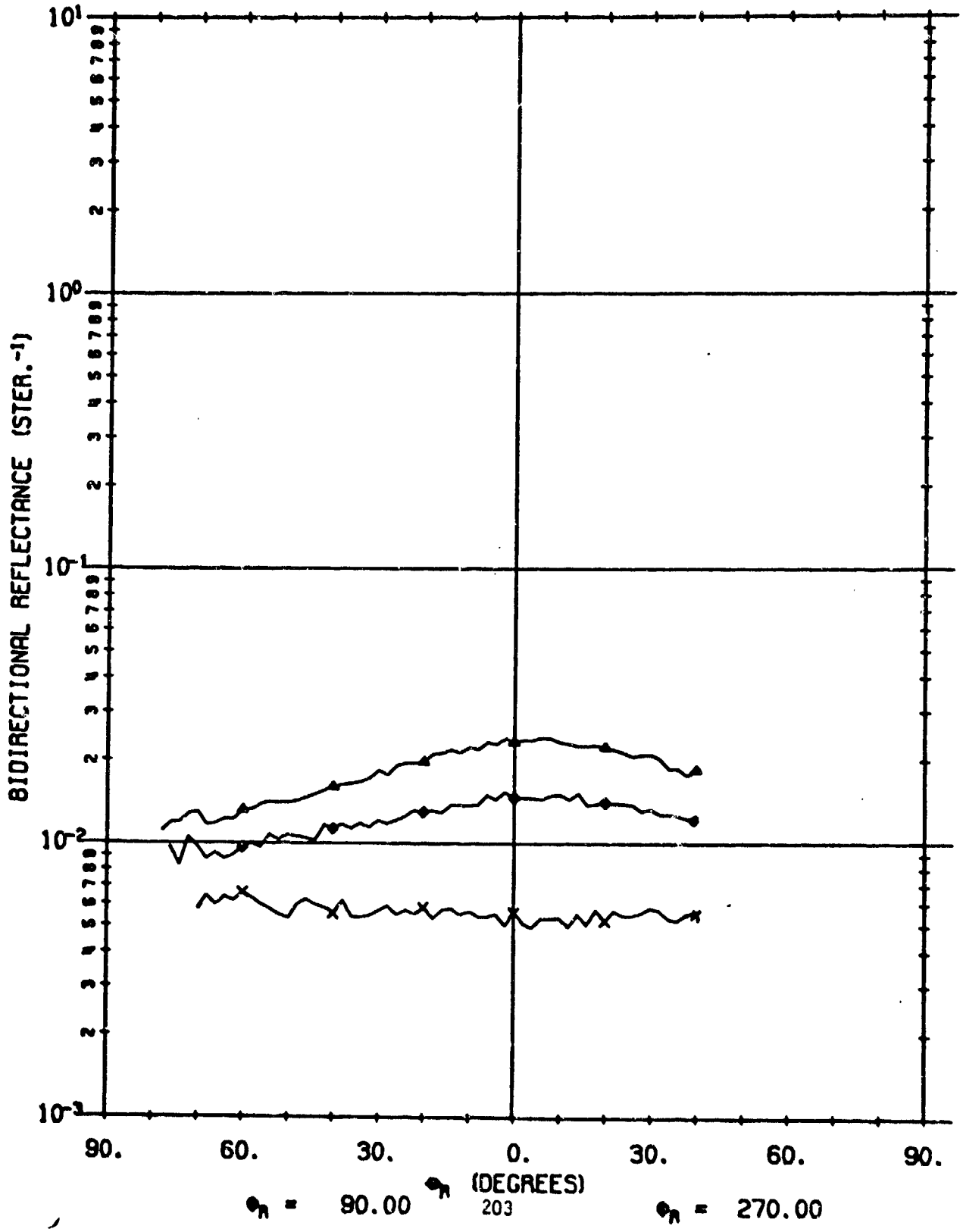

A02022 701

λ = 3.39
Φ_I = 40.0
Φ_I = 180.0

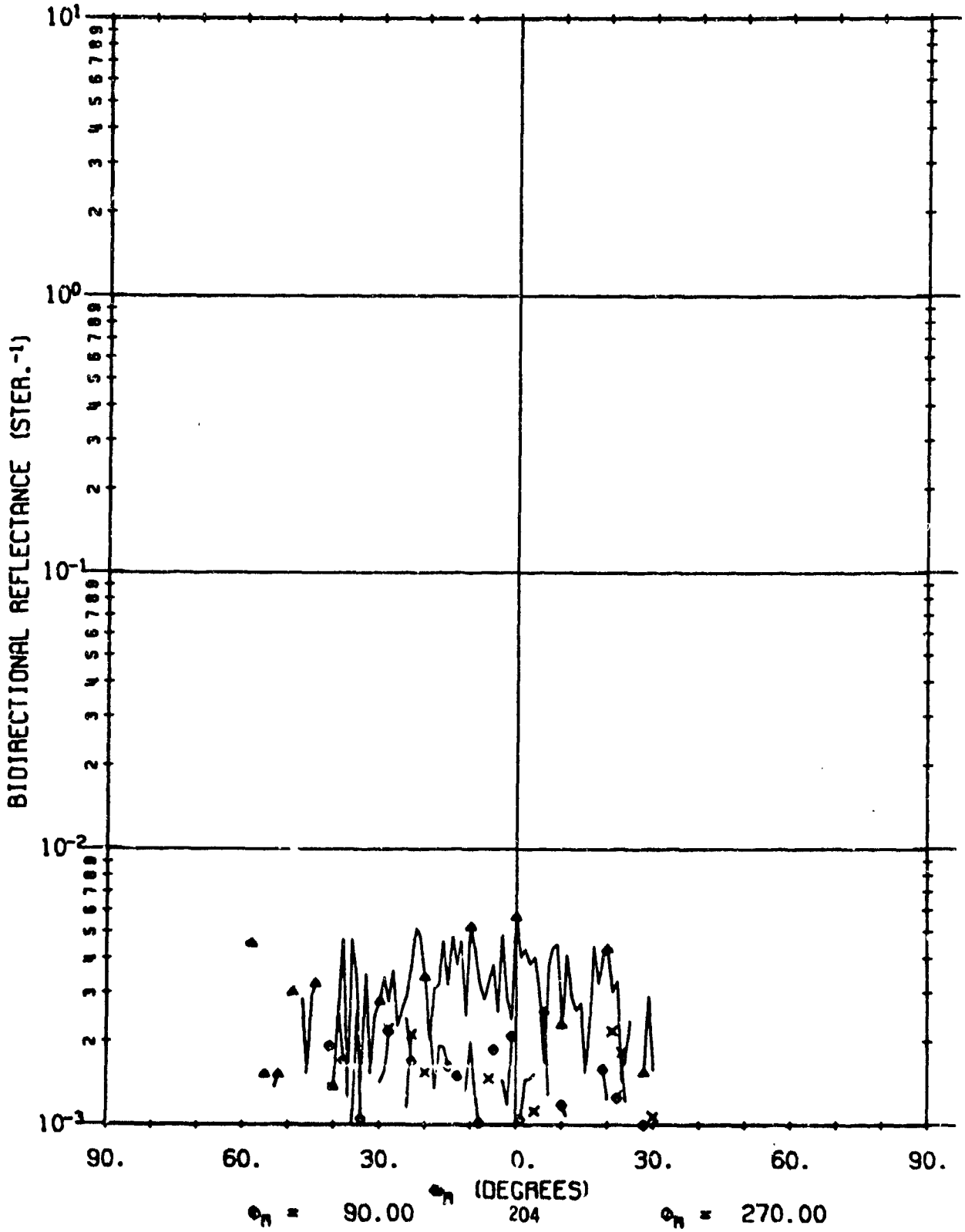

A02022 604

λ = 10.60
θ_I = 40.0
ϕ_I = 180.0

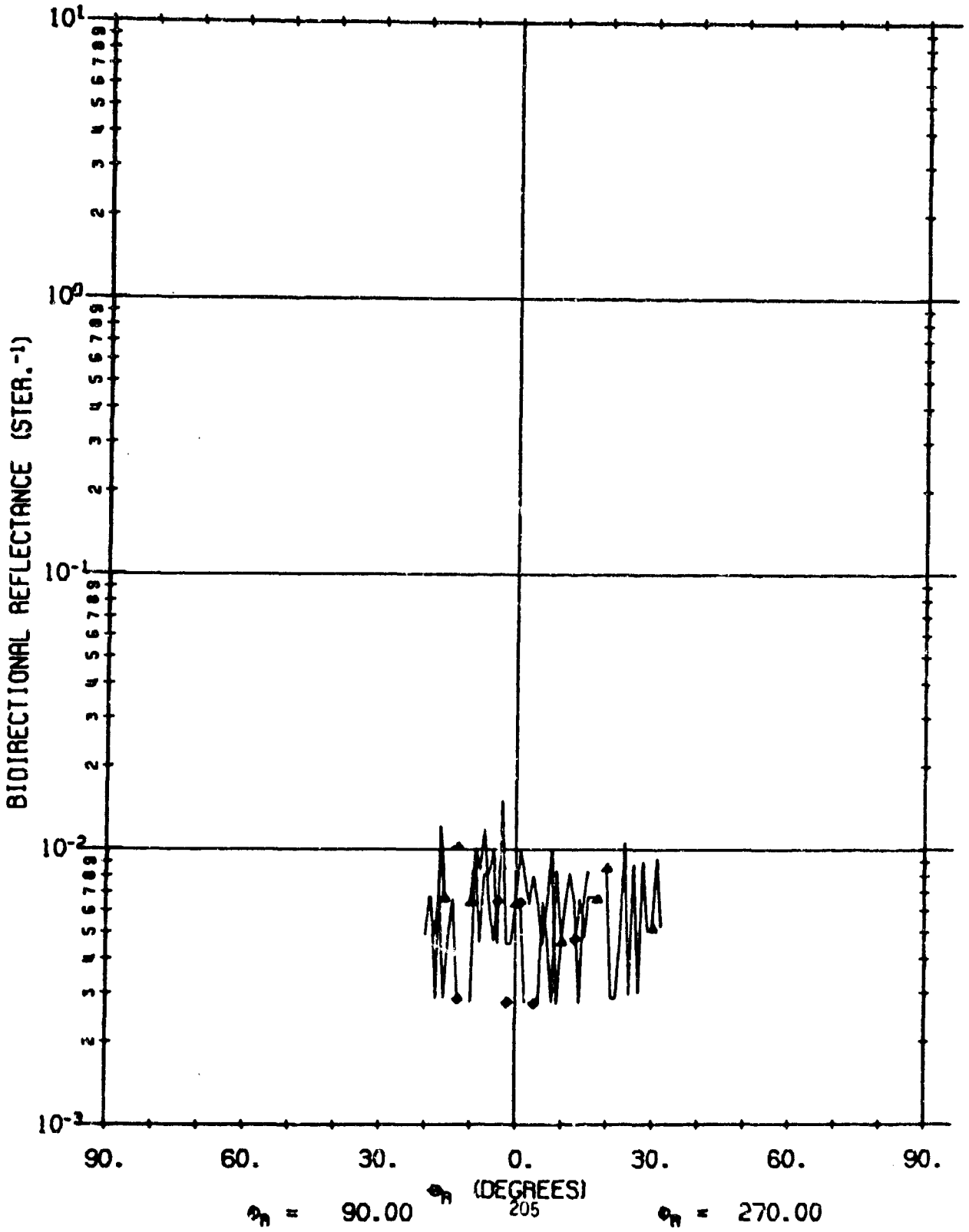

A02022 202

λ = .63
θ_i = 60.0
ϕ_i = 180.0

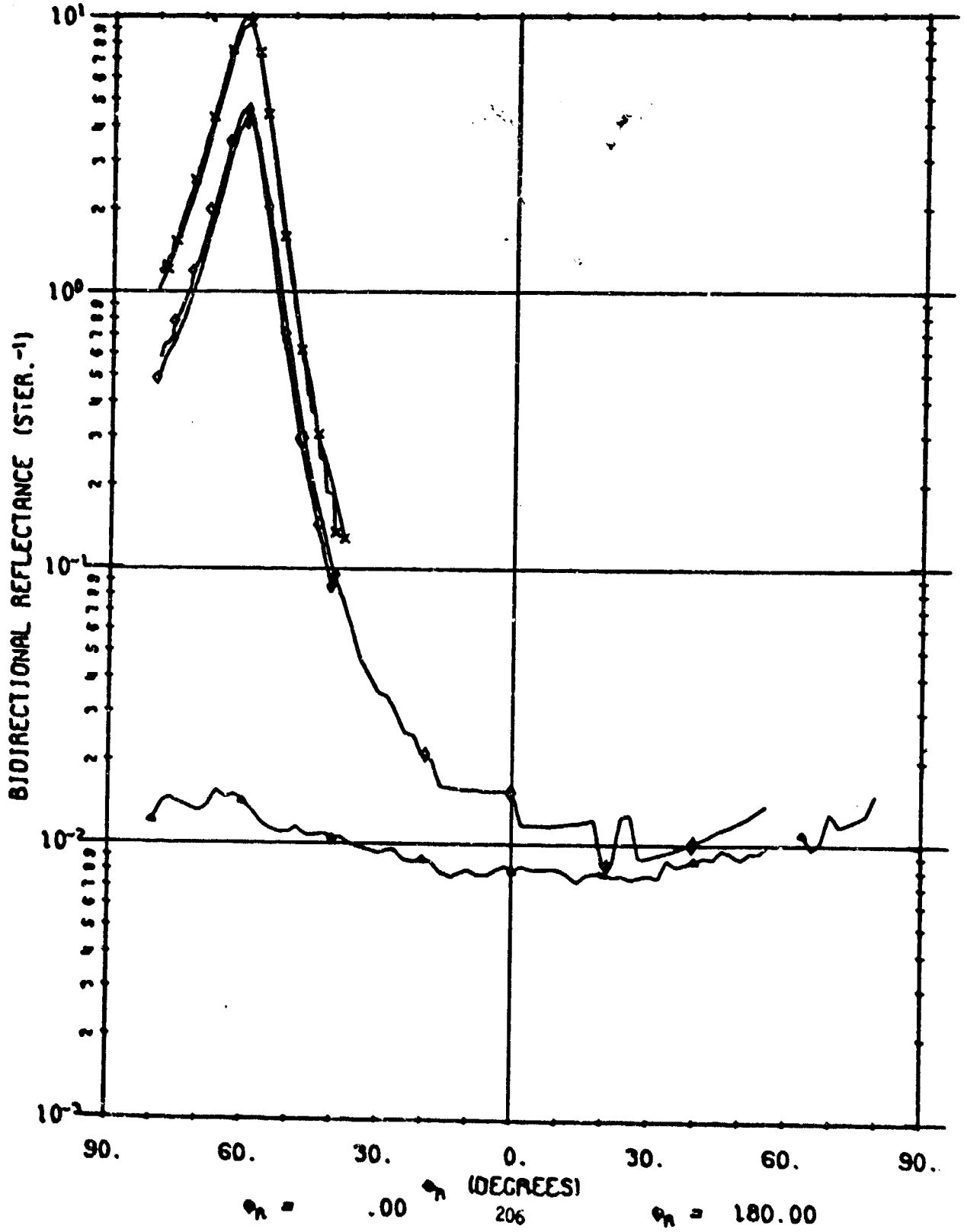

A02022 201

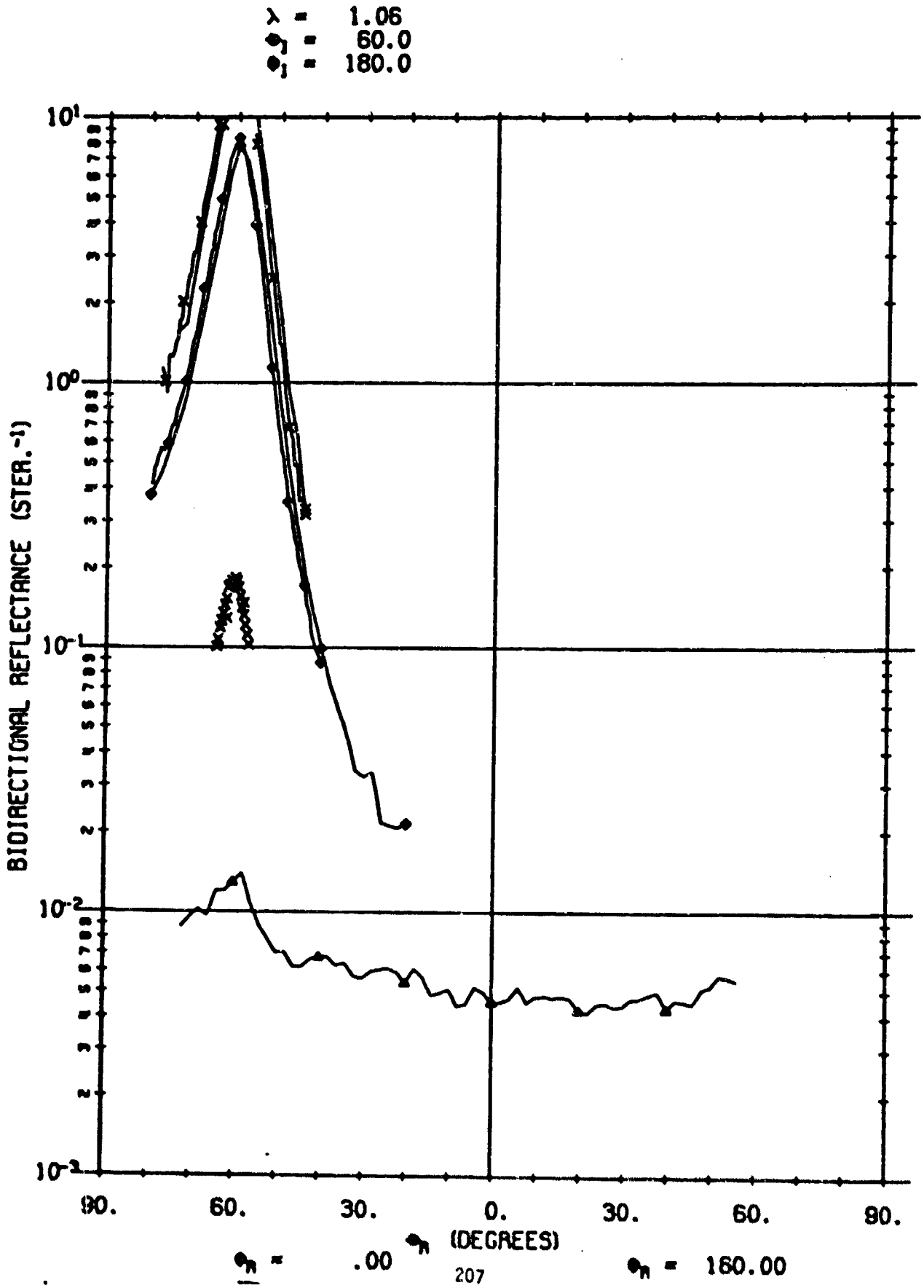
λ = 1.06
θ_i = 60.0
ϕ_i = 180.0
BIDIRECTIONAL REFLECTANCE (STER.$^{-1}$)
10^1
10^0
10^{-1}
10^{-2}
10^{-3}
90.
60.
30.
0.
30.
60.
90.
θ_r (DEGREES)
ϕ_r = .00
ϕ_r = 180.00

A02022 702

λ = 3.39
θ_I = 60.0
Φ_I = 180.0

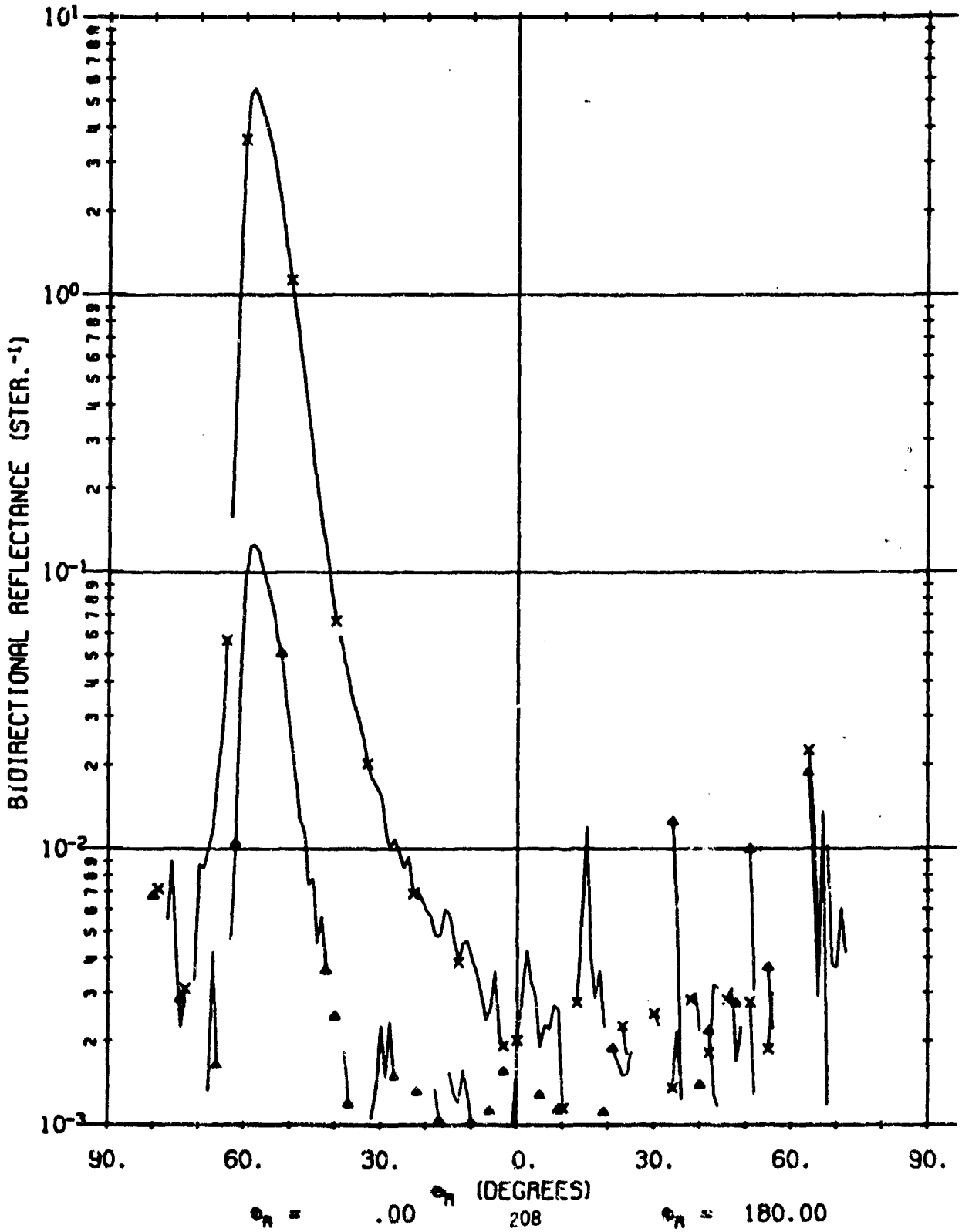

A02022 602

λ = 10.60
θ_I = 60.0
ϕ_I = 180.0

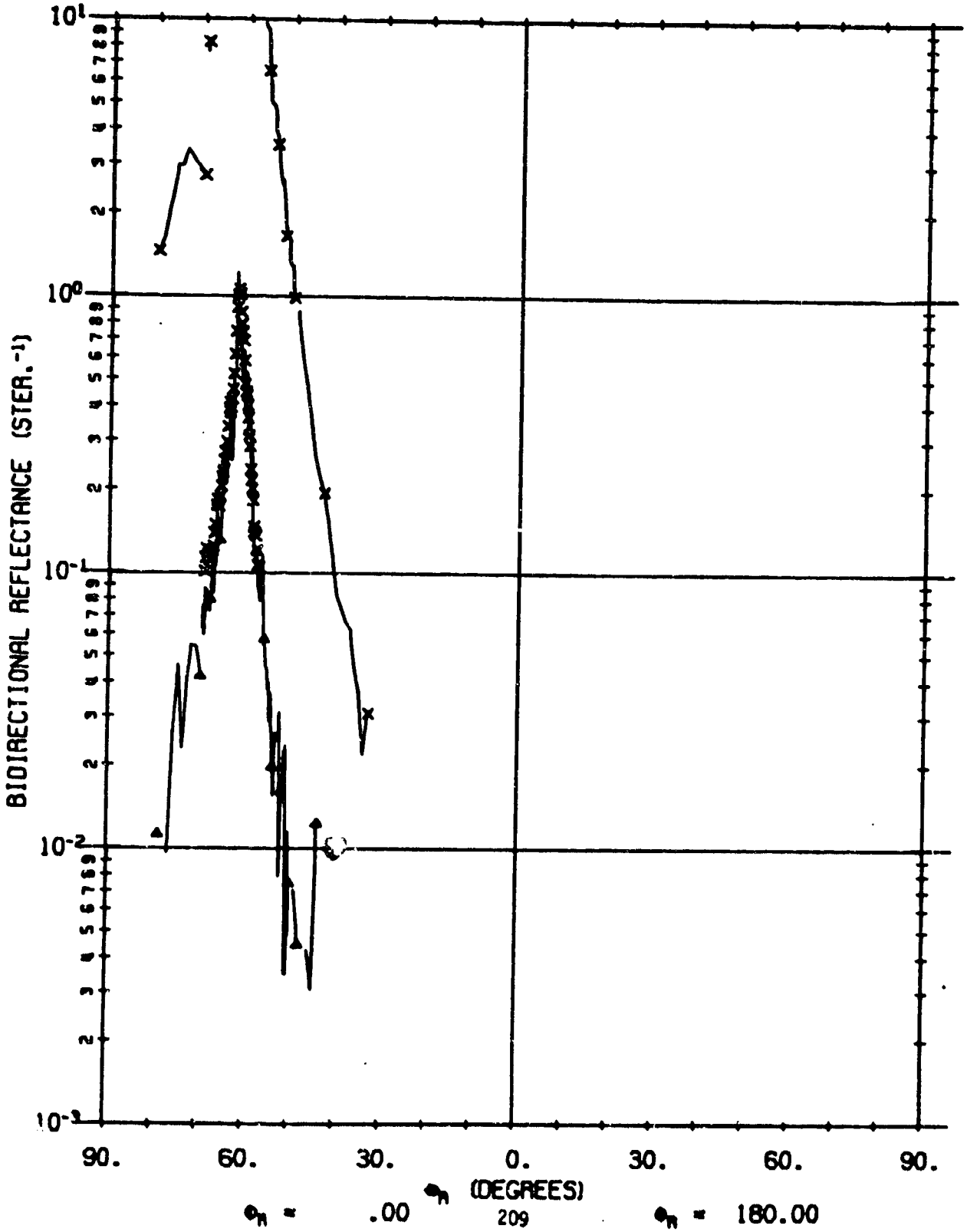

A02022 202

λ = .63
ϕ_t = 60.0
ϕ_i = 180.0

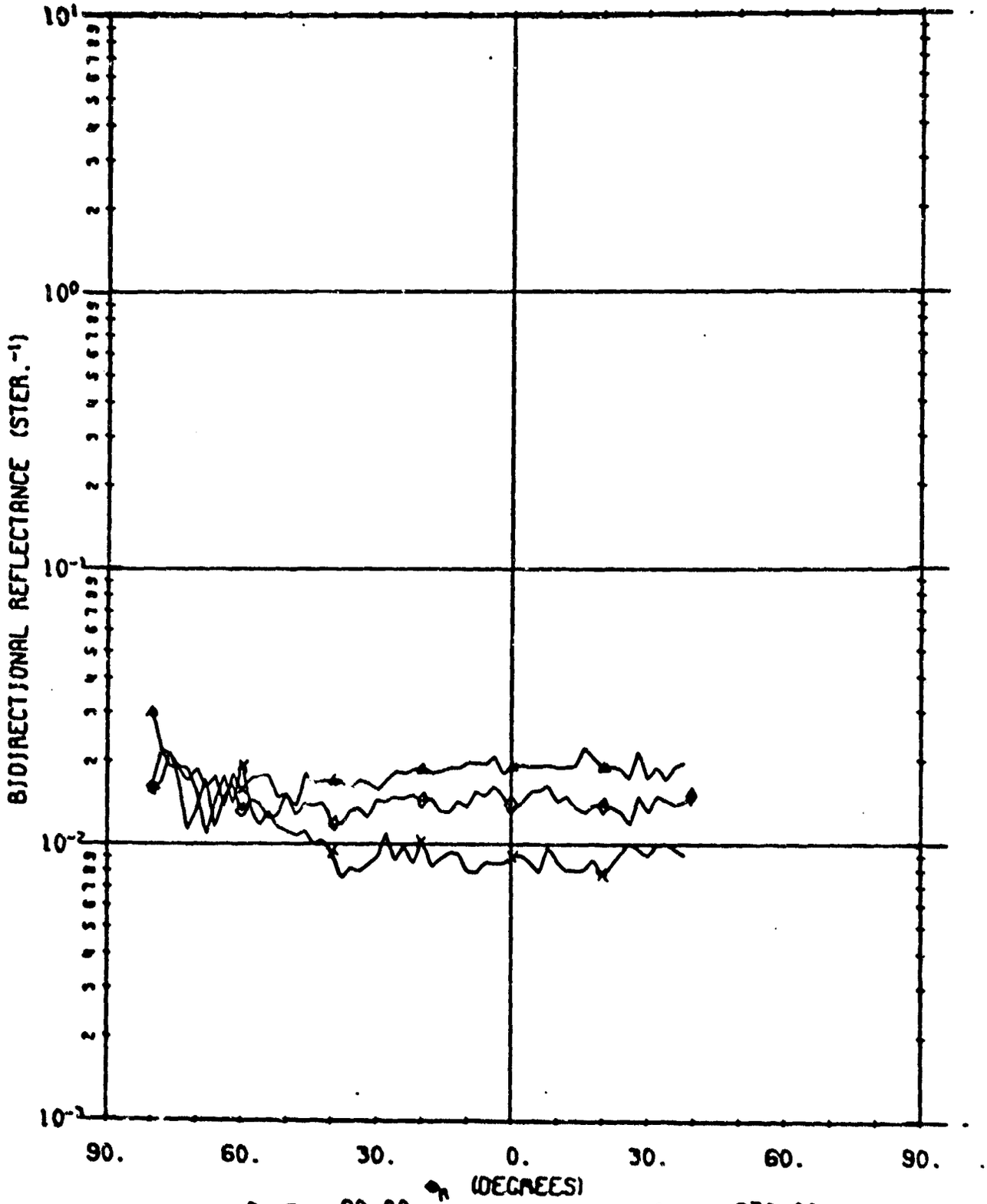

ϕ_r = 90.00 ϕ_r = 270.00

A02022 201

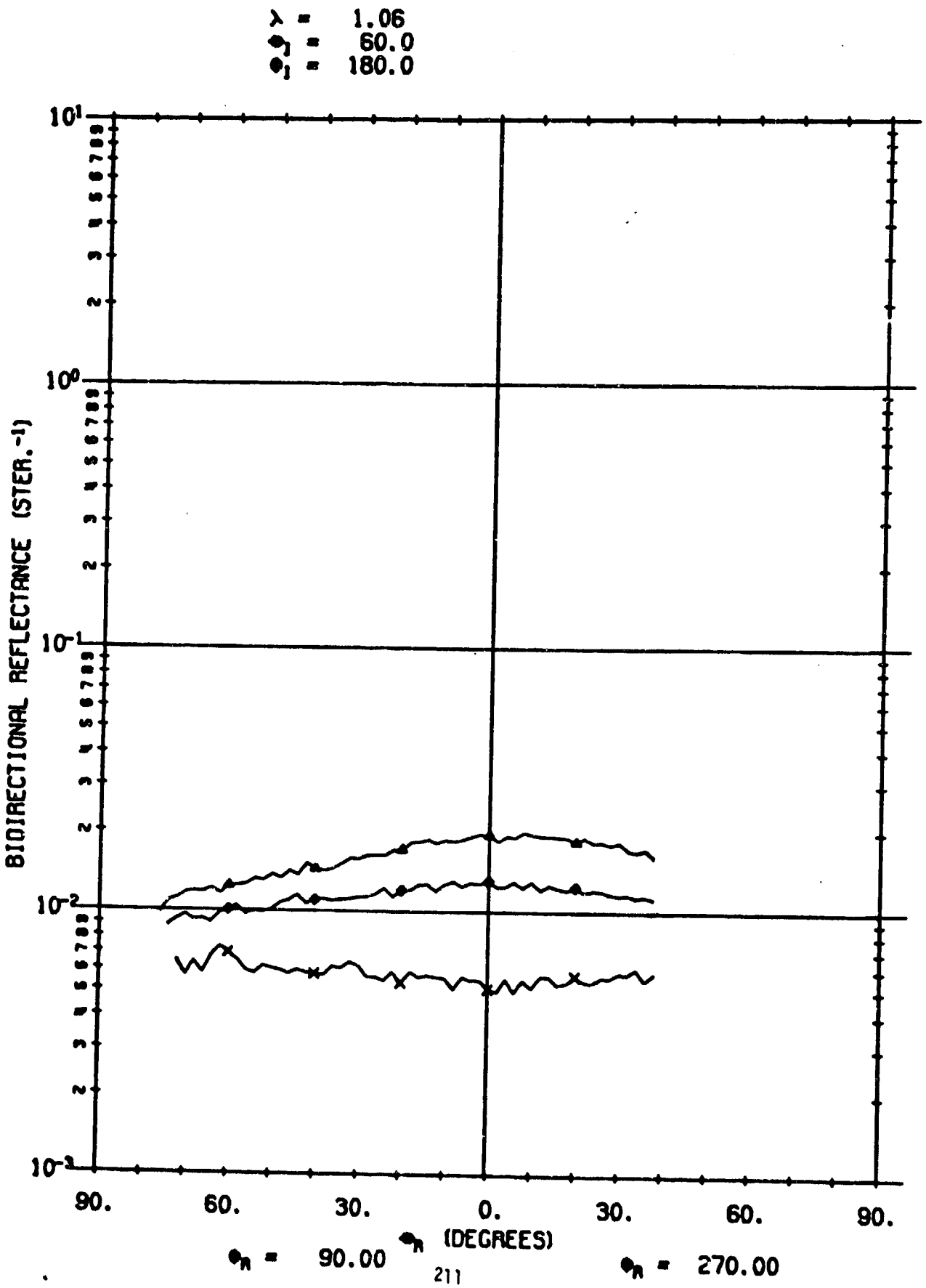
λ = 1.06
θ_i = 60.0
ϕ_i = 180.0
BIDIRECTIONAL REFLECTANCE (STER.$^{-1}$)
10^1
10^0
10^{-1}
10^{-2}
10^{-3}
90.
60.
30.
0.
30.
60.
90.
θ_r (DEGREES)
ϕ_r = 90.00
ϕ_r = 270.00

A02022 701

λ = 3.39
θ_I = 60.0
ϕ_I = 180.0

82

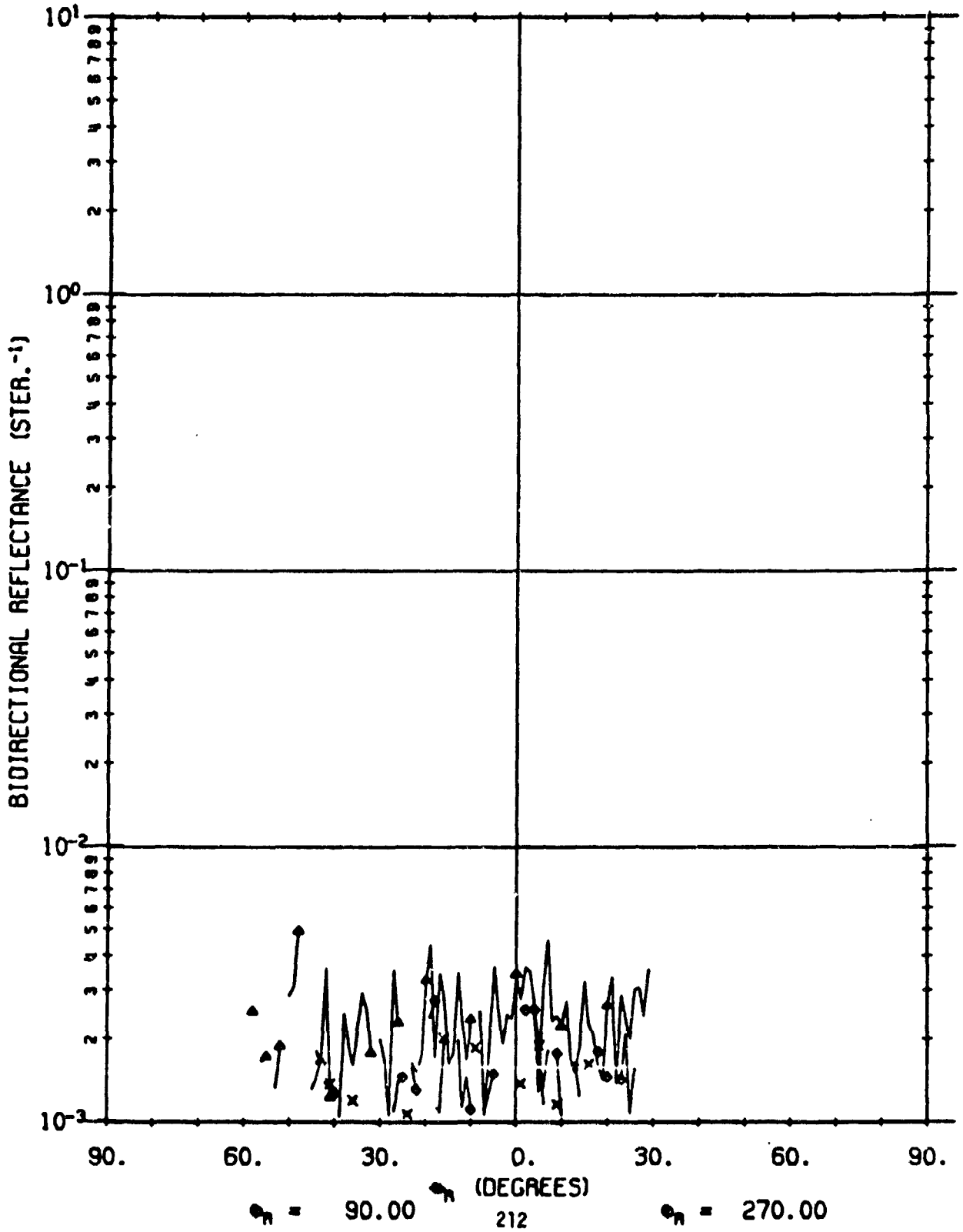

A02022 604

λ = 10.60
ϕ_I = 60.0
θ_I = 180.0

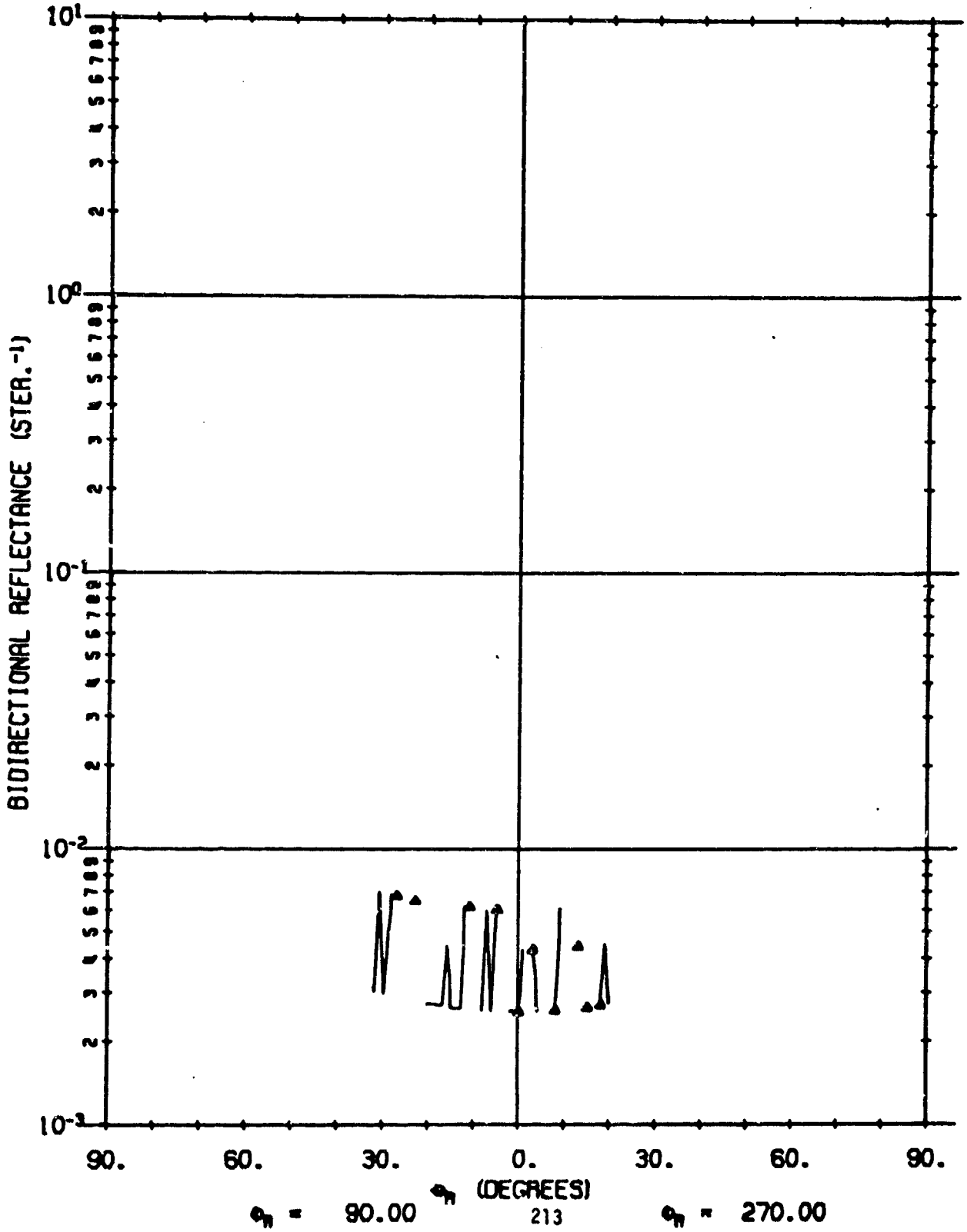

A02022 703

λ = 3.39
Φ_I = .0
Θ_I = 180.0

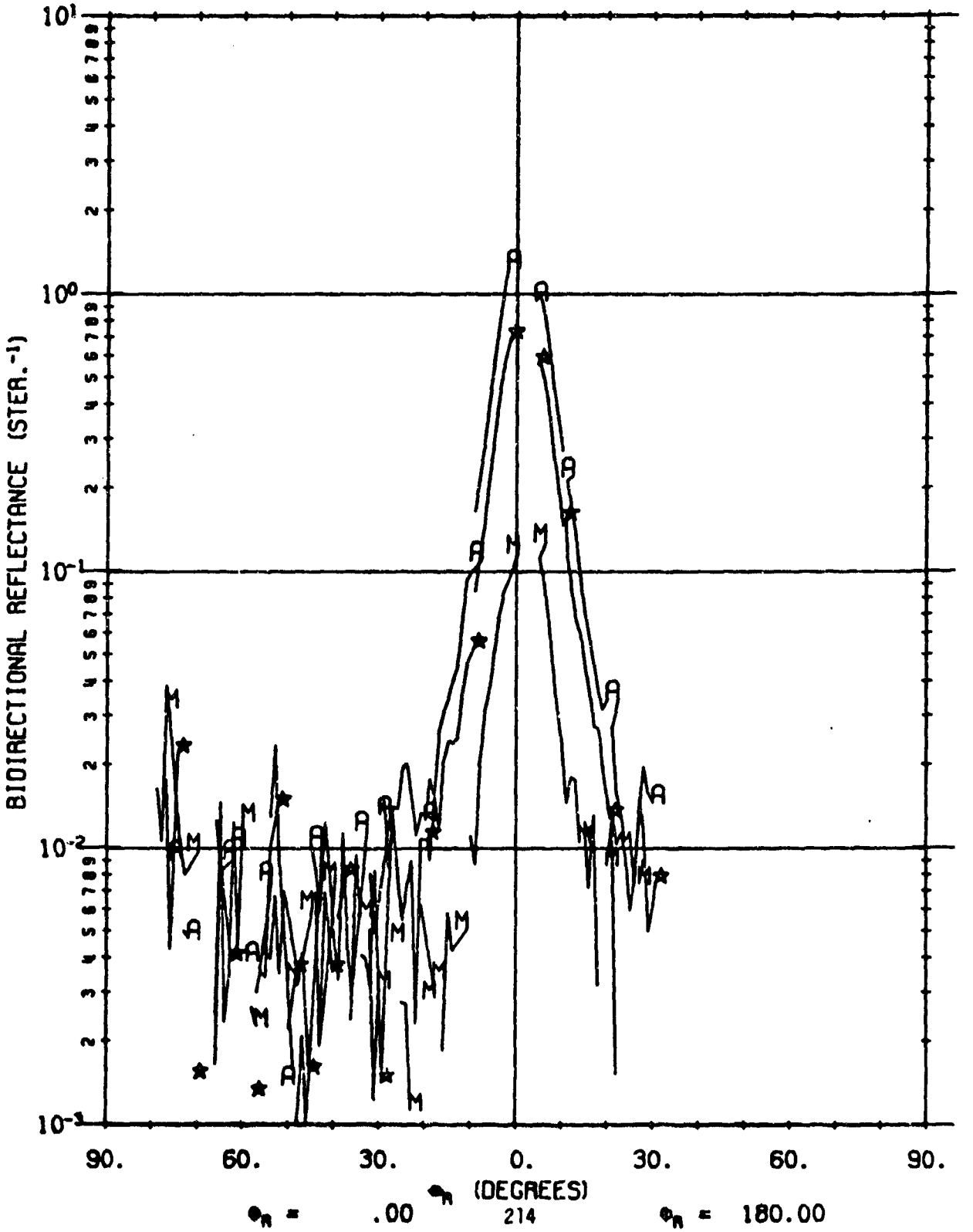

A02022 603

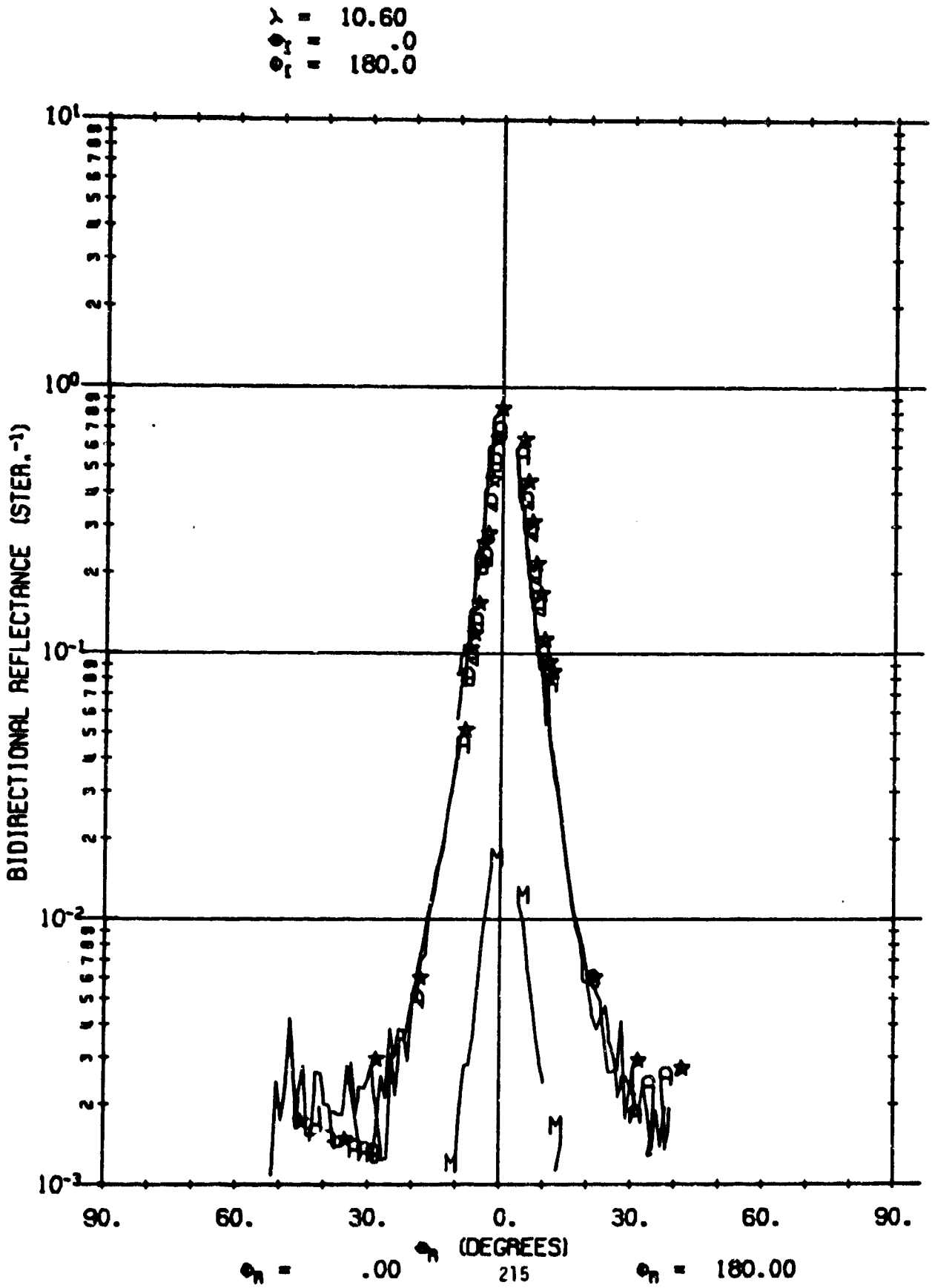
λ = 10.60
ϕ_I = .0
θ_I = 180.0
BIDIRECTIONAL REFLECTANCE (STER.$^{-1}$)
10^1
10^0
10^{-1}
10^{-2}
10^{-3}
90.
60.
30.
0.
30.
60.
90.
θ_n (DEGREES)
ϕ_n = .00
ϕ_n = 180.00

A02022 703

λ = 3.39
θ_I = 20.0
ϕ_I = 180.0

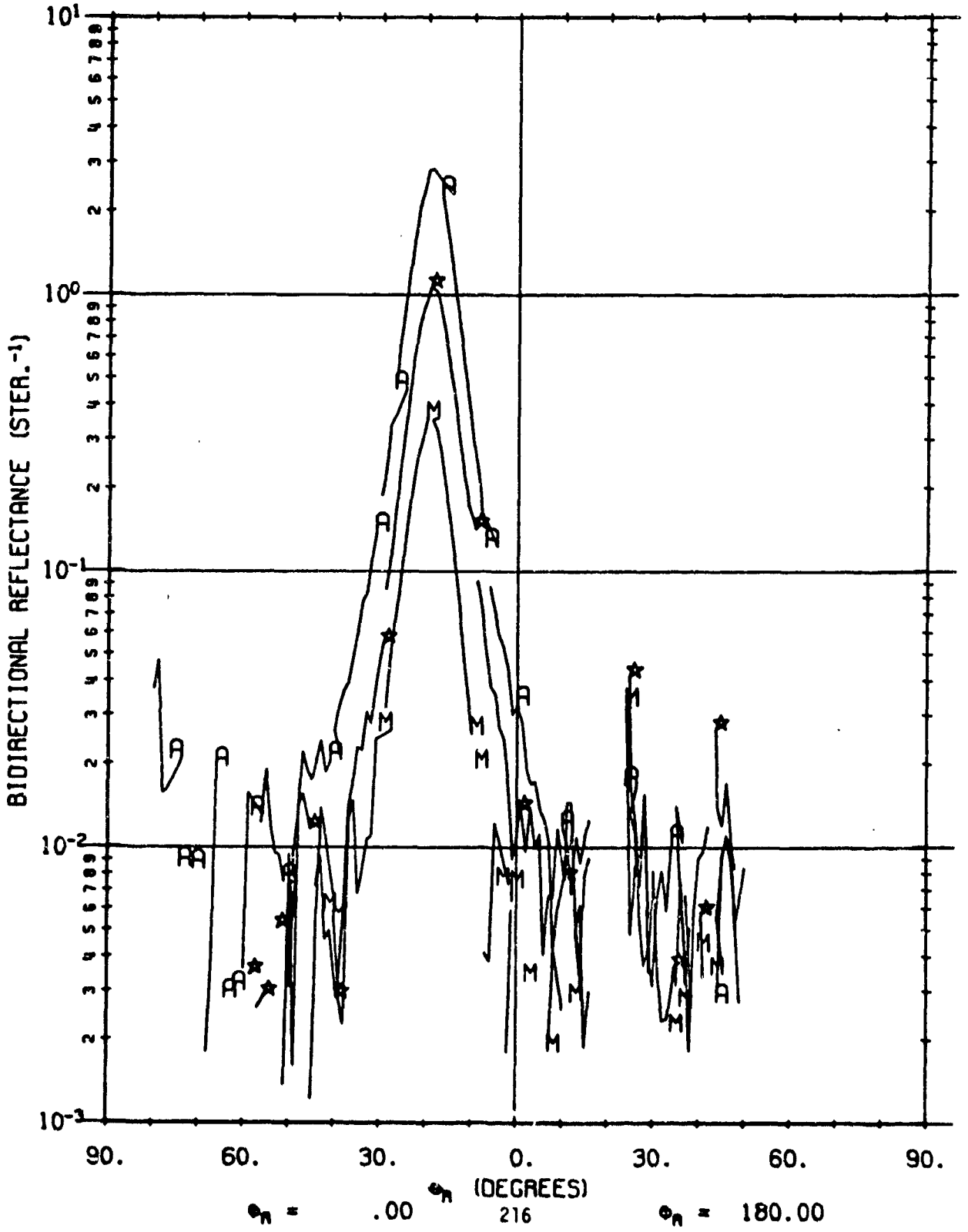

A02022 603

λ = 10.60
ϕ_I = 20.0
θ_I = 180.0

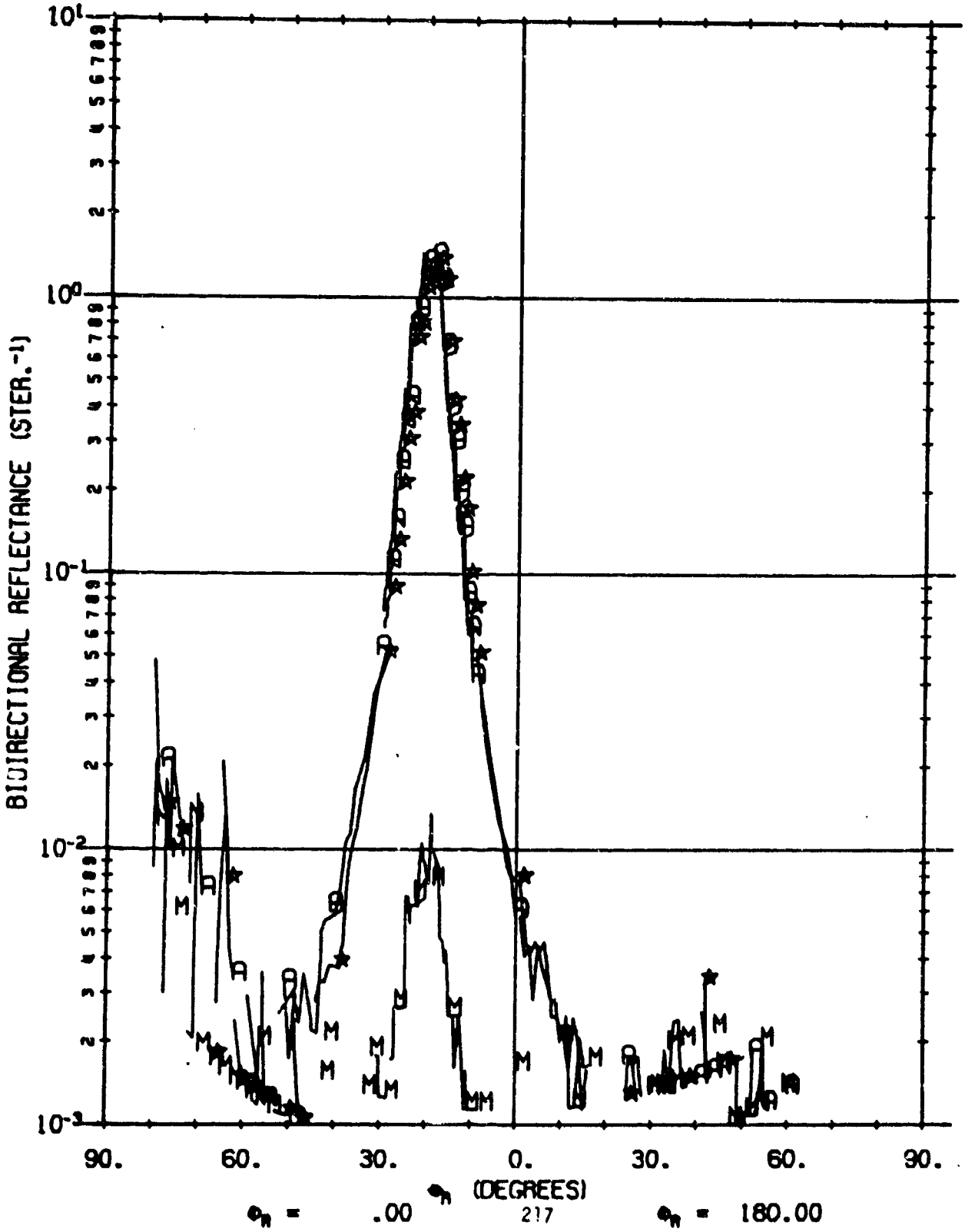

A02022 703

λ = 3.39
Φ_I = 20.0
Φ_I = 180.0

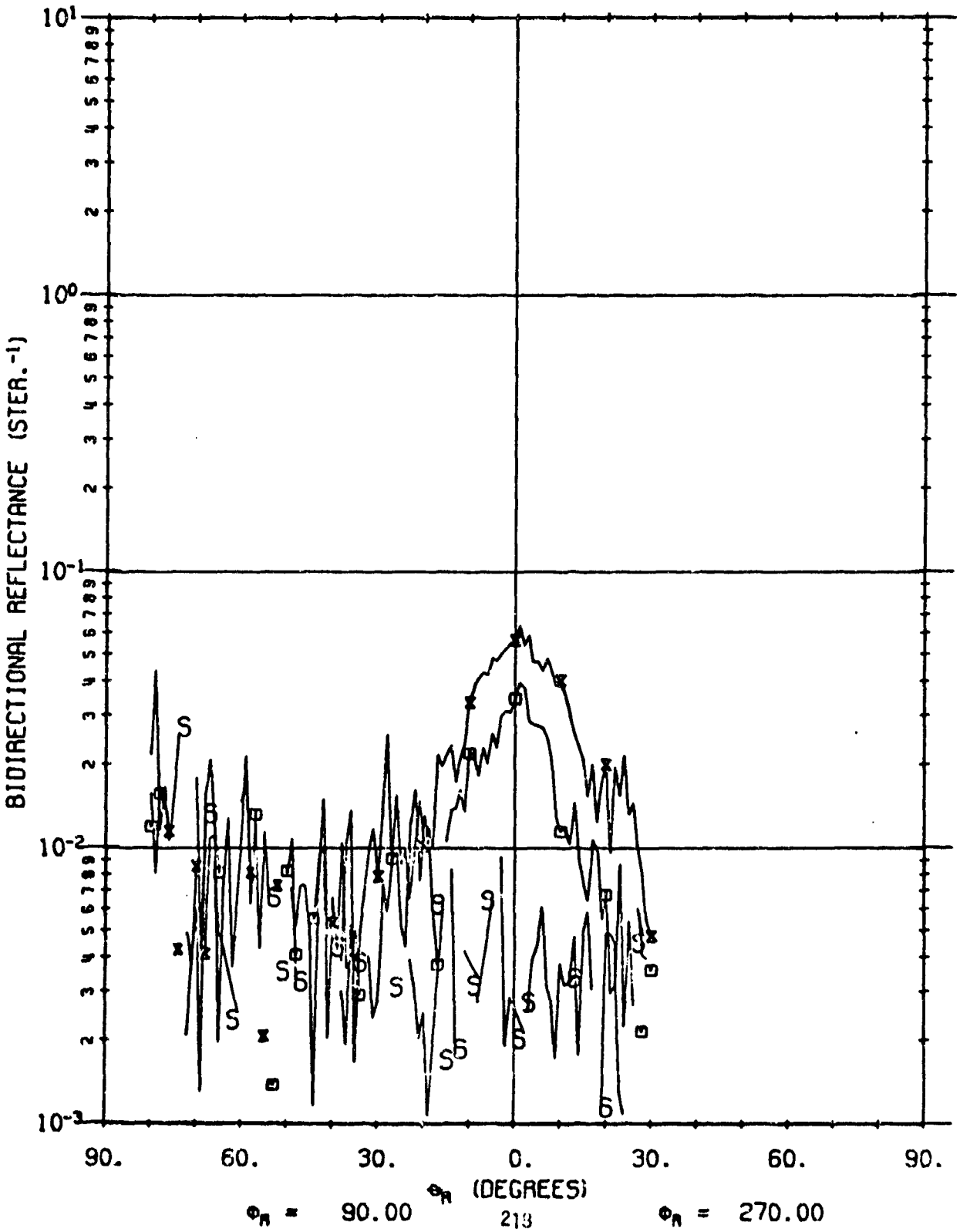

A02022 603

λ = 10.60
θ_i = 20.0
ϕ_i = 180.0

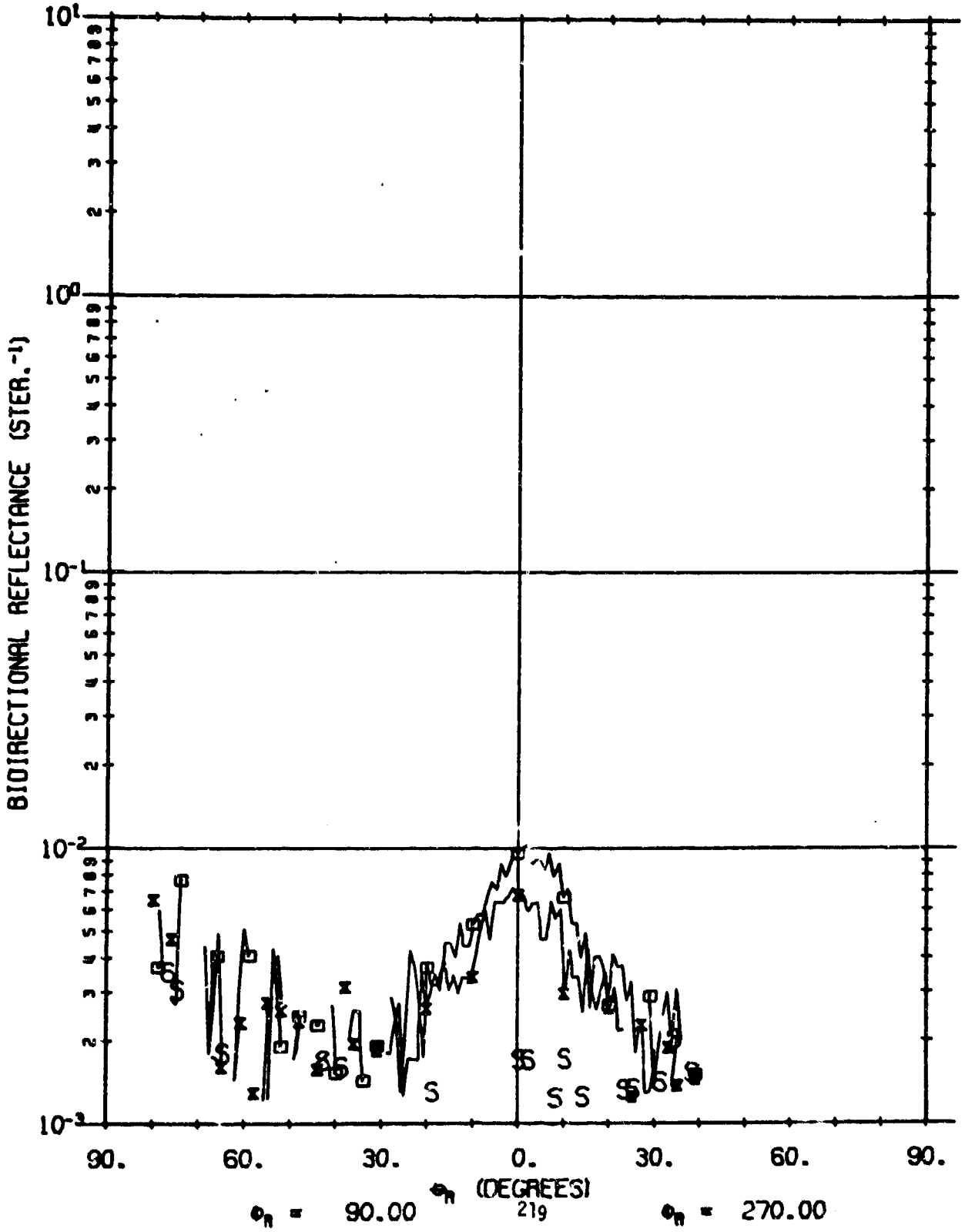

A02022 703

λ = 3.39
Φ_I = 40.0
Φ_I = 180.0

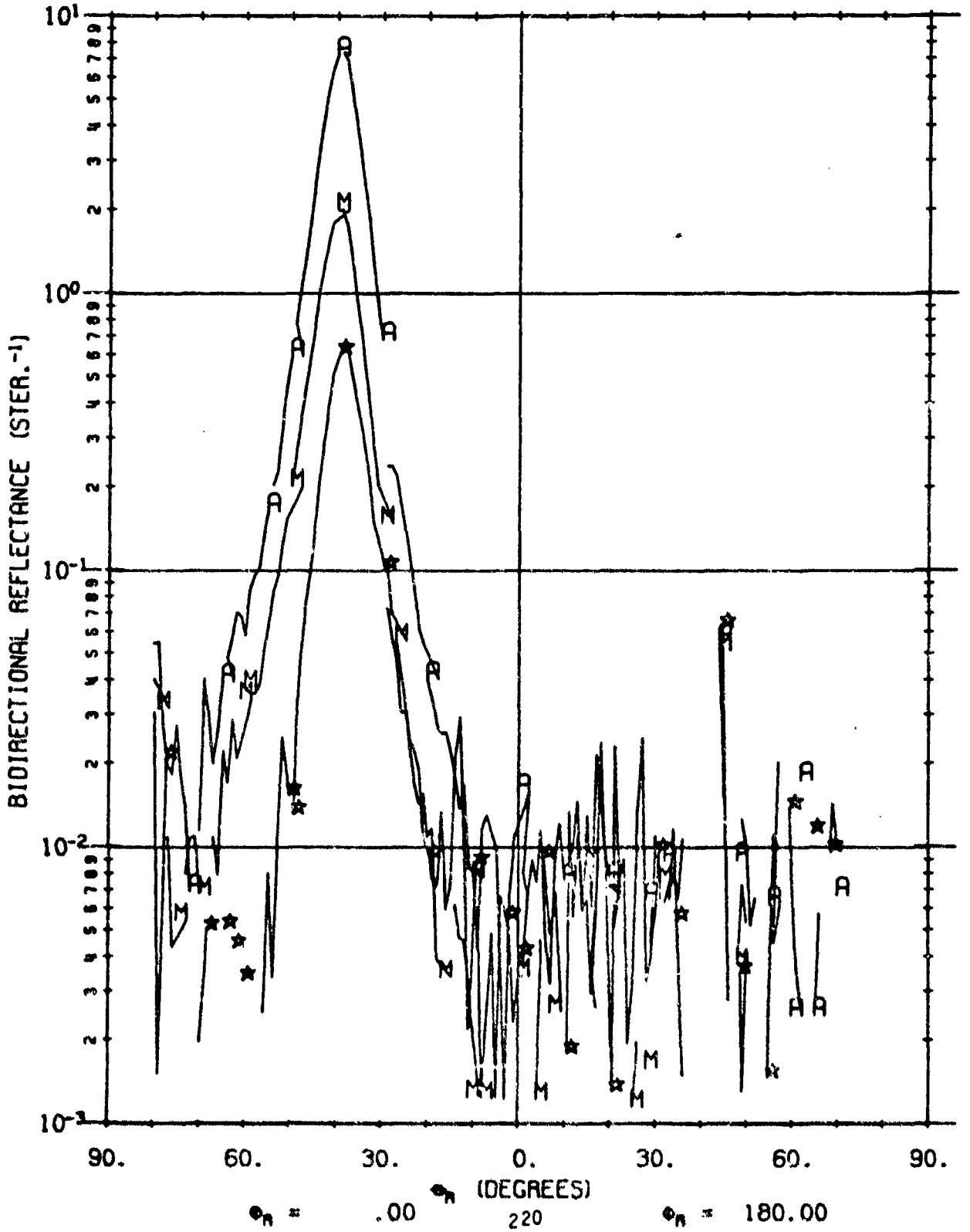

A02022 603

λ = 10.60
ϕ_I = 40.0
ϕ_I = 180.0

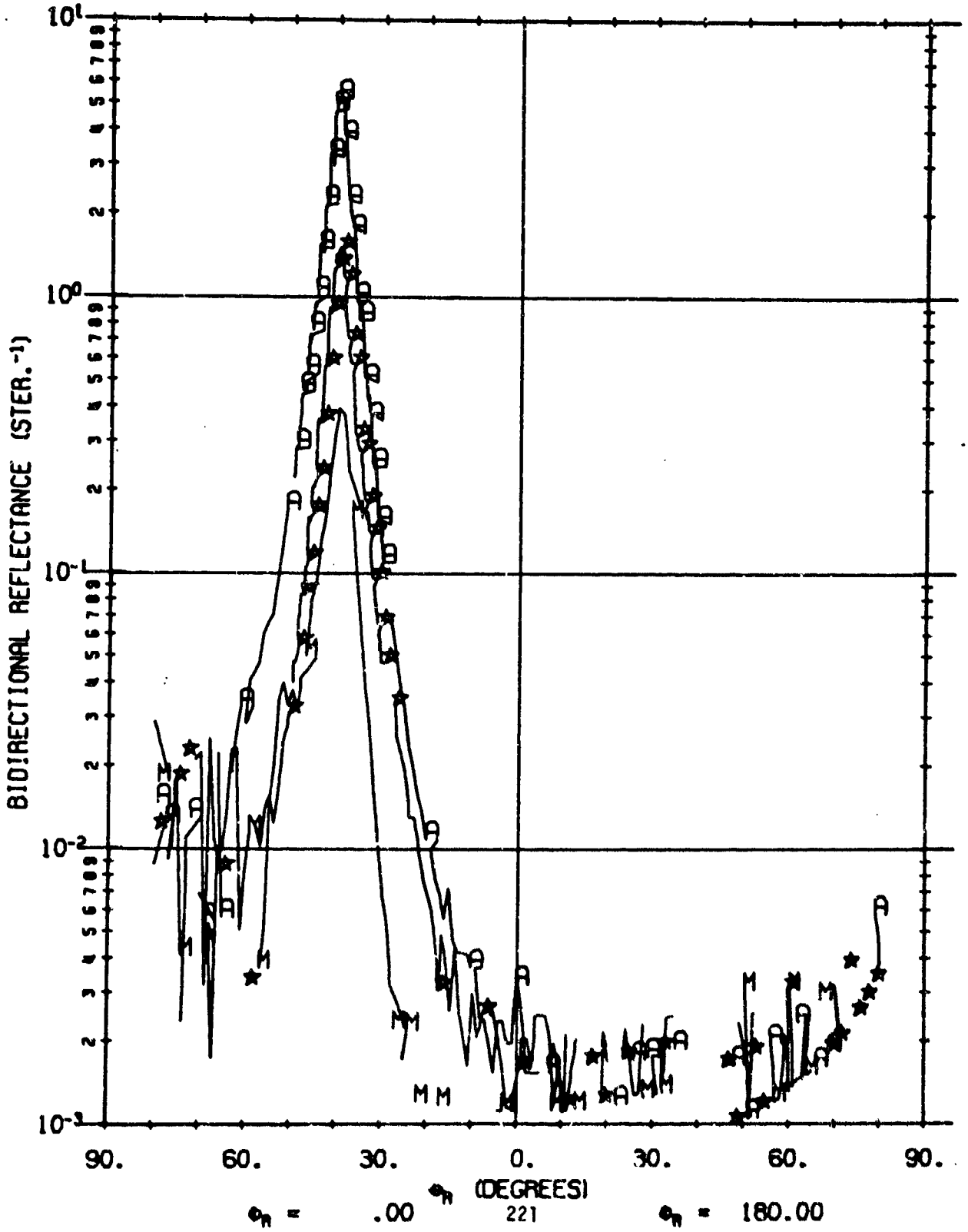

A02022 703

λ = 3.39
Φ_I = 40.0
Φ_I = 180.0

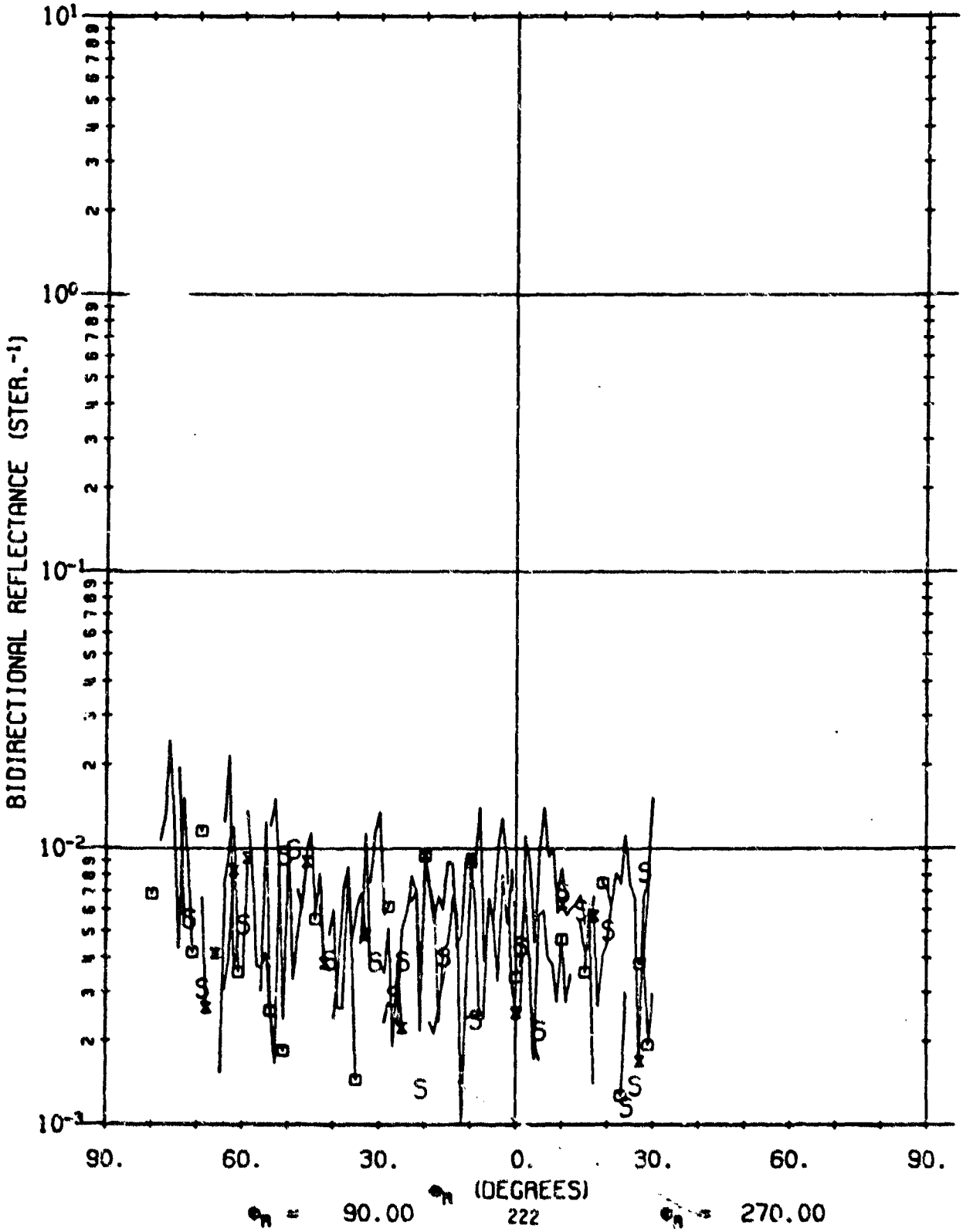

A02022 603

λ = 10.60
Φ_I = 40.0
Φ_I = 180.0

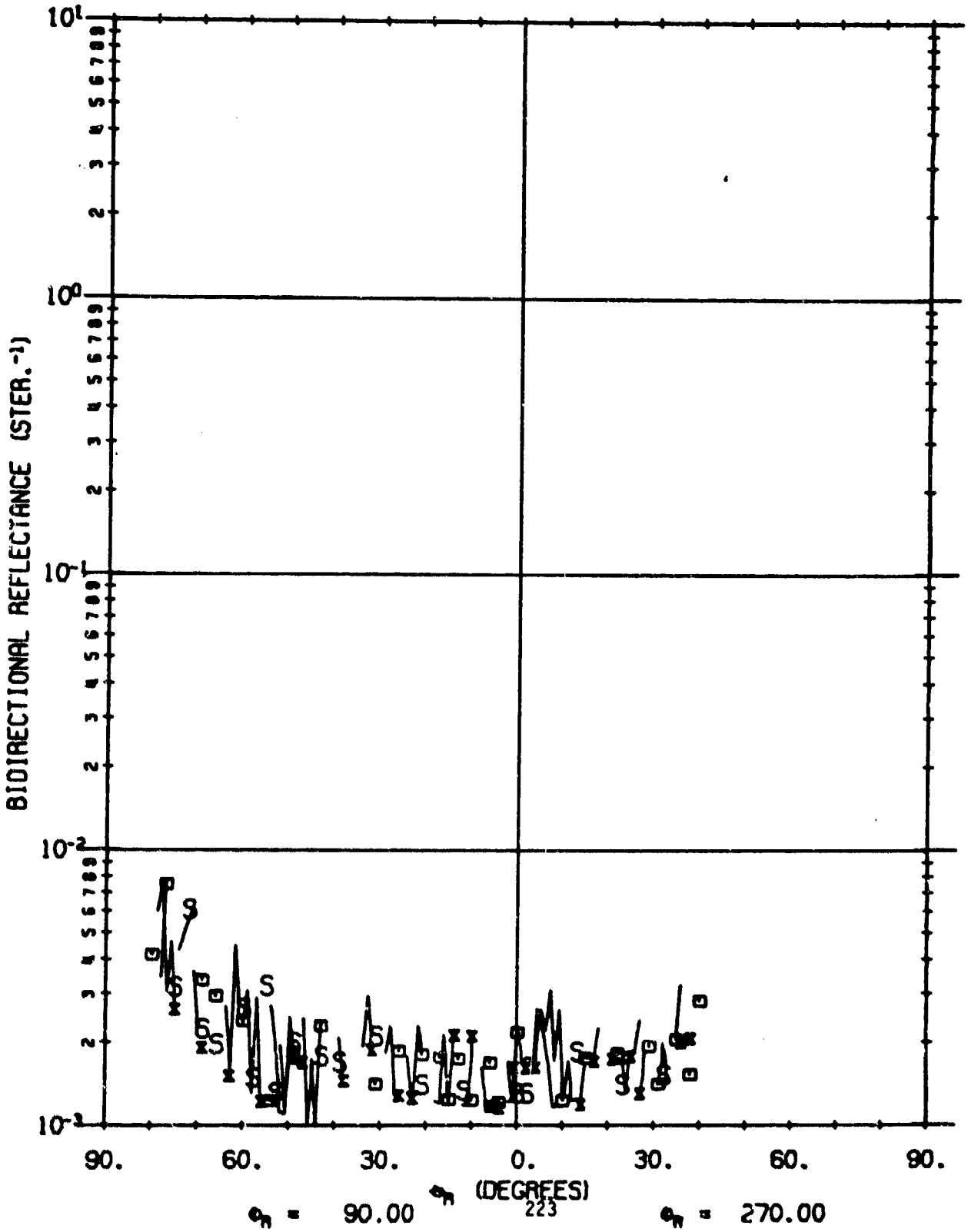

A02022 703

λ = 3.39
Φ_I = 60.0
Φ_I = 180.0

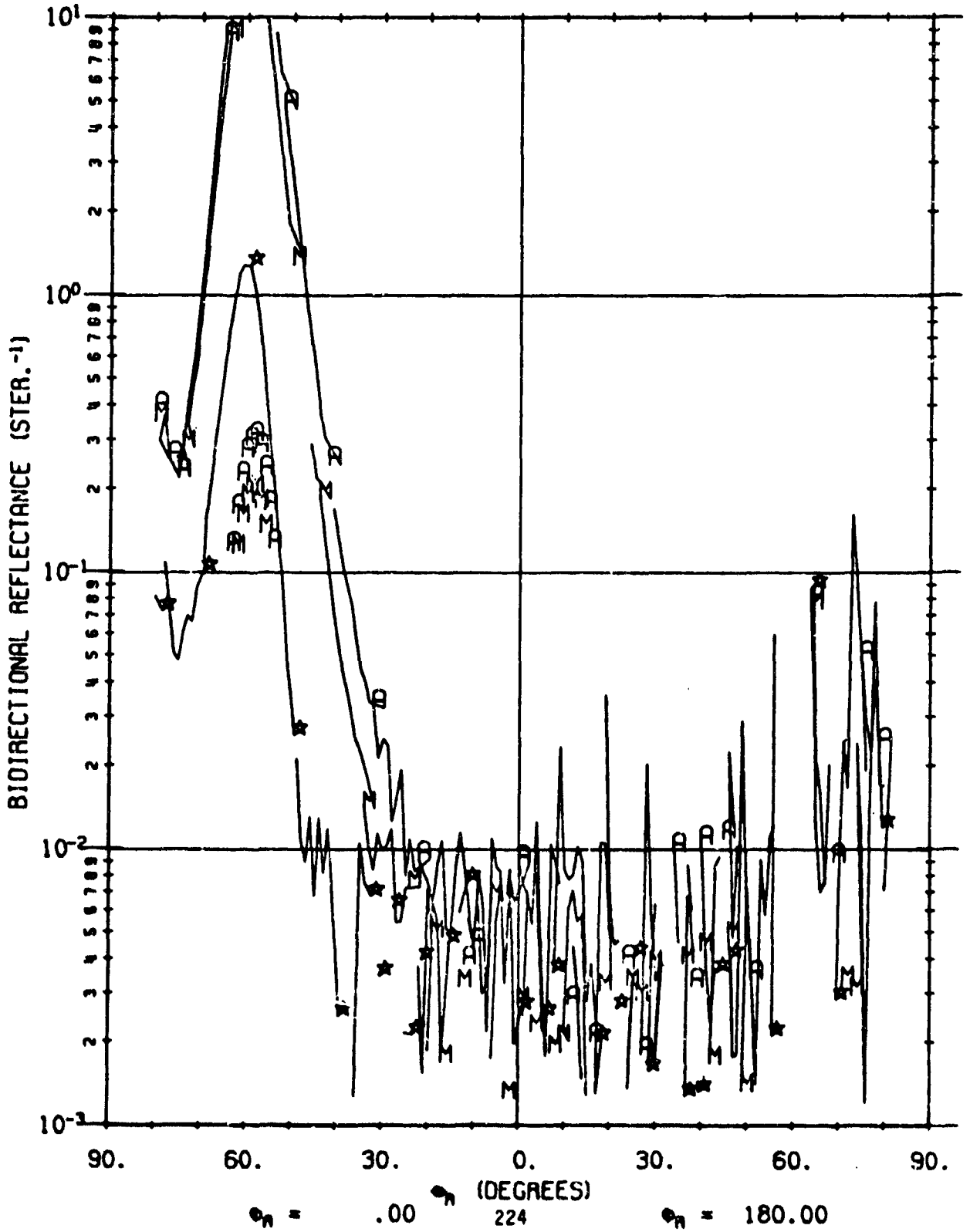

A02022 603

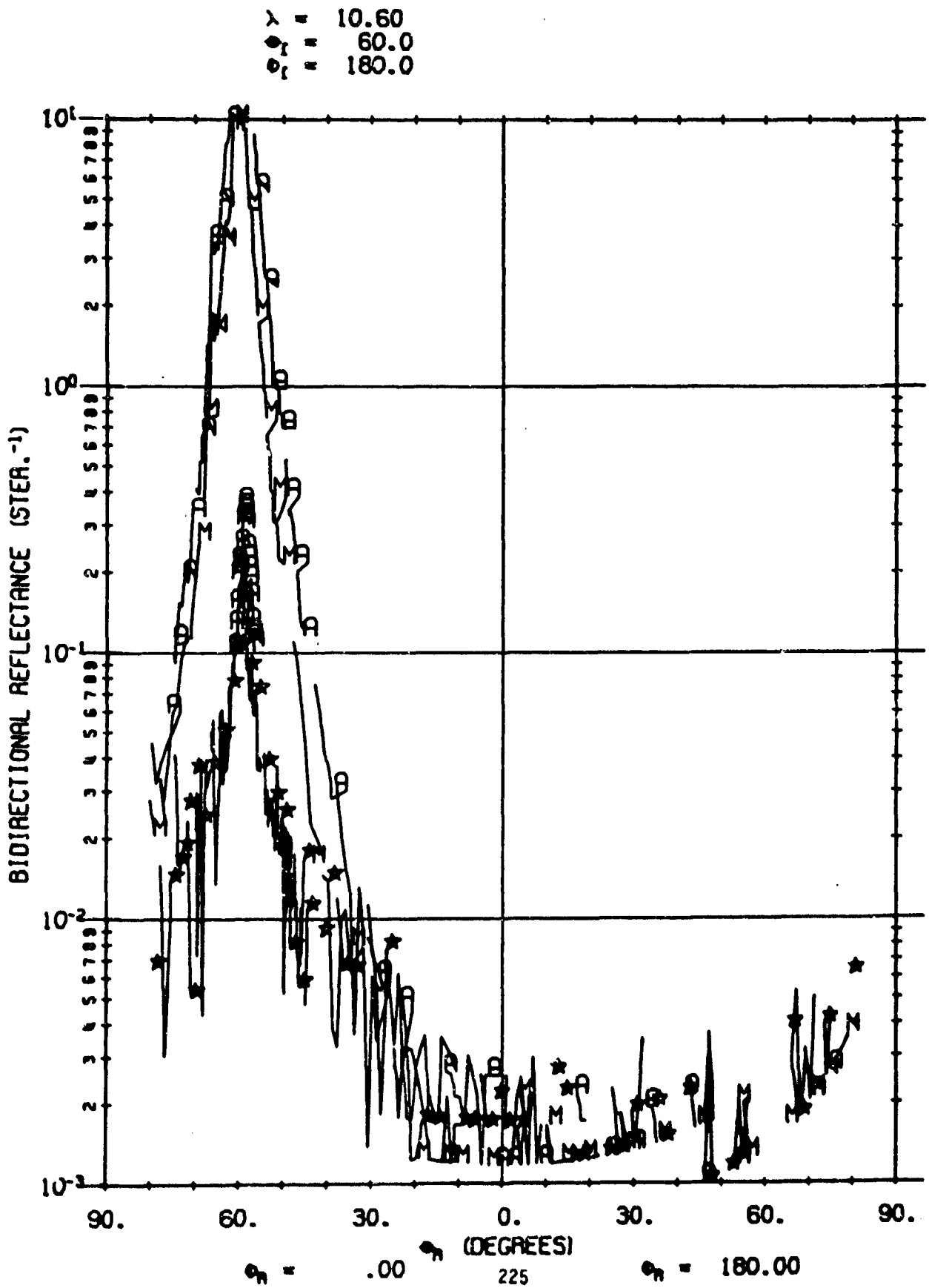
λ = 10.60
θi = 60.0
φi = 180.0
BIDIRECTIONAL REFLECTANCE (STER.-1)
10¹
10⁰
10⁻¹
10⁻²
10⁻³
90.
60.
30.
0.
30.
60.
90.
θr (DEGREES)
φr = .00
φr = 180.00

A02022 703

λ = 3.39
θ_I = 60.0
ϕ_I = 180.0

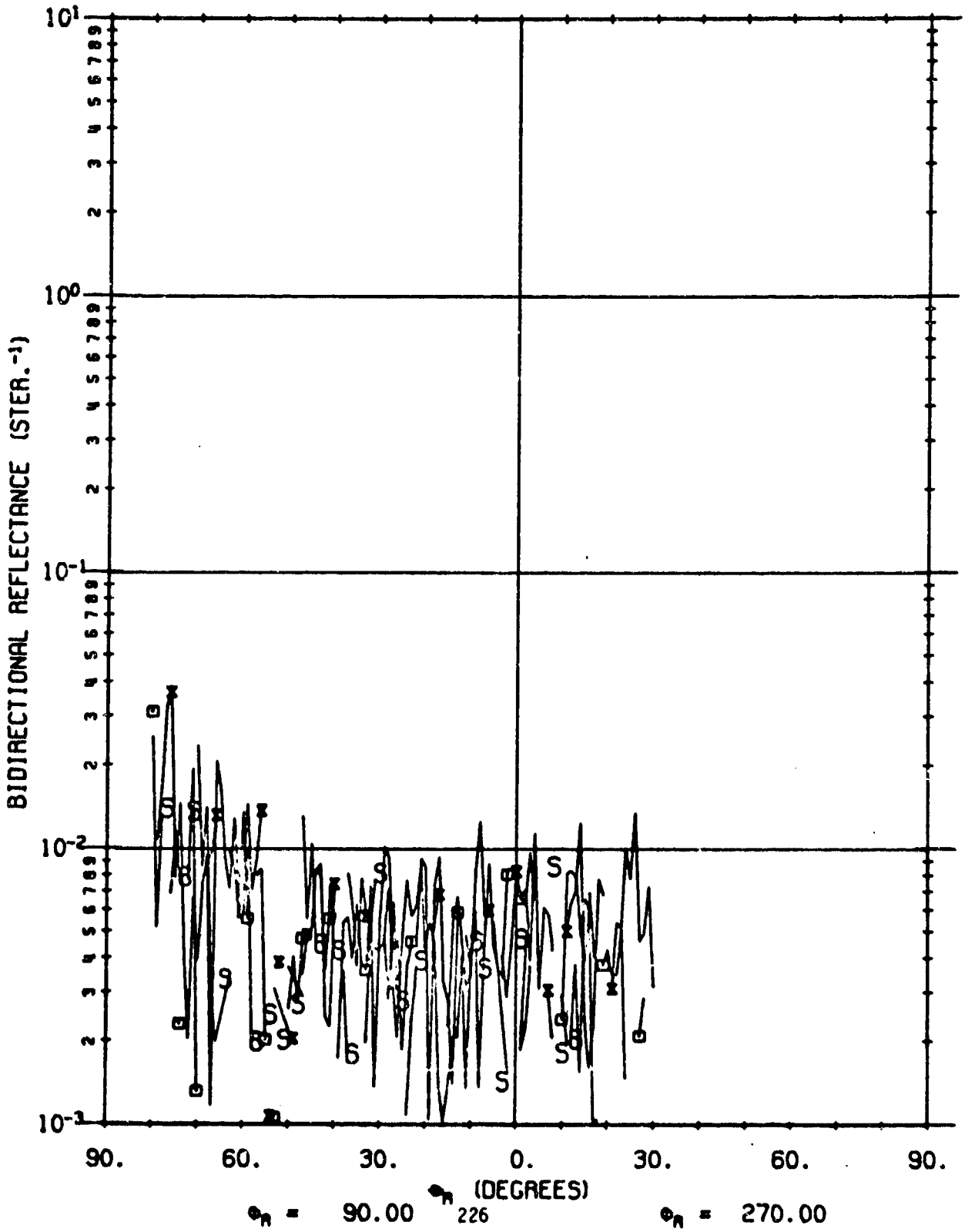

A02022 603

λ = 10.60
θ_i = 60.0
ϕ_i = 180.0

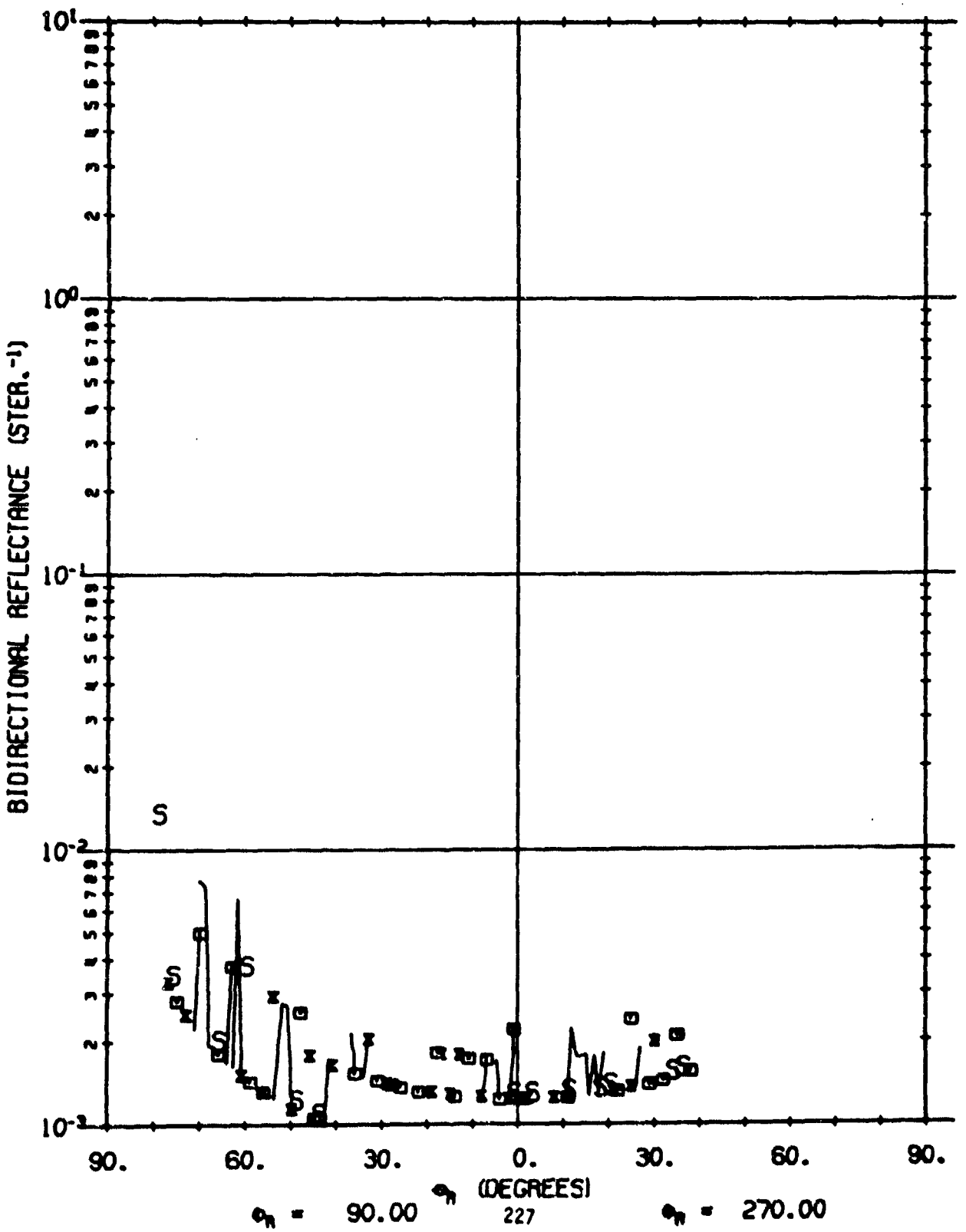

A02022 202

λ = .63
θ_I = .0
ϕ_I = 180.0

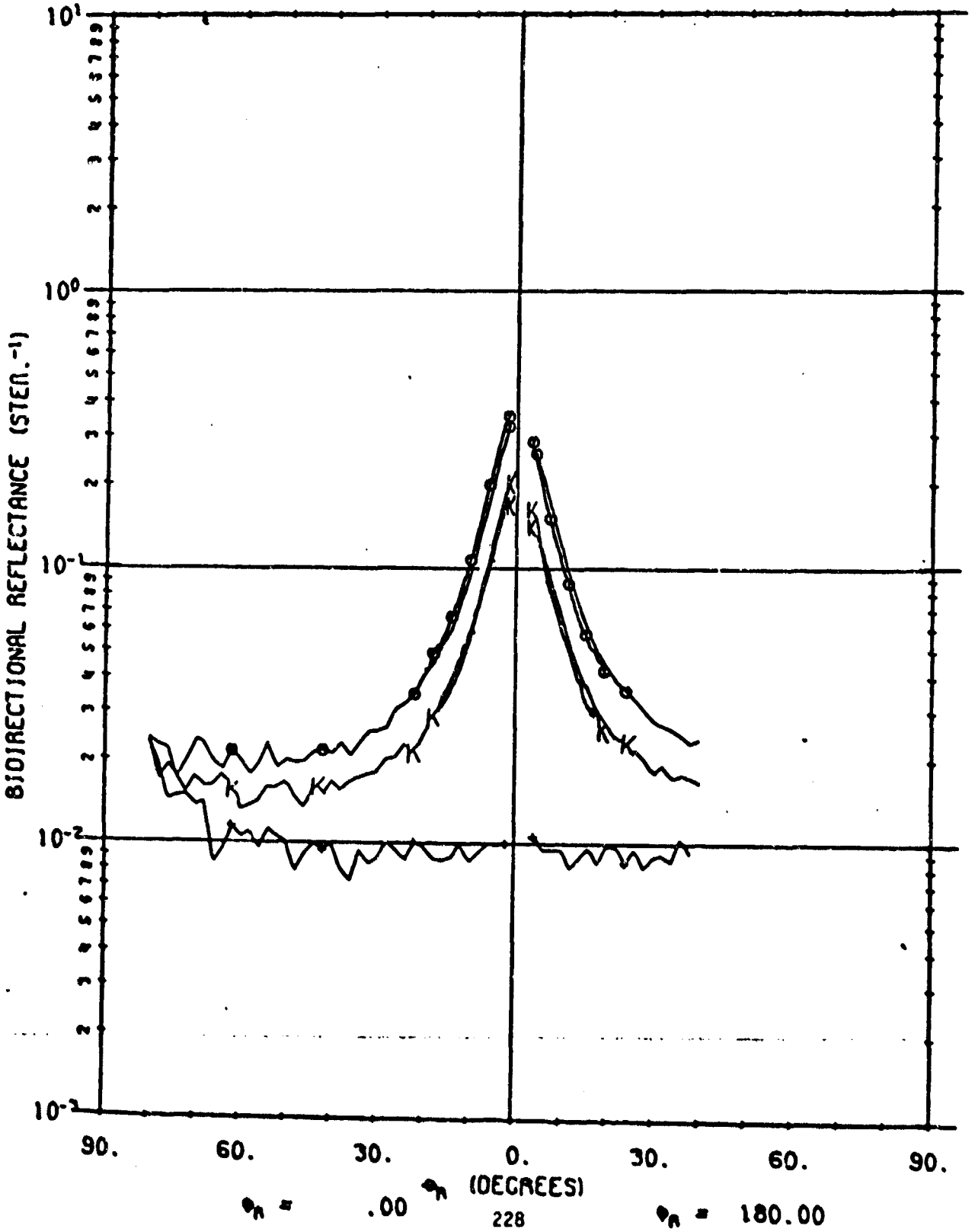

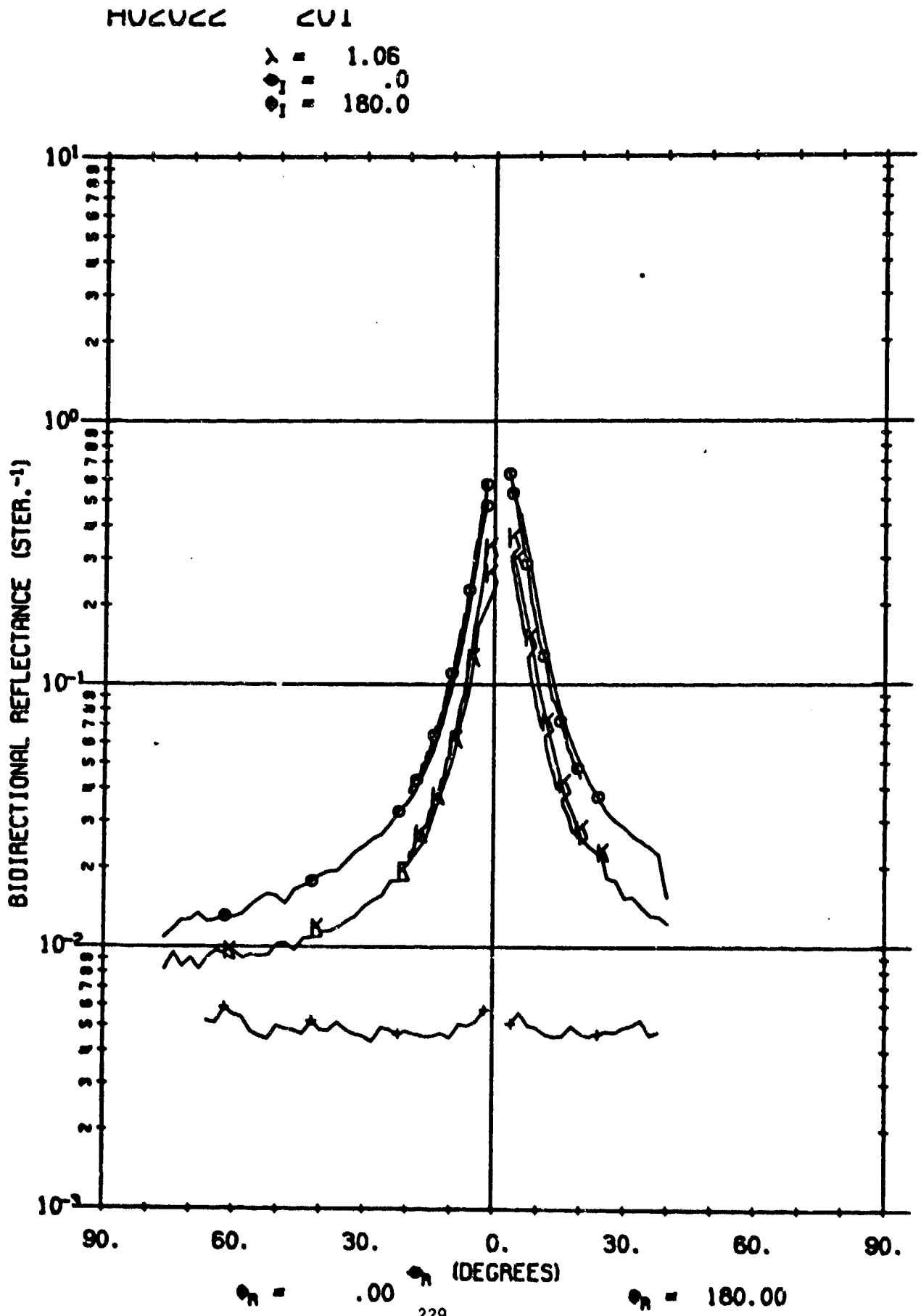
HUCUCC CU1
λ = 1.06
ϕ_I = .0
θ_I = 180.0
BIDIRECTIONAL REFLECTANCE (STER.$^{-1}$)
10^1
10^0
10^{-1}
10^{-2}
10^{-3}
90.
60.
30.
0.
30.
60.
90.
θ_R (DEGREES)
ϕ_R = .00
ϕ_R = 180.00

A02022 701

λ = 3.39
θ_I = .0
ϕ_I = 180.0

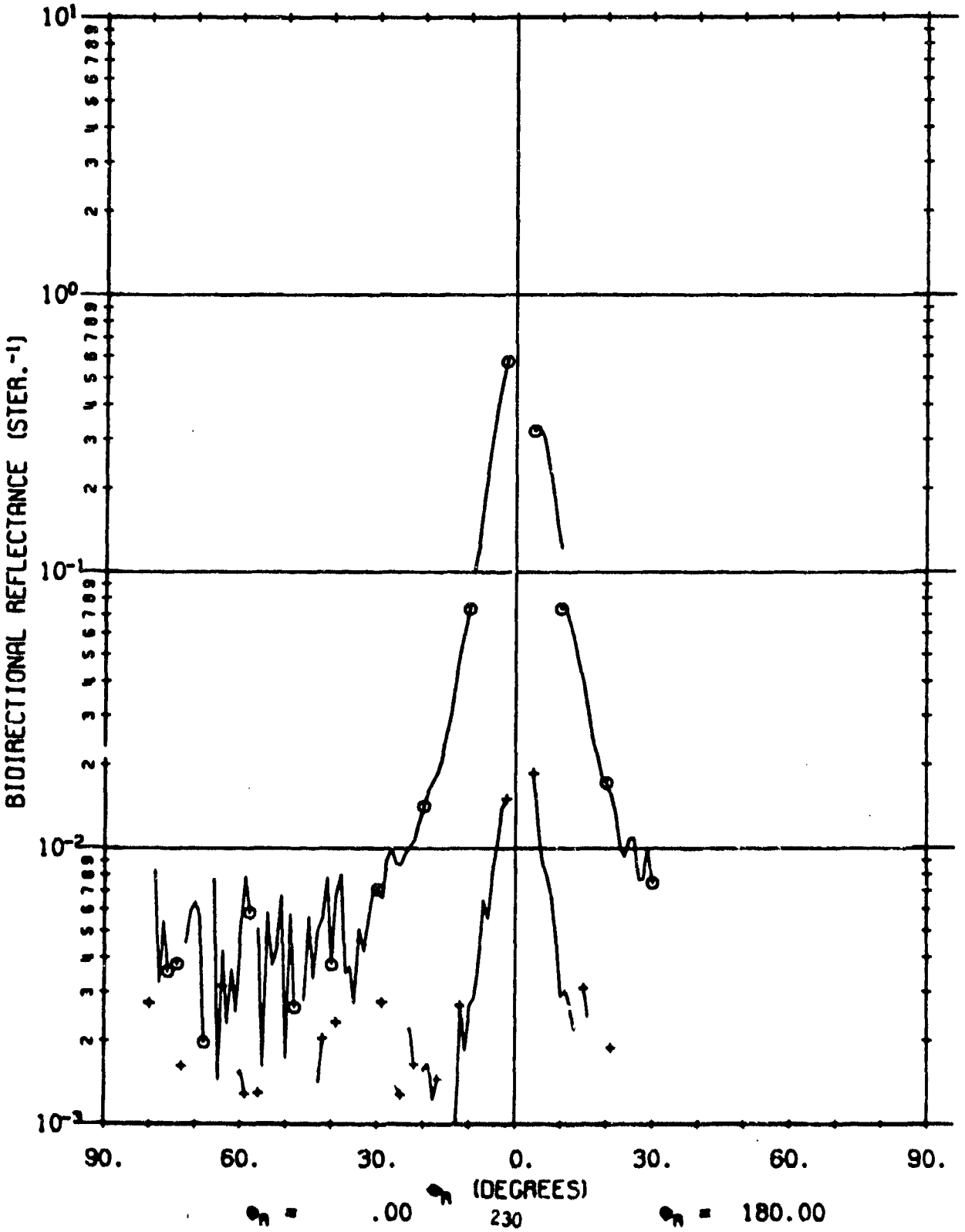

A02022 604

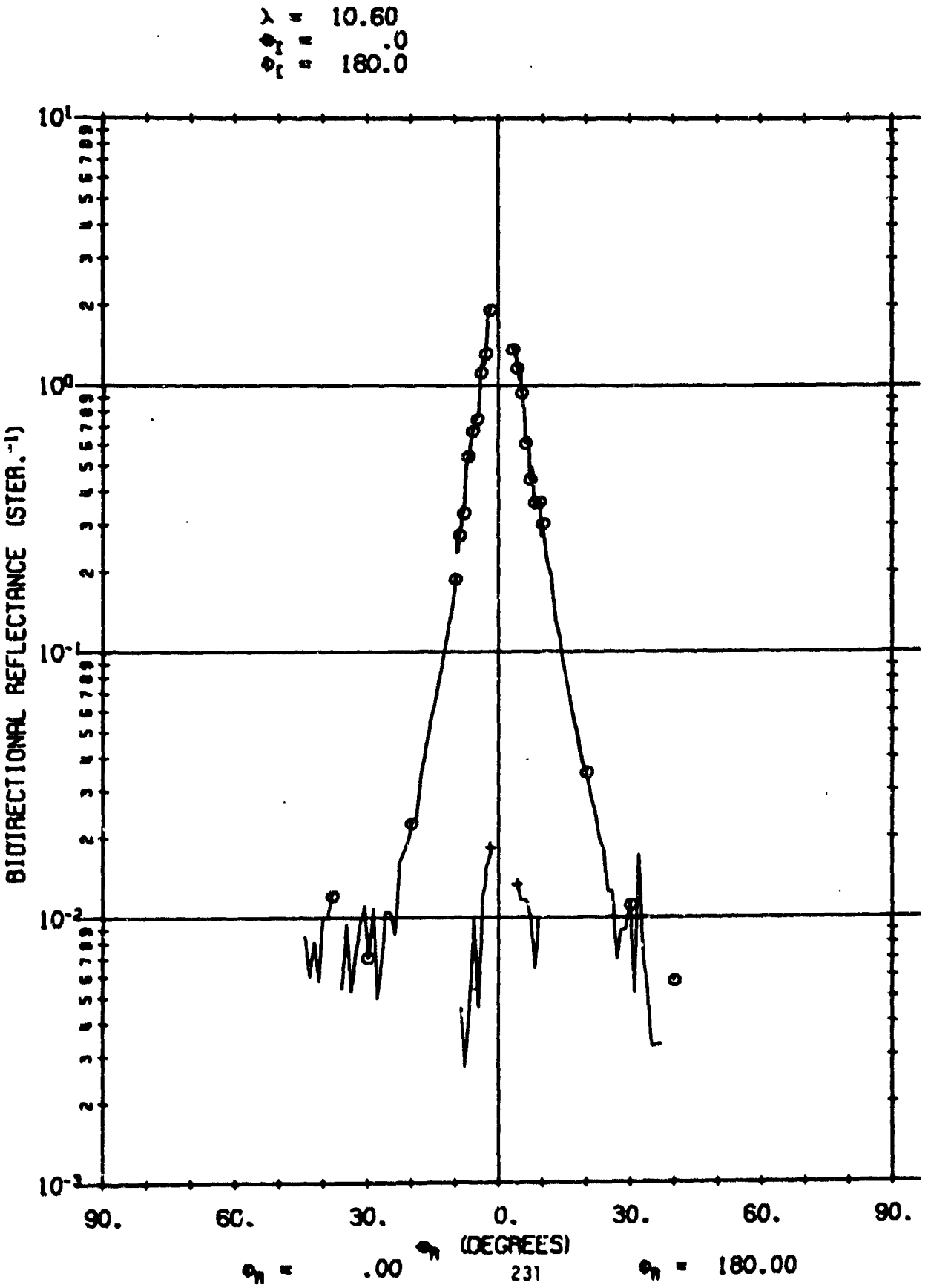
λ = 10.60
ϕ_r = .0
ϕ_i = 180.0
BIDIRECTIONAL REFLECTANCE (STER.$^{-1}$)
10^1
10^0
10^{-1}
10^{-2}
10^{-3}
90.
60.
30.
0.
30.
60.
90.
ϕ_n (DEGREES)
ϕ_n = .00
ϕ_n = 180.00

A02022 202

λ = .63
ϕ_i = .0
θ_i = 180.0

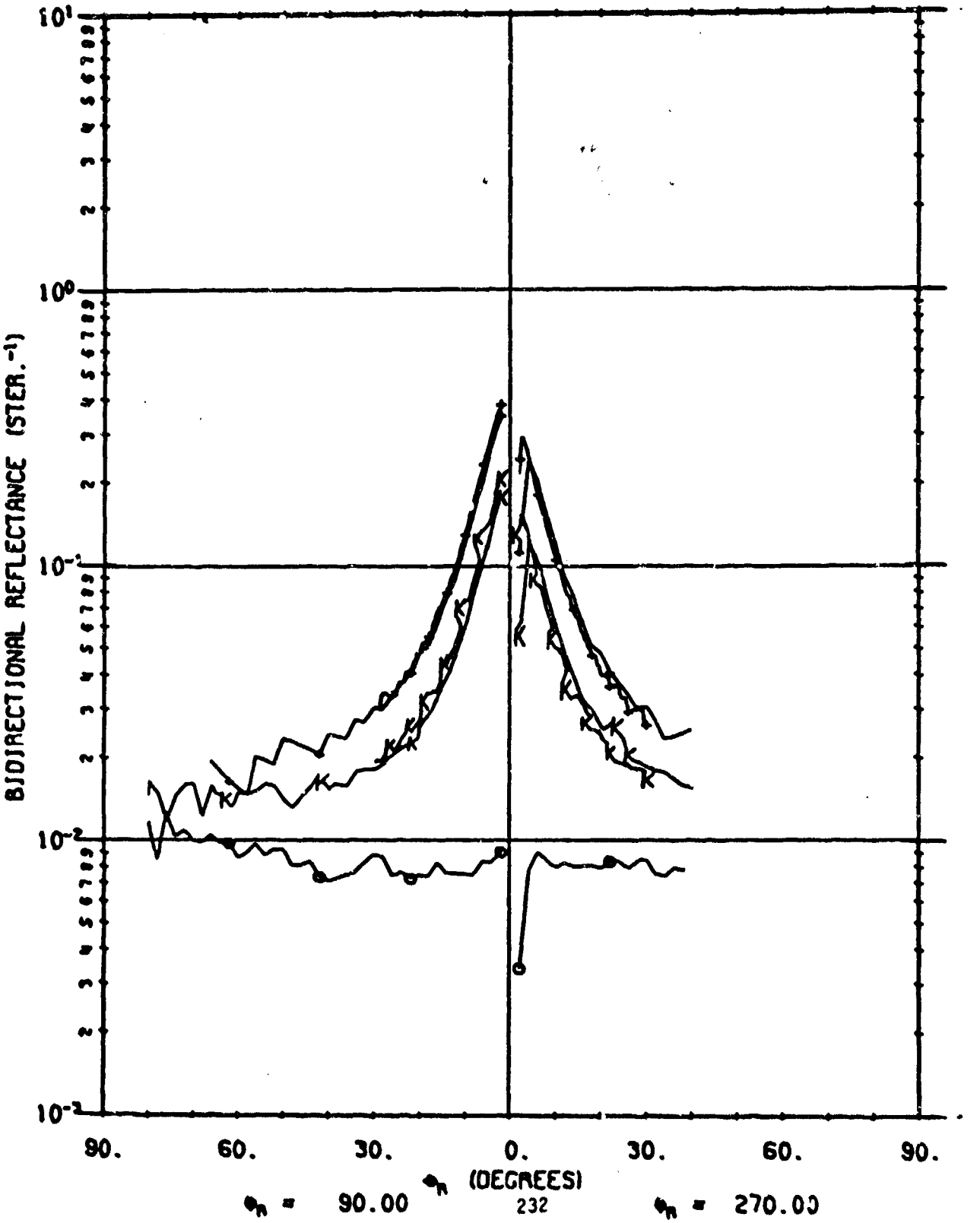

A02022 201

λ = 1.06
θ_i = .0
ϕ_i = 180.0

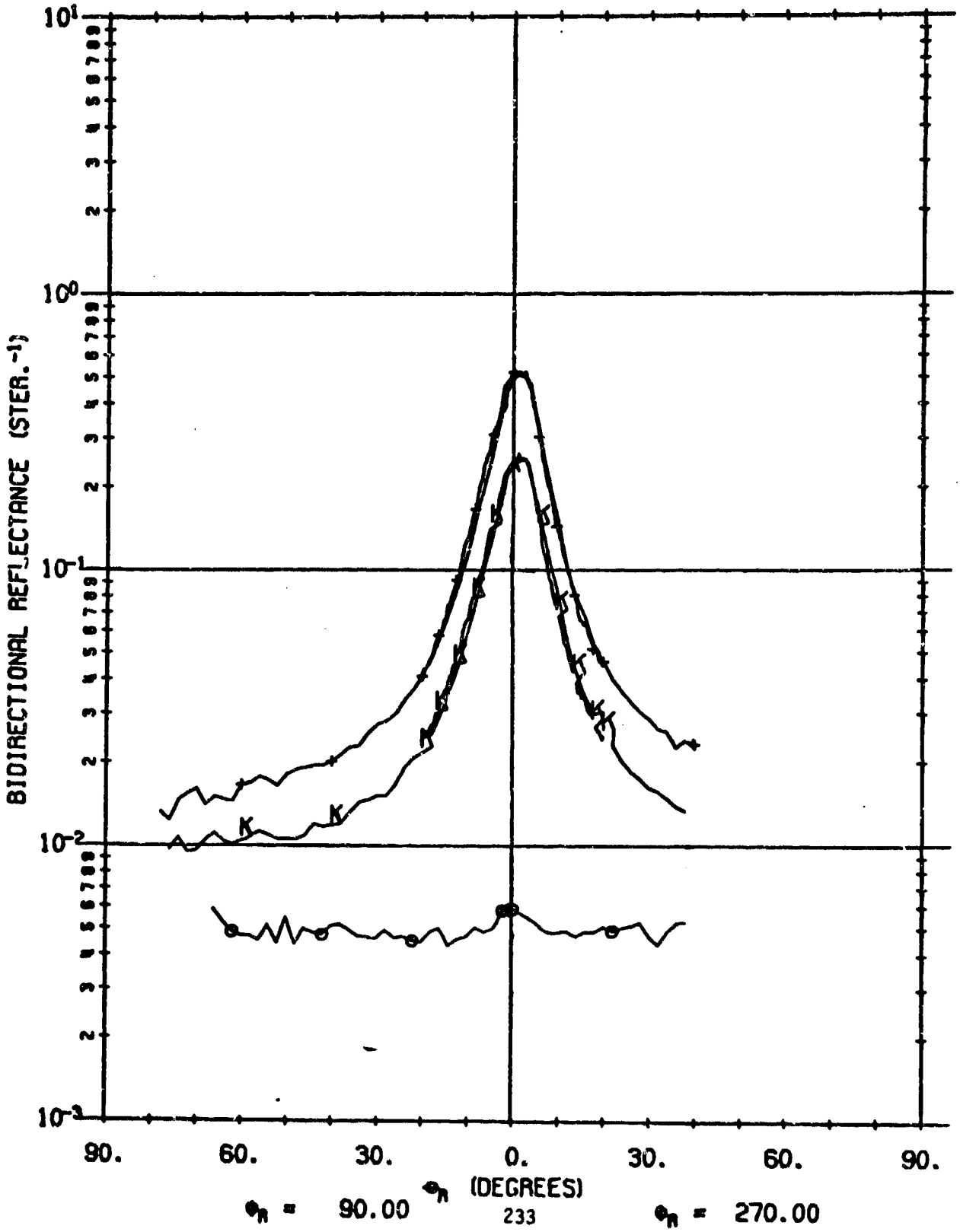

A02022 202

λ = .63
θ_i = 20.0
ϕ_i = 180.0

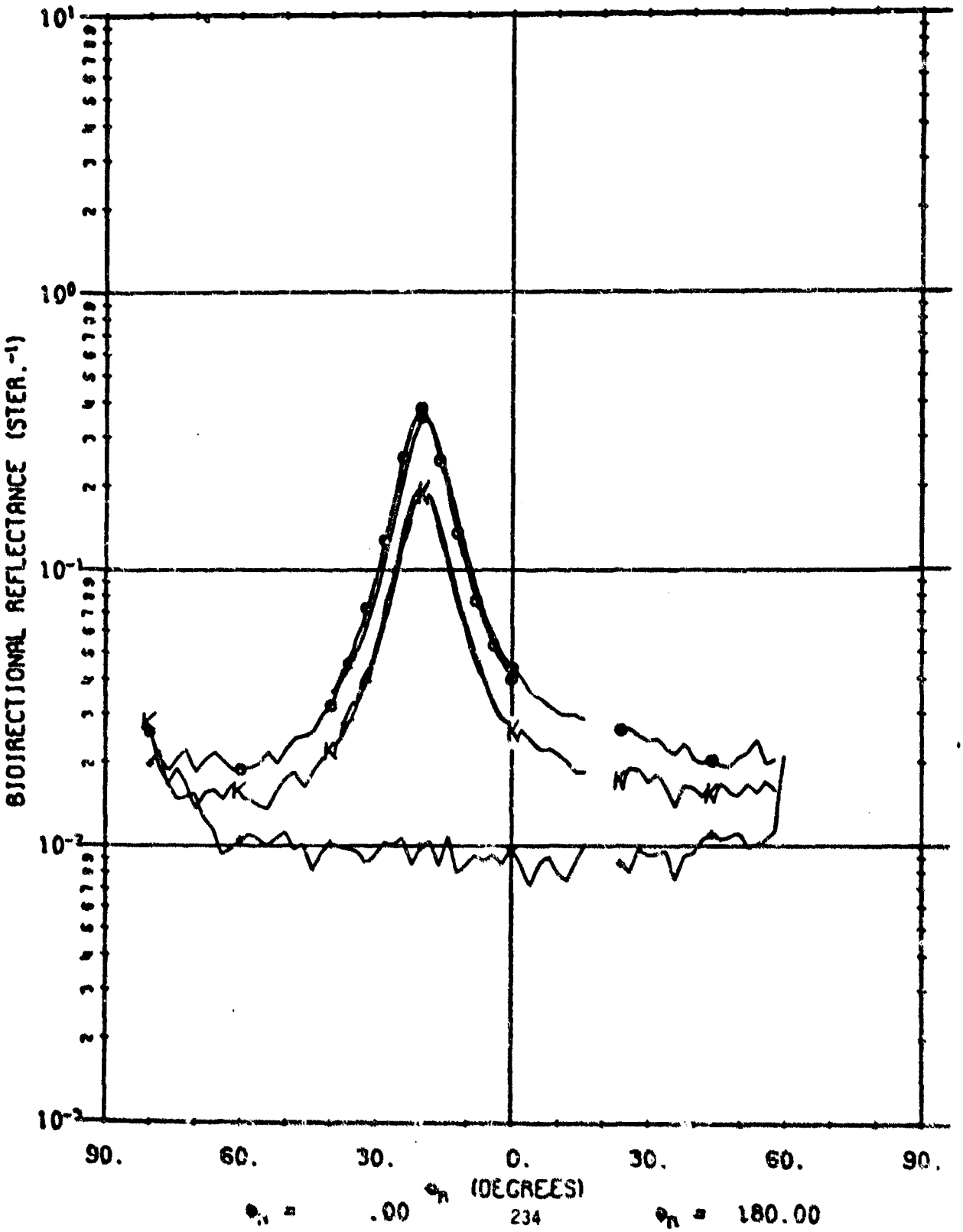

A02022 201

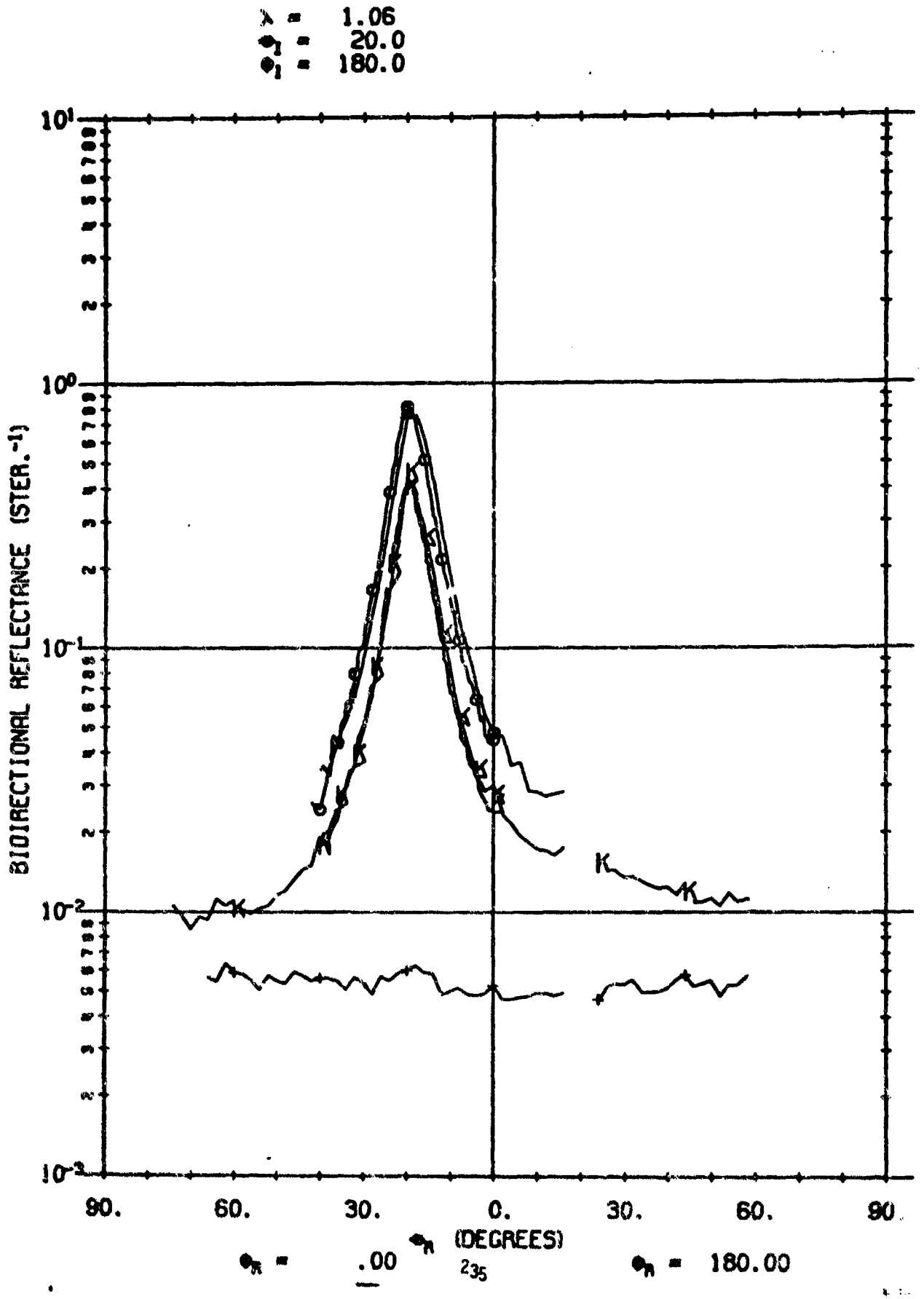
λ = 1.06
θ_i = 20.0
ϕ_i = 180.0
BIDIRECTIONAL REFLECTANCE (STER.$^{-1}$)
10^1
10^0
10^{-1}
10^{-2}
10^{-3}
90.
60.
30.
0.
30.
60.
90.
θ_R (DEGREES)
ϕ_R = .00
ϕ_R = 180.00

A02022 701

λ = 3.39
θ_I = 20.0
ϕ_I = 180.0

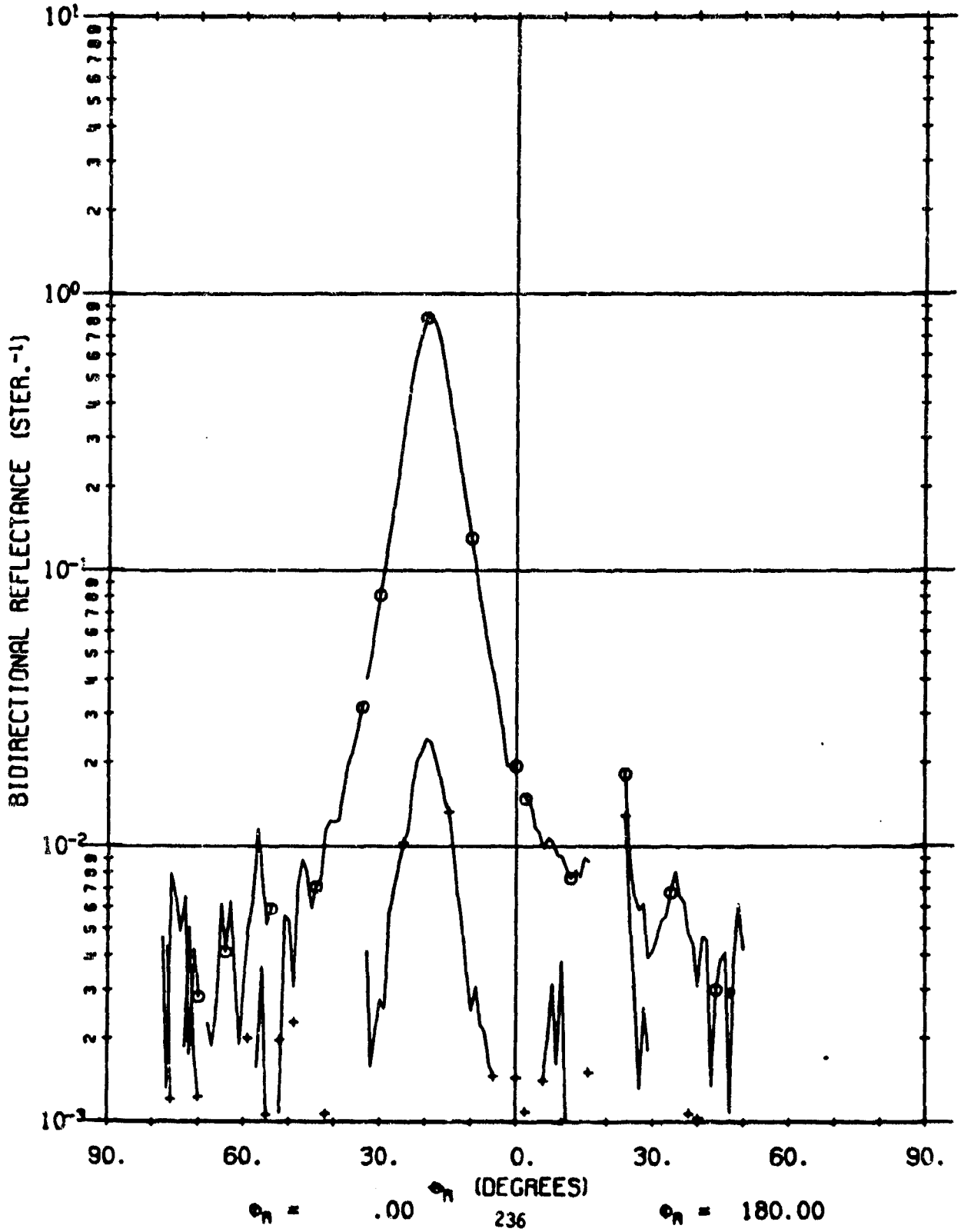

A02022 604

λ = 10.60
Φ_I = 20.0
Φ_I = 180.0

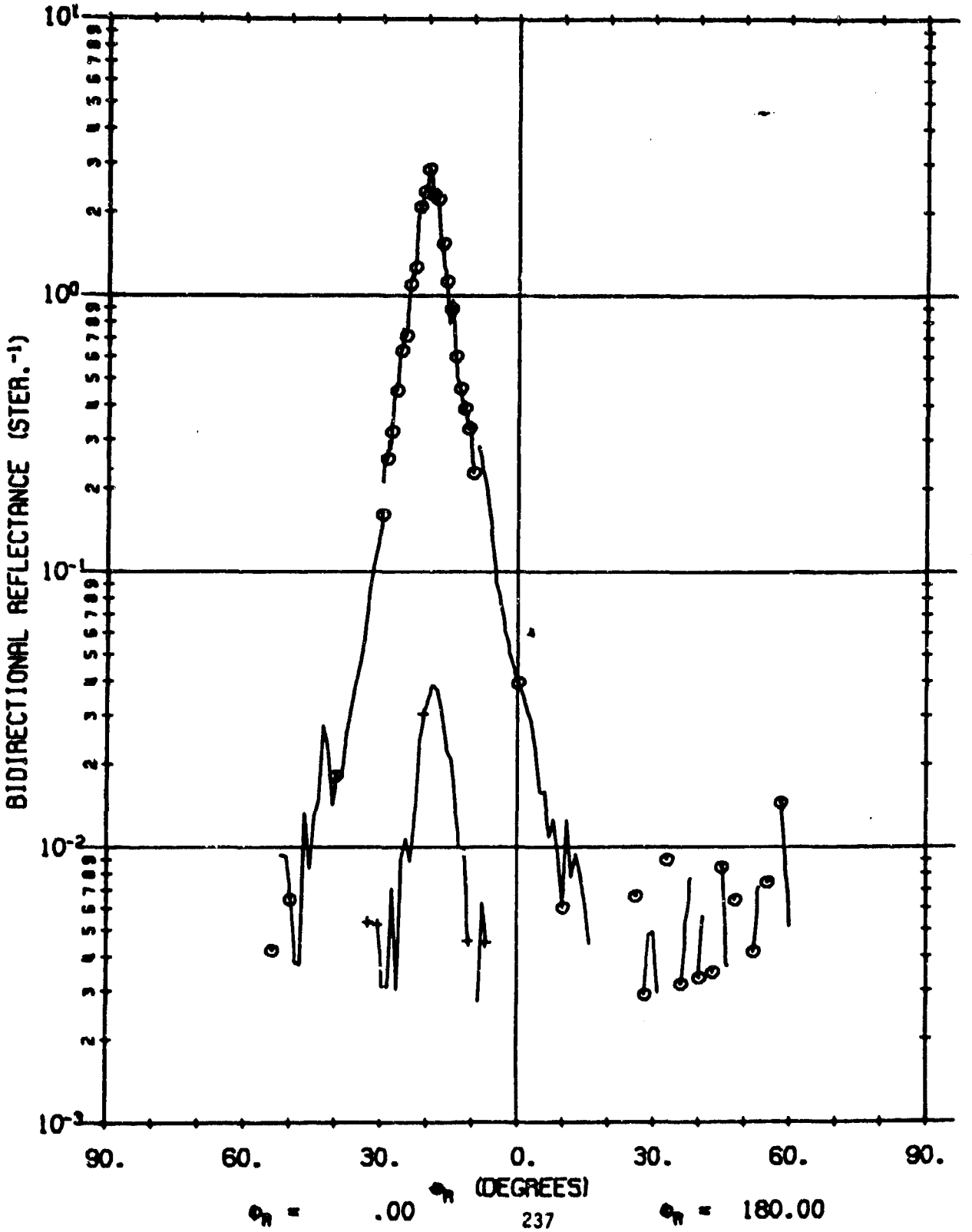

A02022 202

λ = .63
θ_i = 20.0
ϕ_i = 180.0

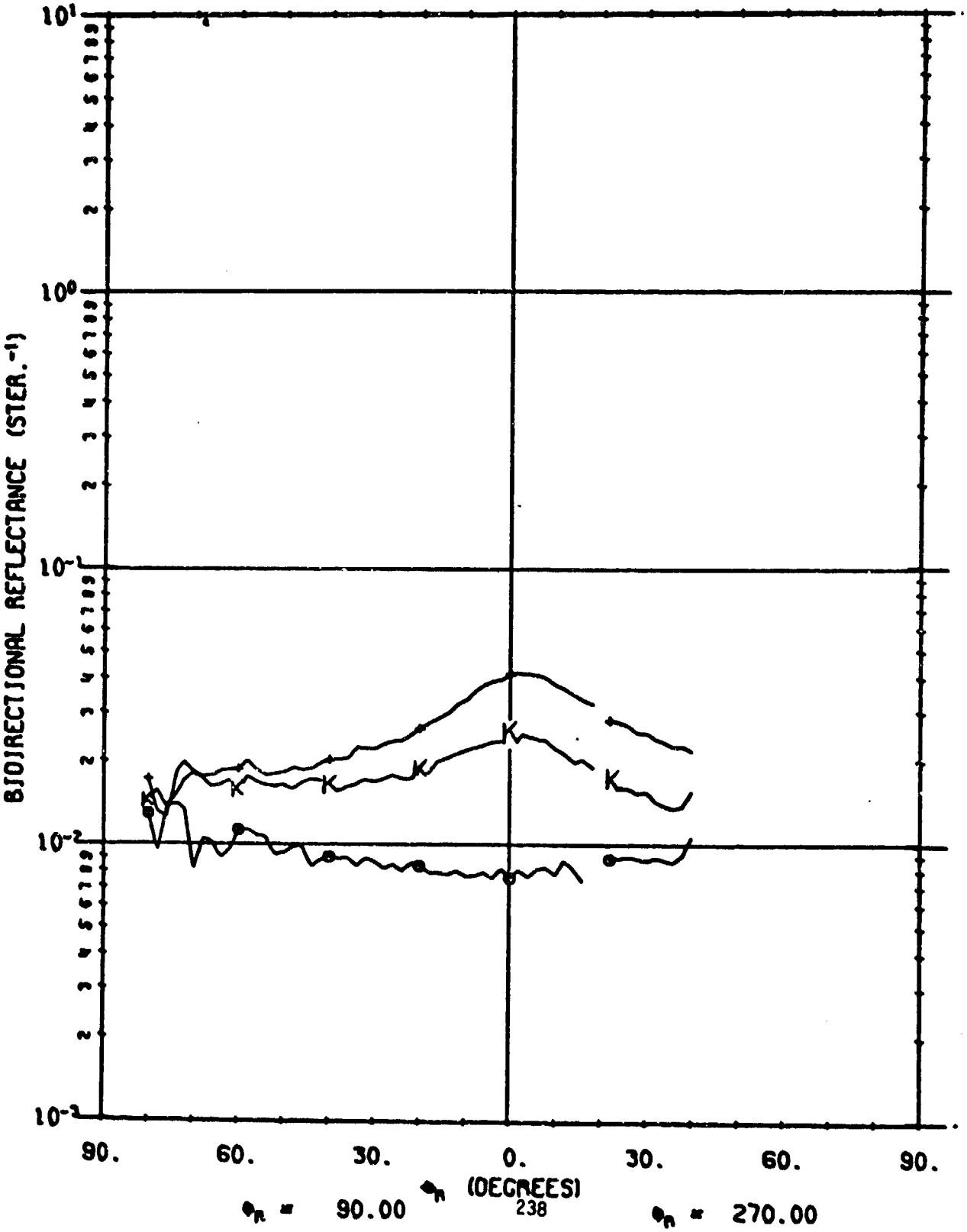

A02022 201

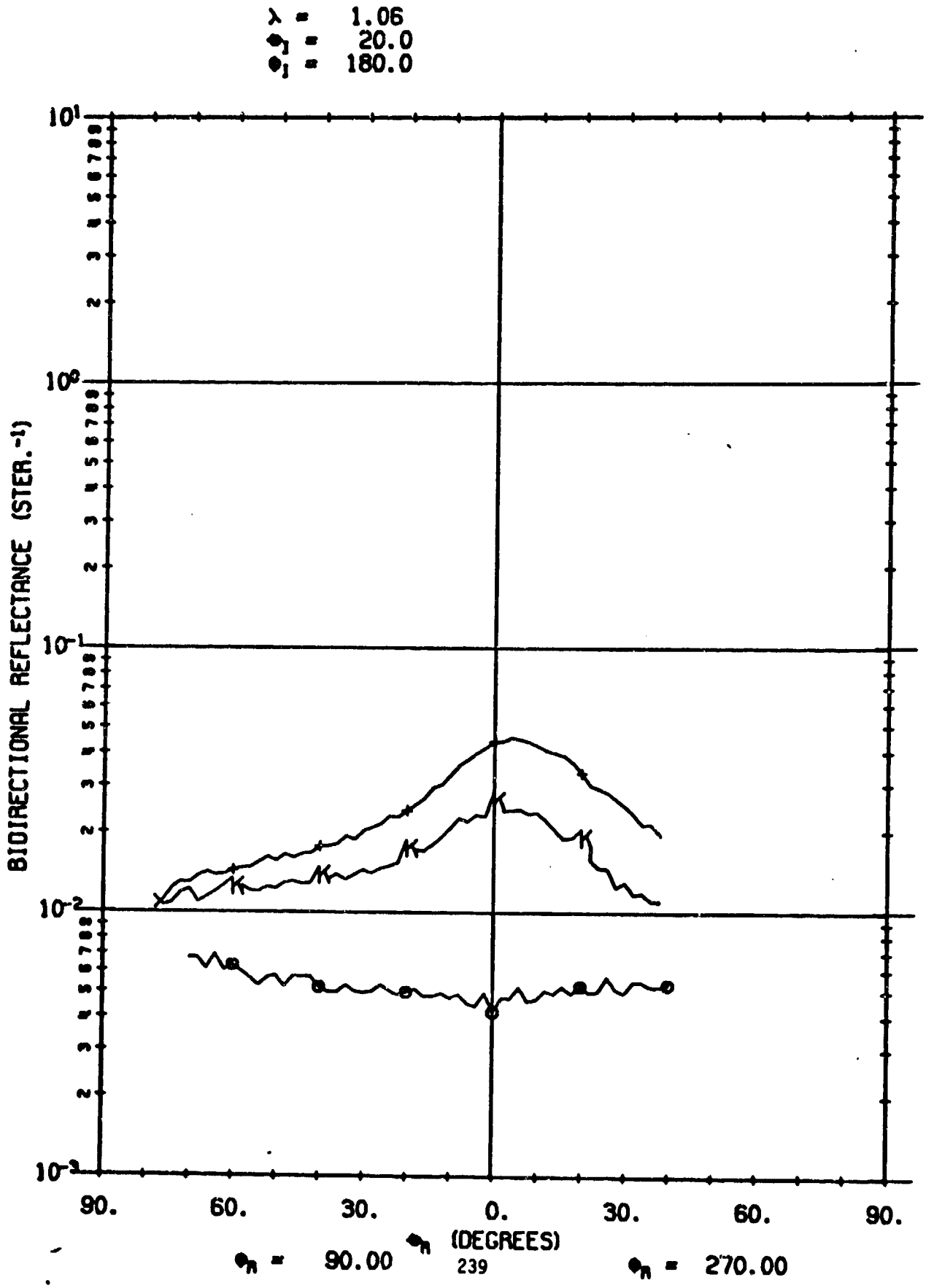
λ = 1.06
θi = 20.0
φi = 180.0
BIDIRECTIONAL REFLECTANCE (STER.-1)
10^1
10^0
10^-1
10^-2
10^-3
90.
60.
30.
0.
30.
60.
90.
θr (DEGREES)
φr = 90.00
φr = 270.00

A02022 702

λ = 3.39
θ_I = 20.0
ϕ_I = 180.0

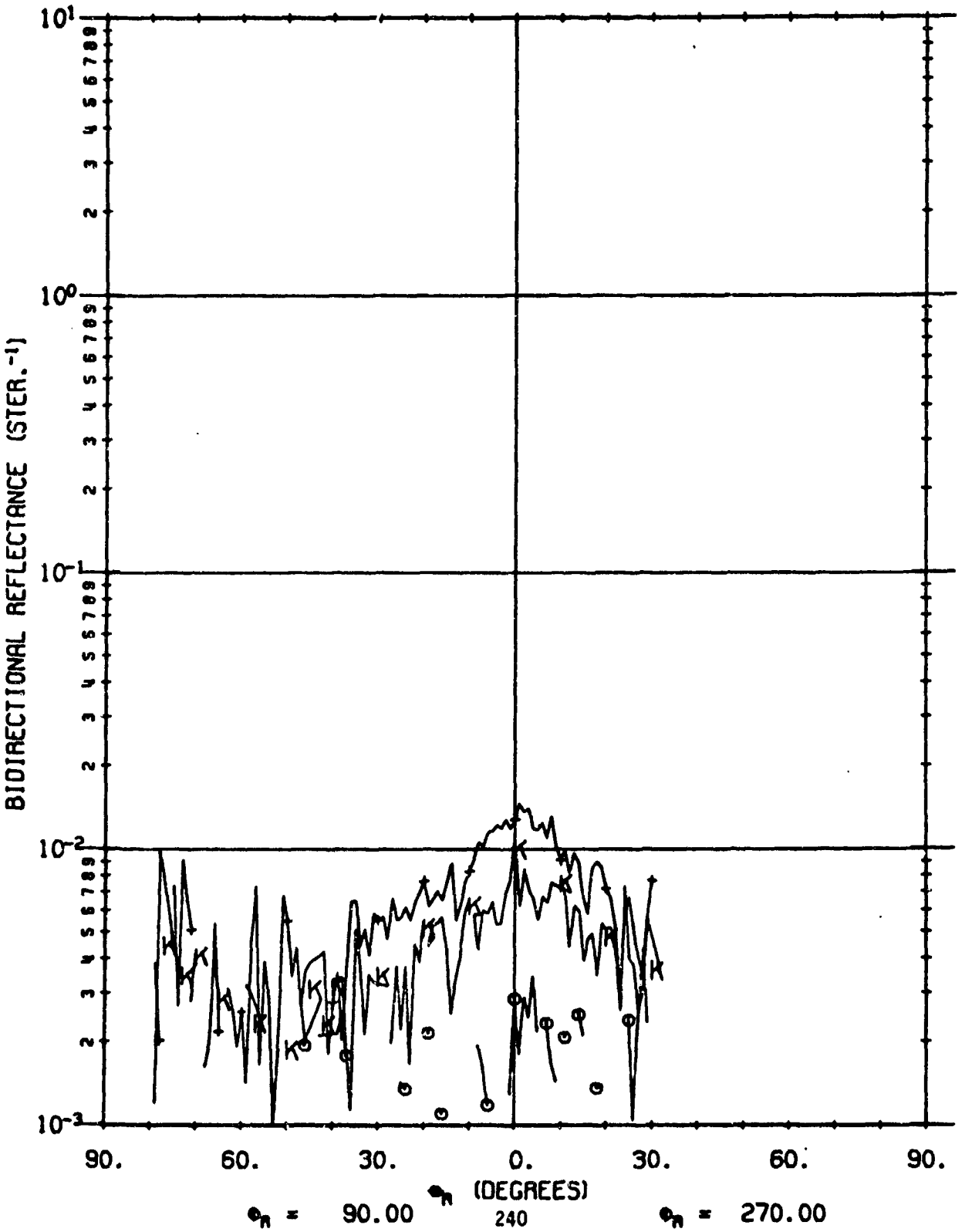

A02022 602

λ = 10.60
θ_I = 20.0
ϕ_I = 180.0

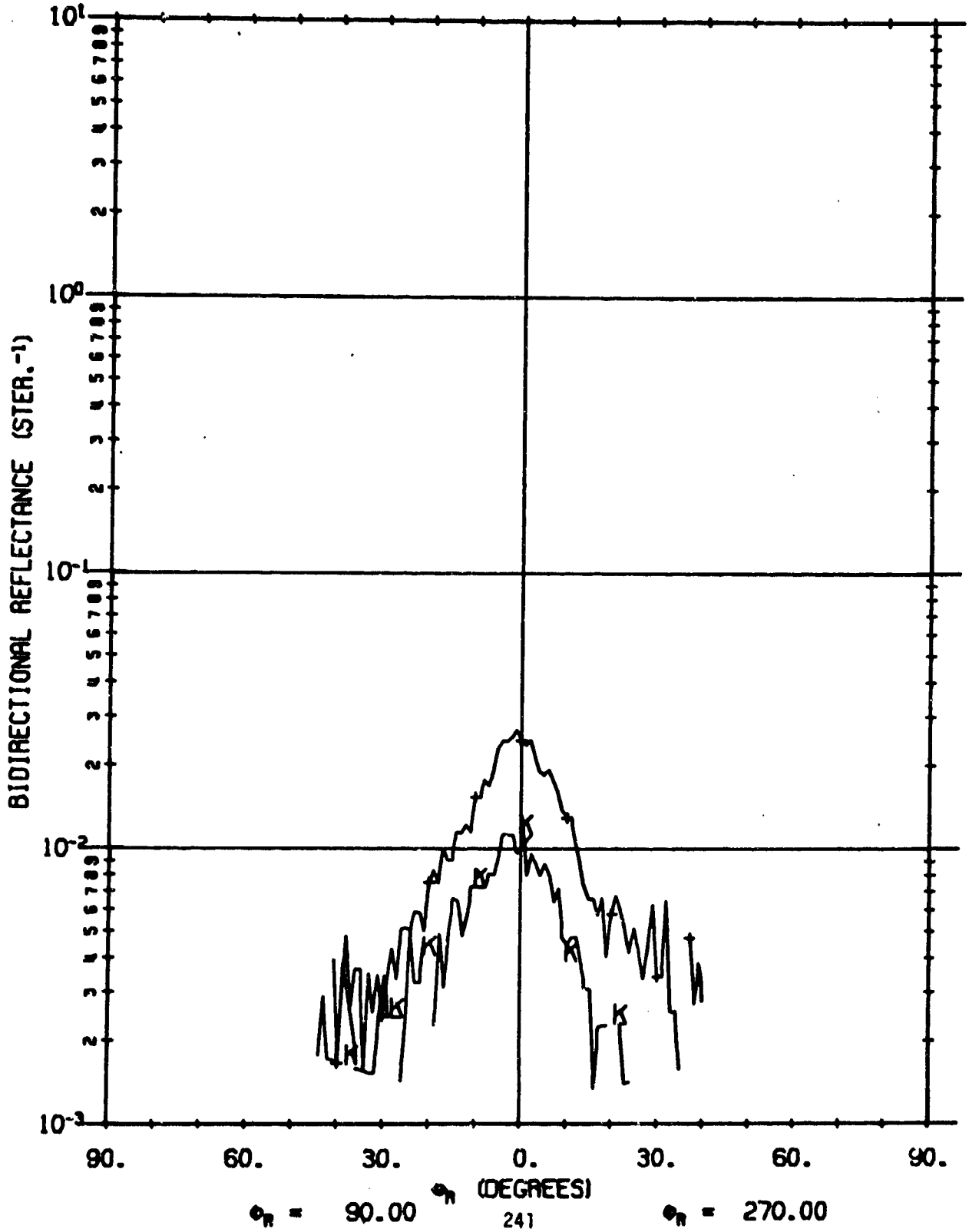

A02022 202

λ = .63
ϕ_i = 40.0
θ_i = 180.0

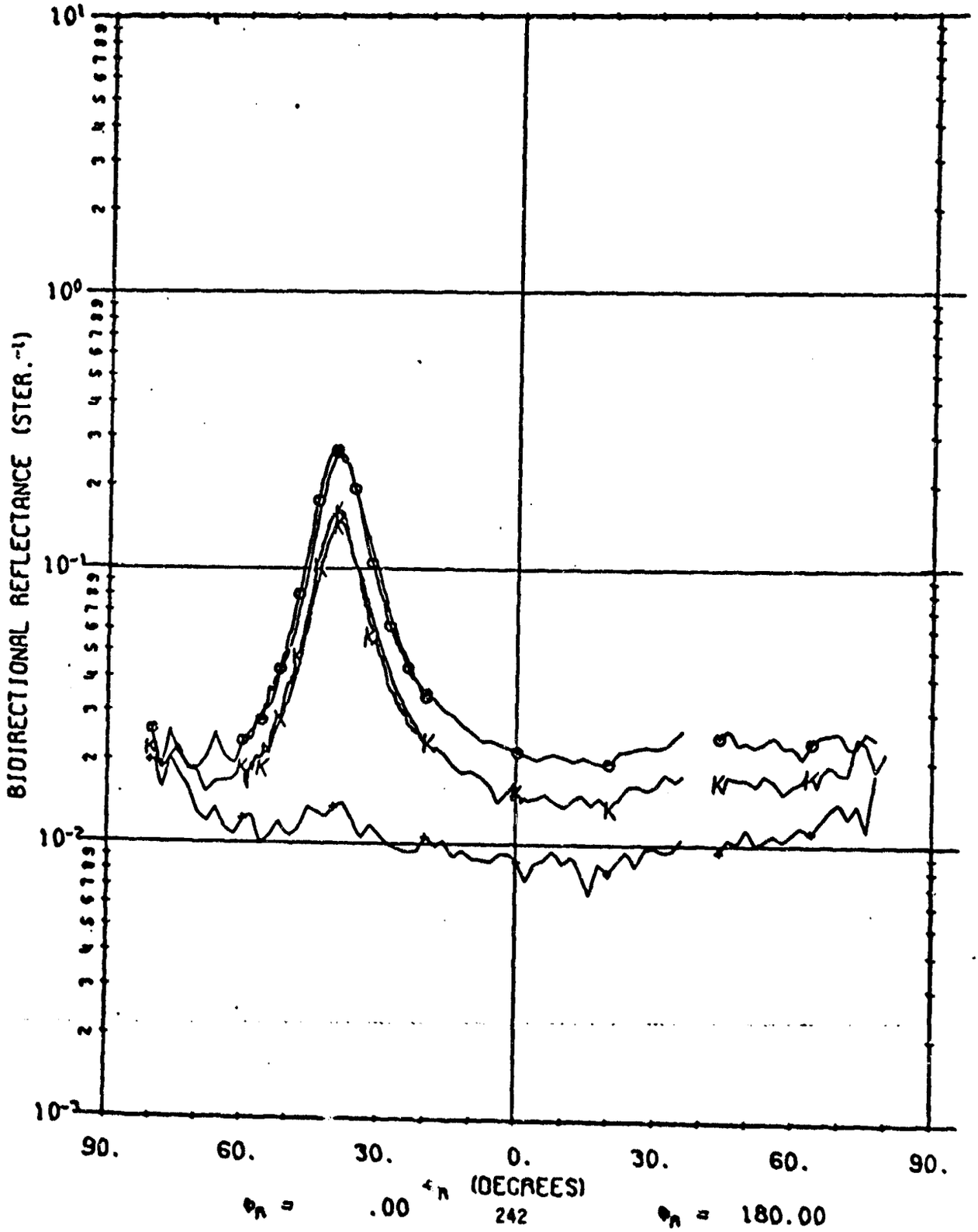

A02022 201

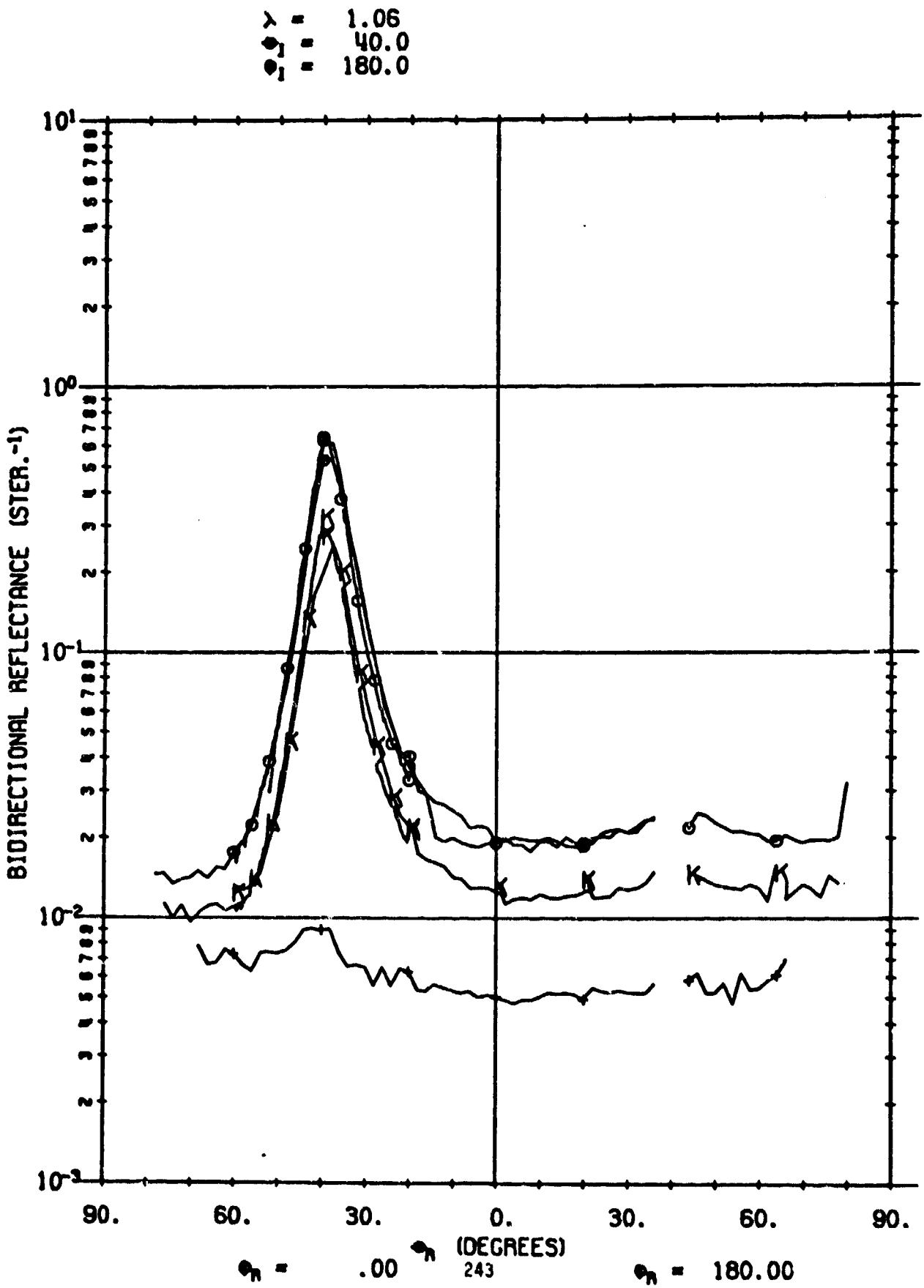
λ = 1.06
θ1 = 40.0
φ1 = 180.0
BIDIRECTIONAL REFLECTANCE (STER.-1)
10¹
10⁰
10⁻¹
10⁻²
10⁻³
90.
60.
30.
0.
30.
60.
90.
θn (DEGREES)
φn = .00
φn = 180.00

A02022 701

λ = 3.39
ϕ_I = 40.0
θ_I = 180.0

77

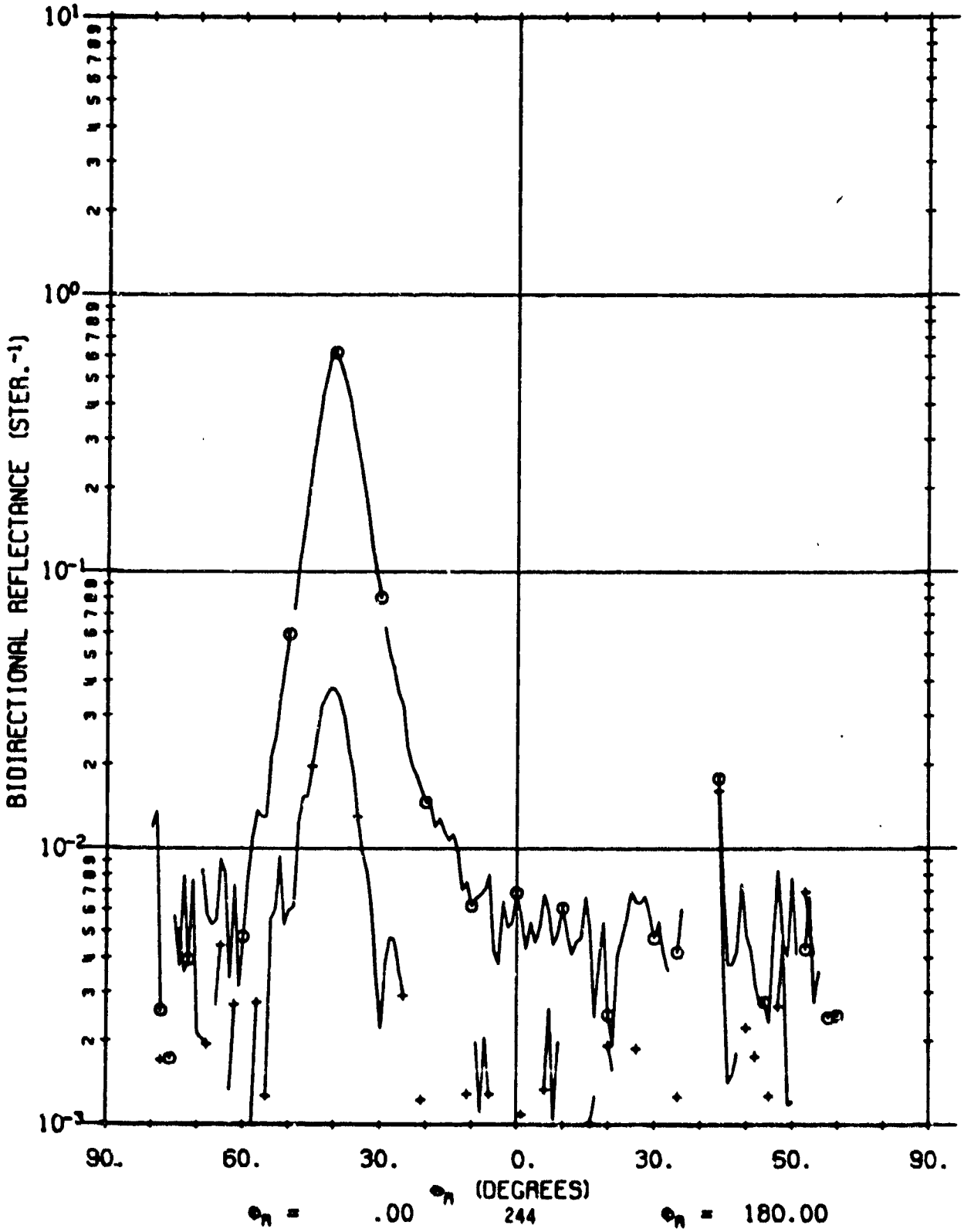

A02022 604

λ = 10.60
θ_i = 40.0
ϕ_i = 180.0

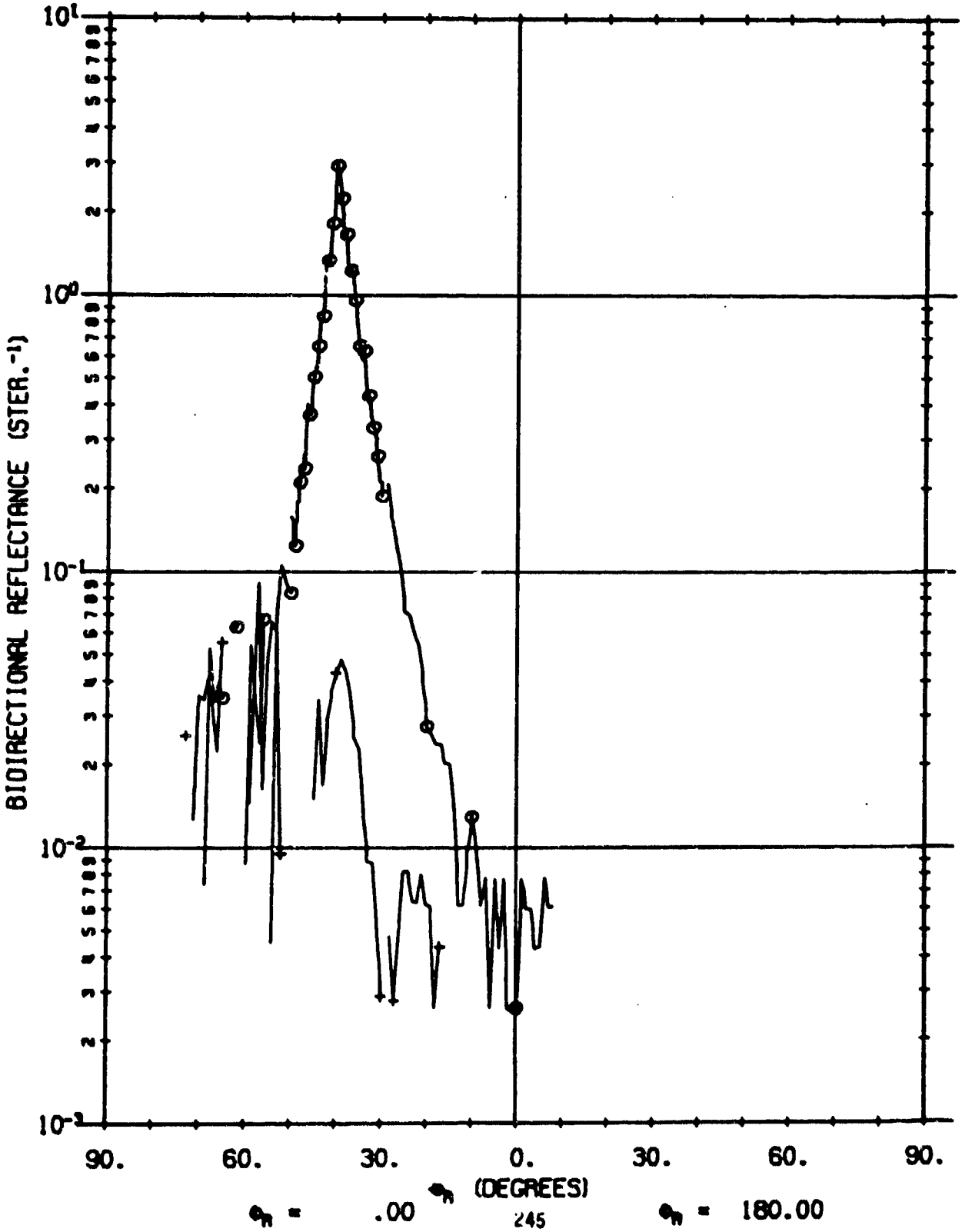

A02022 202

λ = .63
ϕ_i = 40.0
θ_i = 180.0

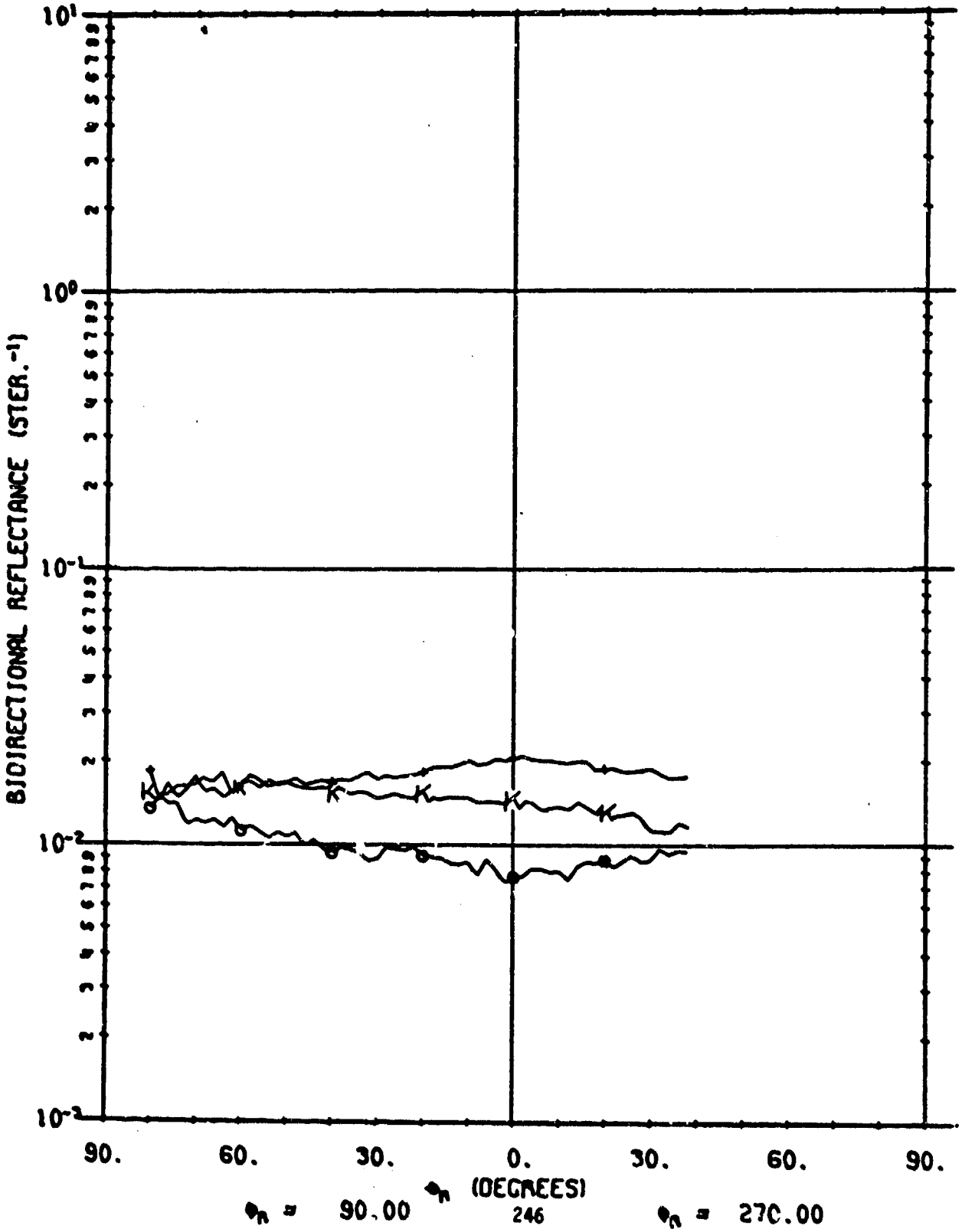

HU2U22 2U1

λ = 1.06
θ_i = 40.0
ϕ_i = 180.0

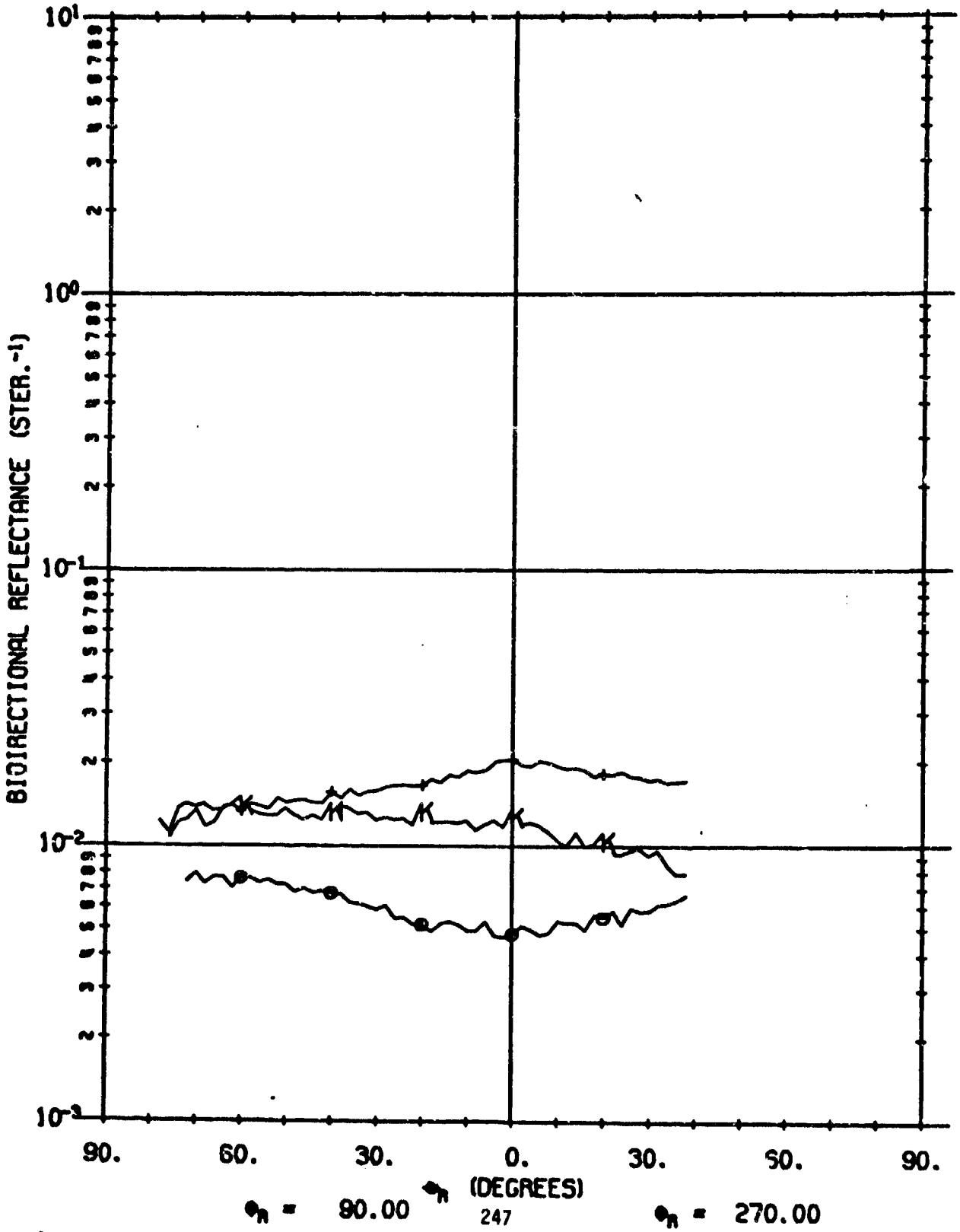

A02022 702

λ = 3.39
ϕ_1 = 40.0
ϕ_1 = 180.0

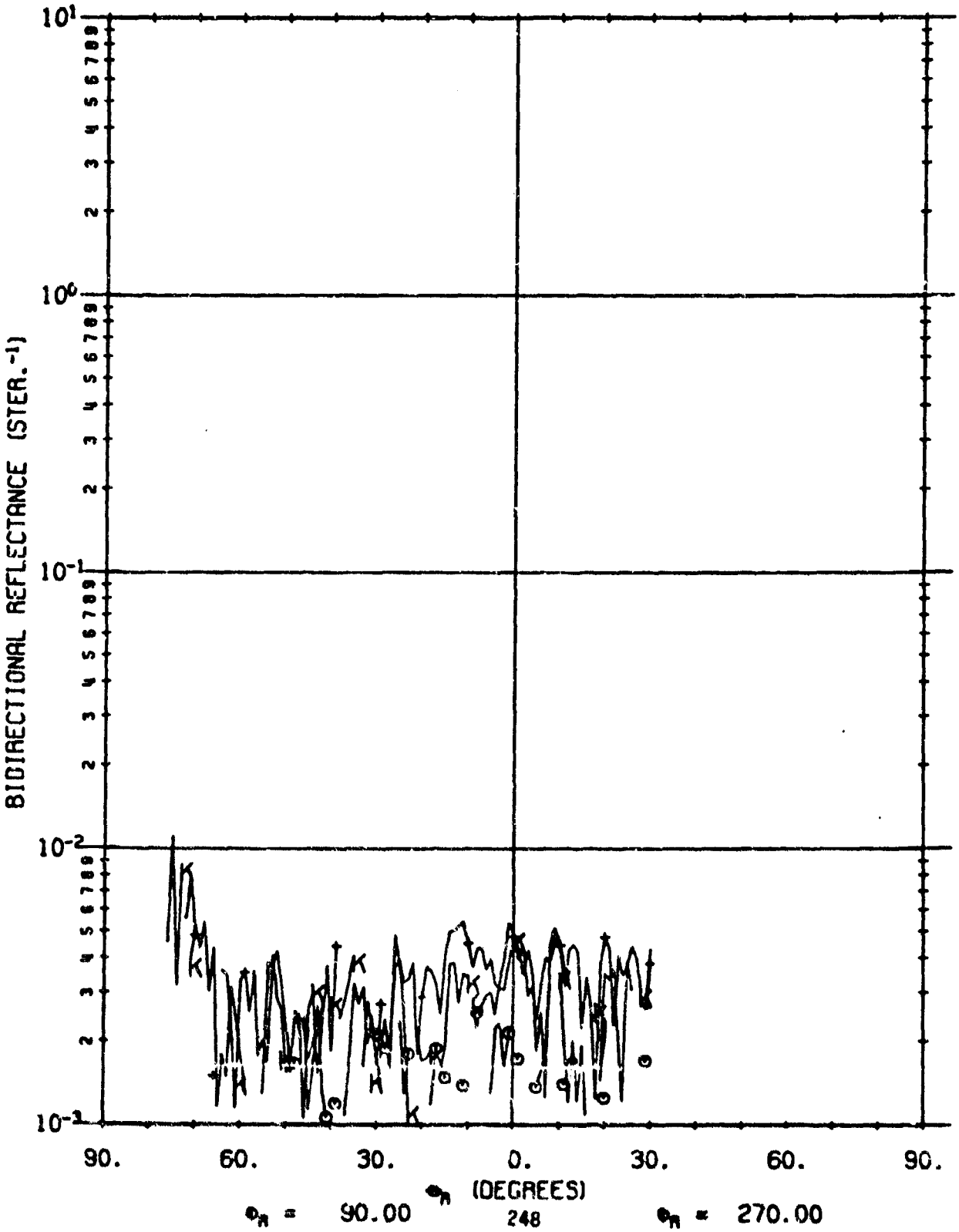

A02022 602

λ = 10.60
ϕ_i = 40.0
ϕ_r = 180.0

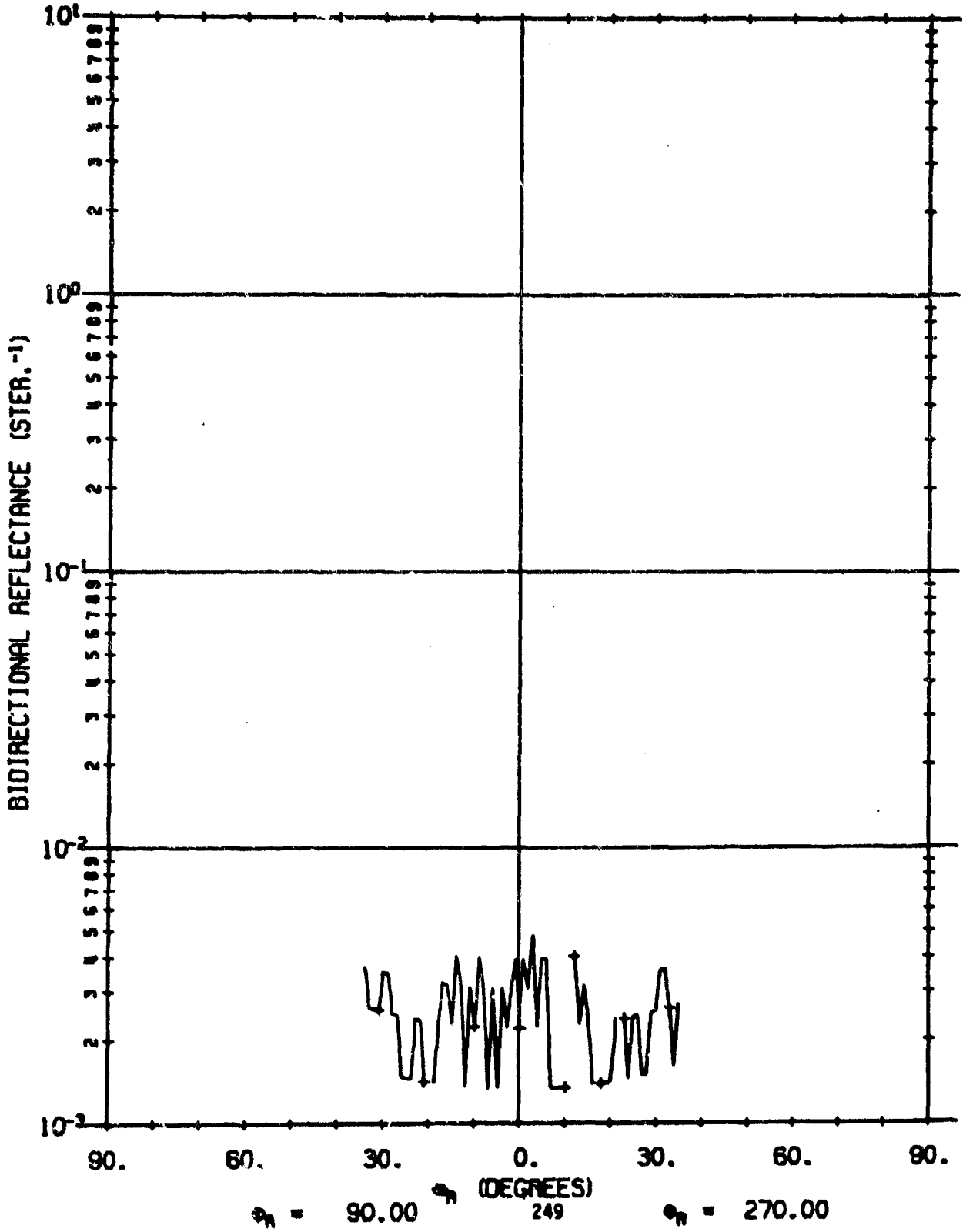

A02022 202

λ = .63
θ_I = 60.0
ϕ_I = 180.0

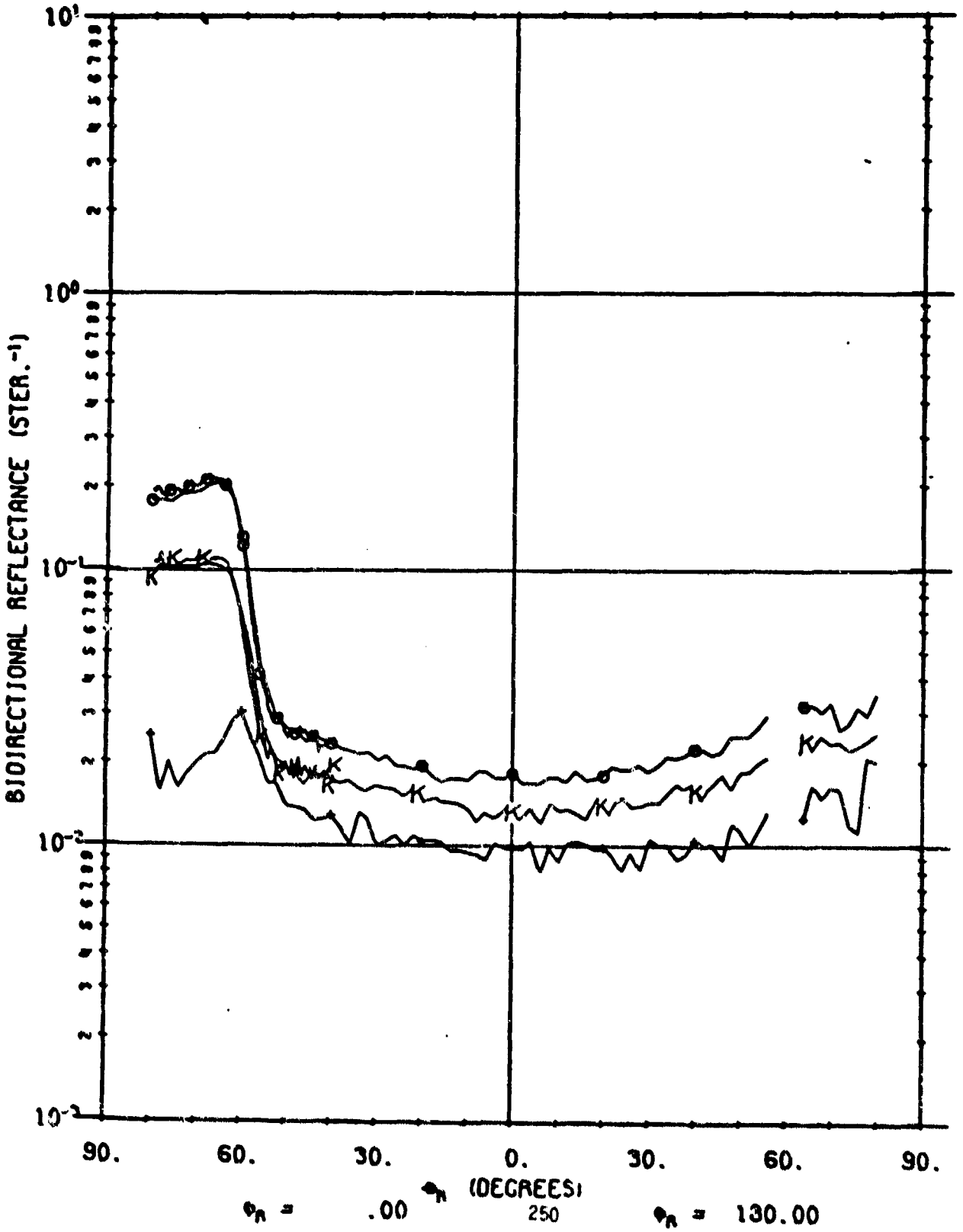

A02022 201

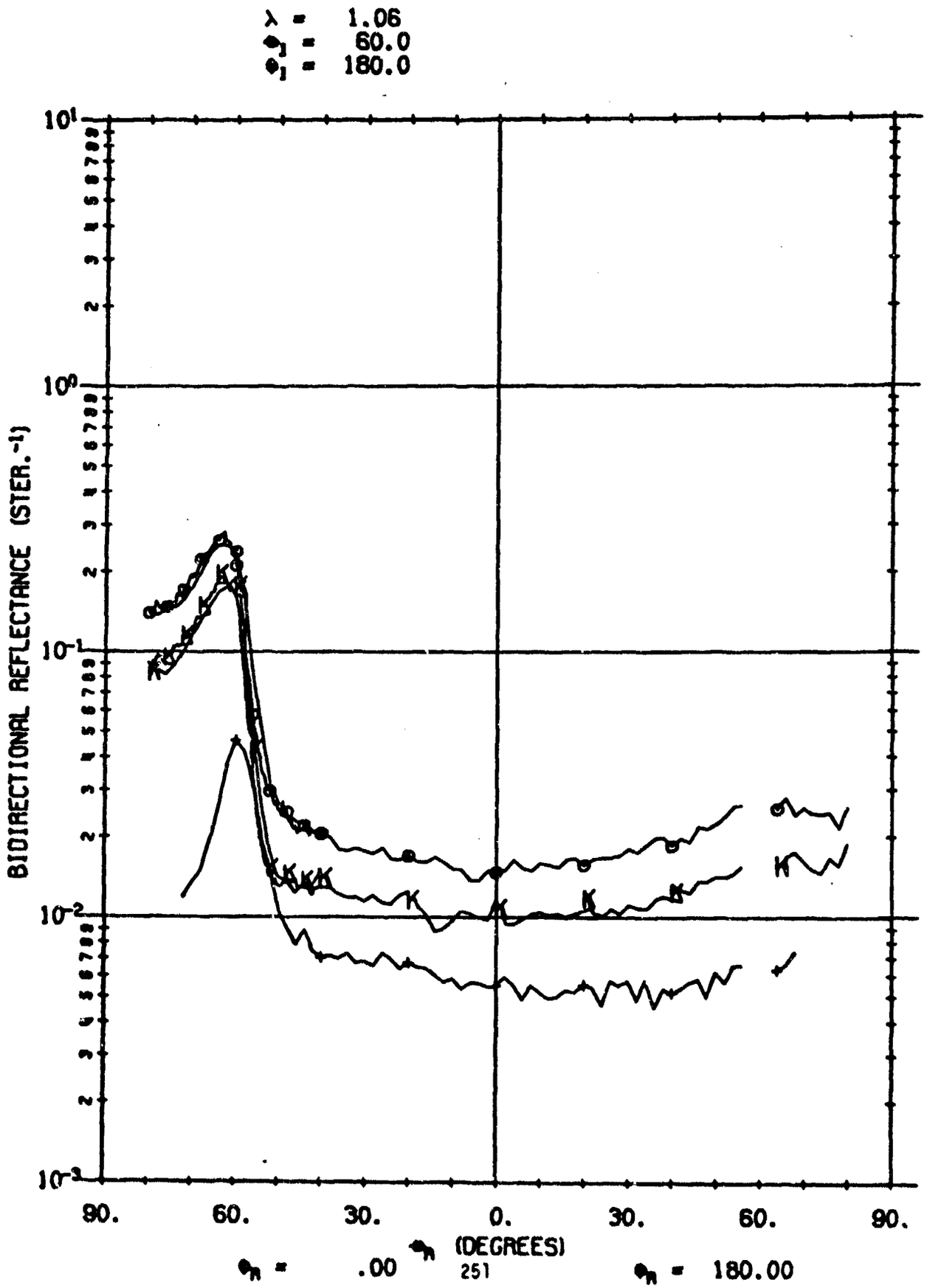
λ = 1.06
θi = 60.0
φi = 180.0
BIDIRECTIONAL REFLECTANCE (STER.-1)
10¹
10⁰
10⁻¹
10⁻²
10⁻³
90.
60.
30.
0.
30.
60.
90.
θr (DEGREES)
φr = .00
φr = 180.00

A02022 701

λ = 3.39
ϕ_1 = 60.0
θ_1 = 180.0

78

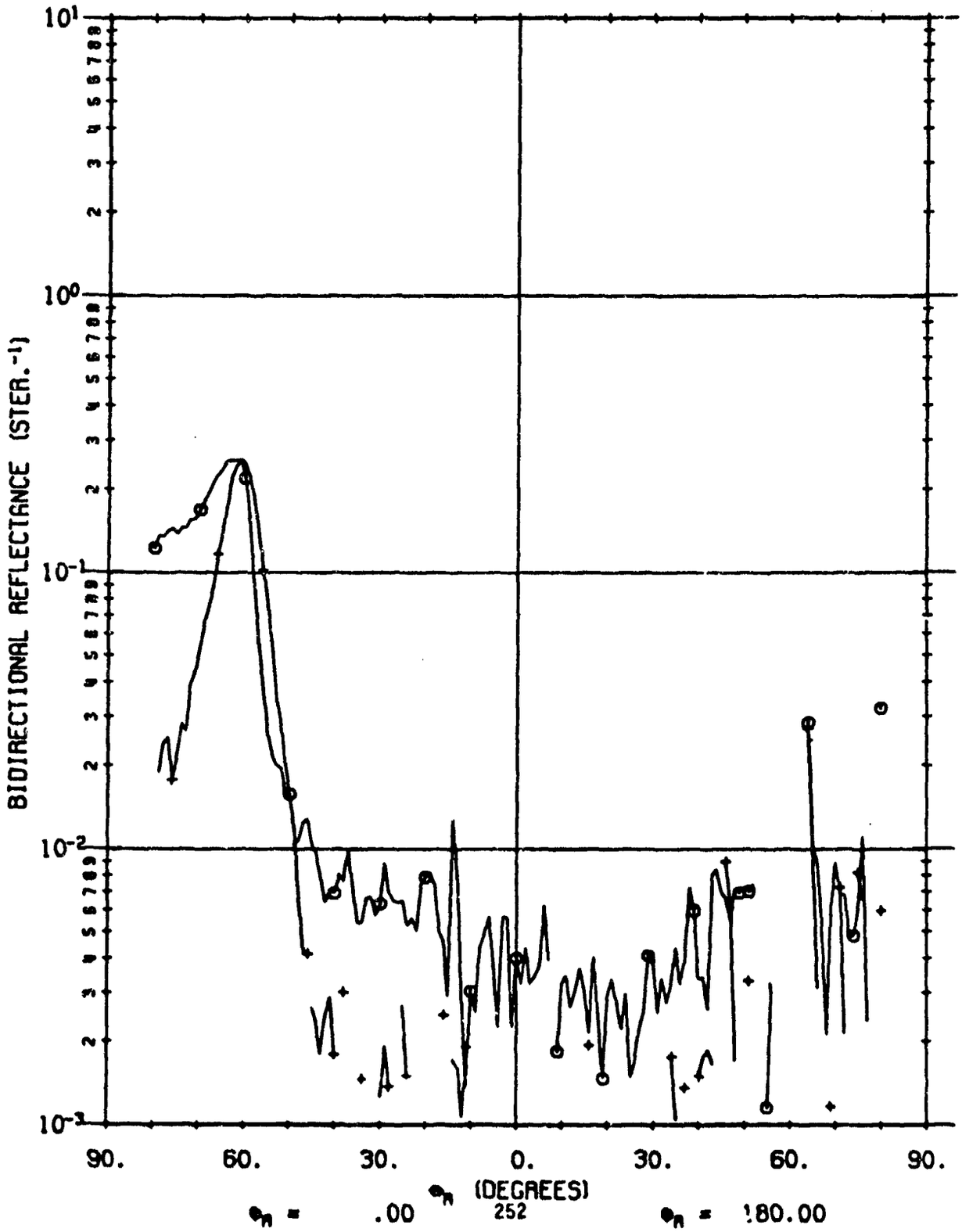

A02022 604

λ = 10.60
ϕ_I = 60.0
ϕ_I = 180.0

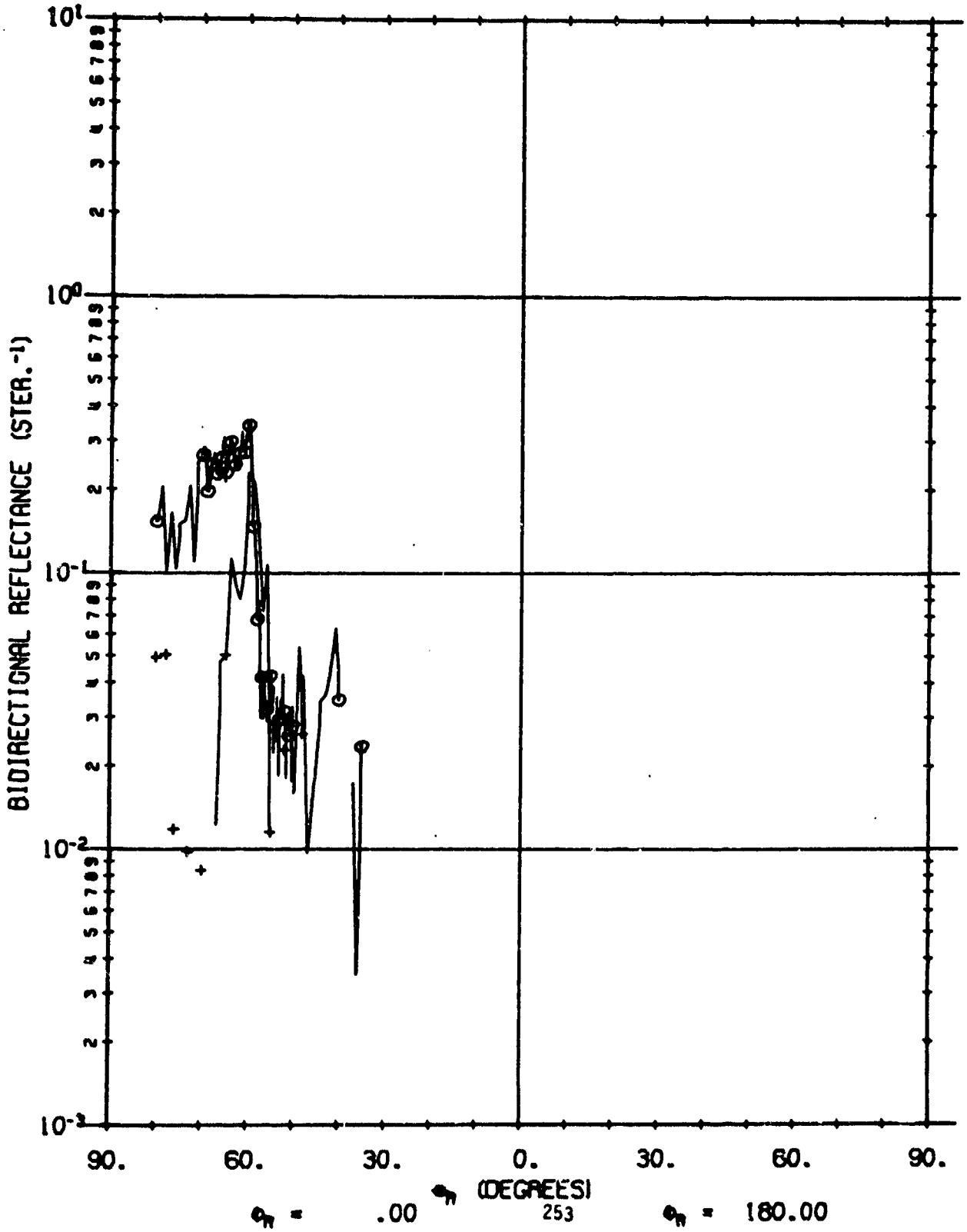

A02022 202

λ = .63
θ_i = 60.0
ϕ_i = 180.0

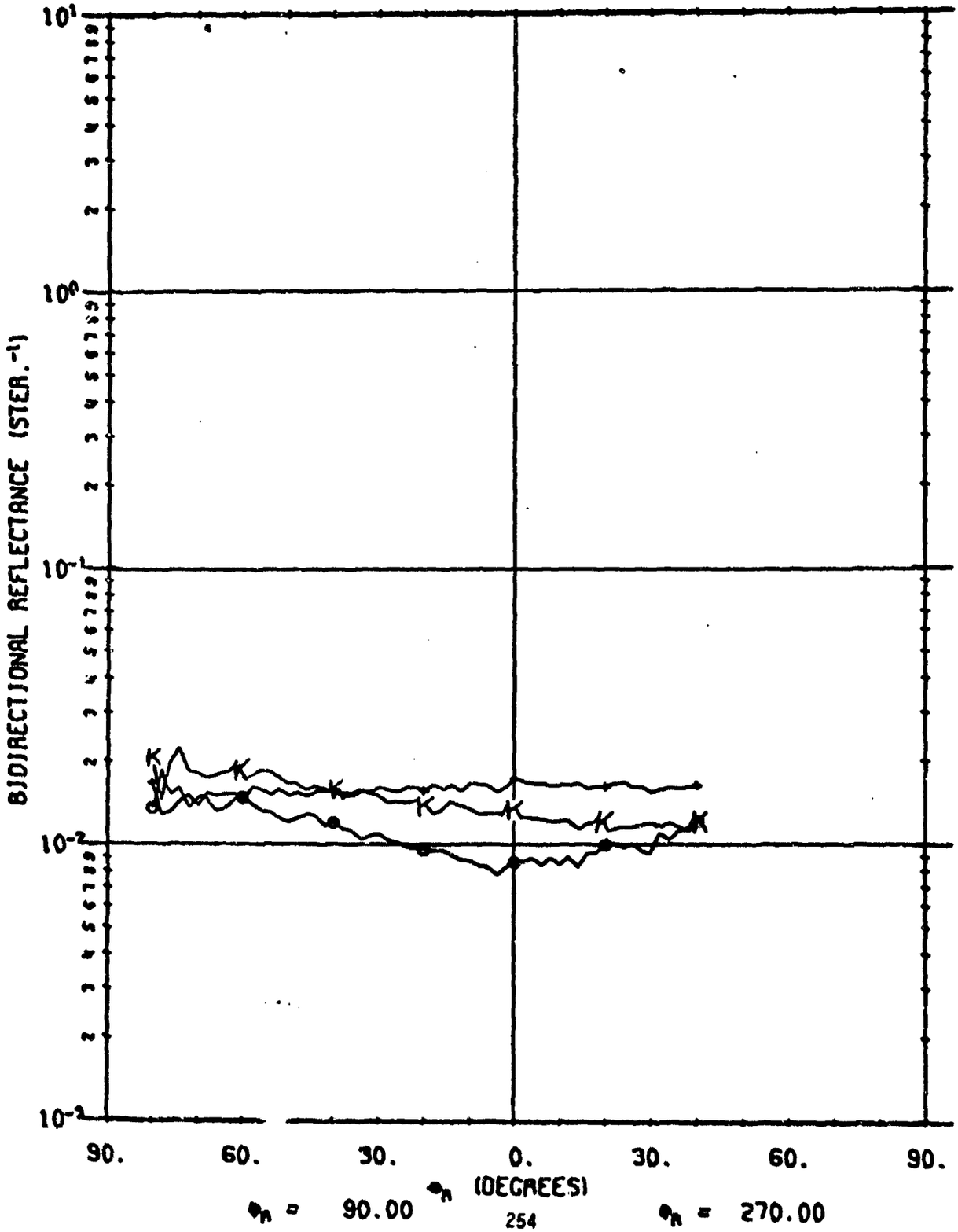

A02022 201

λ = 1.06
ϕ_i = 60.0
θ_i = 180.0

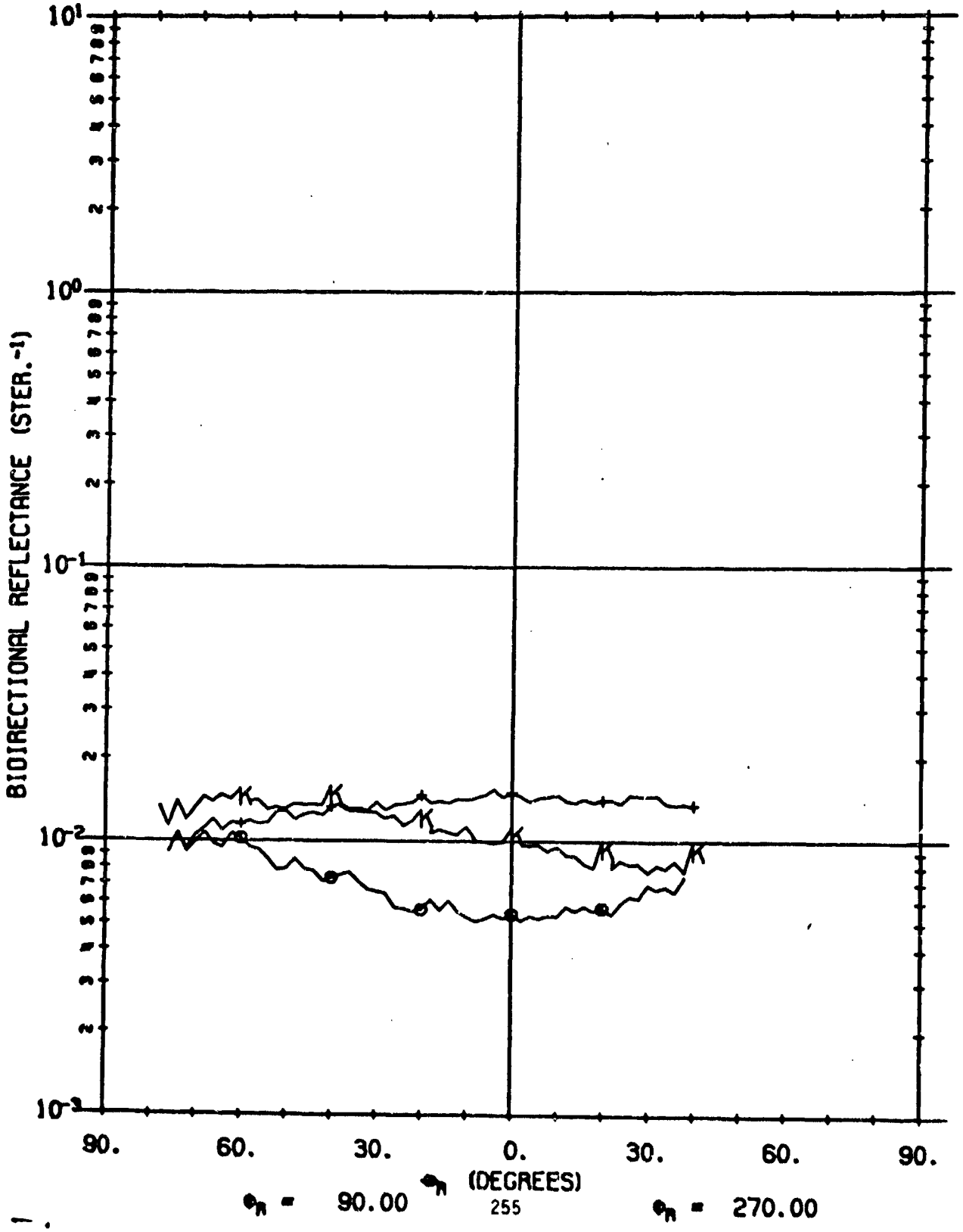

A02022 702

λ = 3.39
θ_I = 60.0
ϕ_I = 180.0

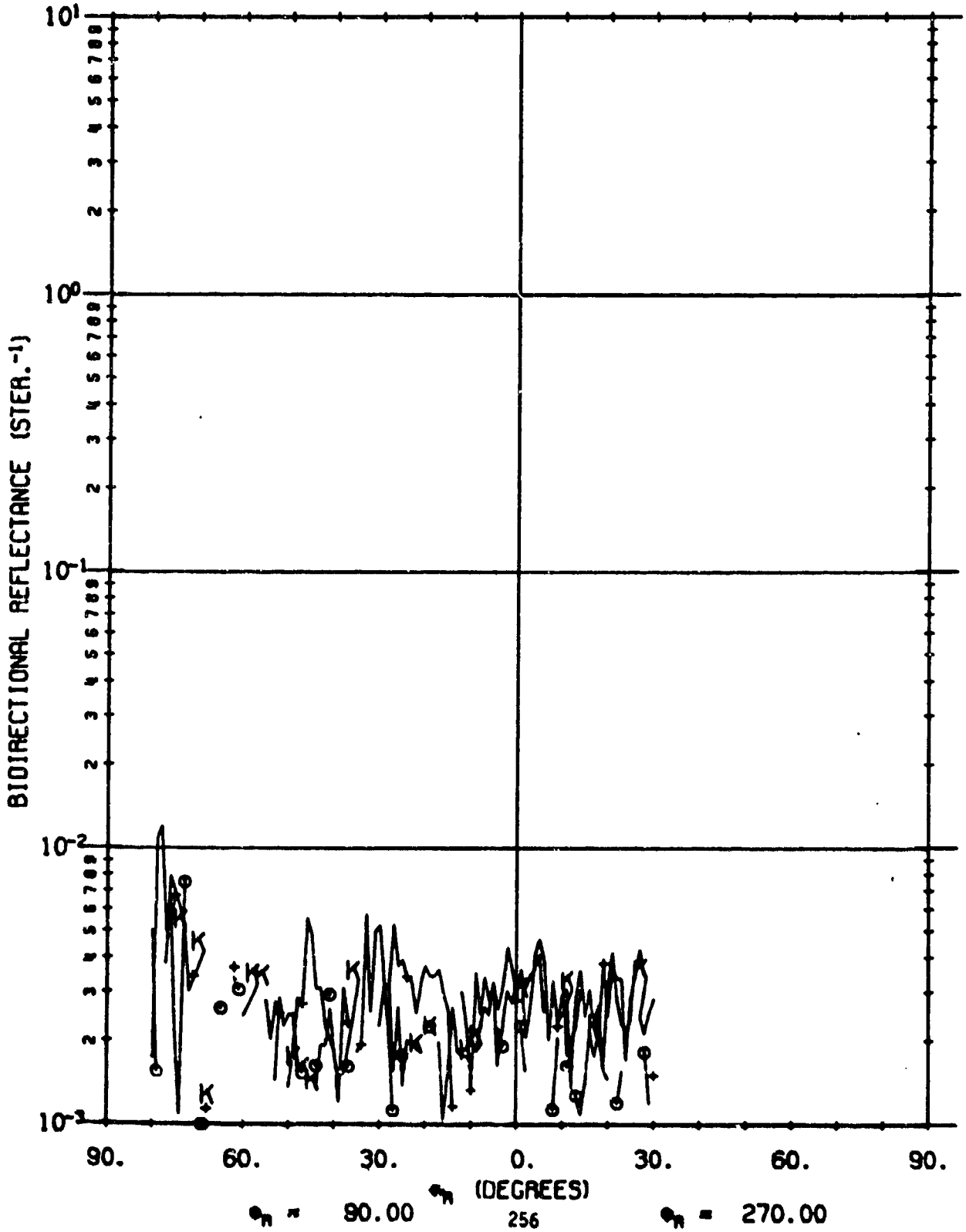

A02023 101

λ = 1.06
θ_i = .0
ϕ_i = 180.0

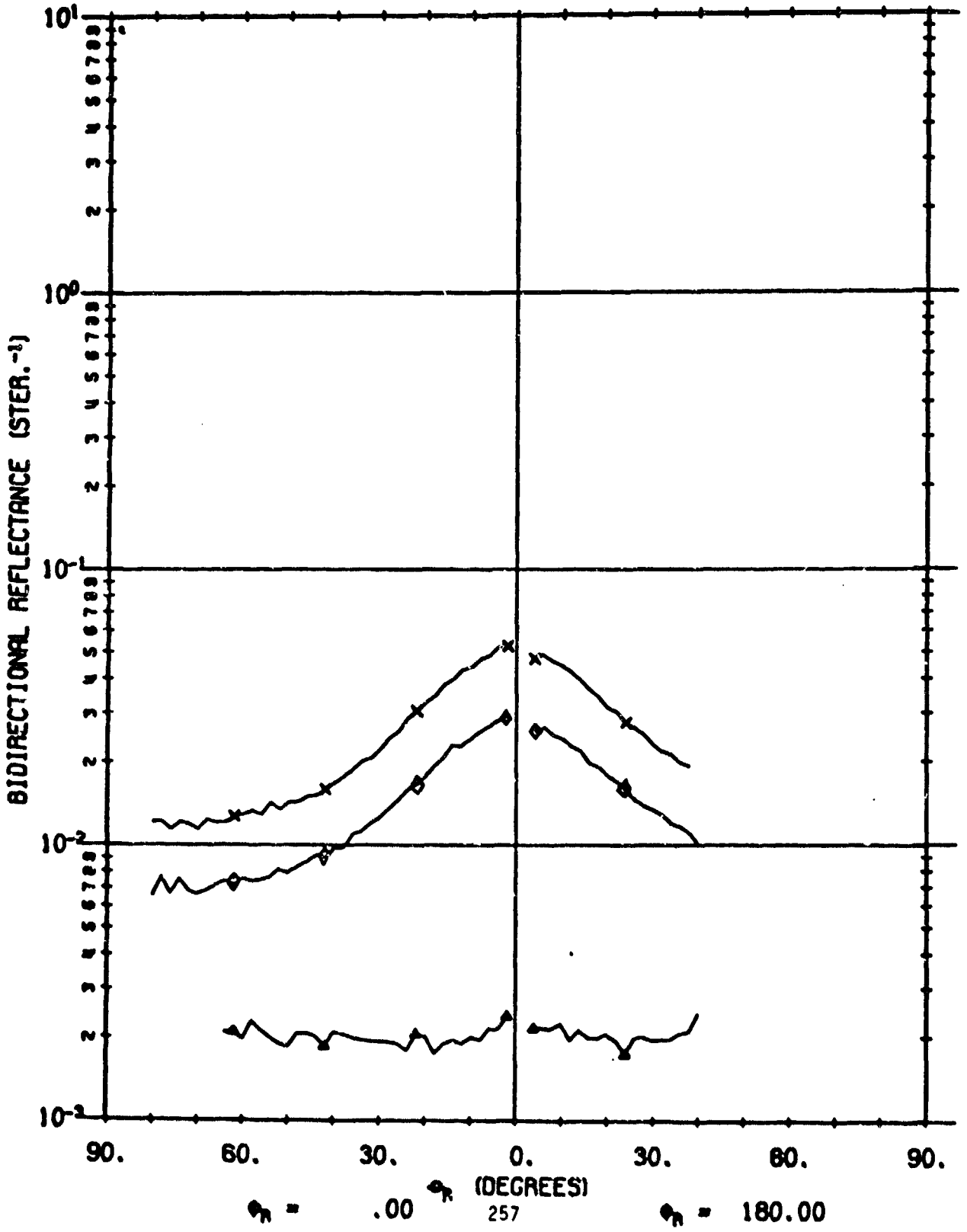

A02023 702

λ = 3.39
ϕ_1 = .0
θ_1 = 180.0

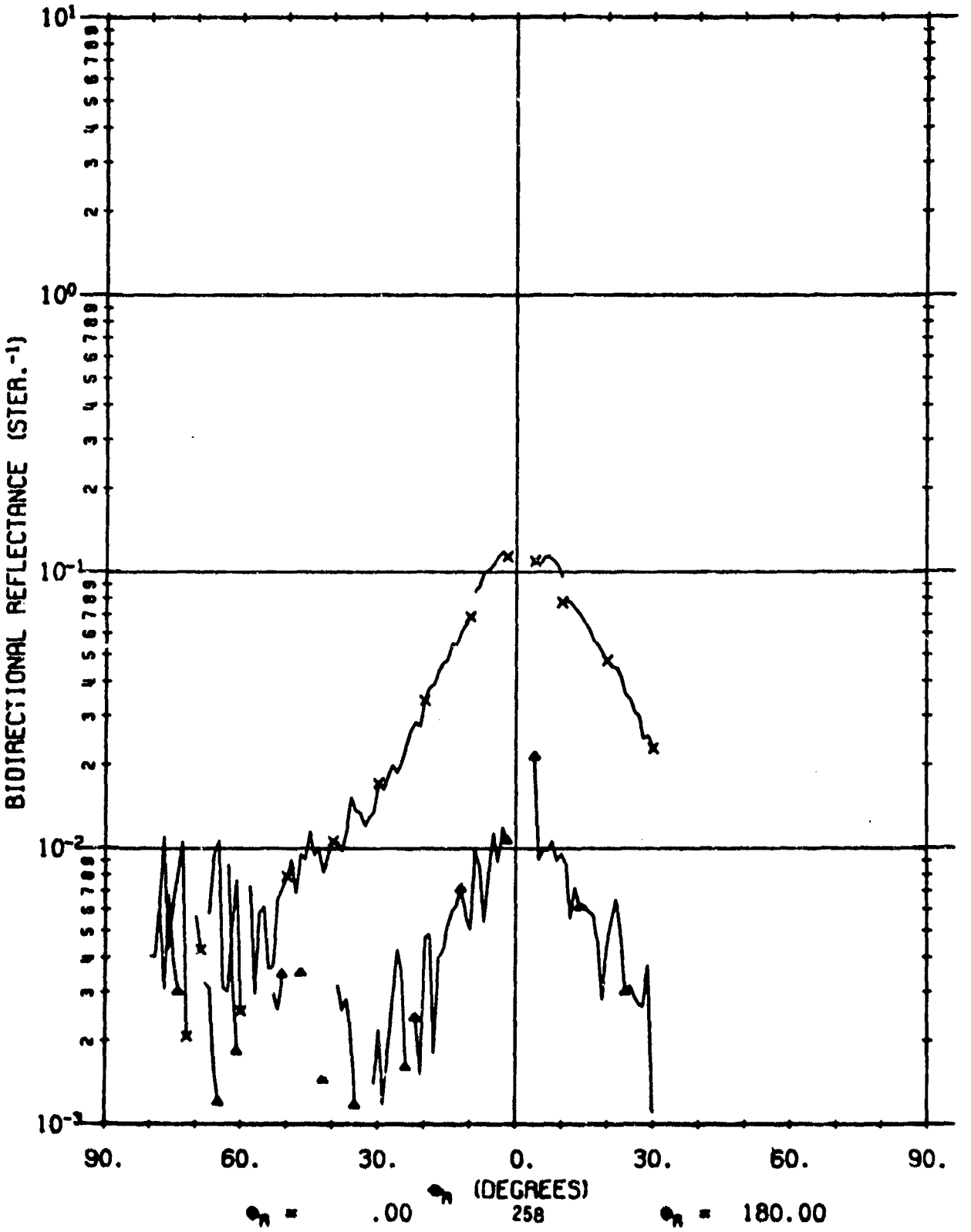

A02023 602

λ = 10.60
θ_I = .0
ϕ_I = 180.0

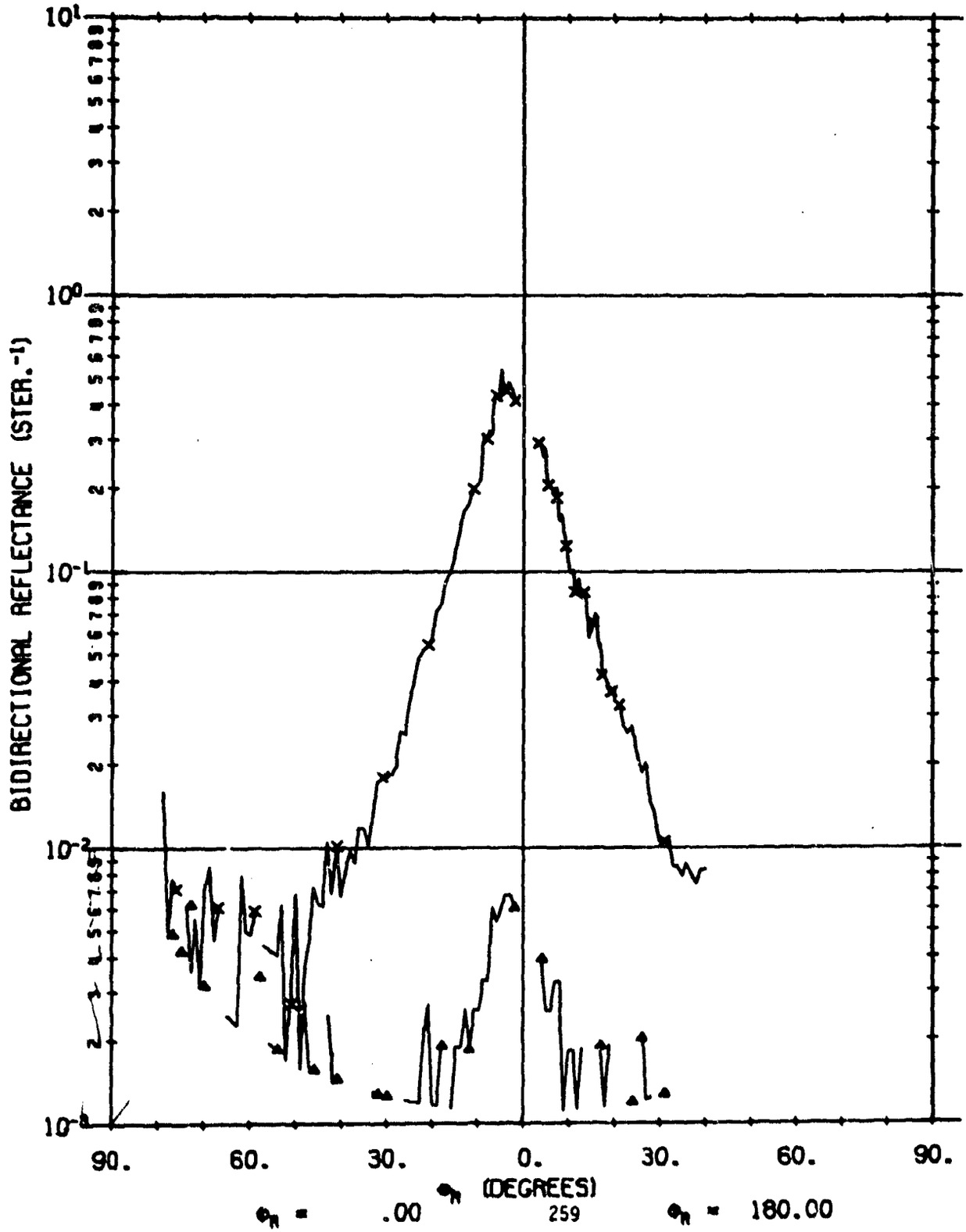

A02023 101

λ = 1.06
θ_i = .0
ϕ_i = 180.0

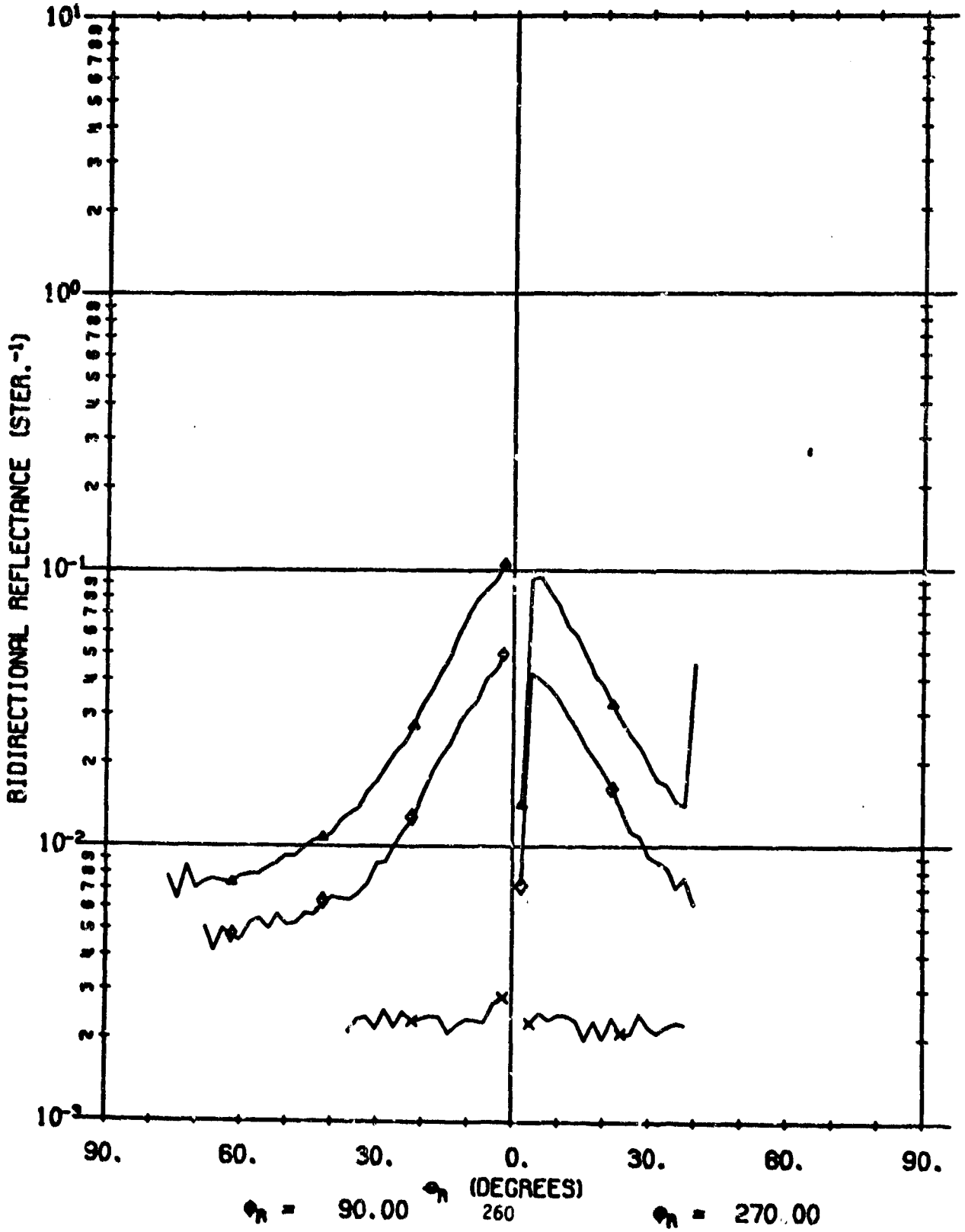

A02023 101

λ = 1.06
θ_i = 20.0
ϕ_i = 180.0

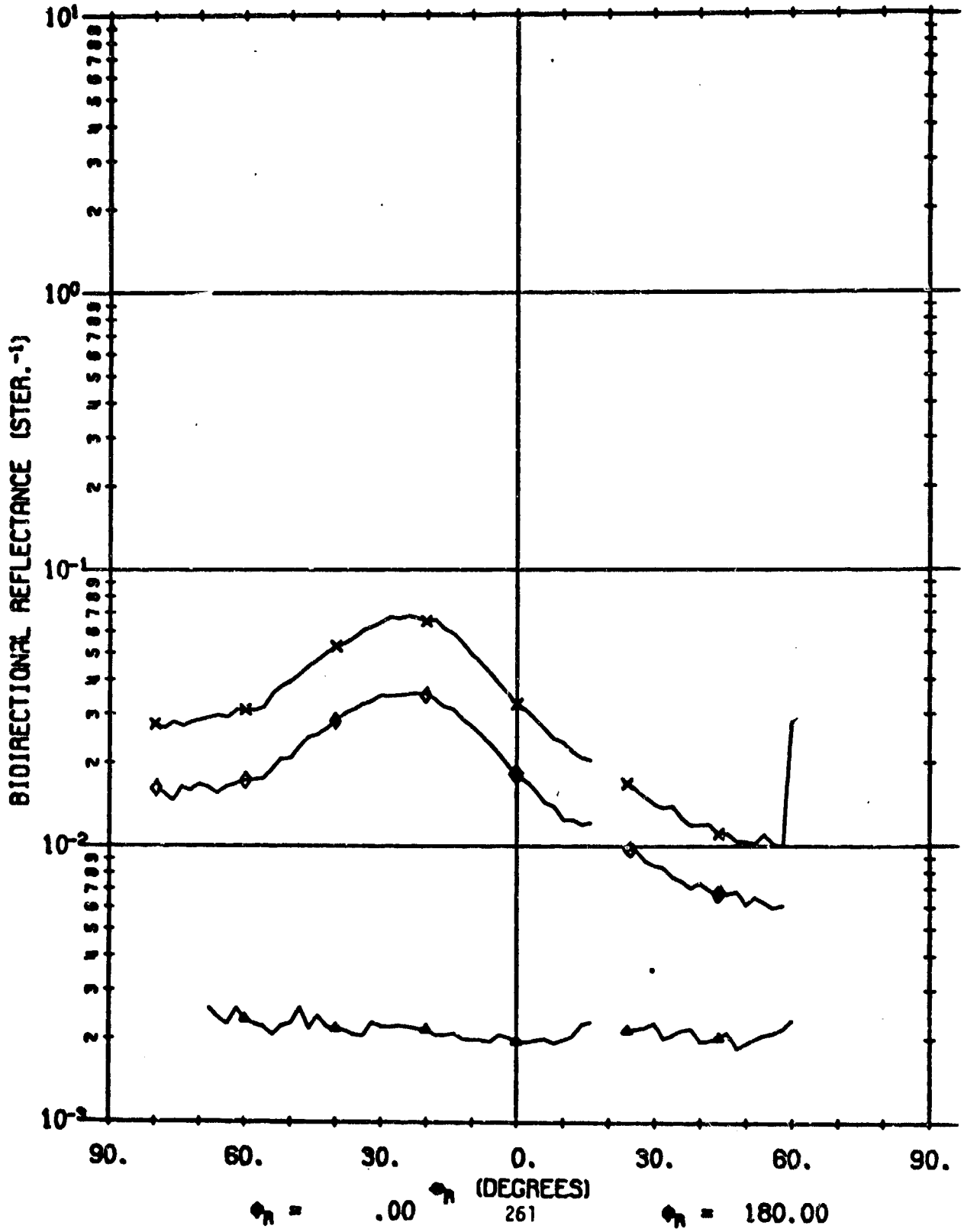

A02023 702

λ = 3.39
Φ_I = 20.0
Θ_I = 180.0

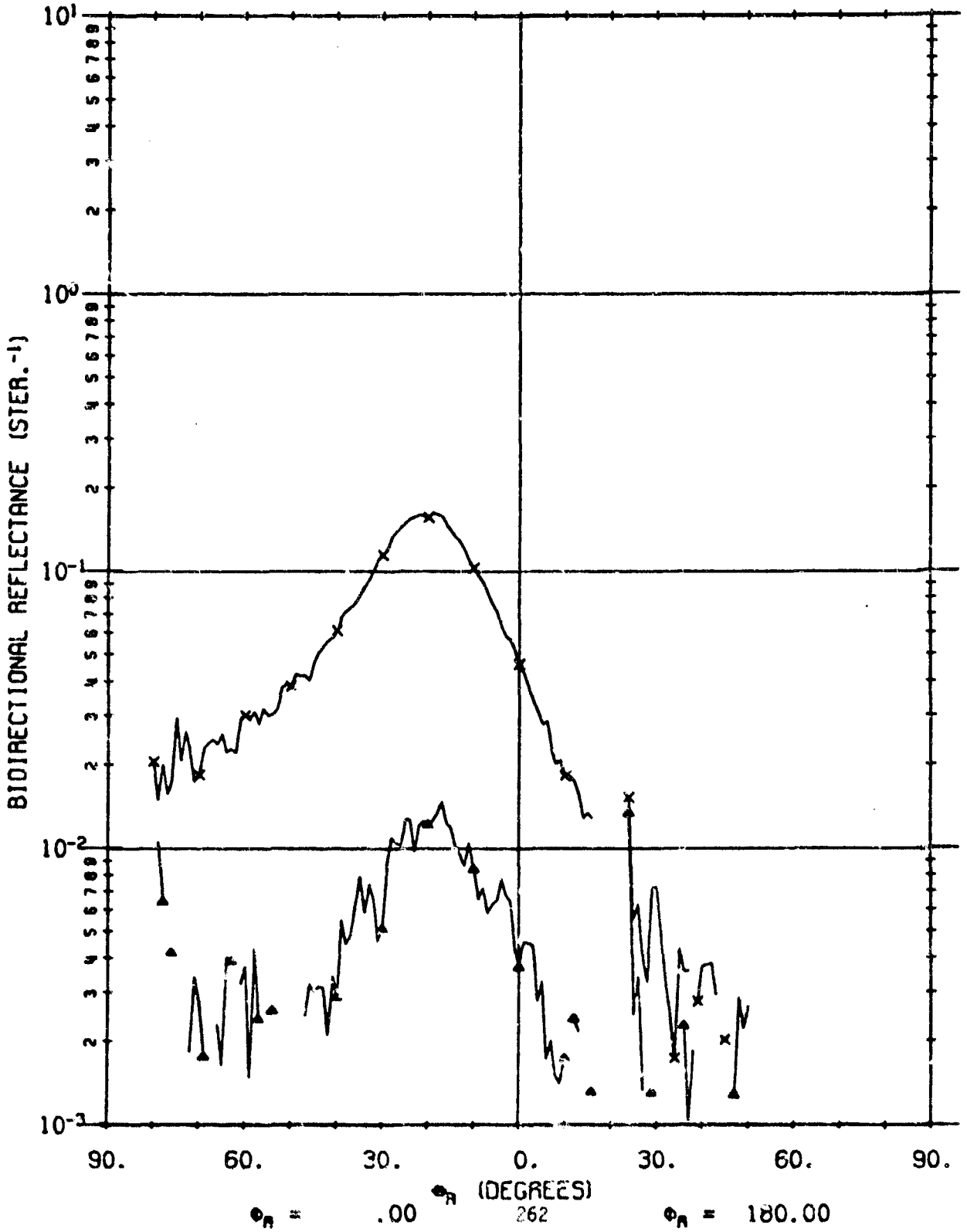

A02023 602

λ = 10.60
θ_i = 20.0
ϕ_i = 180.0

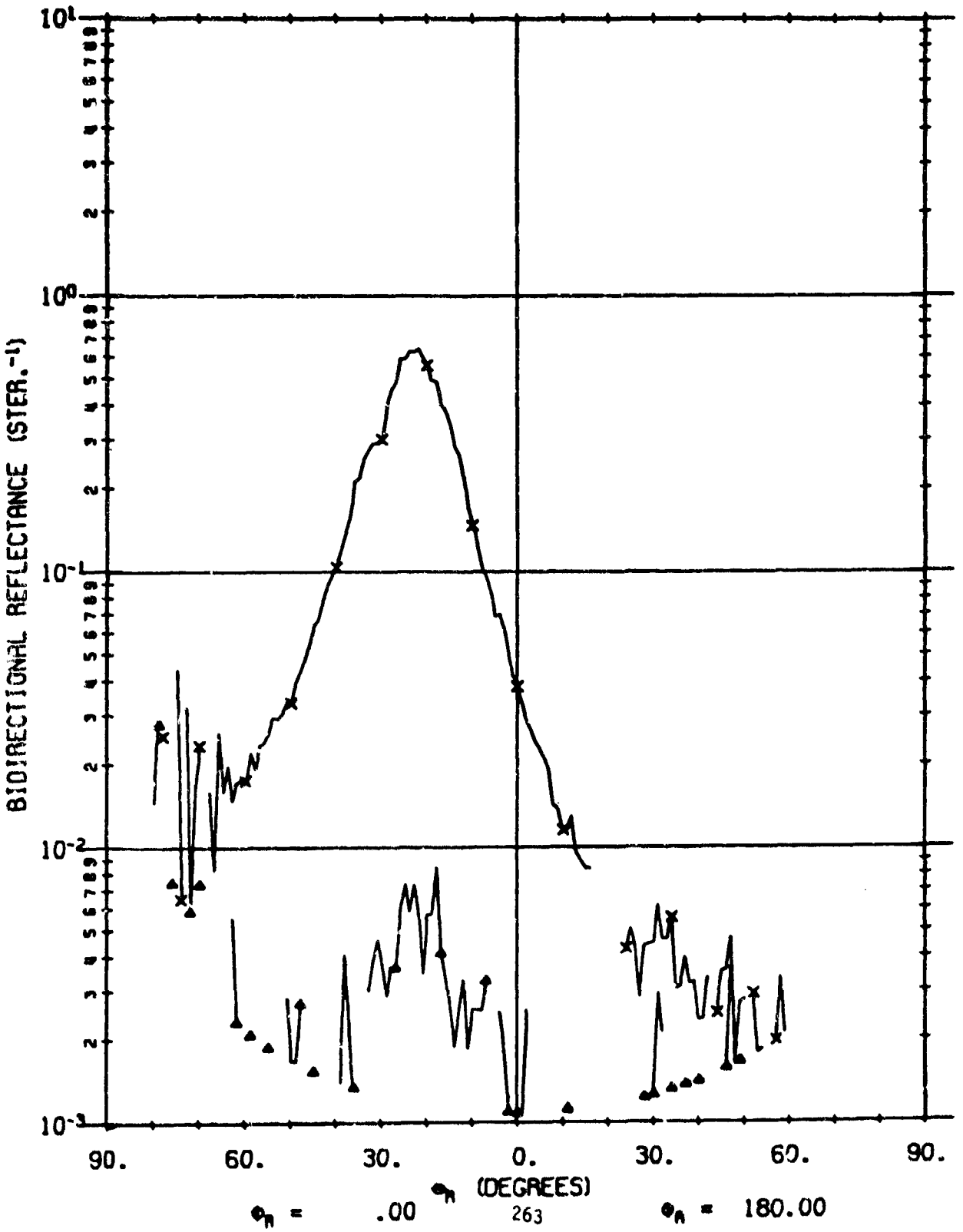

A02023 501

λ = .63
Φ_I = 20.0
Φ_I = 180.0

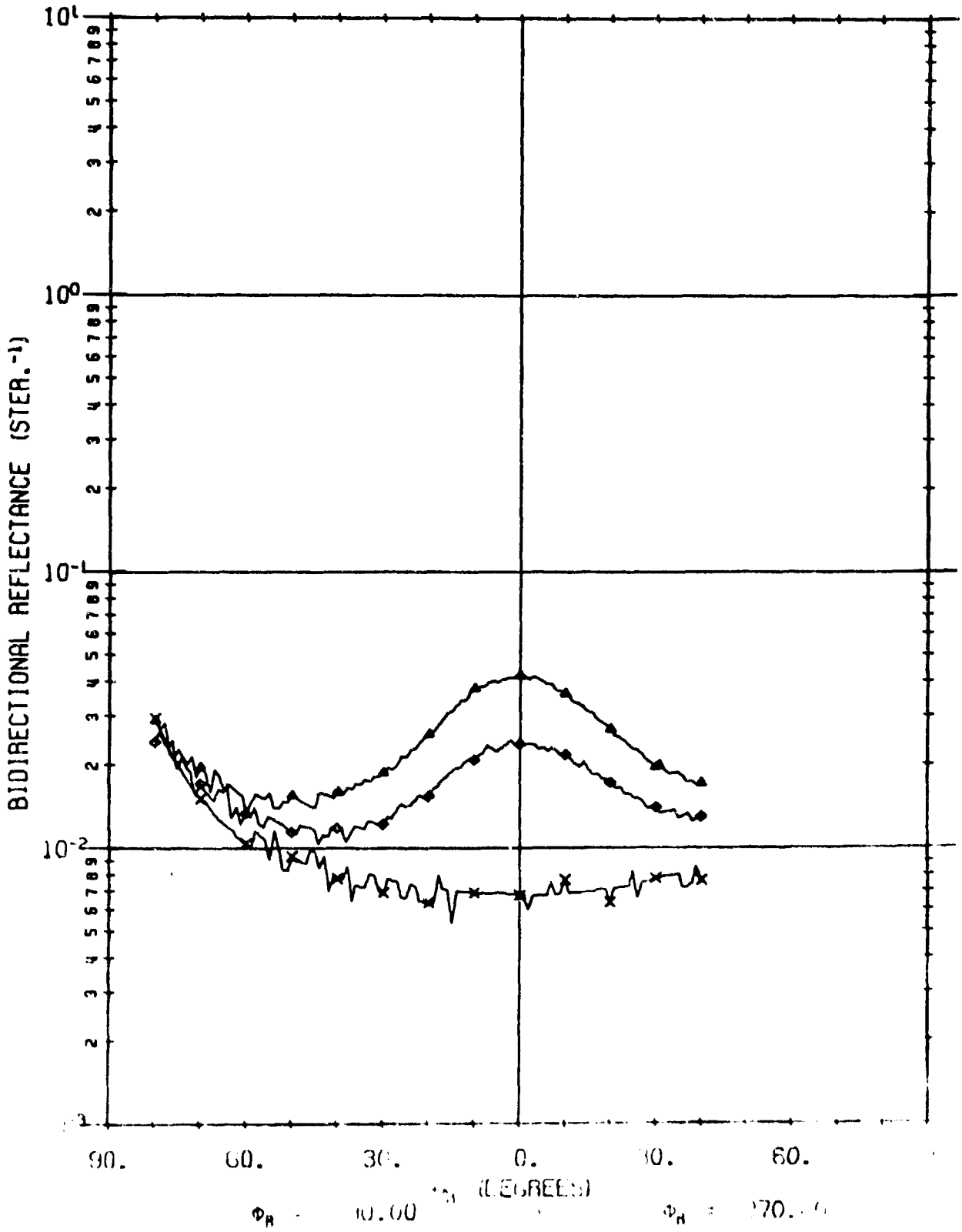

A02023 101

λ = 1.06
θ_I = 20.0
ϕ_I = 180.0

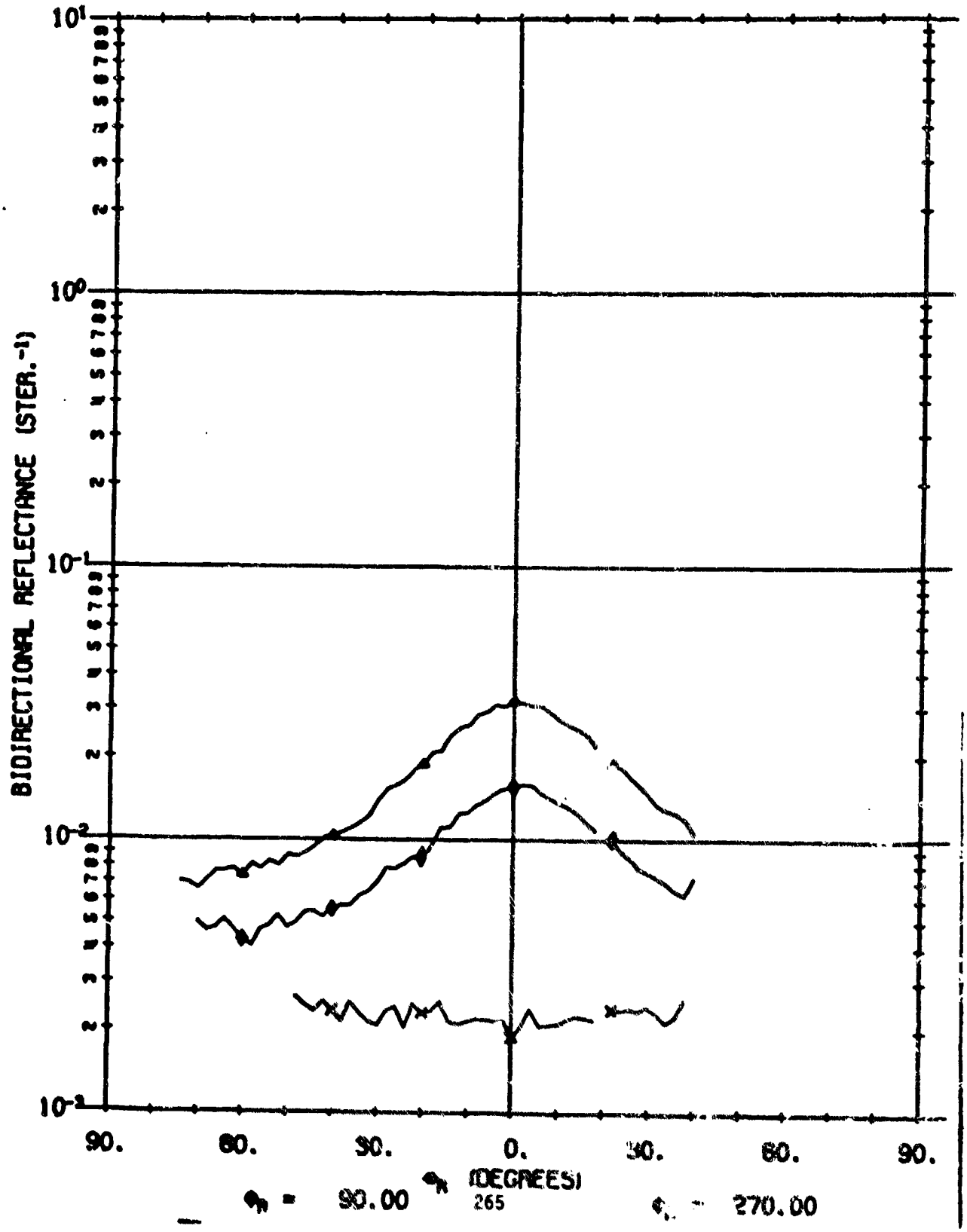

A02023 701

λ = 3.39
Θ_I = 20.0
Φ_I = 180.0

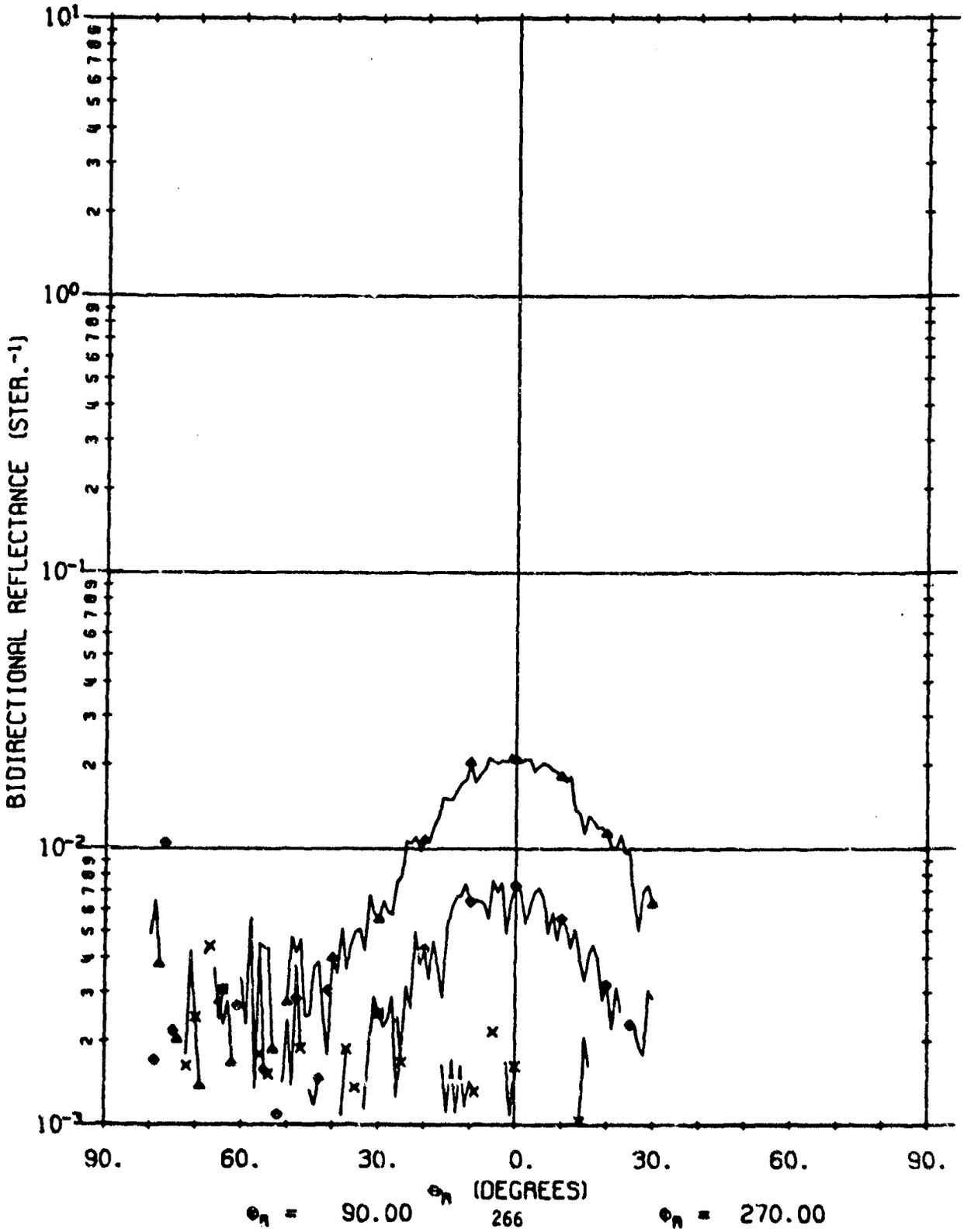

A02023 604

λ = 10.60
ϕ_I = 20.0
θ_I = 180.0

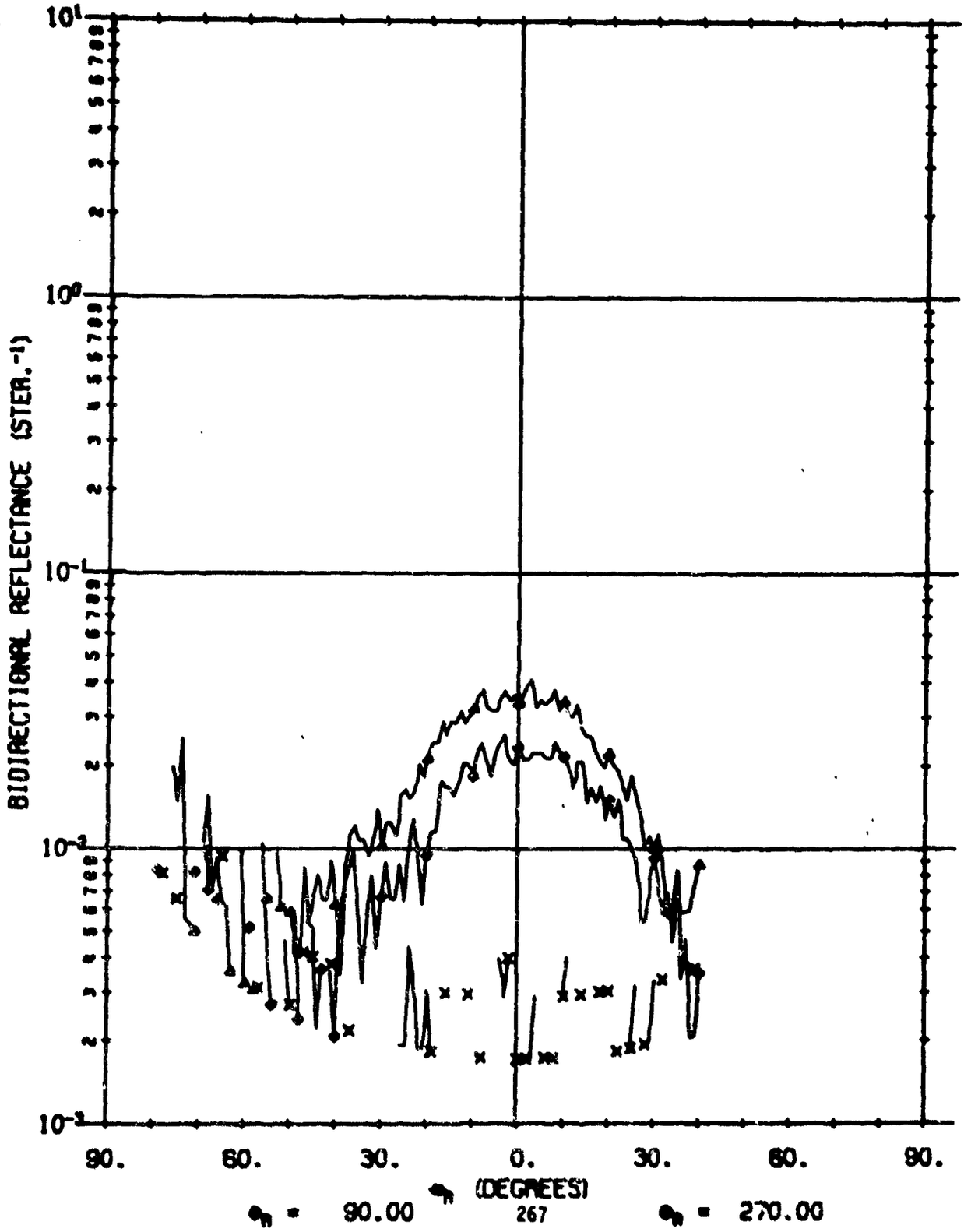

A02023 101

λ = 1.06
ϕ_I = 40.0
θ_I = 180.0

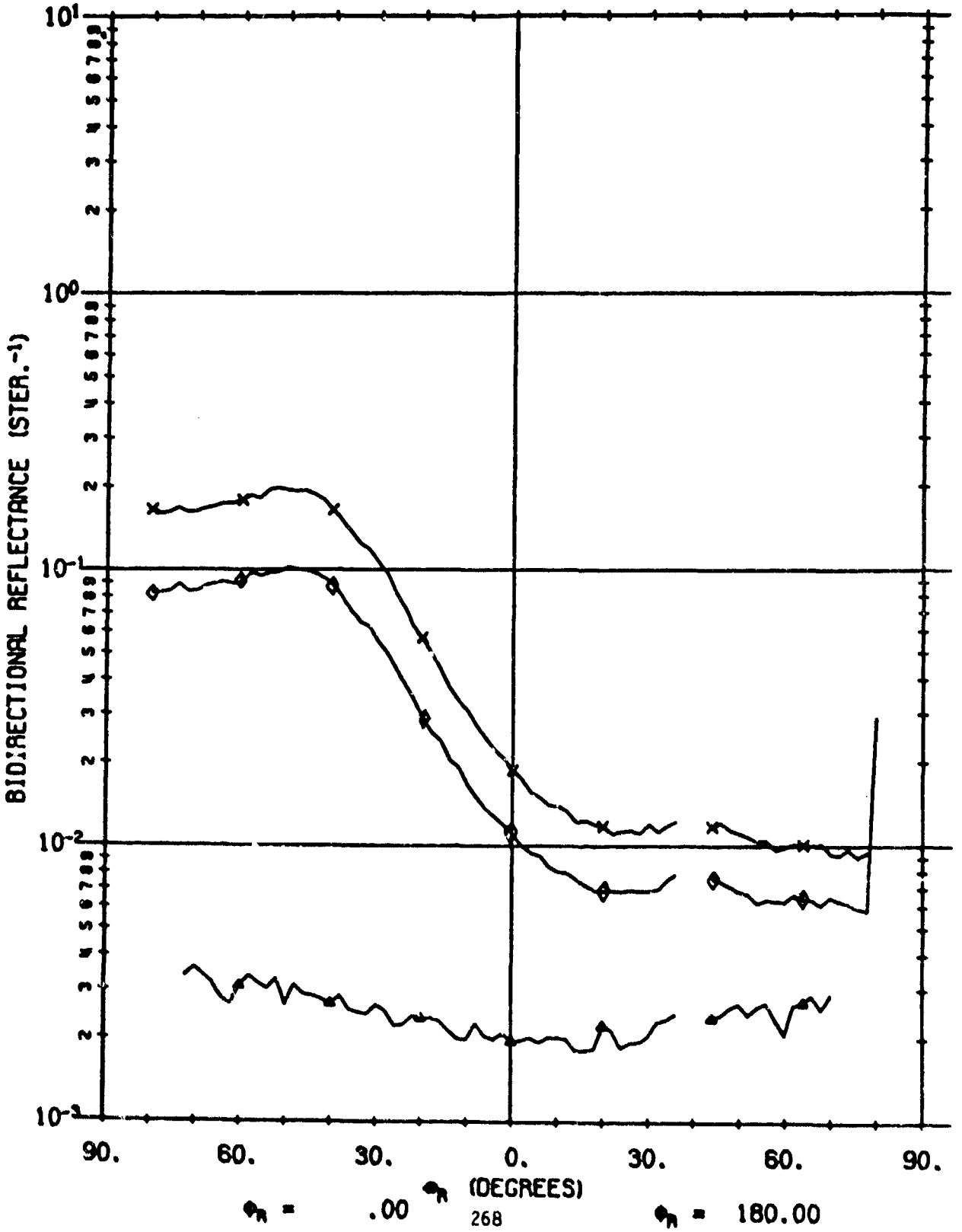

A02023 702

λ = 3.39
Φ_I = 40.0
Φ_I = 180.0

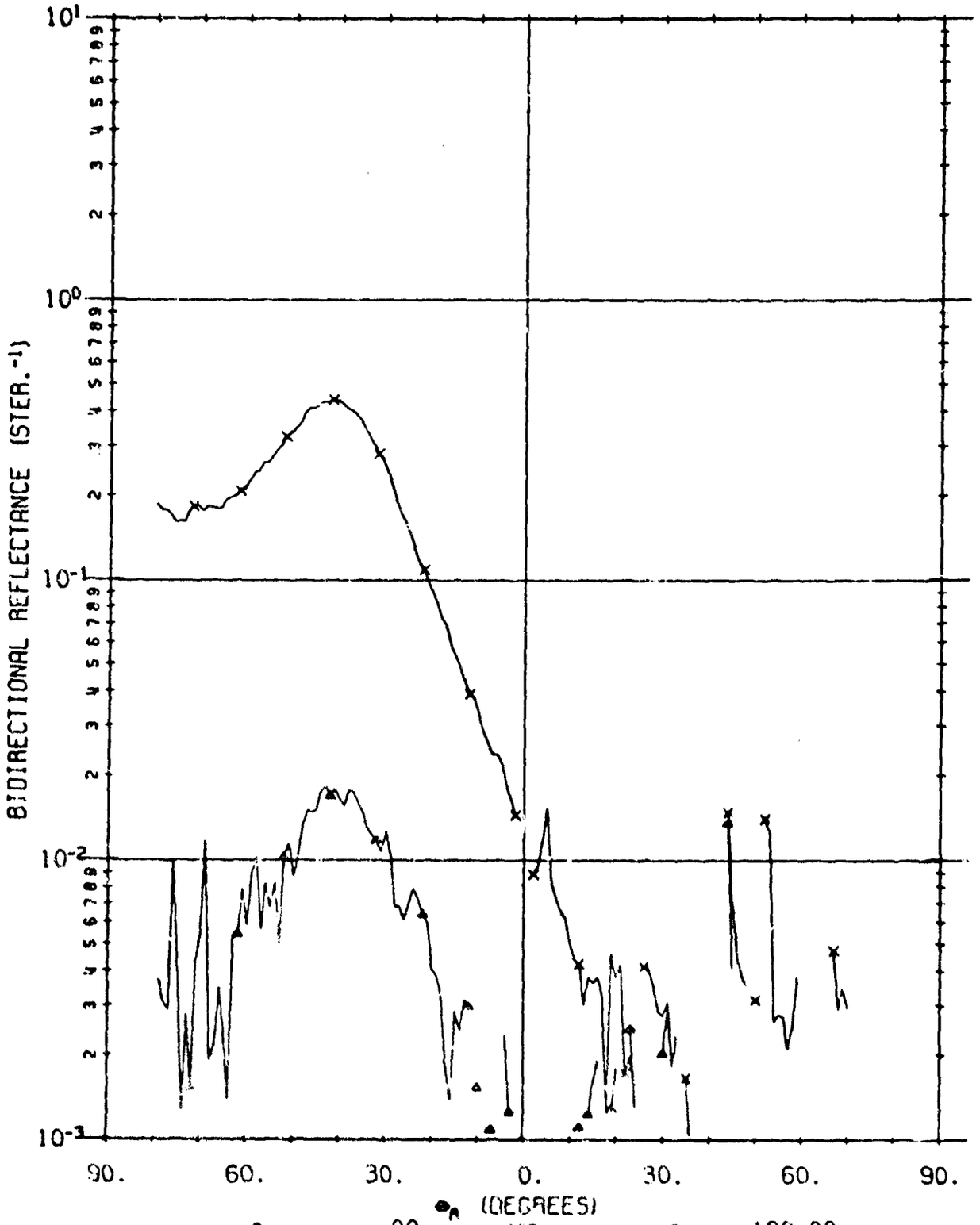

Φ_R = .00 Φ_R = 180.00

A02023 602

λ = 10.60
ϕ_I = 40.0
θ_I = 180.0

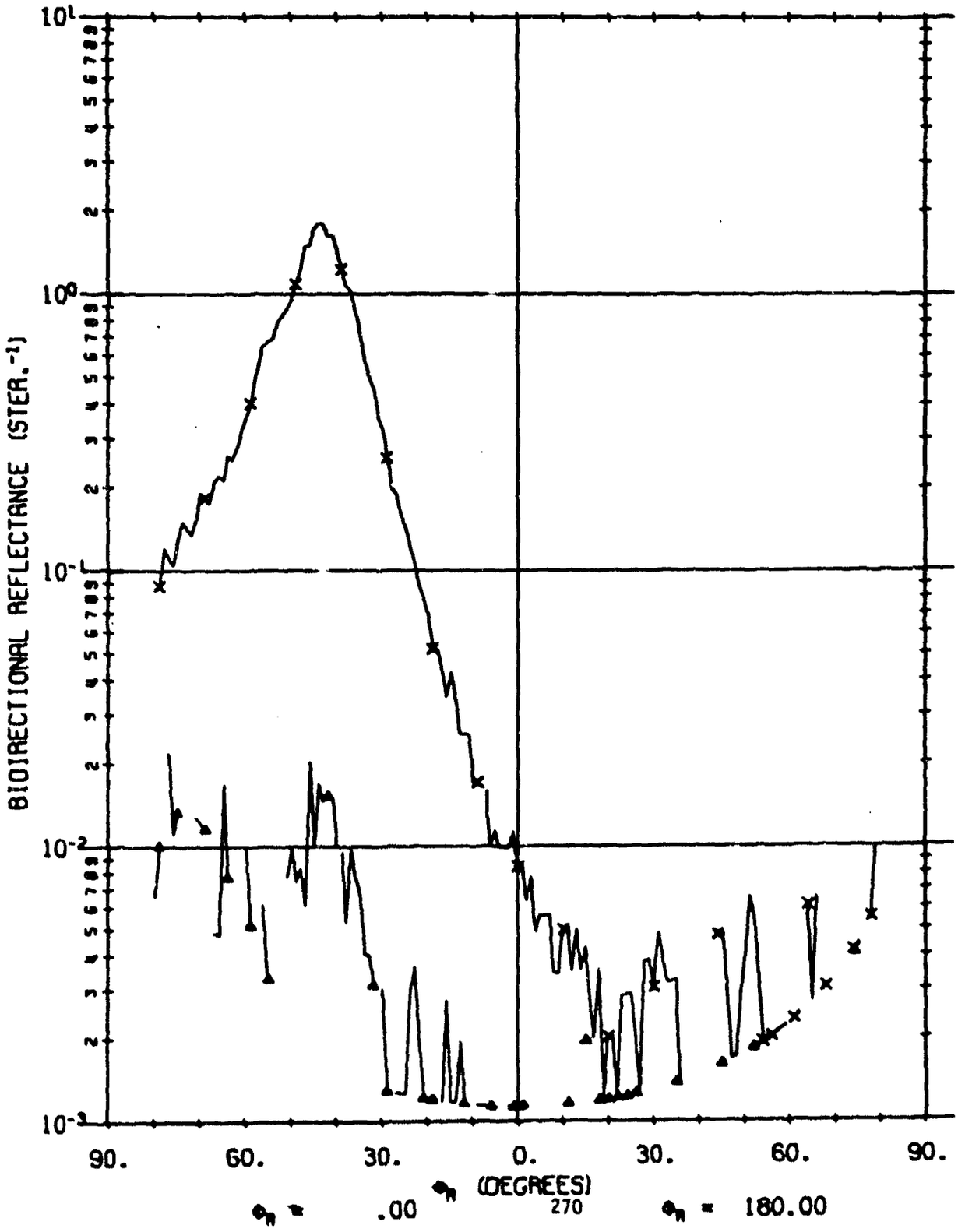

A02023 501

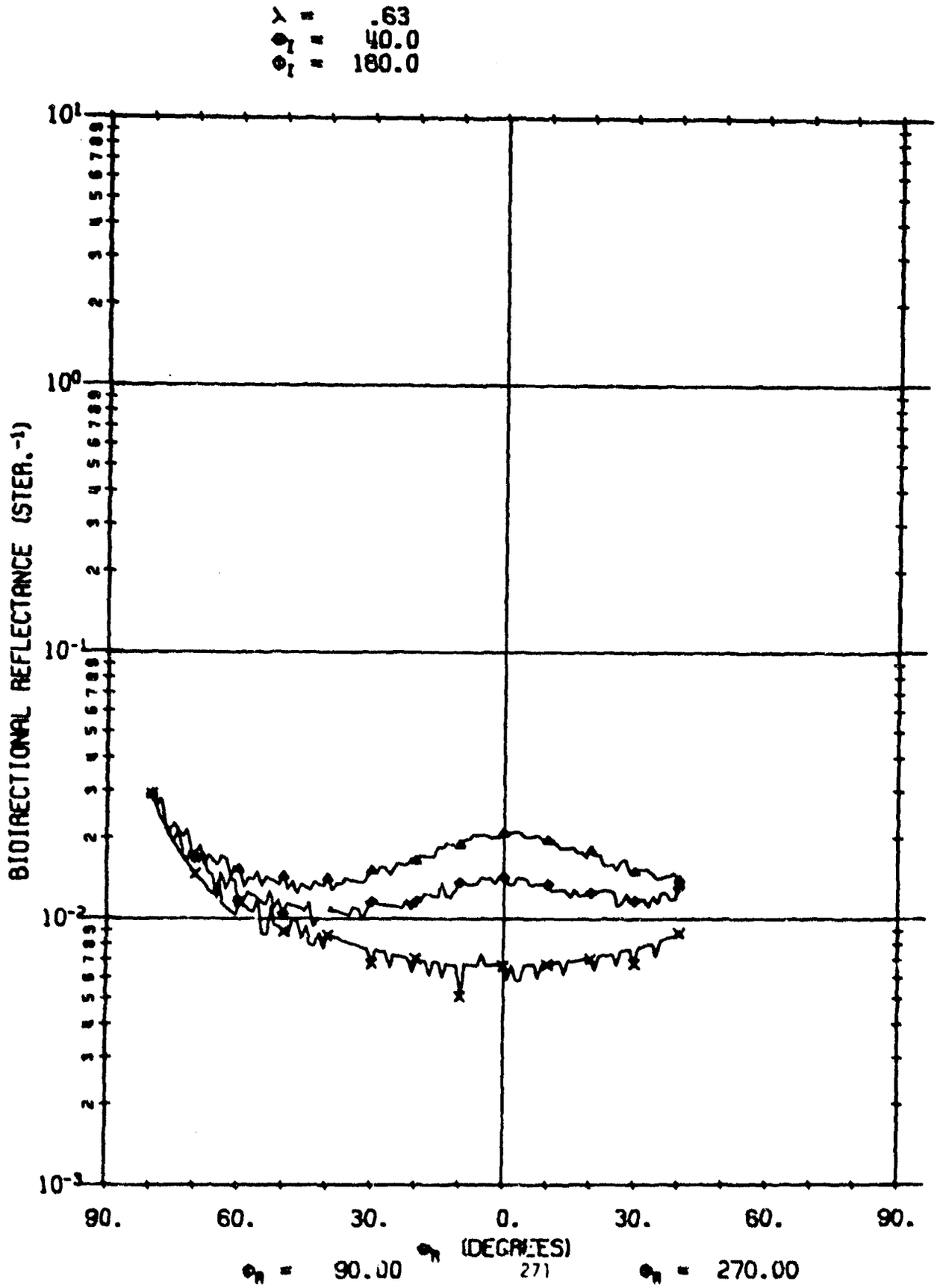
λ = .63
Φ_I = 40.0
Θ_I = 180.0
BIDIRECTIONAL REFLECTANCE (STER.$^{-1}$)
10^1
10^0
10^{-1}
10^{-2}
10^{-3}
90.
60.
30.
0.
30.
60.
90.
Θ_R (DEGREES)
Φ_R = 90.00
Φ_R = 270.00

A02023 101

λ = 1.06
θ_i = 40.0
ϕ_i = 180.0

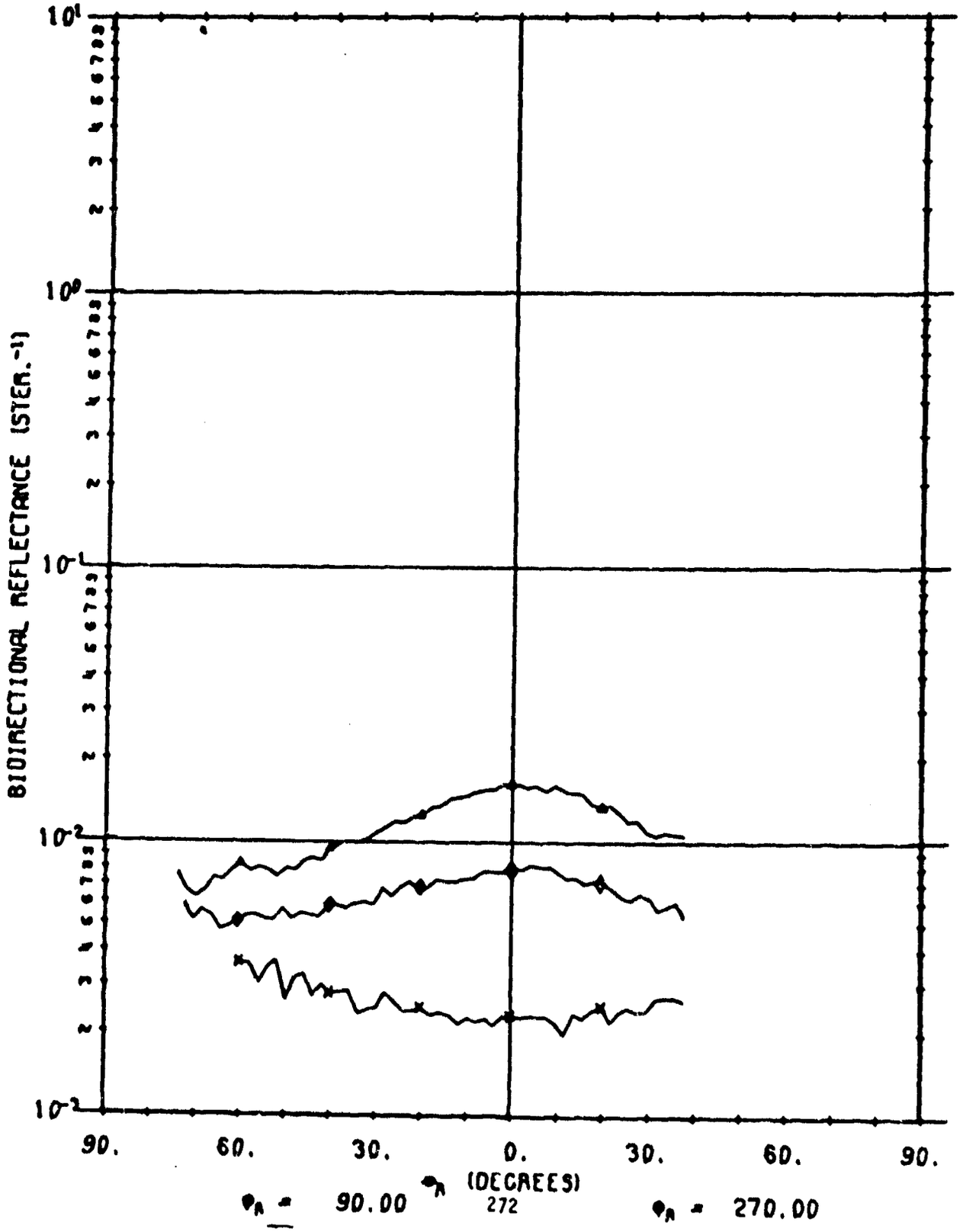

A02023 701

λ = 3.39
Θ_I = 40.0
Φ_I = 180.0

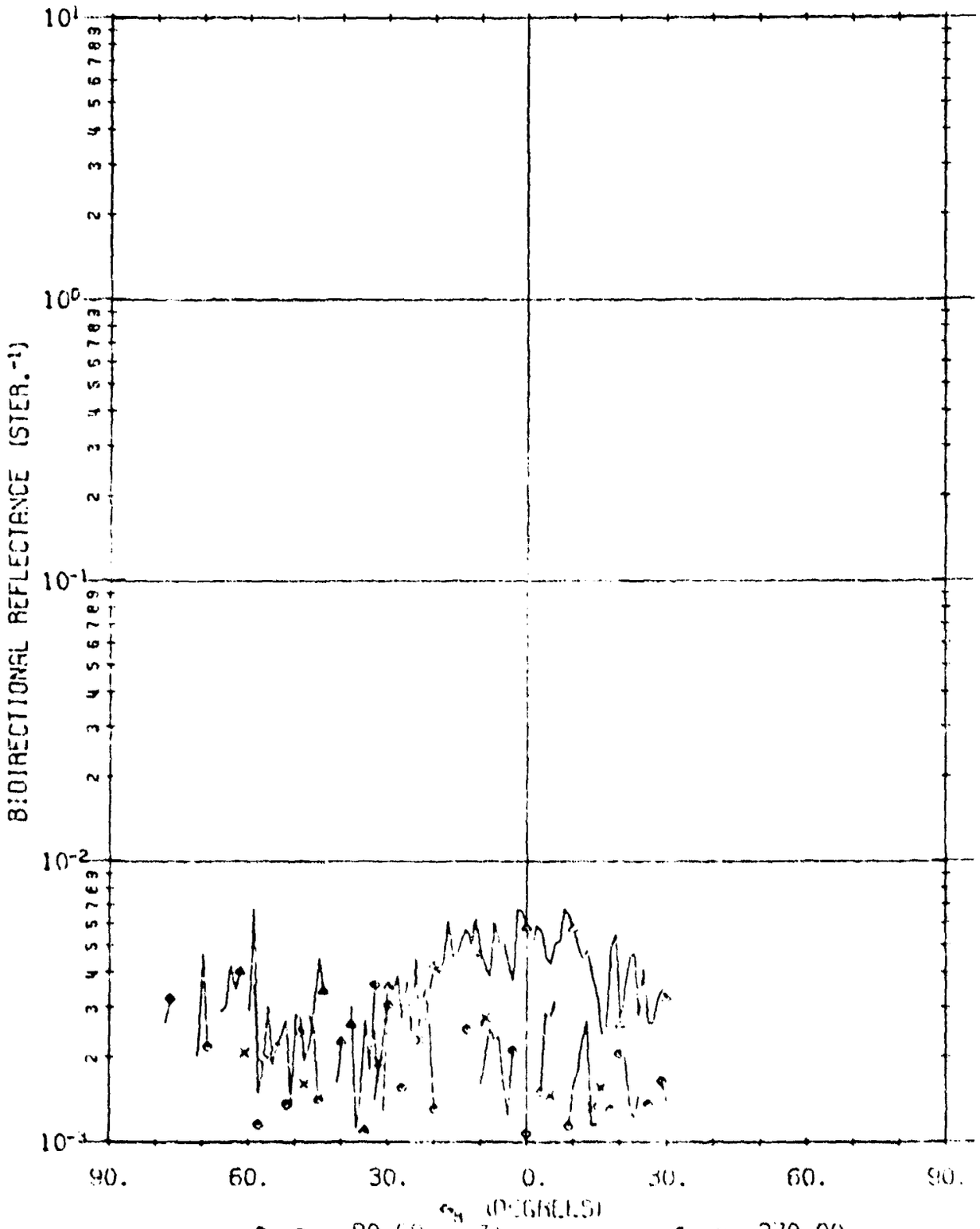

Φ_R = 90.00 Φ_R = 270.00

A02023 604

λ = 10.60
ϕ_i = 40.0
θ_i = 180.0

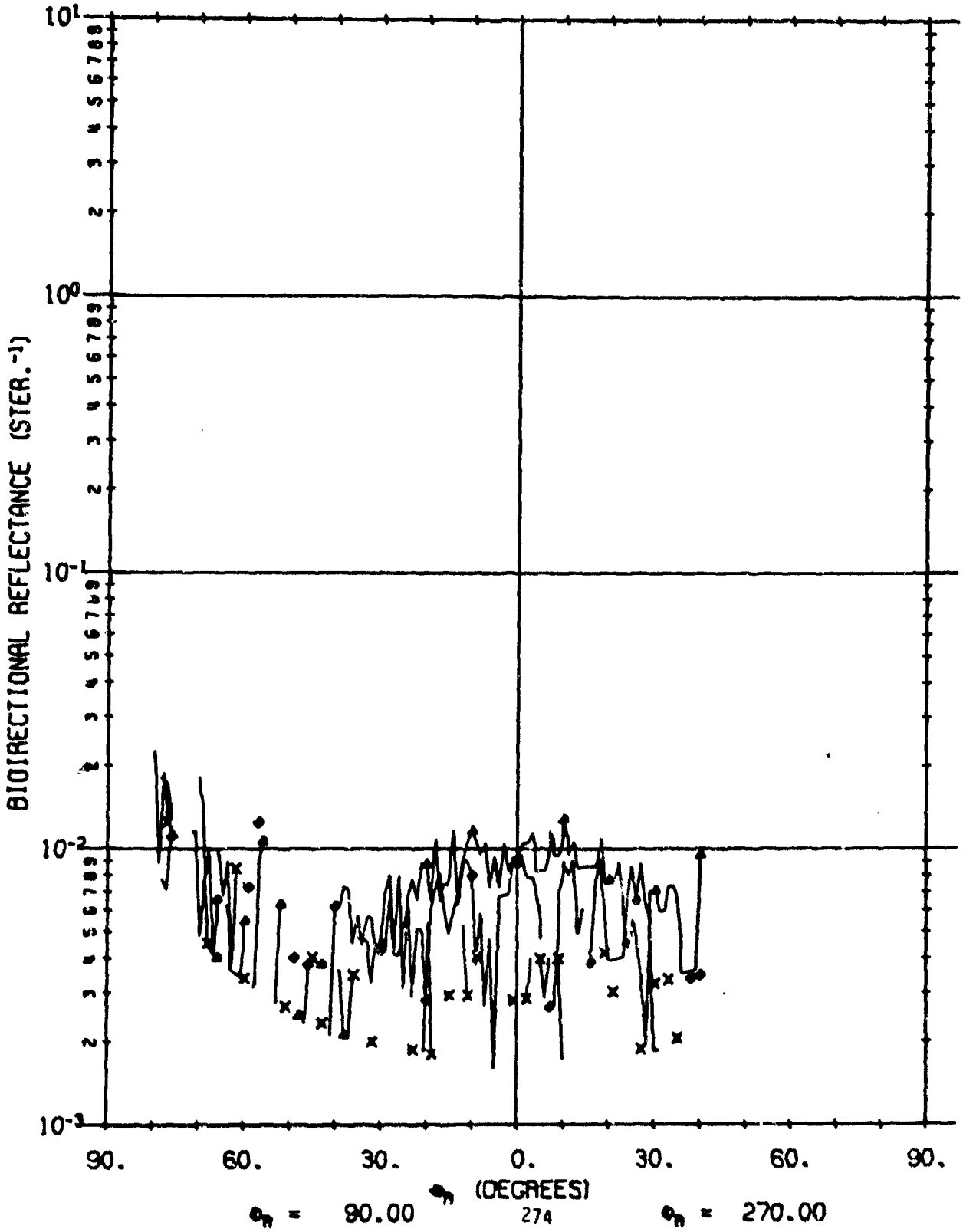

A02023 101

λ = 1.06
ϕ_1 = 60.0
θ_1 = 180.0

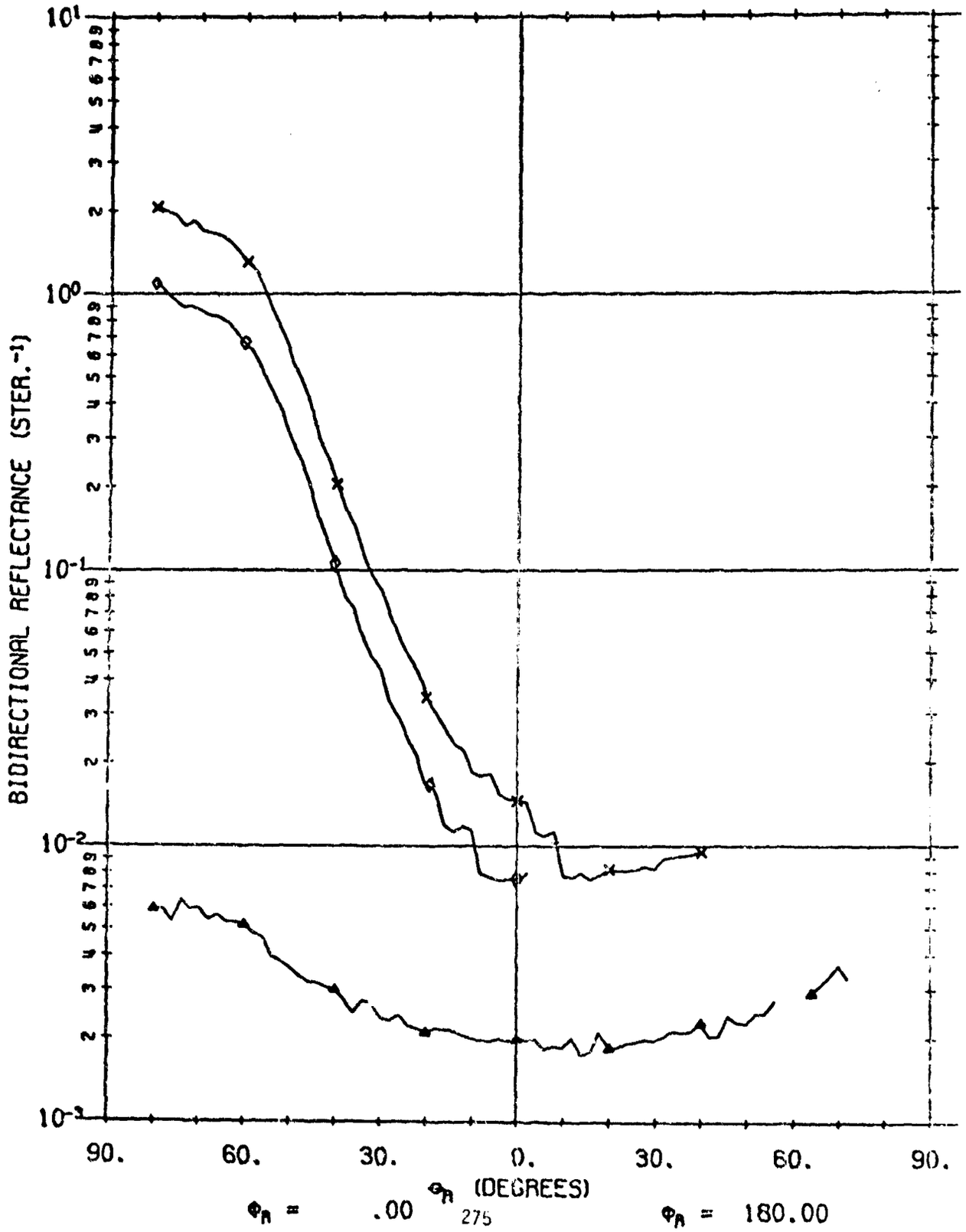

A02023 702

λ = 3.39
Φ_I = 60.0
Φ_I = 180.0

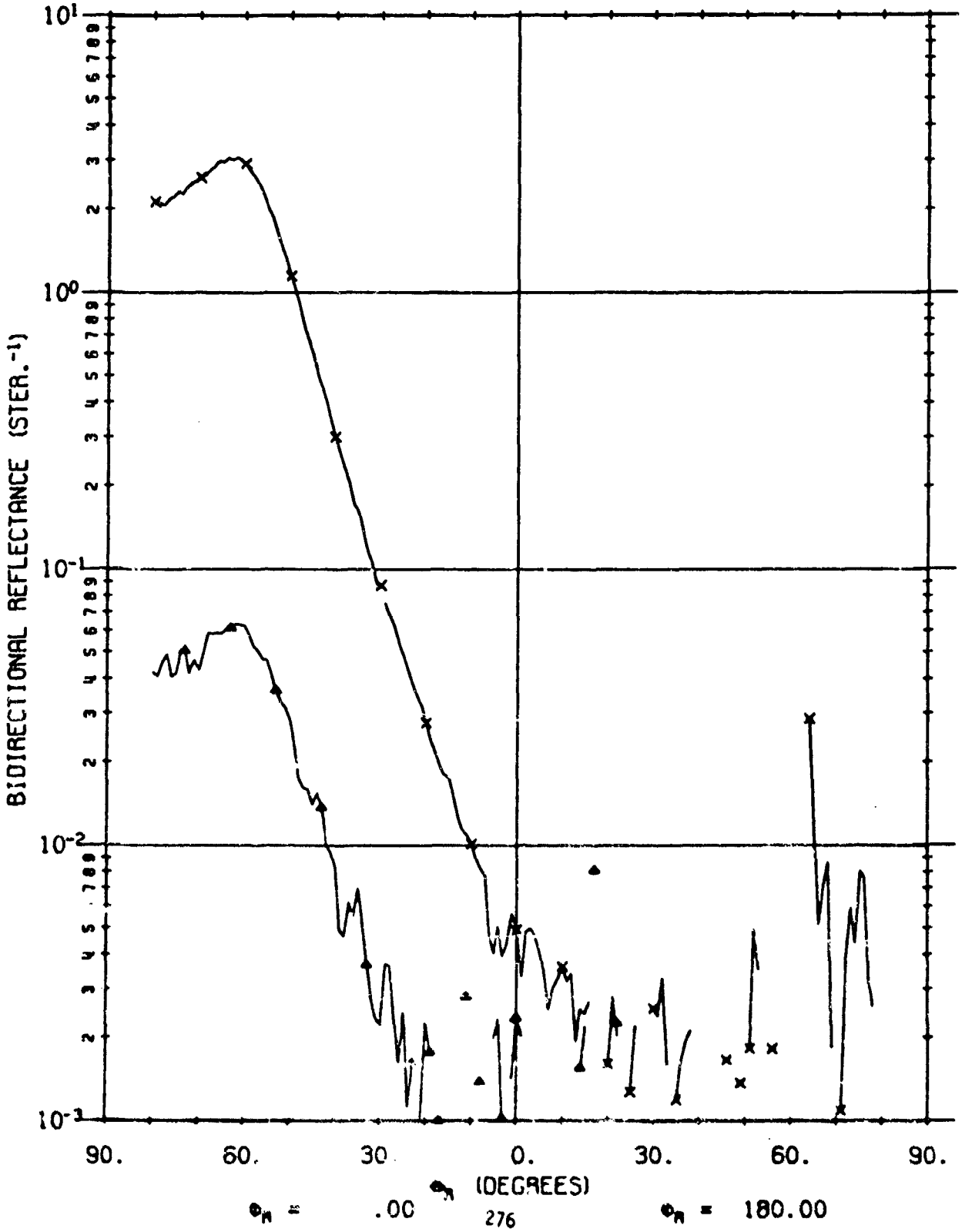

A02023 602

λ = 10.60
Θ_I = 60.0
Φ_I = 180.0

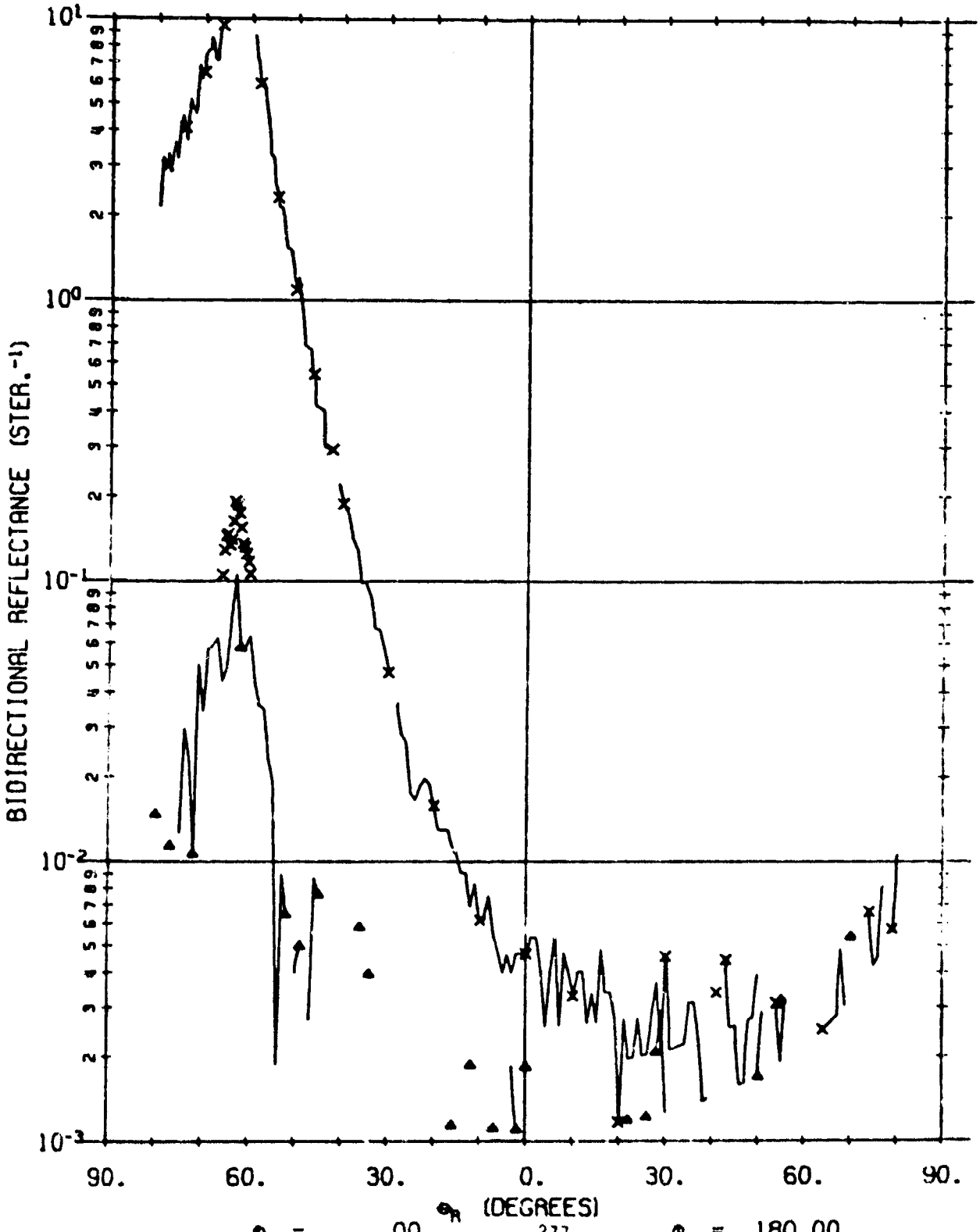

A02023 501

λ = .63
θ_I = 60.0
ϕ_I = 180.0

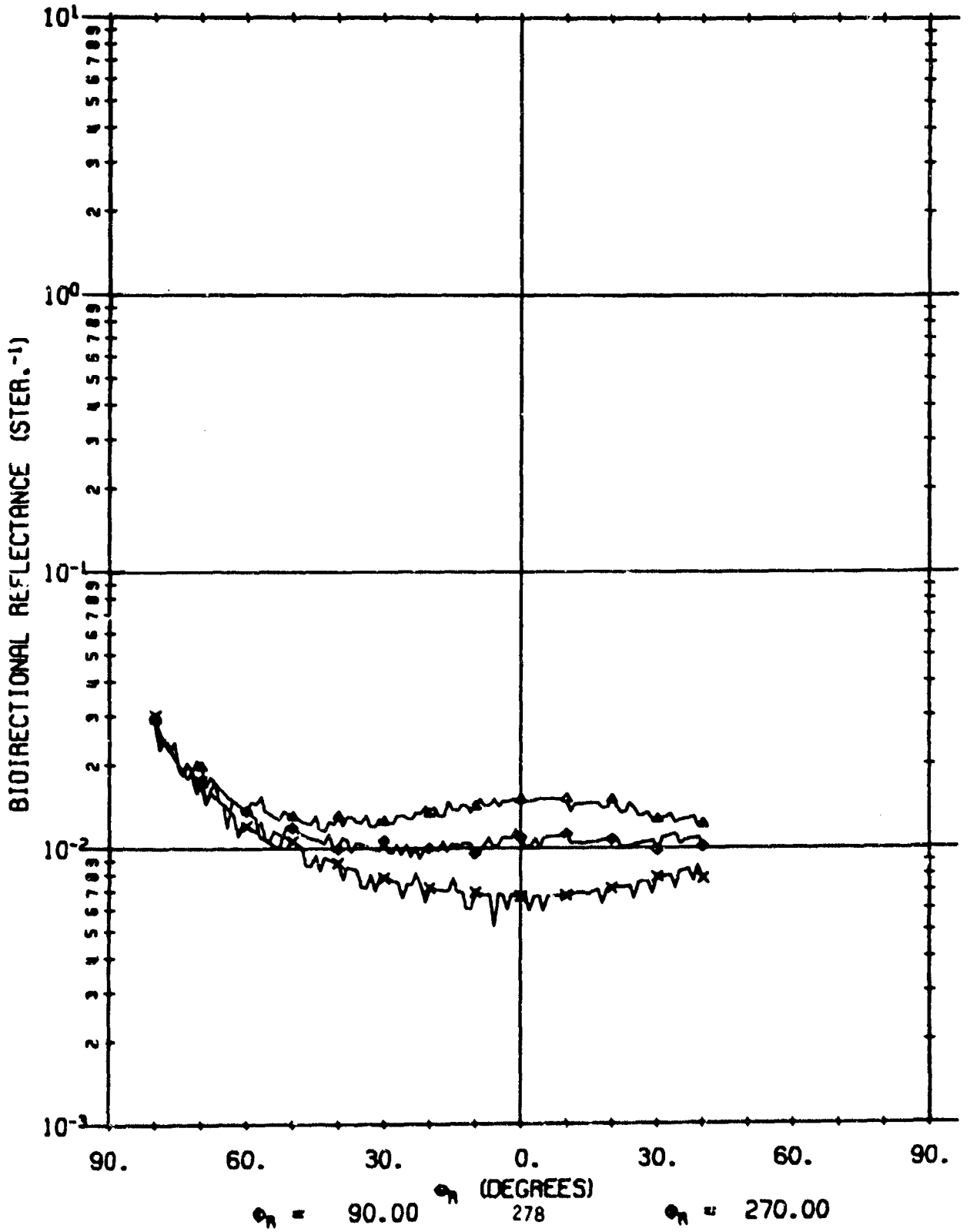

A02023 101

λ = 1.06
θ_i = 60.0
ϕ_i = 180.0

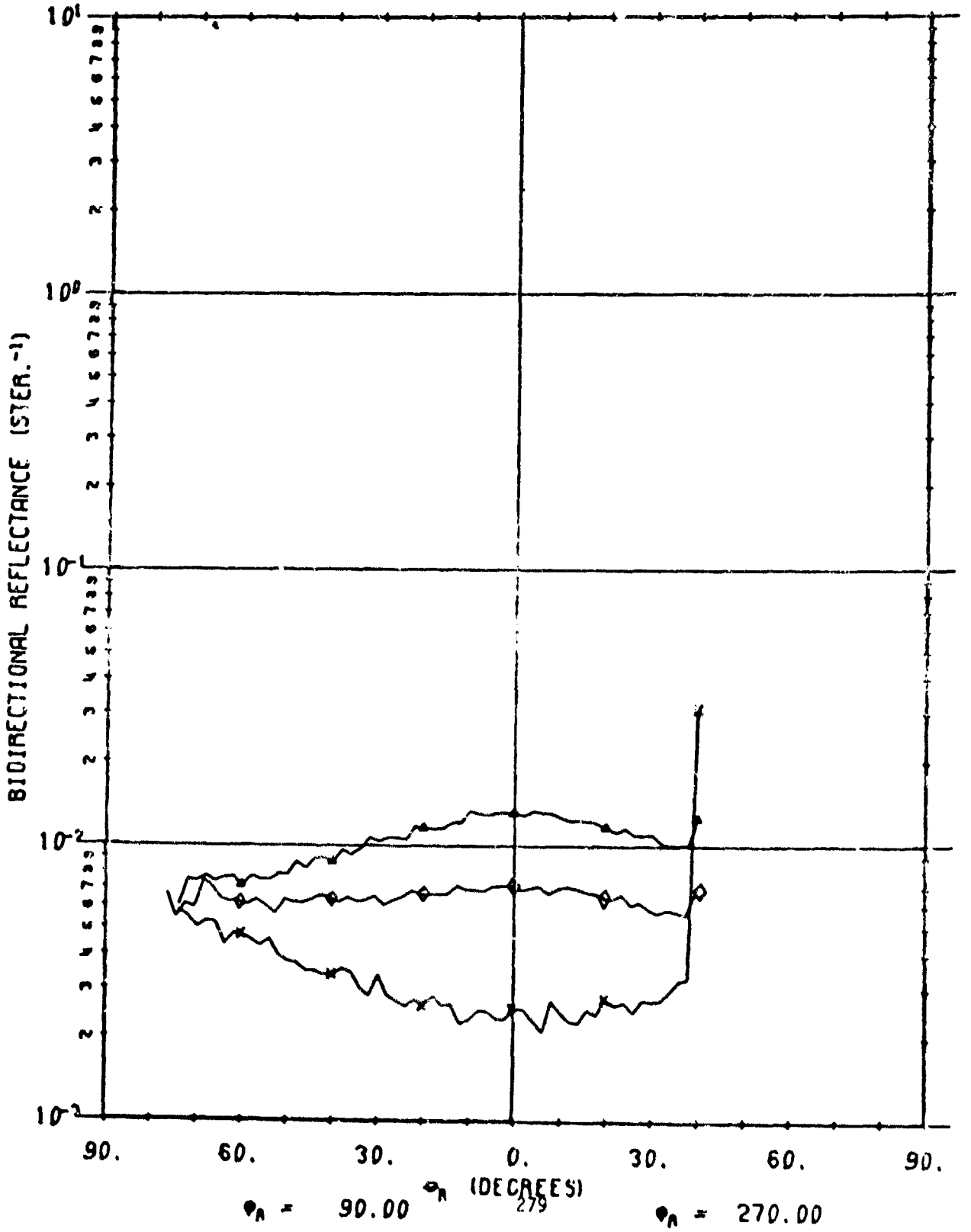

A02023 701

λ = 3.39
θ_I = 60.0
ϕ_I = 180.0

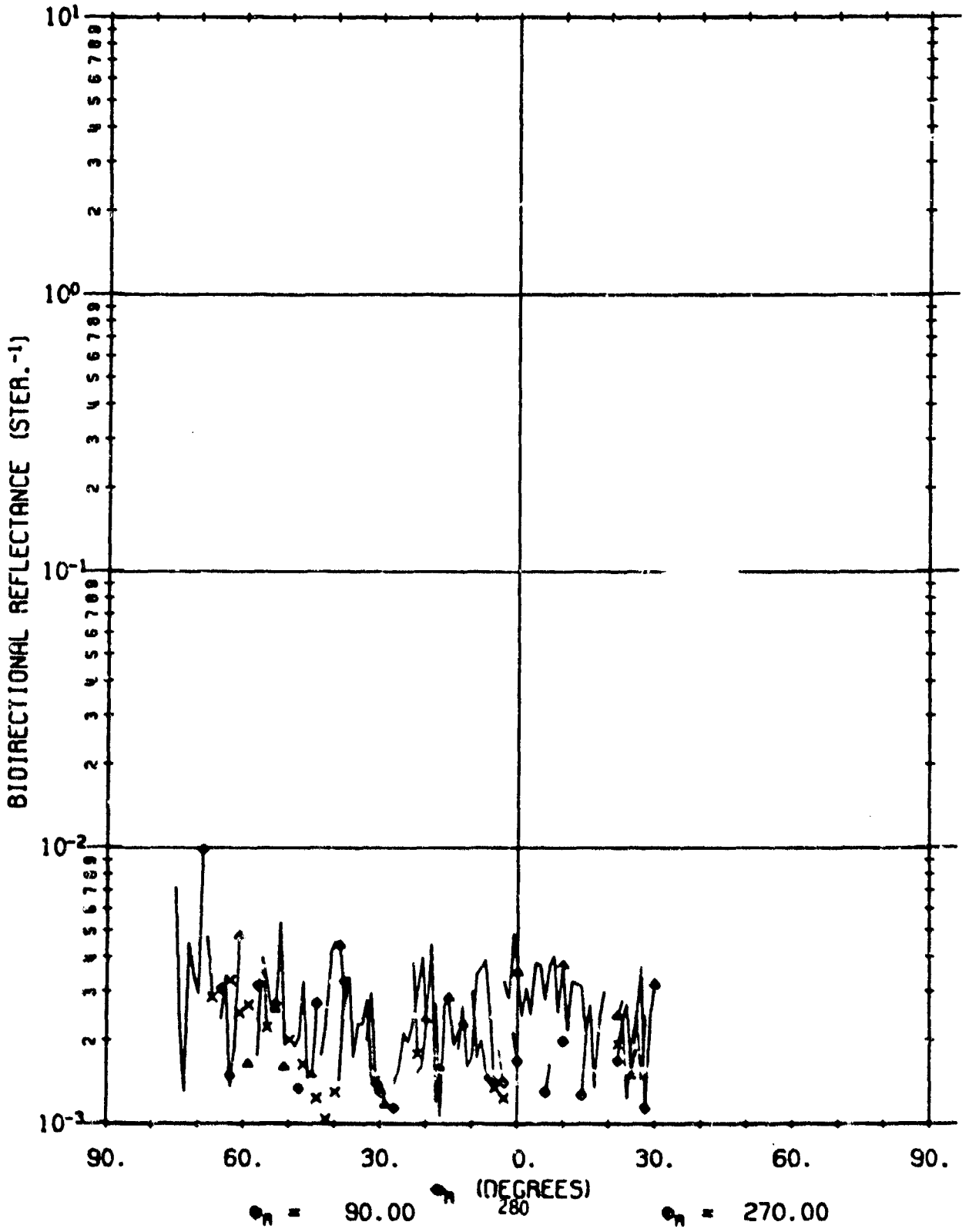

A02023 604

λ = 10.60
Φ_I = 60.0
Φ_I = 180.0

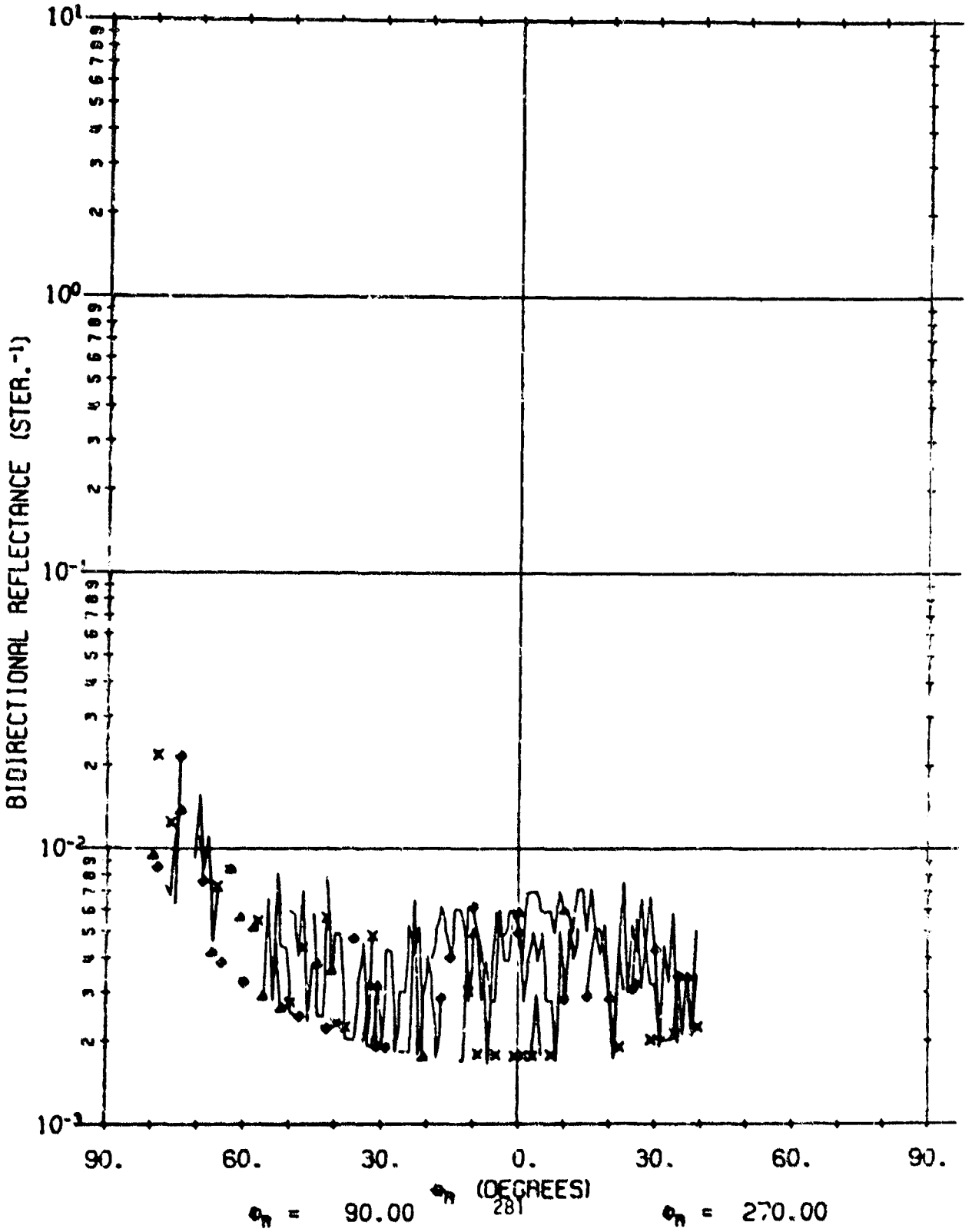

A02023 703

λ = 3.39
Φ_I = .0
Φ_I = 180.0

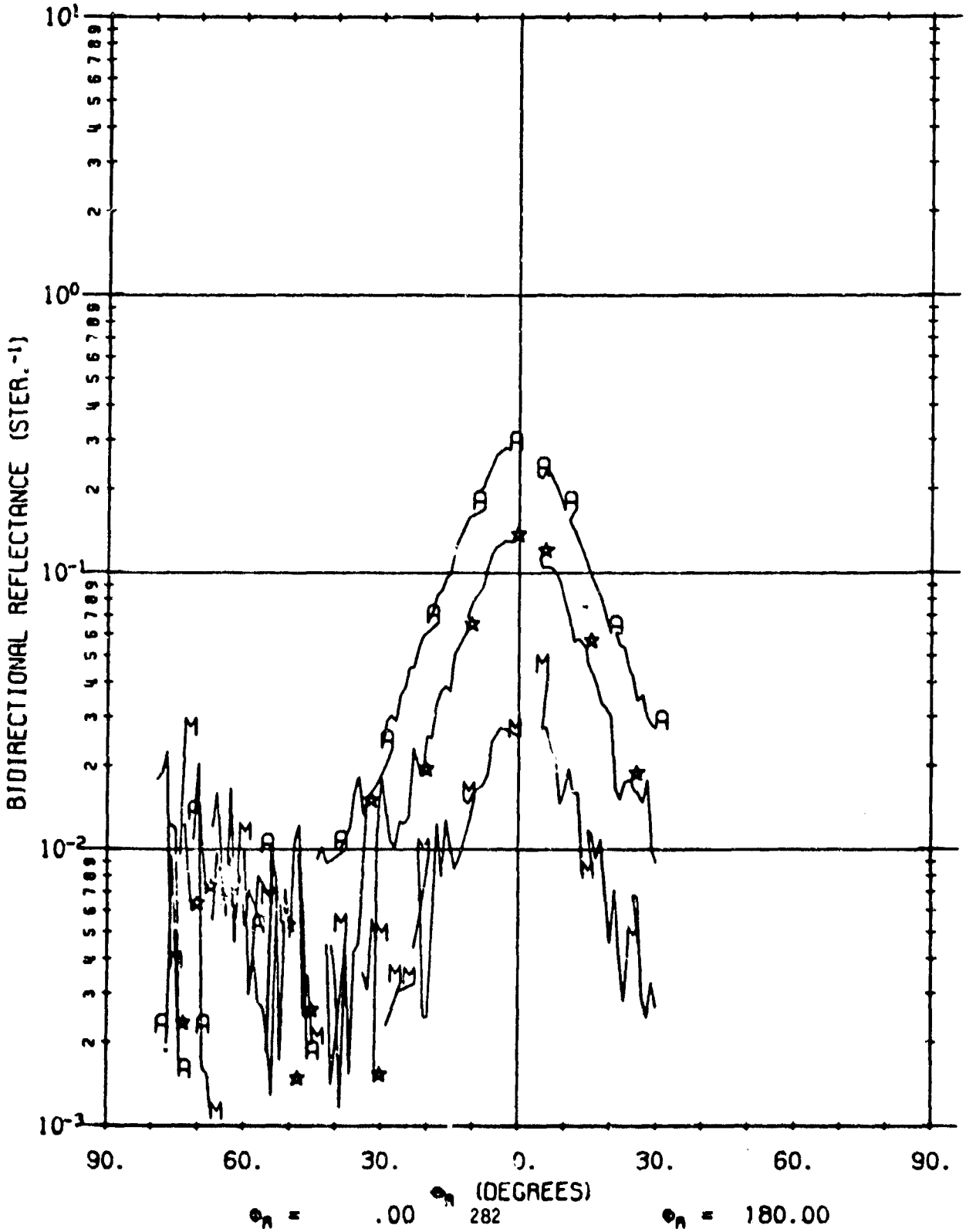

A02023 503

λ = 10.60
θ_i = .0
ϕ_i = 180.0

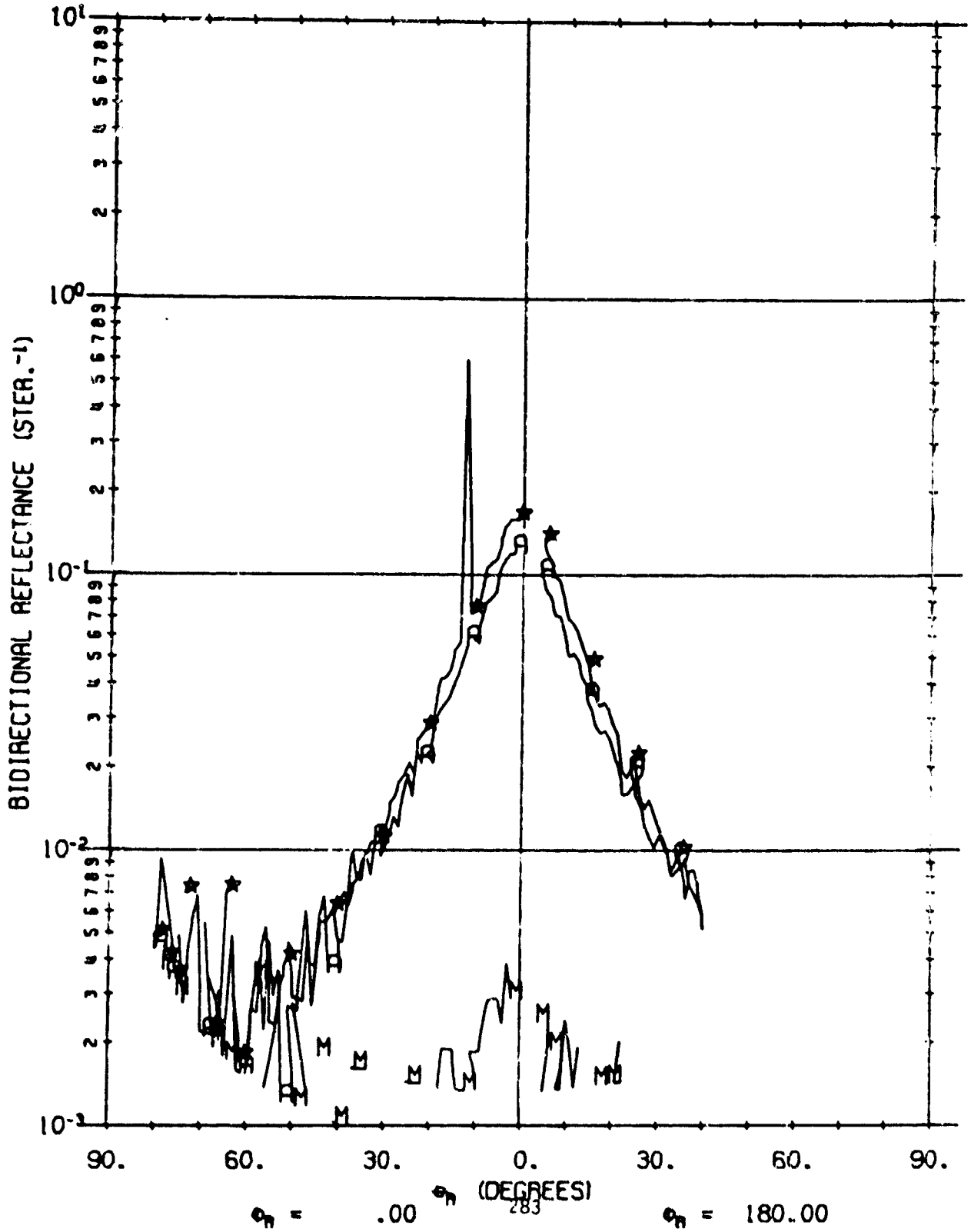

A02023 703

λ = 3.39
Φ_I = 20.0
Φ_I = 180.0

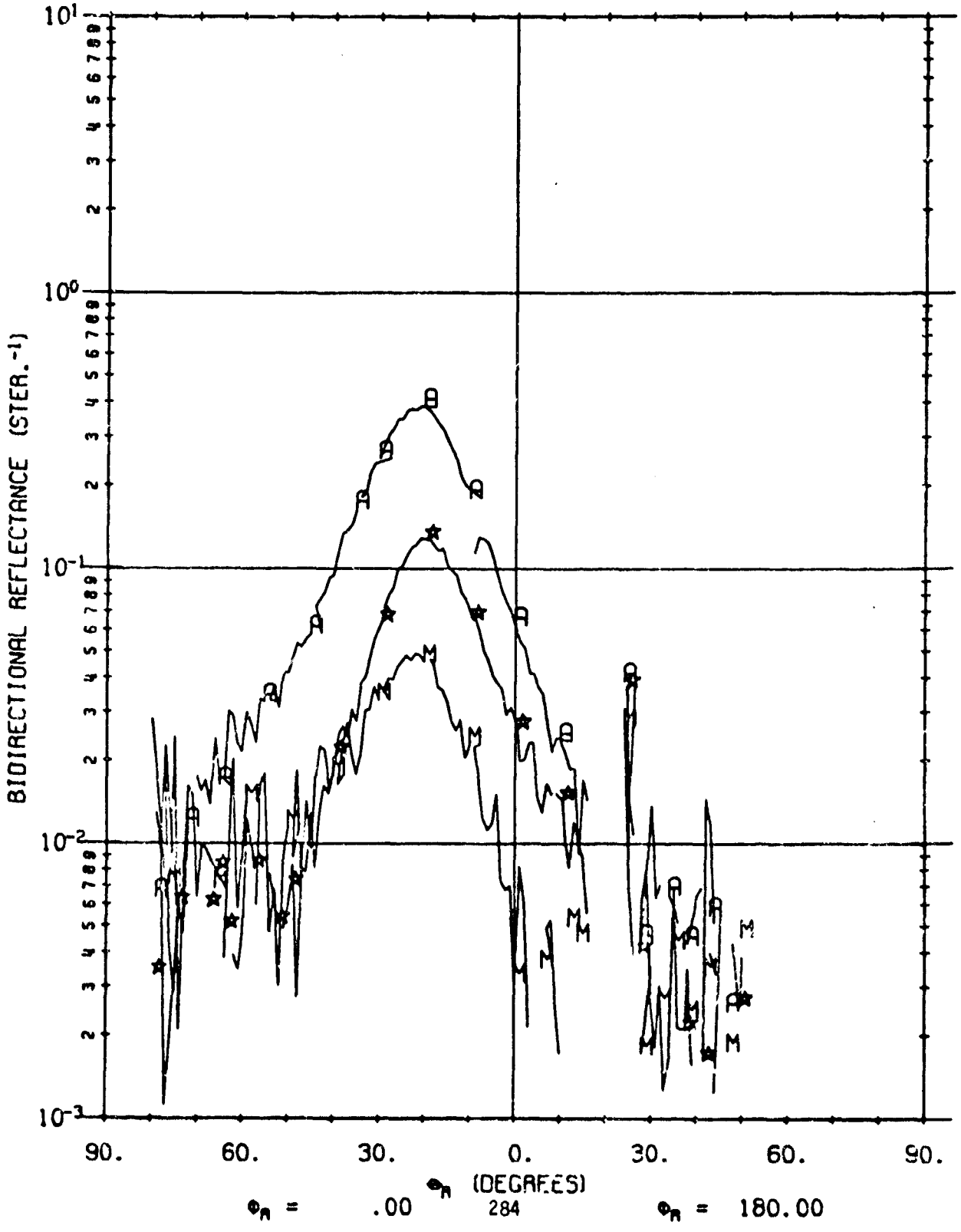

A02023 603

λ = 10.60
Φ_i = 20.0
Φ_i = 180.0

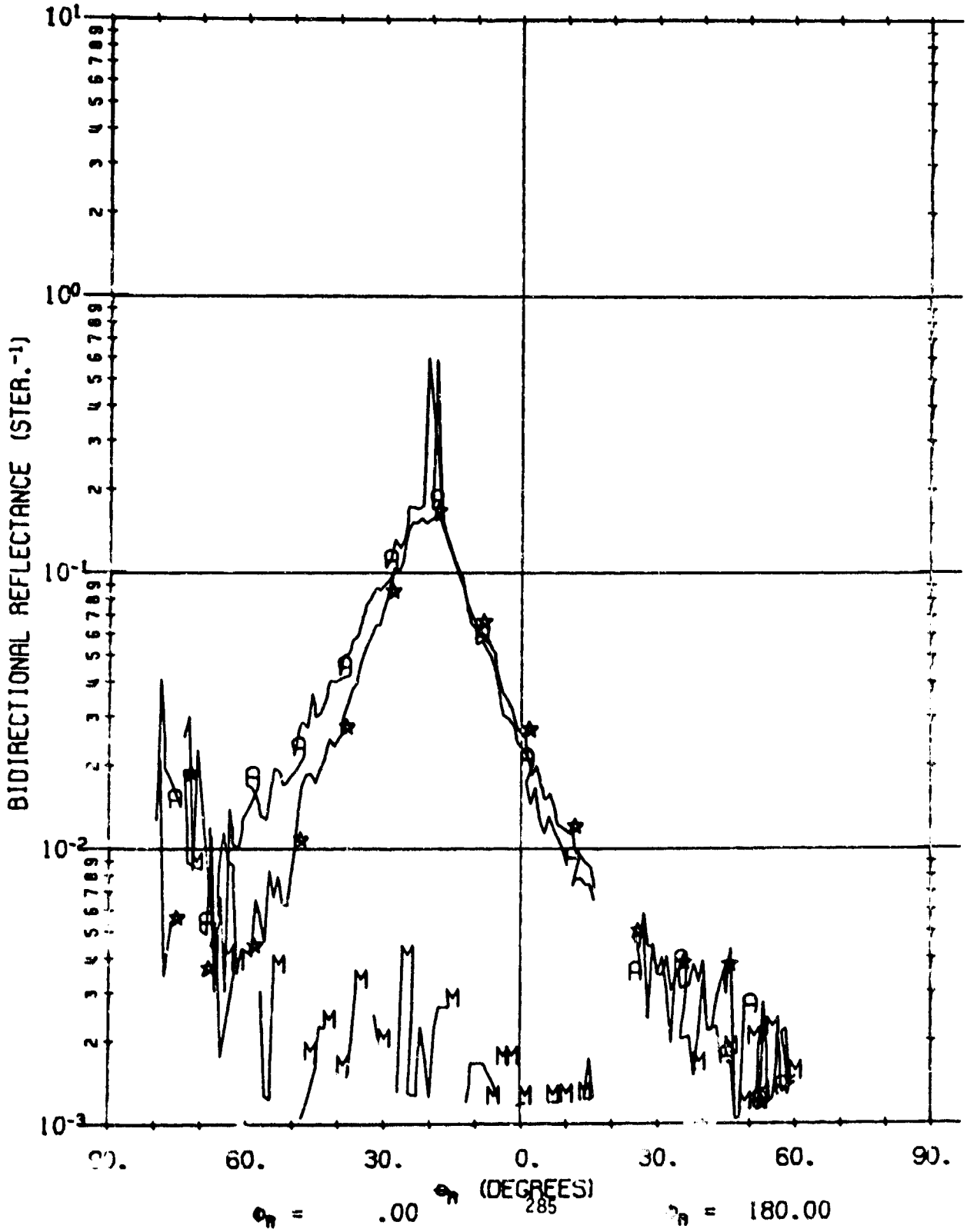

A02023 703

λ = 3.39
Φ_I = 20.0
Φ_I = 180.0

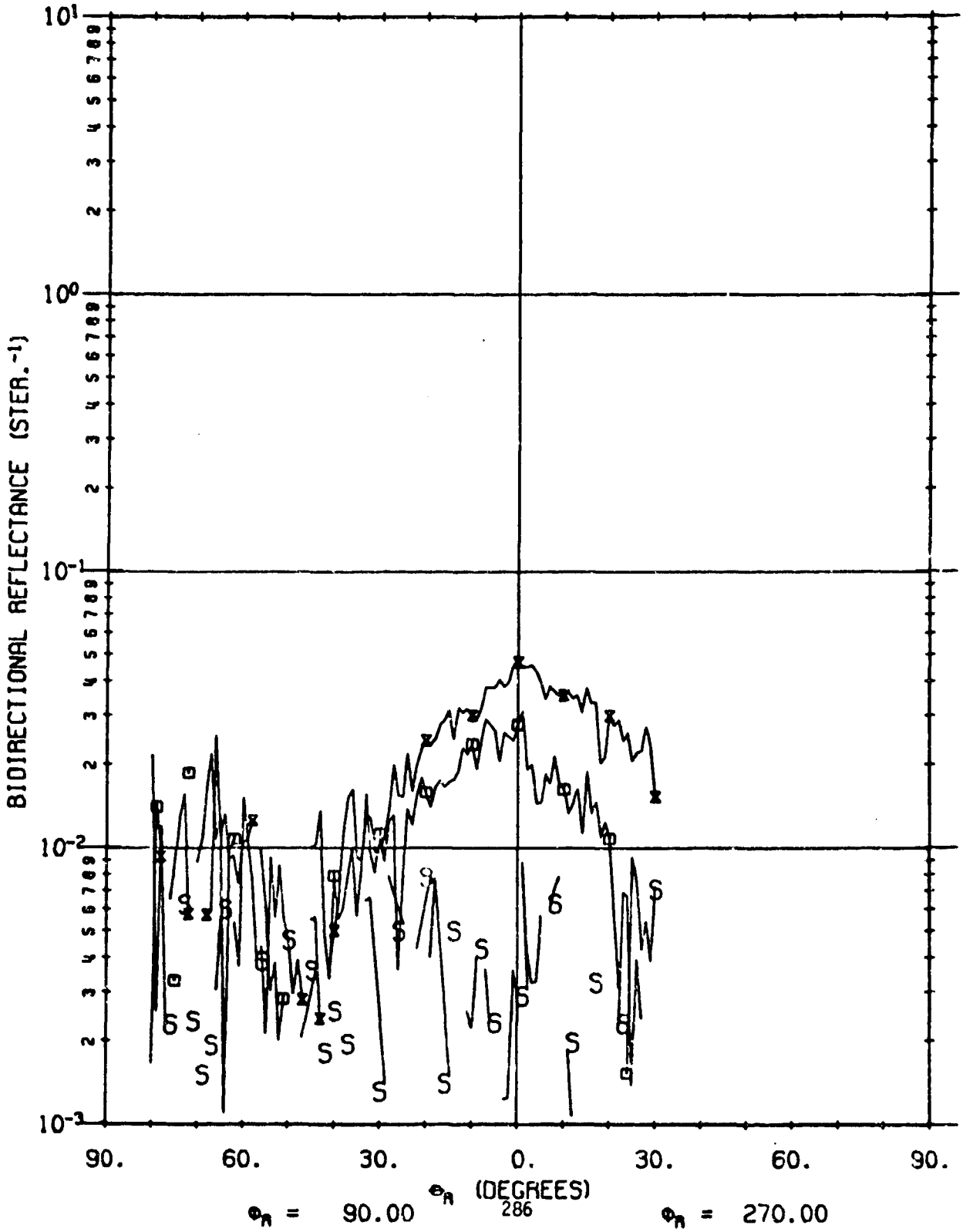

A02023 603

λ = 10.60
Φ_I = 20.0
Φ_I = 180.0

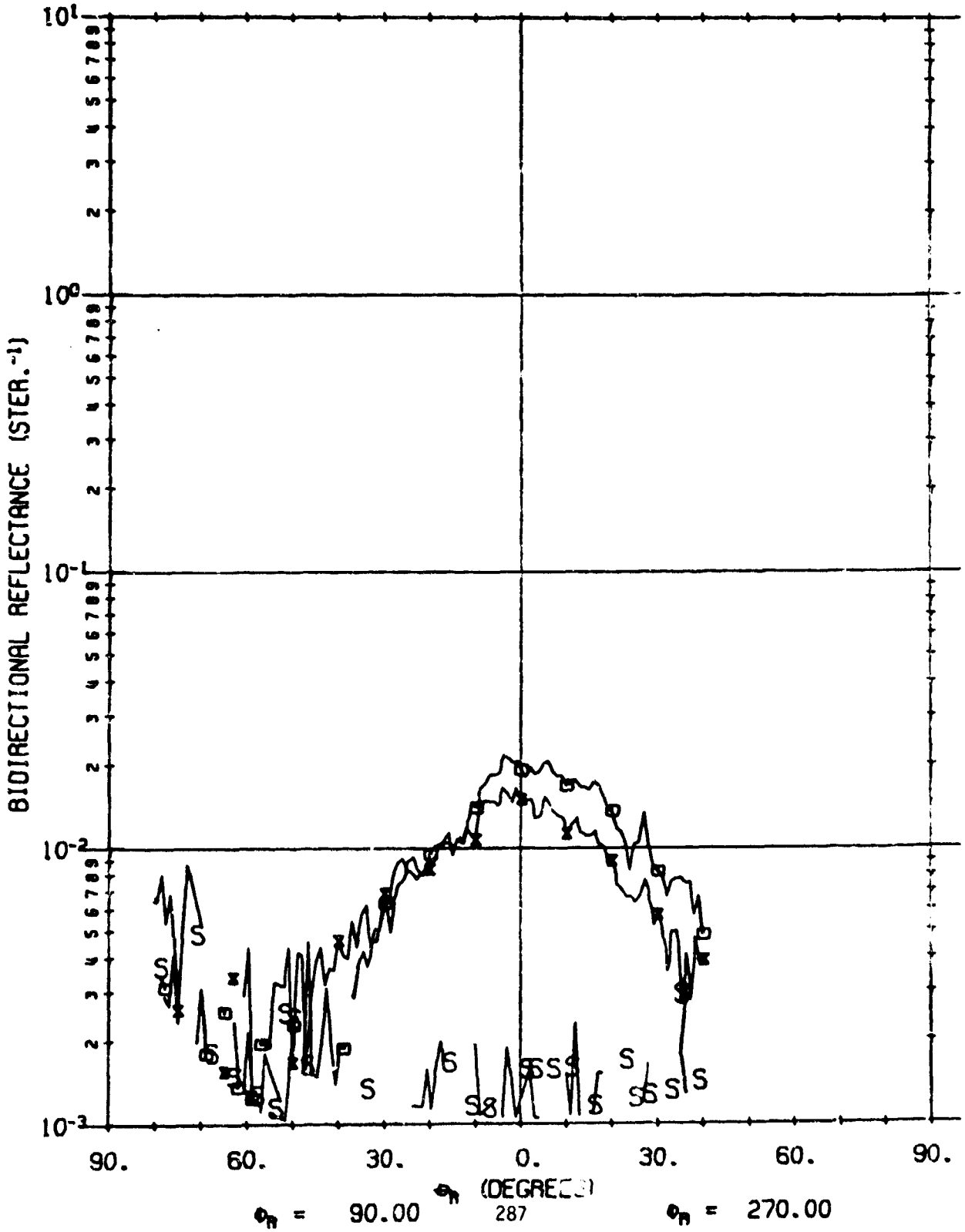

A02023 703

λ = 3.39
Φ_I = 40.0
Θ_I = 180.0

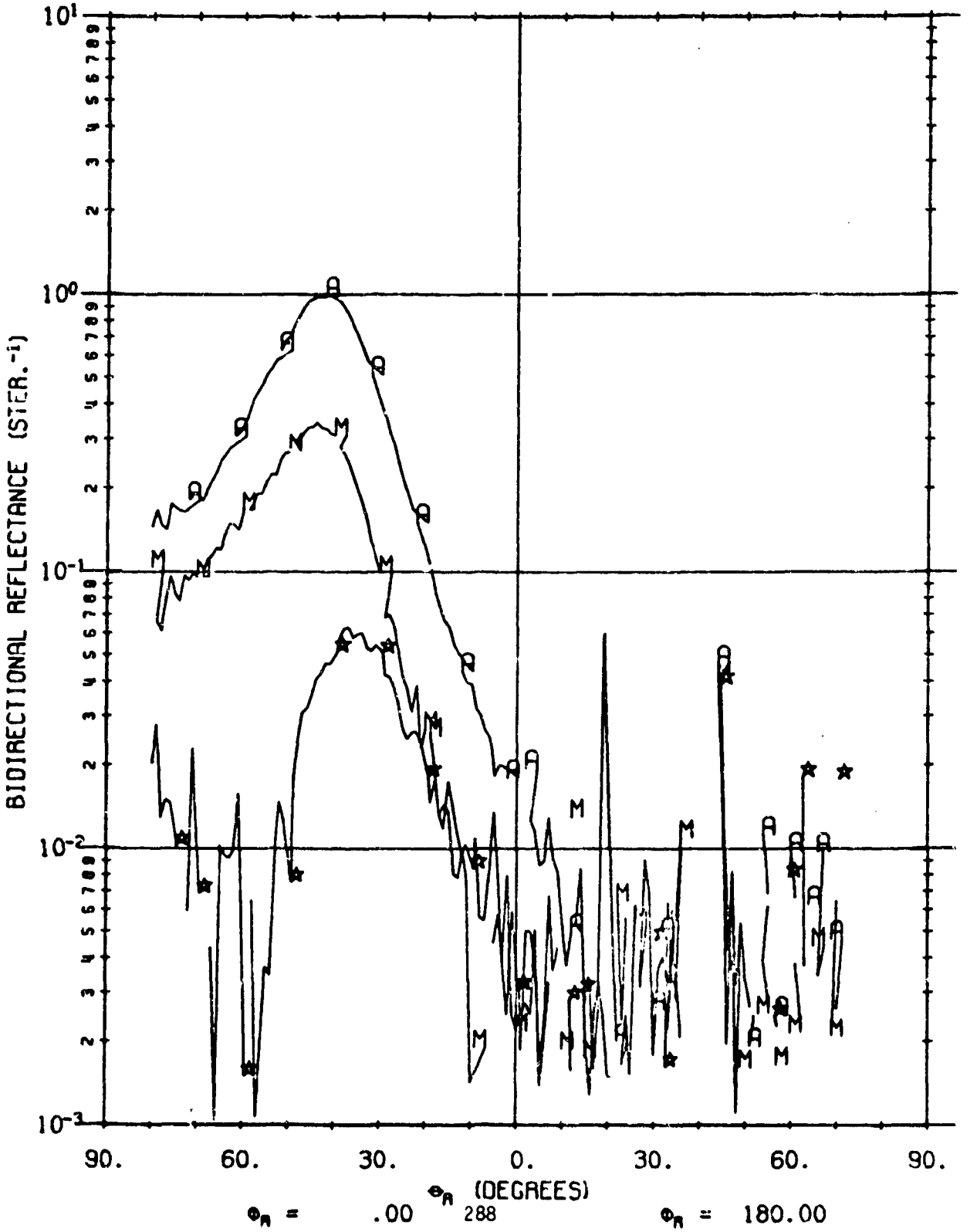

A02023 603

λ = 10.60
Φ_I = 40.0
Φ_I = 180.0

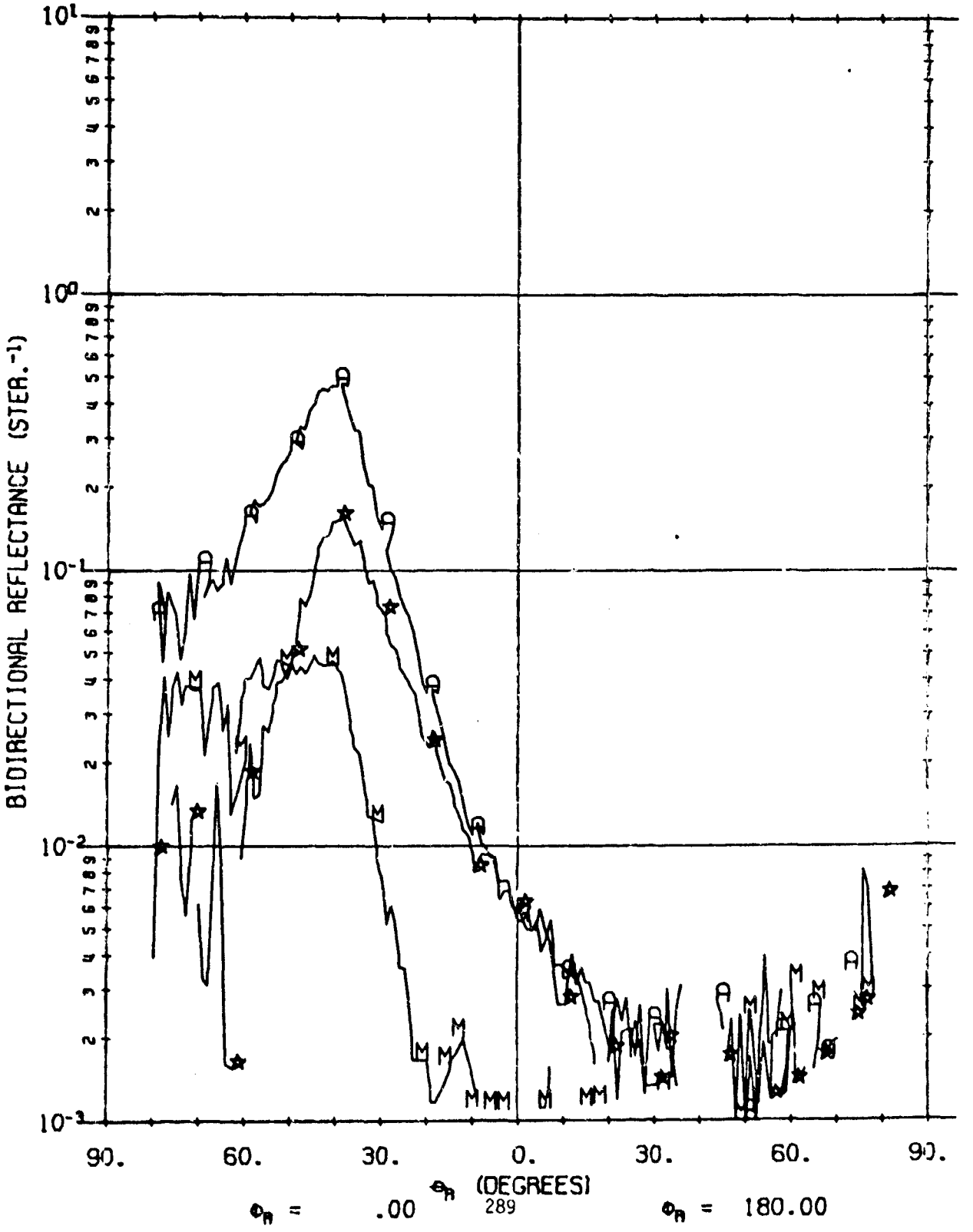

A02023 703

λ = 3.39
Φ_I = 40.0
Φ_I = 180.0

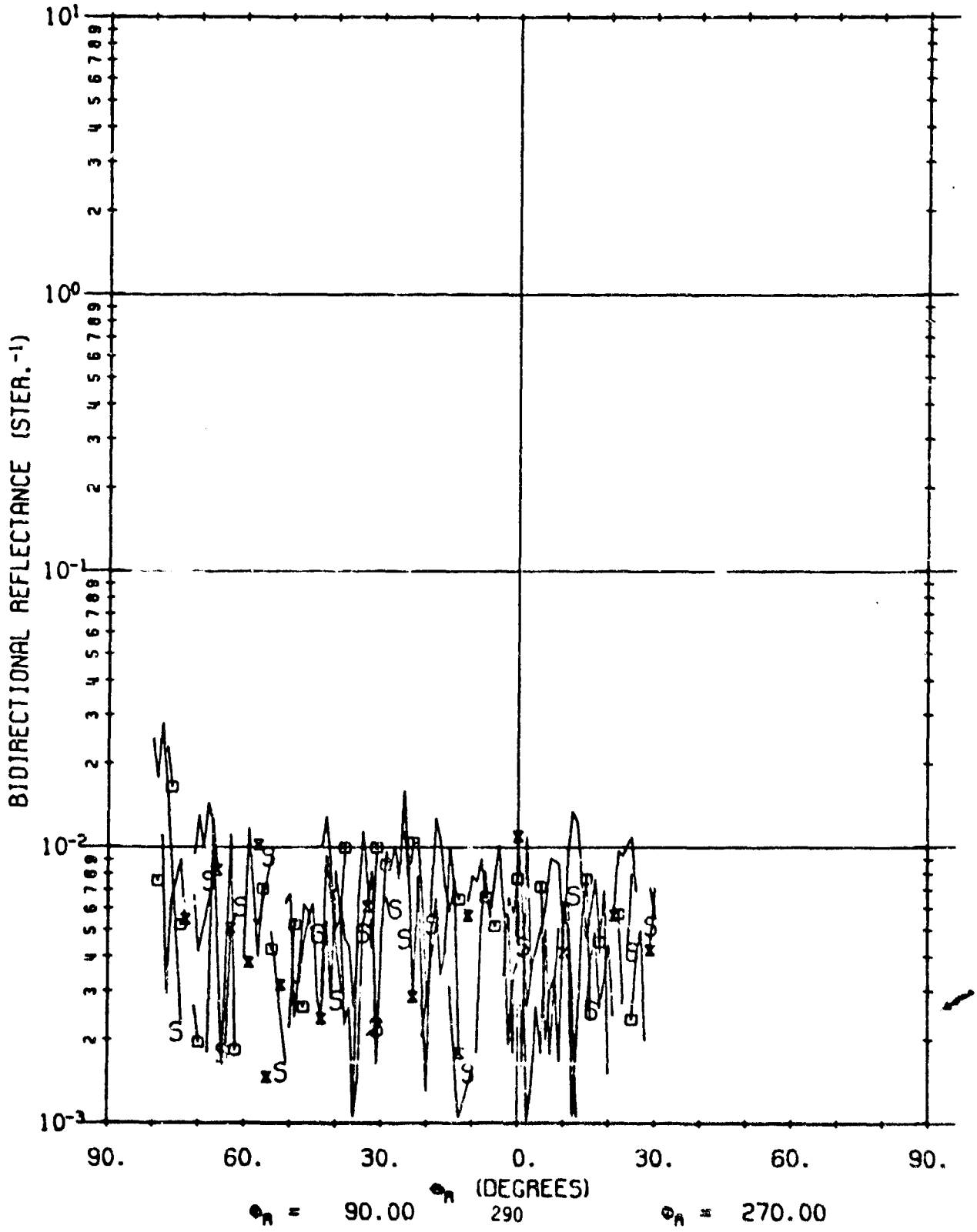

A02023 603

λ = 10.60
Φ_i = 40.0
Φ_i = 180.0

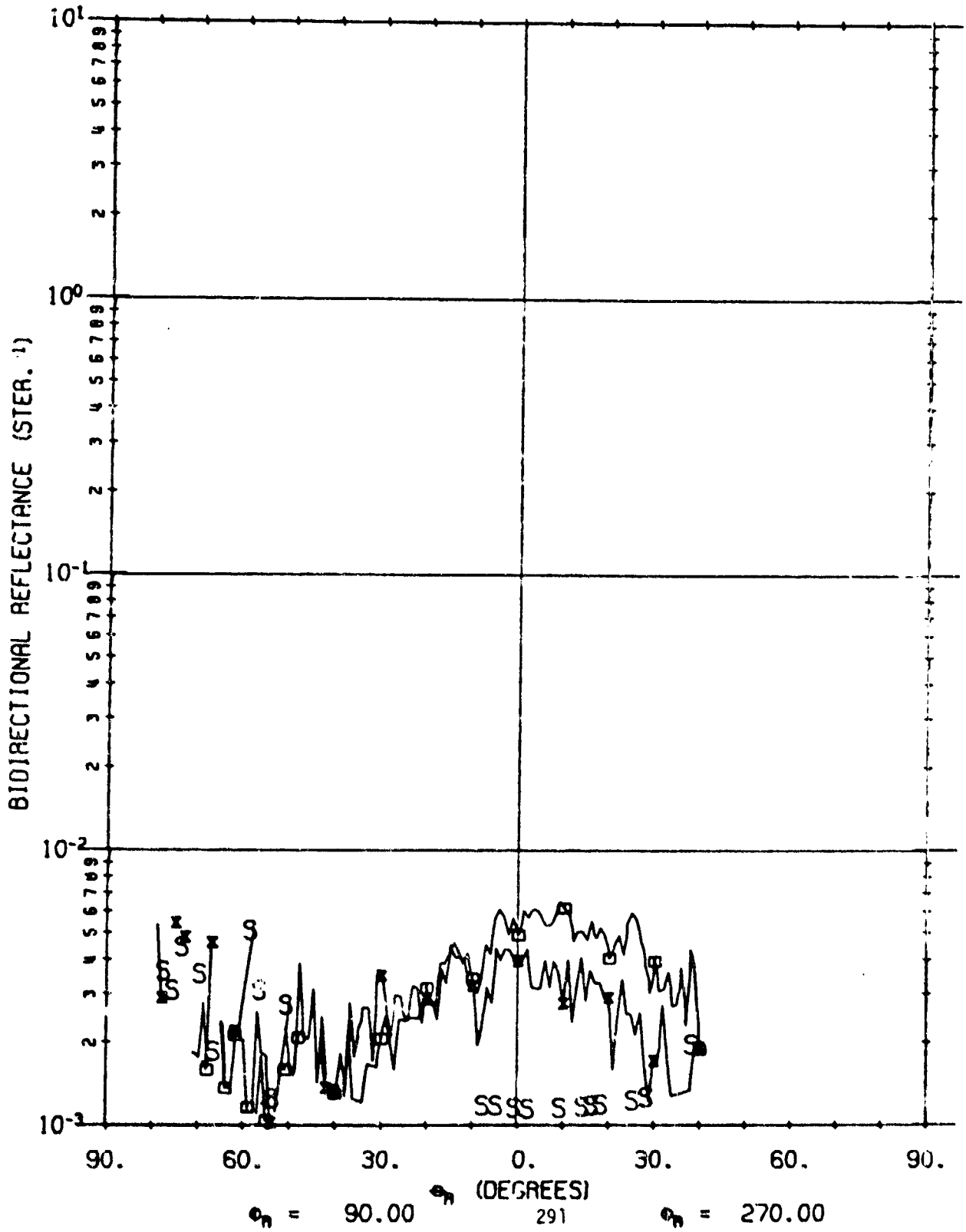

A02023 703

λ = 3.39
Θ_I = 60.0
Φ_I = 180.0

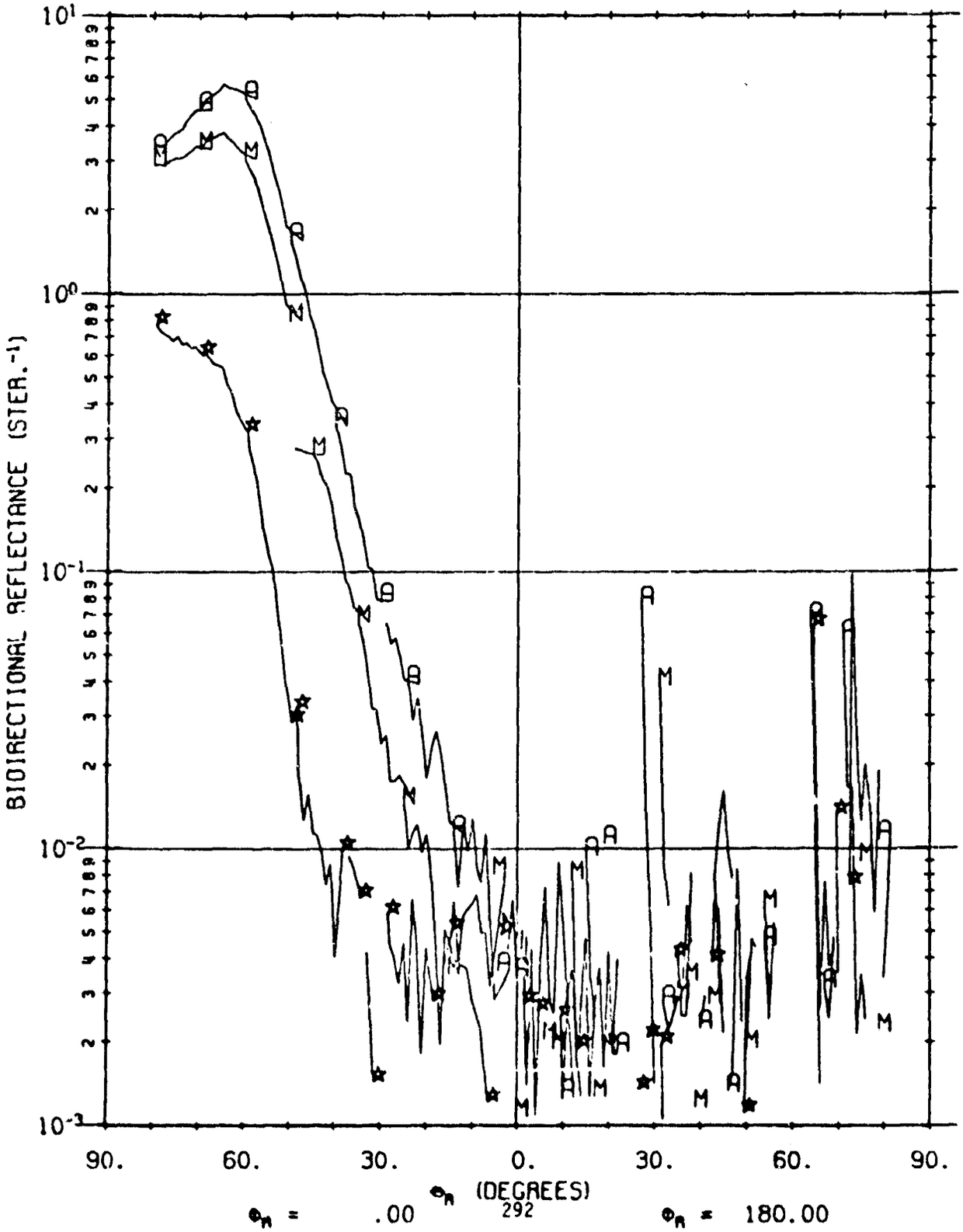

A02023 603

λ = 10.60
Φ_i = 60.0
Φ_i = 180.0

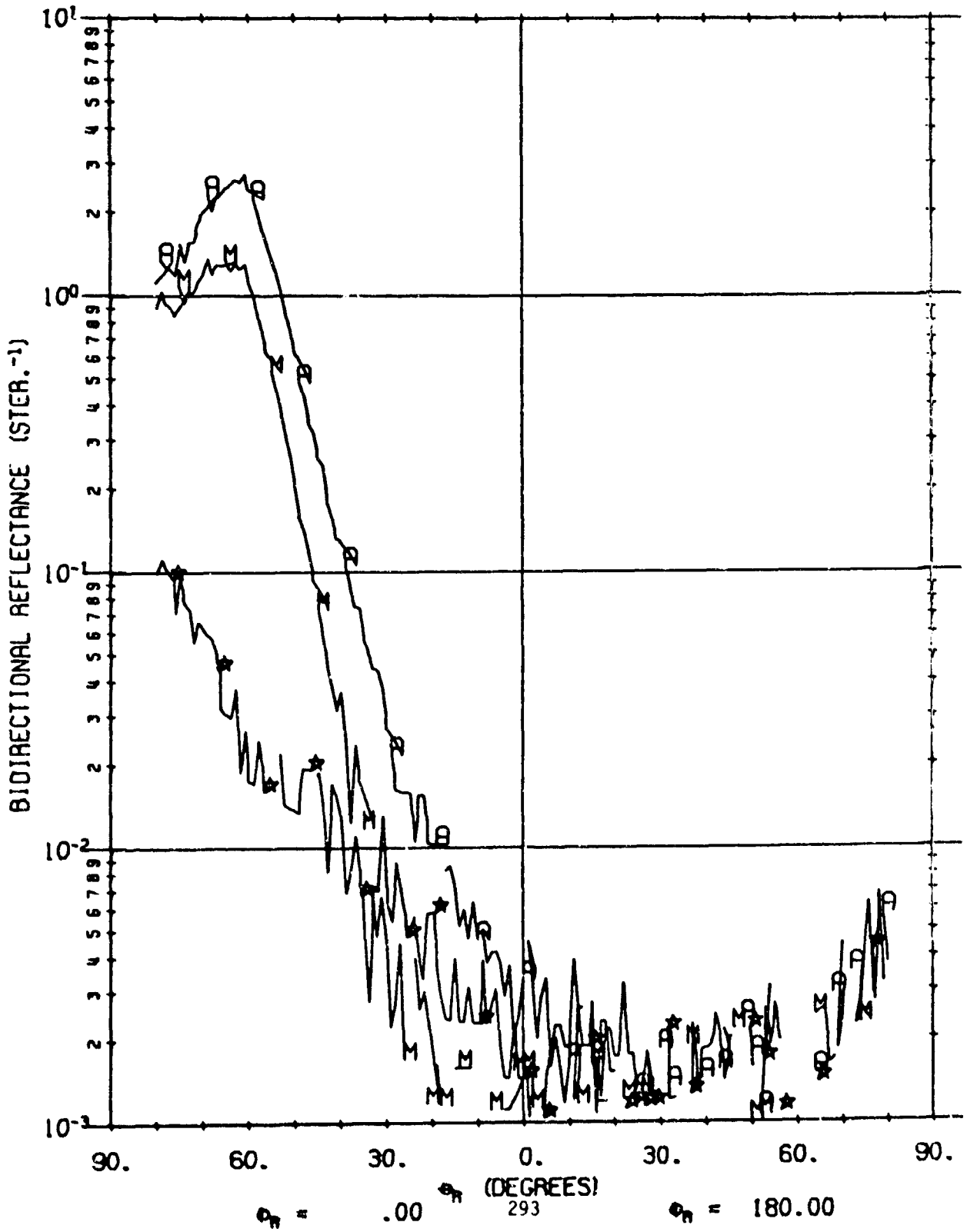

A02023 703

λ = 3.39
Φ_I = 60.0
Φ_I = 180.0

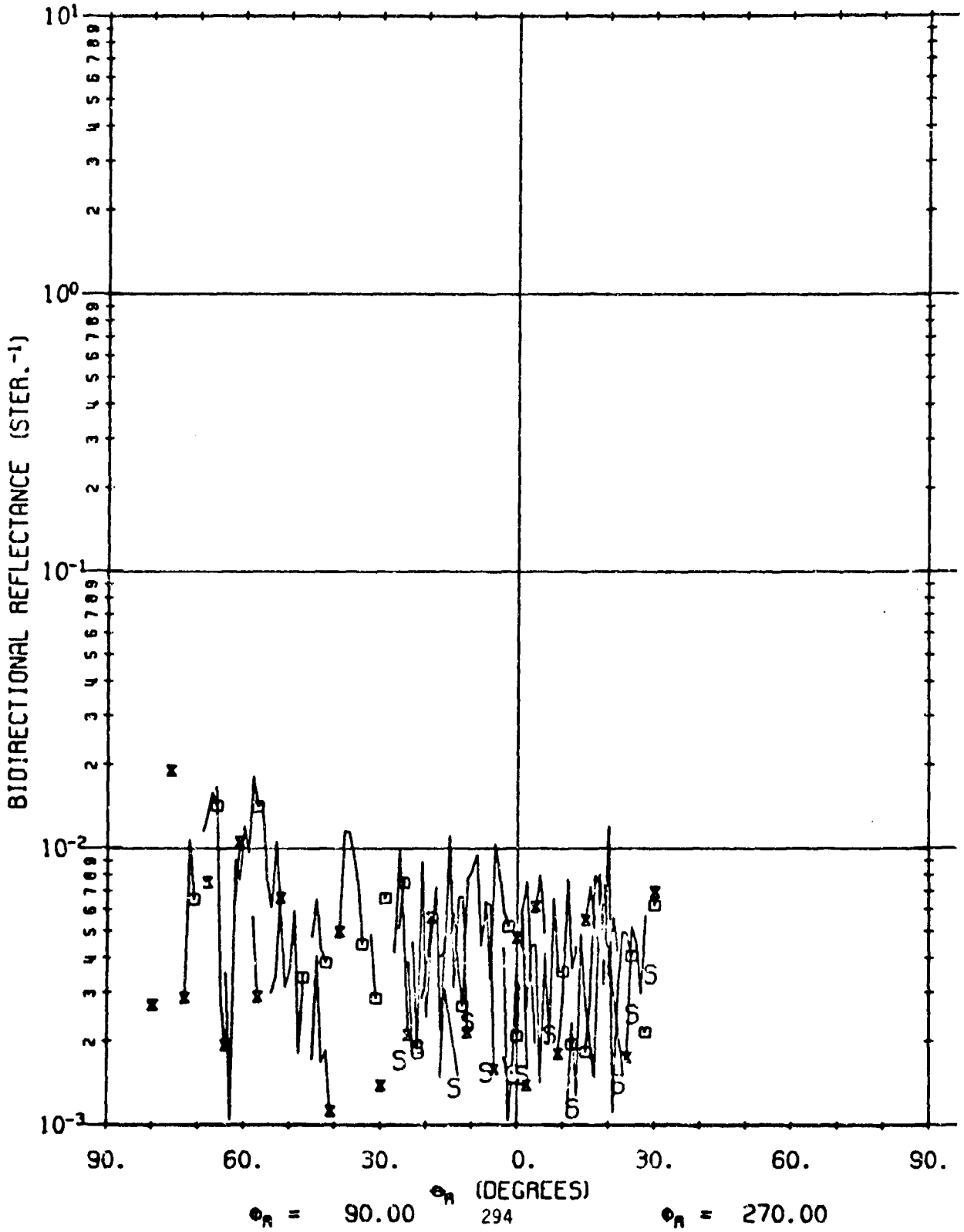

A02023 603

λ = 10.60
θ_i = 60.0
ϕ_i = 180.0

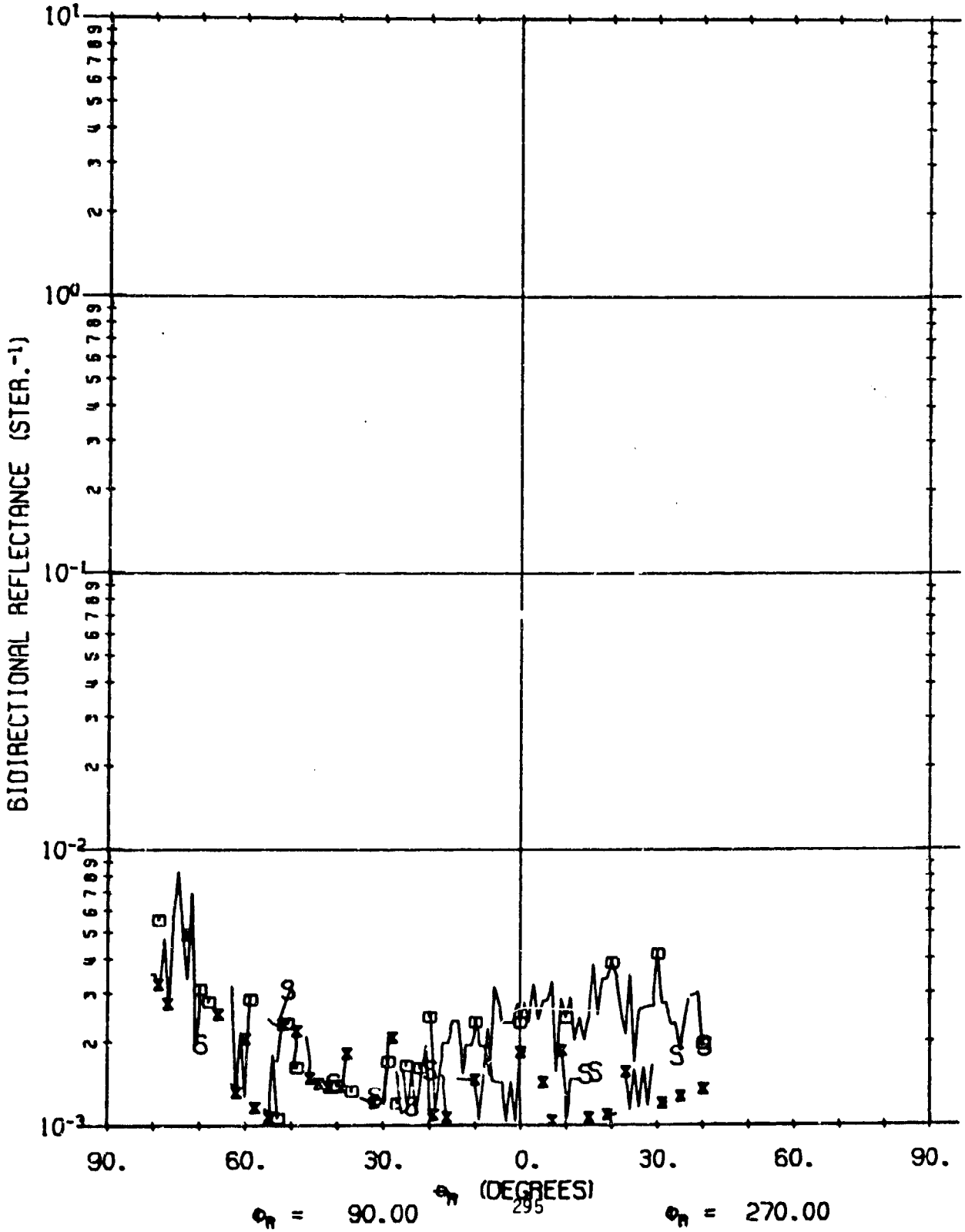

A02023 501

λ = .63
Φ_I = .0
Φ_I = 180.0

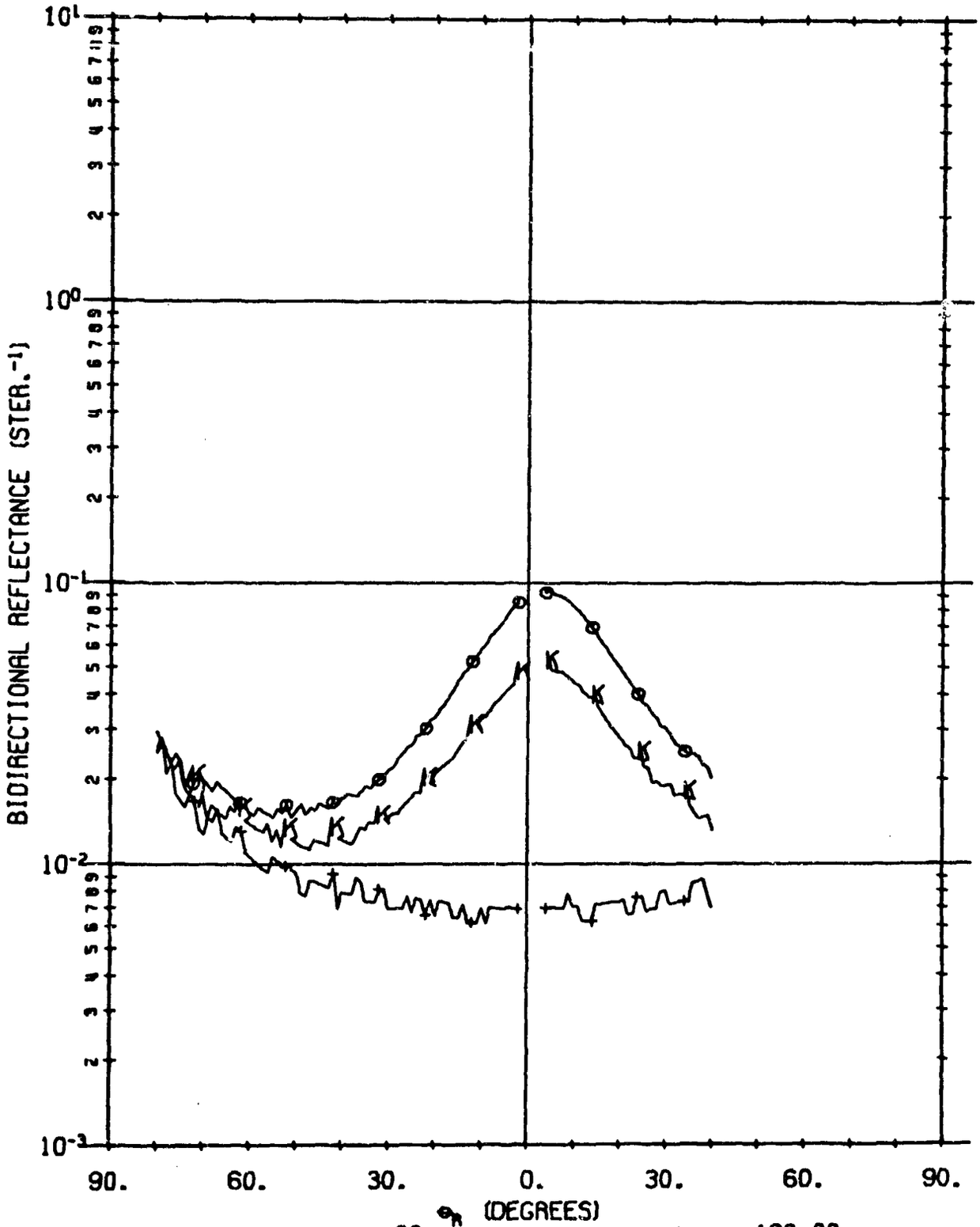

Φ_R = .00 Φ_R = 180.00

A02023 101

λ = 1.06
ϕ_I = .0
θ_I = 180.0

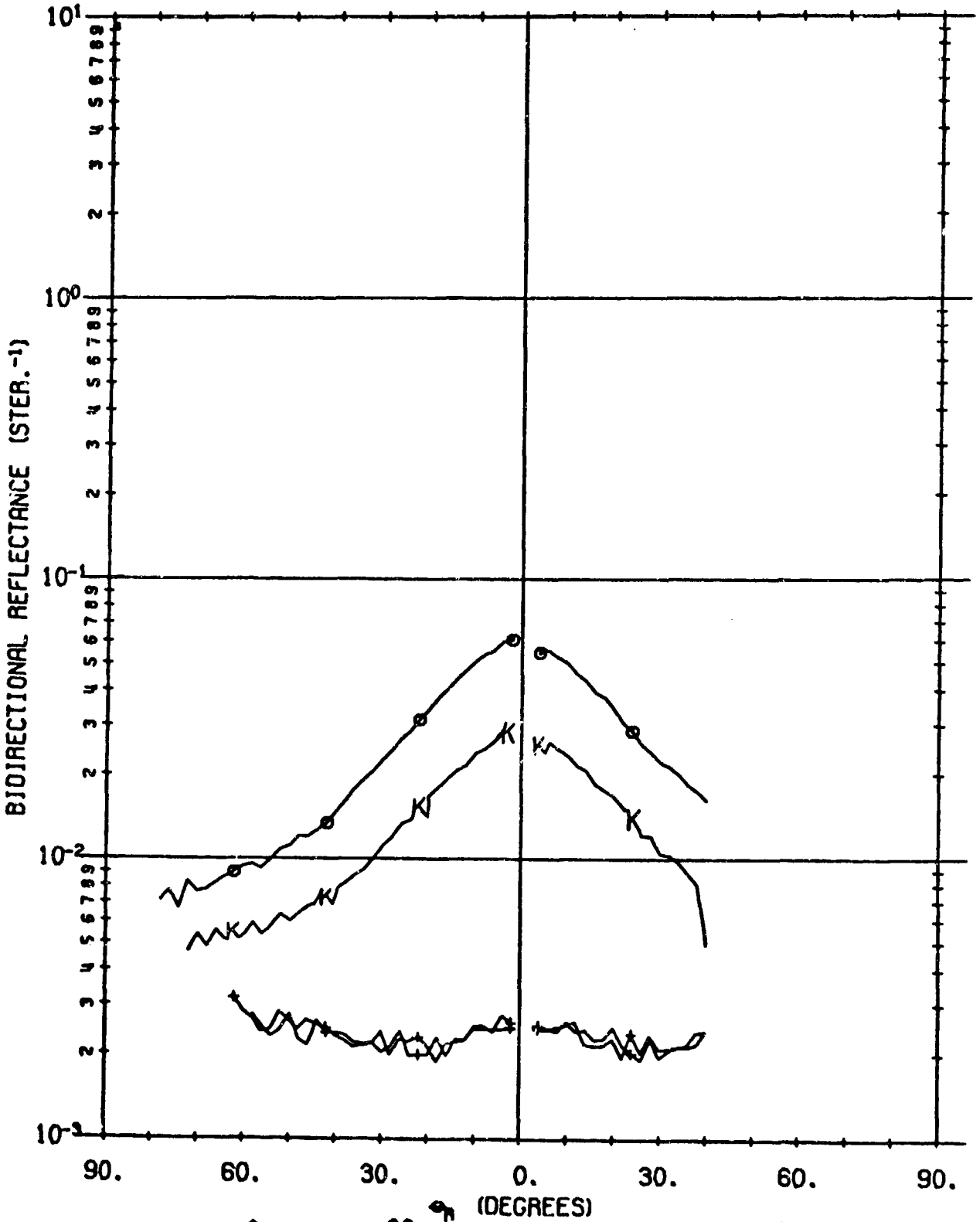

ϕ_R = .00 ϕ_R = 180.00

A02023 701

λ = 3.39
Φ_I = .0
Φ_I = 180.0

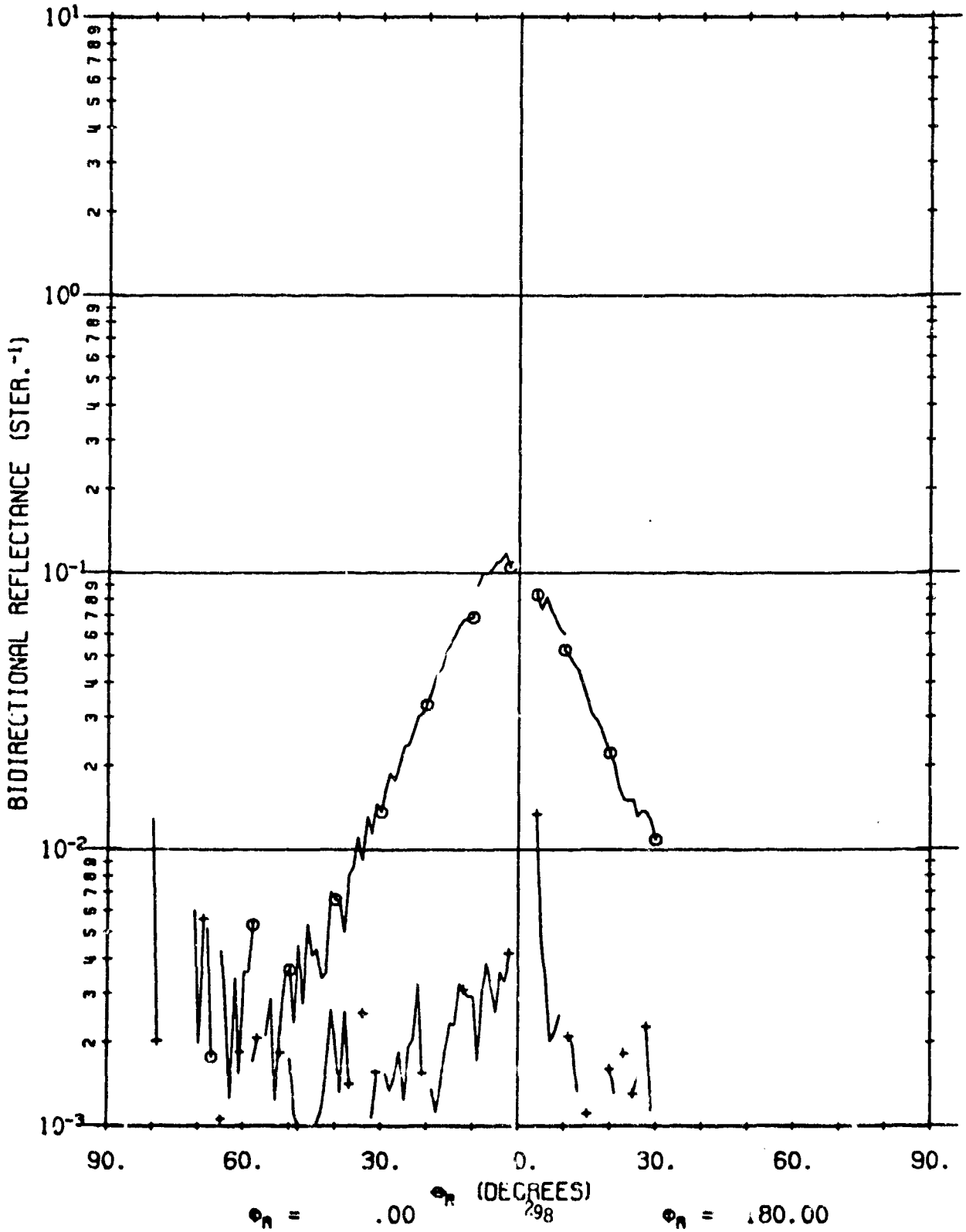

Φ_R = .00 Φ_R = 180.00

A02023 604

λ = 10.60
θ_I = .0
ϕ_I = 180.0

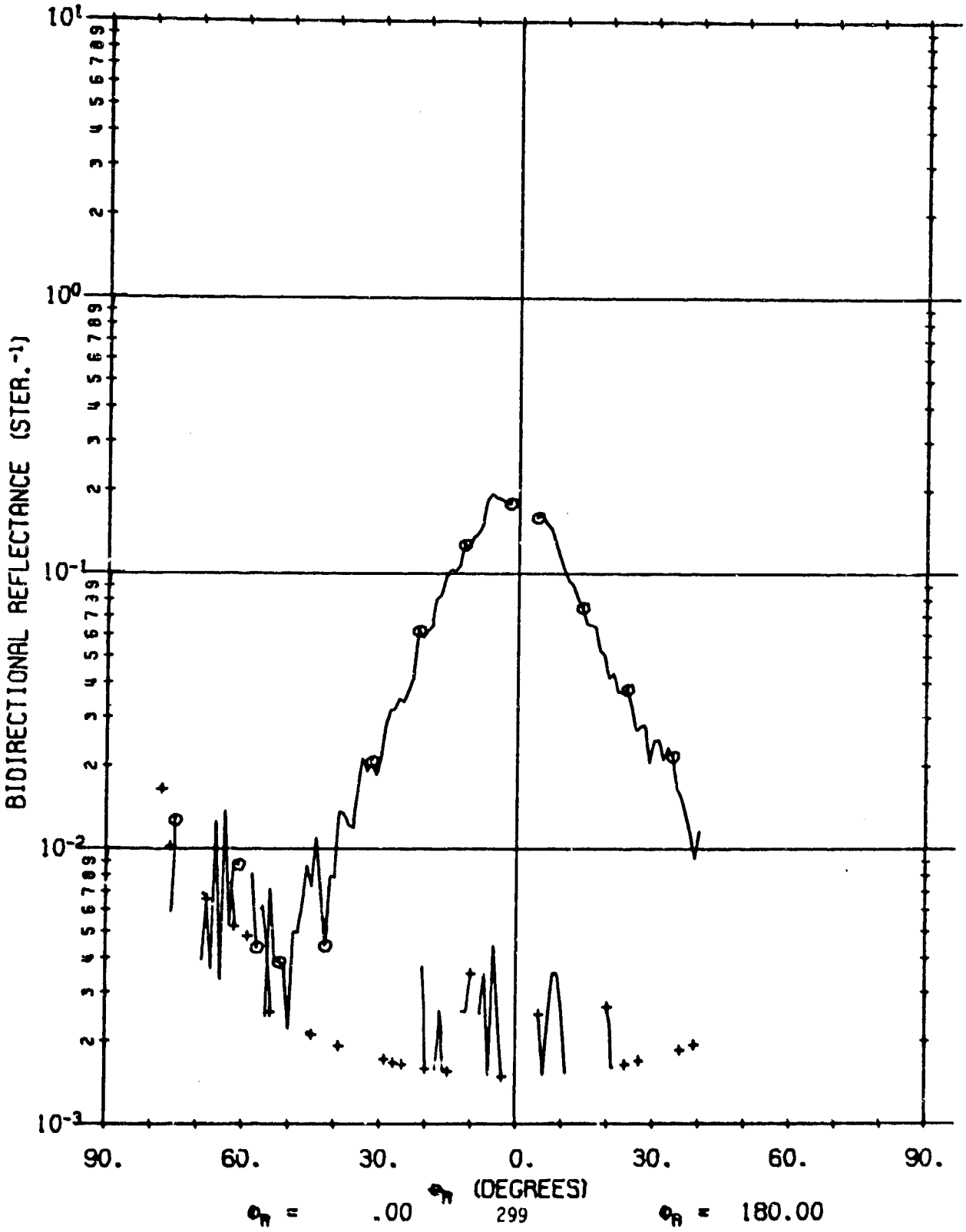

A02023 101

λ = 1.06
Φ_I = .0
Φ_I = 180.0

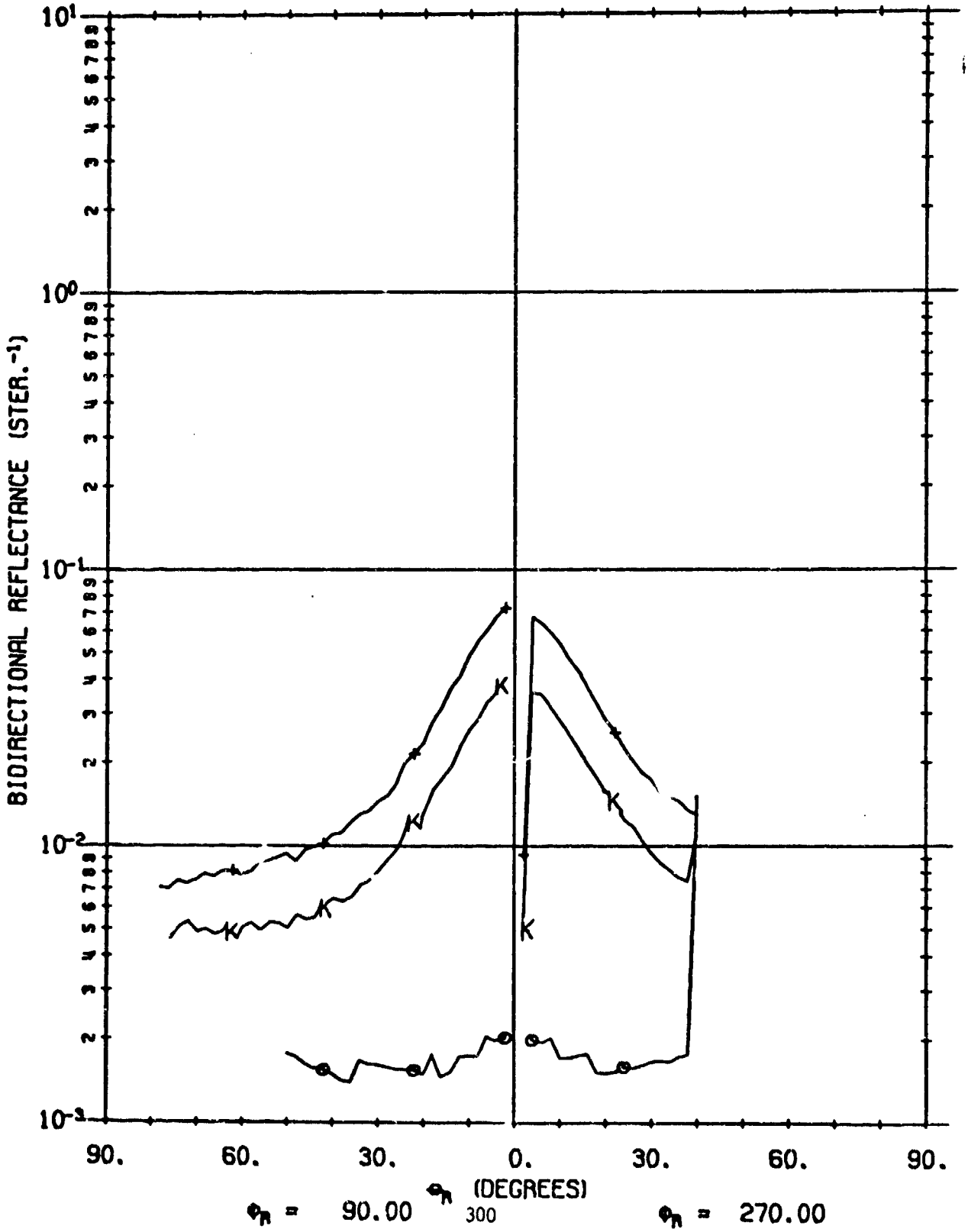

A02023 501

λ = .63
Φ_I = 20.0
Φ_I = 180.0

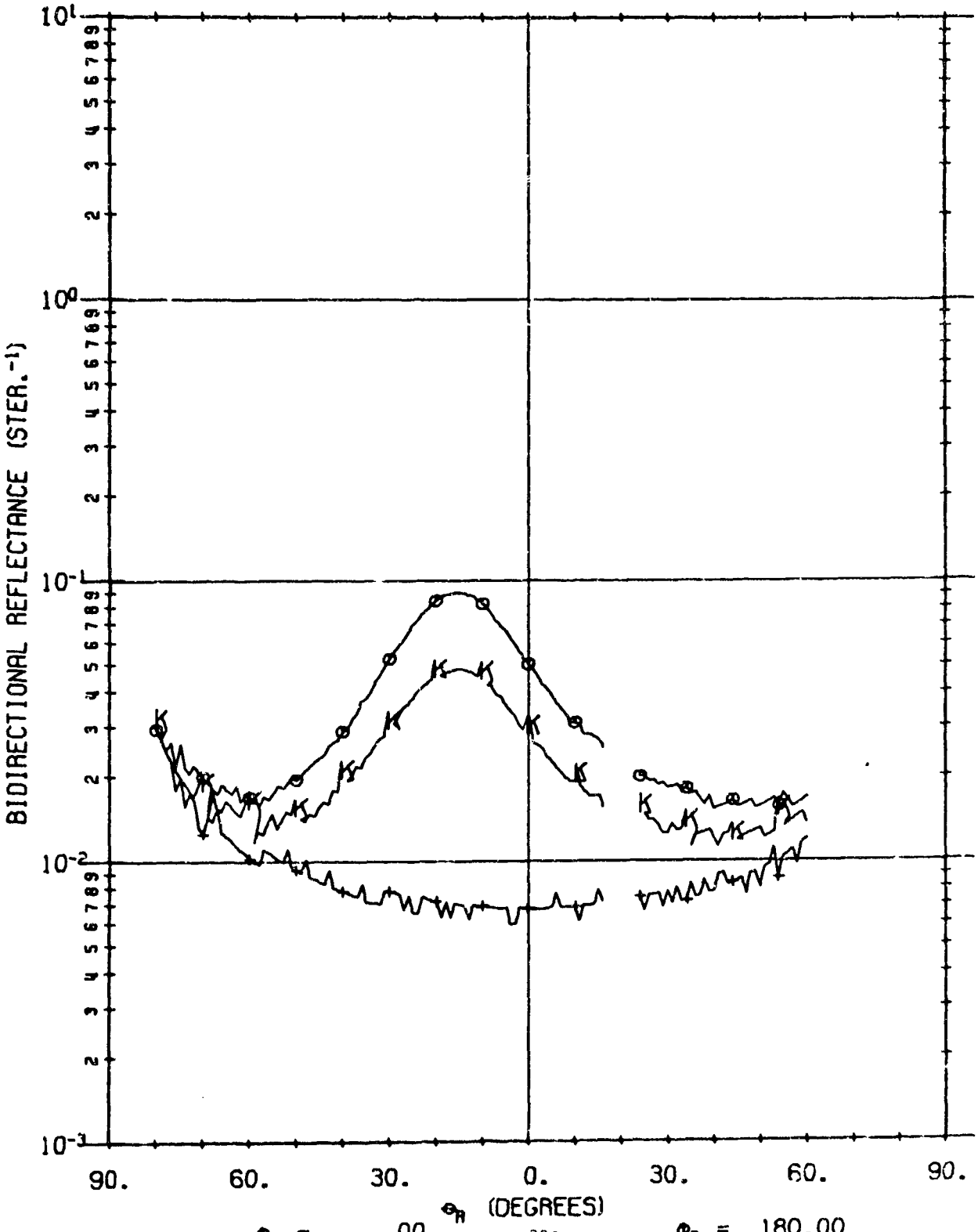

Φ_R = .00 Φ_R = 180.00

A02023 101

λ = 1.06
ϕ_1 = 20.0
ϕ_1 = 180.0

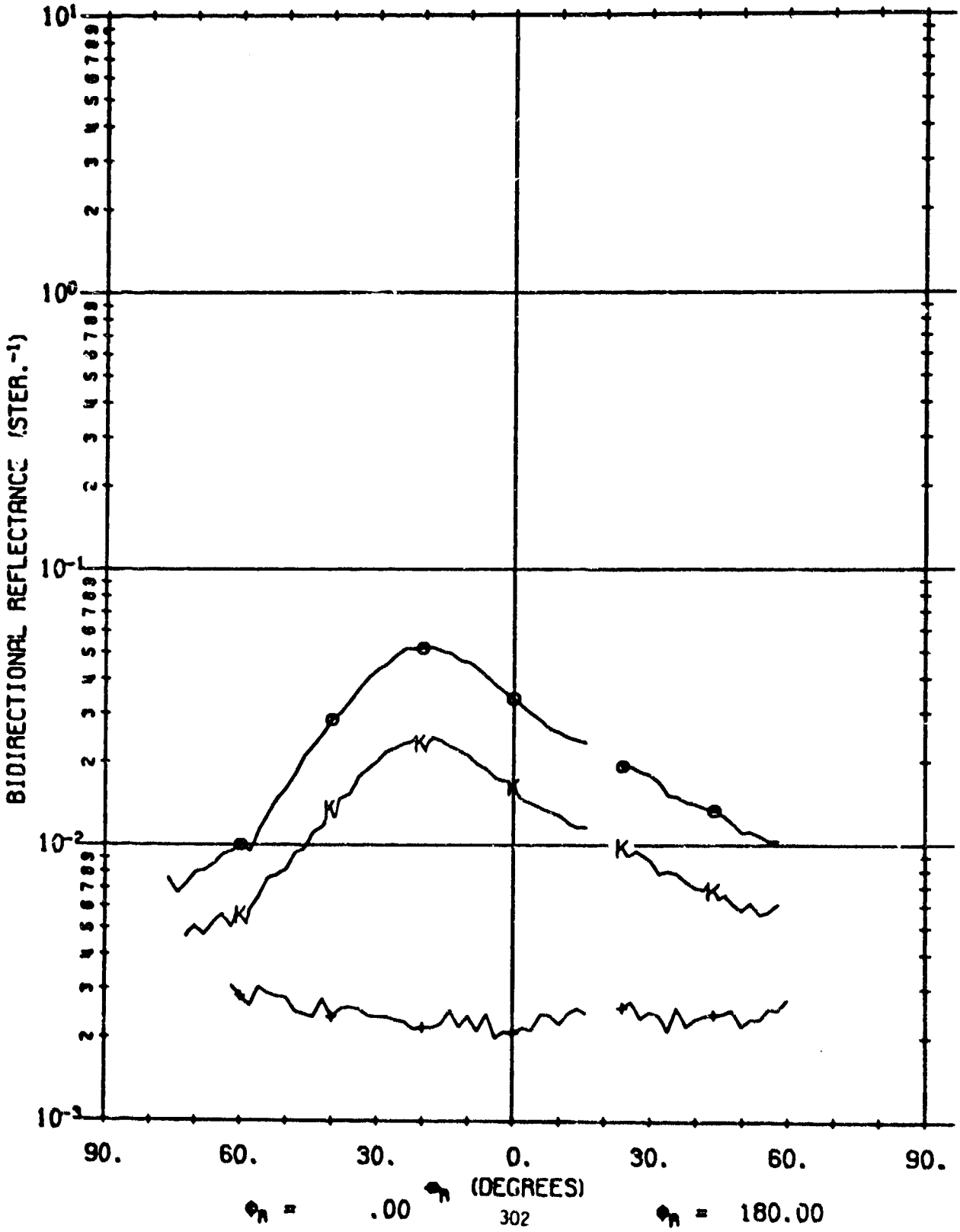

A02023 701

λ = 3.39
Φ_I = 20.0
Φ_I = 180.0

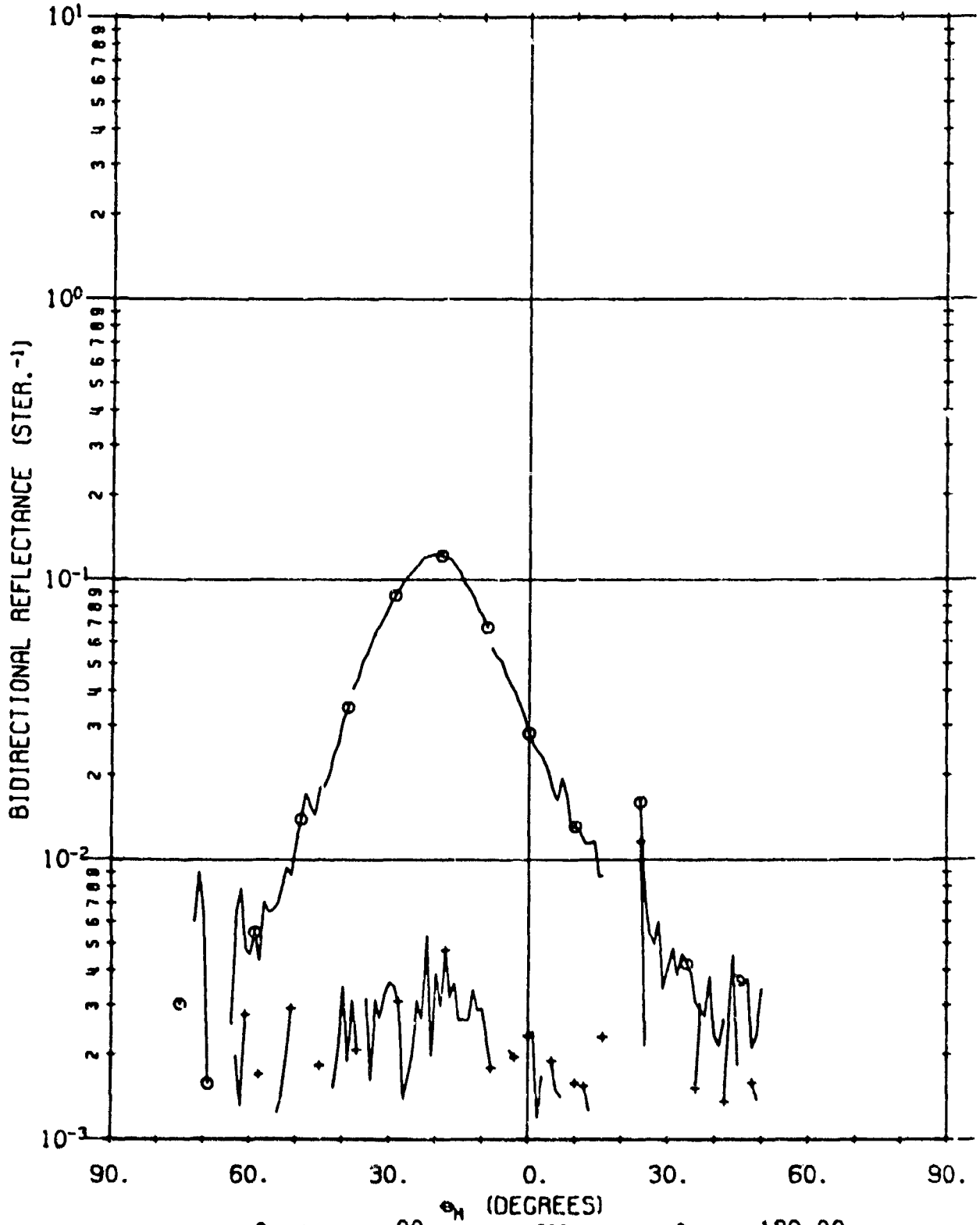

Φ_R = .00 Φ_R = 180.00

A02023 604

λ = 10.60
θ_I = 20.0
ϕ_I = 180.0

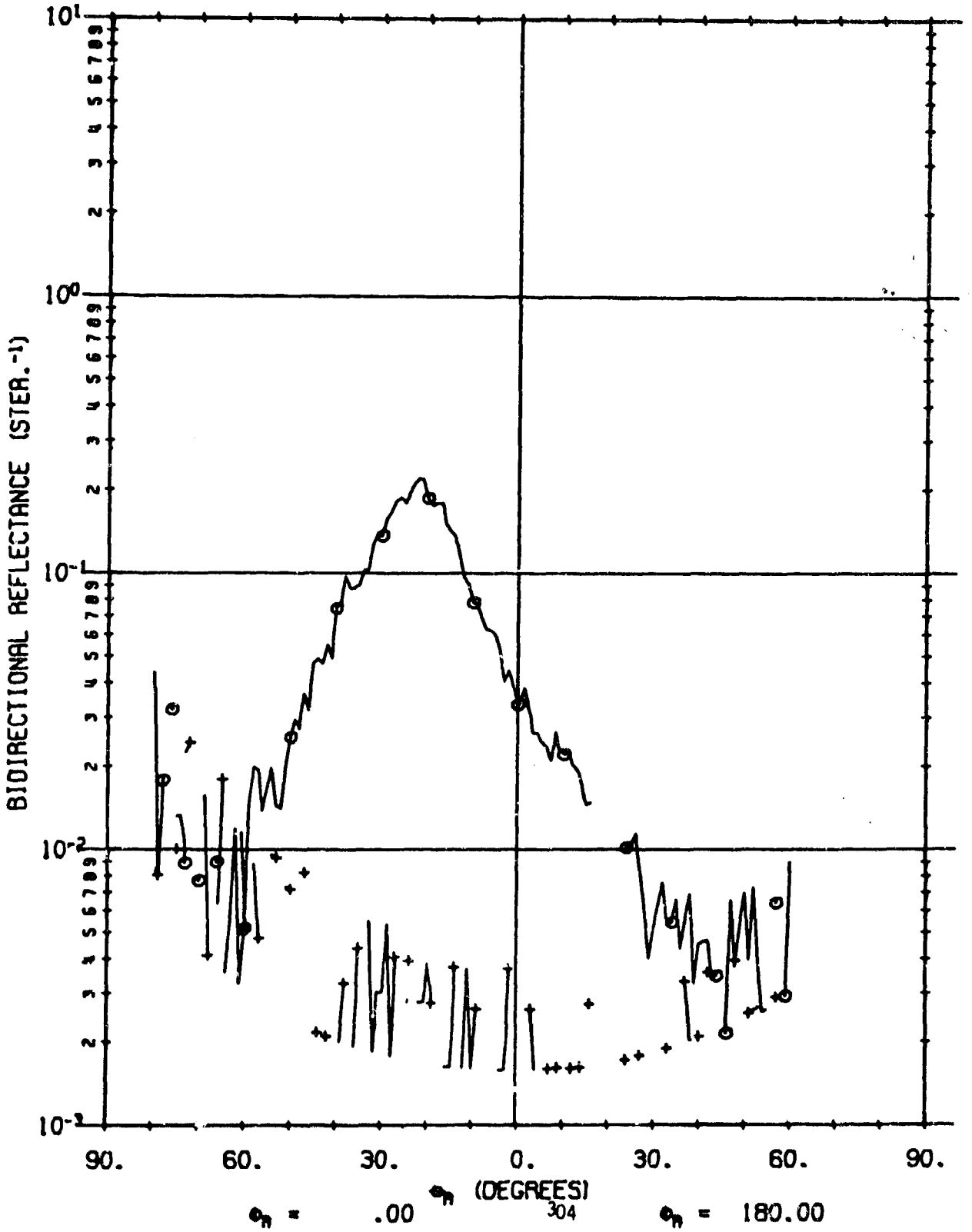

A02023 501

λ = .63
ϕ_i = 20.0
θ_i = 180.0

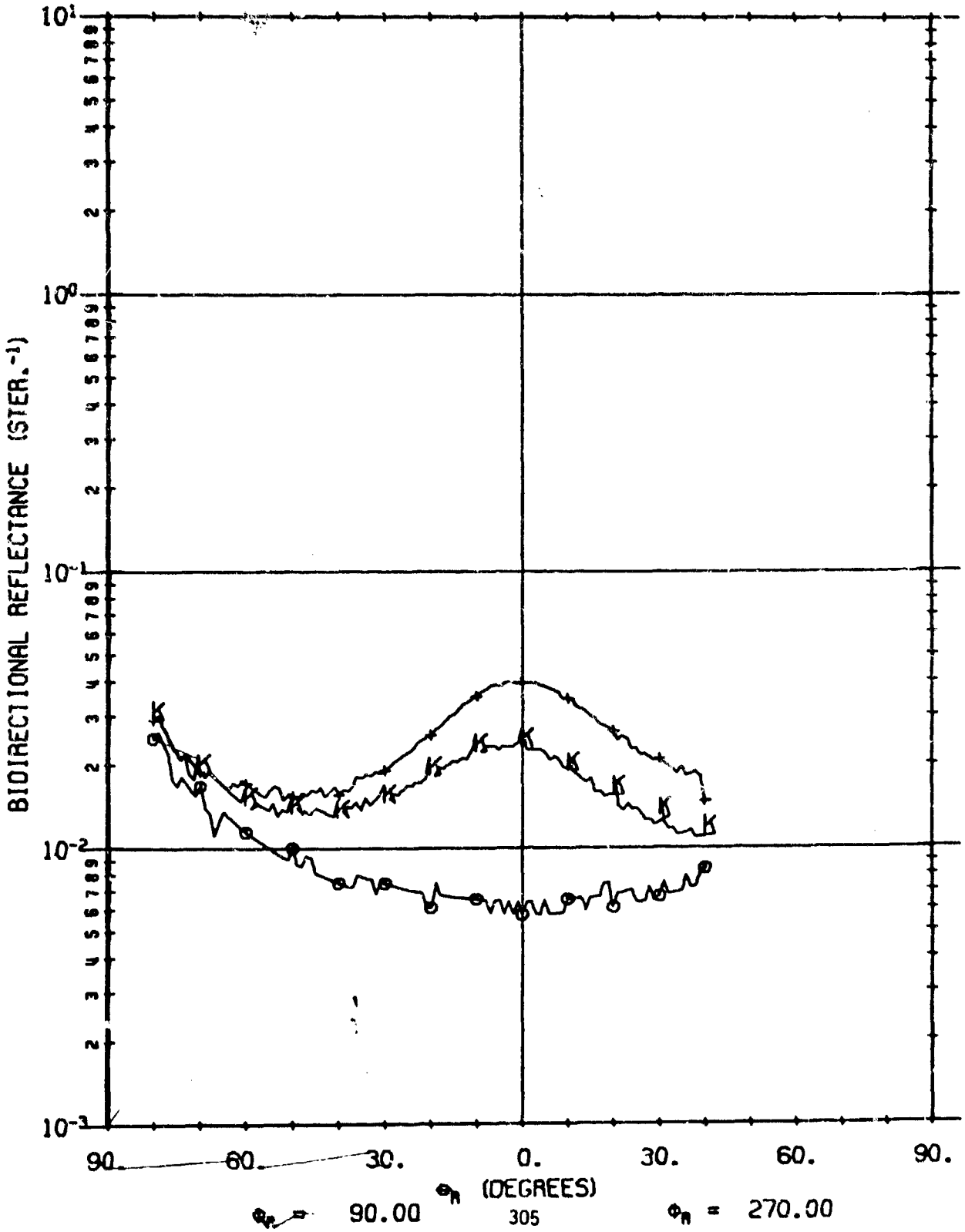

A02023 101

λ = 1.06
θ_i = 20.0
ϕ_i = 180.0

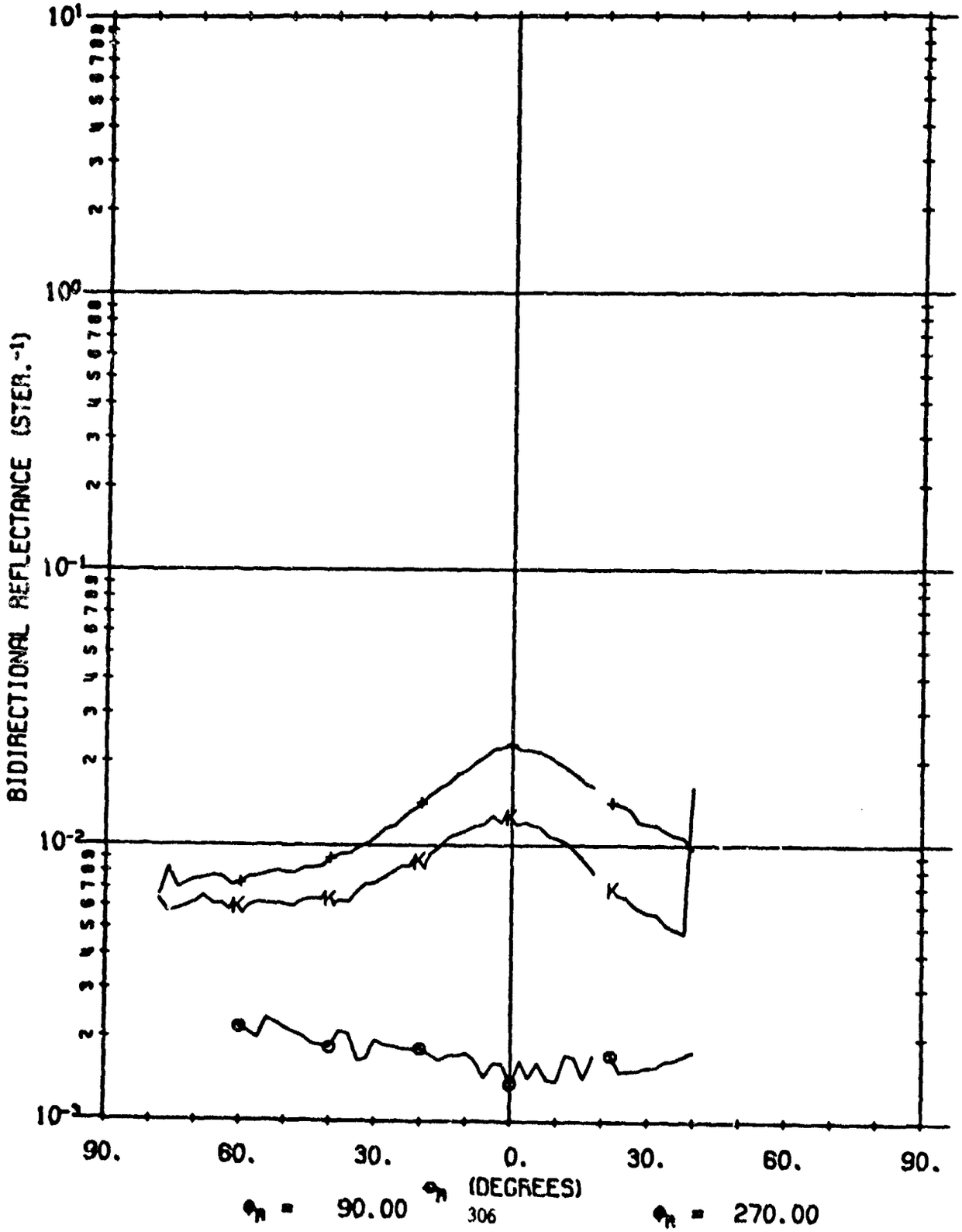

A02023 702

λ = 3.39
θ_I = 20.0
ϕ_I = 180.0

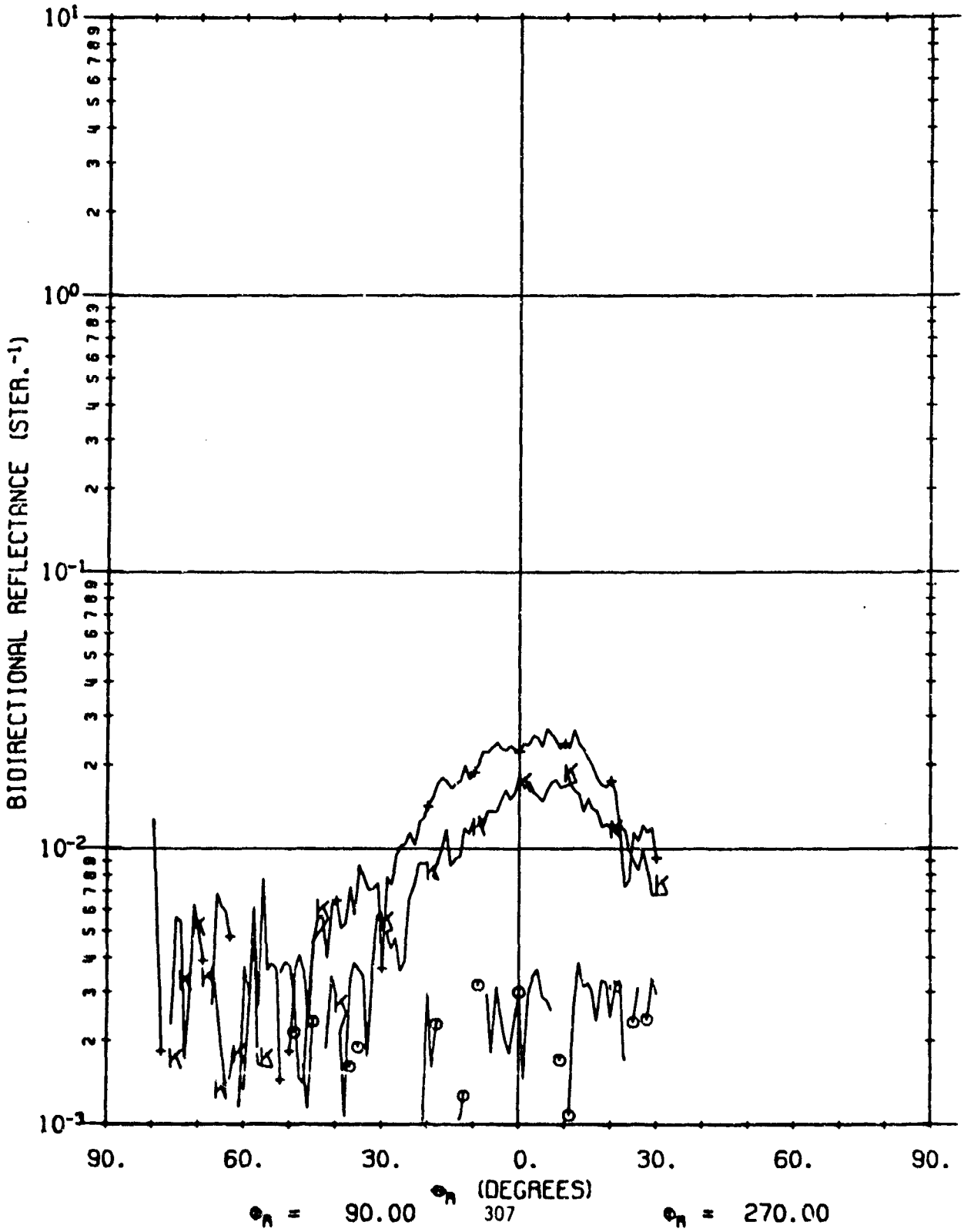

A02023 602

λ = 10.60
θ_I = 20.0
ϕ_I = 180.0

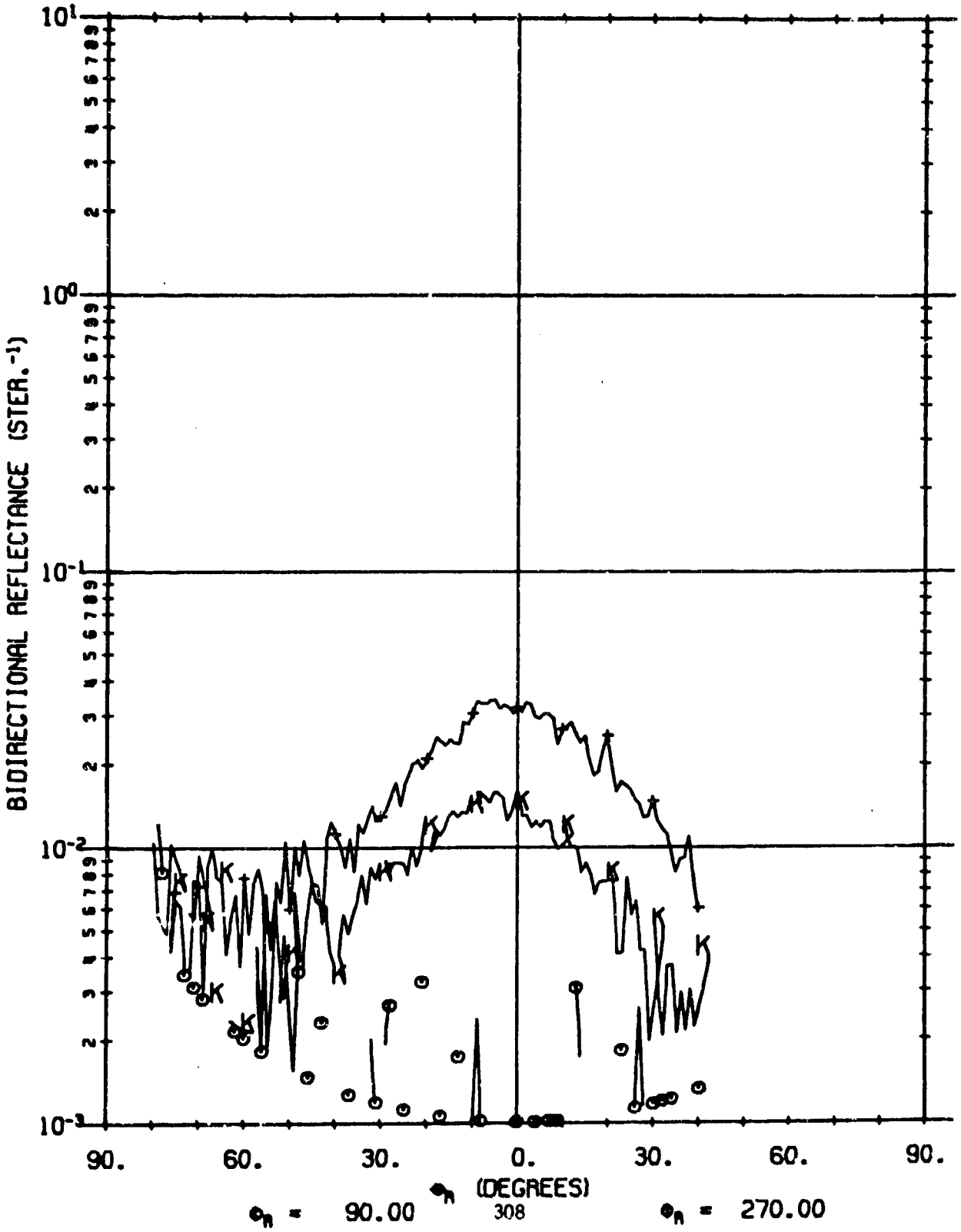

A02023 501

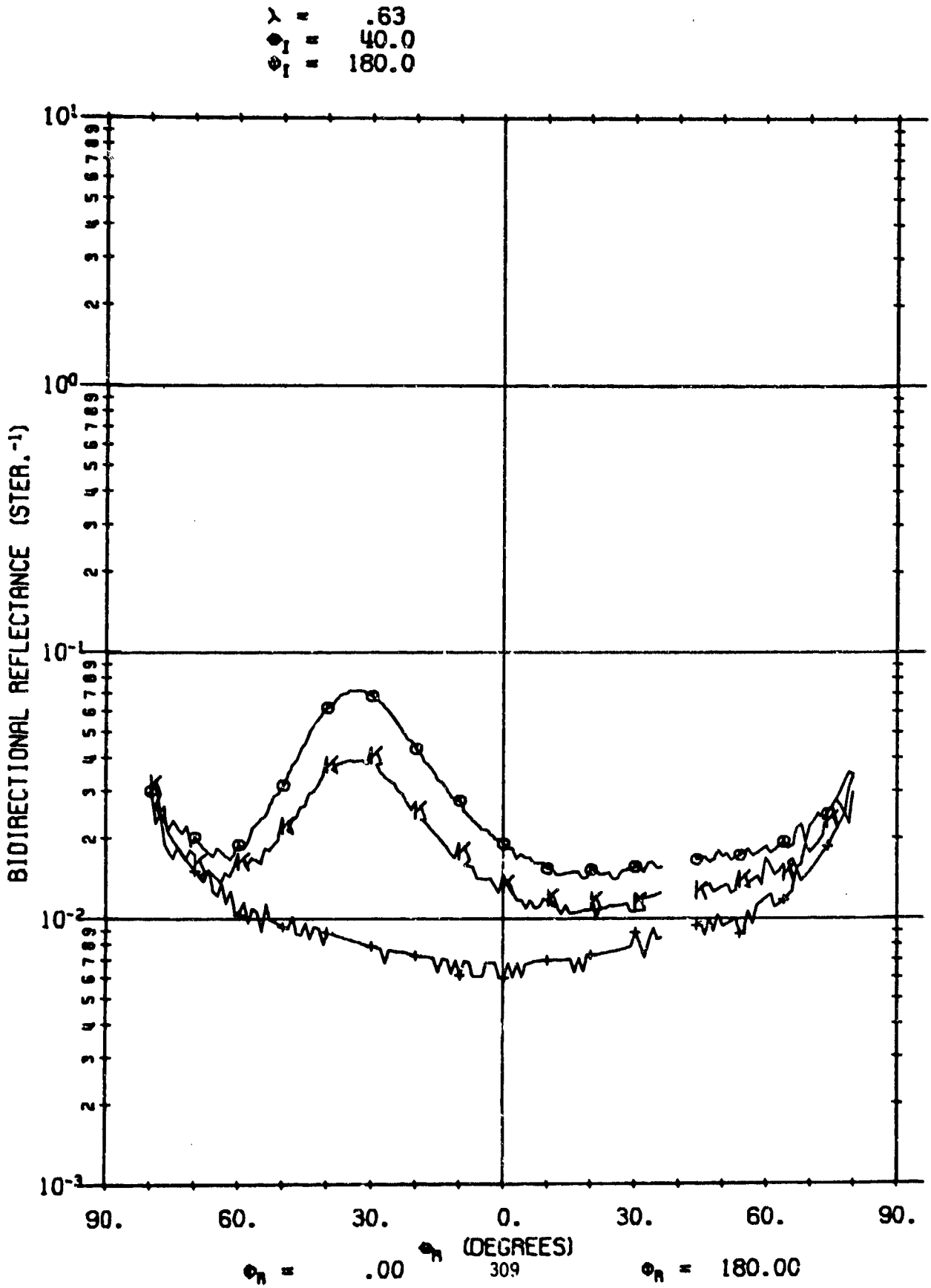
λ = .63
Φ_I = 40.0
Θ_I = 180.0
BIDIRECTIONAL REFLECTANCE (STER.$^{-1}$)
10^1
10^0
10^{-1}
10^{-2}
10^{-3}
90. 60. 30. 0. 30. 60. 90.
Θ_R (DEGREES)
Φ_R = .00
Φ_R = 180.00

A02023 101

λ = 1.06
θ_I = 40.0
ϕ_I = 180.0

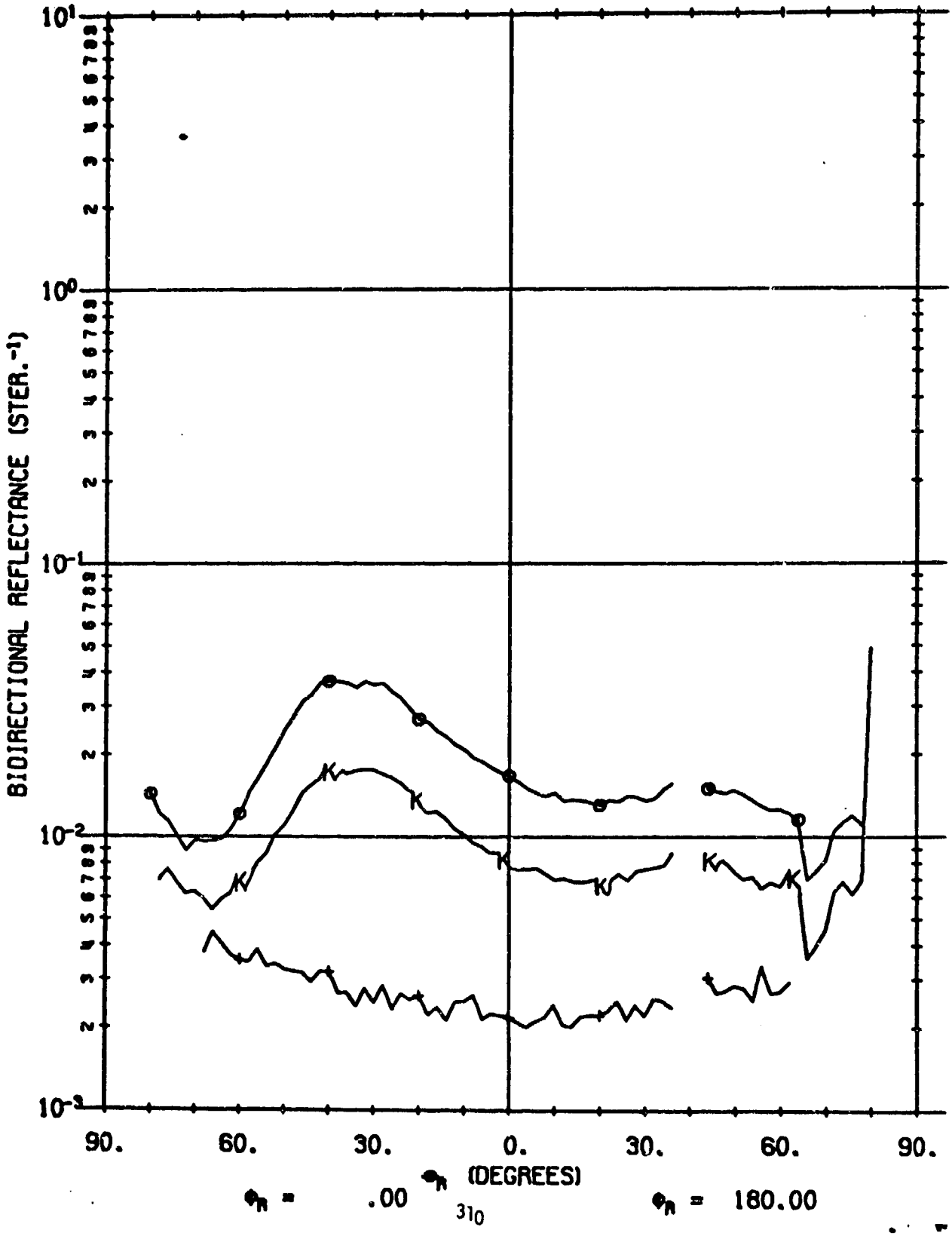

A02023 701

λ = 3.39
Φ_I = 40.0
Φ_I = 180.0

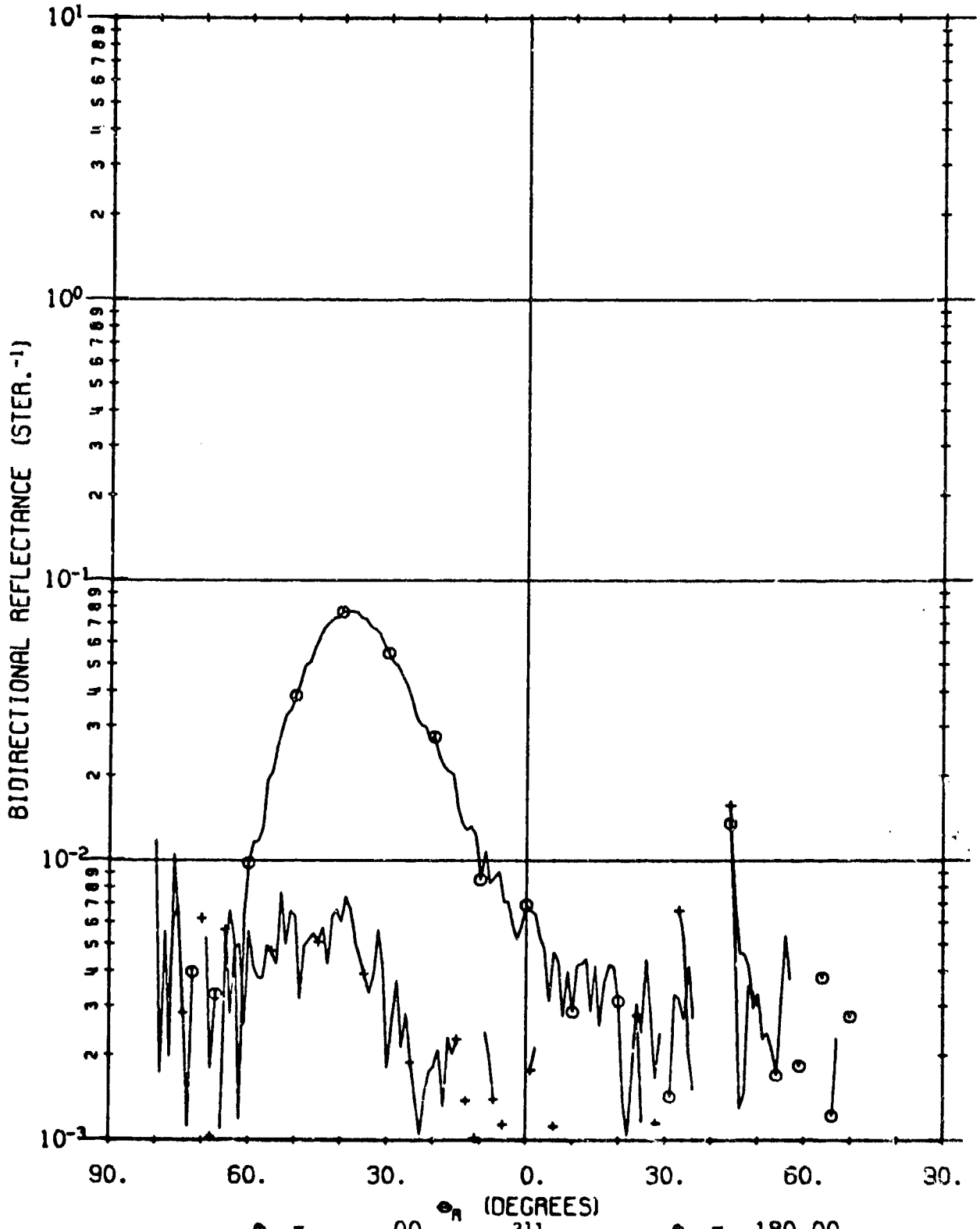

Φ_R = .00 311 Φ_R = 180.00

A02023 604

λ = 10.60
θ_I = 40.0
ϕ_I = 180.0

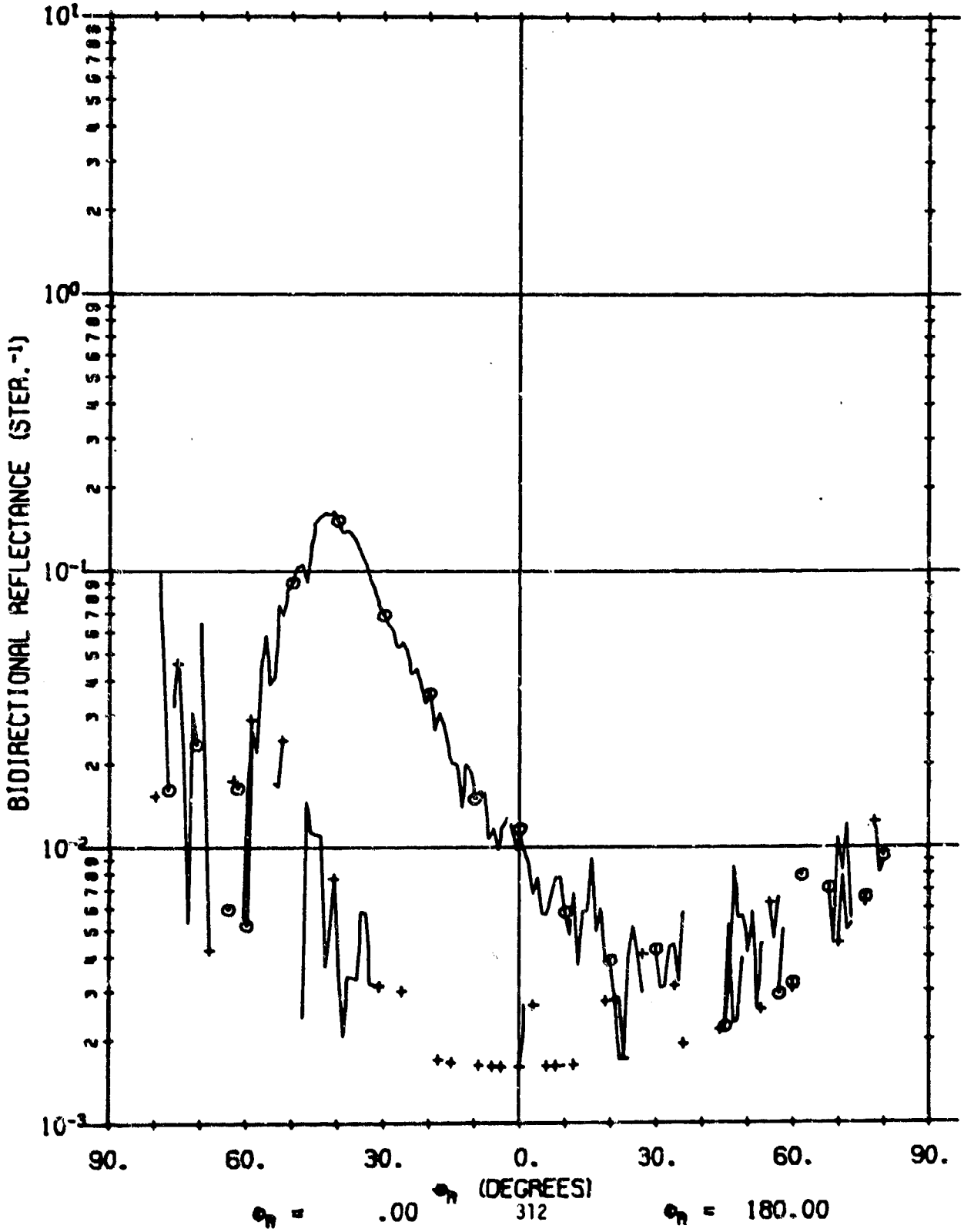

A02023 501

λ = .63
Φ_I = 40.0
Φ_I = 180.0

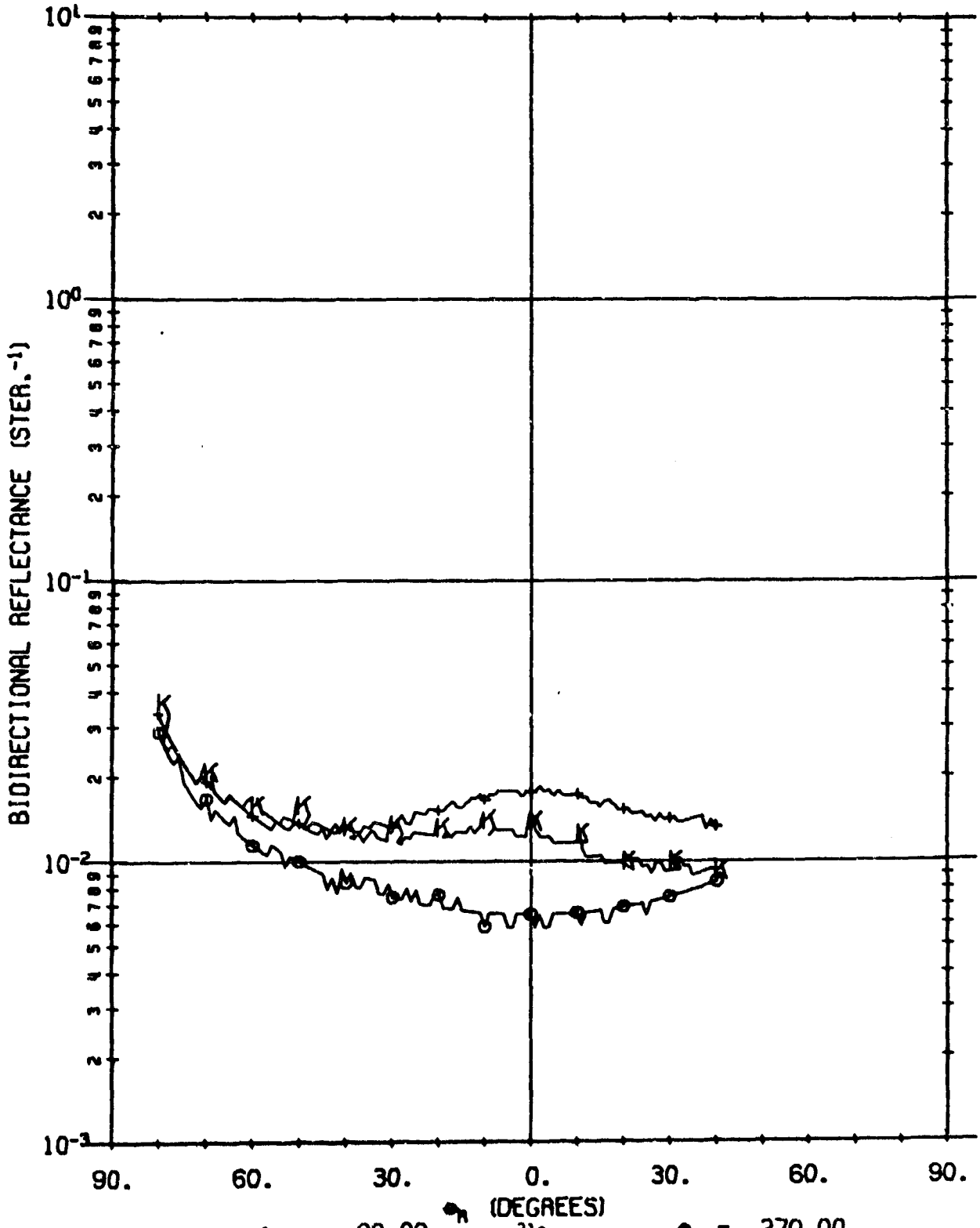

Φ_R = 90.00 Φ_R = 270.00

A02023 101

λ = 1.06
θ_r = 40.0
ϕ_i = 180.0

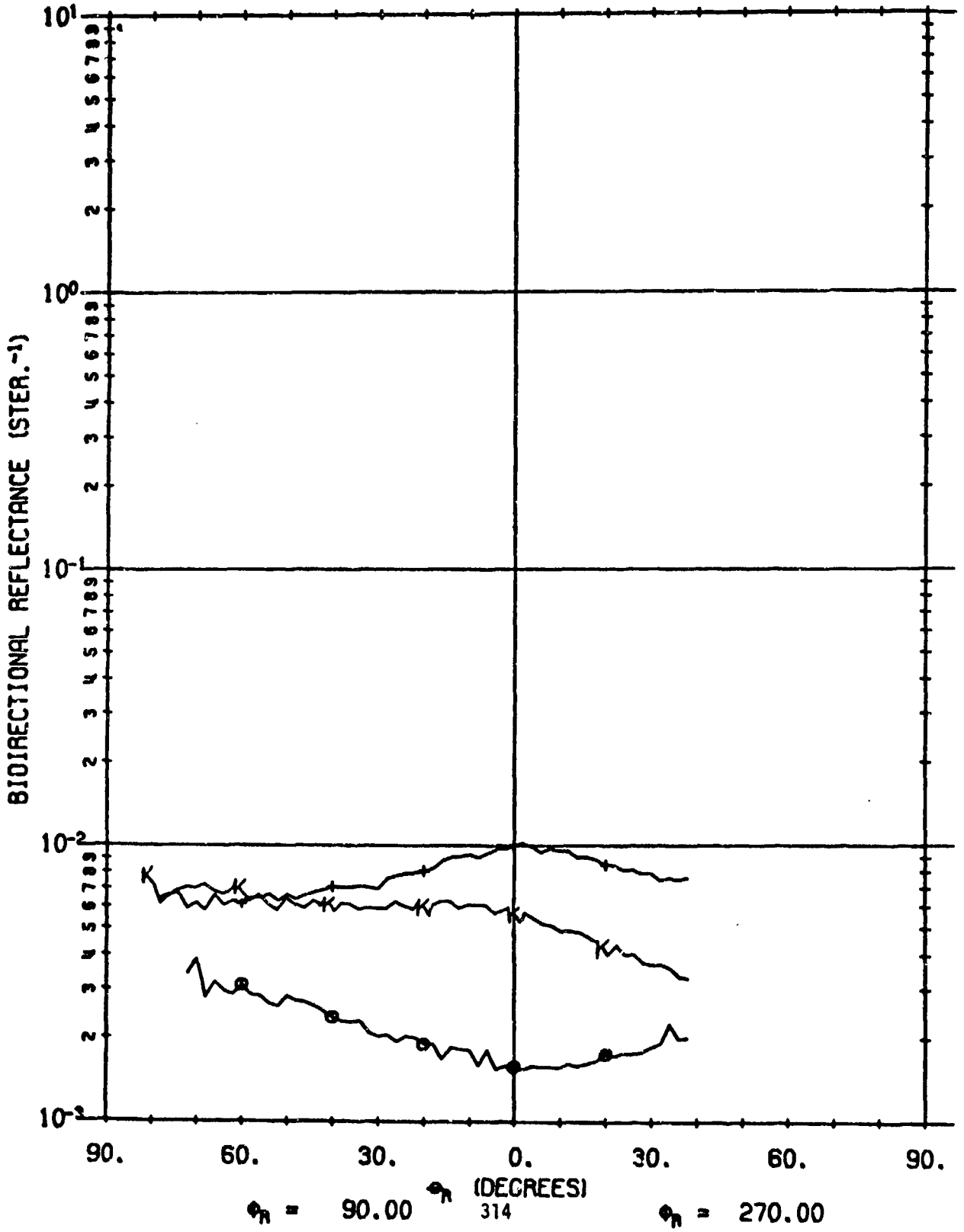

A02023 702

λ = 3.39
Φ_I = 40.0
Φ_I = 180.0

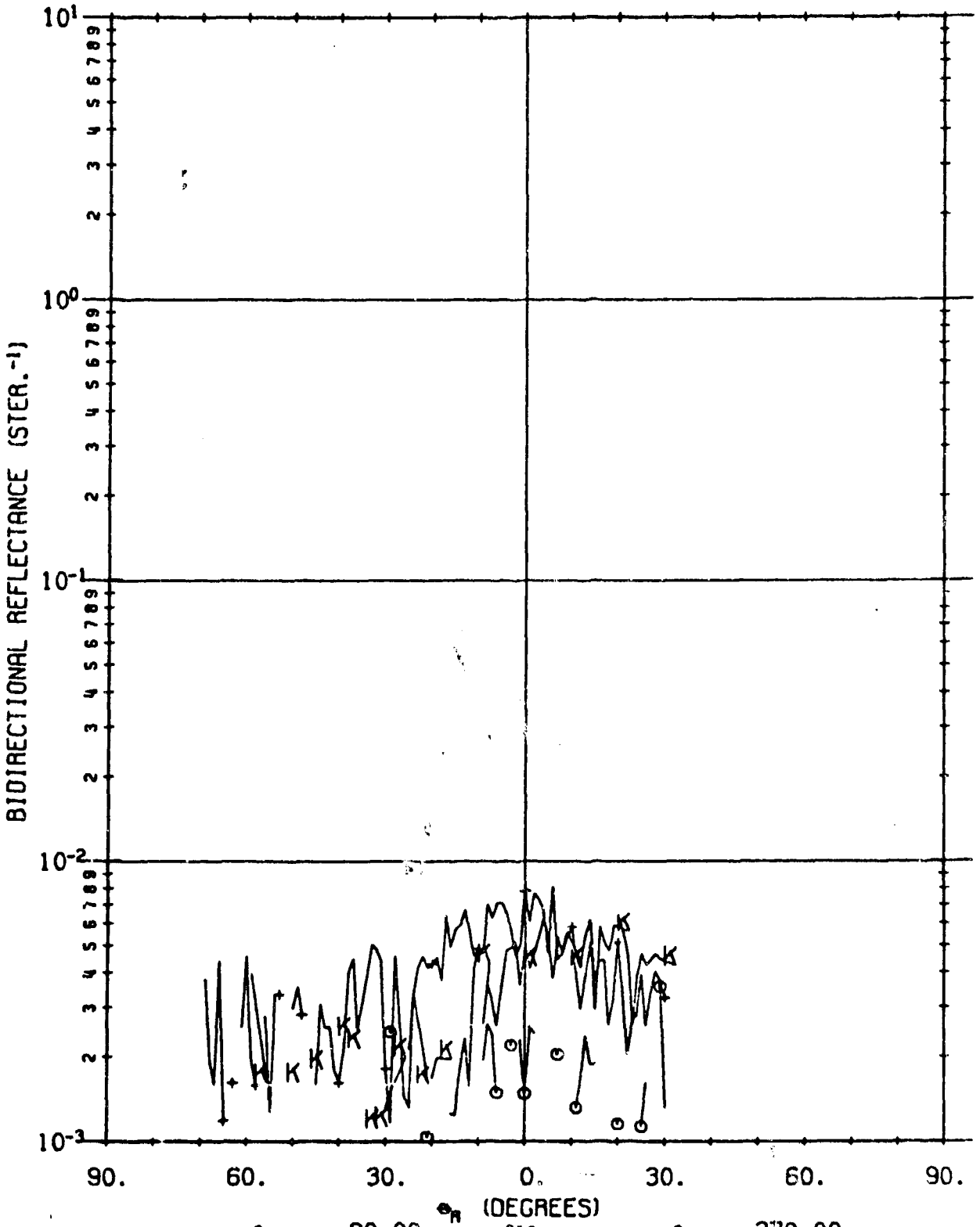

Φ_R = 90.00 Φ_R = 270.00

A02023 602

λ = 10.60
θ_I = 40.0
ϕ_I = 180.0

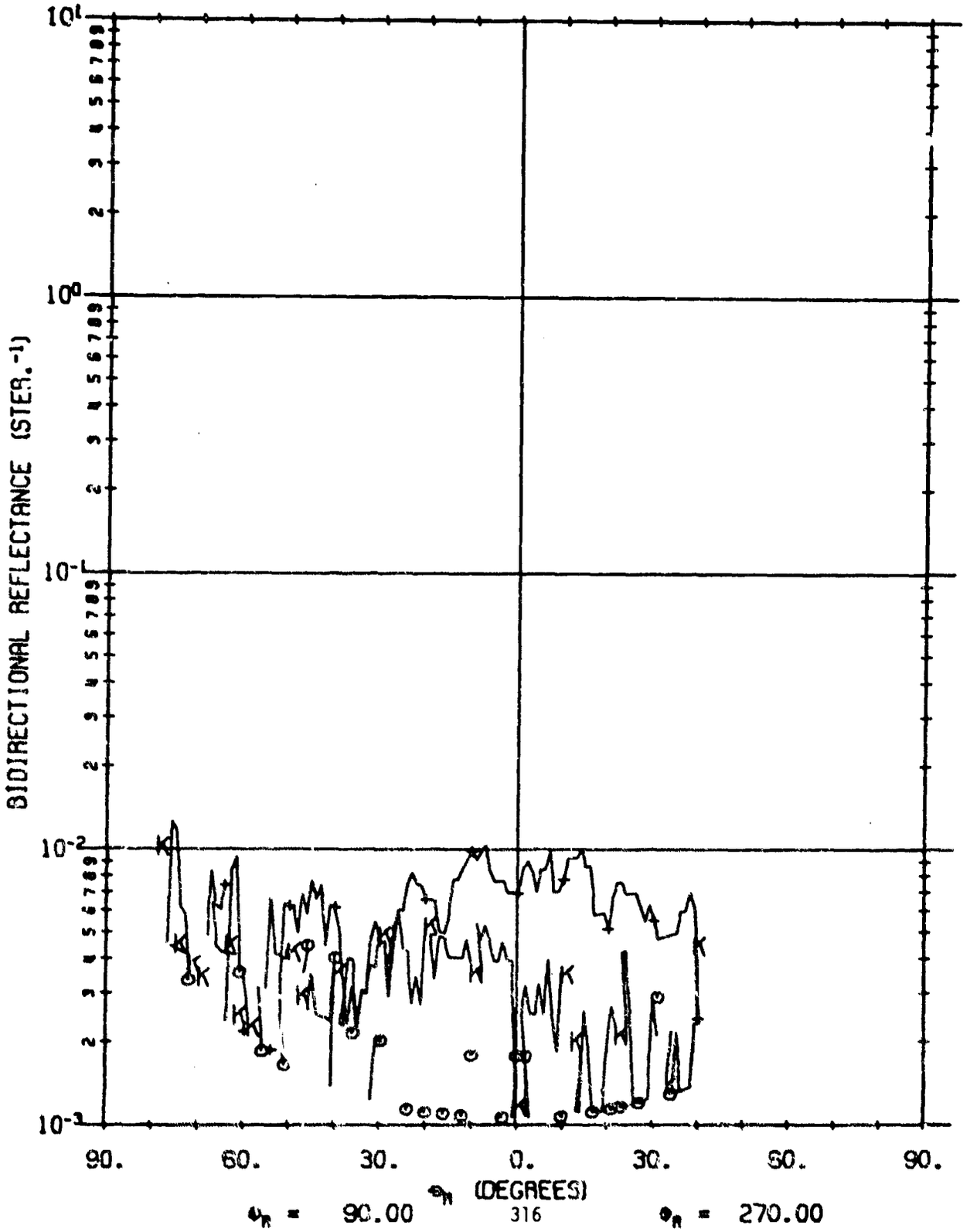

ϕ_R = 90.00 ϕ_R = 270.00

A02023 501

λ = .63
Φ_I = 60.0
Φ_I = 180.0

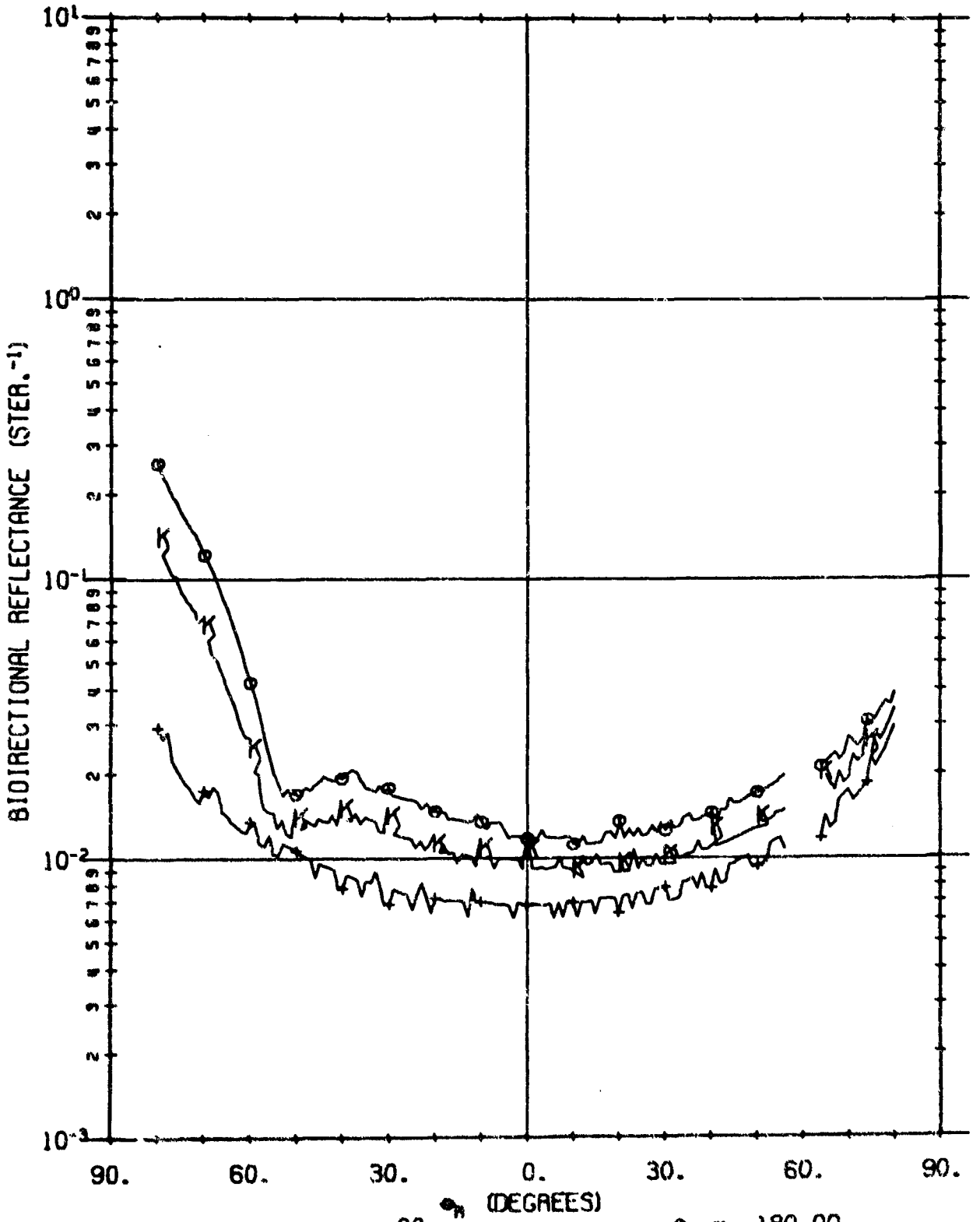

A02023 101

λ = 1.06
θ_I = 60.0
ϕ_I = 180.0

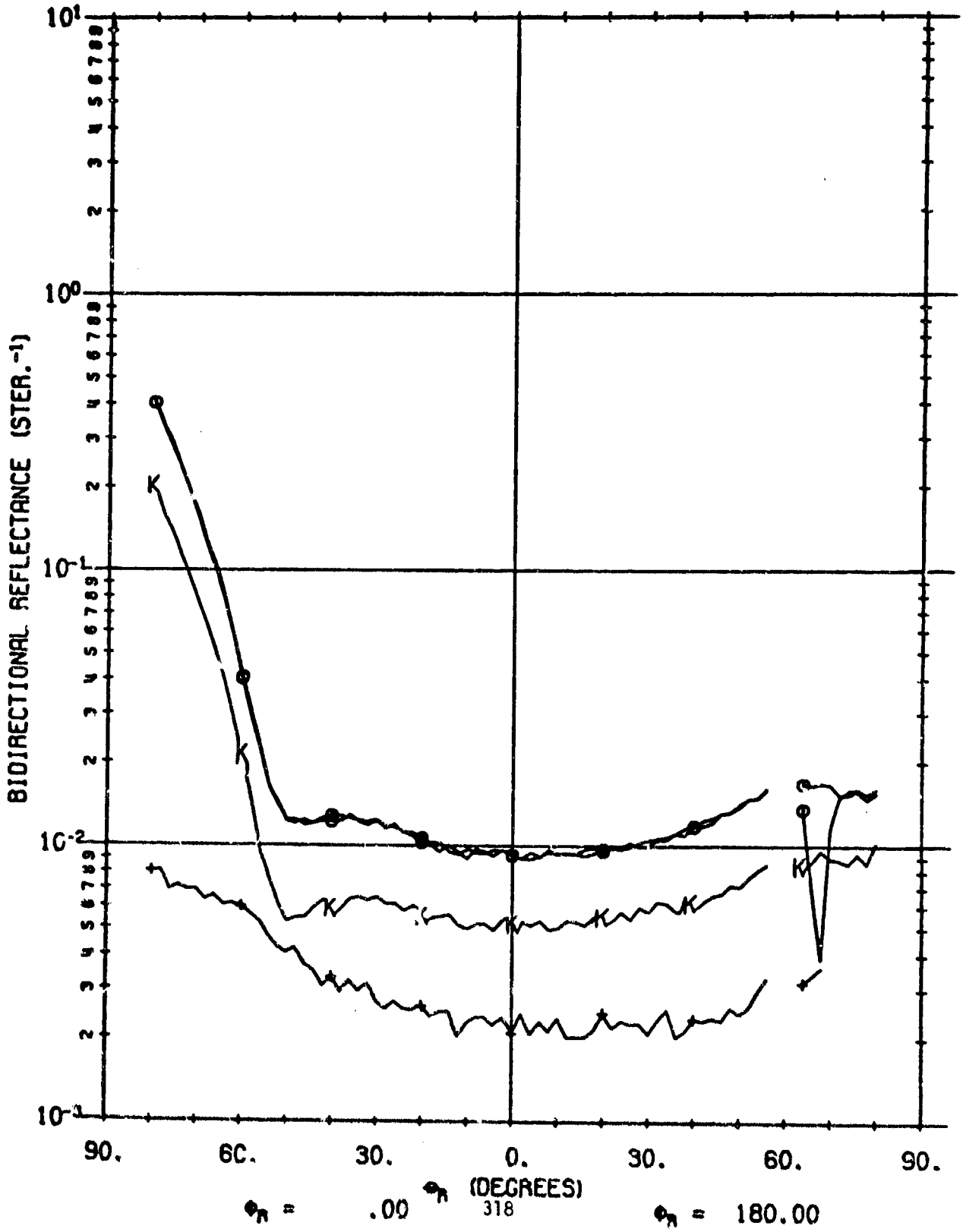

A02023 701

λ = 3.39
Φ_I = 60.0
Φ_I = 180.0

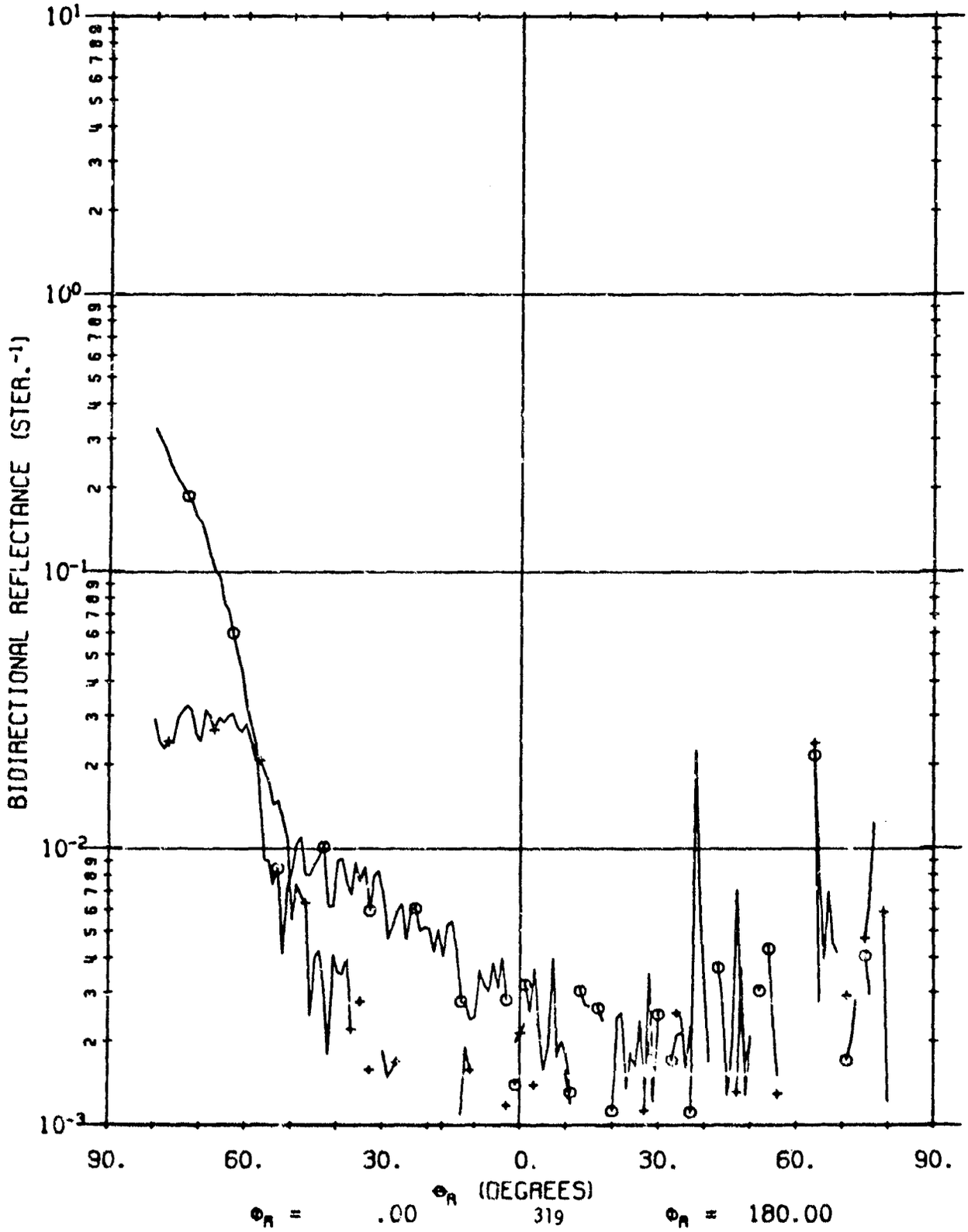

A02023 604

λ = 10.60
Φ_I = 60.0
Φ_f = 180.0

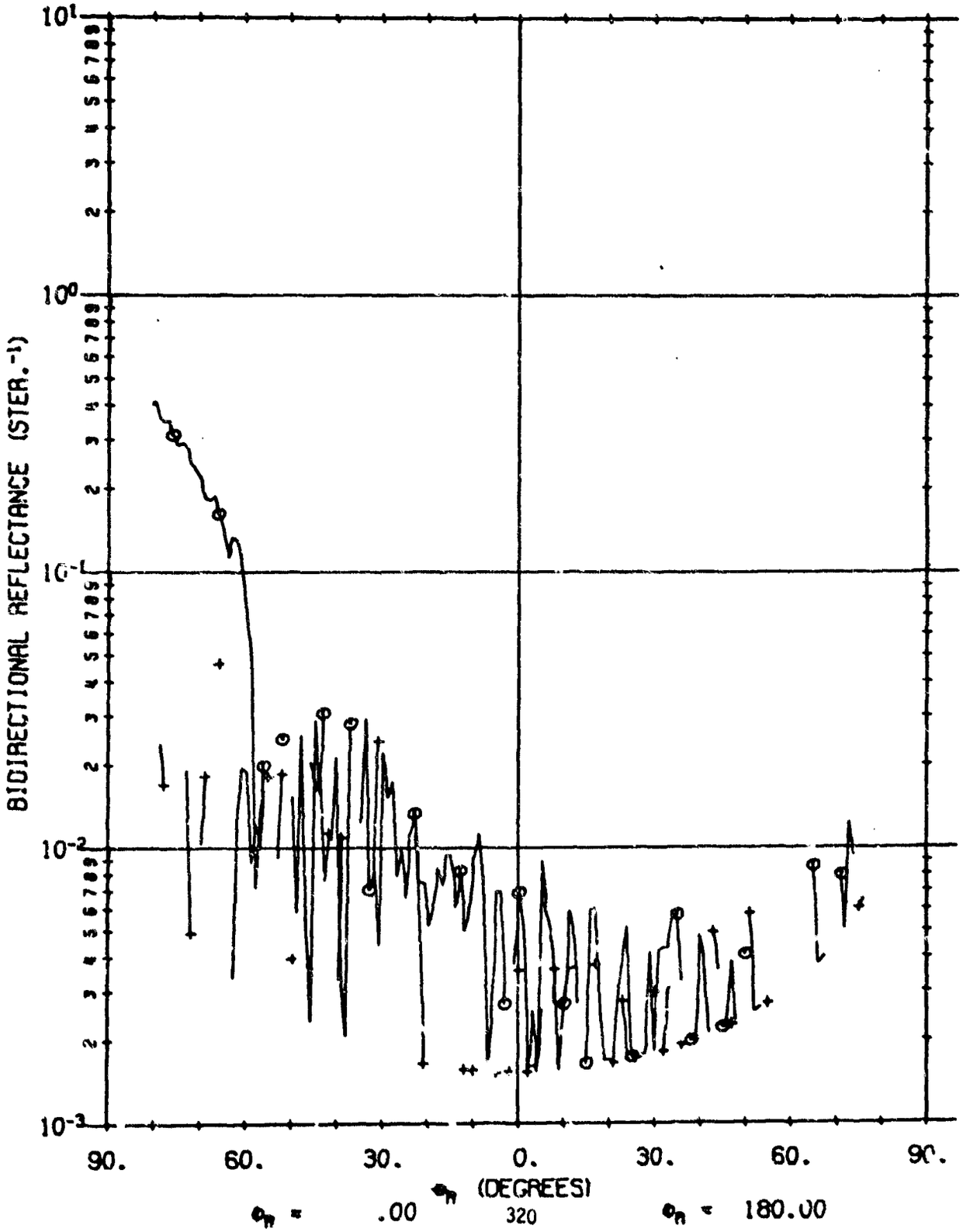

A02023 501

λ = .63
Φ_I = 60.0
Φ_I = 180.0

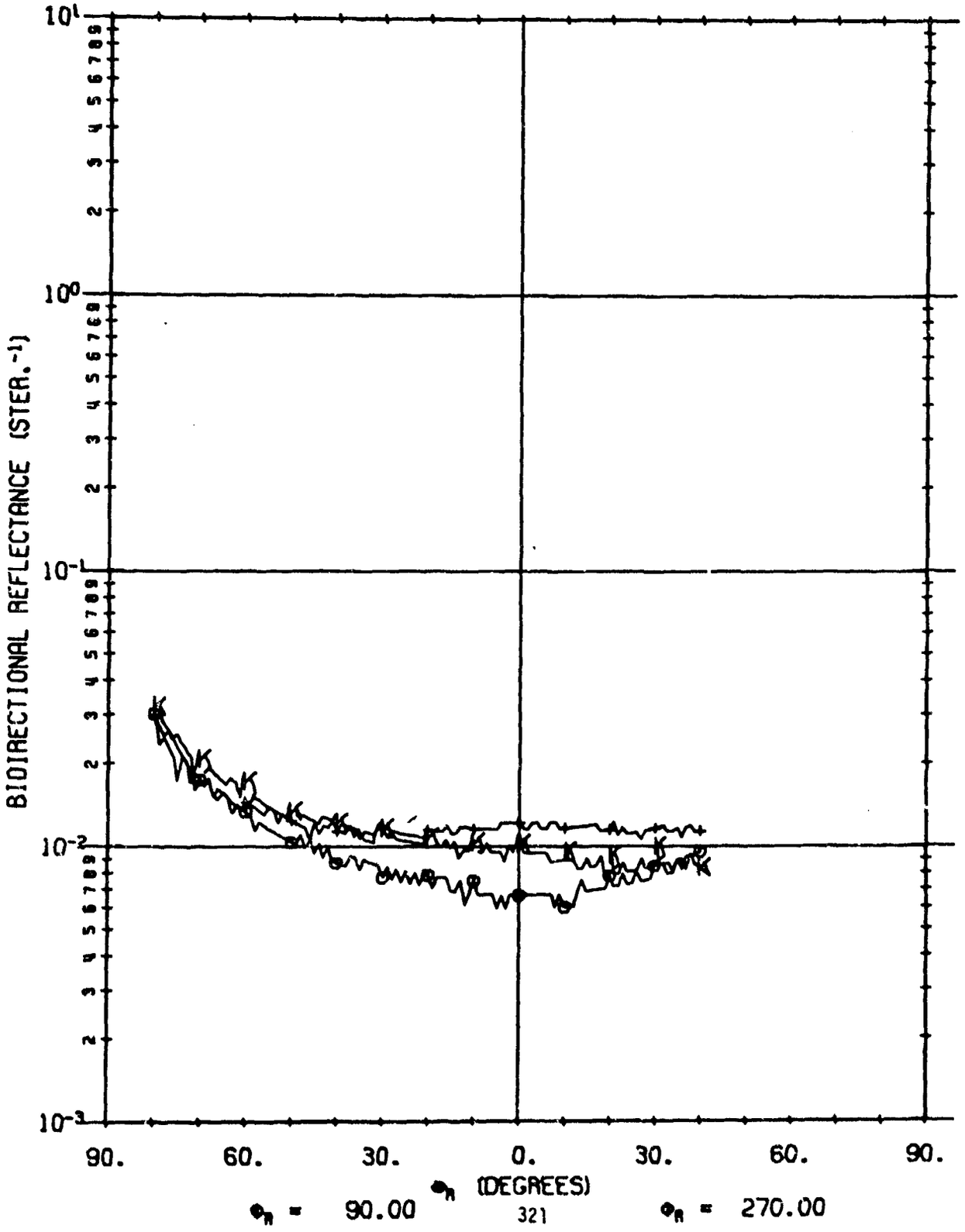

A02023 101

λ = 1.06
ϕ_I = 60.0
θ_I = 180.0

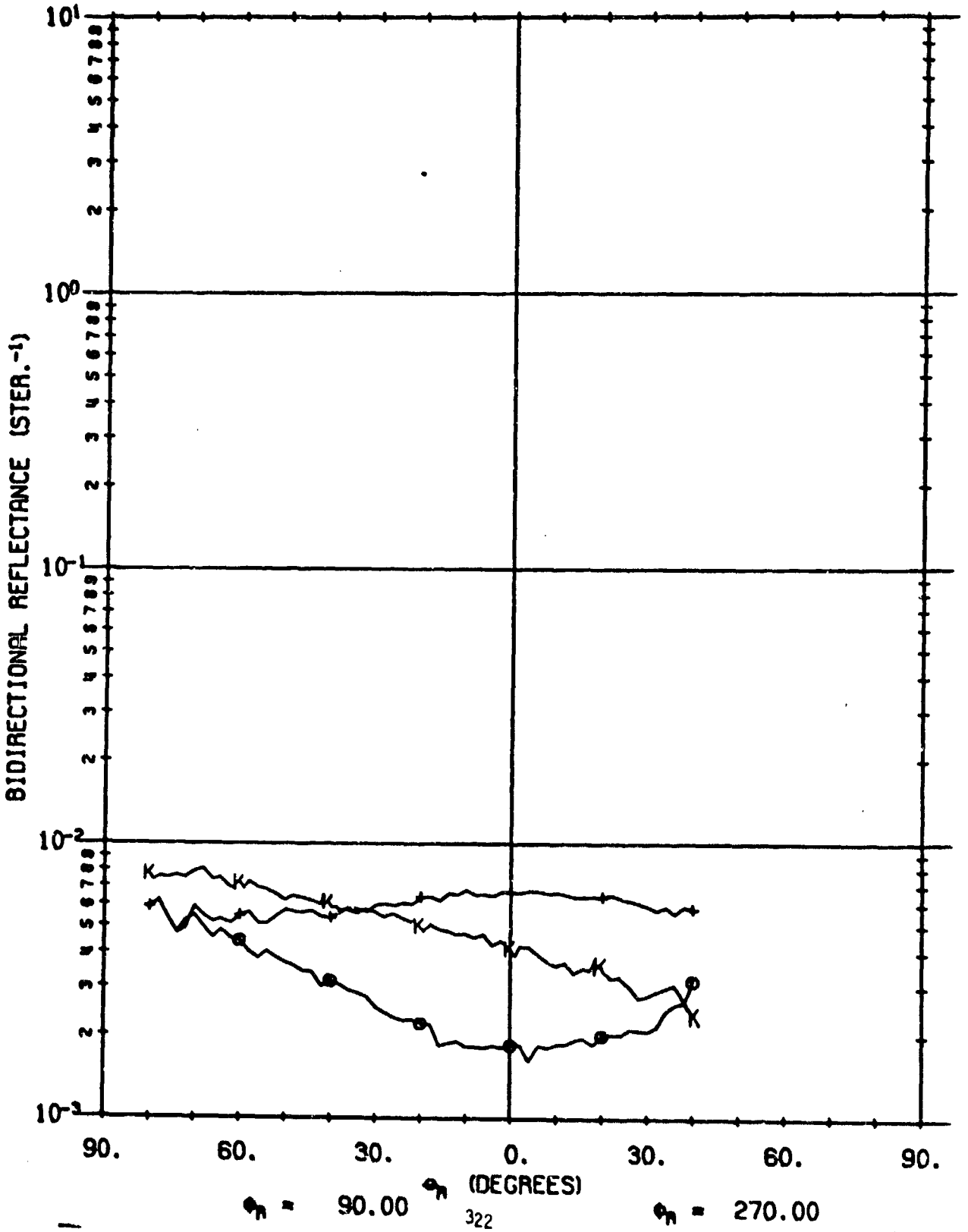

A02023 702

λ = 3.39
Φ_I = 60.0
Φ_I = 180.0

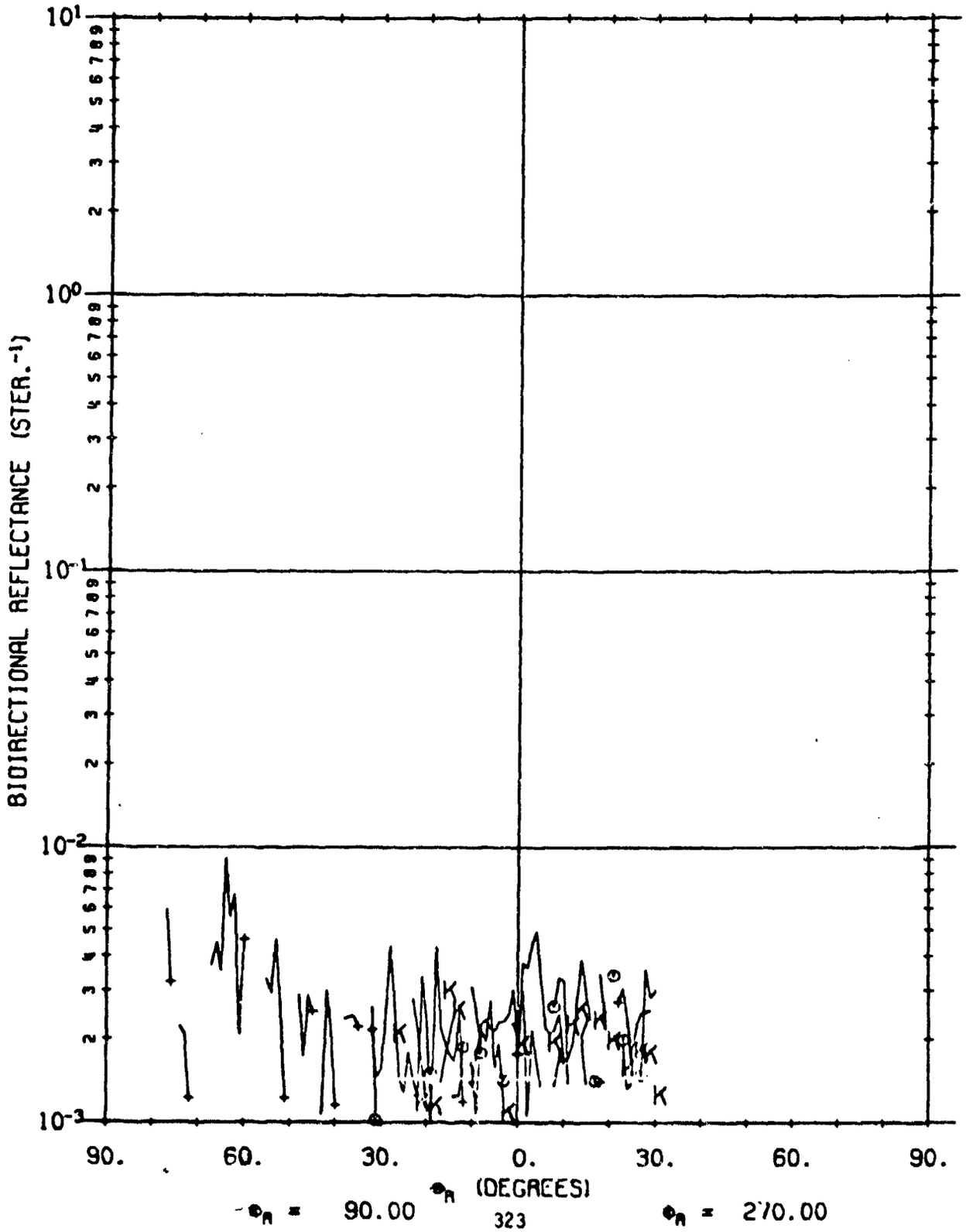

A02023 602
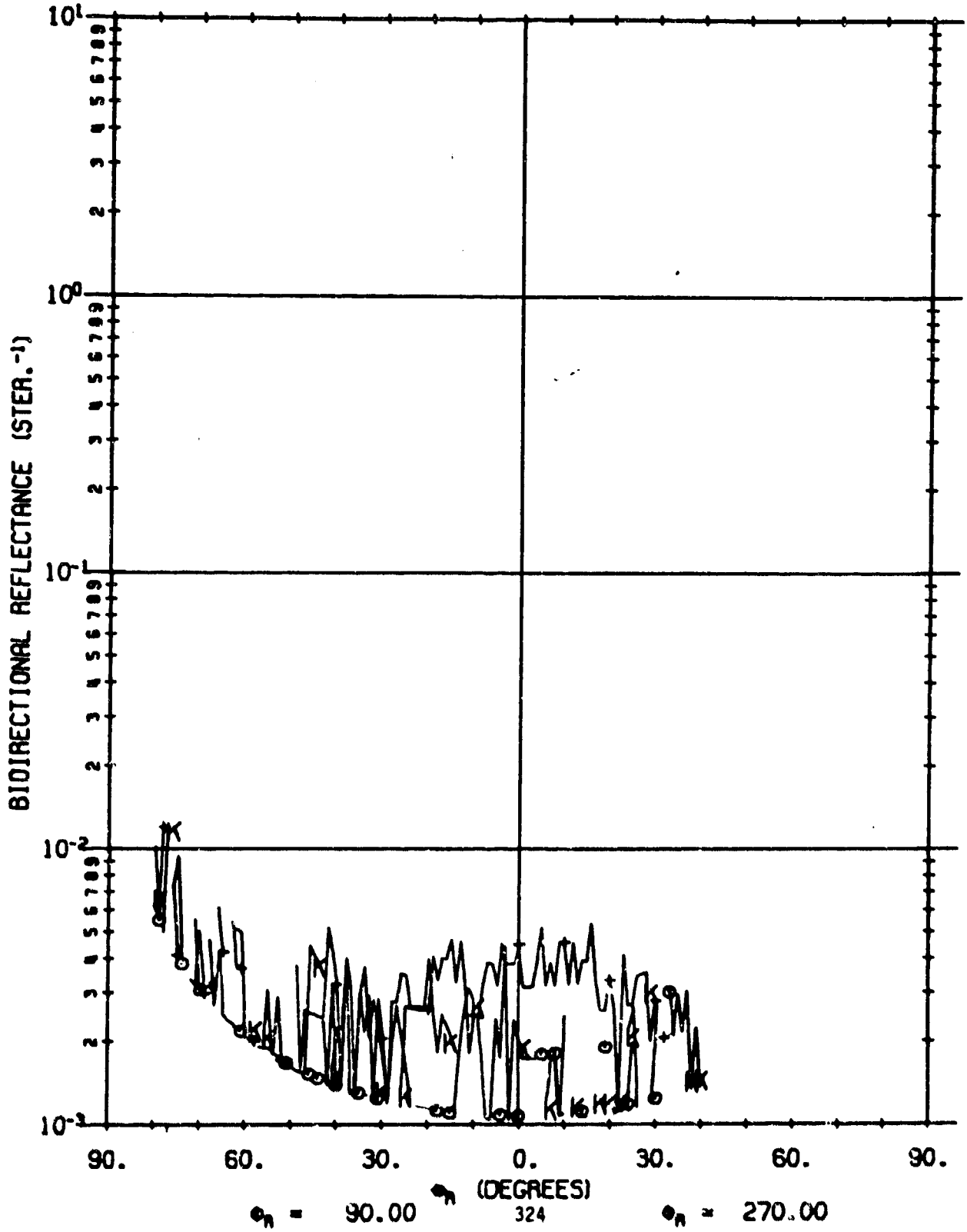
λ = 10.60
θ_I = 60.0
ϕ_I = 180.0